miRNAs as tools to improve CHO cell bioprocess phenotypes

A thesis submitted for the degree of Ph.D.

By Noëlia Sanchez, M.Sc.

The research work described in this thesis was conducted under the supervision of

Dr Niall Barron and Prof. Martin Clynes

National Institute for Cellular Biotechnology

Dublin City University

January 2013

miRNAs as tools to improve CHO cell bioprocess phenotypes

A thesis submitted for the degree of Ph.D.

By Noëlia Sanchez, M.Sc.

The research work described in this thesis was conducted under the supervision of

Dr Niall Barron and Prof. Martin Clynes

National Institute for Cellular Biotechnology

Dublin City University

January 2013

I hereby certify that this material, which I now submit for assessment on the programme of study leading to the award of Ph.D. is entirely my own work, and that I have exercised reasonable care to ensure that the work is original, and does not to the best of my knowledge breach any law of copyright, and has not been taken from the work of others save and to the extent that such work has been cited and acknowledged within the text of my work.

Signed: Noëlia Sanchez ID No: 58114700

Date: 14/01/13

Acknowledgements

I would like to express my sincere gratitude to the director of the National Institute for Cellular Biotechnology, Prof. Martin Clynes, for the opportunity to do my Ph.D. in the center, for encouraging me, particularly in stressful moments, for advising in the redaction of the thesis and for expressing interest in my work.

I would like to thank Dr Patrick Gammell who gave me the opportunity to come in Dublin and to do a six months placement for my master's degree. Despite a panic when he left NICB the week before I arrived, he made sure that I could still come and that I was not left without supervision. I also would like to thank him for his support in job seeking.

For my master degree's placement, I was finally very lucky to be supervised by Dr Niall Barron who also gave me the great opportunity to do a Ph.D. I do not know where to start to describe how an amazing supervisor. I would like to thank him for sharing his scientific knowledge, for his guidance, help and encouragement during the thesis, and also for being patient, available and never angry particularly when he corrected my English. I was also very lucky to work in excellent conditions in his laboratory.

I would like to thank Dr Olga Piskavera and Dr Nga Lao for their help in the laboratory and for teaching me a wide range of molecular biology techniques.

I would like to thank particularly Justine, Serena, Erica and Martin for being very good colleagues and friends and for encouraging me all the time.

I would like to thank all the postgraduate students from the CHO group for sharing their joy as well as their good humour every day and for keeping a good atmosphere in the office as well as in the laboratory.

I would like to thank every single person in the NICB who helped me and encouraged me during my project.

A special thanks to Carol, Yvonne and Mairead for their help regarding the administrative tasks and for being so nice with me.

A big thanks to my parents for their help and support during my studies, for believing in me and understanding my wish to travel even if it implies living far from them.

Last but not least, a huge thanks to Anthony who always believed in me and encouraged me during this journey. I would like to thank him for moving to Ireland and being present to give me his support when I needed him the most.

Table of Contents

Noëlia Sanchez

1 Abstract: miRNAs as tools to improve CHO cell bioprocess phenotypes

miRNAs are small non-coding RNA molecules that are capable of regulating hundreds of genes and are involved in many, if not, all biological pathways. We sought to investigate the utility of these molecules as potential engineering targets in CHO cells and subsequently to identify the mechanisms by which they mediate any observed effect. Previous miRNA profiling studies conducted in our laboratory identified several candidate miRNAs associated with cell proliferation. Functional assessment of several of these miRNAs using mimic and inhibitor molecules showed that miR-30e-5p, miR-29a, miR-10a and let-7e impacted on growth and, despite contrasting results between assays and cell lines could be good candidates to manipulate three main bioprocess-relevant CHO properties, i.e. cell proliferation, cell survival and protein production/secretion.

The functional importance of miR-24 in CHO cell proliferation was also demonstrated. Transient overexpression or knockdown of the three members of the miR-23a~27a~24-2 cluster proved to be a better approach than manipulation of the individual miRNAs due to their presumably cooperative roles in regulating cell growth. Furthermore, stable cell lines expressing antisense transcripts to simultaneously knockdown the miR-23~27a~24-2 cluster members showed increased proliferation of up to 71% compared to control lines.

The anti-proliferative role of miR-7 was verified using mimics in several different CHO cell lines in serum-free medium and we found that the arrest of cell growth upon pm-7 transfection was associated with accumulation in G1 of the cell cycle without induction of apoptosis. Expression profiling and experimental validation revealed that miR-7 targets key regulators of the G1 to S phase transition, including Skp2, Myc and $p27^{Kip1}$ to temporarily arrest cell growth in the G1 phase. The down-regulation via miR-7 of critical pro-apoptotic regulators, including p53, as well as DNA repair factors such as Rad54L, with the concomitant up-regulation of anti-apoptotic factors like p-Akt, promoted cell survival while arrested in G1. Finally, we successfully extended the

longevity of culture and consequently improved CHO cell proliferation by 3.27-fold as well as viability by 28.9% respectively in batch-fed culture using an antisense ‘miRNA sponge’ approach to stably knockdown endogenous miR-7.

2 Abbreviations

Ab - antibody

am - inhibitor for mature miRNA

Amp - ampicilin

ATCC - American Tissue Culture Collection

ATP - adenosine triphosphate

am-neg - negative control for inhibitors

BSA - bovine albumin serum

cDNA - complementary

CDS - coding sequence

CHO - Chinese Hamster Ovary

CMV - cytomegalovirus

DMEM - Dulbecco's Modified Eagle Medium

DMSO - dimethyl sulfoxide

DNA - deoxyribonucleic acid

Dox - doxycyline

FSC - forward scatter

g - gram

G - gravitational force

GAPDH - glyceraldehyde-6-phosphate dehydrogenase

GFP - green fluorescent protein

hrs - -hours

Hyg - hygromycin

LB - Luria-Bertani medium

miR - mature microRNA

miRNA - microRNA

mL - millilitre

mM - milimolar

µL - microliter

µM - micromolar

mRNA - messenger RNA

nM - nanomolar

ORF - open reading frame

P - promoter

PBS - phosphate buffered saline

PCR - polymerase chain reaction

pm - mimic of mature miRNA

pm-neg - negative control for mimics

qRT-PCR - quantitative real time PCR

RISC - RNA-induced silencing complex

RNA - ribonucleic acid

rpm - revolutions per minute

RT - reverse transcription

SDS - Sodium Dodecyl Sulphate

SEAP - Secreted Embryonic Alkaline Phosphatase

SFM - serum-free medium

shRNA - short hairpin RNA

siRNA - small-interfering RNA

Tet – tetracycline

Tet O – tetracycline operator sequences

Tet R – tetracycline repressor

TF – transcription factor

TLDA – TaqMan Low Density Array

TRE – tetracycline response element

TS – Temperature Shift

tTA – tetracycline activator

UHP - Ultra High Pure water

3’UTR - untranslated region at the 3’end

5’UTR - untranslated region at the 5’end

VCP - Valosin-containing protein

ZFN - zinc-finger nuclease

INTRODUCTION

3 Introduction

3.1 The emergence of recombinant proteins as new medecines

The discovery of recombinant DNA technology in 1973 by Cohen and Boyer made possible the emergence of biotechnology and its application in society (Cohen, et al. 1973). The production of recombinant proteins as new medicines is an important area where the use of biotechnology has been essential for both drug development and manufacturing. In 1982, insulin was the first therapeutic made via recombinant protein technology in *Escherichia coli* in application to diabetes mellitus treatment (Butler 2005). In 1986, tissue plasminogen activator, a thrombolytic agent for breakdown of blood clots, was the first biological therapeutic produced in mammalian cells (Vehar, et al. 1986). Since the 1980s many therapeutics have been made using this approach (some examples are listed in **Table 3.1**. Nowadays, monoclonal antibodies (mAbs) represent nearly 70% of all biopharmaceutical products and contribute notably to the success of biomedicines in terms of medical research, diagnosis and therapy (Rodrigues, et al. 2010, Wurm 2004, Jenkins, Parekh and James 1996) (few examples are listed in **Table 3. 2**). The first Mabs were produced using hybridomas which derived from the fusion between immune cells and cancer cells. Recently, more specific drugs have been developed leading to chimeric (murine variable regions fused onto human constant regions of an antibody) and human monoclonal antibodies which bind to specific cell-type receptor and are commercially produced in mammalian cells (Nelson, Dhimolea and Reichert 2010). For clinical purpose, high doses of mAbs are needed during therapy for chronic diseases due to their low potency therefore the cost of these drugs remains quite expensive and not affordable for every country.

Table 3.1 (part 1/2): List of some therapeutic proteins, their commercial name and clinical application

Recombinant protein	Alpha-galactosidase A	Human insulin (BHI)	Follicule-stimulating hormone (FSH)	Factor VIII, Factor IX	Erythropoietin (EPO)	Granulocyte colony-stimulating factor (G-CSF)
Commercial name	Fabrazyme	Humulin Novolin	Follistim	Kogenate	Epogen	Neupogen Neulasta
Clinical application	Fabry disease	Diabetes	Problem of Fertility Ovulation problem	Hemophilia A, Hemophilia B	Anemia (chronic renal failure)	Neutropenia (low number of neutrophils) from chemotherapy, bone marrow
Supplier company	Genzyme	Lilly Novo Nordisk	Serono	Bayer	Amgen	Amgen

Table 3.1 (part 2/2): List of some therapeutic proteins, their commercial name and clinical application

Recombinant protein	Alpha-L-iduronidase	Dornase alpha	Tissue plasminogen activator	Insulin-like growth factor 1 (IGF-1)	Interferon beta-1a	Envelope protein of the hepatitis B
Commercial name	Aldurazyme	Pulmozyme	Activase	Increlex (Mecasermin)	Avonex	Engeric-B (vaccine)
Clinical application	Mucopolysaccharidosis I	Cystic fibrosis	Acute ischemic stroke Heart attacks and acute massive pulmonary embolism	Growth failure due to severe primary IGF-1 deficiency	Multiple sclerosis	Hepatitis B
Supplier company	BioMarin Pharmaceutical	Genentech	Genentech	Tercica Pharmaceuticals	Biogen Idec	GlaxoSmithKline

Table 3.2 (part 1/2): List of some commercially available monoclonal antibodies, their biological target and their clinical application

Commercial name	Abciximab	Adalimumab	Afutuzumab	Bapineuzumab	Benralizumab	Blosozumab
Biological function	Glycoprotein IIb/III receptor antagonist	TNF inhibitor	Immunomodulator	Beta amyloid plaques inhibitor	CD125 inhibitor	Negative regulator of osteoblast activity
Target	CD41 (integrin alpha-IIb)	TNF-α	CDC20	Beta amyloid plaques	CD125	SOST
Clinical application	Platelet aggregation inhibition	Rheumatoid arthritis, Crohn's disease, Plaque Psoriasis	Lymphoma	Alzeihmer's disease	Asthma	Osteoporosis

Table 3.2 (part 2/2): List of some commercially available monoclonal antibodies, their biological target and their clinical application

Commercial name	Brodalumab	Cedelizumab	Edobacomab	Exbivirumab	Ibalizumab	Motavizumab
Biological function	IL-17 inhibitor	CD4 inhibitor	Gram-negative endotoxin inhibitor	Hepatitis B surface antigen	CD4 inhibitor	Respiratory syncytial virus surface inhibitor
Target	IL-17	CD4	Endotoxin	Hepatitis B surface	CD4	Respiratory syncytial virus
Clinical application	Inflammatory diseases	treatment of autoimmune diseases	Sepsis caused by Gram-negative bacteria	Hepatitis B	HIV infection	Respiratory syncytial virus infection (prevention)

3.2 Bioprocess requirements

To answer the increasing market demand (35% per annum), many improvements have been achieved in upstream (cell culture) and downstream (purification) processes for mAb production (Butler 2005, Rodrigues, et al. 2010, Wurm 2004, Jenkins, Parekh and James 1996, Kaufmann, et al. 1999, Kim, Kim and Lee 2012). Most of the improvements have been made in medium formulation and process feeding, including adaptation to serum-free environment. In the 1980s, the maximum cell density achieved in seven days of batch culture was typically 1–2 million cells/ml, with a yield of 50–100mg/l (Wurm 2004) (**Figure 3.2**). Nowadays, a fed-batch culture lasts up to 21 days, with cells reaching 10–15 million cells/ml and producing 1–5g/l of proteins. However, specific cellular productivities, now in the range of 50–60 pg/cell/day, have only been improved by 2-fold since the 1980s (Hacker, De Jesus and Wurm 2009). Recently, CHO cells have been reported to produce up to 10g/L of proteins (Kim, Kim and Lee 2012).

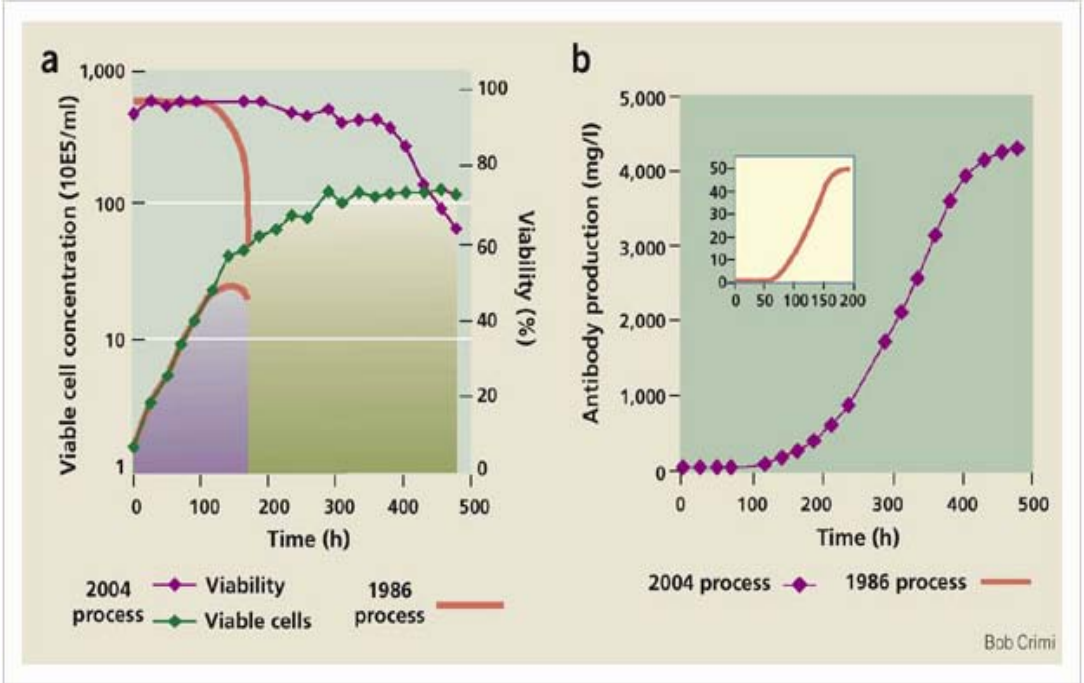

Figure 3.2: Comparison of cell culture processes from 1986 and 2004

The viable cell mass and viability (a) and the productivity (b) of both cell culture processes are shown. The examples are derived from processes comprising suspension cultures of CHO cells. The data from 2004 was generated from a process for the expression of a human recombinant antibody at the 10-liter scale. The hypothetical process from 1986 is based on unpublished results. For clarity the product accumulation data for the hypothetical 1986 process is also represented in the insert in b. Data courtesy of Lonza Biologics, Slough, UK.

Figures and legend were taken from the following paper: 'Production of recombinant protein therapeutics in cultivated mammalian cells' (Wurm 2004).

In cell culture technology, the main desirable characteristics of a cell line are rapid cell growth, sustained viability and high specific productivity (Qp). The improvement of these three cell characteristics leads to the increase of total yield. To achieve high total yield in large-scale culture, different parameters are to be considered.

3.2.1 Choice of host system for recombinant protein production

The choice of the host system is critical and depends on the recombinant protein being produced and its application. Besides mammalian cells, bacteria, yeast, insect cells and plants are also used as expression systems for biopharmaceutical production (Wurm 2004). Among different mammalian cells including baby hamster kidney, mouse myeloma-derived NS0 and human embryonic kidney (HEK)-293, Epithelial-like Chinese Hamster Ovary (CHO) cells are the most widely used host producer. These cells were initiated by T.T. Puck in 1957 (PUCK 1957, Sato, Fisher and Puck 1957). They are fast growing and easily cultivated in large-scale culture. CHO cells are able to synthesize and secrete glycoproteins with similar carbohydrate structures to those found in humans, allowing human-like post-translational modifications particularly glycosylation, proper folding, resulting in correct and efficient biological function. In addition, they are non-human in origin consequently the risk of human viral contamination is importantly reduced (Wurm 2004).

Mammalian cells are the most widely used host system for complex protein production due to their capacity to confer appropriate posttranslational modifications. During the glycosylation process, different carbohydrate structures known as glycans are added to synthesized proteins (Butler 2005, Jenkins, Parekh and James 1996). The production of these glycan structures is essential to the biological activity of the recombinant protein. Variation of glycosylation patterns can lead to immunogenicity (Walsh 2006). Consistency of glycosylation pattern must be maintained over the culture (Restelli, et al. 2006) and for this reason complex protein production is more limited in other systems such as *E.coli*, yeast and insect (baculovirus). Despite the easy manipulation and the low cost of *E.coli*, its cellular machinery does not allow post-translational modifications and proper protein folding. The biological activity and immunogenicity of the recombinant protein may differ from the native protein. Recent reports showed that

post-translational modifications can be achieved by manipulation of *E.coli* particularly by engineering the glycosylation pathway (Wacker, M et al 2002; Zhang Zet al 2004).
Yeast is more difficult to manipulate than *E.coli*, protein purification is not easily feasible as the cell wall is difficult to break and it has different glycosylation patterns than in mammals. Insect cells are not suitable either due to their lack of glycosylation mechanisms thus preventing the protein to be active.

3.2.2 Cell culture parameters

3.2.2.1 Media optimization

Media optimization and serum-free culture development have resulted in large improvements in productivity. Serum is not desirable in cell culture due to its high cost, batch-to-batch variation and the risk of transmitting adventitious agents (viruses, bacteria, mycoplasma and prion contaminations) (Even, Sandusky and Barnard 2006). However, a serum-free medium can contain serum constituents or substitutes derived from animals (e.g: transferrin, albumin, insulin, protein lysates). Other types of serum-free media have been developed and do not contain components of animal origin thus they are referred to as protein-free or chemically-defined.
Feeding optimization in a fed-batch culture is a simple and reliable method consisting of the addition of essential components like glutamine, glucose and amino-acids at appropriate concentrations (Bibila, et al. 1994, Bibila and Robinson 1995). Growth factors (Epidermal Growth Factor, Fibroblast Growth Factor, Insulin Growth Factor), proteins, lipids, carbohydrates, vitamins and small molecules are also added at defined concentrations in serum-free media formulation. Nowadays a lot of chemically-defined serum-free and protein-free media are commercially available.

3.2.2.2 Mode of culture

Different modes of culture of which the most common are batch and fed-batch modes (considered as non-continuous culture) can be used for different applications. Other existing cultures are continuous culture with (perfusion) or without (chemostat or cytostat) cell retention.

3.2.2.2.1 Batch culture

Batch culture mode is a straightforward technique largely used in industry that consists of cells grown in suspension culture with limited nutrient supply and no renewal of medium. Cell growth and viability decline at later stages of culture due to the lack of available nutrients in culture (glucose, glutamine) and the accumulation of waste products (ammonia and lactate) which inhibit cell growth and antibody production (Butler 1987, Hayter, et al. 1992, Newland, et al. 1994). To avoid waste accumulation, a perfusion culture can be considered instead allowing removal of waste and constant nutrient supply (Butler, et al. 1983, Butler 1985).

3.2.2.2.2 Fed-batch culture

An alternative of the batch mode is fed-batch culture, which is a simple and reliable method. This mode of culture can lead to high volumetric productivity (Li, et al. 2005, Dorka, et al. 2009). Nutrients are supplied at appropriate concentrations at different time points of the culture (Bibila and Robinson 1995, Xie and Wang 2006). Through this method waste accumulation can not be avoided but it can be minimized by slow feeding and low concentrations of essential components (Butler 2005, Kim, et al. 2012). Lower levels of glucose and glutamine or replacement by other carbon sources (Duval, et al. 1992, Altamirano, et al. 2004) prevent lactate and ammonia accumulation by improving oxidation of glucose to CO_2 (Xie and Wang 2006, Zhou, et al. 2011, De Alwis, et al. 2007)

3.2.2.2.3 Perfusion

The perfusion culture of non-adherent cells is a very advantageous approach in increasing cell productivity (Tokashiki and Takamatsu 1993). The difference with fed-batch mode is that a perfusion culture allows a constant input of feed solutions and a constant withdrawal of toxic byproducts produced, without disturbing cells in culture. Cells are retained in the bioreactor using filtration, sedimentation or centrifugation. However, with these approaches it is difficult to maintain sterility. In addition, cells can be stressed by shear and potential oxygen depletion resulting in suboptimal product quality and quantity.

3.2.3 Cellular environment parameters

3.2.3.1 Low temperature

To achieve the best cell culture conditions, different parameters can be optimised including temperature, pH, osmolarity, dissolved oxygen and carbon dioxide. Low temperature is a common strategy to improve batch-culture performance in a biphasic culture (Kaufmann, et al. 1999). The shift of temperature from 37°C to 28-31°C applied when cells are actively growing (corresponding to the middle of the exponential phase) causes reduction or arrest of proliferation in the G1 phase of the cell cycle. Consequently, a longer and more viable production phase is maintained by delaying apoptosis (Kaufmann, et al. 1999, Oguchi, et al. 2006, Al-Fageeh, et al. 2006). Cells arrested in this phase are morphologically different and are metabolically more active than non arrested cells. After temperature-shift, levels of recombinant mRNA are increased either due to enhanced transcription or increased mRNA stability (Yoon, Song and Lee 2003). Mammalian cells respond to low temperature by synthesizing specific cold-inducible proteins (CSPs) induced by the change of the initial environmental conditions whereas transcription and subsequent translation of proteins expressed in physiological temperature culture are suppressed. Initially, two proteins were identified from the glycine-rich RNA binding protein family (GRP), the mouse

cold inducible RNA binding protein (CIRP) and the RNA binding motif protein 3 (RBM3) (Nishiyama, et al. 1997b, Nishiyama, et al. 1997a). RBM3 is expressed in a wide variety of human foetal tissues. At low temperature, this latter undergoes regulation at both, transcriptional and translational levels. RBM3 expression may also alter global protein synthesis by having an effect on the levels of small non-coding RNAs known as miRNA, suggesting a role of RBM3 and miRNAs in the mechanisms of homeostatic regulation (Nishiyama, et al. 1997b, Dresios, et al. 2005). However, cold-inducible proteins are not conserved among all species and this effect is extremely variable and appears to be both cell line and expression system dependent . Currently, the detailed cellular and molecular mechanisms of this cold stress response in eukaryotes are not well understood.

3.2.3.2 pH

pH stability is critical to achieve optimal cell culture conditions. Change in pH can affect cell growth, productivity and glycosylation patterns (Oguchi, et al. 2006, Borys, Linzer and Papoutsakis 1993). pH is closely related to other parameters such as temperature, carbon dioxide and glucose content . In addition, the optimal pH slightly differs among cell lines, and some cell lines are less sensitive to variations of pH than others (Kurano, et al. 1990).

3.2.3.3 Dissolved oxygen

Dissolved oxygen (DO) is critical for cell growth and product formation, being closely related to pH in the media (Hanson, et al. 2007). Oxygen is a key requirement for animal cell culture and oxygen limitation can be a major problem when high density is reached leading to lactate production and lower pH (Hanson, et al. 2007). Variations of DO concentration can affect cell metabolism cell growth rate and glycosylation (Thommes, et al. 1993, Kunkel, et al. 1998).

3.3 Bioprocess engineering methods

3.3.1 Generation of a producer cell line

To express an exogenous protein, the protein coding-gene of interest is inserted by cloning in a suitable vector, which contains specific transcriptional elements, and transferred into the cells by transfection. DNA enters the nucleus and integrates at a random location or precise site in the genome, depending of the elements present in the vector. Another gene is inserted in the same vector or a second vector to allow selection of cells that have taken-up the recombinant gene. An antibiotic (neomycin, hygromycin or zeocin) is commonly used for selection of mammalian single cell clones. Besides antibiotic selection, other systems have been developed with dihydrofolate reductase (DHFR) or glutamine synthetase (GS). Following addition of the selection agent, only cells that express the resistance gene survive. There are several methods of transfection that differ in the techniques used or in the transfection reagent formulation. Physical methods include biolistic technology, microinjection or electroporation. Chemical methods include carriers such as lipofection, calcium-phosphate or DEAE-dextran (polycationic derivative of dextran, a carbohydrate polymer). For each cell line and each experiment, the choice of transfection method needs to be determined and should be optimised. These cells that survive selection are referred as mixed population. Then cells are transferred to a fresh culture as single cell clones. Selection of single-cell clones can be performed manually or using fluorescence-activated cell sorting (FACS) if cells express a reporter gene. After expansion in clonal population, different parameters are monitored to select the best clones. To further improve the phenotypes of these clones, an amplification step can be conducted to increase the copy number of the transfected gene (Butler 2005). There are two gene amplification systems in CHO cells, the DHFR system with resistance to methotrexate (MTX) and the GS system with methionine sulfoxamine (MSX) resistance. The DHFR approach is commonly applied to CHO cells deficient in DHFR activity. Methotrexate (MTX) blocks the activity of DHFR leading to considerable cell death. After 2-3 weeks of MTX exposure, only a small number of cells are able to survive by overproducing DHFR due to amplification

of copy number, with this amplification leading to an increase in recombinant protein expression (Pallavicini, et al. 1990, Gandor, et al. 1995). DHFR converts the folate to tetrahydrofolate, this latter being required for synthesis of purine, pyrimidine and glycine (Goeddel 1990). MTX is an analog of folate which competes by binding to DHFR and inhibits the synthesis of tetrahydrofolate thus leading to cell death. During gene amplification, the culture is supplemented with increasing levels of MTX allowing selection of cells that only express high copies of DHFR. The approach taken for the GS/MSX system is based on the same principle.

3.3.2 Targeted integration

The control of DNA insertion in a specific site of the genome is desirable to avoid insertional mutagenesis and to minimize phenotypic heterogeneity due to random integration (Orlando, et al. 2010). Different strategies including Cre/loxP, zinc-finger nucleases and cis-acting elements among others have been shown to promote efficiently site-specific integration, insertion and expression a transgene.

3.3.2.1 Cre/loxP system: recombinase-mediated cassette exchange strategy

The use of gene targeting based on the Cre/loxP system was first described for human monoclonal antibody production in CHO cells by Kito et al., in 2002 (Kito, et al. 2002). The P1 bacteriophage Cre recombinase catalyses a site-specific recombination between two loxP sites (Sadowski 1993). The loxP sites are sequences consisting of an 8-bp core sequence, where recombination takes place, and two flanking 13-bp inverted repeats. Besides the Cre/loxP system, two other systems based on the same principle are used for transgene integration in the mammalian genome, the *Saccharomyces cerevisiae*-derived Flp and the bacteriophage ΦC31-derived integrase which recognise the recombination target sites FRT and attB/attP respectively (Wirth, et al. 2007). This strategy has been applied in CHO cells leading to successful production of recombinant proteins (Kito, et al. 2002, Huang, et al. 2007). Wiberg and co-workers reported the production of a human polyclonal anti-RhD antibody following the integration of 25 individual antibody expression cassettes into a defined FRT target site in CHO cells

(Wiberg, et al. 2006). The repeated insertion of multiple genes into one target site was achieved subsequently to the integration of an accumulative site-specific gene integration using the Cre/loxP system (Kameyama, et al. 2010).

3.3.2.2 Zinc-finger nuclease-based technology

Engineering site-specific nucleases, based on zinc-finger DNA binding motifs, has been reported to stimulate homologous recombination (Pavletich and Pabo 1991). Zinc-finger nucleases (ZFNs) consist of the fusion between zinc-finger DNA binding domains and the nuclease domain of the type IIs restriction enzyme *Fok*I (Kim, Cha and Chandrasegaran 1996). This fusion and the dimerization of zinc-finger DNA binding domain chains induce DNA double strand break (DSB). The new DNA is inserted and ligation occurs via non-homologous end-joining (NHEJ) or by homology-directed repair (HDR) (Weterings and van Gent 2004)(Orlando, et al. 2010). ZFNs have been used to create mutant for GDP-fucose transporter SLC35C1 which regulates the fucosylation of glycans (Zhang, et al. 2012b). The knockout of Bak and Bax, two pro-apoptotic proteins, by this technology increases apoptosis resistance in CHO cells (Cost, et al. 2010). ZFNs have also been used to create glutamines synthetase (GS) gene knockout cells to study the impact of GS on selection efficiency in CHO cell line generation (Fan, et al. 2012).

Recently, other endonuclease-based approaches have also been developed such as meganucleases, transcription activators like effector (TALE-nucleases) and the DNA recombinase-based mammalian artificial chromosome engineering (ACE) system, this latter allowing large cloning capacity (Kennard, et al. 2009a, Kennard, et al. 2009b, Silva, et al. 2011).

3.3.2.3 Cis-acting elements

Scaffold/matrix attachment region (S/MAR) is one the most commonly used cis-acting elements strategy to improve protein production (Harraghy, et al. 2012). This region is involved in chromatin remodelling to maintain an active configuration of the transgene. In CHO cells, S/MARs from different origins have been tested including human β-globin MAR, β-interferon SAR and chicken lysozyme MAR (Girod, Zahn-Zabal and

Mermod 2005, Kim, et al. 2004a, Zahn-Zabal, et al. 2001). Successful increased antibody production has been achieved using another type of cis-acting elements known as ubiquitous chromatin opening elements (UCOEs) combined with a strong viral promoter (Benton, et al. 2002).

3.4 Bioprocess-relevant CHO cell engineering

Recently, CHO cell engineering using single gene manipulation studies has proven to be an efficient method to enhance cell proliferation, secretion capacities and specific productivity as well as to inhibit apoptosis. The advantage of this approach is to turn on the expression of a specific gene using constitutive or inducible system at different phases of culture.

3.4.1 Cell cycle pathway engineering

Overexpression of the oncogene c-Myc, a key node gene involved in cell cycle regulation, has been reported to significantly impact on cell proliferation in attached and suspension CHO-K1 cell culture (Ifandi and Al-Rubeai 2005). Cell productivity can be enhanced using cell-cycle dependent factors such as cyclin-dependent kinase inhibitors $p21^{CIP1}$ and $p27^{KIP1}$ that induce cell cycle arrest and consequently cell productivity increase in CHO-K1 SEAP cells. Overexpression of transcription factors involved in cell cycle progression, cyclin-dependent kinase like 3, cyclin E and E2F-1, successfully improved cell proliferation (Jaluria, et al. 2007, Majors, et al. 2008, Renner, et al. 1995). Up-regulation of mammalian target of rapamycine (mTOR), a serine-threonine kinase involved in many pathways including translation, metabolism, vesicle traffic, cell survival, and cell proliferation, significantly increased viability, robustness, cell size, proliferation and antibody production in CHO cells (Dreesen and Fussenegger 2011). Multigene metabolic engineering using a combination of growth-enhancing factor like Bcl-xL and its stabilizer C/EBPα (CCAAT/enhancer binding protein α) resulted in a further enhancement of cell growth (Fussenegger, et al. 1998).

3.4.2 Apoptosis pathway engineering

3.4.2.1 Single-gene engineering

The accumulation of waste in culture, nutrient deprivation, shear stress and elevated osmolarity promote DNA damage and apoptosis induction leading to poor process performance (Kim, Kim and Lee 2012, Muller, Katinger and Grillari 2008, Arden and Betenbaugh 2004). Apoptosis is a programmed cell death characterized by plasma membrane blebbing, cell shrinkage, nuclear fragmentation, chromosome condensation and chromosome DNA fragmentation (Danial and Korsmeyer 2004). Apoptosis is regulated by the intrinsic pathway (mitochondria, endoplasmic reticulum (ER) and the extrinsic pathway (cellular surface death receptors). Caspases are cysteine proteases that play a key role in the signalling cascades of apoptosis (Majors, Betenbaugh and Chiang 2007).

Over-expression of Bcl-2 and Bcl-xL, two anti-apoptotic factors that regulate apoptosis in the mitochondria, provoked proliferation increase and apoptosis resistance in CHO cells (Kim, et al. 2003, Meents, et al. 2002, Chang, et al. 2005). Knockdown of pro-apoptotic proteins like Bax and Bak has been employed to increase viable cell density (Cost GJ 2010). Another strategy is the suppression of caspases, which regulate apoptosis induction through proteolytic cascades. Apoptosis resistance can also be achieved by overexpression of intracellular caspase inhibitors, such as X-linked mammalian inhibitor of apoptosis (XIAP), an inhibitor of caspase-3/caspase-7/caspase-9 (Sauerwald, Oyler and Betenbaugh 2003, Sauerwald, Betenbaugh and Oyler 2002). Overexpression of other factors, including the human telomerase reverse transcriptase (hTERT), the inhibitor for p53 tumor suppressor protein and Aven, the inhibitor of apoptosome activation via interacting Apaf-1, has been reported to successfully increase apoptosis resistance (Crea, et al. 2006, Arden, et al. 2007, Choi, et al. 2006, Figueroa, et al. 2007).

3.4.2.2 RNAi to improve apoptosis resistance in CHO cells

As described in the previous section, apoptosis is a programmed-cell death that can be promoted by waste accumulation and other stress in the cells. To improve resistance against apoptosis, pro-apoptotic factors can be targeted including proteins from the Bcl-2 family. Using shRNA technology to knockdown Bax and Bak, Lim et al reported the enhancement of cell viability and CHO cell productivity (Lim, et al. 2006) . Following addition of Sodium Butyrate (NaBu) in culture which leads cytotoxicity, simultaneous silencing of caspase-3 and caspase-7 was successful in improving recombinant thrombopoietin production in CHO cells but negatively impacted on cell growth and viability (Sung, et al. 2007, Sung, Hwang and Lee 2005). The knockdown of other pro-apoptotic factors like the apoptosis linked gene 2 (Alg-2) and the zinc finger protein transcriptional factor Requiem have been reported to improve cell viability and recombinant interferon-γ production in CHO cells (Lim, et al. 2010).

3.4.3 Glycosylation pathway engineering

3.4.3.1 Single-gene engineering

The glycan pattern of a recombinant protein is critical to its biological activity. Variations in this pattern can be a problem for protein folding, aggregation or secretion leading to protein degradation and immunogenicity. It can also be an issue with the Food and Drug Act (FDA) regulation which considered the glycosylation very seriously particularly in the case of biosimilars. It can be a challenge to keep the glycan structure patterns consistent between different batches as glycosylation can be dependent on the cell culture process including the recombinant protein itself and extracellular environment (Jenkins, Parekh and James 1996, Reuter and Gabius 1999), the host cell line (Goochee 1992, Goto 2007, Sheeley, Merrill and Taylor 1997) and the method of culture (Jenkins and Curling 1994, Gawlitzek, Conradt and Wagner 1995, Schweikart, et al. 1999). The glycoforms, which represent the different glycoproteins generated

during a culture process, are evaluated for product safety and biological activity. In this regard, the culture parameters are precisely controlled to ensure the reproducibility of the bioprocess culture between the different batches to avoid heterogeneity of glycan patterns (Butler 2006). This pattern is dependent on the expression of various glycosyltransferase enzymes that are present in the Golgi of cells. Over-expression of β1,4 N-acetyl glucosaminoyltransferase, that catalyzes the transfer of N-acetylglucosamine (GlcNAc) to core 2 branched O-glycans, enhances antibody dependent cellular toxicity (ADCC) in CHO cells (Davies, et al. 2001, Umana, et al. 1999). Thus engineered modifications of glycosylation can lead to lower immunogenicity, higher stability of the protein and enhanced its biological activity (Butler 2006).

3.4.3.2 RNAi for glycosylation engineering

The glycan patterns of a recombinant protein are critical to its biological activity. The variation of these patterns can be a problem for protein folding, aggregation, secretion leading to protein degradation and immunogenicity. ADCC is an immune response mediated by recognition of an antigen by the fragment crystallisable (Fc) region of an Immunoglobulin G (IgG). This recognition between antibody and antigen recruits a particular Fc receptor present on natural killers (NK) cells, leading to infected cell destruction. The use of siRNA has been successful in α-1,6 fucosyltransferase (FUT8) mRNA inhibition leading also to enhanced ADCC (Mori, et al. 2004). FUT8 protein catalyzes the addition of fucose to the first GlcNAc residue. The knockdown of both FUT8 and GDP-mannose 4,6-dehydratase (GMD), an enzyme that converts *D*-glucose to GDP-fucose to produce GDP-mannose, had a synergistic effect on ADCC activity (Imai-Nishiya, et al. 2007).

3.4.4 Metabolic pathway engineering

3.4.4.1 Single-gene engineering

Cell engineering can also be applied to improve metabolic phenotypes and overcome environmental stress in the cells (Irani, Beccaria and Wagner 2002, Abston and Miller 2005, Tigges and Fussenegger 2006). Glycolysis pathway can be targeted to increase energy and reduce undesirable byproducts such as lactate. Silencing of lactate dehydrogenase (LDH), an enzyme involved in pyruvate-lactate reaction and NAD^+ formation, has been reported to reduce glycolysis rate (Zhou, et al. 2011, Kim and Lee 2007).

Overexpression of Glutamine synthetase, an enzyme which combines glutamate with ammonia to yield glutamine, has been shown to reduce the amount of ammonia production (Zhang, et al. 2006). Similarly, the overexpression of carbamoyl phosphate synthetase I and ornithine transcarbamoylase involved in urea cycle has been shown to decrease ammonia accumulation (Park, et al. 2000).

3.4.4.2 RNAi for metabolism engineering

To improve cell proliferation and cell viability capacities, the accumulation of byproducts such as lactate produced by glucose and glutamine catabolism should be reduced. The knockdown of lactate dehydrogenase (LDH) the enzyme responsible for the conversion of pyruvate to lactate inhibited lactate production, consequently reduced acidose-mediated apoptosis and improved production of tissue plasminogen activator protein in CHO cells by about 150% (Jeong, et al. 2006). Another study on LDH knockdown using shRNA reported the reduction of glucose consumption rates by 13–46% per cell and lactate production by 21–55%, without any changes in the glutamine consumption rate (Kim and Lee 2007).

3.4.5 Unfolded protein response and secretion pathway engineering

The accumulation of proteins in the endoplasmic reticulum (ER) lumen in addition to environmental perturbations trigger a stress response known as the unfolded protein response (UPR) (Cudna and Dickson 2003, Rutkowski and Kaufman 2004). Following UPR activation, global translation is attenuated while degradation of unfolded proteins is promoted (Chakrabarti, Chen and Varner 2011). These three pathways are regulated by the chaperone protein Bop/Grp78 which promotes proper folding of proteins in the ER. Under ER stress, the interaction of Bop with three transmembrane ER transducers, inositol requiring kinase 1 (IRE1), double-stranded RNA-activated protein kinase (PKR)-like endoplasmic reticulum kinase (PERK) and activating transcription factor 6 (ATF6) is abolished leading to activation of these proteins and subsequent UPR signalling activation (Chakrabarti, Chen and Varner 2011). A prolonged UPR leads to apoptosis-dependent cell death by the activation of the three ER stress-sensing pathways IRE1, PERK, and ATF6 (Forman, Lee and Trojanowski 2003).

To increase the ER capacity and counteract this stress response, the expression of different transcription factors involved in the UPR has been manipulated. Increasing the spliced form of Xbp-1 (Xbp1-(s)) has been shown to enhance SEAP production in CHO cells (Tigges and Fussenegger 2006). Other approaches have focused on reversing the attenuation of translation in response to ER stress. Up-regulation of ATF4, a transcription factor involved in the UPR, triggers phosphorylation of eukaryotic initiation factor-2α (eIF2α) via induction of growth arrest and DNA damage inducible protein 34 (GADD34). This was shown to restore translation and consequently to enhance antithrombin III (AT-III) specific productivity (Ohya, et al. 2008, Omasa, et al. 2008). Targets in the secretion pathway include N-ethylmaleimide-sensitive factor attachment protein receptors (SNAREs) and Sec1/Munc18 (SM) proteins. SNAREs mediate the fusion between transport vesicles and the cell membrane via interaction with SM proteins (Toonen and Verhage 2003). Overexpression of SNAREs or SM proteins improves CHO cell productivity (Peng and Fussenegger 2009).

3.5 The use of RNA interference in CHO cell engineering

Single-gene engineering has been used to successfully improve CHO cell growth, viability, apoptosis resistance as well as to manipulate their metabolic and secretory pathways to adapt the cellular machinery to produce more. However, manipulating one or multiple gene(s) in a specific pathway can negatively impact on other pathways. For instance, if CHO cells are engineered to improve cell proliferation, cell productivity can be compromised. It appears also that single-gene engineering is designed to target key regulators of a cellular function rather than entire pathways. Therefore other approaches have been focused on global changes in DNA, RNA and proteins.

3.5.1 RNA interference mechanism

RNA interference (RNAi) based cell engineering techniques have been developed to knockdown the expression of a target gene in a sequence-dependent manner. The use of ribonucleic acid (RNA) antisense technology as a tool for gene function studies was first applied to the inhibition of thymidine kinase by Izant and co-workers (Izant and Weintraub 1984). Although, sense and antisense RNA were each sufficient to cause interference in *Caenorhabditis elegans* (*C.elegans*), the presence of a double-strand RNA was more effective in silencing the endogenous mRNA transcript, a process that was later called RNAi (Fire, et al. 1998, Fire, et al. 1991). RNAi has also been reported in plants as post-transcriptional gene silencing (PTGS) mechanism (Hamilton and Baulcombe 1999). PTGS is thought to be a mechanism for host protection against viruses and mobile genetic elements like transposons that use double-stranded RNAs (dsRNAs) in their life cycles (Jensen, Gassama and Heidmann 1999, Ratcliff, MacFarlane and Baulcombe 1999). If transposable elements share homology with their host genomes, repression can be induced by the same phenomenon. RNAi since has been discovered in other species such as fungi (mechanism called quelling) (Romano and Macino 1992), drosophila (Hammond, et al. 2000), insects (Kennerdell and Carthew 1998), frogs (Thompson, Goodwin and Wickens 2000), mammals and human (Svoboda, et al. 2000, Wianny and Zernicka-Goetz 2000, Shendure and Church 2002).

RNAi was studied later in more details and described as the degradation of a mRNA, induced by a dsRNA in a sequence-specific manner (**Figure 3.5.1**). This processing is triggered by an endoribonuclease related to the RNase III-like enzyme family, called Dicer. The cleavage induces the production of small interfering RNA (siRNA) duplexes with a length of 21 to 23-nucleotides (nt) and with 3'dinucleotide overhangs (Elbashir, et al. 2001). One strand of the siRNA duplex assembles into the RNA-induced silencing complex (RISC), leading to degradation of the target transcript due to total complementarity between the selected strand and the mRNA sequence. Synthetic chemically-modified siRNAs are often used in reverse genetic experiments to investigate the function of a gene by its knockdown through perfect complementarity (Mac Manus 2002). However, these molecules are expensive and their effect is only temporary therefore short hairpin RNAs (shRNAs) have been engineered in appropriate vectors to allow long-term studies. Expression of shRNA is driven by RNA polymerase II or III promoters and induces stable knockdown for a longer period of time (Kim and Rossi 2007). RNA polymerase III promoters (such as U6) are used for general small RNAs expression whereas RNA polymerase II promoters are used for tissue-specific expression or for the expression of several shRNAs in a single unit and for miRNA (miRNA) precusor expression. miRNAs are another class of small non-coding RNAs involved in post-transcriptional regulation, in a similar manner to siRNAs (Kim and Rossi 2007). Recent publications in bioprocessing have reported the use of RNAi in mammalian cells to improve cell productivity or cell proliferation rate (Wu 2009).

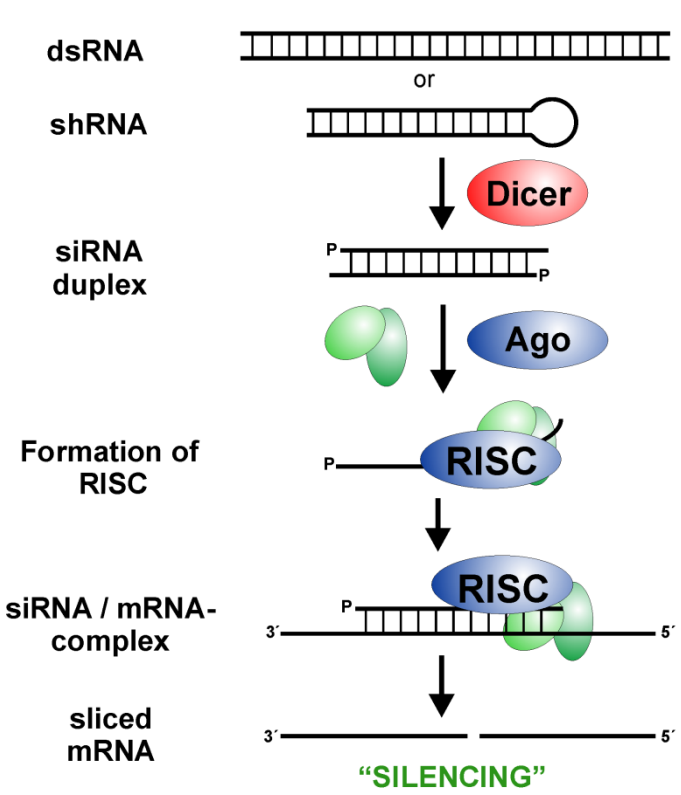

Figure 3.5.1: Mechanism of siRNA silencing RNAi is activated by the presence of a dsRNA or by a shRNA construct in a sequence-specific manner. An RNase III-like enzyme called Dicer recognises the double-stranded molecule and triggers cleavage. This cleavage leads to the production of a small interfering RNA (siRNA) duplexes with a length of 21 to 23-nt characterized by a dinucleotide 3’overhangs. One strand of the siRNA duplex assembles into the RNA-induced silencing complex (RISC) that comprises Argonaute protein. This complex guides the siRNA to its fully complementary target mRNA and this pairing provokes degradation of the transcript due to total complementarity.
(http://www.unikonstanz.de/FuF/chemie/jhartig/)

3.5.2 miRNAs

Similar to siRNAs, miRNAs are another class of small non-coding RNAs involved in post-transcriptional regulation (Kim and Rossi 2007). miRNAs are small non-coding RNAs, involved in many biological pathways and have been shown to be highly conserved between species. Since their discovery, they have expanded the world of small RNAs and given a new perception of post-transcriptional regulation. A single miRNA can potentially regulate hundreds of targets and, in contrast to functional proteins miRNAs do not need to be translated to exert their function (Muller, Katinger and Grillari 2008). This peculiarity of miRNAs make them potentially attractive tools for CHO cell engineering as well as better understanding of the molecular mechanisms regulating CHO behaviour in culture.

3.5.2.1 miRNA discovery

miRNAs were first identified in *C.elegans* with the discovery of linage-4 (lin-4), a critical stage-specific gene, involved in the timing of worm larvae development (Lee, Feinbaum and Ambros 1993)(Lee and Ambros 2001). Lin-4 negatively regulates LIN-14 protein, using an antisense mechanism involving complementarity between lin-14 3'UTR sequence and lin-4 miRNA (Lee, Feinbaum and Ambros 1993). Following this initial discovery, many papers have been published on miRNAs in several species such as worm (Lau, et al. 2001), drosophila, human (Mourelatos, et al. 2002, Lagos-Quintana, et al. 2001), plants, green algae and viruses (Griffiths-Jones 2006). Recently other small non-coding RNAs have been discovered known as Piwi-interacting RNA (piRNAs). PiRNAs bind to Piwi proteins that are one of the two subfamilies of animal Argonaute proteins. They are small RNAs known to be key regulators of germline development in most animals (Aravin, Hannon and Brennecke 2007). Although their biogenesis and their mode of target regulation are different, there is a link between siRNA, miRNA and piRNA pathways. miRNAs are derived from transcripts that form hairpin structures whereas siRNAs are derived from longer hairpins or bimolecular

RNA duplexes and piRNAs originate from precursors that do not seem to have a double-stranded primary structure (Bartel 2004).

3.5.2.2 miRNA biogenesis

Mature miRNAs are single-stranded RNA molecules, of 21-23 nt, that are derived from the transcription of a long primary miRNA (pri-miRNA). Pri-miRNAs can be as long as several kilobases and contain one or more secondary structures consisting of extended stem-loop structures (Lee, et al. 2002). They are usually transcribed by RNA polymerase II (RNA pol II) and like other RNA pol II transcripts, pri-miRNAs undergo similar transcriptional regulation to protein-coding mRNAs such as 5' cap and poly(A) tail (Ding, Weiler and Grosshans 2009). However, for miRNAs located in Alu and other repetitive elements, transcription occurs through RNA polymerase III (Borchert, Lanier and Davidson 2006) These small non-coding RNAs are converted into single-stranded mature miRNAs after a two step cleavage process by RNase III-like enzyme (**Figure 3.5.2.2**). This cleavage, called "cropping" (Ding, Weiler and Grosshans 2009), occurs in the nucleus, by a complex containing Drosha and its cofactor DiGeorge syndrome critical region gene 8 (DGCR8 or Pasha), also known as Microprocessor (Kim, Han and Siomi 2009). The cofactor DGCR8 may recognize a junction, called the SD junction, localized between the single and double-stranded region and the 33-base pair (bp) stem of the pri-miRNA substrate. After recognition, interaction occurs between the dsRNA binding domain (dsRBD) and the stem, leading to RNA duplex cleavage about 11bp from the SD junction (Han, et al. 2009). This cleavage takes place at the stem of the hairpin structure, allowing the formation of a 70-nucleotide hairpin molecule, known as the precursor miRNA (pre-miRNA). The pre-miRNA is exported into the cytoplasm by RanGTP-dependent exportin-5 and processed into a 21-23 nt miRNA duplex, by DICER/transactivation response element RNA-binding protein RNA binding protein (TRBP) complex (Chendrimada, et al. 2005). Like Drosha, Dicer leaves a characteristic two-nucleotide 3'overhang (Hutvagner, et al. 2004). Following cleavage by Dicer, the RNA duplex interacts with an Argonaute (AGO) protein to form the pre-RISC (RNA induced silencing complex).The guide strand is thought to be bound to AGO while the other strand, known as the passenger strand or also called the star strand (miRNA*), is thought to be unwounded from the duplex and degraded leading to the mature RISC

complex (Matranga, et al. 2005, Rand, et al. 2005, Gregory, et al. 2005, Kawamata and Tomari 2010). In mammals there are four Argonaute proteins (AGO1-4 also known as EIF2C proteins). All four can mediate repression of partially complementary target mRNAs through slicer-independent mechanisms but only AGO2 is able to mediate endonucleolytic cleavage (known as 'Slicer' activity) (Peters and Meister 2007). Slicer proteins, by analogy with Dicer, are endonucleases that cleave substrate RNA complementary to the bound small RNA. However, this phenomenon rarely occurs in animals in contrast to plants. Recently, a conserved miRNA biogenesis pathway that requires AGO2 catalysis but not DICER has been identified during mouse (Cheloufi, et al. 2010) and zebrafish development (Cifuentes, et al. 2010). In this study, Dicer-independent cleavage is likely due to the short sequence (17-nucleotide) of pre-miR-451 stem region that can not be recognised and processed by Dicer. In addition, the mature strand sequence starts in the loop region and extends to the complementary strand of the hairpin precursor. This structural feature prevents the miRNA sequence from being recognised by Drosha and Dicer and consequently impairs miRNA maturation (Cheloufi, et al. 2010).

Selection of the strand is dependent on the thermodynamic stability of the 5'end and is followed by target miRNA binding resulting in translation repression and/or mRNA cleavage (Pillai 2005, Valencia-Sanchez, et al. 2006). Recently, studies on miRNA* function revealed that these miRNAs could be play significant functional role and exist in abundance in cells (Okamura, et al. 2008, Ro, et al. 2007, Jagadeeswaran, et al. 2010). It has been demonstrated that miRNA and miRNA* bind to different Argonaute proteins (Okamura, et al. 2008). In drosophila the sequence from the dominant arm (the guide strand or mature miRNA) binds to Ago 1 leading to translational repression and the sequence from the opposite arm, (passenger strand, star strand or miRNA*) binds to Ago 2 and also triggers transcriptional repression (Czech, et al. 2009, Ghildiyal and Zamore 2009). In the same family of miRNAs, the relative ratio of left-arm and right-arm products can differ among members. Some other families show highly asymmetric or more equivalent miRNA hairpin outputs. Thus the mechanism of arm switching is responsible for miRNA* fate and reveals a diversification of miRNA function during miRNA gene evolution (Okamura, et al. 2008, Yang and Lai 2010). The selection of which miRNA strand to incorporate into the RISC complex, may also be tissue and developmental stage dependent (Ro, et al. 2007, Ruby, et al. 2007, Chiang, et al. 2010). In D.*melanogaster* and T.*castaneum*, miR-10 is processed from different arms.

However, the duplex miRNA-miRNA* sequences were the same in both, D.*melanogaster* and T.*castaneum* (Griffiths-Jones, et al. 2011). Using computational prediction, authors have shown that the dominant arm had fewer predicted targets than the other arm (miRNA*), suggesting another level of regulation of miRNA target sites and on miRNA functions by arm switching (Griffiths-Jones, et al. 2011).

In contrast to plants and flies, the mRNA target regulation by miRNAs is more complex in animals and not fully understood.Imperfect complementarity between a miRNA and its target mRNA provokes protein synthesis inhibition or mRNA instability causing deadenylation and degradation, depending of the miRNA/mRNA pair (Behm-Ansmant, et al. 2006). Decay of mRNA is promoted by the recruitment of GW182, CCR:NOT and DCP1:DCP2 deadenylase complexes. GW182 (Glycine-tryptophan protein of 182kDa) belongs to the core of miRISC complexes. GW182 promotes deadenylation and decapping by interacting with AGO1 at its amino-terminal end and its carboxy-terminus interacts with the poly(A) binding protein (PABP), acting downstream of AGO1. Messenger RNA decay occurs in cytoplasmic foci called P-bodies (PBs) where not only Argonaute proteins (AGO1-AGO4), miRNAs, and mRNAs are found but also other molecules such as decapping DCP1:DCP2 complex and cofactors, CCR:NOT deadenylases, the cap-binding protein eIF4E and the RNA helicase Dhh1/Me31B involved in translational repression (Pillai 2005, Valencia-Sanchez, et al. 2006, Jakymiw, et al. 2007, Liu, et al. 2005, Meister, et al. 2005). GW182, required for PBs integrity, also co-localises in these structures. Deadenylation of mRNA at the 3'end is the first step in mRNA decay, followed by the removal of the cap at the 5' end, leading to exonucleolytic cleavage from 5' to 3'. Intracellular localization of a protein or a ribonucleoprotein (RNP) is really important to determine their function and regulation. Moreover, compartmentalization ensures the control of different interactions between partners that act together (Krol, Loedige and Filipowicz 2010). From this observation, several authors suggested a model in which miRNA targets are sequestered and degraded in these P-bodies (Jakymiw, et al. 2007, Sen and Blau 2005). Argonaute proteins are distributed diffusely in the cytoplasm. When cells are subjected to stress, they accumulate into PBs and cytoplasmic aggregations called stress granules (SGs) (Leung, Calabrese and Sharp 2006). In addition to AGO proteins, artificial miRNAs mimic and repressed mRNA are also retained in these SGs (Kedersha, et al. 2005). SG and P-bodies are functionally linked and interact together continuously. The role of PBs

and SGs in translation regulation and the link between miRNA and Argonaute protein localization in SGs and PBs is not yet fully understood.

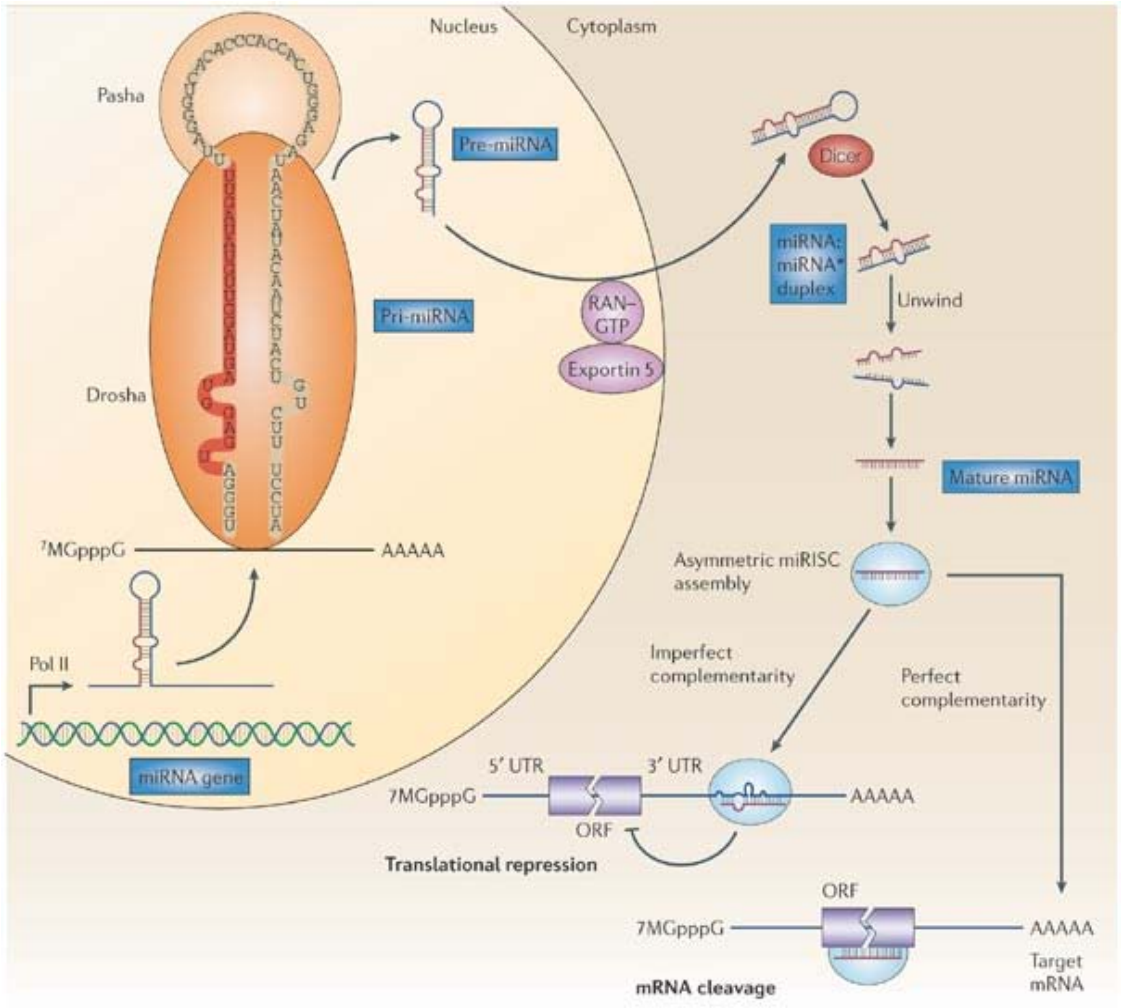

Figure 3.5.2.2: The biogenesis of miRNAs.

miRNA (miRNA) genes are generally transcribed by RNA Polymerase II (Pol II) in the nucleus to form large pri-miRNA transcripts, which are capped (^{7}MGpppG) and polyadenylated (AAAAA). These pri-miRNA transcripts are processed by the RNase III enzyme Drosha and its co-factor, Pasha or DGCR8, to release the ~70-nucleotide pre-miRNA precursor product. RAN–GTP and exportin 5 transport the pre-miRNA into the cytoplasm. Subsequently, another RNase III enzyme, Dicer, processes the pre-miRNA to generate a transient ~ 22-nucleotide miRNA:miRNA* duplex. This duplex is then loaded into the miRNA-associated multiprotein RNA-induced silencing complex (miRISC) (light blue), which includes the Argonaute proteins, and the mature single-stranded miRNA (red) is preferentially retained in this complex. The mature miRNA

then binds to the 3'UTR of its mRNA target via a complementary site known as with its 'seed region' located in positions 2 to 8 nt at the 5'end of mature miRNA (Pillai 2005, Guo and Lu 2010, Doench, Petersen and Sharp 2003, Stark, et al. 2005, Lewis, Burge and Bartel 2005b, Grimson, et al. 2007). This specific binding negatively regulates gene expression in one of two ways depending on the degree of complementarity between the miRNA and its target. Imperfect binding induces a block at the level of protein translation without interfering with the mRNA, whereas perfect (or nearly perfect) complementarity induces target-mRNA degradation.

Figure and legend were taken from the following paper: Oncomirs miRNAs with a role in cancer (Esquela-Kerscher and Slack 2006)

3.5.2.3 Nomenclature of miRNAs

To facilitate access to miRNA information, a database called miRBase was developed to gather together miRNA identity data including sequences, annotation, species affiliation, genomic site origin, target prediction resources and literature references (Griffiths-Jones 2006, Griffiths-Jones, et al. 2008, Griffiths-Jones, et al. 2006).

The first criterion in the miRBase classification is the species affiliation designated by three or four letter prefixes of the species. For example hsa-miR-24 indicates that this miR-24 is found in human (*Homo sapien*s). In addition, "miR" designates the mature form of miRNA in contrast to "mir" for pri-miRNA and pre-miRNA sequences. A star is added to the passenger strand name, hsa-miR-23b*, also known as star strand, in order to distinguish between the guide strand and the passenger strand. Besides the nomenclature that exists for orthologous sequences such as hsa-miR-24 in human and mmu-miR-24 in mouse, there is a specific nomenclature for paralogous sequences. For instance, hsa-miR-24-1 and hsa-miR-24-2 represent the same mature miRNA sequence but their transcripts originate from different genomic loci. In addition, mature miRNAs with only one or two different nucleotides will be given lettered suffixes e.g., hsa-miR-23a and hsa-miR-23b. The excision of mature miRNA sequences from the 5'or 3'end of the hairpin precursor also gives rise to additional terminology such as hsa-miR-30e-3p (3'arm of hairpin) or hsa-miR-30e-5p (5' arm of hairpin). When several miRNAs are organized in a cluster, the terminology is different. For example miR-23a, miR-27a and miR-24-2 are gathered together in miR-23a~27a~24-2 cluster. miRNAs can be grouped by family if they shared a common seed region (Lewis 2003). One example of miRNA family is the let-7 family which reassembles 13 members originated from nine different genomic loci (Roush and Slack 2008, Boyerinas, et al. 2010). Due to their common seed sequence, these members are likely to have shared targets and also common functional roles. Although these principles represent general rules for most species, there are some differences of miRNA nomenclature in plants and viruses.

3.5.2.4 Genomic organization of miRNAs

Transcription of these small non-coding RNAs can be driven by their own promoters or by the promoter of their host gene. miRNA promoters have also been discovered up to several kilobases (kb) away from miRNA sequence, suggesting that primary miRNAs (pri-miRNAs) can be very long trancripts (Corcoran, et al. 2009). miRNAs can be classified as intergenic or intragenic, according to their genomic localization in introns or as independent loci (**Figure 3.5.2.4**). Intergenic miRNAs form their own transcription units (TUs) as initially described (Lau, et al. 2001, Saini, Enright and Griffiths-Jones 2008). Most intergenic human miRNAs have a transcription start site and poly(A) signal (Saini, Enright and Griffiths-Jones 2008, Saini, Griffiths-Jones and Enright 2007). Many of these miRNAs are transcribed as polycistronic transcripts due to their organization in clusters and most clusters are thought to be driven by a common promoter because of their similar expression profiles (Saini, Enright and Griffiths-Jones 2008, Baskerville and Bartel 2005). 36% to 47% of miRNAs are organised in clusters in zebrafish, mouse and human (Griffiths-Jones, et al. 2008, Thatcher, et al. 2008) and approximately 50 distinct miRNAs clusters exist in the human and mouse genomes (Yuan, et al. 2009). Generally, a cluster consists of two or three miRNAs, however larger clusters of six miRNAs such as the human mir-17~92 cluster or eigth miRNAs like miR-302 cluster have been reported (Yuan, et al. 2009). miRNAs in a cluster either share sequence homology or may not be related (Lee and Ambros 2001, Lau, et al. 2001). Sequence homology presents the possibility of targeting the same genes and possibly regulating genes that belong to a unique cellular pathway and interact with each other (Bartel 2004, Yuan, et al. 2009, Olena and Patton 2010, Kim and Nam 2006, Yu, et al. 2006).

Numerous miRNA genes are found in introns of either coding or nonconding transcription units (TUs) (Rodriguez, et al. 2004) and are often processed from unspliced intronic regions (Kim and Kim 2007). Intronic miRNAs are likely to be expressed by their host gene promoter (Baskerville and Bartel 2005) but they can also be transcribed from their own promoter (Aboobaker, et al. 2005). Mirtrons, another class of intronic miRNAs, are spliced and debranched introns that are co-expressed with their host genes. They mimic the structural features of pre-miRNAs to enter the

miRNA-processing pathway without Drosha-mediated cleavage (Ruby, Jan and Bartel 2007). As seen previously, the flanking regions of the miRNA hairpin are crucial for Drosha processing as well as the distance of 11bp that separates the stem and the junction with the flanking sequences (Berezikov, et al. 2007). However, mitrons have canonical splice sites instead of extensive pairing at the base of the hairpin in pri-miRNAs (Ruby, Jan and Bartel 2007) and are processed through splicing instead of Drosha-mediated cleavage.

miRNAs can be located within the exons of genes or overlap between exons and introns which are usually non-coding transcripts. This class is represented only by a small number of miRNAs whereas the other classes are more common (Rodriguez, et al. 2004, Maselli, Di Bernardo and Banfi 2008).

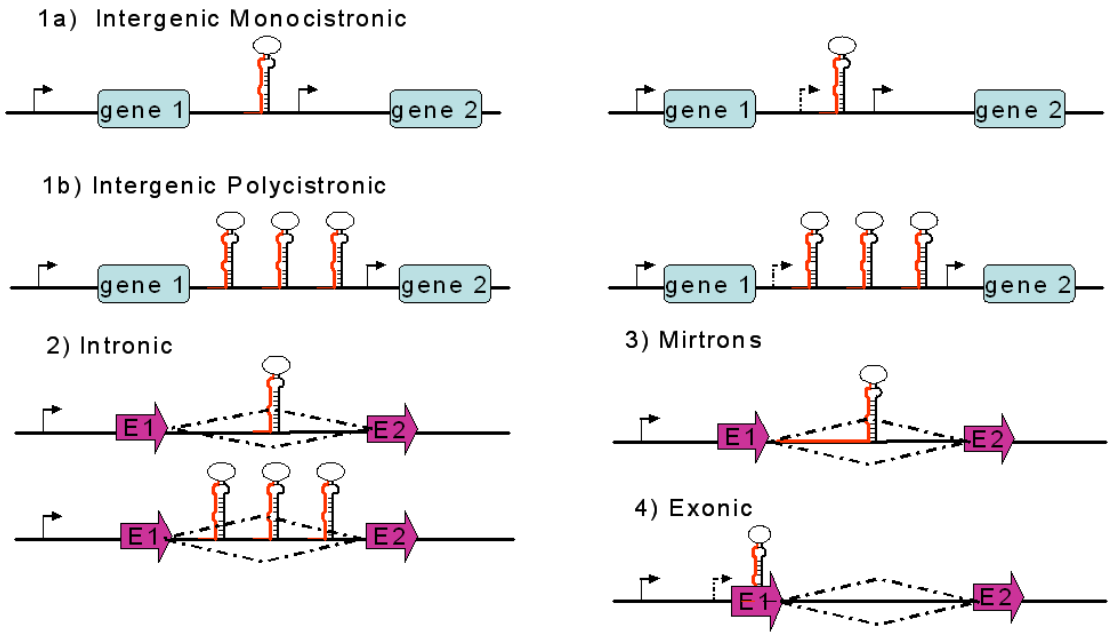

Figure 3.5.2.4: Genomic organization of miRNAs

There are four classes of organization. (1) Intergenic miRNAs, as the name suggests, are located in isolation from other genes and occur as either a monocistronic (a) or polycistronic unit (b). Their transcription is driven by their own promoter upstream and may be either RNA PolII- or PolIII-dependent. (2) Intronic miRNAs are located within an intron of a protein-coding gene, again as monocistronic or polycistronic units. They may be under the control of their own independent promoter or may be co-transcribed with the host gene. In the latter case they are processed into pre-miRNAs by the Microprocessor complex subsequent to intron splicing. (3) Mirtrons exist in short introns and differ from other intronic miRNAs in that they by-pass processing by Drosha and are exported directly to the cytoplasm to engage Dicer. They are co-expressed with the host gene. (4) Exonic miRNAs are located in an exon and are independently transcribed from their own promoter. Black arrow: host gene promoter start site, Black arrow with lines: miRNA promoter start site, Diamond-shape with lines: intron, Purple arrow: exon, Blue Rectangle: gene.

3.5.2.5 Mode of action of miRNA

3.5.2.5.1 Translation regulation through 3'UTR binding

In animals, imperfect complementarity, between a mature miRNA and its target mRNA leads to protein synthesis inhibition and/or mRNA instability causing degradation. Originally, this base-pairing was described by computational prediction studies to occur only between the seed region, located in positions 2 to 8 nt from the 5'end of the mature miRNA and binding to the 3'-UTR of the mRNA (Pillai 2005, Doench, Petersen and Sharp 2003, Stark, et al. 2005, Grimson, et al. 2007, Doench and Sharp 2004, Doench and Sharp 2004, Lewis, Burge and Bartel 2005a) . This feature was also shown later by a proteomic study that confirmed superior protein inhibition capacity for the 3'UTR sites (Baek, et al. 2008). Grimson et al., identified both computationally and experimentally, general features of miRNA-mRNA interaction that are important for the efficacy of repression such as AU-rich nt composition near the seed site and binding site positioning (Grimson, et al. 2007). However, these are general rules and cannot be applied to all miRNA-mRNA pairs. The degree of repression is variable and not all predicted seed sites give rise to repression. Stark et al., showed that genes with a development-related function have long 3'UTRs enriched in miRNA binding sites whereas genes involved in basic cellular processes tend to have shorter 3'UTRs with a lower number of miRNA binding sites (Stark, et al. 2005). miRNAs may impact on 3'UTR length and content and so they likely play a role in 3'UTR evolution of protein-coding genes (Zhang and Su 2009). It has also been suggested that the 3'-end of miRNAs could be involved in mRNA-miRNA interaction by complementing a seed match to enhance target recognition or compensating for a mismatch to the seed (Grimson, et al. 2007, Doench and Sharp 2004, Kiriakidou, et al. 2004, Kloosterman, et al. 2004).

Vasudevan and co-workers have demonstrated that miRNAs can induce translational up-regulation of target mRNAs by AGO_2-3'UTR interaction in non-proliferating cells that are in cell cycle arrest but on the other hand, miRNAs induce repression of translation in proliferating cells (Vasudevan, Tong and Steitz 2007b). These authors

proposed that translation regulation can switch between these two antagonistic mechanisms of repression and activation, depending on the cell cycle phase.

3.5.2.5.2 Tranlsation up-regulation through 5'UTR

Other experimental studies have demonstrated interaction between the 3'end of a miRNA and the 5'UTR of a target mRNA resulting in up-regulation of the target protein-coding gene (Lytle, Yario and Steitz 2007, Lee, et al. 2009, Orom, Nielsen and Lund 2008).

3.5.2.5.3 Non-canonical binding

Recently, Shin and co-workers identified another class of miRNA targets called "centered sites" that lack both perfect seed pairing and 3'-compensatory pairing, and instead have 11-12 contiguous Watson-Crick pairs towards the center of the miRNA (Shin, et al. 2010). Potential miRNA targets have also been computational predicted and experimental genome-wide analyses within open reading frame (ORF) in mammals (Grimson, et al. 2007, Lewis, Burge and Bartel 2005a, Baek, et al. 2008, Farh, et al. 2005) (**Figure 3.5.2.5.3**). The binding of miRNA to the target ORF appears to be less frequent and less effective than 3′-UTR targeting but still much more frequent than 5′-UTR targeting (Bartel 2009).

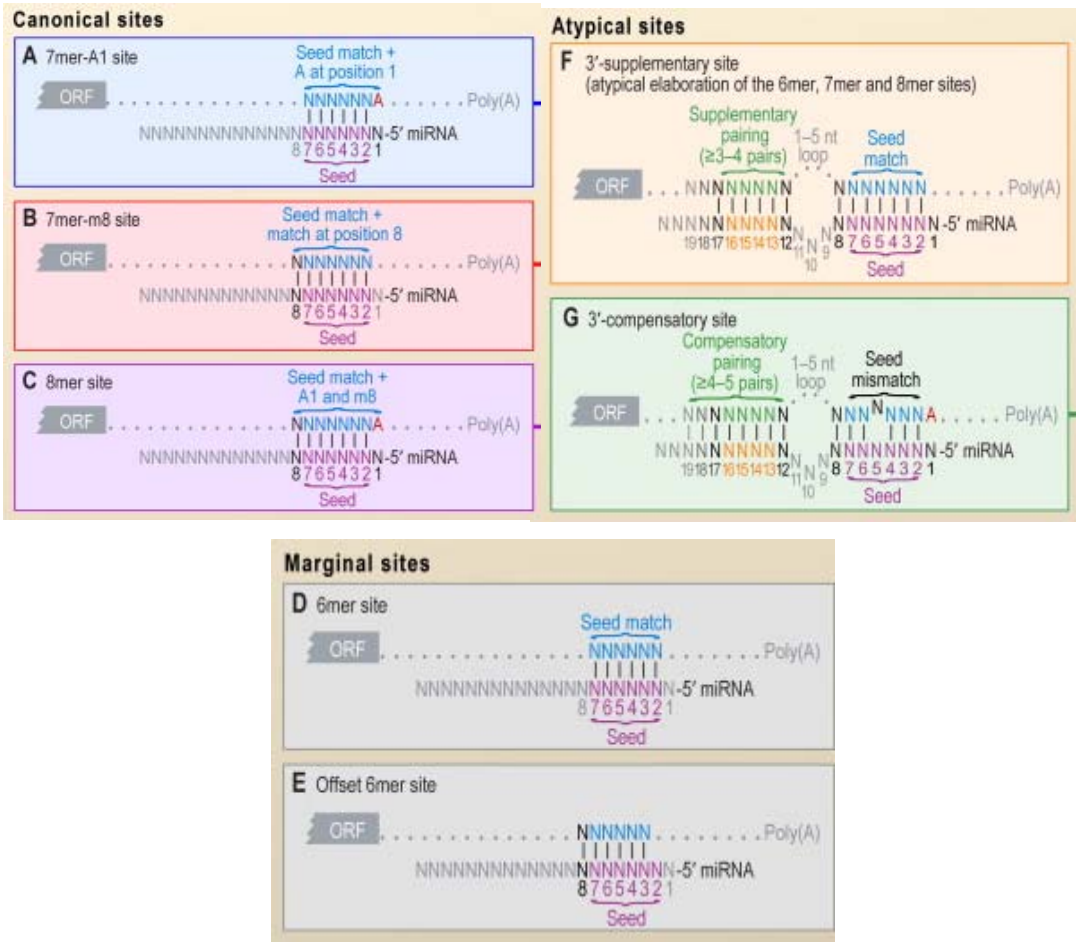

Figure 3.5.2.5.3: Types of miRNA Target Sites

(A–C) Canonical, 7–8 nt seed-matched sites. Vertical dashes indicate contiguous Watson–Crick pairing (D–E). Marginal, 6 nt sites matching the seed region. These 6mer sites typically have reduced efficacy and are conserved by chance more frequently than the larger sites. (F–G) Sites with productive 3 pairing. For 3′ -supplementary sites (F), Watson–Crick pairing usually centering miRNA nucleotides 13–16 (orange) supplements a 6–8 nt site (A–E). At least 3–4 well-positioned contiguous pairs are typically required for increased efficacy, which explains why 3 -supplementary sites are atypical. For 3 -compensatory sites (G), Watson–Crick pairing usually centering on miRNA nucleotides 13–16 (orange) can compensate for a seed mismatch and thereby create a functional site. Figures and legend were taken from the following review: MicroRNAs: Target recognition and regulatory functions (Bartel 2009).

3.5.2.6 miRNA regulation

miRNAs were previously thought to have a long half-life but several examples are now in contrast with this. In plants, the 3'→ 5' small RNA degrading nuclease (SDN1), homolog of the yeast RNA exonuclease 1 (Rexp1), triggers mature miRNA decay *in vitro*. The knockdown of SDN1 induces an increase in miRNA level and developmental defects. Therefore, SDN1 is thought to be an important regulator of miRNA turnover in plant development (Ramachandran and Chen 2008). In C.elegans, the 5'→ 3' exoribonuclease, XRN-2 prompts miRNA degradation and affects functional miRNA homeostasis *in vivo* (Chatterjee and Grosshans 2009). Turnover is an important cellular mechanism to control cell homeostasis and to ensure maintenance of miRNA steady-state levels in the cells. This type of regulation may modulate miRNA expression in different tissues and at a specific stage, for example, during development (Chatterjee and Grosshans 2009). miRNAs enriched in different types of neurons, undergo rapid turnover and degradation but all miRNAs do not undergo turnover in all types of neurons (Krol, Loedige and Filipowicz 2010, Sethi and Lukiw 2009). Another level of regulation, known as RNA editing, has been shown to play an important role in pri-miRNA and pre-miRNA maturation. Pri-miRNAs and pre-miRNAs are thought to be under regulation of A-to-I RNA editing, this mechanism being responsible for miRNA processing alterations (Scadden and Smith 2001). RNA editing is a site-specific modification of an RNA sequence which consequently triggers base-pairing and structural property alteration of transcripts (Blow, et al. 2006). RNA editing is directed by Adenosine deaminases acting on RNAs (ADARs) that can convert adenosine to inosine by deamination, in various dsRNA substrates. For instance, editing can prevent Drosha from pri-miRNA processing (Yang, et al. 2006, O'Connell and Keegan 2006). It can also trigger miRNA functional modulation and extension of miRNA diversity and their targets (Blow, et al. 2006, Heale, et al. 2009). For instance, editing within the seed sequence leads to a big impact on target specificity of edited miRNAs. Editing seems to have different and selective effects on RNAi processes and appears to depend significantly on the RNA-binding activities of ADARs. ADARs can bind to many transcripts without editing them (Klaue, et al. 2003). Besides turnover and editing, miRNA expression may be regulated by feedback loops, recent studies have focused on the regulation network between miRNAs and transcription factors (TFs) (Shalgi, et al.

2007, Hobert 2004, Wang, et al. 2010, Sun, et al. 2012). Maps of transcriptional regulatory networks have been studied in mammals (Boyer, et al. 2005) and other organisms (Fazi, et al. 2005, Johnston, et al. 2005, Varghese and Cohen 2007, Martinez, et al. 2008). These maps have uncovered the existence of feed-forward and feedback loops, promoting robustness and maintenance of homeostasis (Milo, et al. 2002, Shen-Orr, et al. 2002, Alon 2007). An example of a negative feedback loop in miRNA processing is the regulation of Drosha (Han, et al. 2009) and Dicer levels (Tokumaru, et al. 2008, Forman, Legesse-Miller and Coller 2008). Drosha negatively regulates its cofactor DGCR8 by mRNA cleavage and DGCR8 stabilizes levels of Drosha protein leading to Drosha up-regulation (Han, et al. 2009). Another example is the miRNA/mRNA pair let-7/LIN28, involved in double-negative feedback loop regulation where repression of LIN28 protein synthesis is controlled by let-7 and alternatively, LIN28 prevents let-7 maturation (Newman and Hammond 2010, Viswanathan and Daley 2010). miRNA regulation occurs at different levels of miRNA maturation, including regulation of the different forms of miRNA and of the different key regulators of this mechanism such as Dicer and Drosha. Perturbation of miRNA regulation induces defects in development and diseases (Thomson, et al. 2006, Chang, et al. 2004).

3.5.2.7 Computational identification of miRNAs

Mature miRNAs are only 22-23 nt in length, are often expressed at low concentration and they have tissue/cell specific and time-specific expression. Computational programs have been developed based on machine learning techniques in order to be able to identify new miRNA sequences, but the miRNA properties described above make the development of algorithms challenging (Chaudhuri and Chatterjee 2007, Bentwich 2005). These distinct properties are divided in two classes, structural features and sequence features. The structural features include hairpin and hairpin-loop length, thermodynamic stability, base-pairing, bulge size and location, and distance of the miRNA from the loop of its hairpin precursor. Sequence features include nucleotide content and location, sequence complexity, repeat elements and inverted sequence repeats (Bentwich 2005). The different miRNA prediction algorithms often search for sequence and structure conservation in other organisms and give a score to the

prediction depending on the feature similarities they found and on the probability of having found novel miRNAs.

3.5.2.8 Biological role of miRNAs

miRNAs have been demonstrated to be involved in many cellular functions including development (Lee, Feinbaum and Ambros 1993), differentiation (Chang, et al. 2004), cell growth and apoptosis (Cheng, et al. 2005), cell cycle (Chivukula and Mendell 2008, Lal, et al. 2009a, Lal, et al. 2008), DNA-damage response (Pothof, et al. 2009), chromatin-remodelling (Yoo, et al. 2009), DNA methylation (Wu, et al. 2010a), control of signal transduction (Wu, et al. 2010a, Inui, Martello and Piccolo 2010) and cell metabolism (Gao, et al. 2009, Lin, et al. 2009). Some studies have shown that miRNAs can act as a rheostat to maintain homeostasis and limit the response to environmental fluctuations (Stark, et al. 2005, Li, et al. 2009, Hornstein and Shomron 2006). miRNAs have also been found to be deregulated in multiple diseases (Borel and Antonarakis 2008), including cancers (He, et al. 2005, He, et al. 2007b), heart diseases (Papageorgiou, et al. 2012), diabetes (Correa-Medina, et al. 2009) and viral infection (Buck, et al. 2010). miRNAs could be used as biomarkers or therapeutic treatments in several illnesses. However, miRNA regulation networks need to be better understood before achieving these goals. Loss and gain of function approaches are often the method chosen to investigate endogenous miRNA roles.

3.5.2.9 Functional validation

3.5.2.9.1 Loss of function approaches

2'-*O*Me (methylated oligonucleotides)

In short term studies, antisense silencing technology is frequently exploited using chemical modifications for stability and cholesterol conjugation for delivery (Soutschek, et al. 2004). Different silencing technologies have been used such as

inhibitors named 2'-O-methyl-modified oligoribonuleotides (2'-*O*Me) that are complementary to the targeted miRNA (Hutvagner, et al. 2004, Meister, et al. 2004).

AntagomiRs

Other modified molecules developed are cholesterol-conjugated single-stranded RNAs complementary to miRNAs called 'antagomirs' stabilized with a partial phosphorothioate backbone in addition to complete 2'-O-methyl modifications, with dose-dependent and long-lasting effect of at least three weeks (Krutzfeldt, Poy and Stoffel 2006, Krutzfeldt, et al. 2005).

Antisense oligonucleotides

A similar strategy is the use of antisense oligonucleotides (ASOs) (Horwich and Zamore 2008), which are unconjugated single-stranded RNAs and carry phosphorothioate backbones and 2'-Omethoxyethyl modifications. Antagomirs and ASOs have been shown to have similar efficacy of silencing.

LNA-antimiR

More recently, locked –nucleic-acid-modified oligonucleotides (LNA-antimiR) have been developed to efficiently antagonize miRNA *in vivo* after intravenous injection of hypercholesterolemic mice and African green monkeys (Elmen, et al. 2008). This method is dose-dependent, has long-lasting effects and does not seem to cause any associated toxicity. Another advantage of LNAs is their ability to differentiate miRNAs that are derived from the same primary transcript and so specifically silence only one of them.

Mtg-AMOs

Lu et al. have developed a multiple-target technology named MTg- AMOs which are engineered in a single unit to target multiple miRNAs (Lu, et al. 2009). The application of this method in miRNA cluster studies, can overcome problems of miRNA inhibition compensation from other members of the cluster. In this case, this system is more efficient and relevant than targeting a single miRNA as multiple miRNAs have been shown to work together to regulate cellular processes and gene expression.

miRNA sponge

There is also the possibility of more stable long term knockdown using a miRNA "sponge"(miR-SP), by cloning miRNA antisense sequences into an appropriate vector. This construct is usually driven by a strong RNA polymerase II promoter and comprises multiple tandem binding sites for a specific miRNA downstream of a fluorescent reporter gene (Ebert, Neilson and Sharp 2007, Ebert and Sharp 2010). The key advantage of the miR-SP is its ability to inhibit a whole miRNA family (miRNAs that share a common seed region), by using complementary heptameric seed. Inhibition of a unique miRNA may not be phenotypically effective due to compensation by other members of the miRNA family (Loya, et al. 2009, Brown and Naldini 2009).

3.5.2.9.2 Gain of function approaches

Mimic molecules

To mimic endogenous mature miRNAs, double-stranded molecules have been designed. miRNA mimic molecules are often used in parallel to miRNA inhibitors in transient transfection assays. These mimics are chemically modified, short and double-stranded molecules. Their introduction in the cells leads to higher levels of the studied miRNA. Impact of the mimic molecules is not long-lasting therefore these molecules are only used in short-term studies.

shRNA

Instead shRNA-expression vectors can be used for long-term study. It has been demonstrated that the flanking and loop sequences of miR-30 have important features and are sufficient to enhance siRNA/miRNA precursor processing into the mature form (Zeng, Wagner and Cullen 2002, Boden, et al. 2004). Zeng and co-workers reported the artificial expression of precursor miRNA using this approach. The stem sequence of the human miR-30 was replaced with a drosophila-specific gene sequence which was not conserved in human and the chimeric sequence was successful expressed. Thus miR-30-based shRNA vector can be used in transient and stable expression studies. The use of strong promoters and viral vectors can increase the expression of the siRNA/miRNA and it can be applied for knockdown and overexpression. The expression of the transgene can also be controlled in an inducible or spatiotemporal manner using different promoters. Since the report by Zeng and co-workers, many papers have reported efficient expression of miRNA or siRNA using miR-30 backbone in gene function studies but also for gene therapy applications where miR-30-based shRNA contruct is an advantageous approach because it does not trigger cellular immune response (Boden, et al. 2004, Bauer, et al. 2009).

3.5.2.10 Experimental validation for miRNA identification

Novel miRNAs identified by computational prediction can be validated by different experimental techniques. However, for the same reasons described above, validation of miRNAs can be challenging because of their short length, their sequence similarity with other miRNAs, their time- and stage-specific expression and their frequently low level of expression (Chaudhuri and Chatterjee 2007, Bentwich 2005).

3.5.2.10.1 Hybridization techniques

Hybridization techniques including northern blot, RNase protection assay, primer extension and signal-amplifiying ribozyme method are commonly used to validate miRNA expression (Berezikov, et al. 2005)(Lee, et al. 2002, Berezikov, et al. 2005, Hartig, et al. 2004).

Northern blot is used to detect the mature and the precursor form of miRNAs (Lee and Ambros 2001, Lau, et al. 2001, Lagos-Quintana, et al. 2001) and to confirm high-throughput data (Sempere, et al. 2004). However, it is not sensitive and specific enough to capture low expressed miRNAs and for this reason large amount of RNA needs to be extracted from the original sample (Chaudhuri and Chatterjee 2007).

RNase protection assay consists of in vitro transcription of a labelled RNA probe. This RNA probe is complementary to the sequence of interest and hybridized to total RNA (Chaudhuri and Chatterjee 2007). Unhybridized single-strand RNA molecules are digested by a nuclease enzyme whereas the miRNA of interest coupled to the probe is protected. Resulting labelled fragments are run on a gel. This method requires the use of radioisotopes and it is a low-throughput technique (Sandelin, et al. 2007). In the primer extension technique, a labelled DNA primer recognises the 3'end of the miRNA followed by reverse transcription. Products are partially digested and run on a gel to evaluate the product size. This method also is a low-throughput technique and requires the use of radioisotopes (Chaudhuri and Chatterjee 2007).

Ribozymes are nucleases with hairpin structure that cleave RNA molecules in a sequence specific manner (Suryawanshi, Scaria and Maiti 2010). The hammerhead

ribozyme can be easily engineering because of its simple form and size. For these reasons, it can be applied for gene expression inactivation (Michienzi, et al. 2000). Reporter-ribozymes comprised the complementary sequence of the miRNA of interest in their hairpin structure to direct specific binding. A reporter is placed at the 3'-end of the enzyme and a quencher at the 5'end. This binding triggers miRNA cleavage and a fluorescent signal is detected. Different cloning approaches such as random or specific cloning of size-fractioned RNA and amplified-partial sequencing have been developed to validate miRNA identification (Bentwich 2005, Lim, et al. 2005, Takada, et al. 2006).

A recent novel bead-based flow cytometry strategy has been used for miRNA profiling where beads can be coupled to different dyes facilitating simultaneously study of several miRNAs (Lu, et al. 2005).

3.5.2.10.2 Real-time PCR

Real-time PCR is another method for detection of mature and precursor miRNAs (Schmittgen, et al. 2004, Fu, et al. 2006, Tang, et al. 2006) as well as the use of microarrays which are sensitive and specific even for rare miRNAs (Lim, et al. 2005, Schmittgen, et al. 2004, Fu, et al. 2006, Schmittgen, et al. 2008, Barad, et al. 2004, Liu, et al. 2008). The detection of the mature strand is very specific with Real-PCR. In fact, the reverse-transcription (RT) primer can be designed with a stem-loop to distinguish between the mature and the precursor strand and to be specific to the mature miRNA only (Schmittgen, et al. 2008, Chen, et al. 2005). The TaqMan qRT-PCR method uses this system combined with the fluorescence resonance energy transfer (FRET)

Another method is to reverse transcribed the RNA extract with oligodT or random primers and use an intercalator fluorescent dye that binds to double strand DNA during the PCR step such as SYBR green. The detection is monitored by measuring the increase in fluorescence during PCR cycling. This approach is less specific than the TaqMan and can lead to detection of non-specific double-stranded DNA.

3.5.2.10.3 Microarray based-technology

Microarray based-methods are more suitable for miRNA profiling and for high throughput studies. The microarray approach has been applied to the identification of differentially regulated miRNAs upon different conditions (Kantardjieff, et al. 2009, Koh, et al. 2009). A study was conducted in our laboratory to monitor the changes of miRNA expression under temperature-shift in CHO cell culture using human/mouse-miRNA hybridization array (Gammell, et al. 2007). The application of a non-CHO specific microarray was possible to profile miRNAs in CHO cells due to the high conservation of mature miRNAs across species (Bartel 2009).

3.5.2.10.4 Next generation sequencing

Besides qRT-PCR and microarray, next-generation sequencing has proven to be a reliable alternative in miRNA profiling studies. This method does not need as much information as these two approaches therefore it was recently used in CHO cells and led to the identification and annotation of 387 mature miRNAs from six CHO cell lines in different conditions (Hackl, et al. 2011). Another study using the recent release of the whole CHO genome sequencing combined with miRBASE reported the detection of 190 conserved miRNA hairpin precursors (Hammond, et al. 2012).

3.5.2.11 miRNA target identification

3.5.2.11.1 Computational prediction

Initial miRNA target prediction algorithms have been based on seed pairing between miRNA-mRNAs and free energy of binding between each miRNA and its target, leading to high false positive rate. Improvements have been made by incorporation of binding site evolutionary conservation (Lewis, Burge and Bartel 2005a). Other algorithms are now based on folding patterns of RNA sequences conserved between

species such as miRseeker (Lai, et al. 2003) and the RNA folding and the hairpin sequence conservation in MirScan (Lim, et al. 2003). Other programs have taken into account stem-loop structure formation and nucleotide conservation in miRNA precursors (Berezikov, et al. 2005).

In plants, targets of miRNAs are much easier to find than in mammals because of their near-perfect complementarity between miRNA-mRNAs whereas in animals, this perfect match that triggers mRNA cleavage only occurs occasionally. In this regard, miRNA target prediction algorithms in plants minimize high false positive rates (Rhoades, et al. 2002). miRNA target prediction algorithms take into account different features of which the most common is based on Watson-Crick pairing at the seed region (Lewis, Burge and Bartel 2005a, Krek, et al. 2005) and evolutionary miRNA target site conservation (Bartel 2009). Seed sequence evolutionary conservation gives more robustness to target prediction as well as other features such as secondary structure of mRNA for structural accessibility (Kertesz, et al. 2007, Hammell, et al. 2008), nucleotide composition of target sequences and location of the binding sites within the 3'UTR (Grimson, et al. 2007, Baek, et al. 2008, Gaidatzis, et al. 2007). A score is associated with each predicted target to evaluate the authenticity of the prediction. The higher the target score is, the more confident is the prediction. Additional validation using experimental studies, such as transcriptomic or proteomic profiling, increases the discrimination of target rank (Baek, et al. 2008, Selbach, et al. 2008). Alexiou and coworkers, evaluated the prediction performance of five common databases, DIANA-microT 3.0; TargetScan 5.0, TargetScan S, Pictar and EIMMo against genes targeted after miRNA overexpression or knockdown in a study conducted by Selbach et al., in 2008 . The precision of the program (correctly target predicted/ total target predicted) was estimated at 50% and their sensitivity (correctly target predicted/ total correct) between 6 and 12%. These five programs are based mostly on the evolutionary conservation of the seed region and other features including accessibility of the binding site region and thermodynamic stability (Alexiou, et al. 2009). Considering the different properties of each algorithm, it was thought that the combination of several programs could give more accurate target prediction. However, multiple prediction approach appears to be less robust than single prediction program and the enrichment in true targets was very weak (Alexiou, et al. 2009, Alexiou, et al. 2009). To increase accuracy in prediction, Ritchie et al. suggested using a unique algorithm but with different 3'UTR sequences from different databases, to take into account the co-expression of miRNA and its

targets, to consider the presence of different binding sites for these multiple targets and to accept only high p-values for the identification of different genes that share a common biological function and are regulated by a single miRNA (gene ontology (GO) study) (Ritchie, Flamant and Rasko 2009). The use of experimental validation for predicted miRNA targets found *in silico*, has shown that computational predictions cannot be considered as final and conclusive results. To increase miRNA target prediction accuracy, algorithms should not only incorporate conserved 3'UTR-seed base pairing (**Table 3.3**) but also 5'UTR, ORF, 5' or 3' compensatory and multiple binding sites (Peter 2010, Wu, et al. 2010b). To improve these tools for researchers, additional features have been added to these different prediction programs, resulting in new databases such as TarBase or mirZ, where information from different gene, miRNA or protein databases and experimental studies are gathered together and help functional annotation (Min and Yoon 2010).

Table 3.3: Computational prediction of miRNAs

Program	Species specificity	Algorithm description	Webserver
miRNA target at EMBL	Drosophila	Complementarity with 3'UTR	http://www.russell.embl-heidelberg.de/miRNAs/
miRanda	Flies, vertebrates	Complementarity with 3'UTR, thermodynamic stability, duplex species conservation	http://www.miRNA.org/miRNA/home.do
RNAhybrid	Any	Complementarity with 3'UTR, thermodynamic stability, binding conservation	http://bibiserv.techfak.uni-bielefeld.de/rnahybrid/
TargetBoost	Worm and fruit fly	miRNA-mRNA binding site characteristics	https://demo1.interagon.com/targetboost/
psRNAtarget	Plants	Multiple complementary sequence approach	http://bioinfo3.noble.org/psRNATarget/
miRU	Plants	Perfect complementarity sequence, thermodynamic stability, sequence conservation (genome/ESTs)	http://bioinfo3.noble.org/miRNA/miRU.htm
miTarget	Any	Thermodynamic stability and sequence complementarity	http://cbit.snu.ac.kr/~miTarget/
Pictar	Flies Vertebrates Worm	Perfect and partial complementary sequence with 3'UTR, Thermodynamic stability	http://pictar.mdc-berlin.de/
RNA22	Any	miRNA-mRNA binding sites characteristics,Complementarity with 3'UTR, no cross-species conservation	http://cbcsrv.watson.ibm.com/rna22.html
MicroTar	Any	Complementarity with 3'UTR and thermodynamic stability	http://tiger.dbs.nus.edu.sg/microtar/
EIMMo	Humans, mice, fish, Flies, worms	miRNA binding sites conservation	http://www.mirz.unibas.ch/ElMMo2/
GenmiR++	Any	Sequence complementarity,	http://www.psi.toronto.e

		based on expression data sets	du/genmir
PITA	Any	Target site accessibility thermodynamic	http://genie.weizmann.ac.il/pubs/mir07/mir07_data.html
NBmiRTar	Any	Sequence and duplex characterisitics, no sequence conservation,	http://wotan.wistar.upenn.edu/NBmiRTar/login.php
mirWIP	Worm	Structure of target site accessibility, thermodynamic stability, based on experimental data sets	http://146.189.76.171/query.php
Sylamer	Any	Based on microarray data to identify 3'UTR sites	http://www.ebi.ac.uk/enright/sylamer/
miRTarget2	Vertebrates	Based on microarray data to identify 3'UTR sites	http://mirdb.org/miRDB/
TargetScan TargetScan S	Vertebrates	Complementarity with 3'UTR, thermodynamic stability, duplex species conservation	http://www.targetscan.org/

3.5.2.11.2 Experimental validation of miRNA targets

Reporter assays

The most common miRNA target experimental validation is cloning of the 3'UTR of a potential mRNA target downstream of a luciferase or a green fluorescent protein (GFP) ORF sequence (Kiriakidou, et al. 2004). Co- transfection of this construct and the mimic miRNA of interest is performed into cells that endogenously lack this miRNA. Expression of the reporter luciferase or GFP is measured after 24-48 hours (Krutzfeldt, Poy and Stoffel 2006, Kuhn, et al. 2008). However, miRNA overexpression by adding exogenous molecules can trigger "off-target" effects on other genes that miRNA gene targets.

Loss and gain of function studies

To validate a miRNA target, a loss of function study using antisense oligonucleotides or reporter vector technologies can be performed which leads to miRNA inhibition and consequently overexpression of the target gene (Kuhn, et al. 2008). Another strategy is the combination of transient transfections with mimics or inhibitors of mature miRNAs and other methods including microarray assays, western blotting, or proteomics in order to identify targets that are directly or indirectly down-regulated or up-regulated by this miRNA (Lim, et al. 2005).

SILAC

Stable-Isotope labelling by Amino-Acids (SILAC), a common method used in functional and quantitative proteomics in cell culture (Mann 2006), has been used for miRNA target identification in the Hela cell proteome (Vinther, et al. 2006). 12 out of 504 miRNA targets were repressed by miR-1 via their 3'UTR. These genes overlapped with miR-1 regulated genes identified by DNA array and validated by computational prediction databases including miRanda, PicTar and TargetScan S that are based on seed pairing. The other targets were likely to be regulated via non-canonical binding sites or were secondary targets. This technique has been used in addition to mass-spectrometry after miR-223 knockout in mouse neutrophils leading to the identification of 2,773 differentially expressed proteins, including primary and secondary targets

(Baek, et al. 2008). In this paper, in addition to SILAC, microarray profiling was performed to also identify changes at the transcriptional level. The authors showed that mRNA destabilization was the principal mode of endogenous miR-223 inhibition leading to strong repression (> 50%) in contrast to translational repression that led to modest repression (< 33%). A similar study identified targets of let-7b using pulsed SILAC (pSILAC) and microarray techniques after knockdown or overexpression of this miRNA (Selbach, et al. 2008). The conclusions from this study showed that miRNA let-7b represses many proteins and that mRNA and protein levels were down-regulated. Repression of protein was mild as demonstrated previously in other studies (Baek, et al. 2008).

HIT-CLIP

Recently, high-throughput sequencing of RNAs isolated by crosslinking immunoprecipitation (HIT-CLIP) allowed the identification of Argonaute protein-RNA interaction complexes in mouse brain leading to miRNA-mRNA interaction site identification (Chi, et al. 2009). This technique allows identification of direct protein-RNA interaction in a genome-wide manner thus only primary targets are revealed (Licatalosi, et al. 2008). The principle of the method is based on ultraviolet irradiation to induce covalent crosslinks between RNA-protein complexes followed by purification of these RNA-binding proteins and small RNAs, which are amplified and sequenced (Licatalosi, et al. 2008). In the same manner, Chi and co-workers purified Ago bound to mouse brain RNAs, radiolabelled the RNAs, purified the Ago-RNA complexes and visualised them by autoradiography (Chi, et al. 2009). They identified ternary complexes of Ago protein, miRNA and mRNA. A combination of experimental and *in silico* data led to the identification of interaction sites between miRNAs and their target mRNAs. From these interaction sites, genome-wide interaction maps have been generated for miR-124 and for the twenty most abundant miRNAs in mouse brain tissue.

3.5.3 miRNAs as potential tools for CHO cell engineering

The use of single-gene engineering is limited due to the nature of the technology which allows the overexpression of a small number of genes at a time. Multiple overexpression of genes requires co-transfection which increases the production of ectopic proteins and can compete with the endogenous translational machinery. In addition, positive cells which express the different transgenes are selected with different markers that are produced by the translational machinery and possibly overload it. As an alternative to coding-gene engineering approach, miRNAs do not compete with the endogenous translational machinery (Muller, Katinger and Grillari 2008). The capacity of miRNAs to target hundreds of genes makes them very promising tools to target entire cellular pathways such as cell growth and cell cycle, cell metabolism, stress, secretion and apoptosis. For example, overexpression and/or knockdown of different miRNAs using constitutive and inducible promoters might allow mimicking the effect of temperature-shift in a biphasic culture. Stable cell lines could be engineered with miRNAs to increase proliferation and at the middle of the logarithmic growth phase, an inducible system promoting the induction of other miRNAs with suppressive impact on proliferation and positive impact on secretion or metabolism to trigger cell growth arrest and direct the cellular machinery towards production. The participation of miRNAs in different cellular pathways presents exciting opportunities to engineer cells in different ways and to apply all these tools at different time points of the cell culture.

3.5.3.1 Let-7 family

Many miRNAs have been reported to be involved in proliferation including let-7, one of the first studied miRNA. Let-7 has an essential role in the development of C.*elegans*, with its deregulation leading to growth abnormalities (Pasquinelli, et al. 2000). Let-7 sequence and function are well conserved across species (Thomson, et al. 2006, Sempere, et al. 2004, Sempere, et al. 2002, Liu, et al. 2010). Most of let-7 family members act as tumor suppressors in many cancers (Esquela-Kerscher and Slack 2006, Roush and Slack 2008, Slack and Weidhaas 2006). It has been reported that one cluster

of this family that consists of let-7a, let-7d and let-7f is directly down-regulated by Myc overexpression thus promoting tumorigenesis (Chang, et al. 2009). Myc is a transcription factor often deregulated in cancers (Cascon and Robledo 2012, Dang 2012). However, hypomethylation of let-7a-3 triggers its up-regulation in human lung cancer cells causing induction of tumorigenesis (Brueckner, et al. 2007). This is a common characteristic of miRNAs which have been reported to display antagonising role for a same cellular function depending of the cell/tissue-type and the environment conditions (Cheng, et al. 2005).

3.5.3.2 miR-17~92 cluster and its paralogs

The miR-17~92 cluster and its paralogs miR-106b-25 and miR-106a-363 clusters are oncogenes involved in many cancers (He, et al. 2005, Volinia, et al. 2010). They promote proliferation and high survival rate (Hayashita, et al. 2005, Lu, et al. 2007). In B cell lymphoma, induction of the miR-17~92 cluster promotes tumor progression and inhibits apoptosis (O'Donnell, et al. 2005). Interestingly, MYC is responsible for miR-17~92 cluster transactivation. The miR-17~92 cluster directly targets Bim, a pro-apoptotic protein which regulates cell death by antagonizing anti-apoptotic proteins like Bcl-2 (Koralov, et al. 2008). The miR-17~92 cluster and its paralogs are also involved in cell cycle. E2F family members involved in G1/S progression are direct targets of the miR-17~92 cluster and its paralogs and they also regulate the transcription of these miRNAs in a negative feedback loop (O'Donnell, et al. 2005, Sylvestre, et al. 2007, Woods, Thomson and Hammond 2007, Petrocca, et al. 2008). miR-17 has been reported to influence cell cycle progression by targeting p21, a cyclin-dependent kinase inhibitor involved in the G1/S phase (Petrocca, et al. 2008, Ivanovska, et al. 2008).

3.5.3.3 miR-34 family

The tumor suppressor p53 targets miR-34a, miR-34b and miR-34c which in turn repress downstream targets to trigger cell cycle arrest in G1 phase and apoptosis (Hermeking 2010, Hermeking 2007, Tarasov, et al. 2007). p53 is negatively regulated by miR-504 and by miR-125b preventing apoptosis and cell cycle arrest (Hu, et al. 2010). In

addition, miR-34c has been reported to target c-Myc to prevent genomic instability in DNA damage response (Cannell and Bushell 2010).

3.5.3.4 miR-21

miR-21 is very well studied and acts as an oncomiR in many human cancers (Pan, Wang and Wang 2011, Chan, Krichevsky and Kosik 2005) Targets of miR-21 include regulators of tumorigenesis, cell cycle control and apoptosis including p53 pathway components and TGF-β (Papagiannakopoulos, Shapiro and Kosik 2008), the PTEN/AKT signaling pathway (Zhang, et al. 2010), antagonists of the RAS pathway (Frankel, et al. 2008, Zhu, et al. 2008), FasL (Wang and Li 2010) and Cdc25A (Wang, et al. 2009b).

3.5.3.5 miR-24

miR-24 has been previously shown to be involved in cell proliferation, cell cycle , apoptosis and DNA repair genes (Lal, et al. 2009a, Qin, et al. 2010, Mishra, et al. 2009). The up-regulation of miR-24 induces down-regulation of H2AX leading to inhibition of DNA repair in differentiated blood cells (Lal, et al. 2009b). miR-24 up-regulation was reported to trigger cell cycle arrest in G1 phase via targeting key nodes of the cell cycle, MYC and E2F2, and their downstream targets including CCNB1, CDC2, CDK4, p27Kip1 and VHL were also found to be targeted by miR-24 (Lal, et al. 2009a). Other targets involved in other phases of the cell cycle were also differentially regulated including FEN1, MCM4, MCM10, PCNA (S-phase) and AURKB (M-phase).

miR-24-2 is co-transcribed with miR-23a and miR-27a as part of miR-23a~27a~24-2 cluster. In humans, miR-23a~27a~24-2 cluster is intergenic and localized on chromosome 9q22 and its paralog miR-23b~27b~24-1 cluster is localized on chromosome 19p13 and is intronic (Chhabra, Dubey and Saini 2010). It has been reported that it is not uncommon for miRNA clusters to have homologs and paralogs (Yu, et al. 2006) . The role of the whole cluster in cell proliferation and apoptosis has been studied in cancer diseases. Up-regulation of miR-23a~27a~24-2 cluster induced

apoptosis in human embryonic kidney cells (Chhabra, et al. 2009, Chhabra, et al. 2009, Chhabra, Dubey and Saini 2011).

3.5.3.6 miR-23a/b

Recent reports showed the role of c-Myc in glutamine catabolism through repression of miR-23a and miR-23b (Gao, et al. 2009, Dang 2010). c-Myc has been shown to regulate glucose metabolism by promoting glycolysis in transformed cells (Osthus, et al. 2000, Kim, et al. 2004b). Altered glucose metabolism in cancer is known as the Warburg effect. Cancer cells take up excessive amounts of glucose and convert it to lactate even in the presence of adequate levels of oxygen (Dang 2010). c-Myc also regulates Hypoxia-inducible factor 1 (HIF-1) expression, a key regulator of hypoxia (oxygen deprivation), in normal and cancer cells (Doe, et al. 2012). Through the Warbug effect, glucose and glutamine are used as great sources of energy to provide ATP and NAPDH to new cancer cells formed (Dang 2010). As c-Myc is involved in the Warburg effect and it increases the expression of mitochondria glutaminase by repression of miR23a/b in transformed cells, miR-23b could also be involved in the metabolism of CHO cells.

3.5.3.7 miR-27a/b

miR-27 is involved in cell metabolism, through adipogenesis regulation. PPARγ, a key regulator of adipogenesis has been validated as miR-27 target (Lin, et al. 2009). miR-27 has been shown to affect cholesterol homeostasis, fatty acid metabolism and lipogenesis (Sacco and Adeli 2012, Fernandez-Hernando, et al. 2011). miR-27 is also involved in the G2/M checkpoint of the cell cycle in breast cancer cells (Mertens-Talcott, et al. 2007).

3.5.3.8 miR-7

miR-7 is highly conserved across species, from annelids to humans suggesting that its functional role may also be conserved (Prochnik, Rokhsar and Aboobaker 2007). In human, mature miR-7 sequence is derived from three miRNA precursors, miR-7-1,

miR-7-2 and miR-7-3. The miR-7 homolog in mice originates from two precursors, mmu-miR-7a and mmu-miR-7b, whose sequences differ from one or two nucleotides. miR-7 is an intronic miRNA which resides in the first intron of heterogenous ribonuclear protein K gene on chromosome 9 in humans and on chromosome 13 in mice. Generally, the expression of intronic miRNAs is highly correlated to the expression of the host gene (Baskerville and Bartel 2005). However, it is not the case for miR-7 which exhibits differential expression profile to that of its host gene hnRNP-K (Aboobaker, et al. 2005).

3.5.3.8.1 The role of miR-7 in cell proliferation and apoptosis

miR-7 is involved in cell proliferation, apoptosis regulation and its deregulation has been reported in many cancers including breast cancer, pancreatic cancer, glioblastomas, lung cancer and tongue squamous cell carcinoma (Chou, et al. 2010, Kefas, et al. 2008, Ikeda, et al. 2012, McInnes, et al. 2012, Jiang, et al. 2010). In most of these studies, miR-7 acts as a tumor suppressor, its induction causing inhibition of tumor progression. miR-7 has been shown to regulate the phenotypes-associated with cancers by targeting EGFR and IGFR, two signalling pathways involved in the development of tumorigenesis.

Jiang L et al reported the depletion of IGF1R (insulin-like growth factor 1 receptor) at both the mRNA and protein levels upon overexpression of miR-7 in tongue squamous cell carcinoma (TSCC) and confirmed the direct interaction between miR-7 and IGF1R using luciferase-reporter assay (Jiang, et al. 2010, Jiang, et al. 2010). The IGF1 (insulin-like growth factor 1)-dependent activation of Akt (protein kinase B) was repressed as a result of IGF1R inhibition by miR-7 leading to cell proliferation reduction and cell-cycle arrest and on the other hand enhanced apoptotic rate. Recently, the levels of miR-7 have also been shown to anti-correlate with those of IGF1R leading to reduced gastric cancer cell migration and invasion (Zhao, et al. 2012).

In contrast to IGF1R, many studies have focused on the repression of Epidermal Growth Factor Receptor (EGFR) by miR-7 induction. miR-7 has been reported to repress the EGFR pathway, the Akt pathway and extracellular signal-regulated kinase 1/2 (ERK1/2), its downstream effectors which are both activated in glioblastomas, prostate, lung and breast (Kefas, et al. 2008, Giles, et al. 2011, Webster, et al. 2009).

The protein kinase B/Akt, is involved in the control regulation of proliferation, invasion, angiogenesis, and apoptosis resistance in glioblastomas as well as prostate cancers (Giles, et al. 2011). Webster and co-workers showed that miR-7 reduced the expression levels of EGFR mRNA and protein expression in cancer cell lines (lung, breast, and glioblastoma), inducing cell cycle arrest and cell death (Webster, et al. 2009). miR-7 is also involved in the regulation of the phosphoinositide 3-kinase (PI3K)/AKT/mTOR (mammalian target of rapamycin) pathway, another critical pathway downstream of EGFR which is also associated with cell proliferation, survival, and metastasis (Fang, et al. 2012). The negative regulation of the effectors of the PI3K/AKT/mTOR pathway by miR-7 induced G0 /G1-specific cell-cycle arrest and impaired cell migration in hepatocellular carcinoma. It has been suggested that EGFR induces miR-7 expression through the Ras/ERK/Myc pathway (Chou, et al. 2010) Besides EGFR, miR-7 has been shown to also inhibit p21-activated kinase 1 (Pak1), and activated Cdc42-associated kinase (Ack1) signaling pathways in Schwannomas tumors (Saydam, et al. 2011). Recently, Foxp3, a member of the Fork-head family of transcription factors, has been reported to promote miR-7 inducing suppression of oncogene STAB1 by a feed-forward loop in breast cancer (McInnes, et al. 2012). BCL-2, a critical regulator of apoptosis was found to be down-regulated by miR-7 at both mRNA and protein levels leading to growth suppression and apoptosis of in lung carcinoma cell line A549 (Xiong, et al. 2011).

3.5.3.8.2 The role of miR-7 in secretion regulation

miR-7 has been shown to be one of the most abundant miRNA in Langerhans islets, in the endocrine pancreas of rat, human, mice and in neurosecretory cells of zebrafish (Bravo-Egana, et al. 2008, Wienholds, et al. 2005, Lynn, et al. 2007, Tessmar-Raible, et al. 2007). The role of miR-7 in secretion regulation is supported by its increased levels of expression correlated to the increase of insulin transcript during the development/differentiation of human pancreas and in the adult pancreas (Correa-Medina, et al. 2009, Joglekar, Joglekar and Hardikar 2009). In agreement with this, Nieto M et al., reported that miR-7 knockdown attenuated insulin production, decreased β-cell numbers, and glucose intolerance during early embryonic life of mice (Nieto, et al. 2011). Another study showed that insulin receptor substrate 1 (IRS1) expression was

down-regulated as well as insulin-stimulated Akt phosphorylation and glucose uptake upon miR-7 overexpression (Li, et al. 2011).

3.5.3.8.3 The role of miR-7 in robustness

In addition to its involvement in cell proliferation, apoptosis and secretion regulation, miR-7 has been reported to impart robustness during drosophila development. Induction of miR-7 in drosophila cells led to reduction of Notch expression, a gene involved in developmental processes including tissues growth (Stark, et al. 2003). Later, miR-7 was shown to fine-tune the expression of development-specific genes to avoid major cell perturbation and to maintain robustness during environmental flux (Li, et al. 2009, Li and Carthew 2005). Lin X et al., demonstrated that under temperature fluctuation (between 31°C and 18°C), miR-7 is able to buffer specific gene expression and cell fates in the development of *Drosophila* larvae. Upon temperature fluctuation and in presence of miR-7, there were no changes in miR-7 targets expression, Ato (atonal) and Yan, two critical factors for the development of insect sensory organs. Under the same conditions, miR-7 mutant showed strong repression of Ato and high expression of Yan leading to development defects.

3.5.3.8.4 The role of miR-7 in CHO cells

The gathered information from the miR-7 studies described above reported that miR-7 is involved in cell growth, apoptosis, secretion and homeostasis regulation. All these pathways are relevant to bioprocess application and may be subjected to manipulation to improve CHO cell density, viability and recombinant protein production.

We previously reported that transient overexpression of miR-7 induced cell growth reduction and improved normalised productivity in low serum-supplemented CHO-K1 SEAP culture (Barron, et al. 2011). The overexpression of miR-7 was recently reported to impact negatively on ribosomal proteins in CHO cells (Meleady, et al. 2012). Several of these down-regulated proteins, including RPS10, have been shown to be associated with cell proliferation, cell cycle, apoptosis and development regulation (Ren, et al. 2010, Lindstrom 2009, Warner and McIntosh 2009, Wang, et al. 2006). The induction

of miR-7 in CHO cells also promoted the expression inhibition of histone proteins including histones H3 and H4. These recent findings indicate that miR-7 may be a promising target in the improvement of bioprocess-relevant CHO characteristics.

3.5.3.9 Limitations of miRNAs in CHO cells and future perspectives

Until recently with the release of CHO-K1 cell line genome (Xu, et al. 2011), sequence information on CHO cells was not publicly available therefore research on cDNA and miRNAs as tools to engineer CHO cells was based on sequence homology and conservation in similar species such as human, rat and mouse. Although mature miRNA sequences are well conserved across species, notably on the hairpin and the loop of miRNAs, the flanking sequences on either side are not (Berezikov, et al. 2005, Hertel, et al. 2006). Thus the unknown degree of homology with CHO and other species was limiting the panel of tools applicable to CHO cell engineering. In 2007, our laboratory used miRNA bioarrays designed with specific probes to human, rat and mouse RNA to identify differentially regulated miRNAs upon temperature–shift in CHO cells (Gammell, et al. 2007). In this study, the design of primers, based on the identification of a consensus sequence following alignment of pre-mir-21 flanking sequences across different species, allowed the identification and sequencing of miR-21 in CHO cells, listed as cgr-miR-21 in the miRBAse miRNA registry (http://miRNA.sanger.ac.uk/). Based also on miRNA sequence conservation across species, a microarray platform (miRCURY LNA™ miRNA Array) and a qRT-PCR method validated in human and mouse was applied for miRNA profiling in CHO cells (Lin, et al. 2010). The difference with the previous study was the probes which were designed using Locked Nucleic Acid (LNA™) technology increasing binding specificity. More recently, the use of high-throughput sequencing and annotation by homology with human, mouse and rat, resulted in the identification of 350 distinct miRNAs and miRNAs* sequences from four CHO cell lines (Johnson, et al. 2011). Unlike microarray technology, next-generation sequencing allows the identification of novel miRNAs. In addition, read lengths produced are compatible with the length of mature miRNAs and siRNAs (Nobuta, et al. 2010, Morozova and Marra 2008). In a short time, new tools were available to identify and annotate mature miRNAs in CHO cells with no need for sequence information (Hackl, et al. 2011). In one study, the sequencing of 26 validated

targets of miR-17~92 cluster, showed that 19 had their binding sites conserved whereas the 7 others could not be detecte (Hackl, et al. 2012). This is likely due to either incomplete sequencing coverage or due to possible shorter 3'UTRs of CHO-specific mRNA isoforms (Bartel 2009). This knowledge of mature and precursor miRNA sequences will help to develop CHO cell-specific technologies, including microarray and qPCR primers.

AIMS OF THESIS

4 Aims of thesis

The aims of this thesis were as follows:

- **To adapt CHO-K1 SEAP cells in serum-free suspension culture**

- **To validate candidate miRNAs as potential tools to improve CHO cell phenotypes**

Previously in our laboratory, a first miRNA profiling study using TLDA array was performed to investigate the changes of miRNA expression associated with temperature reduction and cell growth decrease and a second one was carried out to identify miRNAs which changes of expression were associated with fast and slow cell proliferation.

We propose to screen these candidate miRNAs in a range of functional assays using transient transfection of mimic or inhibitor molecules where appropriate in order to assess their impact on important bioprocess-relevant phenotypes including cellular growth rate, maintenance of viability and recombinant protein production. The outcome from these assays would allow selection of suitable miRNAs for further investigation and prioritization on their role in CHO cells and their potential to improve CHO phenotypes.

- **To investigate the potential of the individual miR-23a~miR-27a~24-2 cluster members in improving CHO cell characteristics**

A recent study in our laboratory indicated that miR-24-2 could be a useful tool for modifying CHO cell growth. miR-24 is expressed as part of a cluster so we aim to investigate this potential in greater details as well as assessing the utility of the other cluster members miR-23a and miR-27a. We propose to screen these three miRNAs individually and simultaneously in a range of functional assays using transient transfection of mimic or inhibitor molecules and evaluate their potential in ameliorating CHO characteristics. This functional study would unravel the individual and cooperative effects of miRNAs inside the cluster and their impact on CHO phenotypes.

- **To generate CHO cell clones with improved characteristics by stable manipulation of miR-23a~miR-27a~24-2 cluster**

We aim to achieve depletion of miR-23a~miR-27~24-2 cluster and to investigate its impact on cell proliferation. We considered a multiple antisense approach (‘multi-antisense cluster) and propose to generate stable multi-antisense cluster –expressing cell lines to knockdown simultaneously the miR-23a~miR-27~24-2 cluster members.

- **To investigate the potential of miR-7 in improving CHO cell characteristics**

Previous results from our laboratory indicated that miR-7 could be a useful tool for modifying CHO cell growth and productivity. We aim to investigate whether miR-7 could be a target for engineering CHO cell lines. We propose to screen miR-7 in a range of functional assays using transient transfection of mimic or inhibitor molecules and monitor its impact on important bioprocess-relevant phenotypes including cellular growth rate, maintenance of viability and recombinant protein production.

- **To generate CHO cell clones with improved characteristics by stable manipulation of miR-7**

We propose to use an inducible system which would allow overexpression of miR-7 at the middle of the logarithmic phase to stop cell proliferation and consequently turn the cellular machinery towards production. On the other hand, we planned to use an antisense approach known as miRNA sponge to sequester miR-7 and to improve cell proliferation. The generation of stable cell lines would enable the monitoring of cell growth, viability and productivity over a longer period of time, in batch and fed-batch culture.

- **To investigate the functional role of miR-7 in CHO cells**

To understand the molecular mechanisms underlying cell growth arrest upon miR-7 induction, we aim to identify miR-7 targets using microarray approach and validate these targets through real-time PCR, 3’UTR reporter analysis and western blotting. To further understand the network of factors involved in miR-7-dependent regulation of cell proliferation, we propose to identify any changes in expression of other CHO minas subsequent to exogenous miR-7 expression.

MATERIALS AND METHODS

5 Materials and Methods

5.1 GENERAL TECHNIQUES OF CELL CULTURE

5.1.1 Ultrapure water

All solutions were made with ultrapure water. This water was purified by a reverse osmosis system (Millipore Milli-RO 10 Plus, Elgastat UHP) to a standard of 12-18MΩ/cm resistance.

5.1.2 Sterilisation

All glassware, water and thermostable solutions were autoclaved 121˚C for 20 minutes under a pressure of 1bar. Thermolabile solutions (i.e. 10% DMSO, serum) were filtered through a 0.22µm sterile filter (Millipore, millex-gv, SLGV-025BS).

5.1.3 Cell culture cabinet

Cell culture work was performed in a class II laminar air-flow (LF) cabinet (Holten). Cleaning of the LF cabinet was carried out with 70% industrial methylated spirits (IMS) before and after use. Prior to use any items in the LF cabinet, they were also sterilised by IMS. No more than one cell line was brought in the LF cabinet to avoid cross-contamination between cell lines. Before working with another cell line, a 15 min period was given to allow clearance of any possible contaminations. Weekly cleaning of LF cabinet included Virkon, a detergent solution (Virkon, Antec International; TEGO, TH. Goldschmidt Ltd.), followed by water and IMS.

5.1.4 Incubators

Adherent cells were maintained at 37C, in an atmosphere with 5% CO2 and 80% humidity. Cells in suspension were also maintained in these conditions in an ISF1-X (Climo-Shaker) Kuhner incubator with a speed at 130-170 rpm. Weekly cleaning of the incubators followed the same protocol described for the cell culture cabinet.

5.2 Subculture of cell lines

5.2.1 Anchorage-dependent culture

CHO-K1 SEAP cells were split every three days and seeded at $3x10^5$cells/ml in T-75 flask with vented cap. Culture medium consisted of ATCC medium, (DMEM/F-12 Ham containing glutamine and sodium pyruvate; Sigma) supplemented with 5% fetal bovine serum (FBS) (Sigma). Every passage, cells were washed with 3ml PBS and detached using 3ml of pre-warmed trypsin/EDTA (TV). Cells were incubated with TV for five minutes until detachment from the treated flask was observed. 10ml of ATCC medium supplemented with serum were added to the flask to inactivate TV. Cells were spun down at 1000 rpm for 5 min, supernatant was removed and pellet was resuspended with 10ml fresh medium to seed a new flask.

5.2.2 Suspension culture

Suspension-adapted CHO-K1 SEAP cells were passaged every three days and seeded at $2x10^5$cells/ml in 30ml spin tubes (CultiFlask, Sartorius) or 250 mL spinner flasks vented cap. Cells were maintained at 170rpm on spinner platform at 37°C, supplemented with 5% CO_2. Cells were spun down at 1000 rpm for 5 min, supernatant was removed and pellet was resuspended with 10ml fresh medium to seed a new flask. Cells were adapted to serum-free medium in CHO-S-SMF II (Life technologies) and HyClone® (Thermo SCIENTIFIC) media. CHO-S-SMF II is a complete, serum-free

and low protein (<100µg/ml) cell culture medium applied for recombinant protein production in CHO cells. HyClone® is a defined serum-free and protein-free medium, designed for high cell yield and recombinant protein production. For fed-batch culture, CHO CD EfficientFeed™ A was added at 15% of the final volume at day 0 and at 10% of the final volume every 3 days for 13 days. Cells were maintained in the same conditions described for the batch culture but the speed was reduced to 130rpm.

5.2.3 Cell counting and viability determination

5.2.3.1.1 Trypan blue method

Trypan blue is a dye exclusion technique that penetrates and stained dead cells through their damage membrane. This dye is excluded from alive cells which still have an intact membrane. Equal amount of cells and trypan blue were mixed to a final volume of 100 µl and 10µl of this mixture was transferred to a hemocytometer (Neubauer) covered whith a coverslip. The number of cells was evaluated by the cell count average of four grids in the hemocytometer. This number was multiplied by 10^4, which is the volume of the grid and by the dilution factor to get the number of cells/ml in the original sample.

5.2.3.1.2 Cedex Automated Cell Counter

The Cedex Automated Cell Counter (Roche innovatis AG) is an automated cell counting system based on the Trypan Blue exclusion method for determining cell density, cell viability and cell size. This counter is more accurate and precise than the manual count and allows the visualisation of viable, dead cells and aggregates.

5.2.3.1.3 Flow cytometry

Guava Viacount® reagent (Merck-Millipore) distinguishes viable and non-viable cells based on differential permeability of two DNA-binding dyes. The membrane permeant-dye (LDS-751) stains all nucleated cells, leaving nuclear debris unstained. The

membrane impermeant-dye (propidium iodide) stains only damaged cells thus only apoptotic and dying cells are detected. This combination of dyes enables the Guava ViaCount Assay to distinguish viable, apoptotic, and dead cells. Cells were diluted in Guava Viacount® reagent at appropriate concentration and cell counting was performed through Guava EasyCyte flow cytometry system.

5.2.4 Cell freezing

Cells were harvested at the middle of the exponential phase of growth and resuspended in fresh medium few hours prior cryopreservation. Cells were counted, spun down at 1000 rpm for 5 min and resuspended with pre-chilled mixture of 1ml of ATCC/50% FBS and 1ml of 10% filtered cryo-protective agent dimethyl sulfoxide (DMSO). DMSO was added slowly and dropwise to avoid cell membrane damage. This mixture was transferred to a cryovial and was stored at -20°C for one hour, -80°C overnight and placed into liquid nitrogen at -196°C.

5.2.5 Cell thawing

5ml of pre-warmed ATCC + 5%FBS was added quickly to the frozen cells in cryovial to avoid cell toxicity by DMSO. Cells were spun down at 1000 rpm for 5 min. Pellet was resuspended with fresh medium (ATCC + 5%FBS or serum-free medium) and cell counting was carried out to evaluate cell viability. Cells were transferred in an appropriate cell culture vessel and incubated at 37°C for 12 hours. Cells were spun down again and resuspended with fresh medium to eliminate any residual traces of DMSO.

5.2.6 Cell cycle analysis

Cells were washed in 1X PBS, fixed with 200µl ice-cold 70% ethanol and refrigerated for 12hours prior to staining. After overnight incubation at 4°C, the cell pellet was washed in 1X PBS, resuspended in 200µl Guava Cell Cycle reagent containing

propidium iodide (Merck-Millipore) and incubated in the dark at 37˚C for 15min before analysis with a Guava Easycyte96 (Merck-Millipore). For each step, centrifugation was performed at 1000 rpm for 5min at room temperature. The data from the FCS files were analysed using MutliCycle™ DNA analysis in the FCS Express 4 flow cytometry software (De Novo software).

5.2.7 Apoptosis analysis

Cells were harvested and resuspended in 200 µl Guava Nexin reagent (Merck-Millipore) at 72hrs and 120hrs after transfection. Cells were incubated for 20min at room temperature before analysis with a Guava Easycyte96 (Millipore).

5.2.8 Senescence assay

Cells were fixed 72hrs after miR-7 transfection or 96hrs after BrdU addition (Sigma-Aldrich). β -galactosidase activity at pH 6 was assayed as recommended in the senescence β-galactosidase staining kit (#9860 Cell Signalling).

5.3 OTHER TECHNIQUES OF CELL CULTURE

5.3.1 Single cell clone Limited dilution

To obtain one single cell clone, serial dilution was performed in 96-well plates. Cells were cultivated in adherent format for few days until reaching 90% confluence. They were fed with fresh medium few hours before the dilution process. Cells were rinsed and detached with pre-warmed TV after 5 min incubation at 37°C. 9ml of fresh medium were added to the cells and mixing by pipetting up and down was repeated several times to increase the chance of precise dilution. An aliquot was harvested for cell counting and cells were centrifuged at 1000 rpm for 5 min. Cells were resuspended with fresh medium and cell counting was performed three times for accuracy. Serial dilution was carried out with pre-warmed, filtered sterilised conditioned medium taken from 48

hours after culture. Final cell concentration was 5 cells/ml and aliquots of 100µl were transferred to a 96-well plates to get approximately one clone per two wells. Cells were incubated for one week and during this period of time, plates were observed under microscope to ensure the presence of one single colony per well. The number of single cell clones per plate was estimated at around ten.

5.3.2 Single cell clone sorting

Fluorescence-activated cell sorter (FACS) can separate cells on the basis of their size and fluorescence. To increase the amount of single cell clones per plate, cell sorting was done using FACS. Cells are directed into a stream that forms droplets after a laser is directed at the stream. These droplets may contain a cell that results in fluorescence detection. Cells were sorted by rate of fluorescence, medium or high GFP percentage detected by FITC channel, in 96 well plates containing equal amount of conditioned medium and fresh ATCC + 5% FBS medium, supplemented with 50µg sterile-filtered Penicillin/Streptomycin solution (to avoid Gram-negative and Gran-positive bacterial contaminations) and 500µg/ml of G418.
FITC (fluorescein isothiocyanate) is a fluorochrome dye that absorbs ultraviolet or blue light causing molecules to become excited and emit a visible yellow-green light (excitation and emission wavelength are 494 nm and 518 nm respectively). A strict cut off was performed using unstained cells to allow the software to distinguish between GFP negative and positive cells.

5.3.3 Transfection

5.3.3.1.1 Transfection of cDNA molecules using lipid-based reagent

Cells were seeded at $1x10^6$ cells/ml in ATCC + 5% FBS medium, in 6-well plates. Before transfection, medium was replaced by fresh medium without drugs. 11µl of lipid-based transfection reagent (lipofectamine 2000) were diluted into 260µl of serum-free medium and incubated 5min at room temperature. 5µg of plasmid were diluted in

260 µl of serum-free medium and mixed gently to lipofectamine solution for 20min at room temperature. The mixture was transferred drop by drop on the adherent cells and the plate was incubated at 37°C.

5.3.3.1.2 Transfection of cDNA by electroporation

All materials used (plasmid DNA, cells, buffer, cuvettes) were incubated on ice for 30min before starting. Cells were seeded at $8x10^6$ cells/ml in 800µl chilled filtered/sterilised electroporation buffer (2mM HEPES, 15mM K^+PO_4, 1mM $MgCl_2$ and 250mM Mannitol in 50ml final volume) in eppendorf tube and 5µg of plasmid DNA was added to the tube. Appropriate volume of medium needed to resuspend cells after electroporation (5ml in spin tube or 12ml in T75 flask with 1% serum to if the original culture was in serum-free medium) was pre-warmed at 37°C during the assay. The machine was set up at a capacitance of 500µF and 200 volts. High capacitance was chosen for eukaryotic cells (> 50µF). Sample was mixed by pipetting up and down and transferred to the cuvette. After electroporation, actual voltage and time constance were recorded. Electroporated cells were suspended in warm medium by pipetting up and down few times and put in culture at 37°C.

5.3.3.1.3 Selection of transgenic clones

Medium of transfection was replaced by fresh medium 6 hours following the assay. This medium was then replaced by fresh medium supplemented with drugs for positive cell selection 48 hours after transfection. The minimum concentration to kill 90% of cells was found to be 250-350µg of hygromycin, 1000µg/mL of G418. Doxycyclin when required was added 6 hours after transfection at 10µg/mL. The surviving cells were expanded and used for single cell cloning as mentioned.

5.3.3.1.4 Tet OFF gene expression system

The first critical component of the Tet Systems is the regulatory protein, based on TetR. In the Tet-Off System, this 37-kDa protein is a fusion of amino acids 1–207 of TetR and the C-terminal 127 amino acids. of the Herpes simplex virus VP16 activation domain (AD; Triezenberg *et al.*, 1988). Addition of the VP16 domain converts the TetR from a transcriptional repressor to a transcriptional activator, and the resulting hybrid protein is known as the tetracycline-controlled transactivator (tTA). tTA is encoded by the pTet-Off regulator plasmid, which also includes a neomycin-resistance gene to permit selection of stably transfected cells.

The second critical component is the response plasmid which expresses a gene of interest (Gene X) under control of the tetracycline-response element, or TRE. TRE consists of seven direct repeats of a 42-bp sequence containing the *tetO*, located just upstream of the minimal CMV promoter (*P*minCMV). *P*minCMV lacks the strong enhancer elements normally associated with the CMV immediate early promoter. Because these enhancer elements are missing, there is extremely low background expression of Gene X from the TRE in the absence of binding by the TetR domain of tTA or the rTetR domain of rtTA. In the Tet-Off System, tTA binds the TRE and activates transcription in the absence of Tc or Dox.

5.3.3.1.5 Cell transfection with miRNAs/siRNAs

CHO-K1 SEAP cells seeded at $1x10^5$ cells/ml with a viability at minimum 90%, were transiently transfected with a total concentration of 30-100nM mimic molecules (Pre-miR, Applied Biosystems or #M-01-D, double stranded microRNA mimics, GenePharma), inhibitor molecules (Anti-miR, Applied Biosystems or #M-02-D, single stranded microRNA inhibitors) non specific controls (#M-03-D, double stranded microRNA mimic negative control, GenePharma or #M-06-D, single-stranded microRNA negative control) or siRNAs (Custom design, Integrated DNA Technologies) using SiPORT™ NeoFx™ transfection reagent (Ambion), a lipid based transfection reagent. Mimic and inhibitor molecules were diluted into 100µl of serum-

free medium. NeoFX was diluted into 100µl of serum-free medium, mix to the diluted miRNA mixture and incubated 10 min at room temperature. Once the complex formed, it was gently added to the cells in suspension cultured in a 2ml final volume reaction.

5.3.4 3'UTR cloning

RNA was extracted using TRI reagent (Sigma Aldrich) and reverse transcribed using the High-Capacity cDNA Reverse Transcription kit (#4368814, Life technologies), with oligodT or specific reverse primers. PCR amplicons from PSME3, RAD54L and SKP2 were generated using the Platinium® PCR SuperMix High Fidelity (#12532-016, Life technologies). The PCR program consisted of a denaturation step at 95°C for 2min followed by 5 cycles at 95°C for 1min, 58°C for 30sec, 72°C for 2 min and 25 cycles at 95°C for 1min, 55°C for 30sec, 72°C for 2min and 72°C for 10min.

Primers used were the following (Custom design, MWG eurofins):
Psme3 F: AAAACTCGAGAATCAGTATGTCACCCTACA
Psme3 R: AAAAGAATTCGCAGCTTTAGAAAGAGGTC
Rad54L F: AAAACTCGAGCTTCACCTACAGCCATC
Rad54L R: AAAAGAATTCTCCTGGGCTTACCAATC
Skp2 F: AAAACTCGAGCCAGCTGTGTATGAAGTG
Skp2 R: AAAAGAATTCTTGTTCTTCAAAATCAAGT

The PCR products were restriction enzyme digested and inserted between *Xho*I and *EcoR*I sites in the CMV-d2GFP-XE vector (modified vector derived from pcDNA5-CMV-d2eGFP vector, a kind gift from the Sharp lab, MIT). Ligation was performed using Rapid DNA Ligation kit (#11635379001, Roche) at 16°C for 30min.

5.3.5 Evaluation of GFP expression

GFP expression was assessed by Guava EasyCyte flow cytometry system using Guava Express Plus software. Forward scatter gating as well as % fluorescence (log) gating

was fixed at 550-600volts depending on the assay. The data acquired was based on these settings and always maintained for the entire experiment.

5.4 MOLECULAR BIOLOGY TECHNIQUES

5.4.1 RNA extraction using miRVana kit

RNA was isolated from CHO cells using mirVana™miRNA Isolation Kit (Ambion) for total RNA extraction. Cells were spun down at 1000 rpm for 5 min and resuspended in 300-600µl of lysis buffer, depending on the cell density. Cells were disrupted after pipetting up and down. Organic extraction was done by adding 1/10 volume of miRNA Homogenate Additive to the cells followed by 10 min of incubation on ice. Addition of 300-600 µl of Acid-Phenol:Chloroforme to the lysate, vortex step and centrifugation for 5 min at maximum speed, led to RNA extraction. The upper phase (aqueous phase) was removed and 1.25 volumes 100% ethanol kept at room temperature was added to this phase. Lysate/ethanol mixture was applied to a filter cartridge provided in the kit and centrifuged at maximum speed for 15 seconds. Flow-through was discarded and filter was washed once with 700µl of Wash Solution 1 and twice with 500µl of Wash Solution 2/3. A quick spin at maximum speed was applied between each wash steps and flow-through was discarded. Column was spun down 1 min to remove residual fluids from washing steps. Filter cartridge was transferred to a new collection tube and RNA was eluted by applying 100µl of pre-heated (95°C) Elution Solution to the centre of filter and column was spun down 30 sec at maximum speed to recover RNA.

5.4.2 RNA extraction using Tri Reagent

Tri Reagent® is a mixture of guanidine thiocyanate and phenol in a monophase solution which dissolves DNA, RNA, and protein on homogenization or lysis of tissue sample. 1ml is sufficient to lyse 5-10x10^6cells/ml. 200µl of chloroform were added to the lysis to separate DNA, RNA and proteins into 3 phases: an aqueous phase (RNA), the interphase (DNA), and an organic phase (proteins). RNA was then precipitated by

addition of 500µl ispropanol, wash with 500µl of 75% ethanol and after centrifugation the pellet was briefly air-dried under a vacuum and resuspended in appropriate volume (generally 20µl) in nuclease-free water.

5.4.3 RNA and DNA concentration evaluation

Concentration of extracted RNA was measured by NanoDrop 2000 (Thermo scientific), a spectrophotometer for nucleic acid and protein quantitation. A sample volume of 1.5µl was applied to the pedestal of the NanoDrop. A column is formed between the pedestal and the arm of the instrument allowing measurement of nucleic acid at absorbance 260nm and sample purity at 260/280nm.

5.4.4 Reverse transcription

RNA was reverse transcribed into cDNA using High Capacity cDNA reverse transcription kit. 10µl of master mix, containing 10x RT Buffer, 25xdNTP Mix (100mM), 10x Random primers, 1µl of Multiscribe™ Reverse Transcriptase (50U/µl) and 1µl of RNase Inhibitor, was added to 2µg of RNA in 10µl volume. An appropriate volume of nuclease free water was added to have a final volume of 20µl. Tubes were spun down briefly and loaded into the thermal cycler. Conditions of thermal cycler consisted in four steps. Step one was run at 25°C for 10 min, step 2 at 37°C for 120 min, step 3 at 85°C for 5min and temperature was hold at 4°C after the end of the reverse transcription cycle.

5.4.5 Polymerase Chain Reaction

DNA samples were amplified using Platinium® PCR SuperMix High Fidelity kit, a mixture of Taq DNA polymerase and proofreading polymerase Pyroccocus species GB-D (3’ to 5’ exonuclease activity), dNTPs, salts and magnesium. The volume reaction was set up at 50µl, containing 45µl of SuperMix High Fidelity solution, 5µl of primer at concentration of 100nM and DNA at a concentration of 1 to 200ng. For amplification,

30 cycles of PCR were performed with three different steps for each cycle. Denaturation step was run at 95°C for 30 sec, annealing step at 55-60°C for 30sec and extension step at 68-72°C for 1min.

5.4.6 PCR purification

QIAquick PCR kit (QIAgen) was used to purify amplicon products up to 10µg from PCR reaction. In a microcentrifuge tube, five volumes of Buffer PB was added to 1 volume of PCR product and solution was mixed. Then solution was transferred to a column in a microcentrifuge tube and vaccum was applied to allow fluid to go through the column. 750µl of Buffer PE was transferred to the column, vaccum was applied and flow-through was discarded. QIAquick column was spun down 1min to remove any residual fluid and placed into a new microcentrifuge tube. DNA elution was performed by appling 50µl of EB buffer to the centre of the column. The column was let 1 min at room temperature and spun down at maximum speed for 1 min.

5.4.7 Agarose gel

To check the size of DNA samples, agarose gel was performed at different concentrations, between 0.8% for large DNA fragment (5-10kb) and 2% for small DNA fragment (0.2-1kb). Agarose powder was diluted into TAE 1X buffer (made from TAE 50X buffer consisting of 242g if Tris base, 57.1ml of glacial acid and 100ml of 0.5M EDTA in final volume of 1L, pH 8.5) in a 50ml volume. The solution was warmed up for 1min 20sec in a microwave to dissolve the agarose and ethidium bromide at 0.5µg/ml (EtBR) was added to it. This mixture was incubated at room temperature for 30min to set up the gel, transferred to a small gel tank (8-10cm) and run at 90 volts for 30min. DNA samples were diluted at a concentration minimum of 20ng and mixed with 10x loading buffer (made from 25mg of blue bromophenol, 30% of glycerol, 25mg of xilene cyanol and water in a final volume of 6.25ml).

5.4.8 Quantitative Polymerase Chain Reaction (qPCR) using SYBR green method

Fast SYBR Green I dye was used to detect PCR product expression by binding to all double-stranded DNAs formed during the cycling of the PCR reaction. Fluorescent intensity of the intercalant dye is proportional to the amount of PCR product amplified. 10µl of 2x Fast SYBR® Green Master mix were added to a combination of reverse and forward primers (concentration minimal 200nM for each primer), to cDNA (concentration of 20ng) and nuclease-free water in 20µl final volume reaction. Reaction was run for 40 cycles in the thermal cycler using 7500 fast program. For each cycle, the first step of AmpliTaq Fast DNA Polymerase (the activation) was run at 95°C for 20 sec, denaturation was run at 95°C for 1 sec and the last step corresponding to the annealing/extension step was set up at 60°C for 20sec.

5.4.9 MicroRNAs Reverse transcription and real time PCR using TaqMan

5.4.9.1.1 Reverse transcription

Following total RNA extraction using mirVana™miRNA Isolation Kit (Ambion) or Tri regent (Sigma), RNA was quantified by NanoDrop spectrophotometer. RNA was diluted in nuclease-free water at 2ng for the RT reaction. A 10µl reaction solution including 0.15µl of 100mM of dNTPs, 10x reverse transcription buffer, 1µl of Multiscribe™ Reverse Transcriptase (50U/µl), 0.19µl of RNase inhibitor (20U/µl) was added to 5µl of RNA. Solution was mixed gently and spun down briefly. Tubes were transferred to the thermal cycler and program was set up for one cycle, with the first step at 16°C for 30min, the second step at 42°C for 30min and 85°C for 5min.

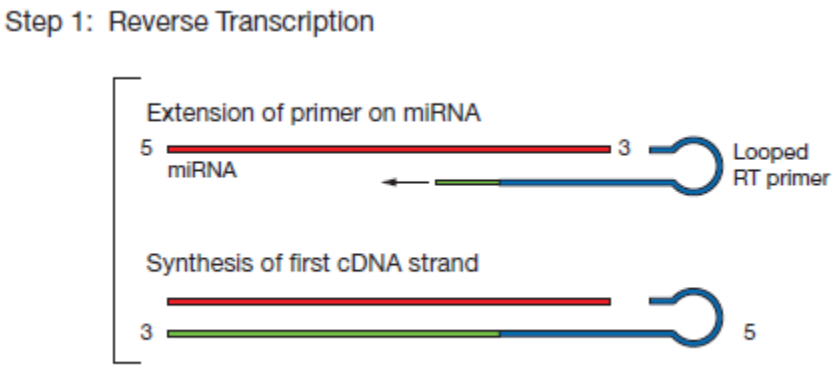

Step 1: **Stem-loop RT**. Stemloop RT primers are annealed to miRNA targets and extended in the presence of reverse transcriptase.

5.4.9.1.2 Real-time PCR

Real-time PCR reaction master mix was done in a 18.67µl reaction with TaqMan® Small RNA Assay 20x, TaqMan® Universal PCR Master Mix 2x and 7.67µl of nuclease-free water and added to 1.33µl of RT reaction sample to get a final volume reaction of 20µl. Solution was mixed by pipetting up and down in a 96-well plate. Plate was placed into thermal cycler and run mode was the standard one. Thermal cycling conditions were set up at 95°C for 10min in the first step followed by 95°C for 15 sec in the second step and 40 cycles at 95°C for 15 sec for the denaturation step and 60°C for 60 sec for the annealing/extension step.

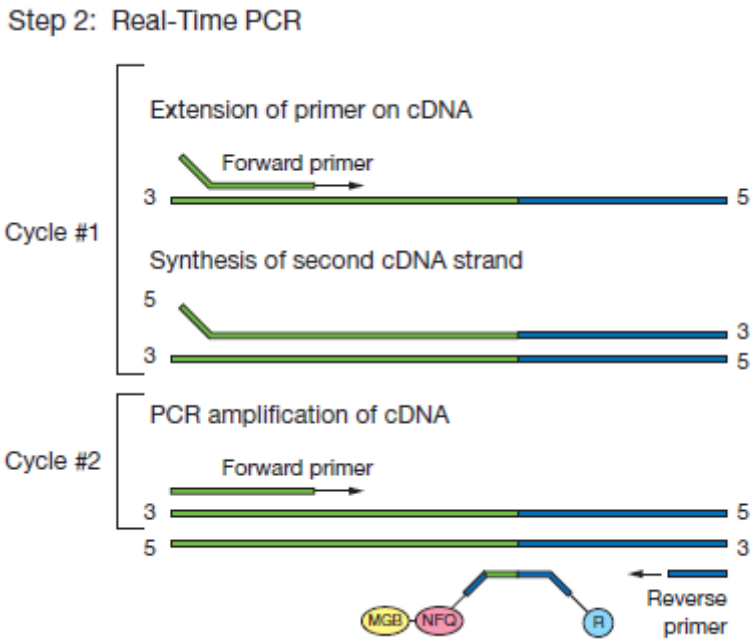

Step 2: Real-time PCR. miRNA-specific forward primer, TaqMan® probe, and reverse primer are used for PCR reactions. Quantitation of miRNAs is estimated based on measured CT values. MGB: minor groove binder; NFQ: non-fluorescent quencher; R: reporter dye (FAM™ dye).

5.4.9.1.3 5'nuclease process

During the amplification of cDNA, the TaqMan® MGB probe anneals specifically to a complementary sequence between the forward and reverse primer sites. The MGB probe at the 3'end of the probe increases specificity through the increase of melting temperature without changes in the probe length (Afonina, et al. 1997, Kutyavin, et al. 1997).

When the probe is intact, the proximity of the reporter dye to the quencher dye results in suppression of the reporter fluorescence, primarily by Förster-type energy transfer (Lakowicz and Maliwal 1983). The lack of fluorescence of the quencher allows a more accurate measurement of the reporter dye. Following recognition of the probe by the DNA polymerase, cleavage occurs and prevents the interaction between the reporter dye and the quencher dye. Consequently signal fluorescence of the reporter is released.

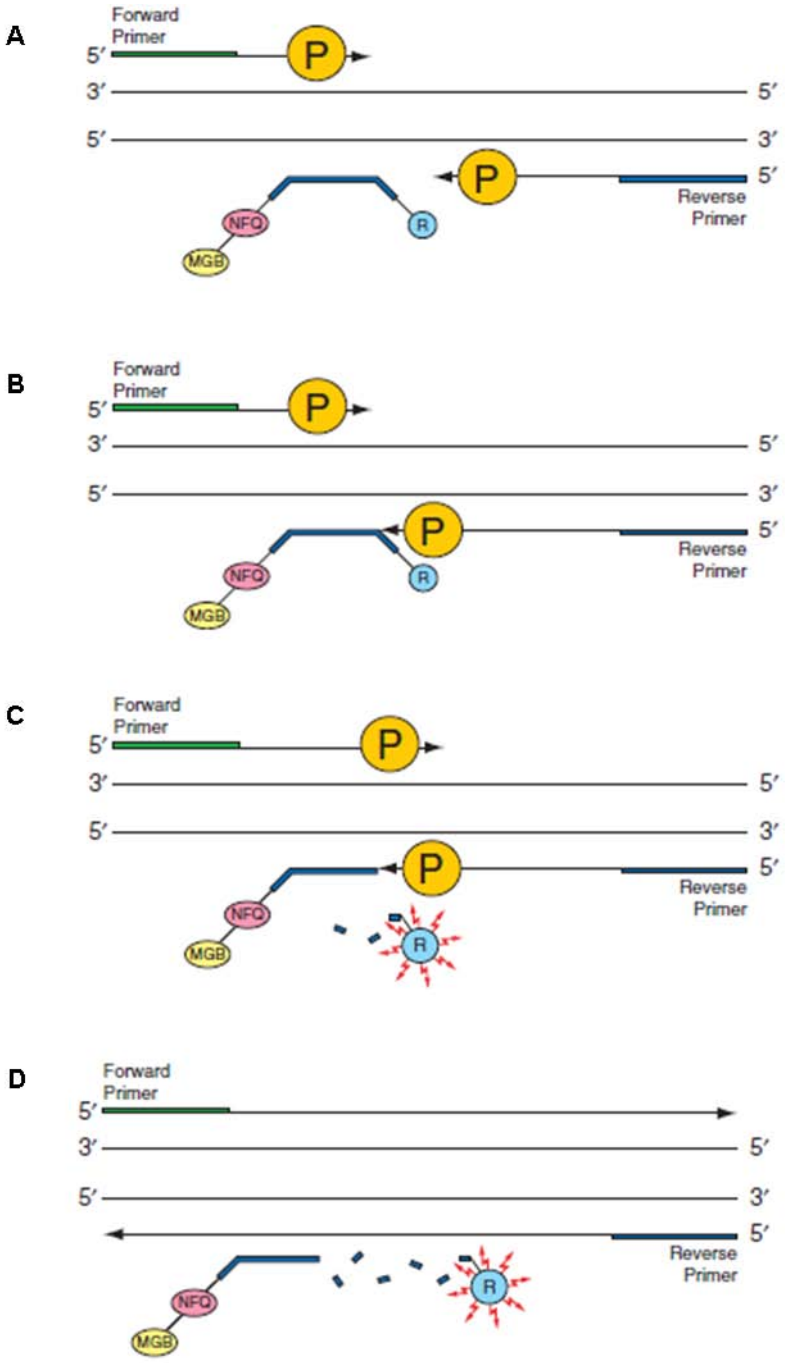

Figure 5.4.9.1.3: Schematic of 5' nuclease assay process.

A: Polymeriszation; B: Strand displacement; C: Cleavage; D: Completion of pol ymerization**.**

5.4.10 Bioanalyzer

Extracted RNA samples quality was checked using Agilent RNA 6000 Nano kit bioanalyzer (Agilent) before microarray assay. Denaturation of samples was performed at 70°C for 2 min and samples were transferred on ice. 9µl of loading gel dye was transferred to the chip in three different wells. 5µl of Agilent marker was loaded into all 12 wells and in the ladder well followed by tranfer of 1µl of ladder and 1µl of samples in the same wells to have a final volume of 6µl in each well of the chip. Chip was placed on a IKA vortex for 1 min at 2400 rpm and transferred to the bionalyser within 5 min to be analysed.

5.4.11 CHO-specific oligonucleotide arrays

Cells were seeded at $1x10^5$ cells/ml and transfected with either 50nM of non-specific control (PM-Neg, Ambion) or miR-7 mimic (PM-7) in a 2ml serum-free suspension culture. Total RNA extraction was performed 24 hours after transfection using the mirVana miRNA Isolation Kit (#AM1560; Life technologies). RNA quality from biological triplicates was checked using an Agilent 2100 Bioanalyzer (Agilent Technlogies). 100 ng of total RNA from each sample underwent cDNA synthesis, followed by cleanup, overnight IVT amplification and labeling using the GeneChip 3' IVT Express Kit (#901229, Affymetrix) according to manufacturer's instructions. cRNA cleanup was carried out using the GeneChip Sample Cleanup Module (#900371, Affymetrix) according to manufacturer's instructions. The custom CHO oligonucleotide WyeHamster3a microarray (Affymetrix) used in these analyses contains a total of 19,809 CHO-specific transcripts, combining library-derived CHO and publicly-available hamster sequences.

5.4.12 Data processing and analysis

Microarray data were pre-processed as described in (Clarke, et al. 2011). Differential expression analysis was carried out using the R package, linear models for microarray

data LIMMA (Wettenhall and Smyth 2004). Genes were considered to be differentially expressed upon observation of a 1.2 fold change in either direction along with a Bonferroni adjusted p-value <0.05. The functional relevance of those differentially expressed genes was determined using the PANTHER (Protein Analysis through Evolutionary Relationships) Classification System.

5.4.13 Real-time PCR of miRNAs using TaqMan Low Density Array

TaqMan Low Density Array is based on the TaqMan PCRmethod in an array format which contains probes for human miRNA signatures. The protocol for the reverse transcription used the High Capacity cDNA reverse transcription (described in the materials and methods). The primers used are the Megaplex™ RT Primers-predefined pools comprising 381 RT primers which bind specifically to the miRNA probes in the 381 wells of the card.

Following reverse transcription, 30-1000ng of cDNA diluted in a final volume of 50 µl is mixed to 50µl of TaqMan® Universal PCR master mix. The 100µl of the mixture is then loaded into the fill reservoir of a 384-well TaqMan array card and two steps of centrifugation at 1200rpm for 1min were performed to ensure complete filling of the card. The TaqMan cards were sealed and miRNA expression was analysed using the ΔΔCt PCR quantification in the Applied biosystems 7900HT Fast Real-Time PCR System. The PCR program consisted in the activation of the AmpliTaq Gold® enzyme for 10min at 95°C for, followed by 40 cycles at 95°C for 15 sec for the denaturation step and 60°C for 60 sec for the annealing/extension step.

5.4.14 Cloning methods

5.4.14.1.1 Oligonucleotide annealing

For annealing of oligonucleotides, 1.5µl of each oligonucleotide was mixed to 5µl of 10x annealing buffer (1M Tris pH 8, 0.5M EDTA pH 8, 2.5M NaCl) and 42µl of nuclease free water. This solution was incubated at 97°C for 5min in heater block.

Heater block was switched off and samples were left in the block to allow the temperature to gently drop for 3 hours to approximately 46°C. Then annealed oligonucleotides were kept on ice for 5 min and kinase treatment was performed. 0.5µl of annealed oligonucleotides were added to 2µl of T4 kinase buffer (ROCHE), 0.4µl of 50Mm ATP at pH 7.5, 17µl of nuclease free water and 0.4µl of T4 polynucleotide Kinase at 10U/µl (ROCHE). The solution was incubated at 37°C for 30min. To stop the reaction, samples were transferred on ice.

5.4.14.1.2 Bacterial Transformation for cloning

One Shot® Max Efficiency® DH5α™-T1® competent cells were transformed using appropriate plasmid-derived vectors. One vial of 50µl DH5α competent cells was thawed for each transformation reaction and 1µl of ligation reaction was added to the cells. Mixture was incubated on ice for 30min followed by a heat shock step at exactly 42°C in water bath for 30 sec. Vial was removed and placed on ice for few minutes. 250µl of pre-warmed S.O.C medium (rich medium) was added to the vial and incubated 1hour at 37°C in a shaking incubator at 225 rpm. Vial was spun down at 1500 rpm for 5min to remove almost all supernatant and 20-30µl was left to be spread into a plate containing LB agar with appropriate antibiotic for clone selection. Plate were incubated at 37°C overnight, transformation efficiency was evaluated by the number of colonies present in the control provided by the kit , pUC19 DNA.

5.4.14.1.3 Purification of plasmid DNA: Miniprep

QIAprep® Spin Miniprep Kit was used to purify up to 20µg of plasmid after transformation. A single colony was harvested from the plate and inoculated into a 5ml LB medium culture supplemented with appropriate antibiotic concentration at 37°C in a shaking incubator. Bacterial Culture was spun down for 5 min at 3000 rpm, pellet was resuspended with 250µl of P1 buffer and transferred to a microcentrifuge tube. 250µl of lysis buffer P2 was added and tube was inverted several times to allow cell lysis. Then 350µl of buffer P3 was added to enhance DNA precipitation and tube was inverted several times and spun down at maximum speed (13,000 rpm) for 10 min. Supernatant

was applied to a QIAprep spin column and vacuum was applied to draw the solution through the column. Column was washed with 500µl of Buffer PB to remove any traces of nuclease activity if using certain strains of bacteria followed by addition of 700µl Buffer PE. After this step, column was centrifuged at maximum speed for 1 min to avoid any residual ethanol from Buffer PE. DNA was eluted by applying 50µl of EB buffer at pH 8, in the centre of the filter. Column was left 1 min at room temperature followed by centrifuge step for 1 min at maximum speed.

5.4.14.1.4 Purification of plasmid DNA: Maxiprep

QIAGEN Plasmid Maxi kit was used to purify up to 500µg of plasmid after transformation.

A single colony was harvested from the plate and inoculated into a 5ml LB medium culture supplemented with appropriate antibiotic concentration at 37°C in a shaking incubator for 8 hours. Bacterial Culture was then transferred to a 250ml culture supplemented with appropriate antibiotic concentration and incubated overnight at 37°C. Culture was harvested and spun down at 6000x*g* for15 min at 4°C. Pellet was resuspended with 10mL of Buffer P1, 10mL of buffer P2 for lysis and tube was mixed by inversion and incubated at room temperature for 5 min. 10mL of pre-chilled Buffer P3 (neutralization buffer) was added to the mixture and tube was mixed vigourously. Buffer P3 enhanced DNA precipitation. Lysate was transferred to a QIAfilter cartridge and incubated for 10 min at room temperature. Plunger was inserted to the cartridge to allow lysate to be filtered. A QIAGEN-tip 500 was equilibrated using 10mL of Buffer QBT that contains detergent leading to reduction in surface tension and fluid to enter through the filter. Cartridge was washed twice with 30 mL of Buffer QC to remove any possible contaminants. DNA was eluted with 15mL of buffer QN, precipitated with 10.5mL of room temperature isopropanol. Tube was mixed and spun down at 15,000 x *g* for 30min at 4°C. Pellet was washed with 5ml 70% ethanol to remove precipitated salts and centrifuges at 15,000 x *g* for 10min. Pellet was air-dried 5-10 min and redissolved in TE buffer (10mM Tris-Cl, pH 8).

5.4.14.1.5 Restriction Enzymatic digestion

For cloning protocol, plasmid DNA at 2µg was doubled digested with appropriate enzymes in 10x buffer and 100x BSA if required in a 60µl final volume reaction. Incubation was performed for 1h at 37°C for simple digestion or several hours if sequential digestion was required.

5.4.14.1.6 Alkaline phosphatase treatment

Alakline phosphatase (New England BioLabs) catalyses the removal of 5'-phosphate groups from DNA or RNA and prevents the CIP-treated DNA fragments to self-ligate because of the lack of 5'-phosphoryl termini groups. This treatment increases the efficiency during cloning assay. 2µg of digested plasmid were transferred to a tube containing 5µl of 10x CIP buffer, CIP enzyme (20U/µl) in a final volume reaction of 50µl. Tube was incubated at 37°C for 1h.

5.4.14.1.7 DNA polymerase I, large (Klenow) Fragment treatment

DNA polymerase I, large (Klenow) Fragment is a proteolytic product of *E.coli* DNA Polymerase I which retains polymerisation and 3'→5' exonuclease activity, but has lost 5'→3' exonuclease activity. A 30µl reaction was set up using 25µl of digested DNA, 10x NEB2 buffer, 33µM of dNTP and 3x Klenow enzyme (5U/µl). Incubation was performed at 25°C for 15 min. Reaction was stopped by adding EDAT at 10Mm followed by incubation at 75°C for 20 min.

5.4.14.1.8 DNA Ligation

Double digested DNA with appropriate enzymes were incubated with T4 DNA ligase and 1x ligation buffer (Roche), at 16°C for 4 hours or overnight in ice/water. T4 DNA

ligase catalyses the formation of phosphodiester bonds between 3'OH and 5'Phosphate ends in double-stranded DNA with sticky or blunt ends.

5.5 Protein assays

5.5.1 SEAP Assay

The enzymatic assay for quantification of SEAP protein was adapted from the method reported previously by Berger and co-workers (Lipscomb, et al. 2005, Berger, et al. 1988). Conditioned medium was collected from cells and was spun down at 13000rpm for 5min. 50µl of cell-free conditioned medium were transferred to individual wells of a 96-well flat bottom plate. 50µl of 2x SEAP reaction buffer (solution stock contains 10.50 g diethanolamine (100%), 50 µl of 1 M MgCl, and 226 mg of L-homoarginine in a total volume of 50 mL) was added to each sample. Plates were incubated for 10 min at 37°C and then 10 µl of substrate solution (158 mg of p-nitrophenolphosphate from Sigma, St. Louis,in 5 mL of 1x SEAP reaction buffer, made fresh for each use) was then added to each well. The change in absorbance per minute (OD 405/min) of each well was monitored by a microplate reader. The change in absorbance per minute was considered as indicator of amount of SEAP present in the sample.

5.5.2 Enzyme-linked immunosorbent (ELISA) assay

To quantify the recombinant Human IgG1 (rHIgG1) antibodies secreted in the culture, cell were spun down at 1000rpm for 5min and supernatant was harvested in a microcentrifuge tube. Supernatant was also spun down again at 13000 rpm for 5 min before the assay to avoid any residual cells. Immunoassay plate (Sigma) was coated using100µl/well of diluted coating antibody (goat anti-Human IgG-affinity purified), overnight at 4°C. To avoid non-specific binding, plate was blocked with 200µl/well of 1% BSA blocking solution for at least 1hour at room temperature. 100µl of supernatant was applied to the plate to allow interaction with the coating antibody. rHIgG1 antibodies were detected by addition of 100µl/well of secondary antibody, a goat anti-

Human IgG linked to horse radish peroxidase (HRP). Between each step of the assay, 3 to 5 washes were done using a wash solution. The enzyme substrate reaction was prepared with 100µl of 3,3',5,5'-Tetramethylbenzidine (TMB) solution. It develops a deep blue product after 15min when reacted with HRP conjugates in ELISA and it is stopped by a H_3P0_4 solution at 2M (100µl/well) which gives a yellow colour. A standard curve with purified rHIgG1 was used to quantify the amount of rHIgG1 present in samples. Absorbance was measured with a reader plate at 450nm.

5.5.3 Western blotting

5.5.3.1.1 Sample preparation

Proteins for analysis by Western blotting were resolved using SDS-polyacrylamide gel electrophoresis (SDS-PAGE). Lysis buffer containing urea was added to cell pellet. Lysis was carried out over twenty min on ice and following vortexing, the lysate was spun at 4˚C for 15 min at maximum speed to remove any insoluble debris. The protein was quantified using the Bradford approach (Bio-Rad; 500-0006). The protein samples were diluted in 2xLaemlli buffer (which contains loading dye, Sigma-Aldrich S#3401) and appropriate volumes of lysis buffer. Before loading into the gel, samples were boiled for 5min and cooled on ice.

5.5.3.1.2 SDS-polyacrylamide gel electrophoresis

5-20µg of protein samples and the molecular weight marker (New England Biolabs) were loaded onto 4–12% NuPAGE Bis Tris precast gradient gels (Life technologies). Electrophoretic transfer, blocking and development of western blots was carried out as described previously. Membranes were probed with the appropriate primary antibodies (anti-PSME3 #ab97576 Abcam, anti-SKP2 #ab68455 Abcam, anti-CMYC #ab31426 Abcam, anti-p53, #M 7001Dako, anti-pAKT #92715 cell signalling, anti-p27 #2552S, anti-IGF1R #3027, Cell signalling) diluted in Tris-buffered saline containing 0.1%-

Tween 20 (TBS-T). An anti-mouse GAPDH monoclonal antibody (#ab8245, Abcam) was used as an internal loading control in all experiments.

RESULTS

6 Results

6.1 Adaptation of CHO-K1 SEAP cells to serum-free medium

CHO-K1 cells were previously engineered in our laboratory to produce human secreted alkaline phosphatase (SEAP). This protein was used as a recombinant protein model in cell productivity assays. The SEAP gene was extracted from pSEAP2-control vector (Professor Martin Fussenegger, Institute for Chemical and Bioengineering, ETH Zurich) and was cloned into pcDNA3.1 (Invitrogen). The final construct was transfected into CHO-K1 cells that were previously adapted to grow in ATCC medium (DMEM / F-12 Ham containing glutamine and sodium pyruvate; Sigma) supplemented with 0.5% serum in suspension culture, in 100ml spinner flasks maintained at 37°C, on a shaker platform at 60rpm (Thesis of Dr Niraj Kumar). However, in commercial processes the cost of serum, the variation of components from batch-to-batch and the risk of viral, fungal or prion contamination have led to the adaptation of cells to serum-free culture.

To start the adaptation, cells were grown in adherent culture of ATCC (DMEM/F12-HAM) medium, supplemented with 0.5% fetal bovine serum (FBS), at 37°C and 5% CO_2. During the first two weeks, cells were not attached but were still alive so they were transferred to suspension culture in disposable 50ml shaker flasks, at 60 rpm. Three serum-free media (SFM) were tested, CHO-S-SFM II (Invitrogen), HyClone SFM4CHO (Thermo Scientific) and CD-OptiCHO (Invitrogen). Although some cells survived in CHO-S-SFM II and HyClone SFM4CHO, cell viability was low. It was likely due to the stress caused by the complete serum-free environment. In addition, the agitation speed used was probably too low causing cells to aggregate. To optimise the speed of agitation, cells were transferred to disposable 5ml spin flasks with vented caps and supplemented with 0.5% FBS. When the rotation speed was set at 100 rpm, the cells grew but they still aggregated. The speed was increased to 130 rpm for one week. At this stage, 2ml of cells were transferred to a tube supplemented with 3ml of fresh medium still containing 0.5% FBS. The speed was increased to 170 rpm for another week. Although half of cells were dead at this stage, the remaining ones were still

dividing. After four passages, cells became healthier and were placed in a disposable 50ml shaker flask with vented lid instead of glass spinner flaks. The glass spinner flasks are time-consuming to prepare. In addition, they are not convenient for routine cell culture work as they do not have a vented cap to allow mixed gas exchange. Following adaptation to high speed agitation in suspension, the process of serum elimination was initiated. A sequential adaptation method was applied to allow cells to recover gently from stress due to serum withdrawal. The principle of this method is to use different ratios of media. Cells are supplemented with a combination of serum and serum-free media until completely adapted to a serum-free environment. Cell culture was performed in 5ml culture, in spin tubes, at 170 rpm, in 25% ATCC media supplemented with 0.5% FBS and 75% serum-free medium. Serum concentration was reduced until the ratio was at 10%/90% between ATCC medium (0.5% FBS) and serum-free medium. Cells were transferred to serum-free culture in CHO-S-SFMII and HyClone SFM4CHO medium for six days. Cells growing in CHO-S-SFMII reached a high cell density at day 2 ($4.93x10^5$ cells/ml) and grew rapidly until day 5 ($48.4x10^5$ cells/ml) (**Figure 6.1.A**). At this time point, cell viability dropped dramatically, likely due to the lack of nutrients that were consumed quickly at the earlier time points as well as the waste accumulation. Cells in HyClone SFM4CHO showed a slower growth from day 2 ($2.77x10^5$ cells/ml) to day 5 ($33.73x10^5$ cells/ml) and consequently sustained a higher cell viability (**Figure 6.1.B**). We choose to prioritise high cell density in a short time therefore CHO-S-SFMII was selected for our cell culture work.

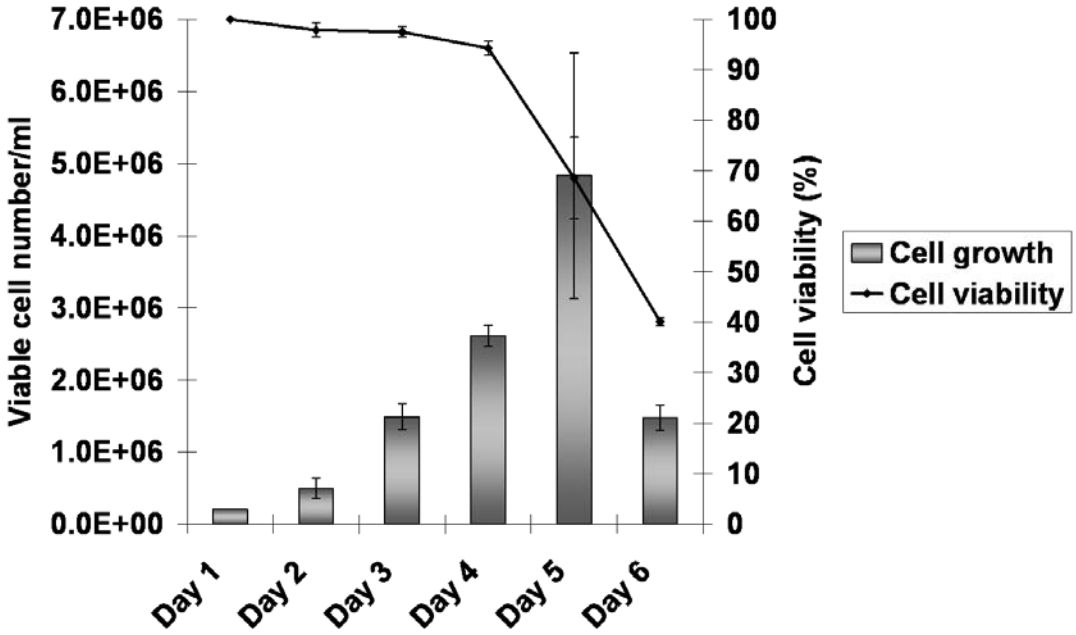

Figure 6.1.A: CHO-K1 SEAP cell growth and viability in CHO-S-SFMII serum-free medium.

Cell growth and viability were assessed in CHO-K1 SEAP cells cultured in CHO-S-SFMII serum-free media in 50ml culture, in shaker flasks. Cells were seeded at $2x10^5$ cells/ml and samples were harvested every day, for six days. Cell number and viability were evaluated manually by exclusion method with trypan blue. Bars represent standard deviations of three biological samples.

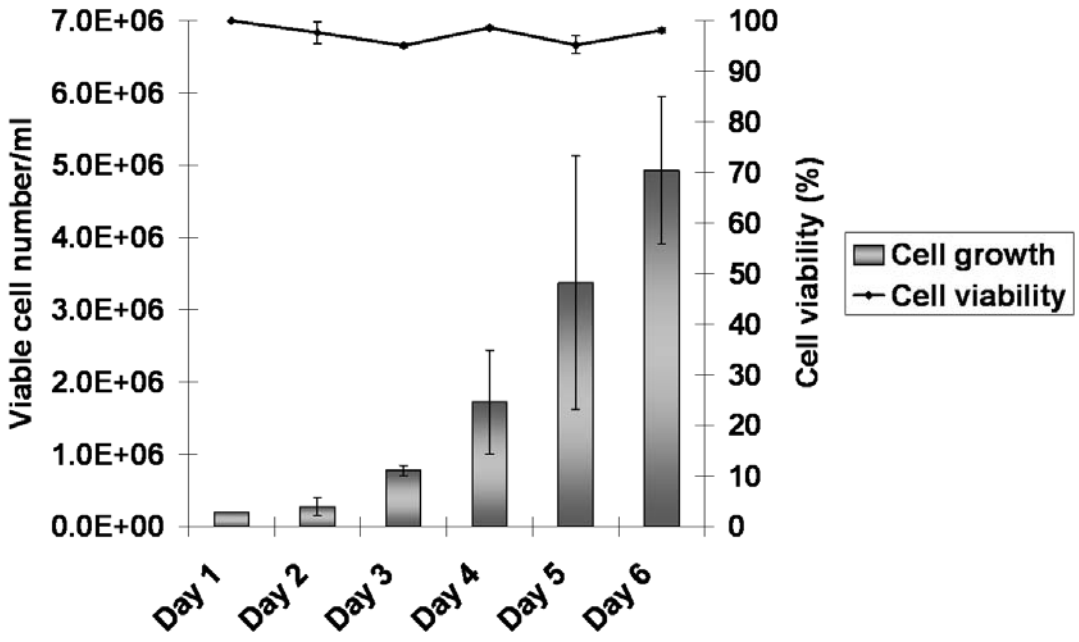

Figure 6.1.B: CHO-K1 SEAP cell growth and viability in HyClone SFM4CHO medium.

Cell growth and viability were assessed in CHO-K1 SEAP cells cultured in HyClone media in 50ml culture, in shaker flasks. Cells were seeded at $2x10^5$ cells/ml and samples were harvested every day, for six days. Cell count and viability were performed manually by exclusion method with trypan blue. Bars represent standard deviations of biological triplicates.

6.2 Functional validation of miRNAs as potential candidates to improve bioprocess-relevant CHO characteristics

6.2.1 Screening of miRNAs in fast growing cells

miRNAs are involved in many cellular functions including cell proliferation, cell cycle, apoptosis, cell metabolism and signal transduction. Therefore they are attractive and potentially useful tools to manipulate important bioprocess-relevant phenotypes including cellular growth rate, maintenance of viability and recombinant protein production. Previously in our laboratory, miRNA profiling using TLDA arrays, a PCR-based technique, was performed to identify differentially expressed miRNAs following temperature-shifted culture (Gammell, et al. 2007). The aim of this study was to investigate the change of miRNA expression associated with temperature reduction and cell growth decrease. A total of 237 miRNA species were detected on TLDA cards of which 17 miRNAs were differentially expressed (Barron, et al. 2011). Although numerous studies have reported on the genes and proteins involved in the cellular response to temperature-shift, we wanted to see whether these miRNAs were responsible for the observed reduction in cellular growth after decreasing the culture temperature. Functional screening of miR-490, miR-34a, miR-34c, let-7e, miR-30e-5p**,** miR-10a and miR-29a was conducted to investigate the impact of these miRNAs on the CHO phenotypes mentioned above. Depending on the data from the profiling experiment and the established role of these miRNAs in other species, we screened for a functional impact using either a mimic or an inhibitor where appropriate (**Table 6.2.1**).

Table 6.2.1: Differentially regulated miRNAs following TS and choice of molecules (mimics or pm/inhibitors or am) for functional validation

miRNAs	TLDA array data	Mimic (pm) or inhibitor (am) molecules
miR-490	Higher expression in the middle of the logarithmic phase at 37˚C	pm-490
miR-34a	Down in TS culture	am-34a
miR-34c	Down in TS culture	am-34c
let-7e	High in TS culture	pm-let-7e
miR-30e-5p	Down in TS culture	pm-30e-5p
miR-10a	Down in TS culture	am-10a
miR-29a	Down in TS culture	am-29a

Functional analysis using mimic (pm) and inhibitor (am) molecules was conducted in a CHO-K1 cell line engineered to produce the Secreted Embryonic Alkaline Phosphatase (CHO-K1 SEAP), cultured in serum-free medium in spin flasks. If the results were promising, the experiment was repeated in recombinant human Immunoglobulin Gamma 1 (rHmIgG1) producing cell lines, CHO1.14 and CHO2B6. Pre-miRs are double-stranded molecules that mimic endogenous mature miRNAs and anti-miRs are single-stranded molecules that inhibit the mature form of endogenous miRNAs by competitively binding to them. Different controls were included in the transient transfection. Pre-miR negative (pm-neg) and anti-miR negative (am-neg) molecules are non-specific sequences that in theory should not match with any sequences in the genome. Non-transfected cells were also included as a control to ensure that cells were growing as expected. The lipid-based transfection reagent (siPORT™ *NeoFx* ™; Ambion) was also used on its own to ensure that there was no non-specific impact on cell growth and cell viability due to the nature of the assay. A siRNA against Valosin-containing protein, a housekeeping gene in CHO cells, was used as a positive control of transfection efficiency and cell death (Doolan, et al. 2010).

6.2.1.1 Screening of miR-490, miR-34a and miR-34c

6.2.1.1.1 Impact on CHO-K1 SEAP cell growth and cell viability

Non-transfected CHO-K1 SEAP cells grew normally and showed high viability (>90%) for the first two days (**Figures 6.2.1.1.A&B**). At day 4, cells reached very high density but maintained a high viability. At day 7, cell density dropped as well as the cell viability (23.34%) likely due to the nature of the batch culture. As expected cells treated with siRNA against VCP had their cell proliferation dramatically decreased and showed a high rate of cell death. Two days after transfection, only 40.76% of cells remained viable (**Figure 6.2.1.1.A**). During the culture period, non-specific impact on cell growth was observed in pre-miR negative (pm-neg) and anti-miR negative molecules (am-neg) transfected cells. The rate of viable cells in these samples was reduced between 6.40% and 6.88% at 48 hours and 96 hours following transfection. The effect of pm-neg and am-neg molecules on cell growth was not observed at day 7 and the viability of cells

treated with these molecules was higher compared to the viability of the non-transfected cells. Thus the effect of pm-neg and am-neg abated at later stages of culture.

Four days following transient up-regulation of miR-490, cell density was decreased by 1.28-fold compared to pm-neg treated cells (**Figure 6.2.1.1.B**). Transient knockdown of miR-34a and miR-34c induced a slight reduction of cell density at the same time point (1.16-fold and 1.08-fold respectively) in comparison to cells transfected with am-neg molecules.

Cell viability was improved in pm-490 and in am-34a treated cells by 9.39% and 6.45% in comparison to their controls at later stages of culture (**Figure 6.2.1.1.B**) likely due to a lower number of cells present in culture at earlier time point**.**

The impact of pm-490, am-34a and am-34c on cell proliferation and cell growth was not reproducible across repeated experiments. Thus these miRNAs were not selected as candidates for further investigation.

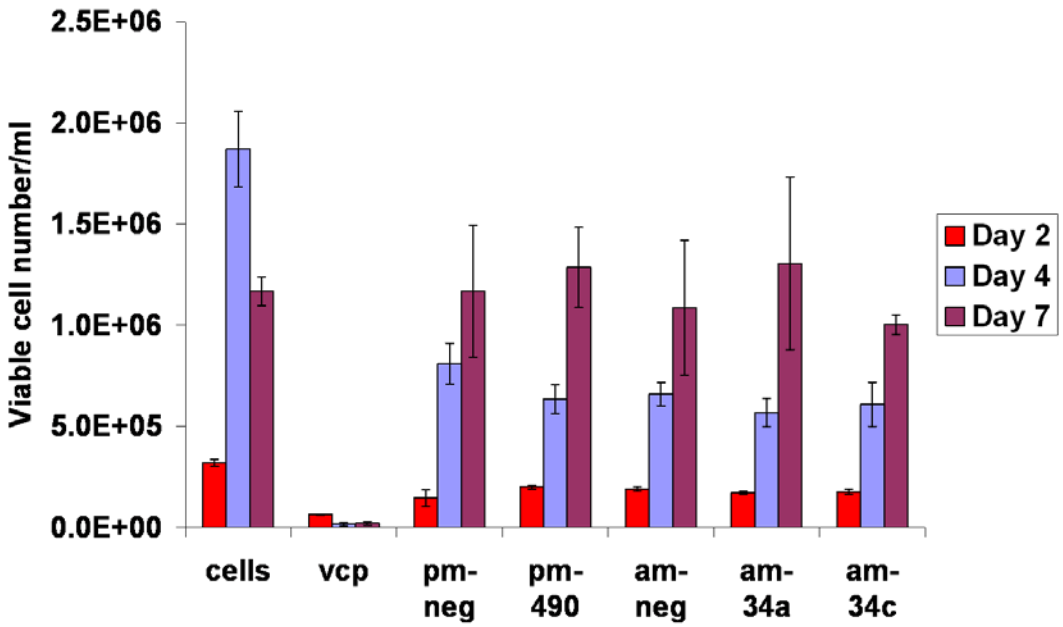

Figure 6.2.1.1.A: Impact of miR-490, miR-34a and miR-34c on CHO-K1 SEAP cell growth.

Cells were seeded at $1x10^5$cells/ml in serum-free medium prior to transfection with 50nM miRNAs. Following transfection, cells were harvested at day 2, day 4, day 7 and stained with GuavaViacount solution to monitor cell growth by Guava flow Cytometer. cells: non-transfected cells cultured at 37°C; vcp: siRNA against Valosin-Containing Protein (positive control of transfection efficiency); pm-neg: negative control for mimics; pm-490; mimic of miR-490; am-neg: negative control for inhibitors; am-34a: inhibitor of miR-34a; am-34c: inhibitor of miR-34c.

At day 2 and day 4, bars represent standard deviations of three biological replicates. At day 7, one sample was used for other assays so only two samples were kept in culture. Bars represent the high and low reading of the two remaining biological replicates. For statistical analysis a student t-test was performed to compare pm-490 with pm-neg and am-34a, am-34c with am-neg. There was no statistically significant difference in growth found in this assay.

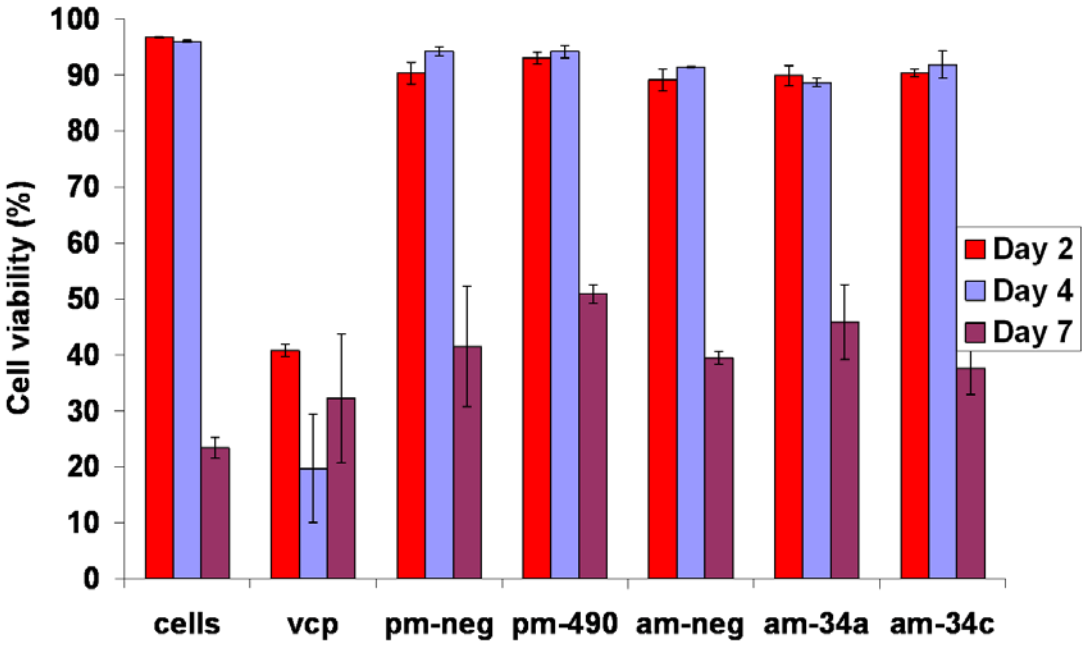

Figure 6.2.1.1.A: Impact of miR-490, miR-34a and miR-34c on CHO-K1 SEAP cell viability.

Cells were seeded at $1x10^5$cells/ml in serum-free medium prior to transfection with 50nM miRNAs. Cells were harvested at day 2, day 4, day 7 and stained with GuavaViacount solution to monitor cell viability by Guava flow Cytometer. cells: non-transfected cells cultured at 37°C; vcp: siRNA against Valosin-Containing Protein (positive control of transfection efficiency); pm-neg: negative control for mimics; pm-490; mimic of miR-490; am-neg: negative control for inhibitors; am-34a: inhibitor of miR-34a; am-34c: inhibitor of miR-34c. At day 2 and day 4, bars represent standard deviations of three biological replicates. At day 7, one sample was used for others assays so only two samples were kept in culture. Bars represent the high and low reading of the two remaining biological replicates. For statistical analysis a Student t-test was performed to compare pm-490 with pm-neg and am-34a, am-34c with am-neg. There was no statistically significant difference in viability levels found in this assay.

6.2.1.1.2 Impact on SEAP total yield and normalised productivity

To investigate the impact of miR-490, miR-34a and miR-34c on SEAP productivity, total yield (change in absorbance/min of p-nitrophenolphosphate into p-nitrophenol) and normalised productivity (change in absorbance/min/cell) were monitored at day 2, day 4 and day 7 after transfection. At 96 hours following transient up-regulation of miR-490, total yield was improved by 1.17-fold (p-value: 0.03267) in comparison to the non-specific control (**Figure 6.2.1.1.C**). However, total yield in these cells was lower than in the non-transfected cells. Transient inhibition of miR-34a and miR-34c slightly increased total yield (1.05-fold to1.15-fold). Normalised productivity was enhanced by 1.5-fold (p-value: 0.04272) after transfection of miR-490 and by 1.44-fold (p-value: 0.02047) following knockdown of miR-34a (**Figure 6.2.1.1.D**). Upon depletion of miR-34c, normalised productivity was slightly improved but it was not statistically significant. However the reproducibility of these assays showed no consistency therefore the investigation of these miRNAs was discontinued.

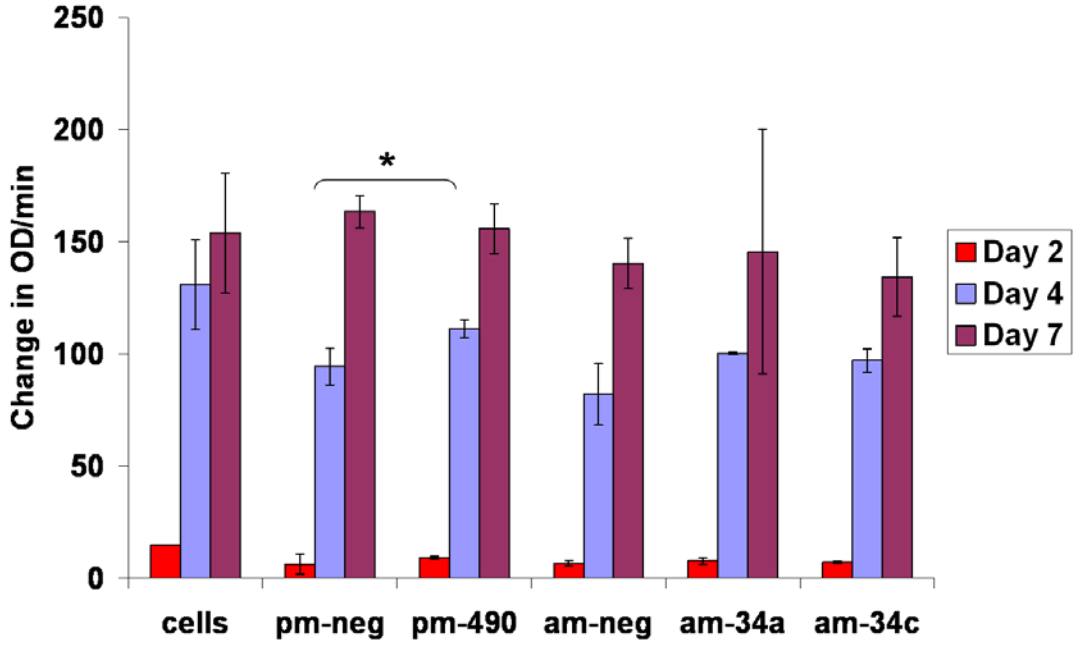

Figure 6.2.1.1.C: Impact of miR-490, miR-34a and miR-34c on CHO-K1 SEAP total yield. Supernatant of cells were harvested at day 2, day 4 and day 7 after transfection. SEAP total yield was analysed by a colorimetric assay. The change in absorbance of SEAP substrate, p-nitrophenolphosphate, was assessed by a spectrophotometer at 405nm in a kinetic assay (see materials and methods for details of SEAP assay in section 6.5.1). cells: non-transfected cells cultured at 37°C; pm-neg: negative control for mimics; pm-490; mimic of miR-490; am-neg: negative control for inhibitors; am-34a: inhibitor of miR-34a; am-34c: inhibitor of miR-34c. For statistical analysis a Student t-test was performed to compare pm-490 with pm-neg and am-34a, am-34c with am-neg. At day 2 and day 4 bars represent standard deviations from three biological replicates, and at day 7 the average total yield was calculated of two biological replicates (one sample was used for others assays). *: p-value< 0.05 (pm-490 compared to pm-neg treatment at four days after transfection).

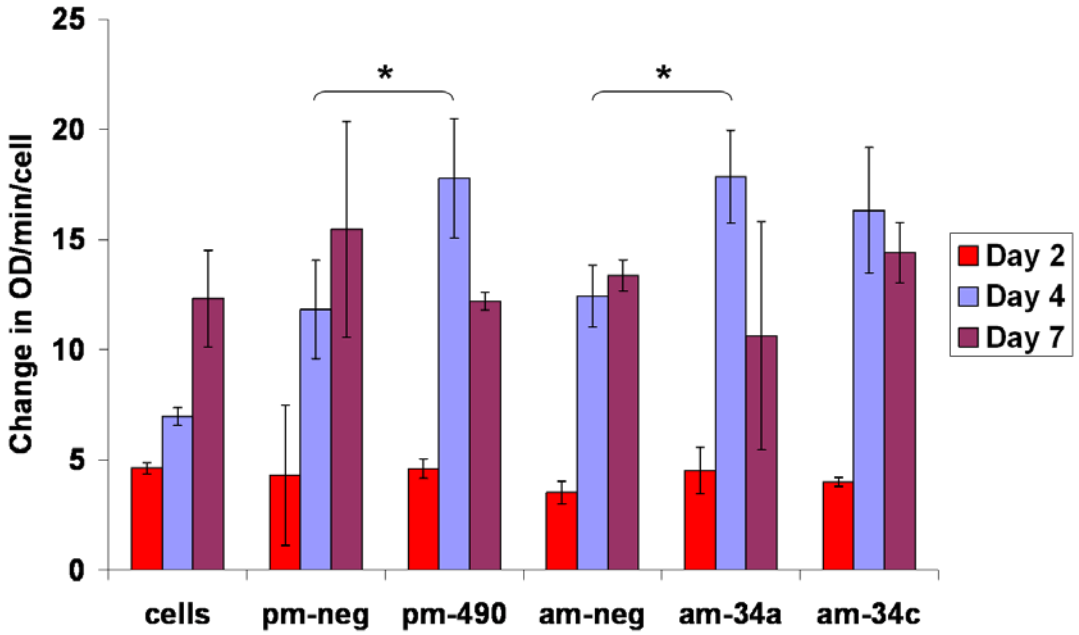

Figure 6.2.1.1.D: Impact of miR-490, miR-34a and miR-34c on CHO-K1 SEAP normalised productivity. Supernatant of cells were harvested at day 2, day 4 and day 7 after transfection. SEAP productivity was analysed by a colorimetric assay. The change in absorbance of SEAP substrate, p-nitrophenolphosphate, was assessed by a spectrophotometer at 405nm in a kinetic assay (see materials and methods for details of SEAP assay in section 6.5.1). cells: non-transfected cells cultured at 37°C; pm-neg: negative control for mimics; pm-490; mimic of miR-490; am-neg: negative control for inhibitors; am-34a: inhibitor of miR-34a; am-34c: inhibitor of miR-34c. For statistical analysis a Student t-test was performed to compare pm-490 with pm-neg and am-34a, am-34c with am-neg. At day 2 and day 4, bars represent standard deviations from three biological replicates. For technical reasons, the average normalised productivity was calculated of two biological replicates at day 7.*: p-value< 0.05 (pm-490 compared to pm-neg treatment four days after transfection; am-34a compared to am-neg treatment at day 4 after transfection).

6.2.1.2 Screening of miR-let-7e, miR-30e-5p, miR-10a and miR-29a in CHO cells

6.2.1.2.1 Impact on CHO-K1 SEAP cell growth and cell viability

As well as being identified in the array profiling experiment, miR-let-7e, miR-30e-5p, miR-10a and miR-29a have been shown to be involved in apoptosis, cell proliferation and cell cycle. In addition, their deregulation has been previously reported in cancers. Therefore these miRNAs were selected for functional validation.

Non-transfected CHO-K1 SEAP cells grew as expected (**Figure 6.2.1.2.A**). VCP knockdown by RNAi induced dramatic cell growth decrease and led to poor viability from day 2 to day 7. The negative control for mimics (pm-neg) had a non-specific impact on cell number at day 2 after transfection (more than 50% reduction) and cell viability was slightly reduced byless than 5%. On the other hand, the negative control for inhibitors led to cell growth decreased during the period of the experiment (**Figure 6.2.1.2.A**). The cell viability dropped by 15.59% compared to the non-transfected cells 48 hours after transfection (**Figure 6.2.1.2.B**). This is routinely observed in transient transfection assays and is a result of the treatment process-i.e., exposure of cells to the lipid-miR complexes.

Four days following transient up-regulation of let-7e, cell density was reduced by 2.97-fold (p-value=0.0048) (**Figure 6.2.1.2.A**) as well as cell viability by 8.70% (p-value= 0.0001) (**Figure 6.2.1.2.B**). At day 7, there was no more suppressive effect of pm-let-7e on cell proliferation and cell viability.

Four days after transfection, overexpression of miR-30e-5p reduced cell density by 1.37-fold but it was not statistically significant and slightly cell viability.

On the other hand, knockdown of miR-10a induced cell density increase of 1.8-fold at day 4 (p-value-= 0.0001) and slightly at later stages of culture without statistical significance (**Figure 6.2.1.2.A**). Cell viability was also increased of 7.71% compared to pm-neg treated cells.

Transient inhibition of miR-29a slightly decreased cell density in the early stages of culture and enhanced cell viability by 9.91% at day 7 (p-value= 0.0358) independently of cell growth (**Figures 6.2.1.2.A &B**).

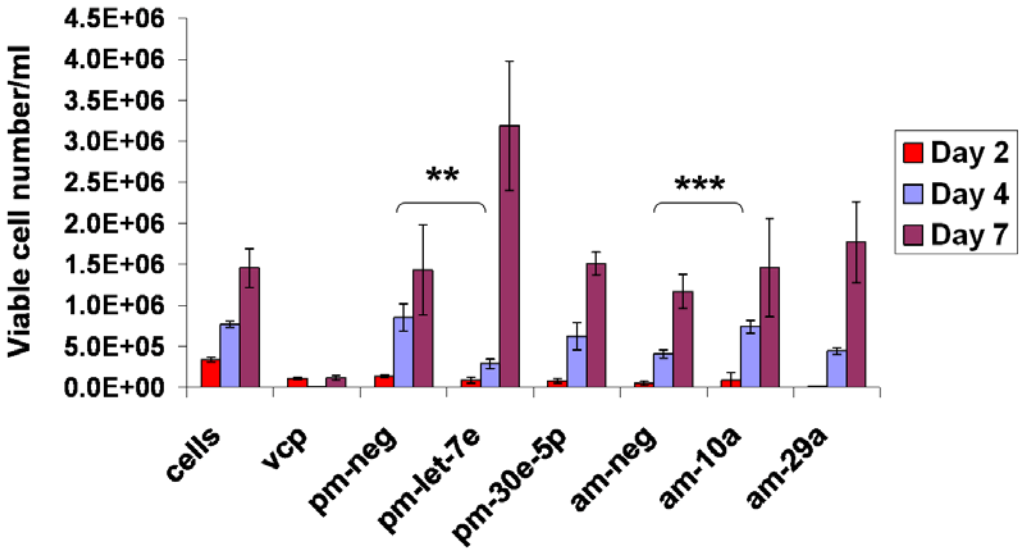

Figure 6.2.1.2.A: Impact of miR-let-7e, miR-30e-5p, miR-10a and miR-29a on CHO-K1 SEAP cell growth. Cells were seeded at $1x10^5$cells/ml in serum-free medium prior to transfection with 50nM miRNAs. Cells were harvested at day 2, day 4, day 7 following transfection and stained with GuavaViacount solution to monitor cell growth by Guava flow Cytometer. cells: non-transfected cells cultured at 37°C; vcp: siRNA against Valosin-Containing Protein (positive control of transfection efficiency); pm-neg: negative control for mimics; pm-let-7e; mimic of let-7e; pm-30e-5p: mimic of miR-30e-5p; am-neg: negative control for inhibitors; am-10a: inhibitor of miR-10a; am-29a: inhibitor of miR-29a. For statistical analysis a Student t-test was performed to compare pm-let-7e and pm-30e-5p with their respective control pm-neg and am-10a, am-29a with their specific control am-neg. Bars represent standard deviations of three biological replicates. **: p-value< 0.01 (pm-let-7e compared to pm-neg 96 hrs after transfection); ***: p-value< 0.001 (am-10a compared to am-neg treatment 96 hrs after transfection).

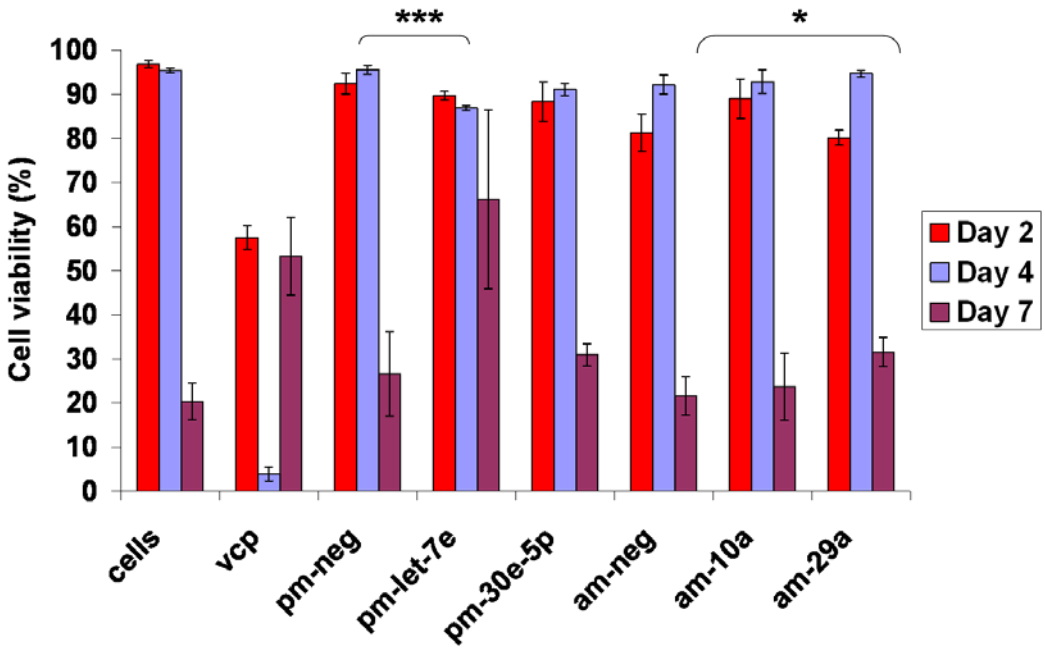

Figure 6.2.1.2.B: Impact of miR-let-7e, miR-30e-5p, miR-10a and miR-29a on CHO-K1 SEAP cell viability. Cells were seeded at $1x10^5$cells/ml in serum-free medium prior to transfection of 50nM miRNAs. Cells were harvested at day 2, day 4, day 7 after transfection and stained with GuavaViacount solution to monitor cell viability by Guava flow Cytometer. cells: non-transfected cells cultured at 37°C; vcp: siRNA against Valosin-containing protein (positive control of transfection efficiency); pm-neg: negative control for mimics; pm-let-7e; mimics of let-7e; pm-30e-5p: mimics of miR-30e-5p; am-neg: negative control for inhibitors; am-10a: inhibitors of miR-10a; am-29a: inhibitors of miR-29a. For statistical analysis a Student t-test was performed to compare pm-let-7e and pm-30e-5p with the specific control for mimics pm-neg and am-10a, am-29a with the specific control for inhibitors am-neg. Bars represent standard deviations of three biological replicates. *: p-value< 0.05 (am-10a compared to am-neg treatment seven days after transfection); ***: p-value< 0.001 (pm-let-7e compared to pm-neg 96 hrs after transfection).

6.2.1.2.2 Impact on SEAP total yield and normalised productivity

To investigate the impact of let-7e, miR-30e-5p, miR-10a and miR-29a on SEAP total yield and normalised productivity, supernatant of samples were harvested at day2, day 4 and day 7.

Transient overexpression of let-7e impacted negatively on total yield and normalised productivity (**Figure 6.2.1.2.C**) likely due to the low number of cells in culture.

Transfection of pm-miR-30e-5p increased total yield by 1.37-fold at later stages of culture (p-value= 0.0346) (**Figure 6.2.1.2.C**) but it did not impact significantly on normalised productivity (**Figure 6.2.1.2.D**).

Transient knockdown of both miR-10a and miR-29a induced a 1.2 to 1.4 fold increase of total yield at day 4 and day 7 (**Figure 6.2.1.2.C**).Two days following inhibition of miR-29a, normalised productivity was significantly increased by 4.93-fold (p-value= 0.0126) (**Figure 6.2.1.2.D**).

The suppressive impact of let-7e on cell growth was reproducible in repeats as well as the advantage in cell growth following inhibition of miR-10a. The increase of total yield and normalised productivity observed after pm-30e-5p and am-10a, am-29a treatment was also reproducible in other assays. Therefore the investigation of miR-let-7e, miR-10a, miR-29a and miR-30e-5p was continued in CHO1.14 cells.

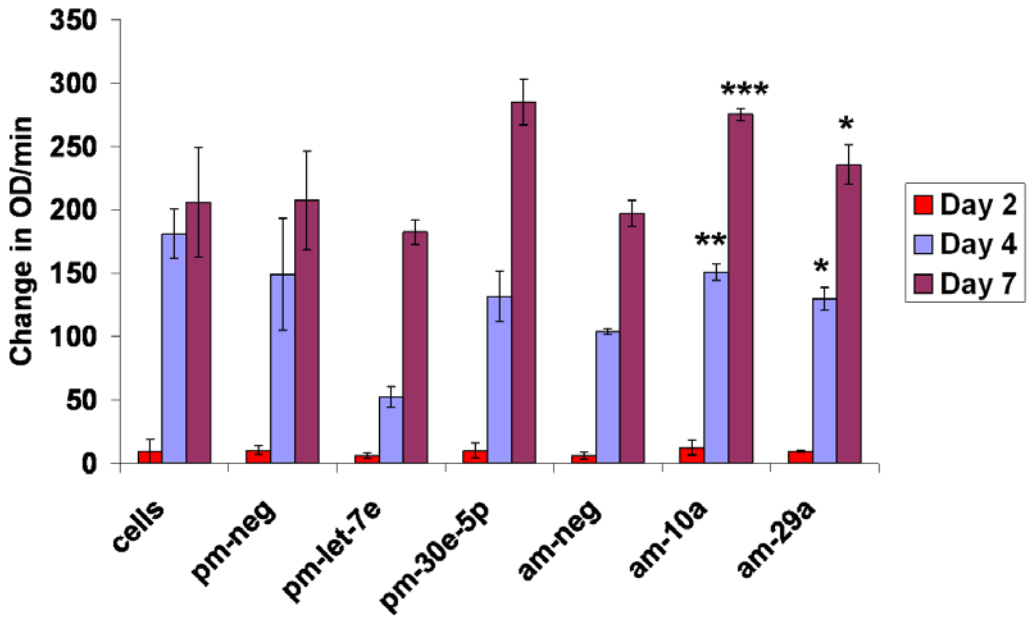

Figure 6.2.1.2.C: Impact of miR-let-7e, miR-30e-5p, miR-10a and miR-29a on CHO-K1 SEAP total yield. Supernatant of cells were harvested at day 2, day 4 and day 7 after transfection. The change in absorbance per min of SEAP substrate, p-nitrophenolphosphate, was assessed by a spectrophotometer (see materials and methods for more details on SEAP assay in section 6.5.1). cells: non-transfected cells cultured at 37˚C; pm-neg: negative control for mimics; pm-let-7e; mimic of let-7e; pm-30e-5p: mimic of miR-30e-5p; am-neg: negative control for inhibitors; am-10a: inhibitor of miR-10a; am-29a: inhibitor of miR-29a. For statistical analysis a Student t-test was performed to compare pm-let-7e and pm-30e-5p with pm-neg and am-10a, am-29a with am-neg. Bars represent standard deviations of three biological triplicates.*: p-value< 0.05 (am-29a was compared to am-neg treatment at day 4 and day 7 after transfection); **: p-value< 0.01 (am-10a was compared to am-neg four days after transfection); ***: p-value< 0.001 (am-10a was compared to am-neg at day 7 after transfection).

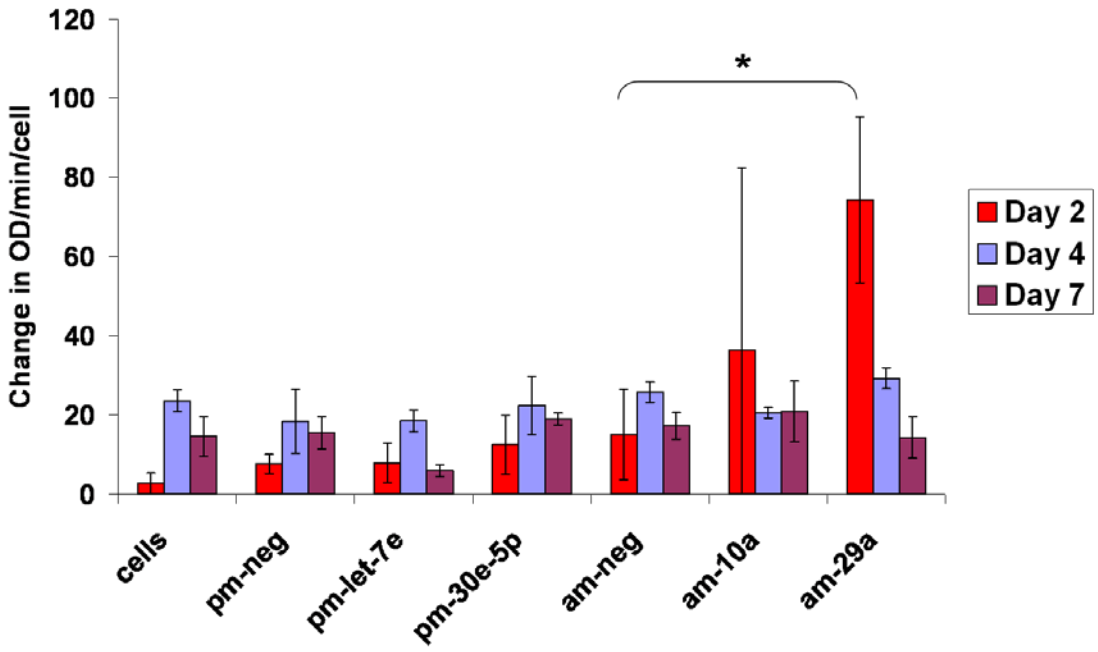

Figure 6.2.1.2.D: Impact of miR-let-7e, miR-30e-5p, miR-10a and miR-29a on CHO-K1 SEAP normalised productivity. Supernatant of cells were harvested at day 2, day 4 and day 7 after transfection. The change in absorbance per min and per cell of SEAP substrate, p-nitrophenolphosphate, was assessed by a spectrophotometer (see materials and methods for more details on SEAP assay in section 6.5.1). cells: non-transfected cells cultured at 37°C; pm-neg: negative control for mimics; pm-let-7e; mimic of let-7e; pm-30e-5p: mimic of miR-30e-5p; am-neg: negative control for inhibitors; am-10a: inhibitor of miR-10a; am-29a: inhibitor of miR-29a. For statistical analysis a Student t-test was performed to compare pm-let-7e and pm-30e-5p with pm-neg and am-10a, am-29a with am-neg. Bars represent standard deviations of three biological replicates. *: p-value< 0.05 (am-29a compared to am-neg treatment 48 hrs after transfection). The high variation observed in am-10a sample at day 2 was likelydue to technical errors.

6.2.1.2.3 Impact on CHO1.14 cell growth and cell viability

To investigate whether the impact of miR-let-7e, miR-30e-5p, miR-10a and miR-29a was reproducible in other cell lines, the transfection assay was repeated in CHO1.14 cells.

Non-transfected cells and vcp siRNA treated cells showed the expected growth and cell viability profiles (**Figure 6.2.1.2.E**). Transfection of pm-neg molecules did not initiate non-specific effects on cell proliferation and cell viability. Treatment of cells with am-neg molecules led to small impact on cell growth two and four days after transfection (**Figure 6.2.1.2.E**).

Transient overexpression of let-7e provoked cell growth increase at day 2 and day 4 by 1.42- and 4.02-fold respectively (p-values=0.0002 and 0.0001). This impact was not present at later stages of culture. The viability of cells transfected with pm-let-7e decreased by 4.59% to 7.87% in the period of the assay (p-values= 0.0210 to 0.0002) (**Figure 6.2.1.2.F**). Cell growth was up-regulated by 1.26-fold 96 hours (p-value= 0.0121) following transient overexpression of miR-30e-5p and cell viability was 20.4% lower (p-value= 0.0026) compared to pm-neg transfected cells at day 7 (**Figure s6.2.1.2.E &F**). These results are in contradiction with what we observed in CHO-K1 SEAP cells.

Knockdown of miR-10a slightly increased cell density at day 4 but it was not statistically significant. Transfection of am-29a did not impact either on CHO1.14 cell growth or on cell viability (**Figures 6.2.1.2.E &F**).

Thus overexpression of let-7e resulted in significant cell growth reduction in CHO-K1 SEAP and CHO1.14 cells and triggered cell death in both cell lines at early stages of culture. Therefore the potential of pm-let-7e was investigated in another cell lines.

Transfection of pm-30e-5p showed inconsistent outcomes across the different repeats and between the cell lines. miR-10a had little impact on cell proliferation. miR-29a did not impact significantly either on cell proliferation or on cell viability.

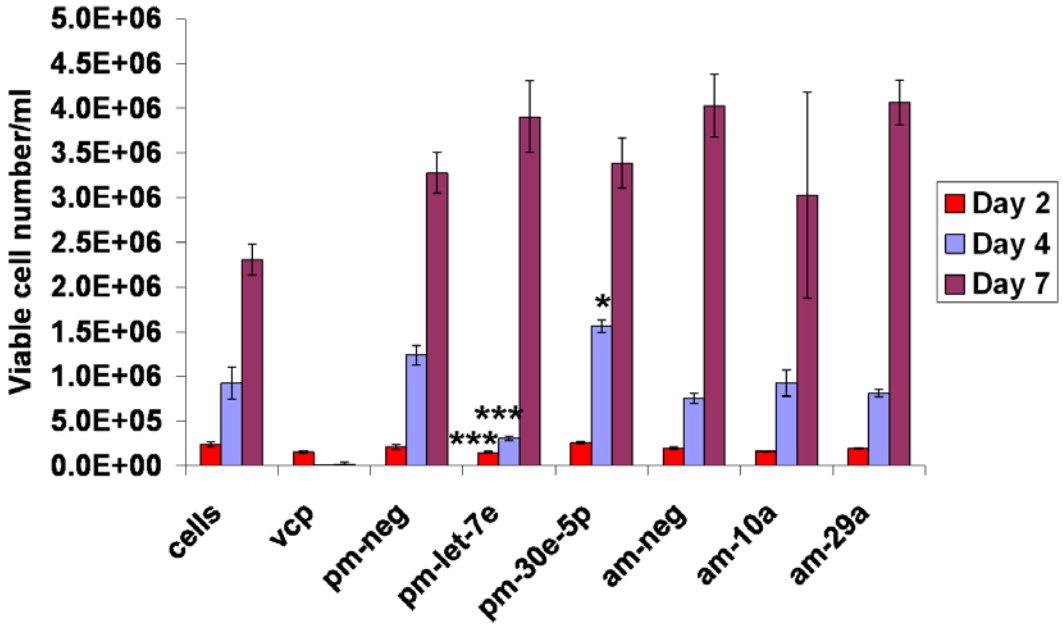

Figure 6.2.1.2.E: Impact of miR-let-7e, miR-30e-5p, miR-10a and miR-29a on CHO-1.14 cell growth. Cells were seeded at $1x10^5$cells/ml in serum-free medium prior to transfection with 50nM miRNAs. Cells were harvested at day 2, day 4, day 7 and stained with GuavaViacount solution to monitor cell growth by Guava flow Cytometry. cells: non-transfected cells cultured at 37°C; vcp: siRNA against Valosin-Containing Protein (positive control of transfection efficiency); pm-neg: negative control for mimics; pm-let-7e; mimic of let-7e; pm-30e-5p: mimic of miR-30e-5p; am-neg: negative control for inhibitors; am-10a: inhibitor of miR-10a; am-29a: inhibitor of miR-29a. For statistical analysis a Student t-test was performed to compare pm-let-7e and pm-30e-5p with pm-neg and am-10a, am-29a with am-neg. Bars represent standard deviations of three biological replicates. *: p-value< 0.05 (pm-30e-5p compared to pm-neg 96 hrs following treatment); ***: p-value< 0.001 (pm-let-7e compared to pm-neg treatment 48 hrs and 96hrs after transfection).

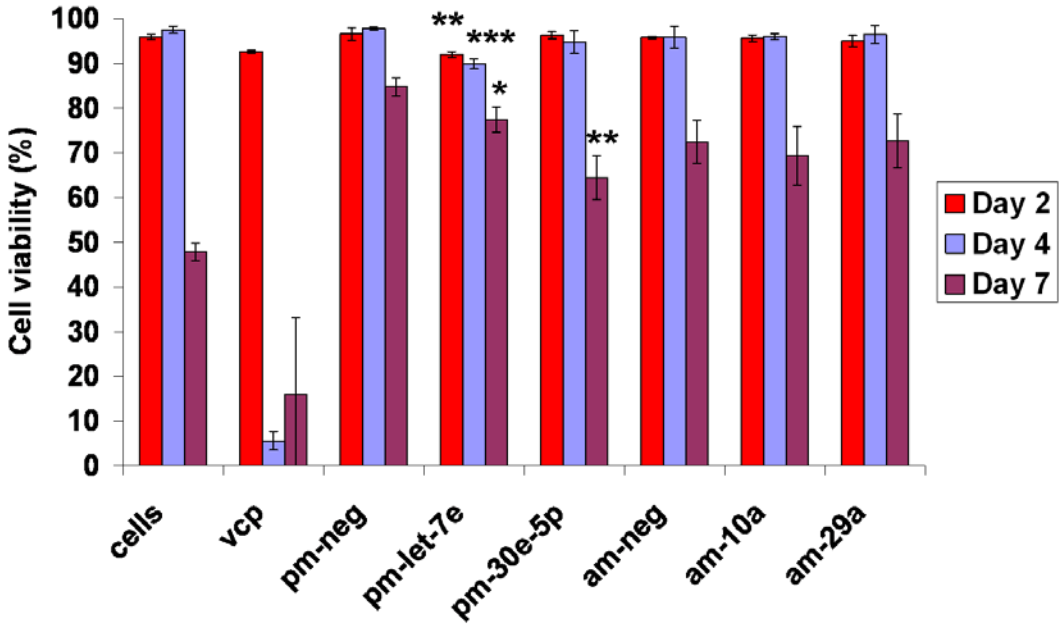

Figure 6.2.1.2.F: Impact of miR-let-7e, miR-30e-5p, miR-10a and miR-29a on CHO-1.14 cell viability. Cells were seeded at $1x10^5$cells/ml in serum-free medium prior to transfection with 50nM miRNAs. Cells were harvested at day 2, day 4, day 7 and stained with GuavaViacount solution to monitor cell viability by Guava flow Cytometry. cells: non-transfected cells cultured at 37°C; vcp: siRNA against Valosin-Containing Protein (positive control of transfection efficiency); pm-neg: negative control for mimics; pm-let-7e; mimic of let-7e; pm-30e-5p: mimic of miR-30e-5p; am-neg: negative control for inhibitors; am-10a: inhibitor of miR-10a; am-29a: inhibitor of miR-29a. For statistical analysis a Student t-test was performed to compare pm-let-7e and pm-30e-5p with pm-neg and am-10a, am-29a with am-neg. Bars represent standard deviations of three biological triplicates. *: p-value< 0.05; **: p-value< 0.01; ***: p-value< 0.001 (pm-let-7e was compared to pm-neg treatment 24 hrs, 48 hrs and 96hrs after transfection and pm-30e5-p was compared to pm-neg at day 7 after transfection).

6.2.1.2.4 Impact on IgG1 total yield and normalised productivity in CHO1.14 cells

To verify whether miR-10a, miR-29a and miR-30e-5p enhanced cell productivity in CHO1.14 cells, total yield and normalised productivity were monitored at day 2, day 4 and day 7 following transfection. Transient up-regulation of miR-let-7e induced a 4.14-fold increase (p-value= 2.66608E-05) of normalised productivity at day 4 after transfection (**Figure 6.2.1.2.G)**.

Transient knockdown of miR-10a resulted in 1.65-fold (p-value= 0.0026) improvement of total yield at day 2 in comparison to the non-specific control (**Figure 6.2.1.2.G**). However, it was lower than the total yield in non-transfected cells and there was no major improvement at later stages of culture. Normalised productivity was also improved 48 hours after am-10a transfection by 1.99-fold (p-value= 0.0027) but it did not exceed the production of non-transfected cells (**Figure 6.2.1.2.H**).

Transfection with am-29a and pm-30e-5p did not impact on total yield and normalised productivity of IgG1 (**Figures 6.2.1.2.G &H**).

In contrast to what we observed in CHO-K1 SEAP cells, transient overexpression of let-7e impacted on normalised productivity of IgG1. This is likely due to a lower number of cells in culture and not due a higer expression of IgG1. The other minas, miR-10a, miR-29a and miR30e-5p had little or no impact on productivity. Thus the investigation of let-7e has a candidate miRNA to manipulate CHO cell proliferation and productivity was pursued in CHO2B6 cells.

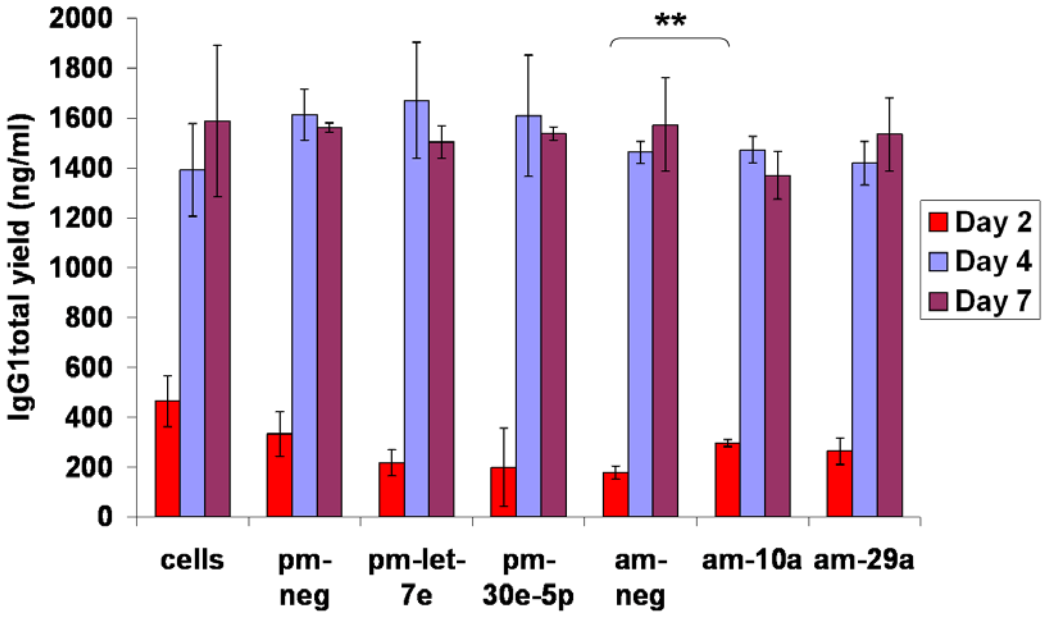

Figure 6.2.1.2.G: **Impact of miR-let-7e, miR-30e-5p, miR-10a and miR-29a on CHO-1.14 total yield**. Supernatant of cells were harvested at day 2, day 4 and day 7 after transfection. The total yield of IgG1 was analysed by ELISA assay. cells: non-transfected cells cultured at 37°C; pm-neg: negative control for mimics; pm-let-7e; mimic of let-7e; pm-30e-5p: mimic of miR-30e-5p; am-neg: negative control for inhibitors; am-10a: inhibitor of miR-10a; am-29a: inhibitor of miR-29a. For statistical analysis a Student t-test was carried out to compare pm-let-7e and pm-30e-5p with pm-neg and am-10a, am-29a with am-neg. Bars represent standard deviations of three biological replicates. **: p-value< 0.01 (am-10a was compared to am-neg 48hrs after transfection).

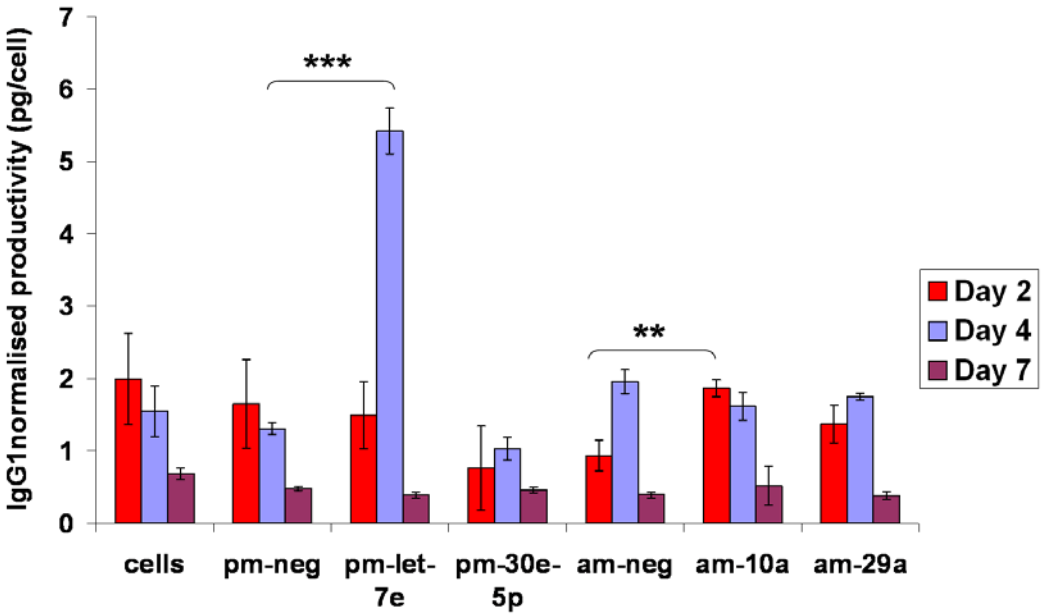

Figure 6.2.1.2.H: Impact of miR-let-7e, miR-30e-5p, miR-10a and miR-29a on CHO-1.14 normalised productivity. Supernatant of cells were harvested at day 2, day 4 and day 7 after transfection. IgG productivity was analysed using ELISA assay. cells: non-transfected cells cultured at 37˚C; pm-neg: negative control for mimics; pm-let-7e; mimic of let-7e; pm-30e-5p: mimic of miR-30e-5p; am-neg: negative control for inhibitors; am-10a: inhibitor of miR-10a; am-29a: inhibitor of miR-29a. For statistical analysis a Student t-test was carried out to compare pm-let-7e and pm-30e-5p with pm-neg and am-10a, am-29a with am-neg. Bars represent standard deviations for three biological replicates. Statistics were evaluated with a Student t-test. **: p-value< 0.01 (am-10a was compared to am-neg 48hrs after transfection); ***: p-value< 0.001 (pm-let-7e was compared to pm-neg 96hrs after transfection).

6.2.1.2.5 Impact of pm-let-7e on CHO2B6 cell growth and viability

Having established that pm-let-7e impacted significantly on CHO-K1 SEAP and CHO1.14 cell growth and viability, we analysed its potential in CHO2B6 cells.
Following transient up-regulation of let-7e, cell growth was arrested from day 2 to day 7 (1.39- to 23.4-fold; p-values= 0.0046 to 1.13279E-06) (**Figure 6.2.1.2.I**). There was a significant reduction in cell viability from day 3 to day 7 (from 11.16% to 46.49%; p-values= 0.0217 to 7.67571E-05) (**Figure 6.2.1.2.J**). It is worth noting that the impact of let-7e on cell proliferation and cell viability was similar to the impact caused by knockdown of VCP, an essential housekeeping gene in CHO cells.

In agreement with the original profiling result, high levels of let-7e are associated with cell density decrease in all three CHO cell lines, suggesting that under temperature-shift let-7e was a mediator of the cell growth arrest. Collectively, these results implied that let-7e is critical in the regulation of CHO cell proliferation and cell death therefore knockdown of let-7e may be a promising route to improve these cell characteristics.

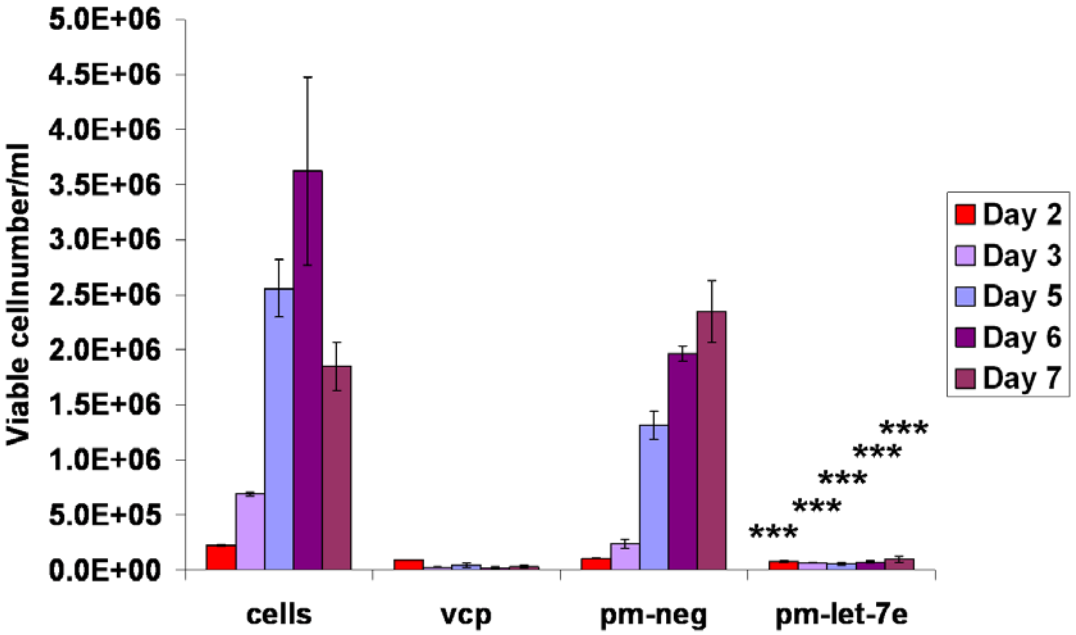

Figure 6.2.1.2.I: Impact of miR-let-7e on CHO2B6 cell growth.

Cells were seeded at $1x10^5$cells/ml in serum-free medium prior to transfection.with 50nM miRNAs. Cells were harvested at day 2, day 3, day 5, day 6 and day 7. Cells were stained with GuavaViacount reagent to monitor cell growth by Guava flow Cytometry. cells: non-transfected cells cultured at 37°C; vcp: siRNA against Valosin-Containing Protein (positive control of transfection efficiency); pm-neg: negative control for mimics; pm-let-7e: mimic of let-7e. For statistical analysis a Student t-test was carried out to compare pm-let-7e with pm-neg from day 2 to day 7. Bars represent standard deviations of three biological replicates. **: p-value< 0.01; ***: p-value< 0.001.

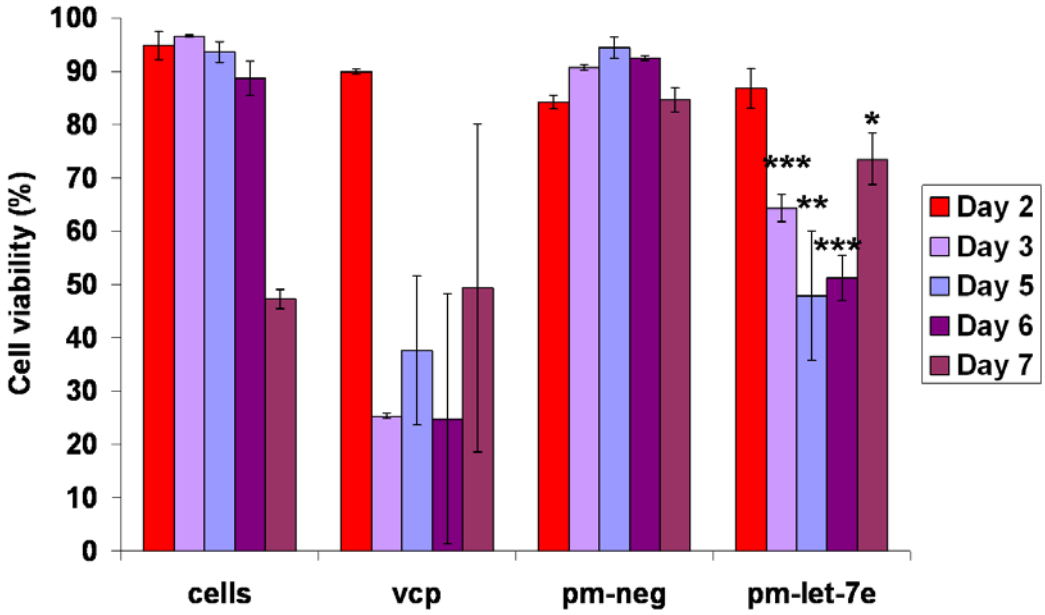

Figure 6.2.1.2.J: Impact of miR-let-7e on CHO2B6 cell viability.

Cells were seeded at $1x10^5$cells/ml in serum-free medium prior to transfection.with 50nM miRNAs. Cells were harvested at day 2, day 3, day 5, day 6 and day 7. Cells were stained with GuavaViacount reagent to monitor cell viability by Guava flow Cytometry. cells: non-transfected cells cultured at 37°C; vcp: siRNA against Valosin-Containing Protein (positive control of transfection efficiency); pm-neg: negative control for mimics; pm-let-7e: mimic of let-7e. For statistical analysis a Student t-test was carried out to compare pm-let-7e with pm-neg from day 3 to day 7. Bars represent standard deviations of three biological replicates. *: p-value< 0.05; **: p-value< 0.01; ***: p-value< 0.001.

6.2.1.2.6 Impact of pm-let-7e on IgG1 total yield and normalised productivity in CHO2B6 cells

To verify whether miR-let-7e impacted on CHO2B6 productivity, IgG1 total yield and normalised productivity were monitored at day 3, day 5 and day 7.

Transient up-regulation of let-7e led to total yield decrease likely due to the low number of cells remaining in culture (**Figure 6.2.1.2.K**). However, it did significantly enhance normalised productivity at day 3, day 5 and day 7 by 3.67-fold, 11.74-fold and 14.47-fold respectively suggesting that the few cells remaining in culture were secreting more IgG1 (**Figure 6.2.1.2.L**).

This confirms that the anti-proliferative role of let-7e and its negative impact on cell viability is conserved between CHO cell lines. Based on these data let-7e is a really promising target to manipulate cell growth and improve normalised productivity in different CHO cell lines.

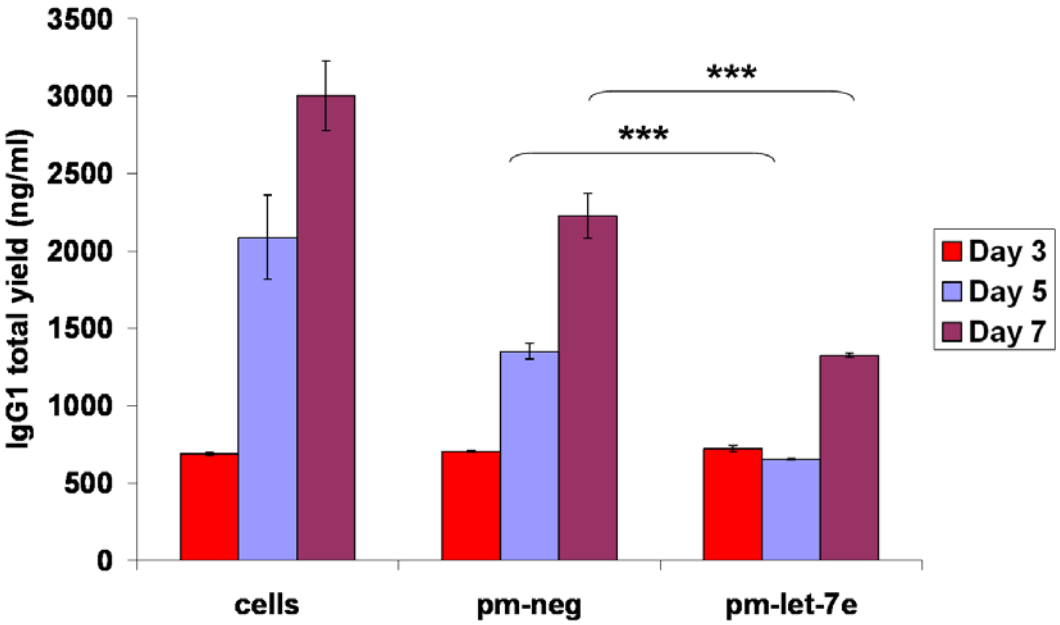

Figure 6.2.1.2.K: Impact of pm-let-7e on CHO 2B6 total yield.

Supernatant of cells were harvested at day 3, day 5 and day 7 after transfection. The total yield of IgG1 was analysed by ELISA (see materials and methods for more details on ELISA protocol in section 6.5.2). Cells: non-transfected cells cultured at 37˚C; pm-neg: negative control for mimics; pm-let-7e; mimic of let-7e. For statistical analysis a Student t-test was carried out to compare pm-let-7e with pm-neg at day 5 and day 7 after transfection. Bars represent standard deviations of three biological replicates. ***: p-value< 0.001.

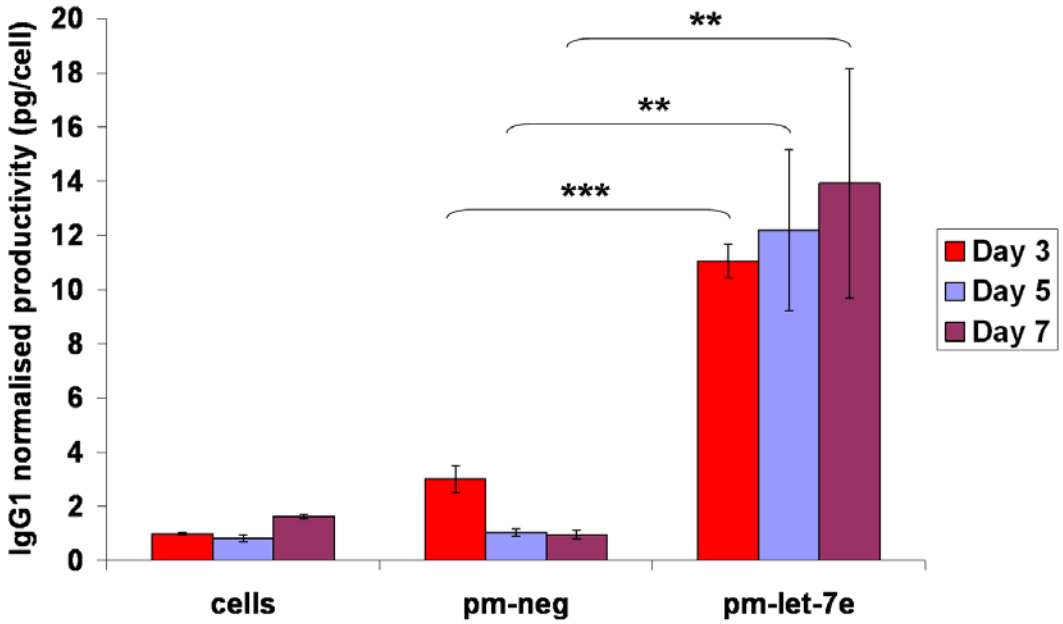

Figure 6.2.1.2.L: Impact of pm-let-7e on CHO 2B6 normalised productivity.

Supernatant of cells were harvested at day 3, day 5 and day 7 after transfection. IgG productivity was analysed by ELISA (see materials and methods for more details on ELISA protocol in section 6.5.2). Cells: non-transfected cells cultured at 37˚C; pm-neg: negative control for mimics; pm-let-7e: mimic of let-7e. A Student t-test was performed allowing the comparison of pm-let-7e to pm-neg at day 3, day 5 and day 7 after transfection. Bars represent standard deviations of three biological replicates. **: p-value< 0.01; ***: p-value< 0.001.

6.2.2 Screening of candidates miRNAs in fast versus slow growing cells

6.2.2.1 Impact on CHO-K1 SEAP cell growth and viability

A miRNA profiling experiment was performed by colleagues in our laboratory in the aim to identify miRNAs associated with rapid cell growth (Clarke, et al. 2012). Five fast growing and five slow growing cell lines were profiled in biological triplicates. These clones were all derived from the same cell line development project by collaborators in Pfizer. They displayed similar recombinant protein production rates and only differed in their cell growth rate. Samples were harvested at day 3, this time point corresponding to the middle of the logarithmic phase of growth and miRNA expression was quantified by TLDA. Following the analysis of data, a list of miRNAs was generated in which miR-23b* was found to be up-regulated in fast growing cells. The expression of miR-216b, miR-409-5p and miR-874 was reduced in these cell lines. Transient overexpression of miR-23b* resulted in cell growth reduction of 1.32-fold at day 3 (p-value= 0.020) and to a lesser extent at day 5 after transfection (**Figure 6.2.2.1.A**). Consequently cell viability was improved at day 7 by 44.25% (p-value= 5.01239E-05) due probably to the smaller number of cells present in this culture (**Figure 6.2.2.1.B**). On the other hand, transient knockdown of miR-216b slightly increased cell density three and five days after transfection and by 1.45-fold at day 7 (**Figure 6.2.2.1.A**). Cell viability was enhanced by 16.57% at later stages of culture independently of cell number (p-value= 0.0001). Transient inhibition of am-874 led to 1.15-fold to 1.31-fold reduction in cell growth and significantly improved cell viability at day 3 and day 5 after transfection (p-value= 0.0002 and 0.0171) (**Figures 6.2.2.1.A &B**). Surprisingly, miR-490-5p did not impact on cell proliferation or cell viability.

Thus miR-23b* significantly reduced cell density and both miR-216b and miR-874 enhanced cell viability at later stages of culture.

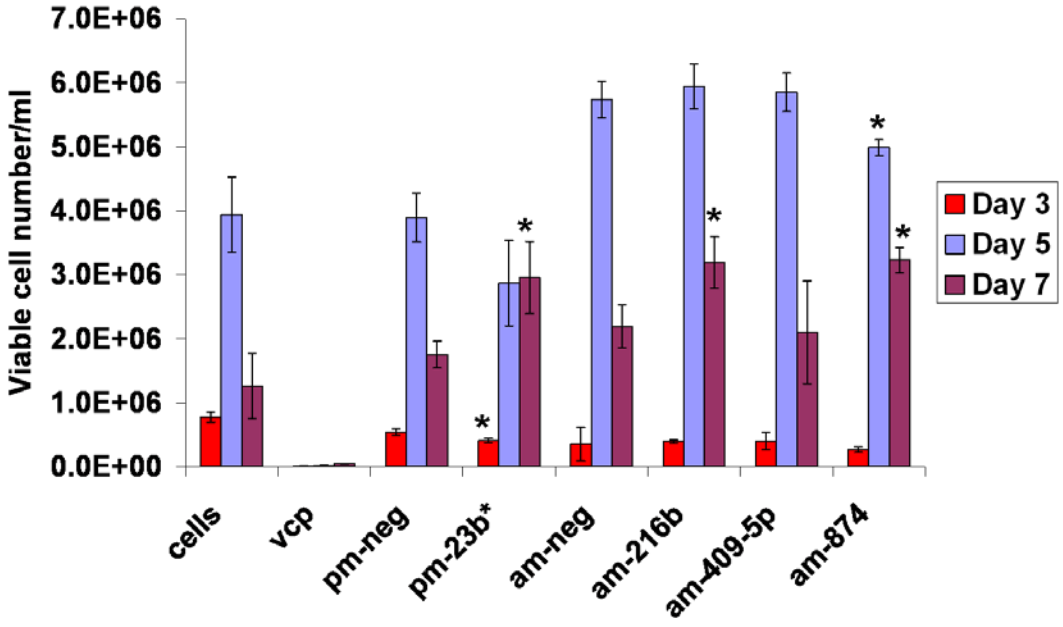

Figure 6.2.2.1.A: Impact of pm-23b*, am-216b, am-409-5p and am-874 on CHO-K1 SEAP cell growth. Cells were seeded at $1x10^5$cells/ml in serum-free medium prior to transfection with 50nM miRNAs. Cells were harvested at day 3, day 5 and day 7 and stained with GuavaViacount reagent to monitor cell growth by Guava flow Cytometry. cells: non-transfected cells cultured at 37°C; vcp: siRNA against Valosin Containing Protein (positive control of transfection efficiency); pm-neg: negative control for mimics; pm-23b*: mimic of miR-23b*; am-neg: negative control for inhibitors; am-216b: inhibitor of miR-216b; am-409-5p: inhibitor of miR-409-5p; am-874: inhibitor of miR-874. Statistical significance was analysed using a Student t-test to compare pm-23b* with pm-neg and am-216b, am-409-5p, am-874 with am-neg. Bars represent standard deviations of three biological replicates.*: p-value< 0.05

.

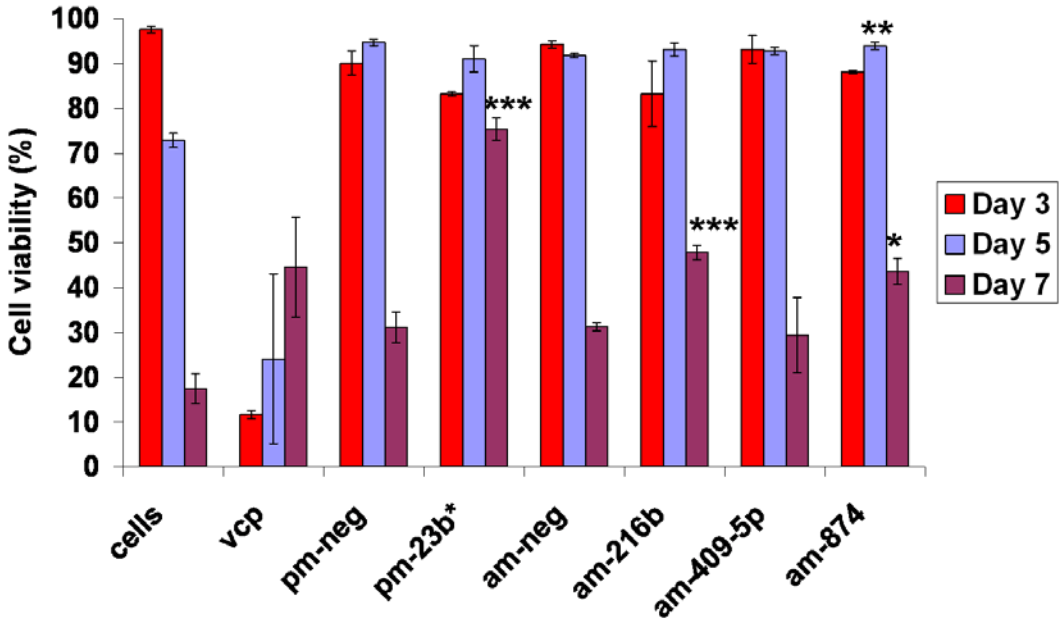

Figure 6.2.2.1.B: Impact of pm-23b*, am-216b, am-409-5p and am-874 on CHO-K1 SEAP cell viability. Cells were seeded at $1x10^5$cells/ml in serum-free medium prior to transfection with 50nM miRNAs. Cells were harvested at day 3, day 5 and day 7 and stained with GuavaViacount reagent to monitor cell viability by Guava flow Cytometry. cells: non-transfected cells cultured at 37°C; vcp: siRNA against Valosin Containing Protein (positive control of transfection efficiency); pm-neg: negative control for mimics; pm-23b*: mimic of miR-23b*; am-neg: negative control for inhibitors; am-216b: inhibitor of miR-216b; am-409-5p: inhibitor of miR-409-5p; am-874: inhibitor of miR-874. Statistical significance was analysed using a Student t-test in which we compared pm-23b* to pm-neg and am-216b, am-409-5p, am-874 to am-neg. Bars represent standard deviations for three biological replicates. *: p-value< 0.05; **: p-value< 0.01; ***: p-value< 0.001.

.

6.2.2.2 Impact on SEAP total yield and normalised productivity

To investigate the impact of miR-23b*, miR-216b, miR-409-5p and miR-874 on SEAP total yield and normalised productivity, supernatant of samples were harvested at day 3, day 5 and day 7.

None of these miRNAs enhanced either total yield of CHO-K1 SEAP cell (**Figure 6.2.2.2.A**).

Due to the high standard deviations displayed in am-neg transfected sample, it was difficult to conclude on any changes in normalised productivity 48 hours after transfection (**Figure 6.2.2.2.B**). However at day 5 and day 7, am-216b, am-409-5p and am-874 did not improved normalised productivity. This assay was conducted only once in CHO-K1 SEAP cells. For statistical significance other repeats need to be done before validation of these miRNAs.

The results for all miRNA screening are summarised in **Table 6.2.2.2**.

.

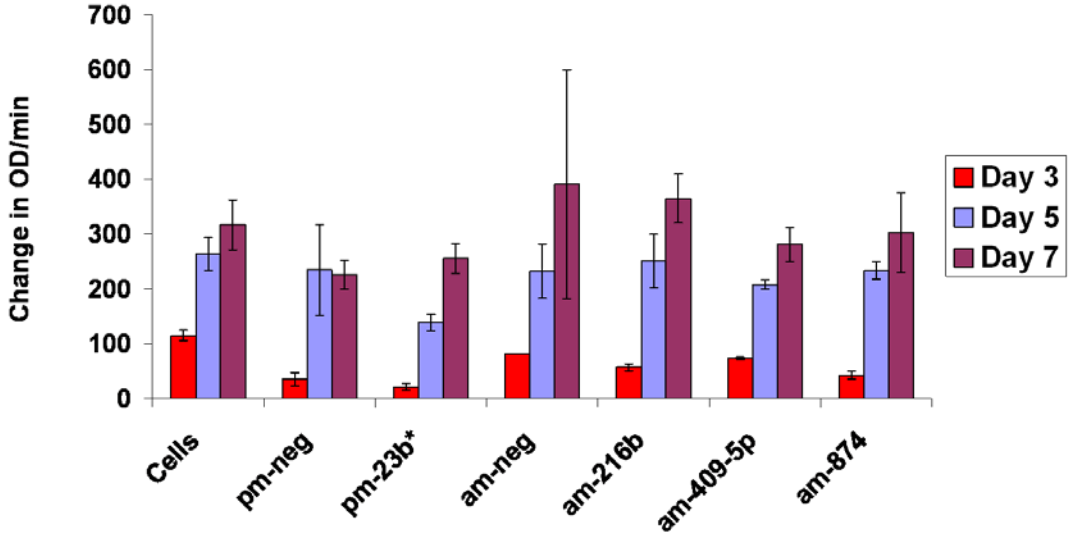

Figure 6.2.2.2.A: Impact of pm-23b*, am-216b, am-409-5p and am-874 on SEAP total yield.

Supernatant of cells were harvested at day 3, day 5 and day 7 after transfection. SEAP total yield was analysed by a colorimetric assay. cells: non-transfected cells cultured at 37˚C; pm-neg: negative control for mimics; pm-23b*; mimic of miR-23b*; am-neg: negative control for inhibitors; am-216b: inhibitor of miR-216b; am-409-5p: inhibitor of miR-409-5p; am-874: inhibitor of miR-874. For statistical analysis a Student t-test was performed to compare pm-23b* with pm-neg and am-216b, am-409-5p, am-874 with am-neg. Bars represent standard deviations for three biological replicates. There was no statistical significance found in this assay.

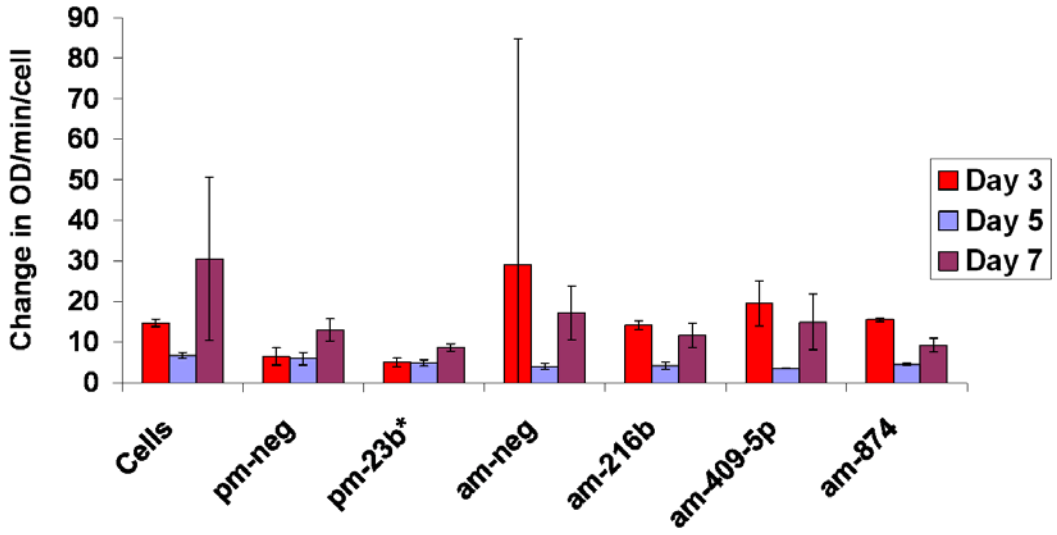

Figure 6.2.2.2.A: Impact of pm-23b*, am-216b, am-409-5p and am-874 on SEAP normalised productivity. Supernatant of cells were harvested at day 3, day 5 and day 7 after transfection. SEAP productivity was analysed by a colorimetric assay. cells: non-transfected cells cultured at 37C; pm-neg: negative control for mimics; pm-23b*; mimic of miR-23b*; am-neg: negative control for inhibitors; am-216b: inhibitor of miR-216b; am-409-5p: inhibitor of miR-409-5p; am-874: inhibitor of miR-874. Statistical significance was assessed by a Student t-test in which pm-23b* was compared to pm-neg and am-216b, am-409-5p, am-874 were compared to am-neg. Bars represent standard deviations for three biological replicates. There was no statistical significance found in this assay.

Table 6.2.2.2: Summary of data of miRNA screening

miRNA	Screening data	Conclusion
miR-490	Inconsistent	Further validation
miR-34a	Inconsistent	Further validation
miR-34c	Inconsistent	Further validation
let-7e	Cell growth arrest, low viability	Knockdown to increase cell density and viability levels
miR-30e-5p	Inconsistent	Further validation
miR-10a	Inconsistent	Further validation
miR-29a	Inconsistent	Further validation
miR-23b*	Low cell density, high viability	Further validation
miR-216b	High viability	Further validation
miR-409-5p	No impact	Further validation
miR-874	Low cell density, high viability	Further validation

6.3 Investigation of the individual miR-23a~miR-27a~24-2 cluster members potential in improving CHO cell characteristics

6.3.1 Screening of miR-24

Previous profiling data from our laboratory indicated that miR-24 could be a useful tool for modifying CHO cell growth. With the intention of manipulating CHO cell phenotypes to improve growth and productivity, the potential of miR-24 as a tool to engineer CHO cells was further studied using mimic and inhibitor molecules. For further details on the description of these molecules and controls used in this study refer to section 6.2.1. Transient transfection using pm-24, pm-neg, am-24 and am-neg molecules was performed in recombinant human monoclonal immunoglobulin gamma 1 (rHmIgG1) producing cells, CHO1.14 and CHO2B6, for seven days of culture in serum-free medium. The concentration of miRNAs used in this experiment was 100nM. Although this concentration may be considered high, this experiment was only to observe if a big change in expression of miR-24 could mimic the cell growth decrease observed subsequent to temperature shift in the profiling study.

6.3.1.1 Screening of miR-24 in CHO1.14 cells

Non-transfected cells had the expected profiles in cell proliferation and cell viability (**Figure 6.3.1.1.A**). Knockdown of vcp using a siRNA led to dramatic cell growth reduction as well as cell viability 96 hours after transfection. The transfection reagent in its own displayed a non-specific impact on cell proliferation at day 2 and day 4 following transfection (**Figure 6.3.1.1.A**). However, it did not impact negatively on cell viability.

Transfection of pm-neg and am-neg molecules induced non-specific decrease of cell growth but it did not impact negatively on cell viability at early stages of culture (**Figures 6.3.1.1.A&B**). This was previously observed in the other transient transfection

assays using lower concentration of miRNAs. At day 4, up-regulation of miR-24 induced cell growth decrease by 1.68-fold and improved cell viability by 14.46% at later stages of culture compared to the non-specific control pm-neg (**Figures 6.3.1.1.A&B**). On the other hand, miR-24 knockdown increased cell growth by more than two-fold and had little impact on cell viability (**Figures 6.3.1.1.A&B**). Although the results were not statistically significant due to the number of replicates, the high and low reading represented by the bars at day 4 and day 7 indicated that the impact of pm-24 on cell proliferation and cell viability was interesting to follow in other cell lines.

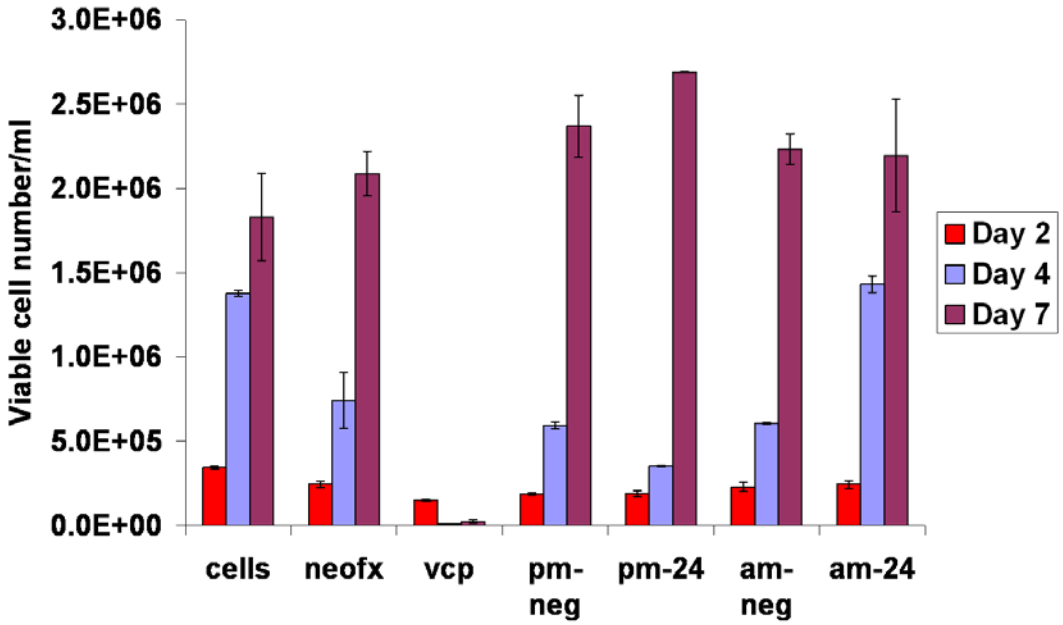

Figure 6.3.1.1.A: Impact of miR-24 on CHO1.14 cell growth.

miR-24 was up-regulated using miRNA mimic (pm) or inhibited using miRNA inhibitor (am) at a concentration of 100nM. Cells were seeded at $1x10^5$cells/ml in serum-free medium and harvested at day 2, day 4 and day 7. Cells were stained with GuavaViacount reagent to monitor cell growth by Guava flow cytometry. cells: non-transfected cells; neofx: transfection reagent; vcp: siRNA against Valosin-Containing Protein (positive control of transfection efficiency); pm-neg: negative control for mimics; am-neg: negative control for inhibitors. At day 2, bars represent standard deviations of three biological replicates. At day 4 and day 7, bars represent the high and low reading of two biological replicates. There was no statistical significance found in this experiment.

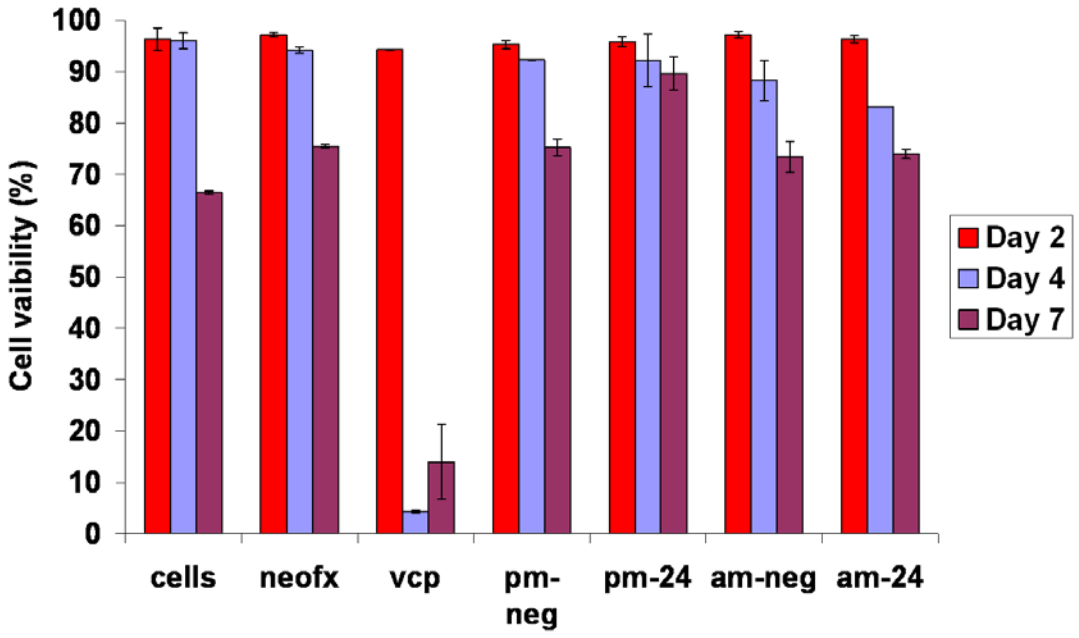

Figure 6.3.1.1.B: Impact of miR-24 on CHO1.14 cell viability.

miR-24 was up-regulated using miRNA mimic (pm) or inhibited using miRNA inhibitor (am) at a concentration of 100nM. Cells were seeded at $1x10^5$ cells/ml in serum-free medium and stained with GuavaViacount reagent to monitor cell viability by Guava flow cytometry at day 2, day 4 and day 7. cells: non-transfected cells; neofx: transfection reagent; vcp: siRNA against Valosin-Containing Protein (positive control of transfection efficiency); pm-neg: negative control for mimics; am-neg: negative control for inhibitors. At day 2, bars represent standard deviations of three biological replicates. At day 4 and day 7, bars represent the high and low reading of two biological replicates. There was no statistical significance found in this experiment.

6.3.1.2 Screening of miR-24 in CHO2B6 cells

To investigate whether the impact of miR-24 observed in CHO1.14 cells was reproducible in other CHO cell lines, functional validation was repeated in CHO2B6 cells.

Non-transfected CHO2B6 cells showed the expected cell growth and viability profiles.

Cells treated with the transfection reagent (neofx) on its own, pm-neg and am-neg molecules showed a cell growth reduction to the same extent. However, no detrimental side effects were observed due to the transfection process over the culture (**Figure 6.3.1.2.A**).

Following transfection of pm-24, cell growth decreased by 3-fold at day 4 and by 14-fold at day 7. Cell viability was also reduced by 1.89-fold to 18.77-fold from day 2 to day 7. Transient knockdown of miR-24 did not impact on cell proliferation or on cell viability (**Figures 6.3.1.2.A &B**).

Although the transient inhibition of miR-24 did not increase CHO2B6 cell proliferation, we had some indications that it may enhance the growth of CHO1.14 cells. In addition, the overexpression of miR-24 led to more consistent results in both cell lines suggesting that miR-24 plays some part in influencing cell growth. Therefore we conducted the same transient assay in CHO-K1 SEAP cells.

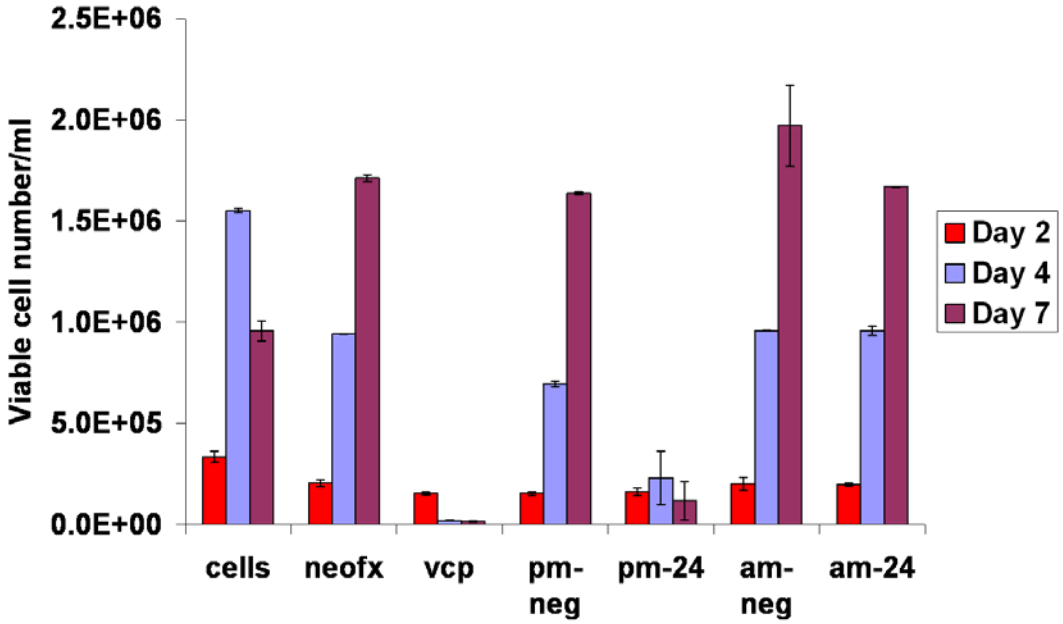

Figure 6.3.1.2.A: Impact of miR-24 on CHO2B6 cell growth.

miR-24 was up-regulated using mimic (pm) or inhibited using inhibitor (am) molecules at a concentration of 100nM. Cells were seeded at $1x10^5$cells/ml in serum-free medium and stained with GuavaViacount reagent to monitor cell growth by Guava flow cytometry at day 2, day 4 and day 7. cells: non-transfected cells; neofx: transfection reagent; vcp: siRNA against Valosin-Containing Protein (positive control of transfection efficiency); pm-neg: negative control for mimics; am-neg: negative control for inhibitors. At day 2, bars represent standard deviations of three biological replicates. At day 4 and day 7, bars represent the high and low reading of two biological replicates. There was no statistical significance found in this experiment.

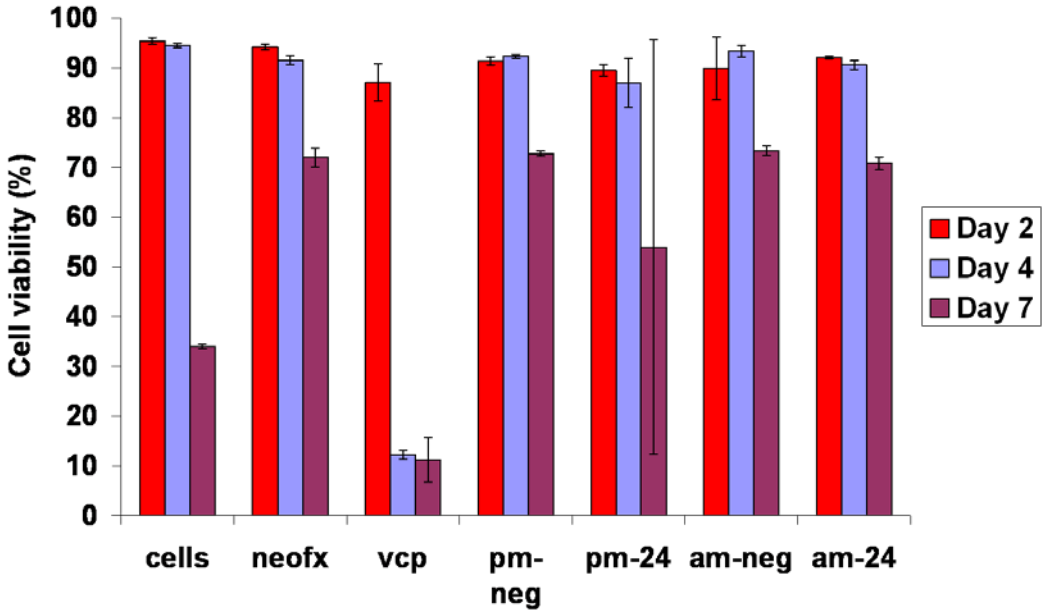

Figure 6.3.1.2.B: Impact of miR-24 on CHO2B6 cell viability.

miR-24 was up-regulated using miRNA mimic (pm) or inhibited using miRNA inhibitor (am) at a concentration of 100nM. Cells were seeded at $1x10^5$cells/ml in serum-free medium and stained with GuavaViacount reagent to monitor cell growth by Guava flow cytometry at day 2, day 4 and day 7. cells: non-transfected cells; neofx: transfection reagent; vcp: siRNA against Valosin-Containing Protein (positive control of transfection efficiency); pm-neg: negative control for mimics; am-neg: negative control for inhibitors. At day 2, bars represent standard deviations of three biological replicates. At day 4 and day 7, bars represent the high and low reading of two biological replicates. There was no statistical significance found in this experiment.

6.3.1.3 Validation of transient overexpression and knockdown of miR-24

Before continuing the investigation on the potential of miR-24 in affecting cell proliferation and viability, we aimed to verify that the phenotypes observed upon pm-24 and am-24 treatment were specific to the changes in expression of miR-24. The expression levels of miR-24 were analysed using quantitative PCR at day 4 after transfection.

Levels of miR-24 were increased by $1.68x10^3$-fold in CHO 1.14 cells and by 469-fold in CHO2B6 cells in comparison to the non-specific control (**Figure 6.3.1.3**).

Surprisingly**,** knockdown of miR-24 led to a small increase of miR-24 levels in CHO1.14 cells. However it induced a 4.01-fold decrease in CHO2B6 cells**.** Knockdown of a particular miRNA could stimulate the cells to produce more of this miRNA. Another possibility is that anti-miR molecules do not induce degradation of the miRNA but rather sequestration so this duplex could be dissociated during RNA extraction process thus the level of this latter would still be detectable.

These results did not prove that miR-24 levels were down-regulated in CHO1.14 cells. Although, it seemed that miR-24 was depleted in CHO2B6 cells, there was no impact on cell proliferation.

Thus we could not conclude on the influence of miR-24 on cell growth.

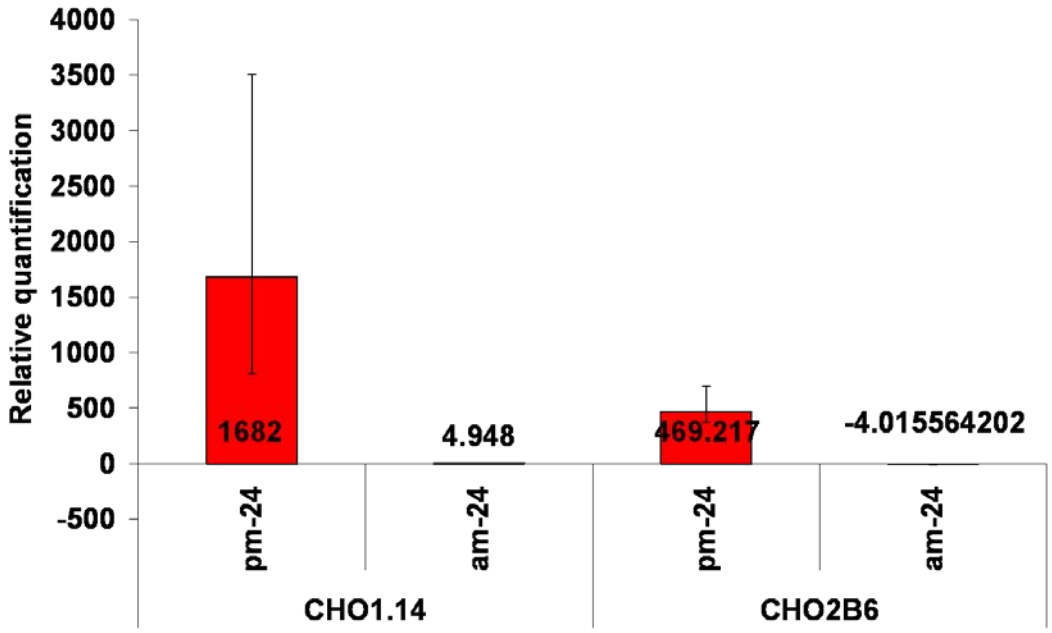

Figure 6.3.1.3: Levels of miR-24 expression in CHO1.14 and CHO2B6 cells.

Changes in miR-24 expression between pm-24/pm-neg and am-24/am-neg were analysed using TaqMan method (see materials and methods for more details on TaqMan assayin section 6.4.9) at day 4 after transfection with pm-neg, pm-24, am-neg and am-24 at a concentration of 100nM. The expression of miRNA was normalised to U6 snRNA as an endogenous control to correct for variation of RNA input. Analysis was performed using the $2^{-\Delta\Delta Ct}$ method with the AB7500 Real Time PCR instrument. Bars represent the maximum and minimum of relative quantification from two biological samples run in three technical replicates.

6.3.1.4 Screening of miR-24 in CHO-K1 SEAP cells

6.3.1.4.1 Impact of pm-24 and am-24 on cell growth and viability

To verify whether the potential of miR-24 impacting cell proliferation was reproducible using lower concentration of pre-miR and anti-miR molecules as well as broadening the screen to a third cell line, functional analysis was repeated in CHO-K1 SEAP cells. A concentration of 50nM was used to reduce the risk of off-target effects. CHO-K1 SEAP growth and viability were analysed at day 3 and day 6 after transfection in serum-free medium. Non-transfected cells showed high viability and grew as usual at early stages of culture. As previously seen, cells treated with siRNA against VCP had their cell growth reduced to very low levels and had poor viability.

Up-regulation of miR-24 reduced cell growth by 1.27-fold and provoked the maintenance of cell viability at later stages of culture (87.35% versus 56.99%; p-value= 0.0004) (**Figures 6.3.1.4.A &B**). Knockdown of miR-24 increased cell density by 1.37-fold (p-value= 0.0372) and improved cell viability significantly at day 3 after transfection (**Figures 6.3.1.4.A &B**).

Thus transfection of pm-24 molecules consistently affect cell proliferation (decrease/increase) and cell viability (improvement) between the different cell lines and assays, even though the extent at low concentration was not as striking as in the previous experiment using high levels of mimics.

Transfection of am-24 led to variability between the assays and cell lines. However, overall there were positive indications that miR-24 plays a role in CHO cell proliferation. Thus other strategies were considered to further investigate this conjecture.

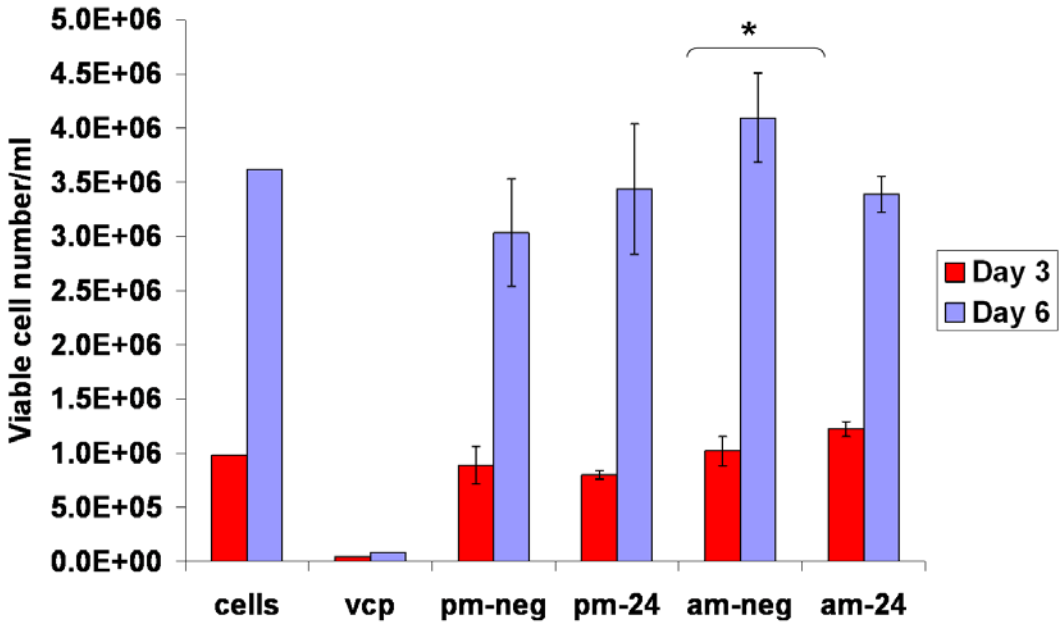

Figure 6.3.1.4.A: Impact of miR-24 on CHO-K1 SEAP proliferation.

miR-24 was up-regulated using pm-24 molecules or inhibited using am-24 molecules at a concentration of 50nM. Cells were harvested at day 3 and day 6 after transfection in serum-free medium and stained with GuavaViacount reagent to monitor cell growth by Guava flow cytometry. cells: non-transfected cells; vcp: siRNA against Valosin-Containing Protein (positive control of transfection efficiency); pm-neg: negative control for mimics; pm-24; mimic of miR-24; am-neg: negative control for inhibitors; am-24: inhibitor of mir-24. A Student t-test was performed to verify the statistical significance of the changes of miR-24 expression in pm-24/pm-neg and am-24/am-neg comparison. Bars represent standard deviations of three biological replicates. There were no replicates for cells and vcp samples. *: p-value< 0.05

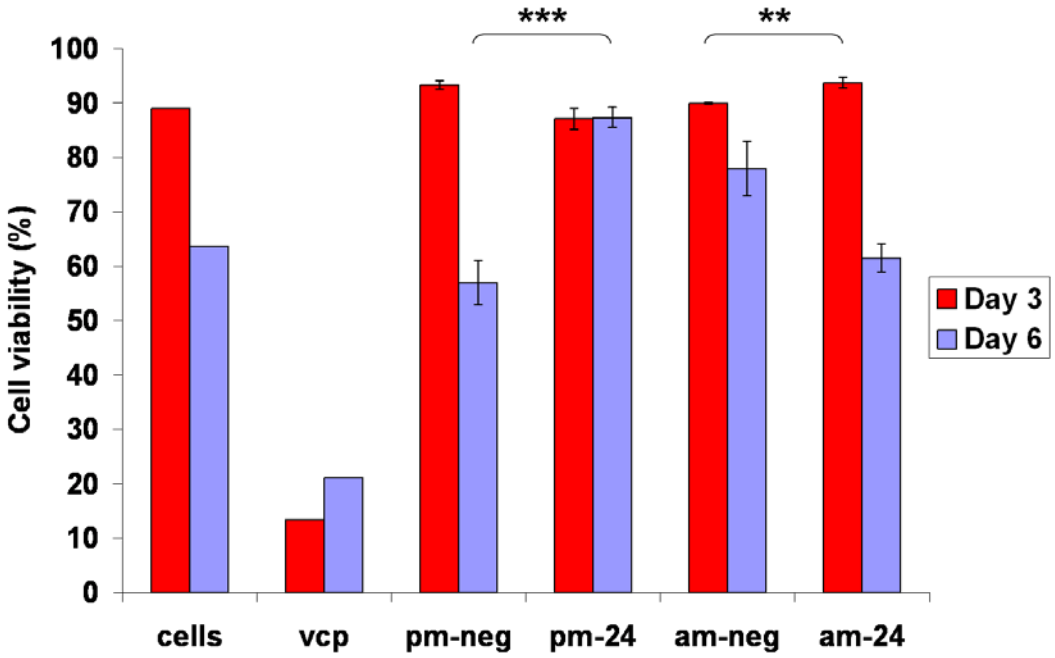

Figure 6.3.1.4.B: Impact of miR-24 on CHO-K1 SEAP viability.

miR-24 was up-regulated using pm-24 molecules or inhibited using am-24 molecules at a concentration of 50nM. Cells were harvested at day 3 and day 6 after transfection and stained with GuavaViacount reagent to monitor cell viability by Guava flow cytometry. cells: non-transfected cells; vcp: siRNA against Valosin-Containing Protein (positive control of transfection efficiency); pm-neg: negative control for mimics; pm-24; mimic of miR-24; am-neg: negative control for inhibitors; am-24: inhibitor of mir-24. For statistical analysis, pm-24 was compared to pm-neg and am-24 was compared to am-neg. A Student t-test was performed to verify the statistical significance of the changes of miR-24 expression in pm-24/pm-neg and am-24/am-neg comparison. Bars represent standard deviations of three biological replicates. There were no replicates for cells and vcp samples. **: p-value< 0.01; ***: p-value< 0.001.

6.3.1.4.2 Impact of pm-24 and am-24 on SEAP total yield and normalised productivity

To study the efficacy of miR-24 overexpression or inhibition in improving SEAP production, supernatant of samples was harvested three days after transfection. Following miR-24 knockdown, total yield was increased by 1.6-fold (p-value=0.0321) in comparison to the negative control and normalised productivity was slightly increased but it was not statistically significant (**Figure 6.3.1.4.C**). Transient overexpression of miR-24 impacted negatively on SEAP production.

These transient transfection assays were repeated several times in CHO-K1 SEAP cells. As discussed previously, variability was noticed in the results. However it may be possible to strengthen the impact of miR-24 on cell proliferation and protein production using other strategies.

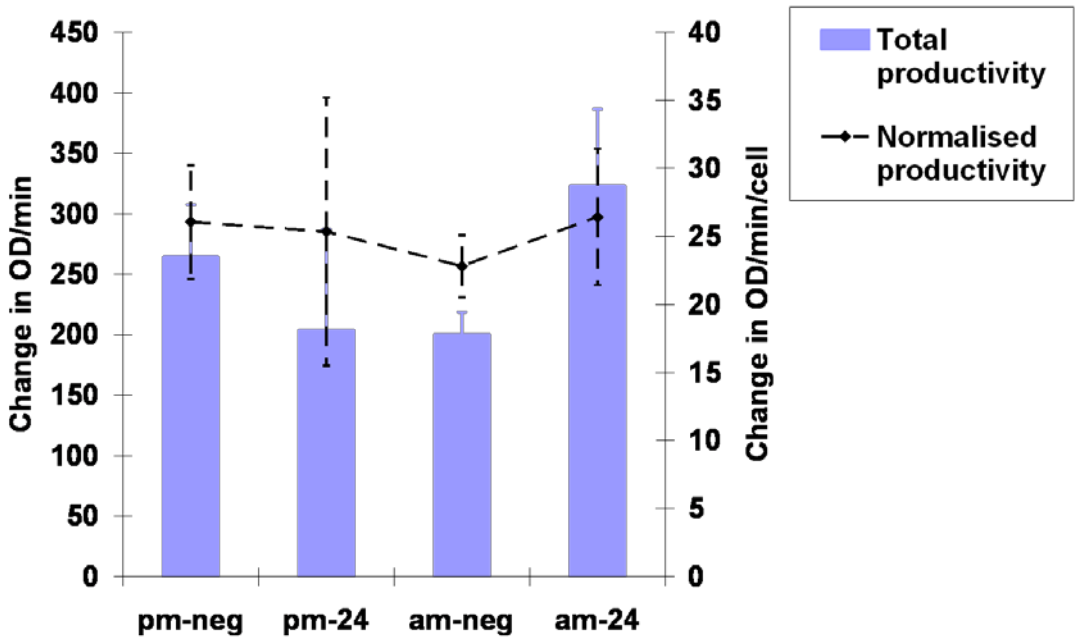

Figure 6.3.1.4.C: Impact of miR-24 on SEAP total yield and normalised productivity at day 3 following transfection.

Supernatant of pm-24 and am-24 treated cells was harvested three days after transfection. Total yield and normalised productivity of the SEAP protein were analysed by a kinetic assay (see materials and methods for details on SEAP assay). pm-neg: negative control for mimics; pm-24; mimic of miR-24; am-neg: negative control for inhibitors; am-24: inhibitor of miR-24. Statistical significance of changes in SEAP production was analysed by a Student t-test in pm-24/pm-neg and am-24/am-neg comparison. Bars represent standard deviations of three biological replicates. Each biological replicate was run in technical duplicates. *: p-value< 0.05.

6.3.2 Inducible overexpression of miR-24

Functional analysis of miR-24 using mimic and inhibitor molecules revealed that the impact on CHO cell growth and productivity was variable but held some promise. It may be that transient transfection of mimics and inhibitors leads to transient impact which typically lasts less than a week. The reproducibility between assays and cell lines was challenging and difficult to achieve even if the conditions of the repeated experiments were kept the same. Therefore we used other tools as an alternative to manipulate miR-24 expression.

6.3.2.1 Inducible overexpression of miR-24 using a tetracycline-inducible cassette

6.3.2.1.1 Description of the inducible system consisting of pMF111 and pSAM200 vectors

In the previous section, we showed that transient overeexpression of miR-24 reduced cell proliferation. To allow cells to grow to a suitable density, an inducible system was considered as an approach to induce miR-24 expression at a desirable time. We were interested in using this system in a transient manner first and if the outcome was promising to generate stable cell lines.

The assay consisted of the co-transfection of two vectors pMF111 and pSAM200 (**Figure 6.3.2.1.A**). pSAM200 vector contains a tetracycline activator (tTA) and the pMF111 vector (Fussenegger, Mazur and Bailey 1997, Mazur, et al. 1998) has a tetracycline-inducible promoter PhCMV*-1. This system allows tight regulation of gene expression by responding to the presence or absence of doxycyline in culture. In *E. coli*, the Tet repressor protein (TetR) negatively regulates the genes of the tetracycline-resistance operon on the Tn*10* transposon. TetR blocks transcription of these genes by binding to the tet operator sequences (*tetO*) in the absence of tetracycline. TetR and *tetO* provide the basis of regulation and induction for use in mammalian experimental systems.

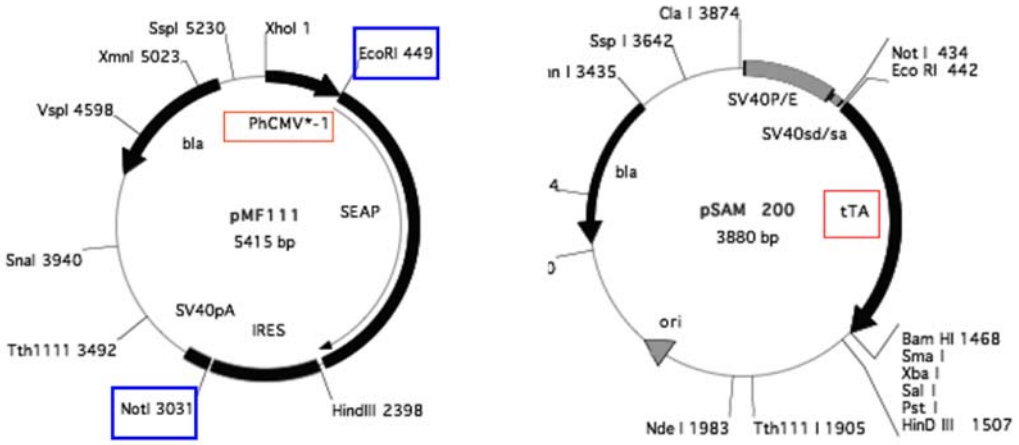

Figure 6.3.2.1.A: Maps of pMF111-SEAP and pSAM200 vectors.

- **pMF111-SEAP vector (left)**: PhCMV*: tetracycline-inducible cytomegalovirus promoter; SEAP: secreated alkaline phosphatase gene; IRES: internal ribosomal entry site allows cap-independent translation initiation; SV40 pA: Simian Virus 40 large T antigen polyadenylation signal which serves for termination of transcription; bla: bla gene encodes β-lactamase and confers resistance to the antibiotic ampicillin. Ampicilin is used in positive colonies selection in transformation assays. The two restriction enzymes, *Eco*RI (5'end) and *Not*I (3'end) used for cloning are highlighted in blue
- **pSAM 200 vector (right)**: SV40 P/E: SV 40 large T antigen promoter/enhancer; SV40 sd/sa: SV40 splice donor/splice acceptor; tTA: tetracycline activator; ori: origin of replication (site of replication initiation). bla: bla gene encodes β-lactamase and confers resistance to the antibiotic ampicillin.

In this assay, we used the Tet-OFF system where tTA binds the Tet response element (TRE) and activates transcription in the absence of doxycyline, a member of the tetracycline antibiotics group (**Figure 6.3.2.1.B**). In the presence of doxycyline, gene expression is turned off and after withdrawal of the drug, gene expression is switch on (described by Gossen & Bujard 1992(Gossen and Bujard 1992).

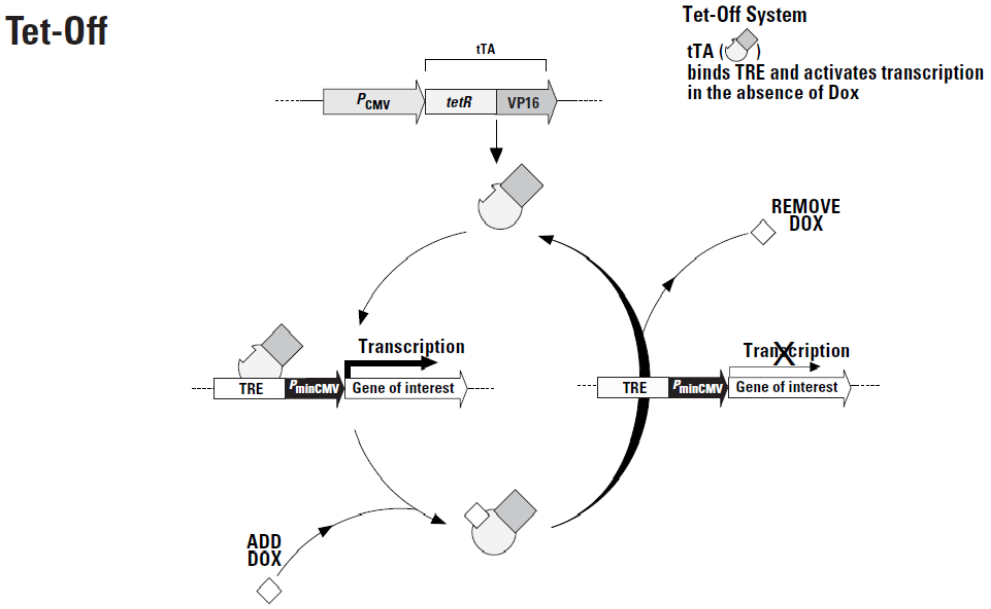

Figure 6.3.2.1.B: Description of Tet OFF gene expression system.

P_{CMV}: cytomegalovirus promoter; tetR**:** Tet repressor protein; VP16: Herpes simplex virus VP16 activation domain to convert TetR from a transcriptional repressor to a transcriptional activator also known as the tetracycline-controlled transactivator (tTA). tTA binds the Tet response element (TRE) and activates transcription in the absence of doxycyline. In the presence of doxycyline, gene expression is turned off and after withdrawal of the drug, gene expression is switch on.

Previously in our laboratory, pMF111-SEAP vector (a gift from Pr Fussenegger's laboratory) was used to stably express the SEAP gene in CHO-K1 cells (For more details refer to the thesis of Dr Niraj Kumar in 2009). The SEAP gene was removed by two restriction enzymes *EcoR*I and *Not*I and replaced by miR-24 precursor. This cloning was done by colleagues using precursor miR-24 which was isolated from CHO cells and amplified by PCR giving an amplicon of 367 bp (**Figure 6.3.2.1.C**). Precursor miR-24 consisted in the mature miR-24 strand with CHO flanking sequences. The size and sequence of the cassette were checked by digestion and sequencing prior to transfection.

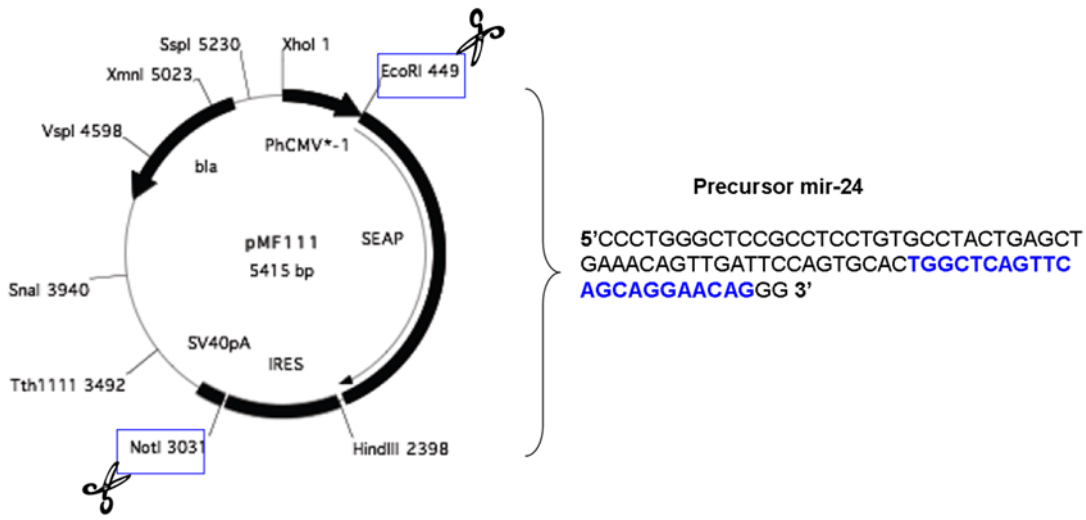

Figure 6.3.2.1.C: Schematic of precursor miR-24 insertion into pMF111 at restriction sites *EcoR*I (5'end) and *Not*I (3'end).

Forward primer: AATAGAATTCGTGTTCACAGTGGCTAAGTTCCGC (designed from human sequence);

Reverse primer: TATTGCGGCCGCGGGAACCACAGAAATCTCAAGGT (designed from mouse sequence).

The sequence shown represents the miR-24 precursor amplicon (78bp). The mature sequence of miR-24 is in blue.

6.3.2.1.2 Inducible overexpression of miR-24 using pMF111-SEAP as a negative control

Several transfection controls were included in the assay, the non-transfected cells, pMF111-SEAP, peGFP-C1 a vector that constitutively expresses enhanced green fluorescent protein (GFP; BD Biosciences) and pmF-GEO, a doxycyline inducible GFP-neomycin fusion vector. The vector pMF111-SEAP consisted of SEAP gene inserted in the vector backbone pMF111. This vector backbone was used as an empty vector control. To overexpress miR-24, the SEAP gene was removed and replaced by the CHO miR-24 precursor. peGFP-C1 and pmF-GEO vectors were used as controls for transfection efficiency and to verify the doxycyline-dependent inducibility.

To evaluate the transfection efficiency, GFP-expression was assessed in peGFP-C1 transfected cells using fluorescent microscopy the day after transfection. There were approximately 60% GFP-positive cells (**Figure 6.3.2.1.D**). The inducibility by doxycyline was also checked by fluorescent microscopy, before and after removal of the drug in pmF-GEO+ pSam200 co-transfected cells. In the presence of doxycyline, faint GFP expression was detectable thus the system was not completely turned off (**Figure 6.3.2.1.D**). After withdrawal of the drug, more GFP protein was expressed in the cells (**Figure 6.3.2.1.D**) suggesting that the co-transfection worked well. The leaky GFP expression observed in the presence of doxycyline showed that the Tet OFF system was not optimal but satisfactory for the purpose of first screening.

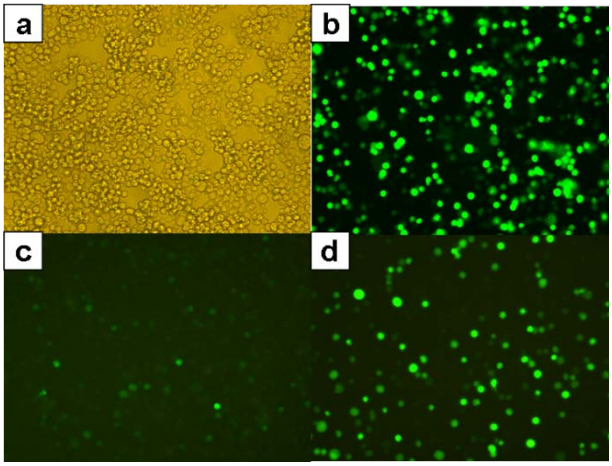

Figure 6.3.2.1.D: Detection of GFP fluorescence. a: non-transfected CHO1.14 cells; b: CHO 1.14 cells transfected with peGFP-C1; c: CHO 1.14 cells co-transfected with pmF-GEO+ pSam200 and cultured with doxycyline; d: CHO 1.14 cells co-transfected with pmF-GEO+ pSam200 and cultured without doxycyline. Magnification x10.

6.3.2.1.3 Investigation of pMF111-miR-24 impact on CHO2B6 growth and viability

To study the impact of miR-24 up-regulation on CHO phenotypes, cell growth and cell viability were monitored at day 1, day 4 and day 6 after transfection in CHO1.14 cells.
Unexpectedly, the co-transfection had a detrimental impact on cell growth in all samples cultured with doxycyline, especially four days after transfection (**Figure 6.3.2.1.E**).This impact was not detectable at earlier time point and it was abated at day 6 likely due to the loss of plasmids. In absence of doxycyline, cell growth was further reduced in all samples.
Due to the detrimental impact of transfection on cell growth, these data were difficult to analyse. Surprisingly, CHO1.14 viability was not dramatically affected by the transfection despite the impact on cell number (**Figure 6.3.2.1.F**). Non-transfected cells had a viability of 80% at day 1 whereas in other assays they usually maintained their viability around 90% at early time points. Therefore this assay was repeated in another cell line.

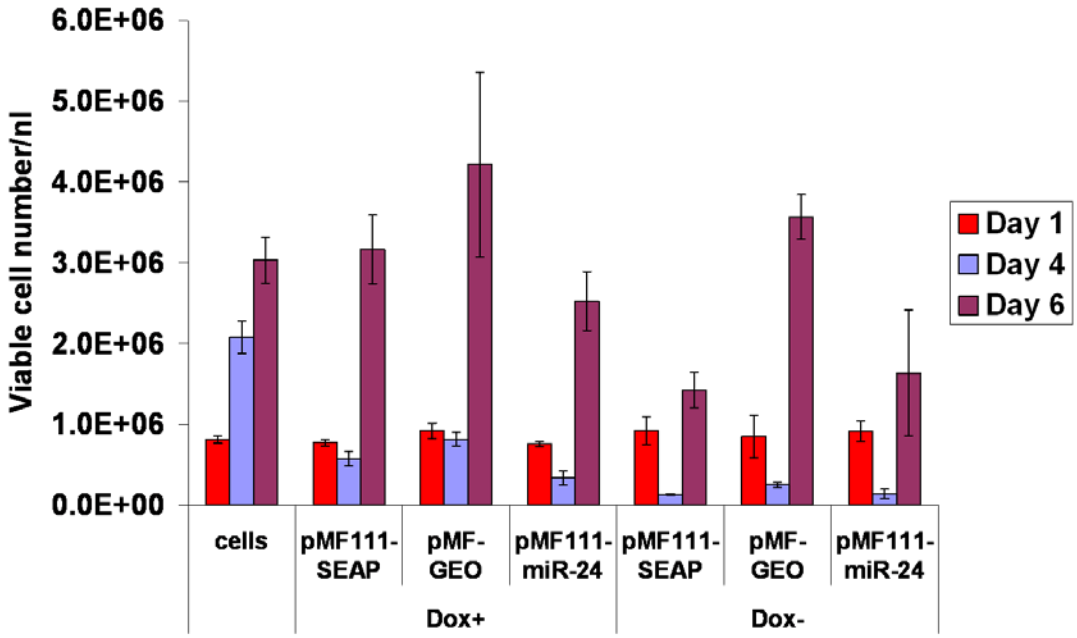

Figure 6.3.2.1.E: Impact of pMF111-miR-24 transfection on CHO1.14 growth.

Transfection was performed in suspension with 2µl of lipofectamine 2000 reagent (Invitrogen), using 1µg of plasmids, in cells seeded at a concentration of $1x10^6$cells/ml in 1ml final volume. Doxycyline was added six hours after transfection, at a final concentration of 1µg/ml. Cells were harvested and stained with GuavaViacount reagent at day 1, day 4 and day 6 to monitor cell density by Guava flow cytometry. Bars represent standard deviations of three biological replicates. Dox+: culture with doxycyline; Dox-: culture with no doxycyline.

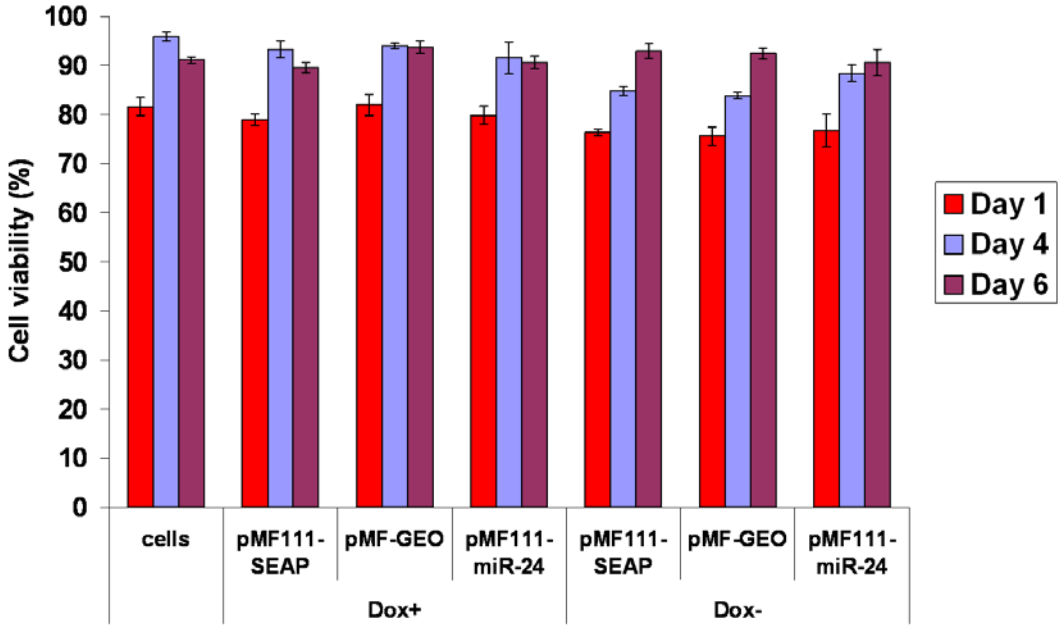

Figure 6.3.2.1.F: Impact of pMF111-miR-24 transfection on CHO1.14 viability.

Transfection was performed in suspension with 2µl of lipofectamine 2000 reagent (Invitrogen), using 1µg of plasmids, in cells seeded at a concentration of $1x10^6$cells/ml in 1ml final volume. Doxycyline was added six hours after transfection, at a final concentration of 1µg/ml. Cells were harvested and stained with GuavaViacount reagent at day 1, day 4 and day 6 to monitor cell density by Guava flow cytometry.Bars represent standard deviations of three biological replicates. Dox+: culture with doxycyline; Dox-: culture with no doxycyline.

6.3.2.1.4 Investigation of pMF111-miR-24 impact on CHO2B6 growth and viability

Transfection of pMF111-SEAP, pMF-GEO and pMF111-miR-24 was repeated in CHO2B6 cells.

Again the transfection of these vectors impacted in a non-specific manner on cell proliferation in presence of doxycyline, particularly at day 4 (**Figure 6.3.2.1.G**). However, this impact was much less pronounced than in CHO1.14 cells. Similarly, the presence of doxycyline appeared to confer some kind of protective effect compared to the culture without doxycyline.This was also more obvious on day 4, though it could be seen at day 1 also (**Figure 6.3.2.1.G**). The decrease of cell viability levels following withdrawal of doxycyline, suggested also that doxycyline protected cells against transfection toxicity (**Figure 6.3.2.1.H**).

Following removal of doxycline from the cell culture, cell growth was decreased in all samples (**Figure 6.3.2.1.G**). Surprisingly, the reduction of cell growth observed four days after pMF111-miR-24 transfection was not as obvious as for the controls. However the viability of these cells was reduced to the same extent (**Figure 6.3.2.1.H**).

Together these results revealed the non-specific impact of the transfection and doxycyline on cell proliferation and cell viability. For this reasons, it was difficult to decipher any impact of miR-24.

To eliminate the possibility of the induction of the transgene (SEAP or GEO) expression causing the observed reduction in cell numbers after doxycyline removal, the experiment was repeated in the same cell lines using pMF111 empty vector.

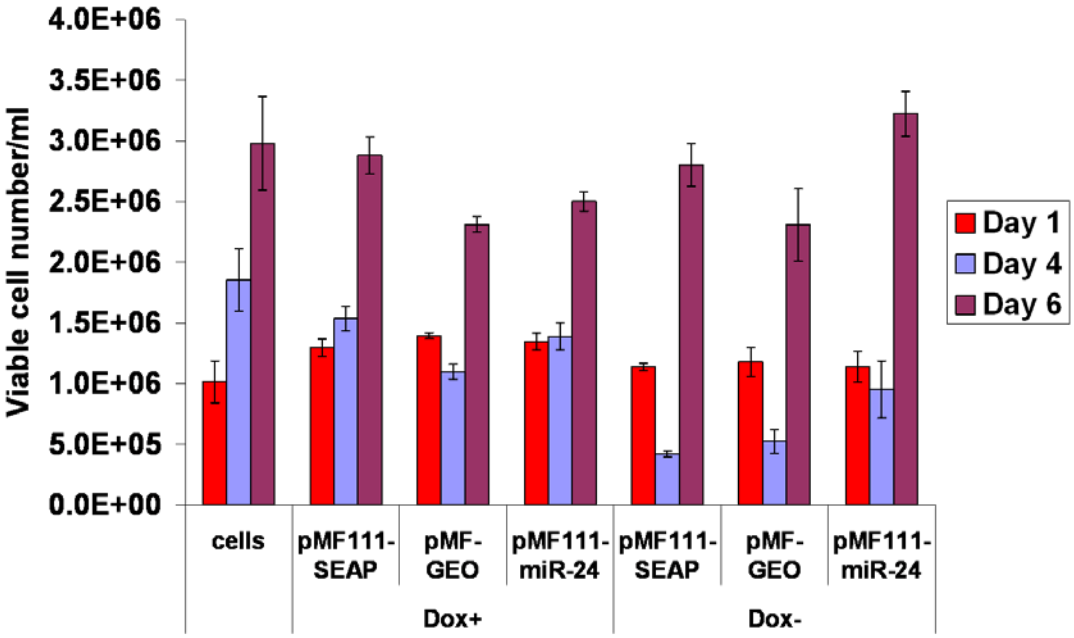

Figure 6.3.2.1.G: Impact of pMF111-miR-24 transfection on CHO2B6 growth.

Transfection was performed in suspension with 2µl of lipofectamine 2000 reagent (Invitrogen), using 1µg of plasmids, in cells seeded at a concentration of $1x10^6$cells/ml in 1ml final volume. Doxycyline was added six hours after transfection, at a final concentration of 1µg/ml. Cells were harvested and stained with GuavaViacount reagent at day 1, day 4 and day 6 to monitor cell density by Guava flow cytometry. Bars represented standard deviations of three biological replicates. Dox+: culture with doxycyline; Dox-: culture with no doxycyline.

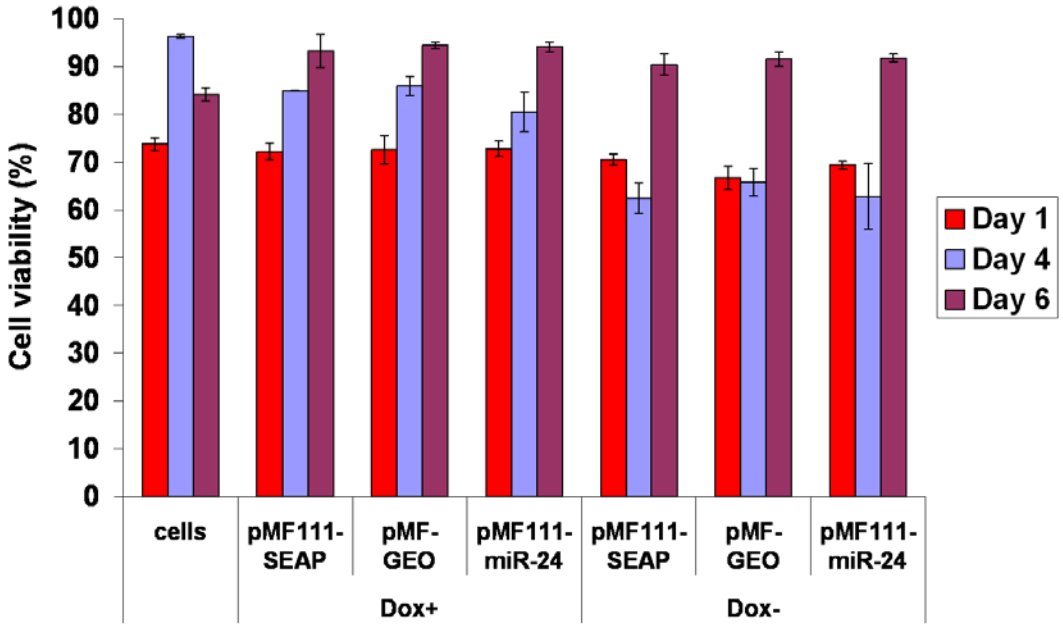

Figure 6.3.2.1.H: Impact of pMF111-miR-24 transfection on CHO2B6 viability. Transfection was performed in suspension with 2µl of lipofectamine 2000 reagent (Invitrogen), using 1µg of plasmids, in cells seeded at a concentration of $1x10^6$cells/ml in 1ml final volume. Doxycyline was added six hours after transfection, at a final concentration of 1µg/ml. Cells were harvested and stained with GuavaViacount reagent at day 1, day 4 and day 6 to monitor cell density by Guava flow cytometry. Bars represented standard deviations of three biological replicates. Dox+: culture with doxycyline; Dox-: culture with no doxycyline.

6.3.2.1.5 Inducible overexpression of miR-24 using pMF111 backbone as a negative control

In the previous attempt to overexpress miR-24 using pMF111-SEAP/pSAM200 Tet OFF system, the non-specific effect of both the transfection and doxycyline made the interpretation of the data difficult. In an effort to enhance the quality of the assay, transfection was repeated in CHO 1.14 and CHO 2B6 cells, using pMF111 empty vector as negative control. The culture conditions were kept as described in the previous section.

Prior to transfection, the plasmid pMF111-SEAP (5415bp) was digested with *EcoR*I and *Not*I to remove the SEAP gene and the digested samples were run in an agarose gel for visualisation (**Figure 6.3.2.1.I**). The size of the vector backbone and the SEAP gene were expected at 2833bp and 2582bp respectively. Due to the size of the DNA, the two bands ran very close to each other on the gel.

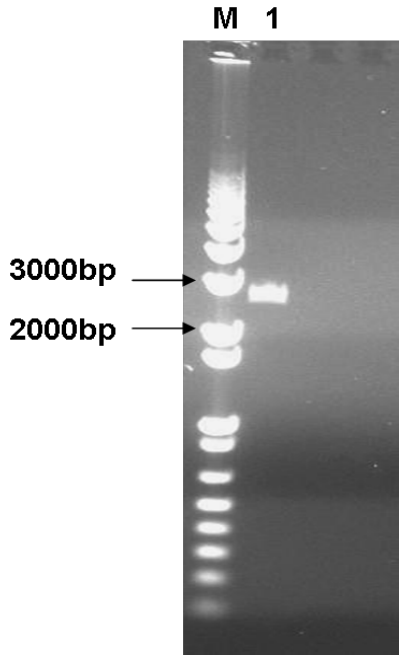

Figure 6.3.2.1.I: Digestion of pMF111-SEAP with *EcoR*I and *Not*I.

The vector pMF111-SEAP (5415bp) was digested with *EcoR*I and *Not*I to remove the SEAP gene. Following digestion, samples was run in a 1% agarose gel. Two bands were expected at 2833bp for pMF111 vector and at 2582bp for SEAP gene. M: 1kb Plus DNA ladder. Lane 1: digested pMF111-SEAP.

The plasmid was recircularised after treatment with DNA polymerase I, Large (Klenow) Fragment which creates blunt ends. The resulting colonies were miniprepped and plasmid linearised using *Eco*RI and *Not*I to verify correct size (**Figure 6.3.2.1.J**).

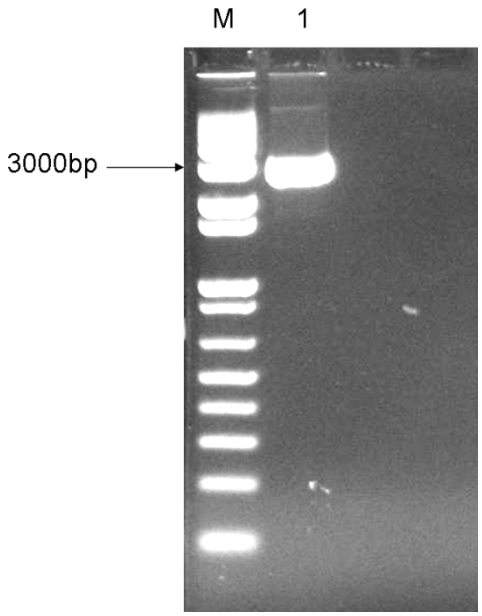

Figure 6.3.2.1.J: Linearization of pMF111 by *Eco*RI and *Not*I.

The vector pMF111 (2833bp) was linearised with *Eco*RI and *Not*I. Following digestion, samples was run in a 1% agarose gel. M: 1kb Plus DNA ladder. Lane 1: linearised pMF111.

6.3.2.1.6 Impact of pMF111-miR-24 transfection on CHO1.14 growth and viability

Although pMF111 empty vector and pMF111-miR-24 resulted in non-specific impact on cell growth in presence of doxycyline particularly at day 4, it was to a lesser extent than in the previous assay (**Figures 6.3.2.1.K &L**). Following doxycyline withdrawal, the non-specific impact on cell proliferation was further enhanced four days after transfection. In this assay, cell viability was negatively affected by the transfection in presence and in absence of doxycyline.

6.3.2.1.7 Impact of pMF111-miR-24 transfection on CHO2B6 growth and viability

In CHO2B6 cells, transfection reduced extensively cell growth in all samples in presence and after removal of doxycyline (**Figures 6.3.2.1.M &N**). Unlike the previous assays, cell viability was higher in the non-transfected cells as well as in the other samples and doxycyline withdrawal did not affect cell viability.

The results from this assay corroborated the conclusions made in the previous assay. The transfection impacted negatively on cell proliferation and often on cell viability. Doxycyline removal prevented further cell growth and usually promoted cell death increase. In most cases, the non-specific impact diminished at day 6 likely due to the loss of the plasmid. To verify whether precursor miR-24 was processed into the mature form by the cellular machinery, we investigated the levels of expression of miR-24.

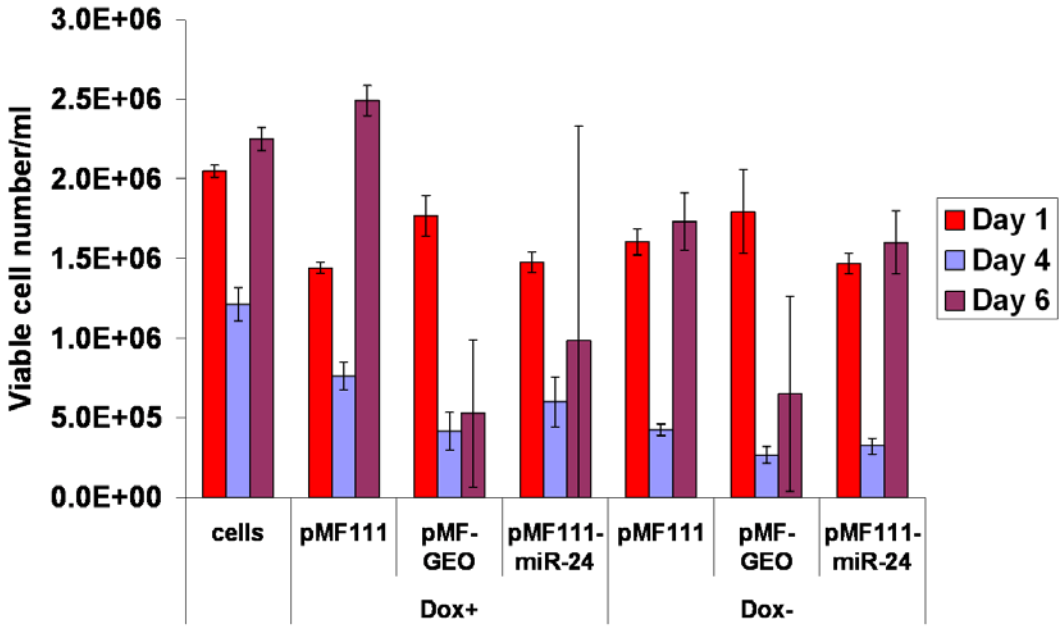

Figure 6.3.2.1.K: Impact of pMF111-miR-24 transfection on CHO1.14 growth.

Transfection was performed in suspension with 2µl of lipofectamine 2000 reagent (Invitrogen), using 1µg of plasmids, in cells seeded at a concentration of $1x10^6$cells/ml in 1ml final volume. Doxycyline was added six hours after transfection, at a final concentration of 1µg/ml. Cells were harvested and stained with GuavaViacount reagent at day 1, day 4 and day 6 to monitor cell density by Guava flow cytometry. Bars represented standard deviations of three biological replicates. The high standard deviations observed in some of the samples at day 6 are likely due to cell clumping. Dox+: culture with doxycyline; Dox-: culture with no doxycyline.

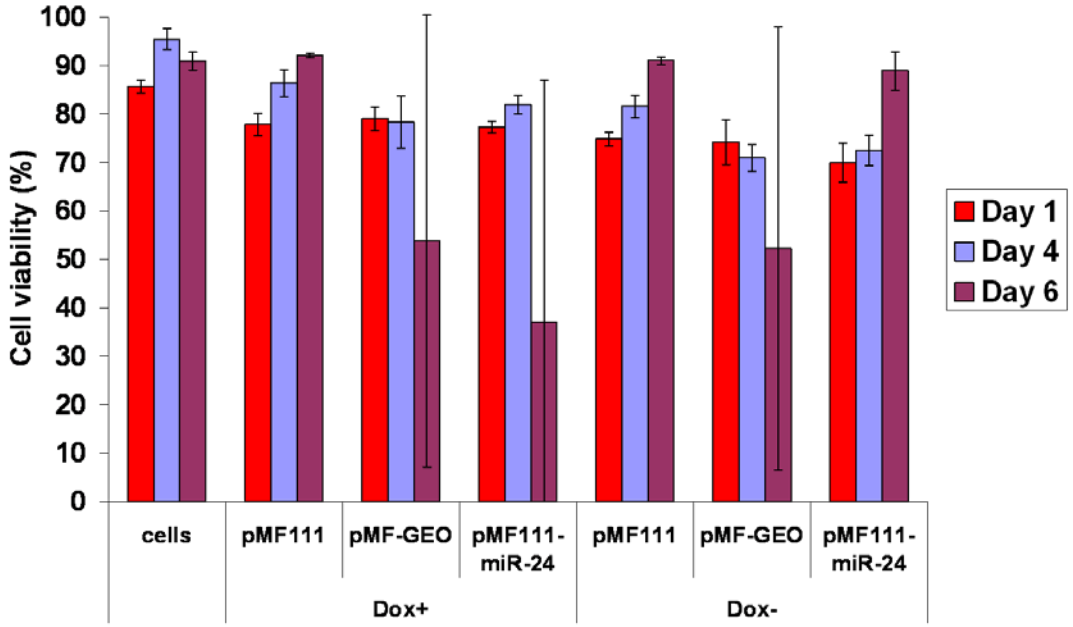

Figure 6.3.2.1.L: Impact of pMF111-miR-24 transfection on CHO1.14 viability. Transfection was performed in suspension with 2µl of lipofectamine 2000 reagent (Invitrogen), using 1µg of plasmids, in cells seeded at a concentration of $1x10^6$cells/ml in 1ml final volume. Doxycyline was added six hours after transfection, at a final concentration of 1µg/ml. Cells were harvested and stained with GuavaViacount reagent at day 1, day 4 and day 6 to monitor cell density by Guava flow cytometry. Bars represented standard deviations of three biological replicates. The high standard deviations observed in some of the samples at day 6 are likely due to cell clumping. Dox+: culture with doxycyline; Dox-: culture with no doxycyline.

.

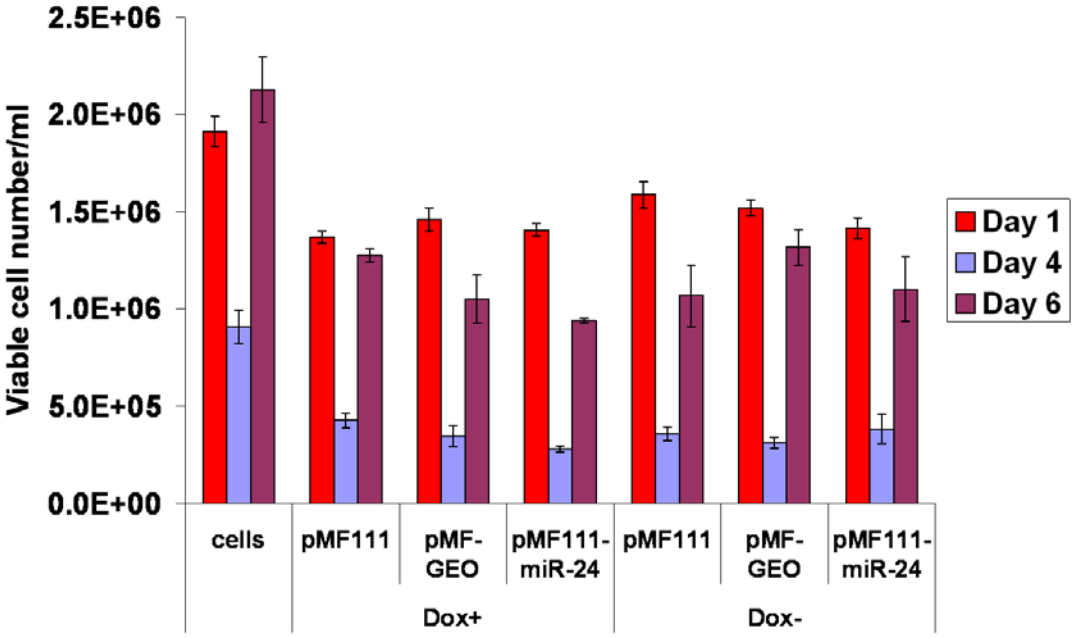

Figure 6.3.2.1.M: Impact of pMF111-miR-24 transfection on CHO2B6 growth.

Transfection was performed in suspension with 2µl of lipofectamine 2000 reagent (Invitrogen), using 1µg of plasmids, in cells seeded at a concentration of $1x10^6$cells/ml in 1ml final volume. Doxycyline was added six hours after transfection, at a final concentration of 1µg/ml. Cells were harvested and stained with GuavaViacount reagent at day 1, day 4 and day 6 to monitor cell density by Guava flow cytometry. Bars represented standard deviations of three biological replicates. Dox+: culture with doxycyline; Dox-: culture with no doxycyline.

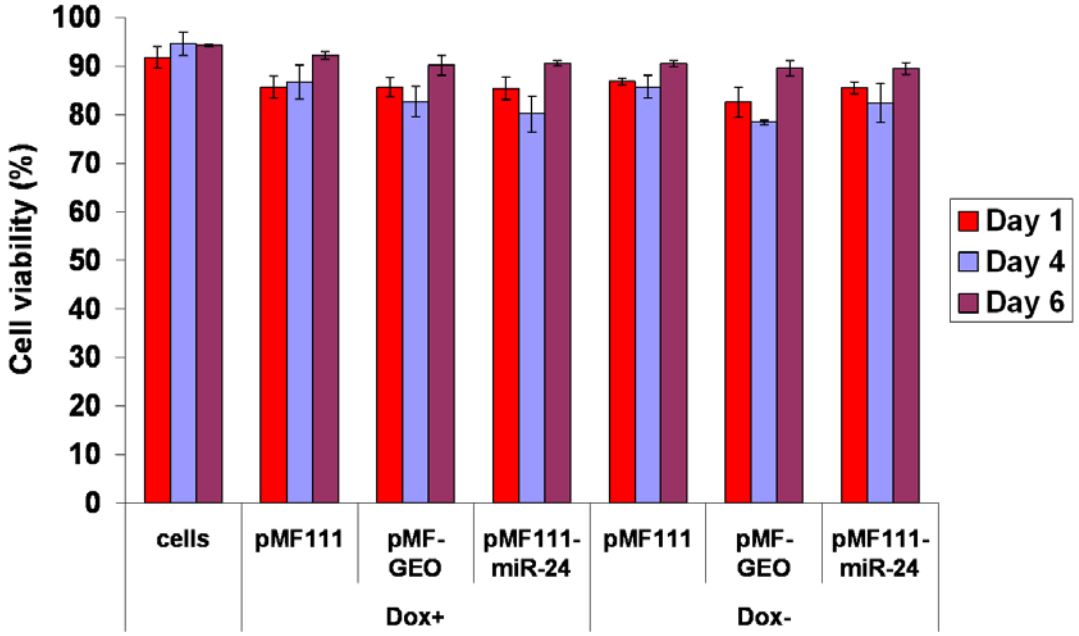

Figure 6.3.2.1.N: Impact of pMF111-miR-24 transfection on CHO2B6 viability. Transfection was performed in suspension with 2µl of lipofectamine 2000 reagent (Invitrogen), using 1µg of plasmids, in cells seeded at a concentration of $1x10^6$cells/ml in 1ml final volume. Doxycyline was added six hours after transfection, at a final concentration of 1µg/ml. Cells were harvested and stained with GuavaViacount reagent at day 1, day 4 and day 6 to monitor cell density by Guava flow cytometry. Bars represented standard deviations of three biological replicates. Dox+: culture with doxycyline; Dox-: culture with no doxycyline.

6.3.2.1.8 Investigation of miR-24 levels in pMF111-miR-24 transfected cells

To confirm that miR-24 precursor was processed correctly into the mature form and overexpressed following transfection of pMF111-miR-24 in absence of doxycyline, the levels of miR-24 expression were assessed using real-time PCR in CHO1.14 and CHO2B6 cells, in presence or absence of doxycyline.

Surprisingly, the levels of miR-24 were increased in CHO1.14 cells (**Figure 6.3.2.1.O**). In CHO2B6 cells, there was a slight decrease of the levels of miR-24 (**Figure 6.3.2.1.O**).

Although these results were not statistically significant, this suggests that miR-24 precursor was processed into miR-24 mature form in CHO1.14 cells but not in CHO2B6 cells. From previours studies, we knew that the endogenous levels of expression of miR-24 were high in both cell lines (Ct~23-24), however it is unlikely that the attempt to further overexpress miR-24 might not be successful. The issues with the Tet OFF system pMF111/pSAM200 could not be resolved at the time of the study so we considered other approaches to investigate the impact of miR-24 on cell proliferation and cell viability.

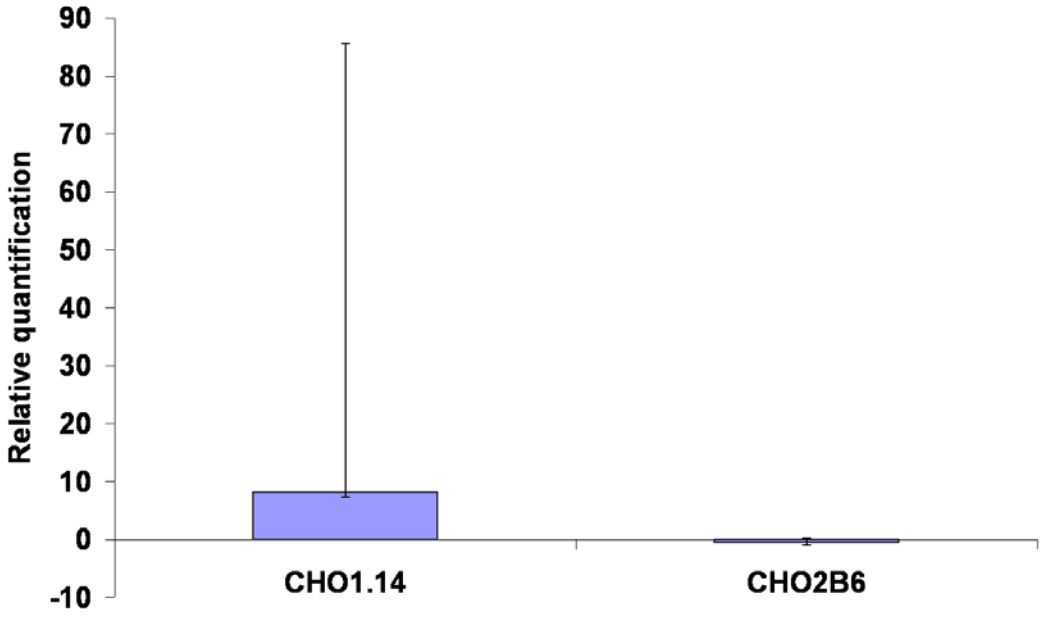

Figure 6.3.2.1.O: Levels of miR-24 expression in pMF111-miR-24 expressing CHO1.14 and CHO2B6 cells at day 4 after transfection.

Changes in miR-24 expression in pMF111-miR-24 transfected cells were analysed after removal of doxycyline at day 4 after transfection in CHO1.14 and CHO2B6 cell lines. The expression of miRNA was normalised to RNU6B as an endogenous control to correct for variation of RNA input. Analysis was performed using the AB7500 Real Time PCR instrument. Bars represent the high and low reading from two biological samples.

6.3.3 Screening of miR-23a and miR-27a

In the functional validation of miR-24 using mimic and inhibitor molecules, the changes of miR-24 expression led to variable impacts on cell proliferation and cell viability as well as between the cell lines. Overall there was a positive indication that miR-24 may influence these phenotypes particularly when using mimics. The attempt to transiently overexpress miR-24 using an inducible system was not effective due to transfection and miR-24 processing issues. Therefore we sought other approaches to continue the functional validation of miR-24.

miR-24 is co-transcribed with two other miRNAs, miR-23a and miR-27a, to form the miR-23a~miR-27~24-2 cluster. It is thought that these three miRNAs cooperate together to regulate the same cellulae pathways. It is possible that manipulating miR-24 independently of the other members of the cluster, miR-23a and miR-27a, could lead to compensation by these miRNAs. Thus this counteraction may result in restoring the original phenotype and so little or no effect might be seen. In addition, as these miRNAs are expressed at different levels in the cells, one may be more impactful on the phenotype than the others. Therefore the utility of the other cluster members, miR-23a and miR-27a, was assessed by individual or simultaneous transfection.

6.3.3.1 Screening of miR-23a in CHO-K1 SEAP cells

Mimics and inhibitors of miR-23a were transfected at 50 nM in CHO-K1 SEAP cells. Samples were harvested at day 2, day 4 and day 7 to monitor cell growth, viability and productivity.

CHO-K1 SEAP cells grew as expected for seven days. Cells treated with siRNA against VCP had their cell growth and cell viability dramatically reduced. Transfection of pm-neg and am-neg molecules provoked a decreased of cell growth at day 2 and to a lesser extent 96 hours after transfection. At day 7, cells grew rapidly in am-neg treated cells. This is possibly due to a technical problem with the preparation of the sample dilution or with the cell count.

At day 4, transfection of pm-23a led to lower cell density ($6.5x10^5$cells/ml) than in the non-specific control treated cells ($1.05x10^6$cells/ml) (**Figure 6.3.3.1.A**). At this time

point, cell viability was also reduced by nearly 10% (**Figure 6.3.3.1.B** Transient knockdown of miR-23a did not impact on cell density but slightly enhanced cell viability at day 4 after transfection (**Figures 6.3.3.1.A &B**).

As mentioned in the previous screening assays, mimics had more pronounced impact than the inhibitor molecules on the phenotypes mentionned above. This assay was repeated in the same cell lines and the same cell proliferation and viability profiles were observed. Like miR-24, miR-23a may affect cell proliferation.

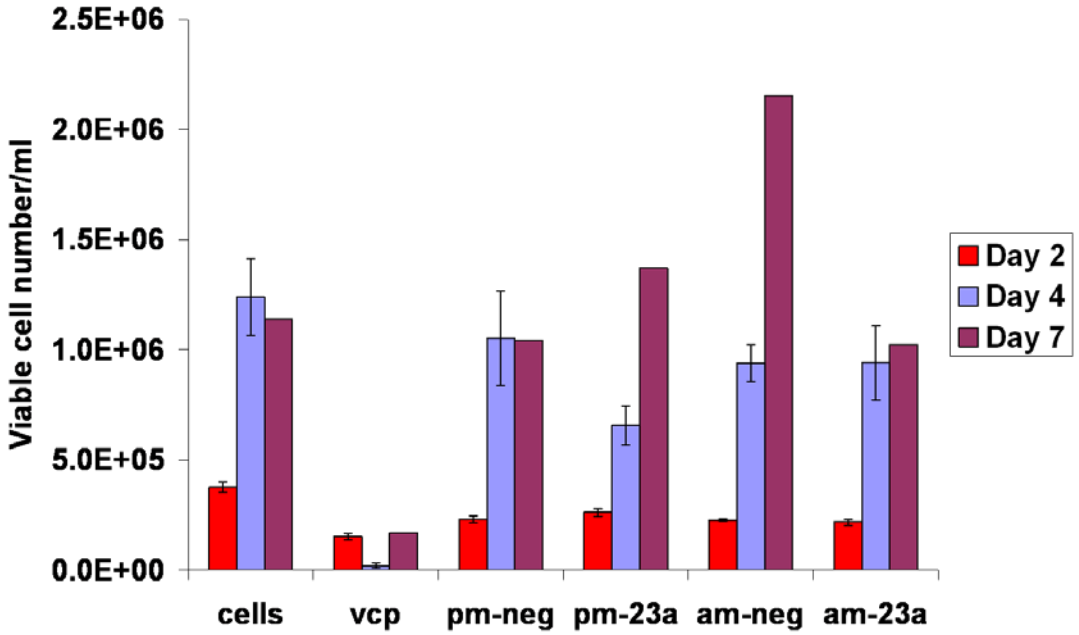

Figure 6.3.3.1.A: Impact of miR-23a on CHO-K1 SEAP growth.

miR-23a was up-regulated using pm-23a molecules or inhibited using am-23a molecules at a concentration of 50nM. Cells were harvested at day 2, day 4 and day 7 after transfection in serum-free medium and stained with GuavaViacount reagent to monitor cell growth by Guava flow cytometry. cells: non-transfected cells; vcp: siRNA against Valosin-Containing Protein (positive control of transfection efficiency); pm-neg: negative control for mimics; pm-23a; mimic of miR-23a; am-neg: negative control for inhibitors; am-23a: inhibitor of mir-23a. At day 2, bars represent stardard deviations of biological triplicates. At day 4, bars represent the high and low reading of two biological replicates. At day 7, one biological sample was monitored.

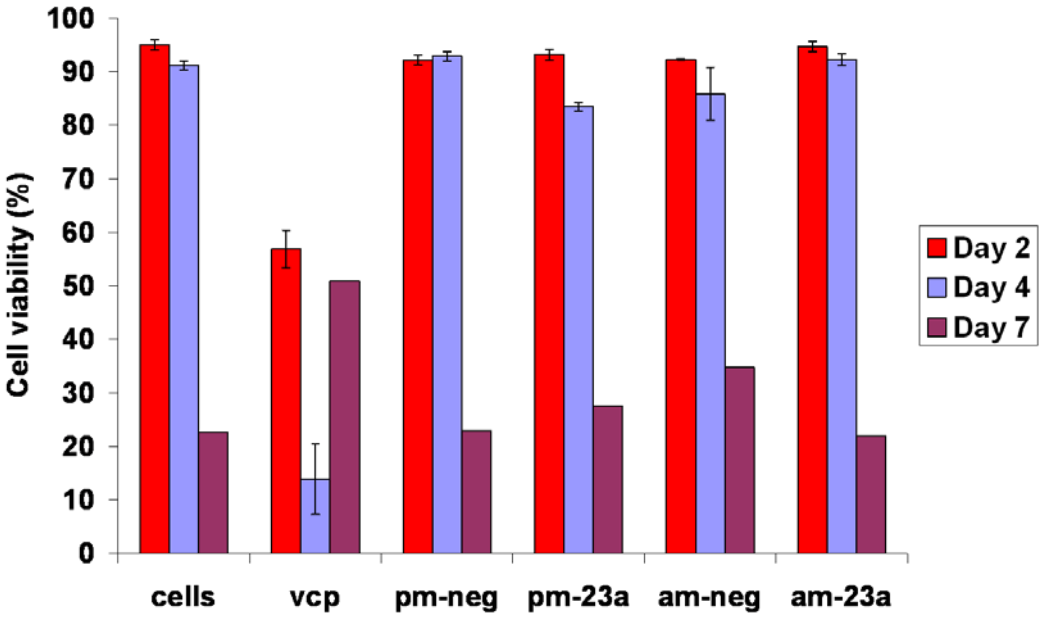

Figure 6.3.3.1.B: Impact of miR-23a on CHO-K1 SEAP viability.

miR-23a was up-regulated using pm-23a molecules or inhibited using am-23a molecules at a concentration of 50nM. Cells were harvested at day 2, day 4 and day 7 after transfection and stained with GuavaViacount reagent to monitor cell viability by Guava flow cytometry. cells: non-transfected cells; vcp: siRNA against Valosin-Containing Protein (positive control of transfection efficiency); pm-neg: negative control for mimics; pm-23a; mimic of miR-23a; am-neg: negative control for inhibitors; am-23a: inhibitor of mir-23a. At day 2, bars represent stardard deviations of biological triplicates. At day 4, bars represent the high and low reading of two biological replicates. At day 7, one biological sample was monitored.

6.3.3.2 Screening of miR-27a

6.3.3.2.1 Screening of miR-27 a in CHO1.14 cells

Screening of miR-24 and miR-23a showed a potential impact of both miRNAs on cell proliferation. To investigate whether miR-27a expressed at high concentration (100nM) would also affect cell proliferation and possibly viability, a transient transfection of pm-27a and am-27a was carried out in CHO1.14 cells and samples were harvested at day 2, day 4 and day 7 to monitor the phenotypes of interest. Non-transfected cells showed the usual profile of growth with rapid cell proliferation and appeared to maintain high viability at early stages of culture (**Figure 6.3.3.2**). As expected, knockdown of VCP impacted dramatically on cell growth and viability. Transfection of pm-neg, am-neg and the transfection reagent (neofx) on its own appeared to have a non-specific effect on these phenotypes particularly at day 4. This impact was abated after seven days of culture.

Transient overexpression of miR-27a induced a 1.35-fold cell density increase 48 hrs after transfection (p-value= 0.000257) (**Figure 6.3.3.2.A**). This advantage in cell growth was maintained at day 4 after transfection, though it was to a lesser extent. Cell viability was enhanced by 8.23% at later stages of culture (**Figure 6.3.3.2.B**).

Transient inhibition of miR-27a slightly decreased cell growth two days after transfection (**Figure 6.3.3.2.A**). Surprisingly, it increased cell density by 1.43-fold four days following transfection and enhanced CHO1.14 viability by 7.34% at the same time point (**Figures 6.3.3.2.A &B**). Despite inconsistency, these results indicated that manipulation of miR-27a expression could influence cell proliferation.

To further investigate the potential of miR-27a, we repeated the same experiment in CHO2B6 cells.

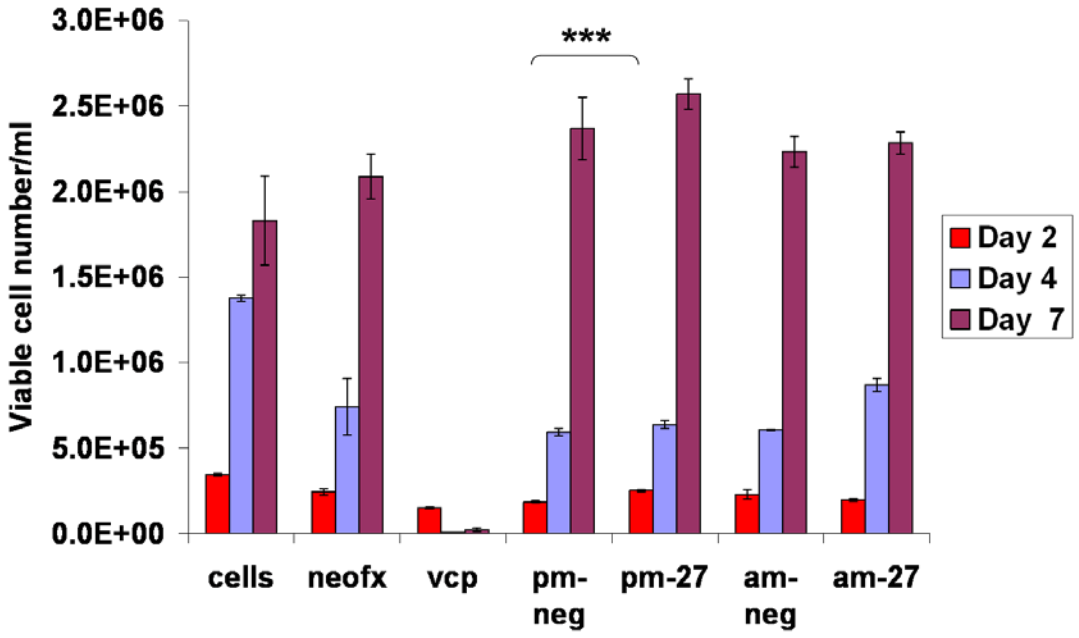

Figure 6.3.3.2.A: Impact of miR-27a on CHO1.14 growth.

miR-27a was up-regulated using pm-27a molecules or inhibited using am-27a molecules at a concentration of 100nM. Cells were harvested at day 2, day 4 and day 7 after transfection in serum-free medium and stained with GuavaViacount reagent to monitor cell growth by Guava flow cytometry. cells: non-transfected cells; neofx: lipid-based transfection reagent; vcp: siRNA against Valosin-Containing Protein (positive control of transfection efficiency); pm-neg: negative control for mimics; pm-27a; mimic of miR-27a; am-neg: negative control for inhibitors; am-27a: inhibitor of mir-27a. A Student t-test was performed to analyse the statistical significance of the impact of miR-27a overexpression or knockdown on cell proliferation compared to pm-neg and am-neg. At day 2, bars represent stardard deviations of biological triplicates. At day 4 an day 7, bars represent the high and low reading of two biological replicates. ***: p-value< 0.001 (pm-27 was compared to pm-neg at 48 hrs following transfection).

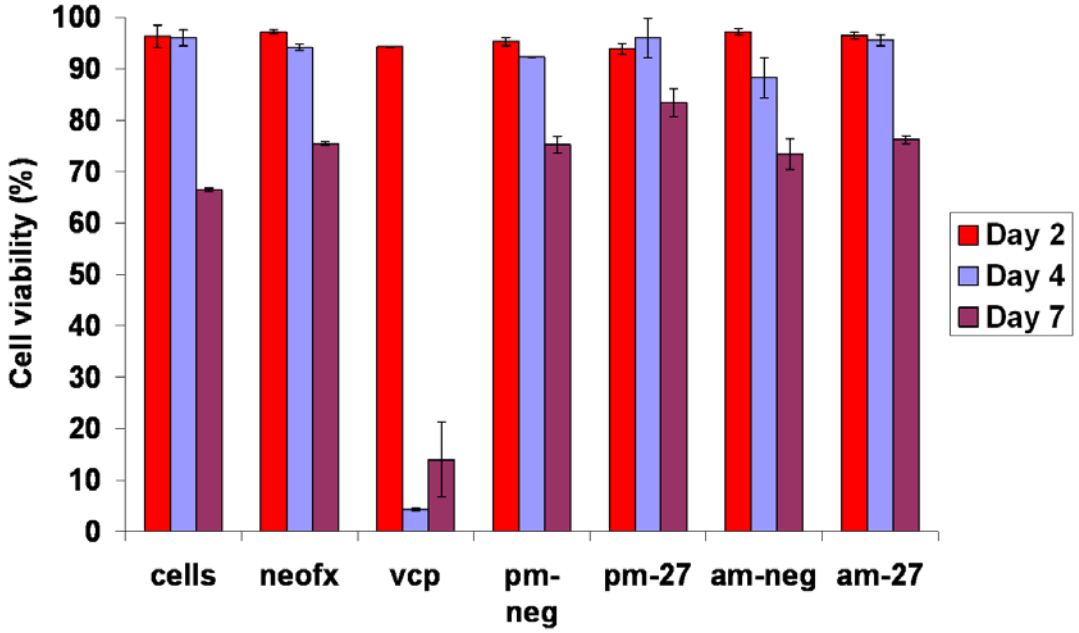

Figure 6.3.3.2.B: Impact of miR-27a on CHO1.14 viability.

miR-27a was up-regulated using pm-27a molecules or inhibited using am-27a molecules at a concentration of 100nM. Cells were harvested at day 2, day 4 and day 7 after transfection in serum-free medium and stained with GuavaViacount reagent to monitor cell viability by Guava flow cytometry. cells: non-transfected cells; neofx: lipid-based transfection reagent; vcp: siRNA against Valosin-Containing Protein (positive control of transfection efficiency); pm-neg: negative control for mimics; pm-27a; mimic of miR-27a; am-neg: negative control for inhibitors; am-27a: inhibitor of mir-27a. A Student t-test was performed to analyse the statistical significance of the impact of miR-27a overexpression or knockdown on cell viability compared to pm-neg and am-neg. At day 2, bars represent stardard deviations of biological triplicates. At day 4 an day 7, bars represent the high and low reading of two biological replicates.

6.3.3.2.2 Screening of miR-27 a in CHO2B6 cells

To investigate whether the potential of miR-27a was reproducible, a transient assay was performed in CHO2B6 cells, using mimic and inhibitor molecules at a concentration of 100nM. Samples were harvested at day 2, day 4 and day 7 to assess cell growth and viability.

The observations made in the previous assays for the controls were valid in this experiment. There was a non-specific impact of the transfection reagent in its own (neofx), pm-neg and am-neg molecules on cell proliferation but the viability was maintained at high levels.

Following transient up-regulation of miR-27a, cell density was improved at day 2 by 1.6-fold (p-value= 0.000328) and at day 4 by 1.35-fold (**Figure 6.3.3.2.C**)**.** Cell viability was reduced by 4.67% (p-value**=** 0.03097) and by 7.52% two and four days after transfection (**Figure 6.3.3.2.D**)**.** On the other hand, miR-27a knockdown had little impact on cell proliferation and viability (**Figures 6.3.3.2.C &D**).

Thus mimics of miR-27a improved cell growth significantly at early stages of culture, this increase being maintained at day 4 after transfection for two replicates in both CHO1.14 and CHO2B6 cell lines. Variability in the impact on both cell proliferation and viability was noticed following knockdown of miR-27a. This transient assay was repeated at lower concentration in CHO1.14 cells but the manipulation of miR-27a showed little and variable outcomes.

As mentionned previously, miR-27a, miR-24-2, miR-23a are co-transcribed to form miR-23~27a~24-2 cluster. Therefore we considered monitoring the impact of the entire cluster on CHO phenotypes rather than monitoring individual miRNA.

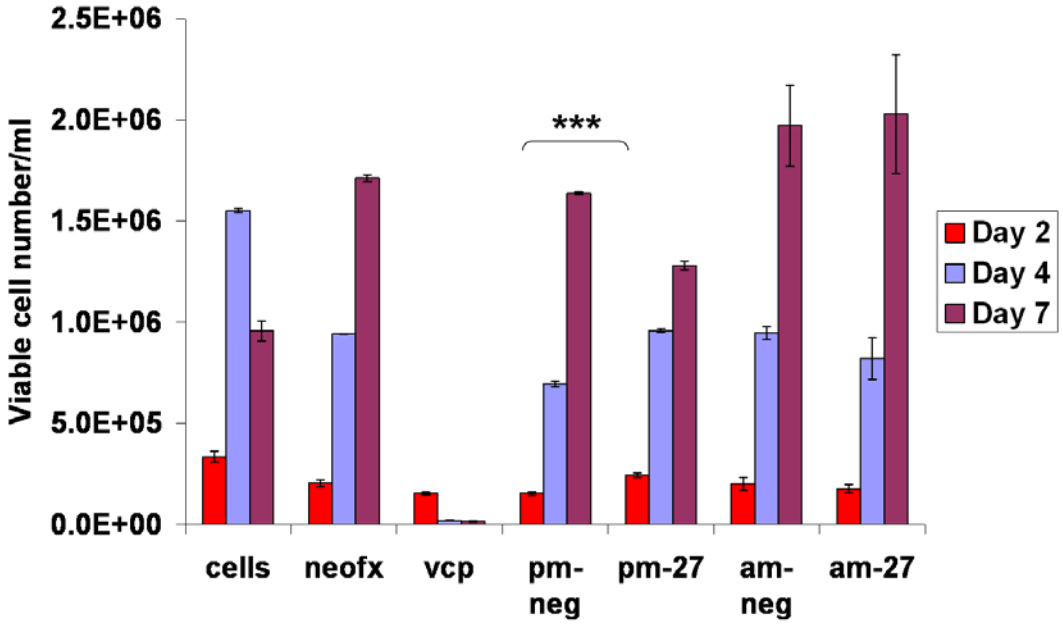

Figure 6.3.3.2.C: Impact of miR-27a on CHO2B6 growth.

miR-27a was up-regulated using pm-27a molecules or inhibited using am-27a molecules at a concentration of 100nM. Cells were harvested at day 2, day 4 and day 7 after transfection in serum-free medium and stained with GuavaViacount reagent to monitor cell growth by Guava flow cytometry. cells: non-transfected cells; neofx: lipid-based transfection reagent; vcp: siRNA against Valosin-Containing Protein (positive control of transfection efficiency); pm-neg: negative control for mimics; pm-27a; mimic of miR-27a; am-neg: negative control for inhibitors; am-27a: inhibitor of mir-27a. A Student t-test was performed to analyse the statistical significance of the impact of miR-27a overexpression or knockdown on cell proliferation compared to pm-neg and am-neg. At day 2, bars represent stardard deviations of biological triplicates. At day 4 an day 7, bars represent the high and low reading of two biological replicates. ***: p-value< 0.001 (pm-27 was compared to pm-neg treatment 48 hrs after transfection).

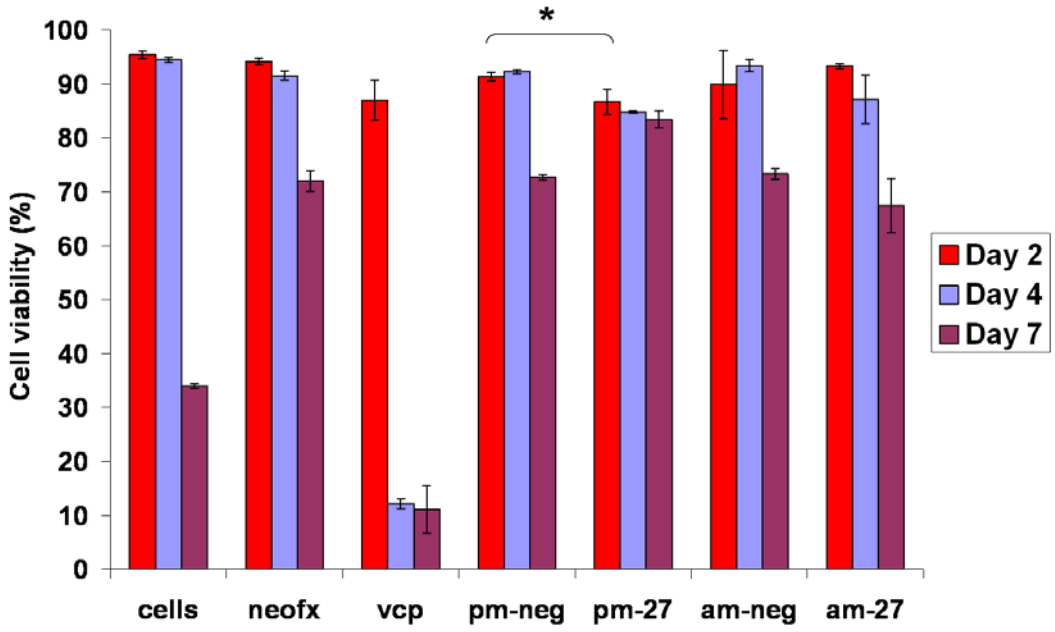

Figure 6.3.3.2.D: Impact of miR-27a on CHO2B6 viability

miR-27a was up-regulated using pm-27a molecules or inhibited using am-27a molecules at a concentration of 100nM. Cells were harvested at day 2, day 4 and day 7 after transfection and stained with GuavaViacount reagent to monitor cell viability by Guava flow cytometry. cells: non-transfected cells; neofx: lipid-based transfection reagent; vcp: siRNA against Valosin-Containing Protein (positive control of transfection efficiency); pm-neg: negative control for mimics; pm-27a; mimic of miR-27a; am-neg: negative control for inhibitors; am-27a: inhibitor of mir-27a. A Student t-test was performed to analyse the statistical significance of the impact of miR-27a overexpression or knockdown on cell viability compared to pm-neg and am-neg. At day 2, bars represent stardard deviations of biological triplicates. At day 4 an day 7, bars represent the high and low reading of two biological replicates. *: p-value< 0.05 (pm-27 was compared to pm-neg treatment 48 hrs after transfection).

6.4 Screening of miR-23a~27a~24-2 cluster on CHO phenotypes

6.4.1 Impact of miR-23~27a~24-2 cluster on CHO-K1 SEAP growth and viability

Individual transfection of miR-23a, miR-27a or miR-24-2 showed positive indications that manipulation of their expression may affect cell proliferation and possibly viability. However, variability was present between the cell lines and the assays. Therefore we considered transfecting miR-23a, miR-27a and miR-24-2 simultaneously in CHO-K1 SEAP cells. To avoid saturation of the RNA interference machinery, the final combined concentration of transfected miRNAs was 50 nM. Samples were harvested at day 2, day 4 and day 7 for cell growth and viability.

Cells grew as expected while maintaining high viability (**Figure 4.4.1.A**). Cells treated with pm-neg and am-neg had their cell growth reduced, particularly at day 2. This non-specific impact was not noticed at day 7 after transfection and had no major impact on cell viability (**Figures 6.4.1.A &B**).

At day 4 following up-regulation of miR-23~27a~24-2 cluster members, cell growth was decreased by 2.11-fold and had recovered by day 7 (**Figure 6.4.1.A**). Simultaneous knockdown of miR-23a, miR-27a and miR-24-2 did not impact on cell proliferation. CHO-K1 SEAP viability was enhanced slightly at day 2 following up-regulation of the miR-23~27a~24-2 cluster members and also at day 4 by 4.47% after simultaneous knockdown of miR-23a, miR-27a and miR-24 (**Figure 6.4.1.B**).

Thus simultaneous overexpression of miR-23~27a~24-2 cluster members resulted in further reduction of cell proliferation compared to the individual effect. The anti-proliferative effect of these miRNAs was noticed four days after transfection and was abated at day 7. Although the statistical significance of this impact was not demonstrated, the two biological samples had very similar cell density. This suggested that these three miRNAs may act cooperatively to influence cell growth.

Surprisingly, knockdown of the miR-23~27a~24-2 cluster members did not impact on cell proliferation and had little impact on cell viability thus suggesting that knockdown was not optimal using transient inhibitor molecules.

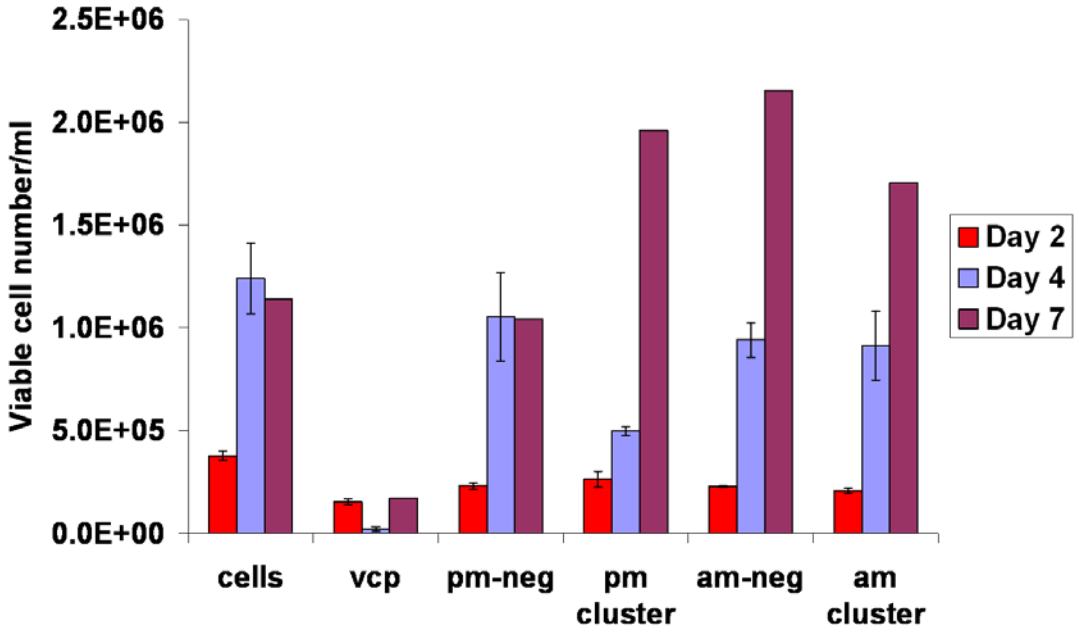

Figure 6.4.1.A: Impact of miR-23a~27a~24-2 cluster on CHO-K1 SEAP growth. Simultaneous transient transfection of miR-23a, miR-27a and miR-24-2 was performed at a final concentration of 100nM in CHO-K1 SEAP cells in serum-free medium. Samples were harvested at day 2, day 4 and day 7 and cells were stained with GuavaViacount reagent to monitor cell growth by Guava flow cytometry. cells: non-transfected cells; vcp: siRNA against Valosin-Containing Protein (positive control of transfection efficiency); pm-neg: negative control for mimics; pm cluster: mimics of miR-23a/miR-27a/24-2; am-neg: negative control for inhibitors; am cluster; inhibitors of miR-23a/27a/24-2 cluster. At day 2, bars represented standard deviations for biological triplicates. At day 4, the bars indicated the high and low reading of two biological replicates.At day 7, one biological sample was analysed.

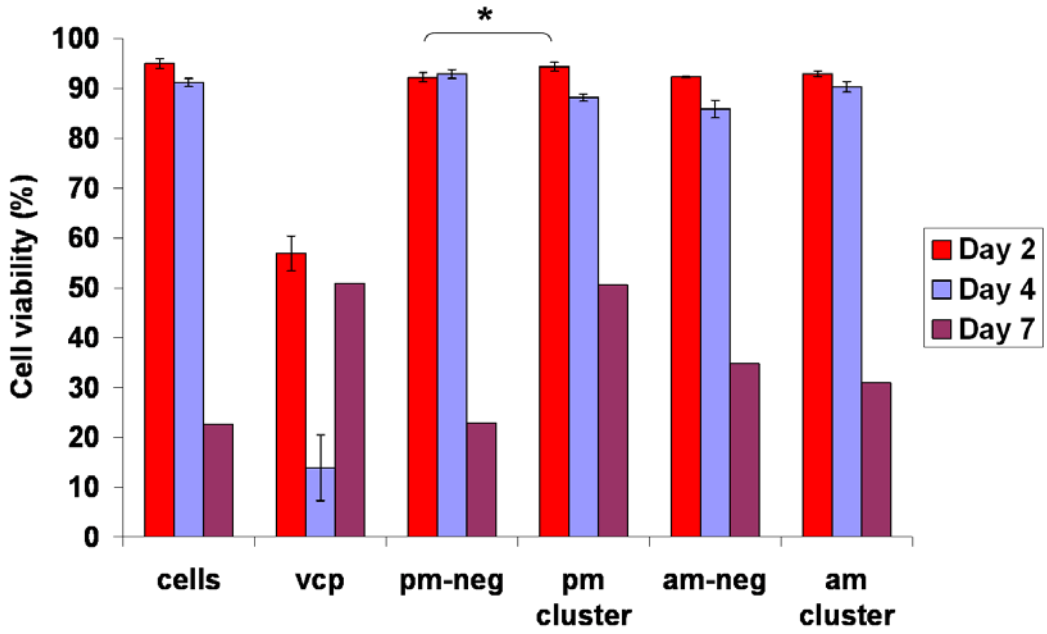

Figure 6.4.1.B: **Impact of miR-23a~27a~24-2 cluster on CHO-K1 SEAP cell viability.** Simultaneous transient transfection of miR-23a, miR-27a and miR-24-2 was performed at a final concentration of 100nM in CHO-K1 SEAP cells in serum-free medium. Samples were harvested at day 2, day 4 and day 7 and cells were stained with GuavaViacount reagent to monitor cell viability by Guava flow cytometry. cells: non-transfected cells; vcp: siRNA against Valosin-Containing Protein (positive control of transfection efficiency); pm-neg: negative control for mimics; pm cluster: mimics of miR-23a/miR-27a/24-2; am-neg: negative control for inhibitors; am cluster; inhibitors of miR-23a/27a/24-2 cluster. At day 2, bars represented standard deviations for biological triplicates. At day 4, the bars indicated the high and low reading of two biological replicates.At day 7, one biological sample was analysed. *: p-value< 0.05 (pm cluster was compared to pm-neg treatment at 48 hrs after transfection).

6.4.2 Impact of miR-23~27a~24-2 cluster on SEAP total yield and normalised productivity

To investigate the impact of the miR-23a~27a~24-2 cluster on total yield and normalised productivity supernatants were harvested at day 2, day 4 and day 7.

Total yield was negatively impacted two and four days following simultaneous overexpression of the miR-23a~27a~24-2 cluster members (**Figure 6.4.2.A**). This can be explained by the low cell number present in culture at day 4. However at day 2, cells grew as well as the control and showed increased viability. Thus it is possible that the transfection of the three inhibitor miRNAs provoked a reduction of total yield independently of cell density at early stages of culture. On the other hand total yield was enhanced by 1.44-fold at day 7 likely due to the loss of mimics at this stage and the consequent higher cell number in culture (**Figure 6.4.2.A**). Transient knockdown of the miR-23a~27a~24-2 cluster members also reduced total yield at day 2 and day 4 and recovered by day 7 (**Figure 6.4.2.A**). Total yield decrease was independent of cell density at both time points suggesting that transfection of the three mimic miRNAs impacted negatively on total yield. However, both overexpression and knockdown showed the same impact. Thus the effect may not be specific to the changes of miRNA expression but rather may be a non-specific impact induced by the transfection process.

Normalised productivity was improved by 1.84-fold at day 4 following simultaneous up-regulation of miR-23a, miR-27a and miR-24-2 and by 1.71-fold following knockdown of the cluster at later stages of culture (**Figure 6.4.2.B**). This latter was likely due to the recovery of cells following the loss of the inhibitor molecules. Considering the lack of biological replicates in this experiment, the impact of miR-23a~27a~24-2 cluster on total yield and normalised productivity was unclear. The results from the cluster member knockdown in this assay and in the previous one indicated that knockdown was not optimal using transient inhibitor molecules. Therefore we envisaged to knockdown miR-23a~27a~24-2 cluster using another antisense approach.

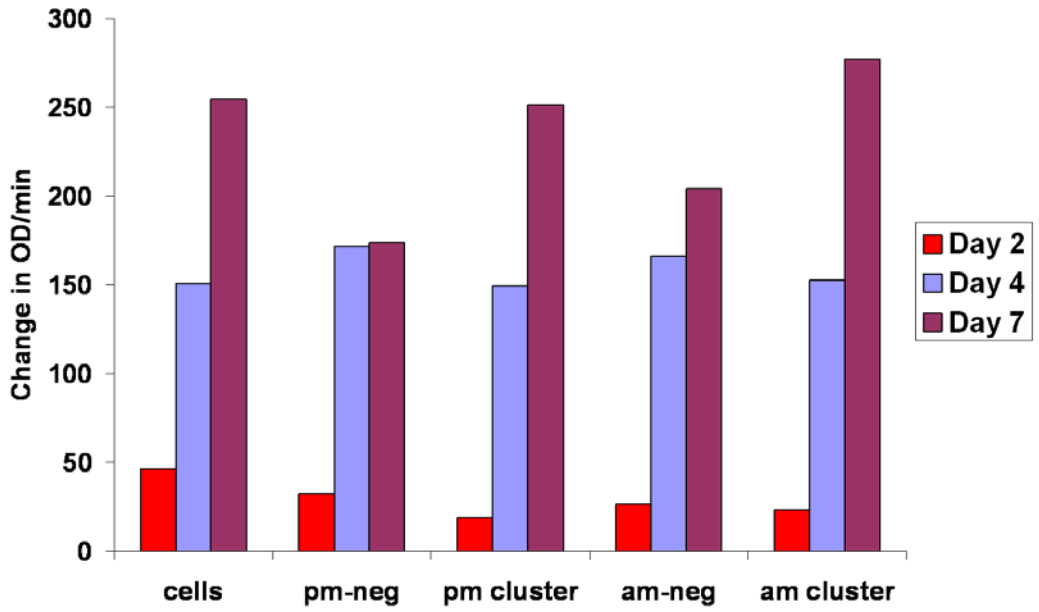

Figure 6.4.2.A: Impact of miR-23a~27a~24-2 cluster on total yield in CHO-K1 SEAP cells.

Supernatants were harvested at day 2, day 4 and day 7 after transfection in serum-free medium. SEAP total yield was analysed by a kinetic assay (see materials and methods for more details on SEAP assay in section 6.5.1). The change in absorbance of SEAP substrate, p-nitrophenolphosphate, was assessed by a spectrophotometer at 405nm. cells: non-transfected cells; pm-neg: negative control for mimics; pm cluster: mimics of miR-23a, 27a and 24-2; am-neg: negative control for inhibitors; am cluster: inhibitors of miR-23a, 27a and 24-2. One biological sample was tested in this experiment.

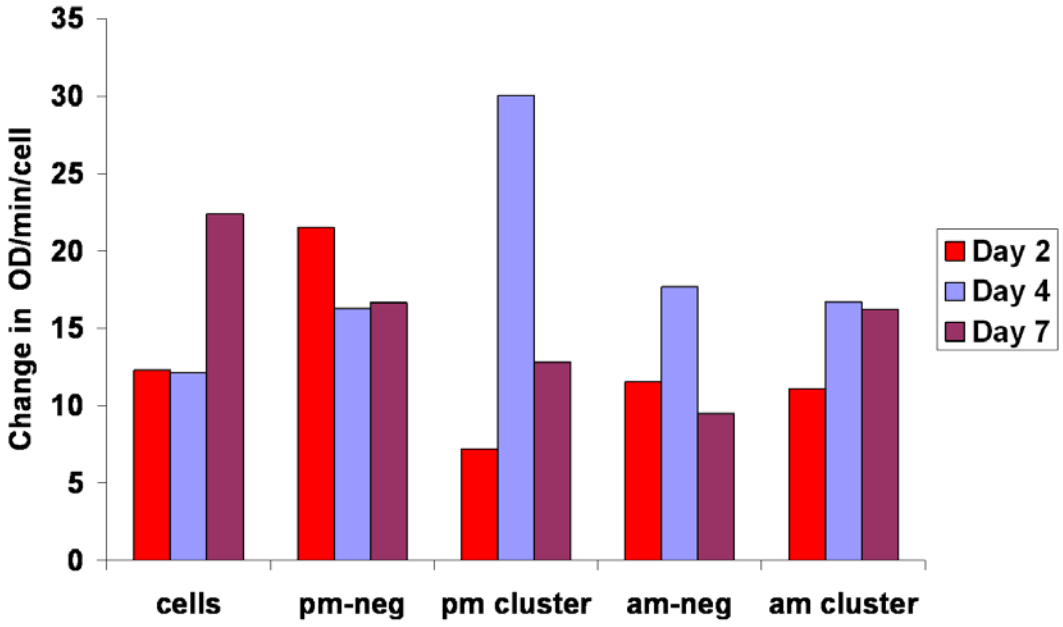

Figure 6.4.2.B: Impact of miR-23a~27a~24-2 cluster on SEAP normalised productivity. Supernatants were harvested at day 2, day 4 and day 7 after transfection. SEAP total yield was analysed by a kinetic assay (see materials and methods for more details on SEAP assay in section 6.5.1). The change in absorbance of SEAP substrate, p-nitrophenolphosphate, was assessed by a spectrophotometer at 405nm. cells: non-transfected cells; pm-neg: negative control for mimics; pm cluster: mimics of miR-23a, 27a and 24-2; am-neg: negative control for inhibitors; am cluster: inhibitors of miR-23a, 27a and 24-2. One biological sample was tested in this experiment.

6.4.3 Investigation of miR-24 targets

miR-24 has been previously shown to be involved in cell proliferation, cell cycle, apoptosis and DNA repair (Lal, et al. 2009a, Qin, et al. 2010, Mishra, et al. 2009). Our results further demonstrated the association of miR-23a~miR-27a~miR-24-2 cluster members with cell proliferation. Therefore we considered the validation of previously identified targets of miR-24 to verify whether they were conserved in CHO cells. Screening of miR-24 targets was done using several genes cited in a recent publication by Lal and co-workers (Lal, et al. 2009a) including Cyclin A, MCM4 (minichromosome maintenance complex component 4), MYC, FEN1 (Flap structure specific endonuclease I) and PCNA (proliferating cell nuclear antigen). It had been reported that these genes did not involve canonical seed pairing with miR-24 and were not predicted by seed recognition computational prediction method. However, miR-24 is a well conserved miRNA in several species so we chose the genes described in this paper to identify any changes in expression after treatment with pm-24 or am-24 at a concentration of 50nM. PABPNI (polyA binding protein, nuclear 1) was used as endogenous control. This gene was previously identified as a suitable endogenous control for qPCR studies in CHO cells (Bahr, et al. 2009). However, the expression of PABPNI was variable between samples and therefore was not a suitable endogenous control for our study. We repeated the qPCR assay using β-ACTIN as the endogenous control and PABPNI as a target. Transient knockdown of miR-24 led to up-regulation of MCM4, MYC, PCNA and PABPNI by 2- to 3.3-fold (**Figure 6.4.3.A**). Levels of FEN1 were slightly down-regulated and Cyclin A expression was not detected. On the other hand, transient up-regulation of miR-24 induced knockdown of MCM4, MYC, FENI and PABPNI by 1.25- to 4-fold (**Figure 6.4.3.B**). PCNA was slightly up-regulated. Thus MCM4, MYC, FEN1, PABPNI and CyclinA may be directly or indirectly targeted by miR-24 in CHO cells. This suggests that the role of miR-24 in the regulation of cell proliferation, cell cycle and DNA repair may be conserved in CHO cells.

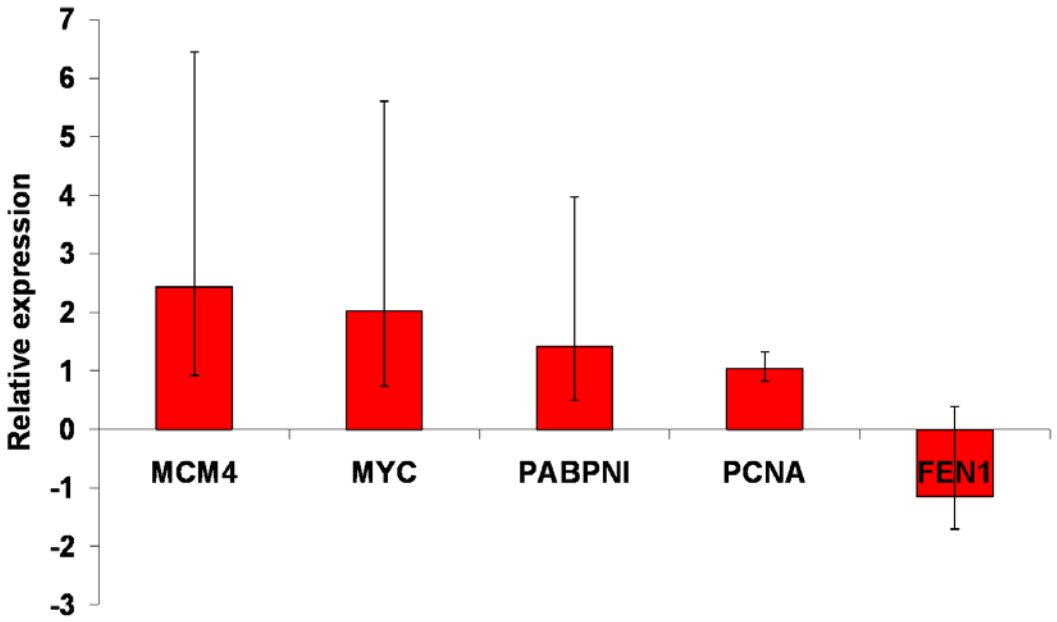

Figure 6.4.3.A: Changes in expression levels of miR-24 targets following miR-24 knockdown. Transient knockdown of miR-24 was achieved using inhibitors of miR-24 at a concentration of 50nM. Levels of expression of CyclinA, MCM4, MYC, FEN1, PCNA and PABPN1 were analysed at day 4 after transfection using the AB7500 Real Time PCR instrument. Bars represent the minimum and maximum of two biological samples run in technical triplicates.

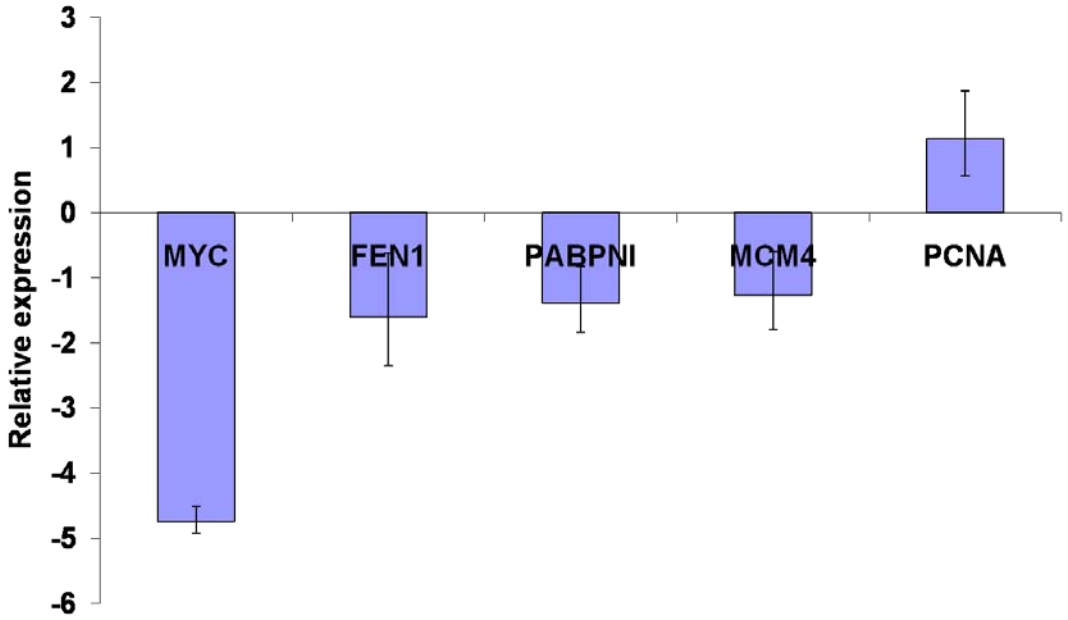

Figure 6.4.3.B: Changes in expression levels of miR-24 targets following miR-24 overexpression. Transient up-regulation of miR-24 was achieved using mimics of miR-24 at a concentration of 50nM. Levels of expression of CyclinA, MCM4, MYC, FEN1, PCNA and PABPN1 were analysed at day 4 after transfection using the AB7500 Real Time PCR instrument. Bars represent the minimum and maximum of two biological samples run in technical triplicates.

6.5 Stable knockdown of miR-23a~27a~24-2 cluster

In an attempt to circumvent the issues associated with transient transfections, we used a multiple antisense approach to simultaneoulsy inhibit the three miR-23a~27a~24-2 cluster members. This technology is similar to miRNA sponge technology but instead of targeting the seed sequence of a miRNA, the antisense transcripts are the exact antisense sequences of the mature miR-23a, miR-27 and miR-24-2.

This approach is derived from the Mtg-AMOs (multiple target anti-miRNA antisense oligonucleotideoxyribonucleotides) technology which gives the possibility to simultaneously knockdown several miRNAs as well as to impact on their mRNA targets (Lu, et al. 2009). We called this approach‘multi-antisense cluster’.

6.5.1 Vector design

Two constructs were designed one containing the exact antisense sequences of miR-23a, miR-27a and miR-24-2 cluster members (wild-type (wt) cluster) and the other containing random sequences in place of the miRNA sequences (mutant (mut) cluster) (**Figure 6.5.1.A**). miR-23a, miR-27a and miR-24-2 were linked together by a 8 nucleotide linker. At the time of the study, there was no CHO genome sequence available so the random sequence was aligned with other miRNA sequences from human, rat and mouse to minimise the potential for any off-target effects. Two restriction enzyme sites, *Xho*I and *EcoR*I were added to the 5’ and 3’end of the oligonucleotides for insertion into pd_2EFP-Hyg2 vector.

miR-23a~27a~24-2 wild type (wt cluster): Wt Cluster sense strand

5’**TCGAG**GGAAATCCCTGGCAATGTGATCTAAATGAGCGGAACTTAGCCACT GTGAACTAAATGACTGTTCCTGCTGAACTGAGCCA**G** 3’

miR-23a~27a~24-2 wild type (wt cluster): Wt Cluster antisense strand

5’**AATTC**TGGCTCAGTTCAGCAGGAACAGTCATTTAGTTCACAGTGGCTAAG TTCCGCTCATTTAGATCACATTGCCAGGGATTTCC**C** 3’

miR-23a~27a~24-2 mutant (mutt cluster): Mutt cluster sense strand

5’**TCGAG**GGAAATCCCTGGCCGCTTCAGCTAAATGAGCGGAACTTAGCCTTC CGACGCTAAATGACTGTTCCTGCTGAATCGTGATC**G** 3’

miR-23a~27a~24-2 mutant (mutt cluster): Mutt cluster antisense strand

5’**AATTC**GATCACGATTCAGCAGGAACAGTCATTTAGCGTCGGAAGGCTAAG TTCCGCTCATTTAGCTGAAGCGGCCAGGGATTTCC**C** 3’

Figure 6.5.1.A: Design of the antisense transcripts and the negative control

Underlined purple letters represent the restriction enzyme overhangs, *Xho*I and *Eco*RI. Underlined blue letters represent the 8 nt linker. Black letters represent the antisense mature miRNA sequences. The length of the four oligonucleotides was 86bp.

To obtain pd$_2$EGFP-Hyg2 vector (**Figure 6.5.1.B**), a colleague from our laboratory, Dr Nga Lao engineered different vectors derived from pcDNA5-FRT vector (Invitrogen) and pCMV-d$_2$EGFP (a gift from Pr Sharp laboratory, MIT). The pd$_2$EGFP-Hyg2 vector contains a constitutive CMV promoter, a hygromycin gene for selection and a destabilized enhanced GFP (dEGFP). This modified EGFP consists of the fusion of the ornithine decarboxylase degradation domain from mouse (MODC) and the C-terminal of an enhanced variant of GFP (EGFP). The resulting reporter is very unstable with a short half-life of 2hrs. The change of dEGFP fluorescence induced by the binding of the miRNA to the antisense transcripts cloned downstream of the d$_2$EGFP can be correlated to the changes in miRNA expression. By binding to the antisense transcripts, the miRNA prevents dEGFP from being translated so the dEGFP acts as a reporter of miRNA depletion. Once the miRNA binds to its antisense, its active levels are decreased in the cell and less miRNA molecules are available to bind to their cognate mRNA targets.

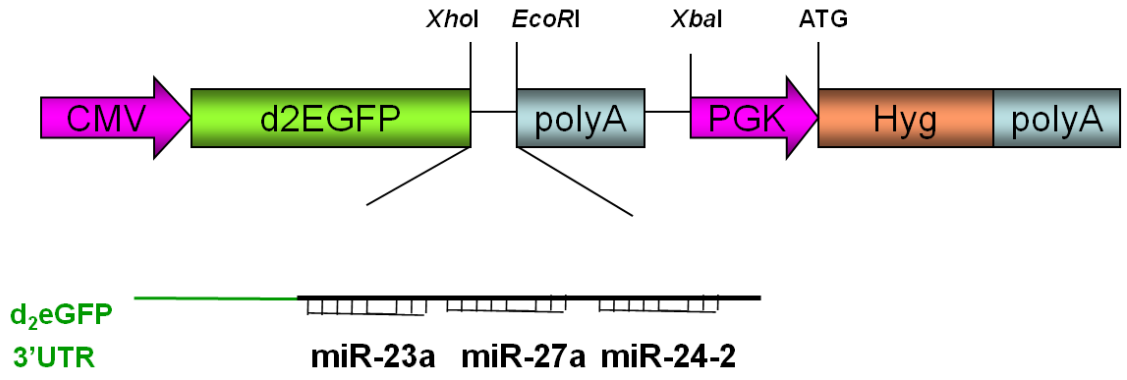

Figure 6.5.1.B: Design of pd$_2$EGFP-Hyg2 vector for miR-23a~27~24-2 cluster stable knockdown. CMV: cytomegalovirus promoter; d2EGFP: destabilized enhanced Green Fluorescent Protein; polyA: signal of polyadenylation for transcriptional termination; PGK: phosphoglycerate kinase promoter; Hyg: hygromycin (antibiotic for selection of positive clones).

Following oligonuclotide annealing and cloning of the wt and mut cluster cassettes into pd_2EFP-Hyg vector, band sizes of the two constructs were checked by digestion with *BamH*I *and Xba*I. Vector size was expected to be at 6884bp and insert at 1428bp for the wt and mutt cluster constructs (**Lane 1-3, Figure 6.5.1.C**) and bands were expected at 6884bp and 1345bp for the control (empty vector), (**Lane 4, Figure 6.5.1.C)**.

Nucleotide sequences were confirmed by sequencing and aligned against BLAST nucleotide database (**Figure 6.5.1.D**)

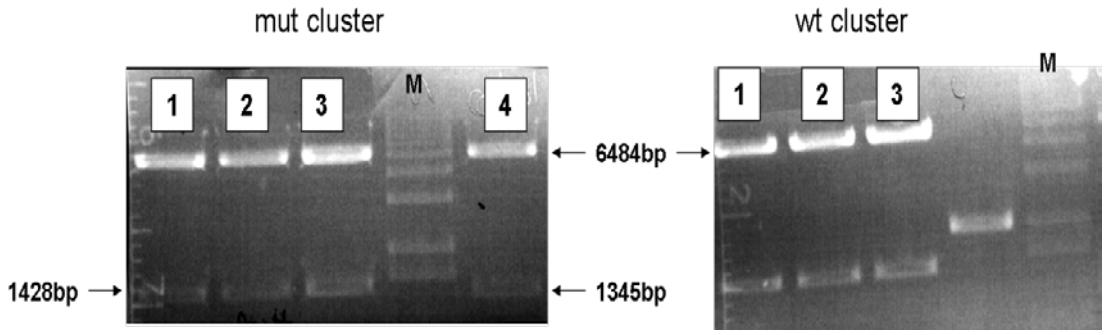

Figure 6.5.1.C: Mutant (mut) and wild-type (wt) cluster digestion with *BamHI*/*Xba*I in a 1% agarose gel.

Lanes1-3: three positive clones containing mut cluster (left panel) or wt cluster (right panel) inserted between *Xho*I and *EcoR*I. Lane 4: negative clone. M: 1kb Plus DNA ladder (Invitrogen) used to determine vector and insert sizes.

Mut cluster

GTGCTTCTGCTAGGATCAATGTGTAGGCGGCCG**CTCGAGGGAAATCCCTG**
GCCGCTTCAGCTAAATGAGCGGAACTTAGCCTTCCGACGCTAAATGACT
GTTCCTGCTGAATCGTGATCGAATTCTCGATGCATGCCTCGACTGTGCCTT
CTAGTTGCCAGCCATCTGTTGTTTGCCCCT

Wt cluster

CTTCTGCTAGGATCAATGTGTAGGCGGCCG**CTCGAGGGAAATCCCTGGCA**
ATGTGATCTAAATGAGCGGAACTTAGCCACTGTGAACTAAATGACTGTT
CCTGCTGAACTGAGCCAGAATTCTCGATGCATGCCTCGACTGTGCCTTCTA
GTTGCCAGCCATCTGTTGTTTGCCCCTCCC

Figure 6.5.1.D: Mutant (mut) and wild-type (wt) cluster sequencing

Sequencing was done by MWG eurofins using a primer that recognises a specific part of the dEGFP sequence, situated 630bp upstream of the mut and wt cluster cassette. In red are the restriction enzyme sites used for cloning, *Xho*I for the 5'end and *Eco*RI for the 3'end. The blue letters are the antisense sequences of miR-23a, miR-27a and miR-24-2 that are linked together by a 8nt linker (purple letters). The black letters represent the flanking sequencing from the pd2EGFP-Hyg2 vector.

6.5.2 Analysis in mixed population

The two constructs, mut cluster as a negative control and wt cluster, were then transfected at a concentration of 5µg/well into CHO-K1 SEAP cells, in a 6-well plate using 10µl of lipofectamine reagent. The pEGFP-C1 vector was also transfected as a control of transfection efficiency (estimated at approximately 60% by guava flow cytometry). The next day two wells were used to evaluate the levels of expression of miR-24 using real-time PCR and one well was kept to generate stable cell lines (**Figure 6.5.2**). miR-24 was down-regulated by 1.81-fold in the wt cluster transfected cells in comparison to the mutt cluster expressing cells. Thus this was a good indication that miR-24 was targeted by the wt cluster.

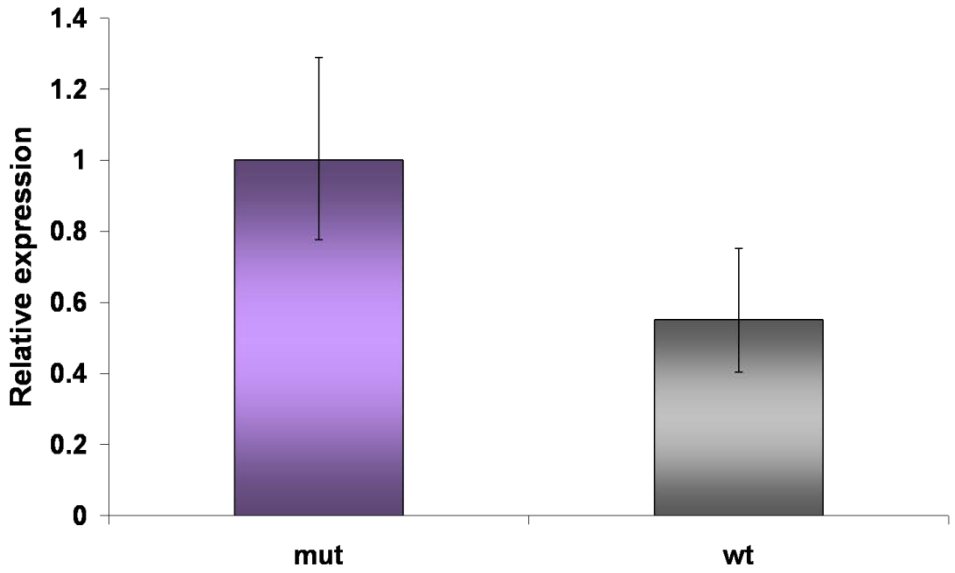

Figure 6.5.2: Evaluation of miR-24 expression in mut and wt cluster transfected cells. Changes in miR-24 expression in mut and wt cluster expressing cells were analysed 24 hours after transfection with the AB7500 Real Time PCR instrument. The expression of miR-24 was normalised to U6 snRNA as an endogenous control to correct for variation of RNA input. Mut: miR-24 expression in mutant cluster transfected cells; wt: miR-24 expression in wild type cluster transfected cells. Bars represent the high and low reading of two biological samples run in technical triplicates.

To generate stable mut and wt cluster expressing cell lines drugs were added two days after transfection. G418 was added at 1000µg/ml to maintain SEAP-producing cells and hygromycin was added at 350µg/ml for selection of mut cluster or wt cluster expressing cells.

Cells were transferred to a T-25 flask then scaled-up to a T-75 flask once confluent. Having generated a stable population, samples were taken to monitor cell growth, cell viability and GFP positivity.

6.5.2.1 Investigation of GFP fluorescence

The number of GFP-positive cells was measured using Guava Express Plus software on a Guava benchtop flow cytometry. In wt cluster expressing cells, the average GFP positivity in three biological triplicates was significantly lower (10-30%) than in mut cluster expressing cells (30-50%) at every time point of the cell culture (**Figure 6.5.2.1**). Thus the reduction of GFP positivity suggested that the miR-23a~27a~24-2 cluster members were binding to the wt cluster.

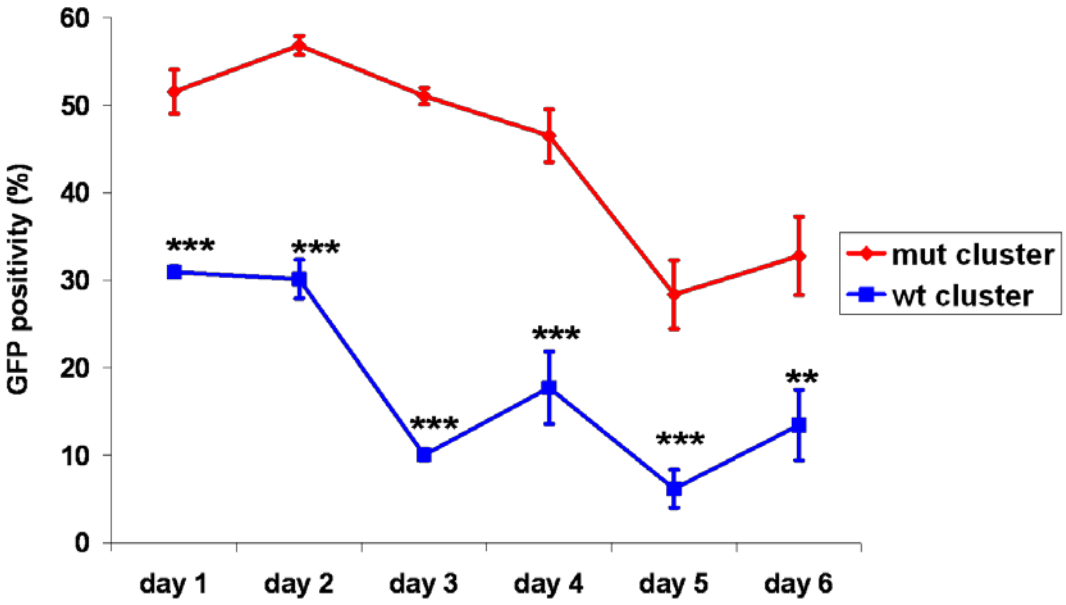

Figure 6.5.2.1: Investigation of GFP positivity in wt and mut cluster in mixed populations. Cells were seeded at $2x10^5$cells/ml in T-75 flasks in biological triplicates. Samples were harvested everyday for six days to monitor GFP positivity by Guava Flow cytometry. Bars represented standard deviations of three biological samples. A Student t-test was performed to analyse the statistical significance of any changes in GFP fluorescence. **: p-value< 0.01; ***: p-value< 0.001.

6.5.2.2 Investigation of wt cluster on cell growth and viability of mixed populations

Cell growth and viability were monitored in the same populations for six days. Overall, the wt cluster transfected cells showed increased cell proliferation compared to the control cells (**Figure 6.5.2.2.A**). At day 5, cell density was improved by 2.87-fold. However, due to high standard deviations between the three biological samples especially towards the end of the culture, this difference was only significant at day 1. The high variations may have been due to aggregation. Cell viability was reduced by 5.26% (p-value= 0.0084) at day 2 and this reduction was maintained until the fifth day (**Figure 6.5.2.2.B**). It seemed that the negative impact on cell viability was abated by day 6. However, the high standard deviations masked the real levels of cell viability particularly at later stages of culture.

Although high standard deviations were displayed towards the end of the assay, the four first days provided good indications on the positive impact of the wt cluster in mixed populations.

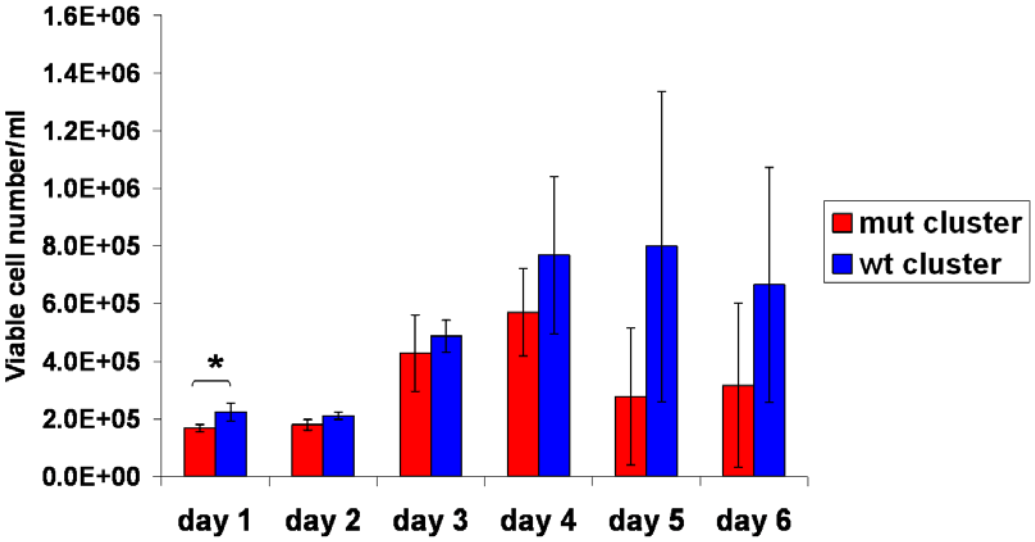

Figure 6.5.2.2.A: Profile of cell growth in wt and mut cluster transfected cells in mixed populations. Cells were seeded at $2x10^5$cells/ml in T-75 flasks in biological triplicates. Samples were harvested everyday for six days and resuspended into GuavaViacount reagent to monitor cell growth using Guava Flow cytometry. Bars represented standard deviations of three biological samples. A Student t-test was performed to analyse the statistical significance of the difference in cell density observed upon wt cluster transfection and mut cluster. *: p-value<0.05.

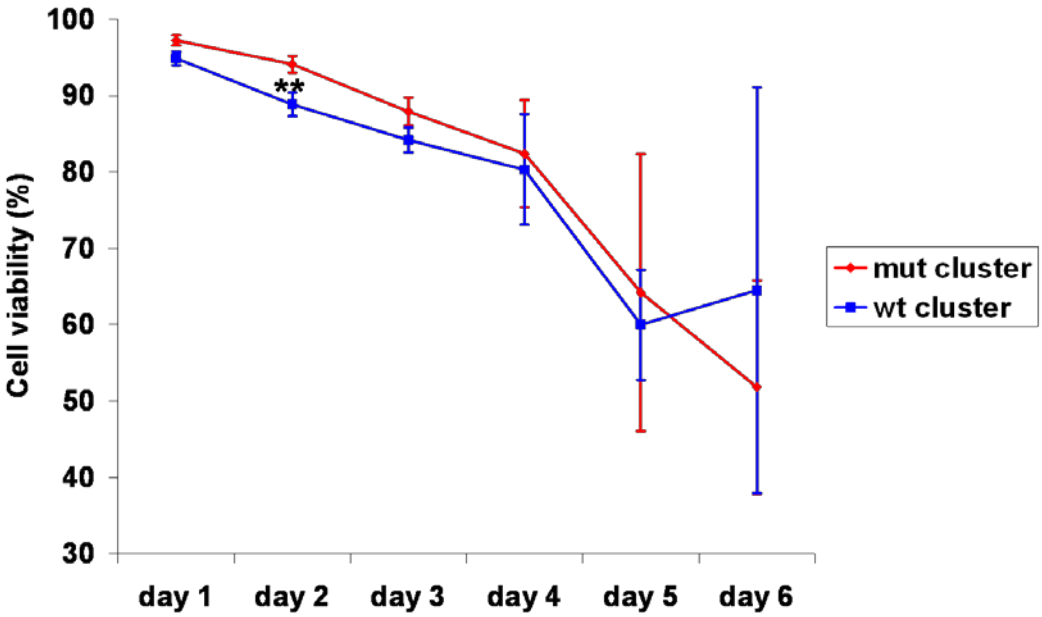

Figure 6.5.2.2.B: Profile of cell viability in wt and mut cluster transfected cells in mixed populations. Cells were seeded at $2x10^5$cells/ml in T-75 flasks in biological triplicates. Samples were harvested everyday for six days and resuspended into GuavaViacount reagent to monitor cell viability using Guava Flow cytometry technology. Bars represented standard deviations of three biological replicates. A Student t-test was performed to analyse the statistical significance of the difference in cell viability observed upon wt cluster transfection and mut cluster.

**: p-value< 0.01.

6.5.3 Analysis in single cell clones in 24-well-plate

These promising results encouraged us to pursue our investigation of stable knockdown of the miR-23a~27~24-2 cluster.

Single cell cloning was performed in 96 well plates with ATCC+5% FBS. Colonies were transferred to a 24-well plate subjected to drug selection medium. When cells reached confluence they were transferred to a 24-well plate in 1ml suspension culture. GFP fluorescence, cell growth and cell viability were monitored in 8 randomly chosen clones from the wt and the mut group by flow cytometry.

The data distribution for each group demonstrated that the median of GFP expression, representing the 50^{th} percentile (middle of the box), was lower in the wt cluster expressing cells from day 1 to day 3 (**Figure 6.5.2.3.A**). It is worth noting that there was a considerable variability in GFP fluorescence between the clones (whiskers). The median cell density was higher in wt cluster expressing cells from day 1 to day 5 with an improvement of 1.4-fold on day 5 (p-value=0.013) (**Figure 6.5.2.3.B**). In addition, the 25^{th} and 75^{th} percentiles of the data confirmed the cell growth advantage of wt cluster expressing clones particularly after day 4. The median cell viability was slightly lower in wt cluster expressing cells than in the control cells from day 1 to day 4 (**Figure 6.5.2.3.C**) but was enhanced by 12.5% by day 5 in these cells in comparison to the mutt cluster expressing cells.

The trend towards lower GFP expression and increased growth across several clones in these experiments suggested that the multi-antisense cluster was successfully depleting one or more members of the miR-23a~27~24-2 cluster in these cells.

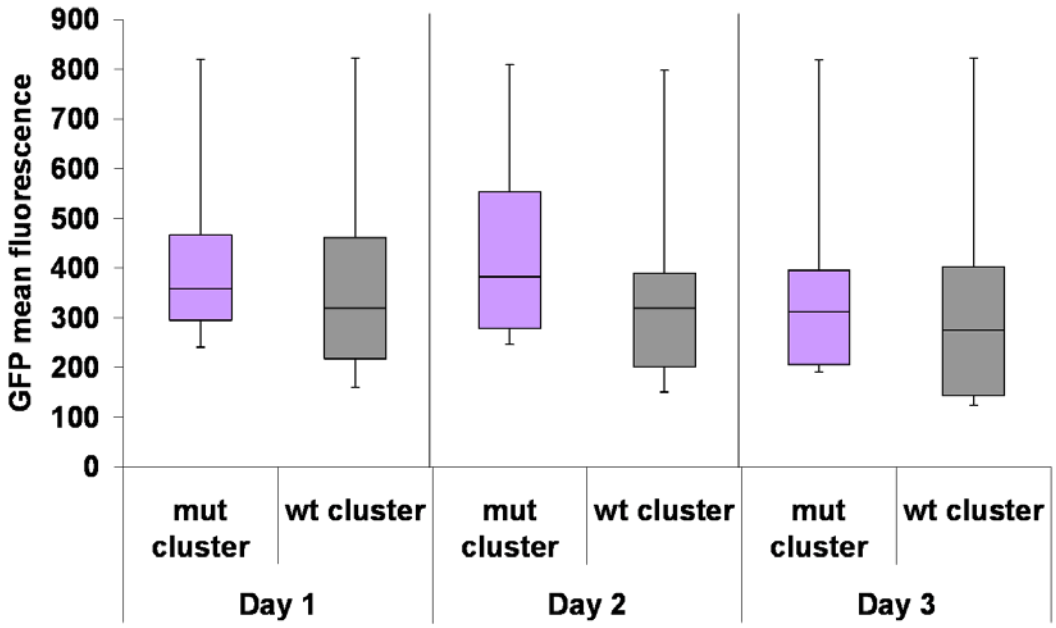

Figure 6.5.2.3.A: Distribution of GFP fluorescence in mut and wt cluster expressing CHO-K1 SEAP cells. GFP mean fluorescence was analysed using Guava Flow cytometry for 3 days. Distribution of all data was analysed for each group using the minimum, the 25%, the 75% and the maximum of all the data. The bottom and top of the box represented the 25th and 75th percentile (the lower and upper quartiles, respectively), the band near the middle of the box is the 50th percentile (the median) and the ends of the whiskers represent the minimum and the maximum of all the 8 clones for each group.

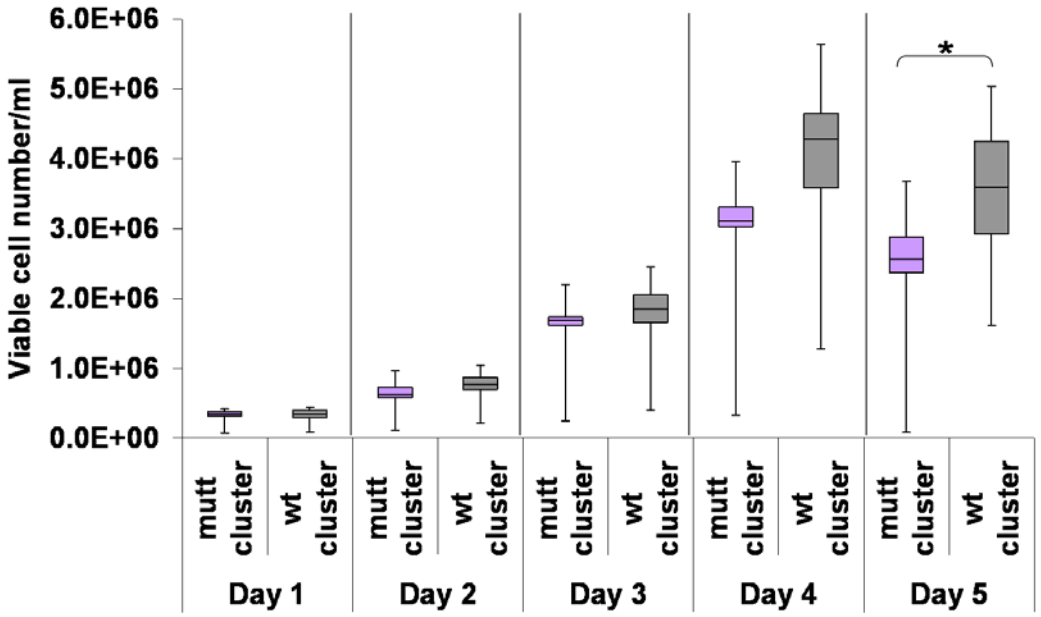

Figure 6.5.2.3.B: Distribution of cell density in mut and wt cluster expressing CHO-K1 SEAP cells. Cells were harvested every day for 5 days and stained with GuavaViacount solution to monitor cell growth by Guava Flow cytometry. Distribution of all data was analysed for each group using the minimum, the 25%, the 75% and the maximum of all the data. The bottom and top of the box represents the 25th and 75th percentile (the lower and upper quartiles, respectively), the band near the middle of the box is the 50th percentile (the median) and the ends of the whiskers represent the minimum and the maximum of all the 8 clones for each group. Statistical analysis of the mean was performed using a Student t-test. *: p-value< 0.05.

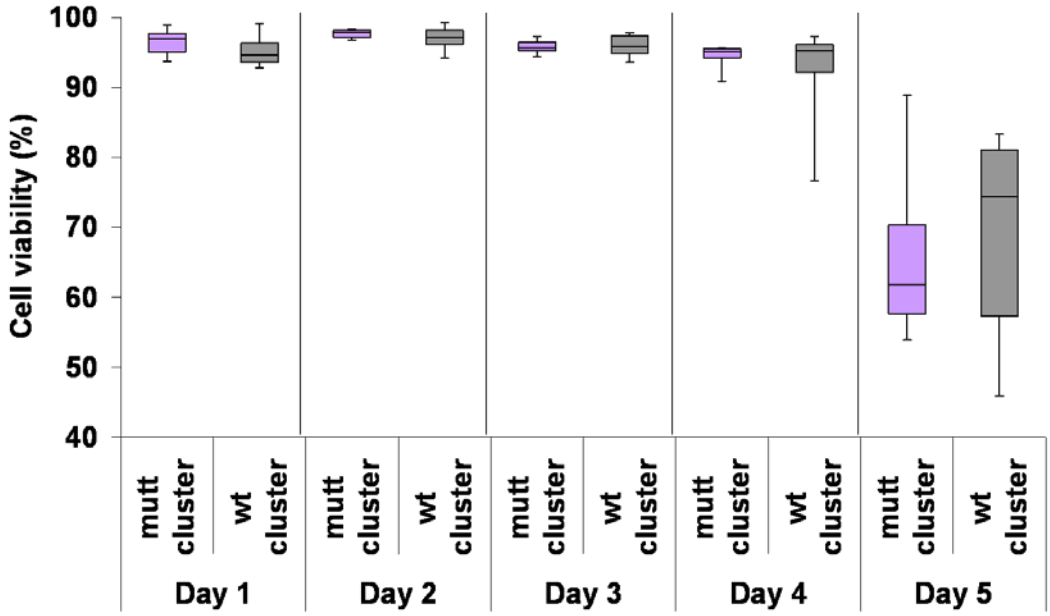

Figure 6.5.2.3.C: Distribution of cell viability in mut and wt cluster expressing CHO-K1 SEAP cells. Cells were harvested every day for 5 days and stained with GuavaViacount solution to monitor cell viability by Guava Flow cytometry. Distribution of all data was analysed for each group using the minimum, the 25%, the 75% and the maximum of all the data. The bottom and top of the box represents the 25th and 75th percentile (the lower and upper quartiles, respectively), the band near the middle of the box is the 50th percentile (the median) and the ends of the whiskers represent the minimum and the maximum of all the 8 clones for each group.

6.5.4 . Analysis in single cell clones in 5ml spin flasks

To scale up the culture, the three best performing clones from the mut and the wt cluster single populations were transferred to a 5ml suspension culture in vented flasks at 170rpm. We previously demonstrated that the cell density was improved at later stages of culture so cell density and viability were monitored from day 3 to day 6 of culture. At day 3, cells were resuspended in fresh medium to extend the period of the culture. The cell growth profile across the three clones of a same group was very similar (**Figure 6.5.4.A**). The average cell density was enhanced at day 5 by 1.71-fold in the wt cluster expressing clones in comparison to the mut cluster clones (p-value: 0.0040) (**Figure 6.5.4.B**). This advantage was still maintained at day 6 (p-value= 0.0156). Regarding cell viability, there was no major difference between the two groups (**Figure 6.5.4.C**).

Thus these results suggested that stable knockdown of miR-23a~miR-27a~miR-24-2 cluster promoted significant advantage in cell proliferation from day 3 to day 6 of culture.

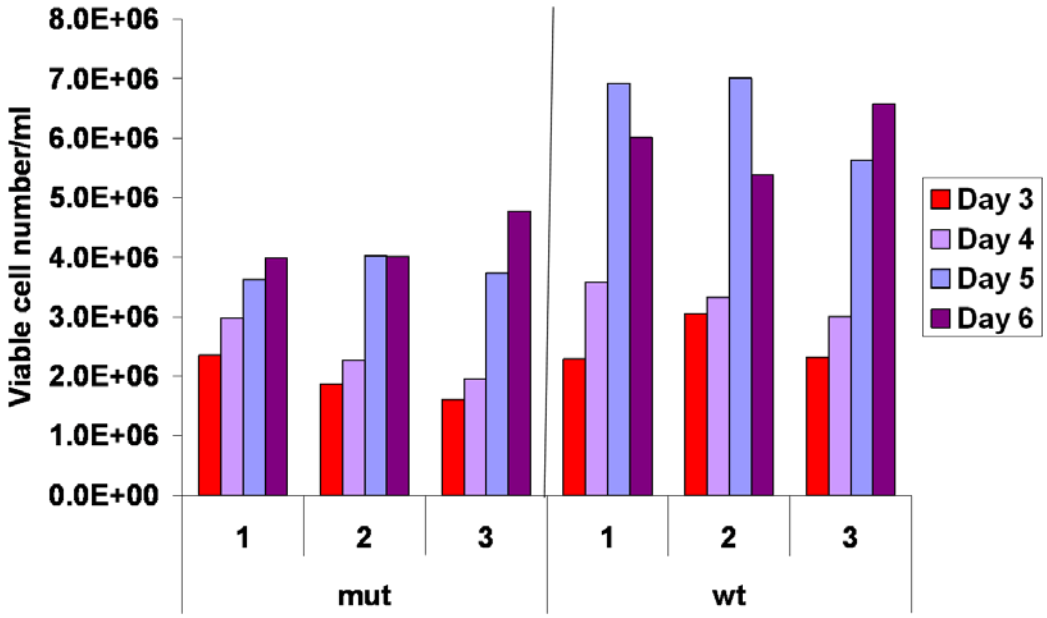

Figure 6.5.4.A: Cell growth profile of each mut and wt cluster clone in 5ml suspension culture.

Cells were harvested from day 3 to day 6 of culture and stained with trypan blue solution to evaluate cell density by the Cedex Automated Cell Counter (Roche). mut: mut cluster expressing clones; wt: wt cluster expressing clones.Three clones from each group were tested.

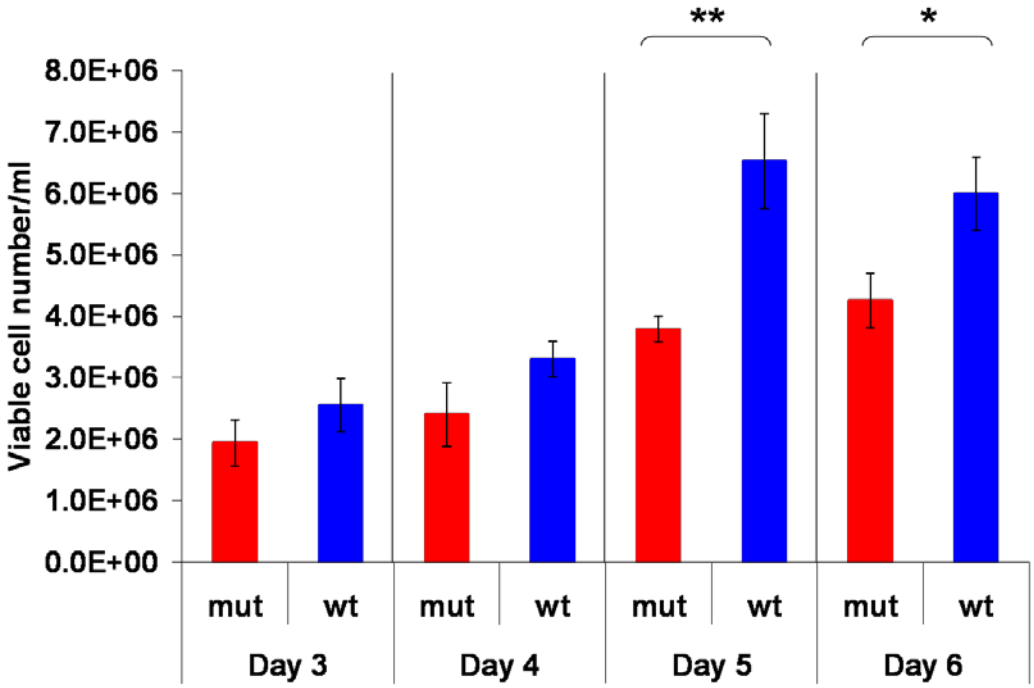

Figure 6.5.4.B: Profile of the mean cell density of mut and wt cluster expressing clones in 5ml suspension culture. Cells were harvested from day 3 to day 6 of culture and stained with trypan blue solution to evaluate cell density by the Cedex Automated Cell Counter (Roche). mut: mut cluster expressing clones; wt: wt cluster expressing clones. Bars represent standard deviations of three clones. Statistical significance of the changes in cell density was analysed using a Student t-test. *: p-value <0.05; **: p-value <0.01

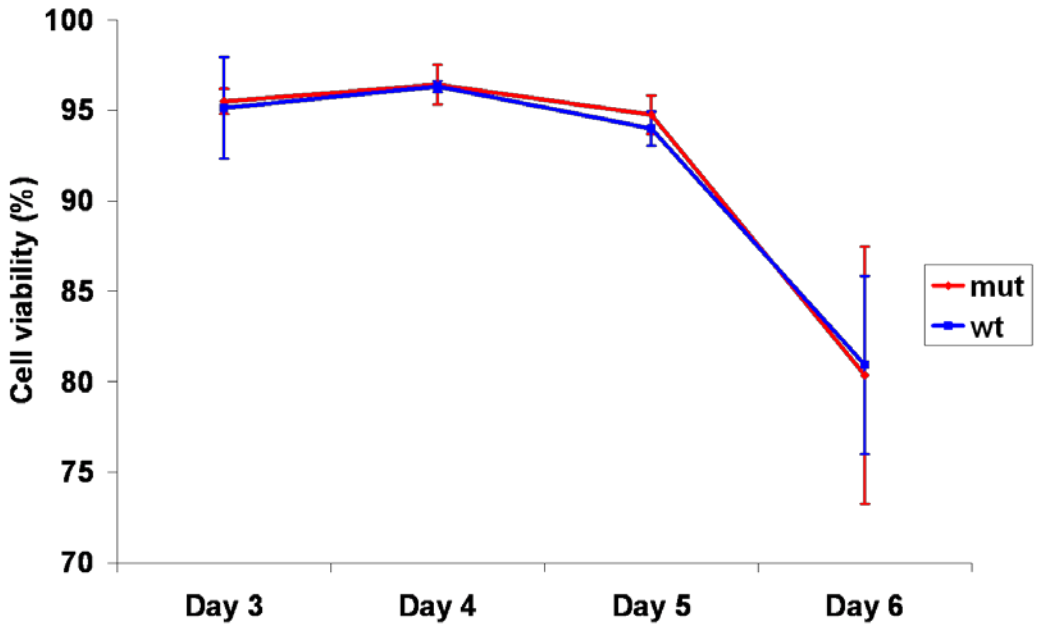

Figure 6.5.4.C: Profile of mean viability of mut and wt cluster expressing clones in 5ml suspension culture. Cells were harvested from day 3 to day 6 of culture and stained with trypan blue solution to evaluate cell viability by the Cedex Automated Cell Counter (Roche). Bars represent standard deviations of three clones. mut: mut cluster expressing clones; wt: wt cluster expressing clones.Bars represent standard deviations of three clones.

6.5.5 Validation of the multi-antisense cluster approach

To verify that the wt cluster was actually targeting endogenous miR-23a~27~24-2 cluster in a specific manner, a transient transfection was performed with pm-neg, pm-23a, pm-27a and pm-24-2 molecules at a concentration of 50nM in mut and wt cluster expressing CHO-K1 SEAP cells. The six clones selected in the previous assay were subjected to this treatment. In theory, these mimics should bind a functioning antisense transcript and further repress GFP expression.

Transient up-regulation of miR-23a, miR-27a and miR-24-2 did not impact on GFP fluorescence in mut cluster expressing clones (**Figure 6.5.5**). However, a reduction of GFP fluorescence was observed in two wt cluster clones (wt clones 1&2). In addition, the impact was stronger after pm-24-2 or pm-27a transfection.

Thus the efficiency of the multi-antisense cluster approach was verified in two clones tested out of three. The wt cluster was able to sequester exogenous miRNAs in an efficient manner. It is not obvious why the third clone did not show GFP fluorescence reduction as an improvement in cell density was demonstrated earlier (**Figure 6.5.5**). It is possible that in clone 3 the Mtg-AMO was expressed at lower level than in the other clones. After binding efficiently to endogenous miRNAs it was saturated and could not target the exogenous miRNAs delivered in the cells. These results also suggested that miR-23a, miR-27a and miR-24-2 depletion contributed to the observed phenotype to a different extent which may be due to the differences in their endogenous expression levels or the specific mRNAs that each one targets. This validation confirmed that the increase of cell growth observed in wt cluster expressing clones was specific to miR-23a~27~24-2 cluster knockdown. Thus we speculated that miR-23a~27~24-2 cluster members may play a role in the regulation of cell proliferation

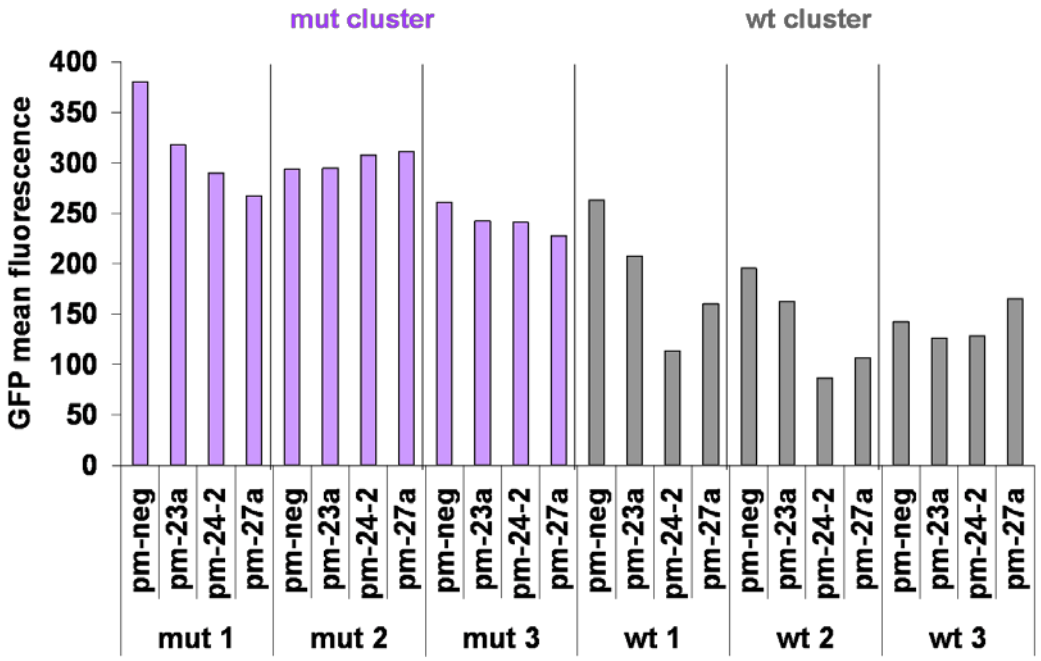

Figure 6.5.5: Analysis of GFP fluorescence in mut and wt cluster expressing clones after transfection with pm-neg, pm-23a, pm-27a and pm-24-2. Cells were seeded at $1*10^5$cells/ml prior to transfection with pm-neg, pm-23a, pm-27a or pm-24-2 molecules at a concentration of 50nM. GFP mean fluorescence was analysed using GFP Express Plus software by Guava flow cytometry 24 hrs after transfection. pm-neg: negative control for mimics; pm-23a: mimic of miR-23a; pm-24-2: mimic of miR-24-2; pm-27a: mimic of miR-27a.

6.6 Screening of miR-7 and its impact on CHO phenotypes

Recently, we reported that transient overexpression of miR-7 induced cell growth arrest for 96hrs while maintaining high cell viability in low-serum culture (Barron, et al. 2011). Consequently normalised productivity was enhanced in CHO-K1 SEAP cells. To investigate whether the effect of miR-7 was reproducible in other cell lines, functional validation was performed in CHO-K1 SEAP, CHO1.14 and CHO2B6 cells. The presence of serum is not desirable in protein production therefore all assays were conducted in serum-free culture.

6.6.1 Screening of miR-7 in CHO1.14 cells

Transient transfection of pm-7, pm-neg, am-7 and am-neg molecules at a concentration of 100 nM was performed in CHO1.14 cells. As previously discussed for miR-24, this concentration may be considered high, possibly leading to off-target effects. However, this experiment was only designed to get some indication of miR-7 potential before being repeated at a lower concentration.

Following transfection, cell growth, cell viability and cell productivity were monitored at day 2, day 4 and day 7. Cells treated with the transfection reagent (neofx) on its own, pre-miR or anti-miR controls showed high viability at early time points so no detrimental side effects were observed due to the transfection process (**Figure 6.6.1.A**). As previously shown, cell density was negatively impacted particularly four days after transfection. A siRNA against Valosin-containing protein was used as a positive control of transfection efficiency. Inhibition of VCP protein has been previously shown to have detrimental impact on CHO cell growth and viability (Doolan, et al. 2010). As expected, VCP knockdown led to a dramatic cell growth and cell viability reduction over the period of the assay (**Figure 6.6.1.B**).

At day 4, transient up-regulation of miR-7 led to a 4-fold decrease in cell density. This phenotype was maintained at day 7 where cell density was further reduced by 20-fold compared to pm-neg treated cells (**Figures 6.6.1.A &B**). Low number of healthy cells (with high levels of viability) suggested that cells were arrested rather than growing and

being killed. On the other hand, transient inhibition of miR-7 increased cell growth more than two-fold (**Figure 6.6.1.B**).

Thus the suppressive impact of miR-7 on cell proliferation seems to be conserved in CHO1.14 cells cultured in serum-free medium. In addition, miR-7 is likely to impact directly on cell viability.

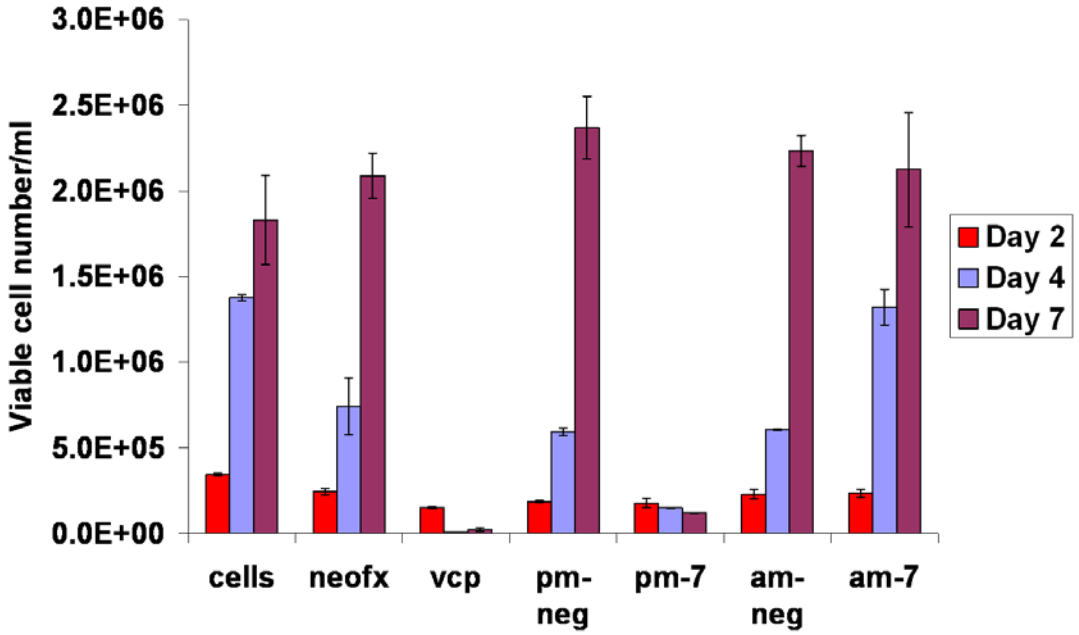

Figure 6.6.1.A: Impact of pm-7 and am-7 transfection on CHO1.14 growth.

miR-7 was transiently up-regulated or inhibited using mimics (pm) or inhibitors (am) at a concentration of 100nM. Cells were harvested at day2, day 4 and day 7, and stained with GuavaViacount reagent to monitor cell growth by Guava flow cytometry. cells: non-transfected cells; neofx: transfection reagent; vcp: siRNA against Valosin-Containing Protein (positive control of transfection efficiency); pm-neg: negative control for mimics; pm-7; mimic of miR-7; am-neg: negative control for inhibitors; am-7: inhibitor for mir-7. At day 2, bars represent standard deviations of three biological samples. At day 4 and day 7, bars represent the high and low reading of two biological duplicates. In the absence of triplicates the significance of the impact of treatment could not be assessed.

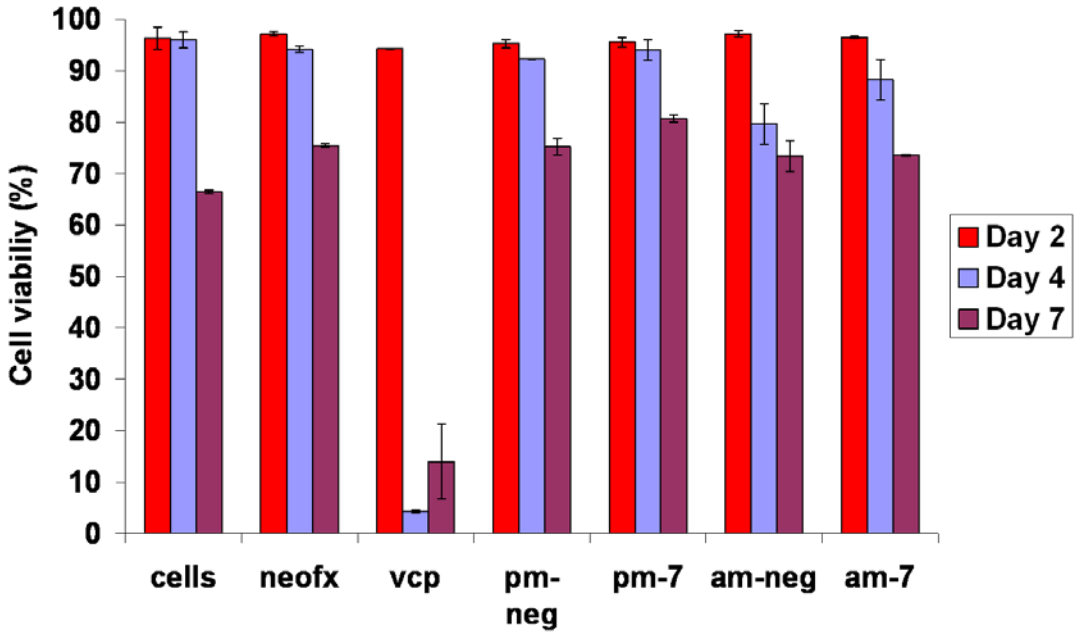

Figure 6.6.1.B: Impact of pm-7 and am-7 transfection on CHO1.14 viability.

miR-7 was transiently up-regulated or inhibited using mimics (pm) or inhibitors (am) at a concentration of 100nM. Cells were harvested at day2, day 4 and day 7, and stained with GuavaViacount reagent to monitor cell viability by Guava flow cytometry. cells: non-transfected cells; neofx: transfection reagent; vcp: siRNA against Valosin-Containing Protein (positive control of transfection efficiency); pm-neg: negative control for mimics; pm-7; mimic of miR-7; am-neg: negative control for inhibitors; am-7: inhibitor for mir-7. At day 2, bars represent standard deviations of three biological samples. At day 4 and day 7, bars represent the high and low reading of two biological duplicates. In the absence of triplicates the significance of the impact of treatment could not be assessed.

6.6.2 Screening of miR-7 in CHO2B6 cells

Functional validation was repeated in CHO2B6 cells using the conditions that were previously described in section 6.6.1. VCP knockdown induced cell growth arrest and reduced cell viability at day 4 and day 7 following transfection (**Figure 6.6.2.A**). Transient overexpression of miR-7 reduced cell density by 3-fold and by 2.5-fold at day 4 and day 7. In contrast to pm-7 transfection in CHO1.14 cells, cell viability was reduced from day 2 by 4.35% (p-value= 0.0010) to day 4 in CHO2B6 cells (**Figure 6.6.2.B**). Surprisingly, knockdown of miR-7 did not impact on cell proliferation.

Thus the potential of miR-7 in impacting cell proliferation when transiently overexpressed was also conserved in CHO2B6 cells.

This transient transfection assay was repeated several times at the same concentration in CHO1.14 and CHO2B6 cells. The same profiles were observed for miR-7 up-regulation. However, the impact of miR-7 knockdown was variable across repeats.

Taken together these results suggested that miR-7 may influence cell proliferation and possibly cell viability at later stages of culture.

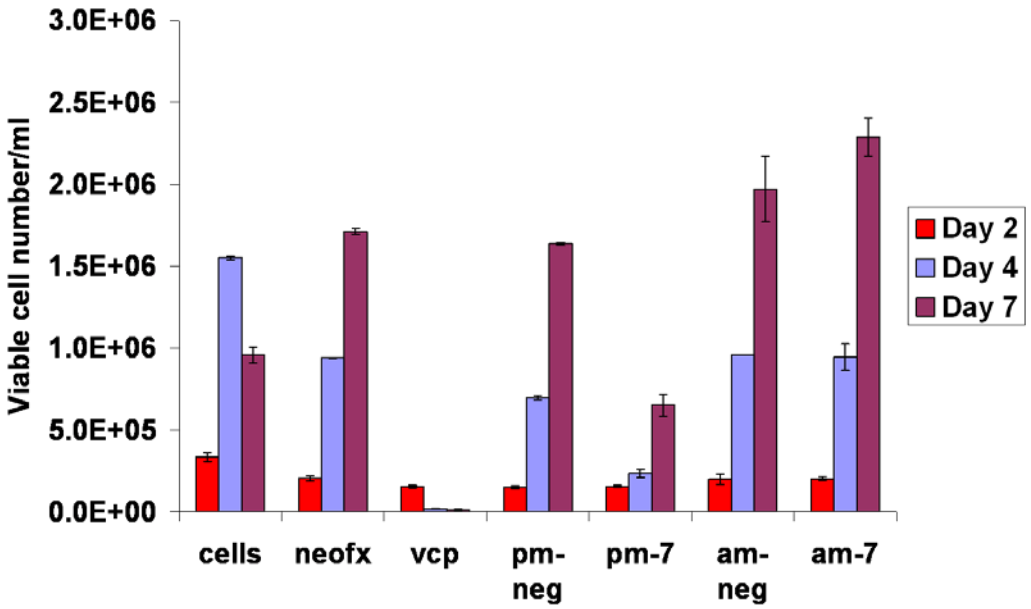

Figure 6.6.2.A: Impact of pm-7 and am-7 transfection on CHO2B6 growth.

miR-7 was transiently up-regulated or inhibited using mimics (pm) or inhibitors (am) at a concentration of 100nM in serum-free medium. Cells were harvested at day 2, day 4 and day 7, and stained with GuavaViacount reagent to monitor cell density by Guava flow cytometry. cells: non-transfected cells; neofx: transfection reagent; vcp: siRNA against Valosin-Containing Protein (positive control of transfection efficiency); pm-neg: negative control for mimics; pm-7; mimic of miR-7; am-neg: negative control for inhibitors; am-7: inhibitor for mir-7. At day 2, bars represent standard deviations of three biological samples. At day 4 and day 7, bars represent the high and low reading of two biological duplicates. In the absence of triplicates the significance of the impact of treatment could not be assessed. .

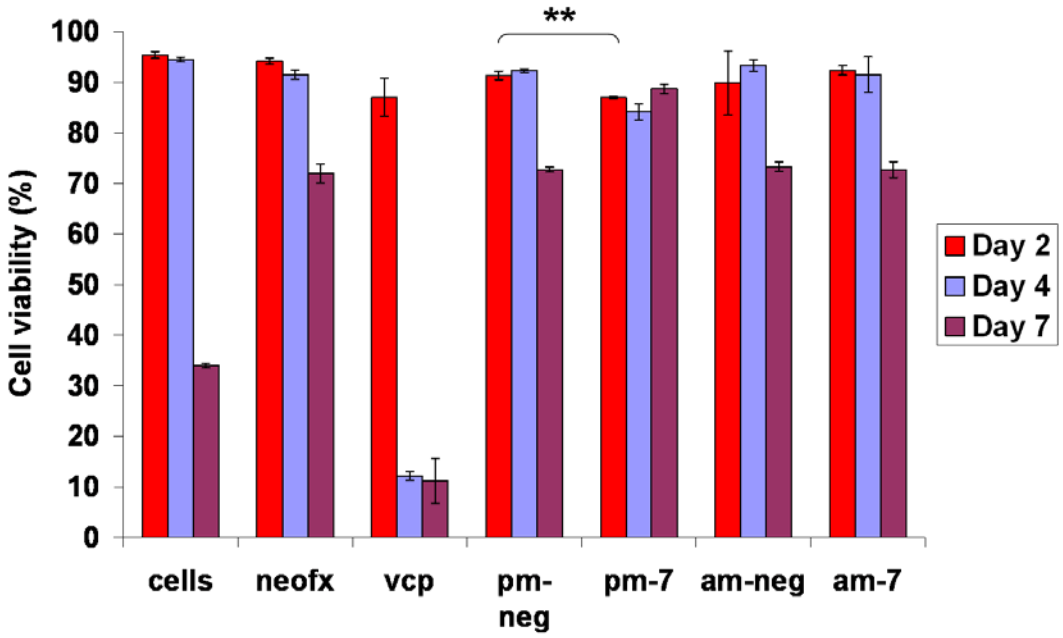

Figure 6.6.2.B: Impact of pm-7 and am-7 transfection on cell viability in CHO2B6 cells. miR-7 was transiently up-regulated or inhibited using mimics (pm) or inhibitors (am) at a concentration of 100nM. Cells were harvested at day2, day 4 and day 7, and stained with GuavaViacount reagent to monitor cell viability by Guava flow cytometry. cells: non-transfected cells; neofx: transfection reagent; vcp: siRNA against Valosin-Containing Protein (positive control of transfection efficiency); pm-neg: negative control for mimics; pm-7; mimic of miR-7; am-neg: negative control for inhibitors; am-7: inhibitor for mir-7. At day 2, bars represent standard deviations of three biological samples. At day 4 and day 7, bars represent the high and low reading of two biological duplicates. A Student t-test was performed to compare pm-7 and pm-neg treatment at 48 hrs after transfection. **: p-value<0.01.

6.6.3 Validation of miR-7 overexpression and knockdown

To verify that the impact on CHO cell growth and cell viability was triggered by miR-7 up-regulation or inhibition, the levels of miR-7 expression were analysed by real-time PCR four days after transfection. At this time, miR-7 levels were increased by 6 $x10^4$ in CHO1.14 cells and by 1.52$x10^4$-fold in CHO2B6 cells *(***Figure 6.6.3.A).**

After transient transfection of miR-7 inhibitors, miR-7 was undetectable in CHO1.14 cells thus suggesting that all molecules of endogenous miR-7 were targeted for degradation *(***Figure 6.6.3.B**). Surprisingly, transfection of am-7 molecules provoked only a 6% decrease in CHO2B6 cells. As previously discussed for miR-24 inhibitor molecules, there are several possible explanations for this result. Knockdown of a particular miRNA could trigger the cells to produce more of this miRNA. However it is more likely that anti-miR molecules that are single-stranded molecules could be dissociated from their target miRNA during the RNA extraction process. The reverse transcription primer could compete with anti-miR molecules for binding to miRNA so the level of this miRNA would still be detectable. Another possibility is that anti-miR could be degraded in the cells before binding to their cognate miRNA because of their single-stranded structure.

These data supported the results from the functional validation with mimics and suggested that the growth reduction observed in CHO1.14 and CHO2B6 cells was provoked by transient miR-7 overexpression.

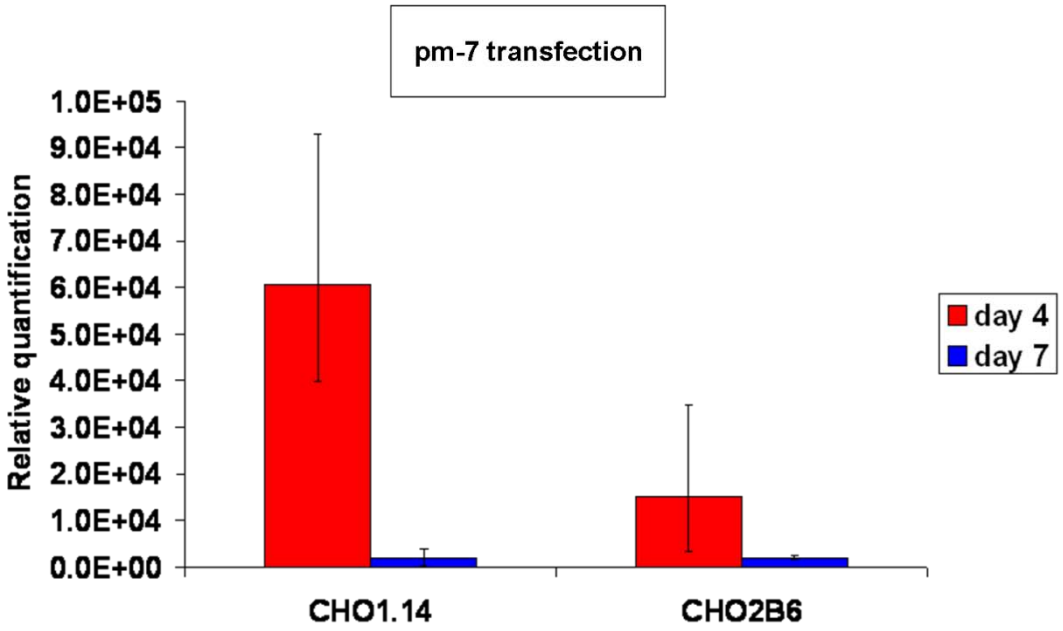

Figure 6.6.3.A: Levels of miR-7 expression in CHO1.14 and in CHO2B6 cells at day 4 following pm-7 transfection. Changes in miR-7 expression were analysed at day 4 after miR-7 mimic transfection with 100nM of pm-7 molecules using an AB7500 Real Time PCR instrument. The expression of miR-7 was normalised to snRNAU6 to correct for variation of RNA input. Bars represented the minimum and maximum value of two biological replicates. Each sample was run in three technical replicates. Relative quantification was evaluated using normalisation to pm-neg (pm-neg=1).

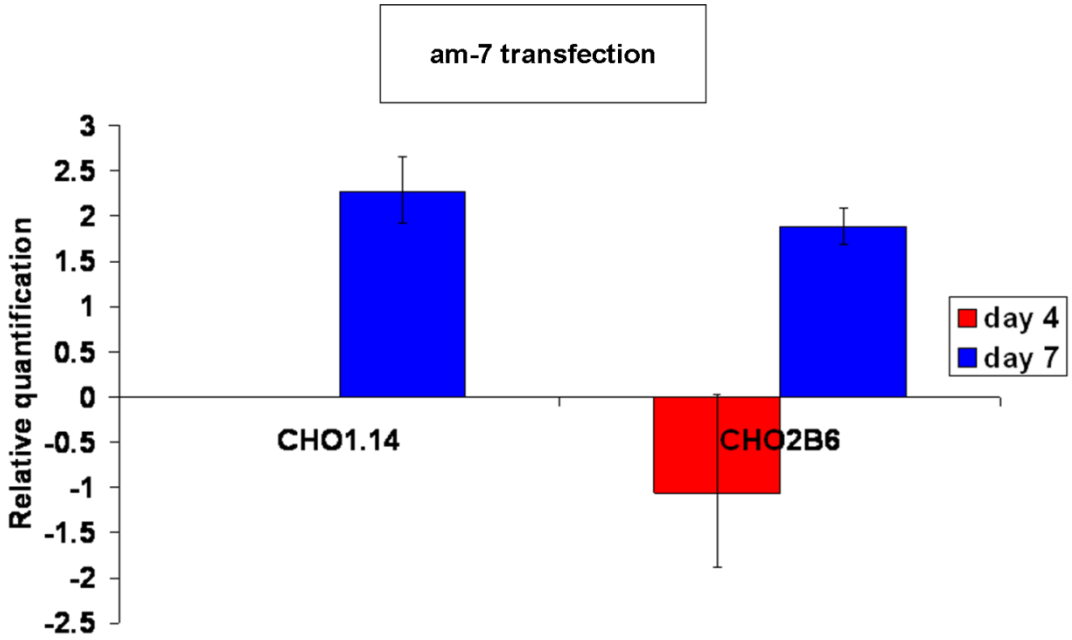

Figure 6.6.3.B: Levels of miR-7 expression in CHO1.14 and in CHO2B6 cells at day 4 after am-7 transfection. Changes in miR-7 expression were analysed at day 4 after miR-7 inhibitor transfection with 100nM of am-7 molecules using an AB7500 Real Time PCR instrument. The expression of miR-7 was normalised to snRNAu6 to correct for variation of RNA input. Bars represent the minimum and maximum value of two biological replicates. Each sample was run in three technical replicates. Relative quantification was evaluated using normalisation to pm-neg (pm-neg=1).

6.6.4 Screening of miR-7 in CHO-K1 SEAP cells

6.6.4.1 Impact of miR-7 on cell growth and cell viability

To validate the potential of miR-7 on cell proliferation and cell viability, functional analysis was repeated in CHO-K1 SEAP cells in CHO-S-SFMII media. The concentration of pre-miR and anti-miR molecules was reduced to 50nM to minimise the risk of off-target effects. CHO-K1 SEAP cell growth were analysed at day 3 and day 6 after transfection.

Non-transfected cells had the usual cell proliferation and viability profile (**Figure 6.6.4.1.A**). VCP siRNA also performed as expected by impairing cell growth and inducing high levels of cell death. In contrast to the previous functional validation studies, the two controls, pm-neg and am-neg molecules, did not trigger non-specific effects on cell proliferation (**Figure 6.6.4.1.A**). The am-neg molecules appeared to protect cells against death (**Figure 6.6.4.1.B**).

Transient overexpression of miR-7 induced a 1.85-fold to 1.87-fold reduction of cell growth at three (p-value= 0.0028) and six days (p-value= 0.017) after transfection (**Figure 6.6.4.1.A**). As observed previously in CHO1.14 and CHO2B6 cells, cell viability was 37% higher in pm-7 treated cells in comparison to the negative control treated cells at later stages of culture (p-value= 0.0002) (**Figure 6.6.4.1.B**). In addition there was no negative impact at earlier time points.

Inhibition of miR-7 did not impact on cell density but it enhanced cell viability the third day after transfection (p-value= 0.0005).

Thus we demonstrated that the cell growth reduction detected upon pm-transfection was reproducible in the different repeats. Therefore we speculated that the anti-proliferative role of miR-7 is conserved across CHO cell lines. There are also promising indications that miR-7 may exert a control on cell viability.

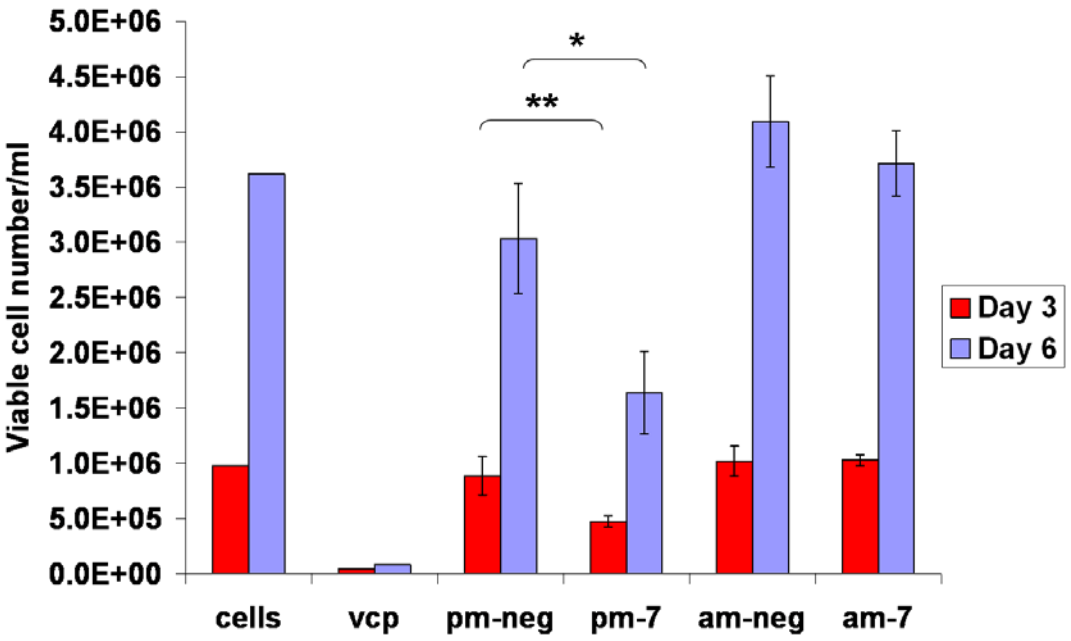

Figure 6.6.4.1.A: Impact of miR-7 on CHO-K1 SEAP growth in serum-free medium.

miR-7 was transiently up-regulated using pm-7 molecules or inhibited using am-7 molecules at a concentration of 50nM in serum-free culture. Cells were harvested at day 3 and day 6 and stained with GuavaViacount reagent to monitor cell density by Guava flow cytometry. cells: non-transfected cells; vcp: siRNA against Valosin-containing protein (positive control of transfection efficiency); pm-neg: negative control for mimics; pm-7: mimic of miR-7; am-neg: negative control for inhibitors; am-7: inhibitor for mir-7. For statistical significance, a Student t-test was carried out to comapre pm-7 with pm-neg and am-7 was with am-neg. Bars represent standard deviations of three biological samples. One biological sample was tested for non-transfected cells and vcp treated cells. *: p-value< 0.05; **: p-value< 0.01.

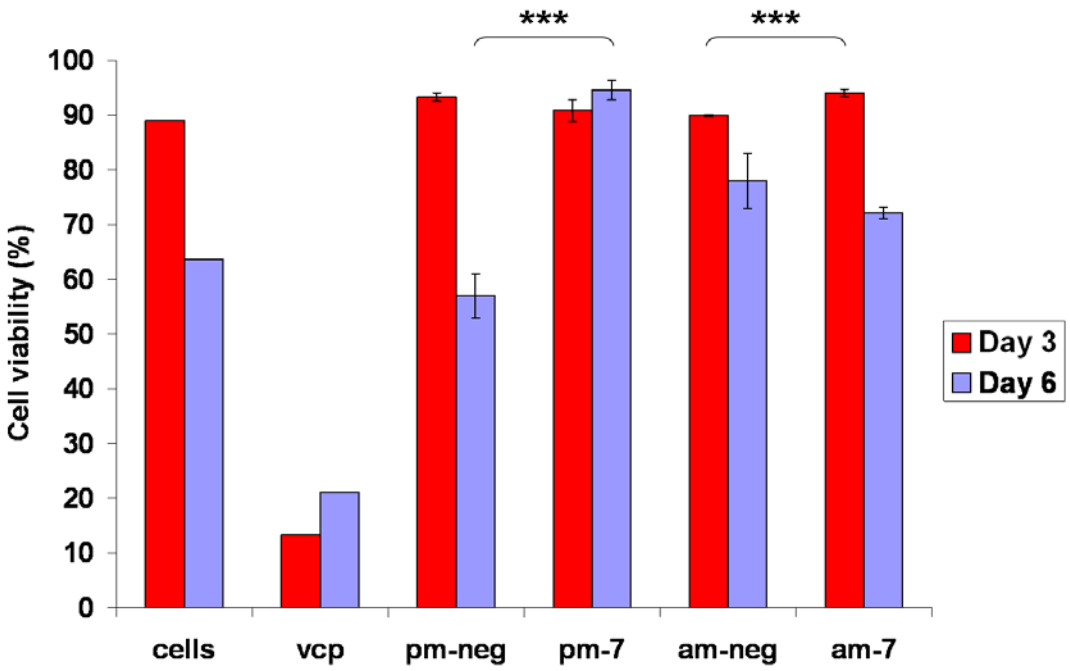

Figure 6.6.4.1.B: Impact of miR-7 on CHO-K1 SEAP viability in serum-free medium.

miR-7 was transiently up-regulated using pm-7 molecules or inhibited using am-7 molecules at a concentration of 50nM in serum-free medium. Cells were harvested at day 3 and day 6 and stained with GuavaViacount reagent to monitor cell viability by Guava flow cytometry. cells: non-transfected cells; vcp: siRNA against Valosin-containing protein (positive control of transfection efficiency); pm-neg: negative control for mimics; pm-7: mimic of miR-7; am-neg: negative control for inhibitors; am-7: inhibitor for mir-7. For statistical significance a Student t-test was carried out to compare pm-7 with pm-neg and am-7 was with am-neg. Bars represent standard deviations of three biological samples. One biological sample was tested for non-transfected cells and vcp treated cells. ***: p-value< 0.001.

6.6.4.2 Impact of miR-7 on SEAP total yield and normalised productivity

To assess the effect of miR-7 on SEAP total yield and normalised productivity, supernatants were harvested at day 3 after transfection. Total yield was negatively affected subsequent to transient overexpression of miR-7 (**Figure 6.6.4.2**). This is likely due to the small number of cells present in culture at this time point. Transient knockdown did not impact on total yield.

Normalised productivity was slightly increased after miR-7 induction by 1.19-fold (**Figure 6.6.4.2**). However, it was not statistically significant.

Thus the suppressive impact on cell proliferation and the maintenance of cell viability observed upon pm-7 transfection in CHO1.14 and CHO2B6 cells is also verified in CHO-K1 SEAP cells. Although the concentration of exogenous miR-7 was lower in this assay, the phenotype is still reproducible thus it is specific to miR-7 and not likely due to off-target effects.

Together these results suggest that miR-7 may be a potential target for cell growth manipulation and cell viability improvement. The cell productivity might be improved following manipulation of miR-7 expression using other approaches than transient assays to extend the culture period.

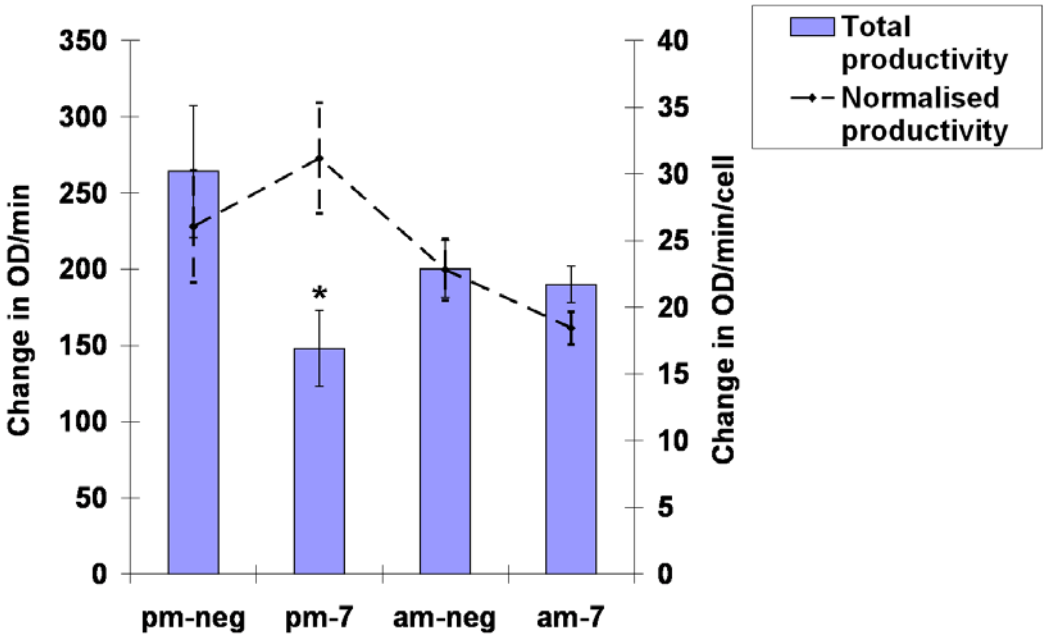

Figure 6.6.4.2: Impact of miR-7 on SEAP total yield and normalised productivity in serum-free medium at day 3 following transfection.

Supernatants of miR-7 treated cells were harvested at day 3 after transfection. The change in absorbance of SEAP substrate, p-nitrophenolphosphate, was assessed by a spectrophotometer at 405nm in a kinetic assay. pm-neg: negative control for mimics; pm-7: mimic of miR-7; am-neg: negative control for inhibitors; am-7: inhibitor for mir-7. Bars represent standard deviations of three biological samples. Each sample was run in technical duplicates. For statistical significance a Student t-test was carried out to compare pm-7 with pm-neg and am-7 was with am-neg. *:p-value<0.05

6.6.5 Screening of miR-7 in CHO cells cultured at high cell density

To establish whether the high cell survival rate observed upon pm-7 treatment was specific to miR-7 up-regulation or whether it was due to a lower cell number in culture, transient transfection was repeated at high cell density. CHO-K1 SEAP and CHO1.14 cells were seeded at $2x10^5$cells/ml and cultured for three days. Transfection was performed the third day, which corresponds to the middle of the logarithmic growth phase. At this time point, cell density reached approximately $1x10^6$cells/ml. The volume of transfection reagent used was the same as in the previous assays (2µl per tube) in a 2ml final volume culture. A siRNA against VCP was used as a positive control to monitor cell growth reduction and cell death. In a previous study, we showed that CHO-K1 SEAP cells shifted to lower temperature induced cell growth arrest and viability improvement (Barron, et al. 2011). Therefore cells cultured at 31°C were included as a positive control to assess cell viability maintenance.

6.6.5.1 Screening of miR-7 in CHO-K1 SEAP cells cultured at high cell density

Non-transfected cells grew well until day 3 after transfection. However, the next three days, cell density and viability decreased dramatically (**Figure 6.6.5.1.A**). In this assay, day 3 corresponds to six days of batch culture (three days before and three days after transfection). Thus it suggests that at day 3 after transfection cells are not healthy due to waste accumulation and nutrient deprivation in the culture. In addition, cells grown at 31°C showed a similar growth profile with no indication of cell growth arrest as expected (**Figure 6.6.5.1.A**). Cells did not show an increase in viability for the three first days. There was a small improvement at later stages but it was not statistically significant.

Following knockdown of VCP, cell growth was reduced by 4.44-fold to 9.18-fold in comparison to the non-transfected cells cultured at 37°C from day 3 to day 5 (5.61882E-05 <p-values <8.69549E-06) (**Figure 6.6.5.1.A**)**.** Levels of cell viability were decreased by 54.83% at day 3 in comparison to cells exposed at 37°C (9.34389E-07 <p-value< 1.74995E-05) **(Figure 6.6.5.1.B**). Thus siRNA molecules were efficiently transfected in high cell density conditions.

Up-regulation of miR-7 reduced cell growth by 1.53-fold to 2.92-fold from day 3 to day 5 after transfection (0.0010 <p-value<0.0021) **(Figure 6.6.5.1.A)**. There was no indication of cell viability improvement in these conditions.

Although the transfection of the siRNA against VCP was efficient in CHO-K1 SEAP cells seeded at high density, pm-7 treated cells did not improve cell viability. In addition, cells exposed to low temperature culture did not either show improvement in cell viability and their viability decreased dramatically at day 3.

These data suggested that the transfection conditions were not optimal to assess cell viability enhancement upon miR-7 overexpression. Thus we could not exclude the possibility that the maintenance of high viability was due to the low number of healthy cells in culture.

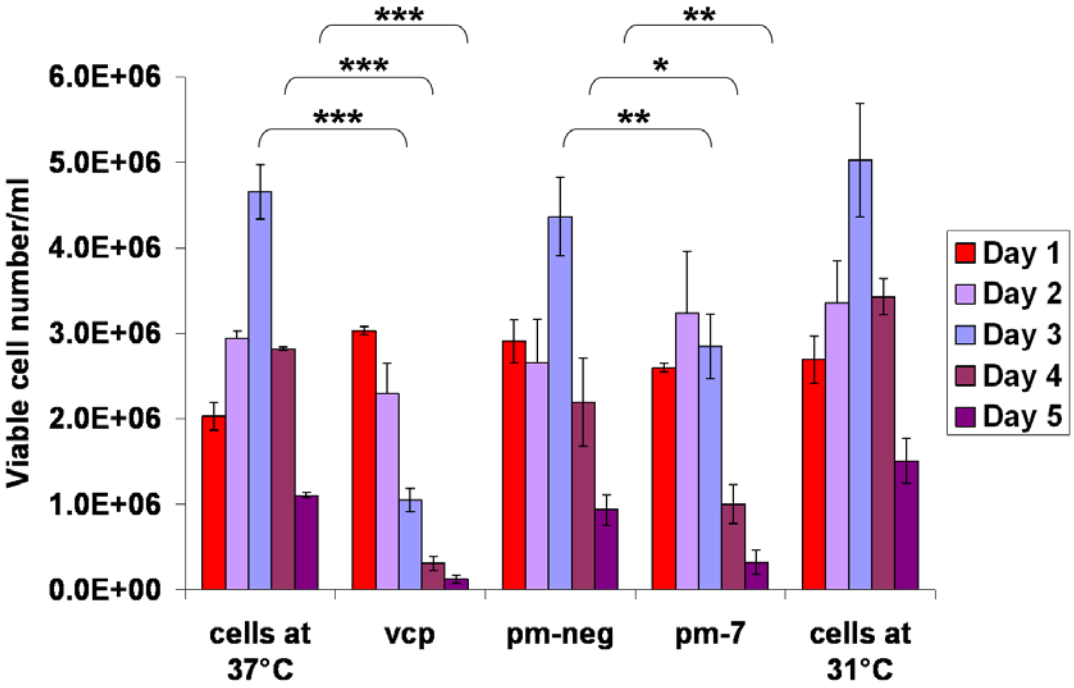

Figure 6.6.5.1.A: Impact of pm-7 on CHO-K1 SEAP growth at high density culture. Cells were seeded at $2x10^5$cells/ml and cultured for three days at 37˚C before transfection or transferred to 31˚C. miRNAs were transfected at a concentration of 50nM. Cells were stained with GuavaViacount reagent to monitor cell growth by Guava flow Cytometry. cells 37˚C: non-transfected cells cultured at 37˚C for the whole assay; vcp: siRNA against Valosin-containing protein; pm-neg: negative control for mimics; pm-7: mimic of miR-7; cells 31˚C: cells cultured at 37˚C for three days and at 31˚C for the next five days. For analysis of statistical significance a Student t-test was performed. In this analysis, vcp and cells at 31˚C were compared to cells grown at 37˚C; pm-7 was compared to pm-neg. Bars represent standard deviations of biological replicates. *: p-value< 0.05; **: p-value< 0.01; ***: p-value< 0.001.

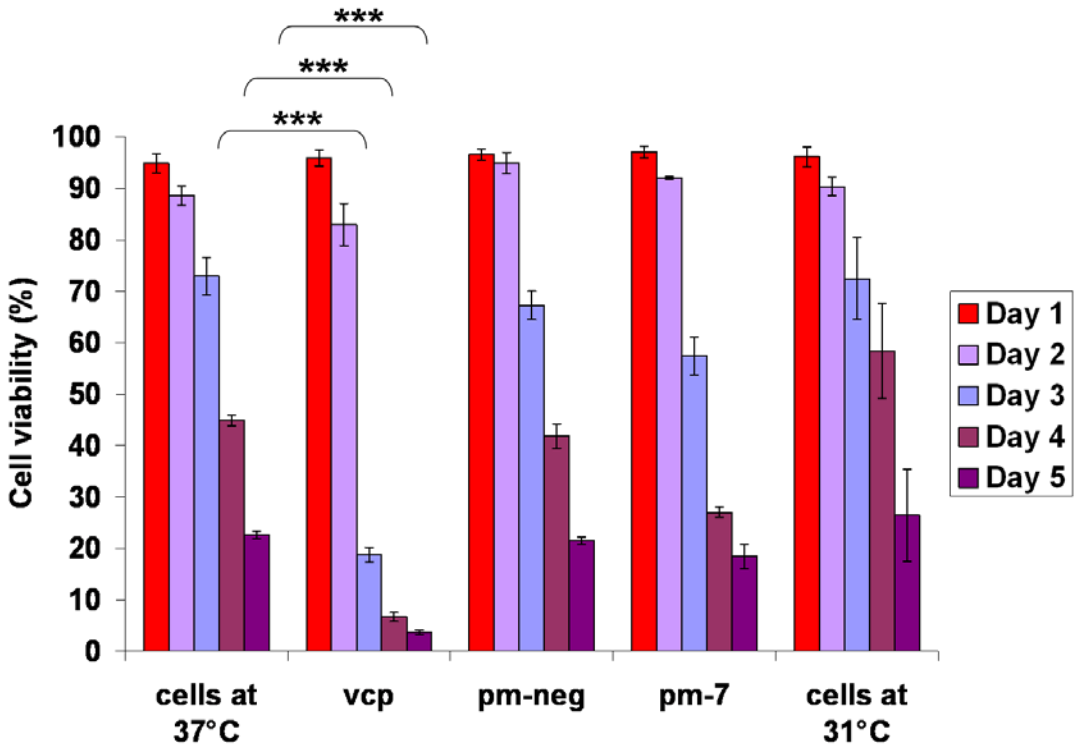

Figure 6.6.5.1.B: Impact of pm-7 on CHO-K1 SEAP viability at high density culture. Cells were seeded at $2x10^5$cells/ml and cultured for three days at 37˚C before transfection or transferred to 31˚C. miRNAs were transfected at a concentration of 50nM. .Cells were stained with GuavaViacount reagent to monitor cell viability by Guava flow Cytometry. cells 37˚C: non-transfected cells cultured at 37˚C for the whole assay; vcp: siRNA against Valosin-containing protein; pm-neg: negative control for mimics; pm-7: mimic of miR-7; cells 31˚C: cells cultured at 37˚C for three days and at 31˚C for the next five days. For analysis of statistical significance a Student t-test was performed. In this test, vcp and cells at 31˚C were compared to cells exposed at 37˚C; pm-7 was compared to pm-neg. Bars represent standard deviations of biological triplicates. *: p-value< 0.05; **: p-value< 0.01; ***: p-value< 0.001.

6.6.5.2 Screening of miR-7 in CHO1.14 cells cultured at high cell density

To verify that the maintenance of cell viability was directly associated with high levels of miR-7 expression in the cells, transient transfection at high density was repeated in CHO1.14 cells. The conditions of transfection and controls used in this assays were the same as in CHO-K1 SEAP cell transfection (section 6.6.5.1).

Non-transfected cells grew exponentially for two days but by day 3 their growth declined as well as their viability (**Figure 6.6.5.2.A &B**). Cells grown at 31°C showed a 1.6-fold decrease of cell growth from day 1 to day 5 compared to cells cultured at 37°C , with an exception at day 3 (**Figure 6.6.5.2.A**). However, there was no major improvement of cell viability (**Figure 6.6.5.2.B**).

Knockdown of VCP reduced cell density by 2.80-fold at day 3 (p-value= 0.0002) and 3.86-fold at day 4 (p-value= 0.0058) (**Figure 6.6.5.2.A**). The cell viability levels were also significantly reduced (1.79096E-07 < p-value < 3.98937E-05) (**Figure 6.6.5.2.B**). On day 5, mostly healthy cells remained in culture. This could be due to the loss of VCP siRNA molecules or transfection efficiency thus leading to survival of a few cells in culture. This suggested that the transfection of siRNA molecules worked efficiently at high density in CHO1.14 cells.

Transient overexpression of miR-7 provoked a 1.13-fold and a 1.45-fold cell density decrease at day 2 (p-value= 0.0130) and day 3 (p-value= 0.0017) respectively (**Figure 6.6.5.2.A**).

Cell viability was improved by 52% at later stages of culture in comparison to the control (p-value= 0.0003) and by 5.83% in comparison to the cells grown at 37°C (**Figure 6.6.5.2.B**).

The transient transfection at high density was repeated three times in CHO-K1 SEAP cells and CHO1.14 cells with different outcomes across the assays and the cell lines. The potential of miR-7 to reduce cell growth was not reproducible in all assays. Cells at 31°C did not show cell survival improvement in all the repeats. Thus these results indicated that the maintenance of cell viability imparted by miR-7 overexpression could not overcome or counteract the lack of nutrients and waste accumulation in culture. This theory is supported by the significant drop in cell viability in most of the samples only three days after transfection. Usually at low density, transfection of miR-7 impacts on cell growth by day 2 or day 3 while cells still maintain high cell viability. However, we

cannot rule out that the higher rate of cell viability observed previously was due to a lower cell number leading to healthier culture environment or due to reduced intracellular delivery caused by the unchanged concentration of miR-7 as well as the transfection reagent (neofx) .

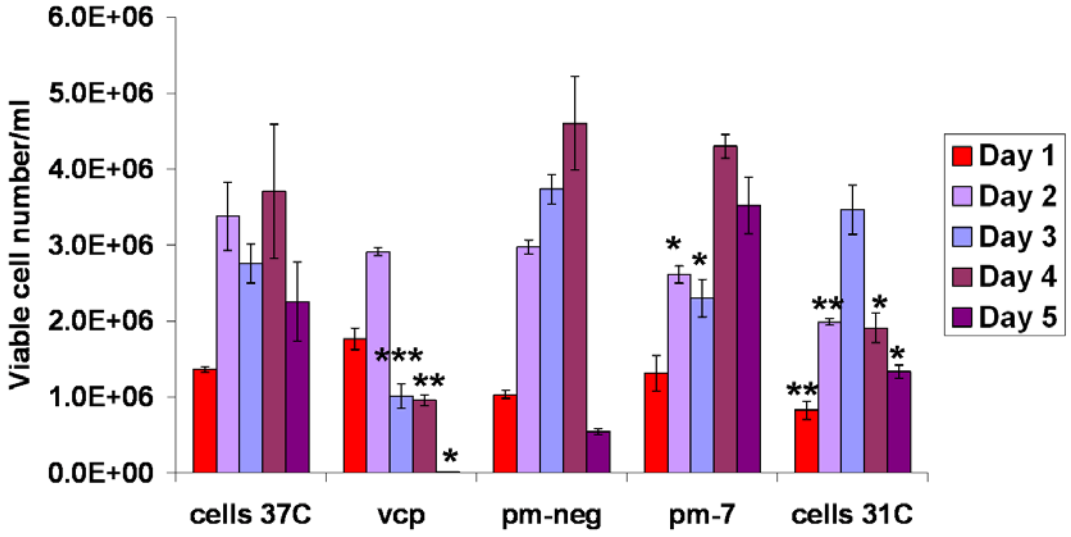

Figure 6.6.5.2.A: Impact of pm-7 on CHO1.14 growth at high density culture.

Cells were seeded at $2x10^5$cells/ml and cultured for three days at 37˚C before transfection or transferred to 31˚C. miRNAs were transfected at a concentration of 50nM .Cells were stained with GuavaViacount reagent to monitor cell growth by Guava flow Cytometry. cells 37˚C: non-transfected cells cultured at 37˚C for the whole assay; vcp: siRNA against Valosin-containing protein; pm-neg: negative control for mimics; pm-7: mimic of miR-7; cells 31˚C: cells cultured at 37˚C for three days followed by 31˚C for five days. A Student t-test was performed to analyse the statistical significance of the results. In this test, vcp and cells at 31˚C were compared to cells grown at 37˚C; pm-7 was compared to pm-neg. Bars represent standard deviations of three biological replicates. *: p-value< 0.05; **: p-value< 0.01; ***: p-value< 0.001.

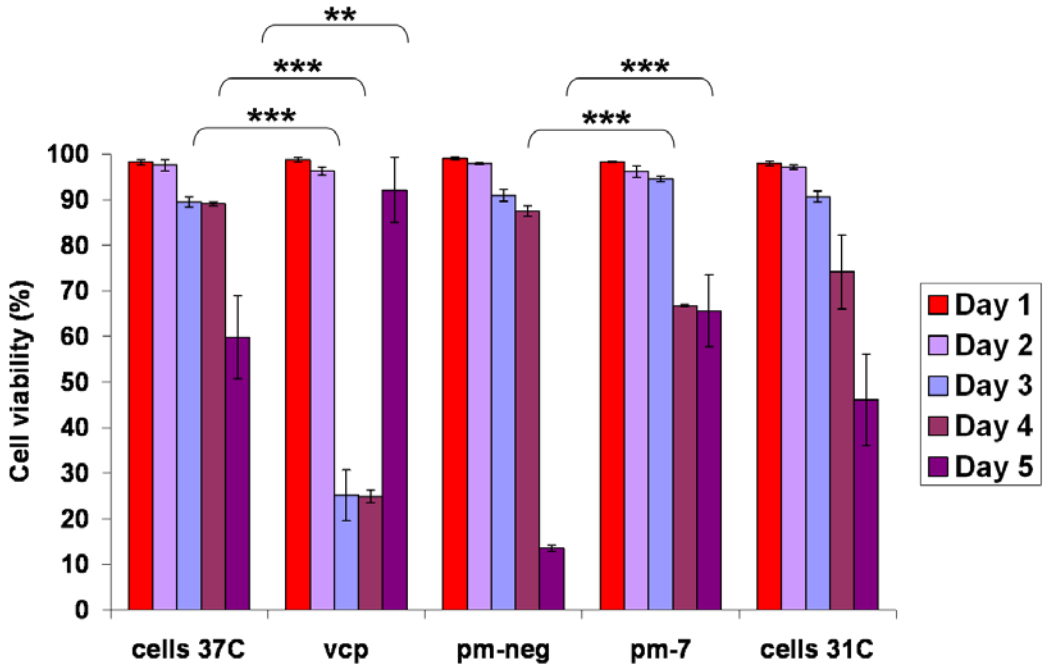

Figure 6.6.5.2.B: Impact of pm-7 on CHO1.14 viability at high density culture. Cells were seeded at $2x10^5$cells/ml and cultured for three days at 37˚C before transfection or transferred to 31˚C. miRNAs were transfected at a concentration of 50nM .Cells were stained with GuavaViacount reagent to monitor cell viability by Guava flow Cytometry. cells 37˚C: non-transfected cells cultured at 37˚C for the whole assay; vcp: siRNA against Valosin-containing protein; pm-neg: negative control for mimics; pm-7: mimic of miR-7; cells 31˚C : cells cultured at 37˚C for three days followed by 31˚C for five days. A Student t-test was performed to analyse the statistical significance of the results. In this test, vcp and cells at 31˚C were compared to cells grown at 37˚C; pm-7 was compared to pm-neg. Bars represent standard deviations of three biological replicates. ***: p-value< 0.001.

6.7 CHO cell engineering using miR-7

In the previous sections, we showed that the transient up-regulation of miR-7 using mimic molecules decreased cell growth, promoted high cell viability and had little impact on normalised productivity in three different CHO cell lines. Due to the nature of the batch culture, it was difficult to prove that high cell viability was directly associated with high levels of miR-7 in the cells. As seen earlier for miR-24 knockdown, the inhibition of miR-7 using inhibitors was difficult to achieve and/or did not impact on CHO phenotypes. In addition, mimics and inhibitors are transient so are only applicable to short-term studies rather than long-term studies. Therefore to further validate the potential of miR-7 in cell proliferation control and to better evaluate its impact on cell viability and productivity, we decided to transiently overexpress miR-7 using an inducible vector. If the outcomes were promising, CHO cells would be engineered to facilitate the constitutive and reproducible induction/knockdown of miR-7.

6.7.1 Overexpression of miR-7 using a tetracycline inducible system: pMF111/pSAM200

The observed impact of miR-7 on cell growth led us to pursue the use of an inducible system. This system would allow cells to grow until the middle of the logarithmic growth phase and being turned on at this time point it would promote cell growth arrest and protein production. In this assay, we used the Tet-OFF system where a tetracycline activator (tTA) binds to a Tet response element (TRE) and activates transcription in the absence of doxycyline (a member of the tetracycline antibiotics group) (**Figure 6.7.1.A**). In the presence of doxycyline, gene expression is turned off and after withdrawal of the drug, gene expression is on. For this pupose, pMF111 (containing precursor miR-7) and pSAM200 vectors were co-transfected into cells (refer to section 6.3.2 for more details on the system and vector description).

Cloning of precursor miR-7 into pMF111 vector

Precursor miR-7 (pre-miR-7) was previously amplified from CHO cells using the following primers.

F: AATAGAATTCAGAGGCAGGAAACTCAGGTGTCA

R: TATTGCGGCCGCATGTCCTTGTTTCTGGAGAAGTCC

These primers were designed in conserved sequence loci of human and mouse pre-miR-7. Prior to cloning, precursor miR-7 and pMF111 were digested with *EcoR*I and *Not*I. Following ligation (**Figure 6.7.1.A**) and amplification by transformation, another digestion was done to verify the size of the insert and the plasmid (**Figure 6.7.1.B**). The nucleotide sequence was checked by sequencing to ensure there were no mistakes in the cloning.

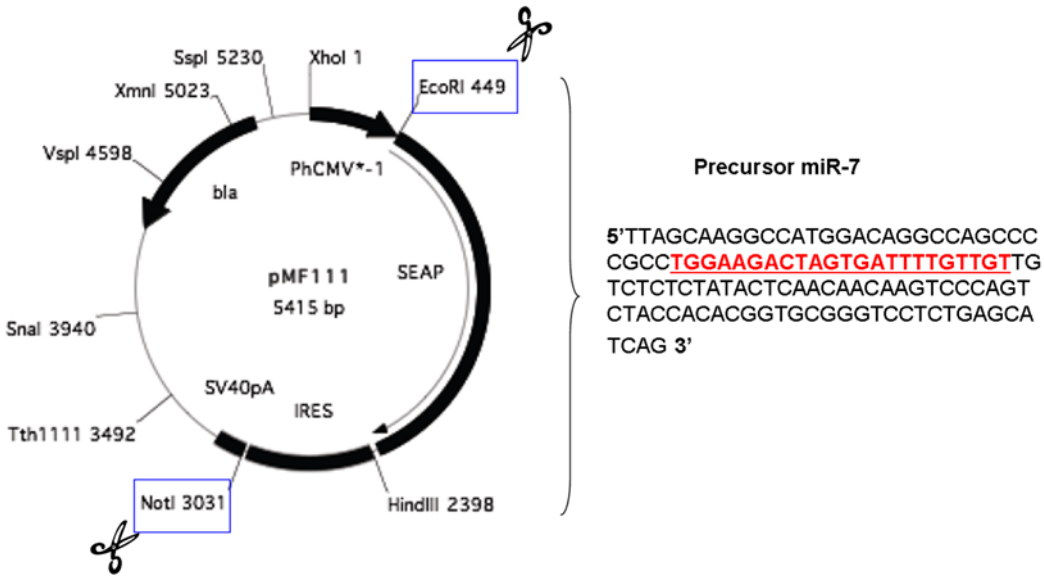

Figure 6.7.1.A: Map of pMF111 vector and features of cloning

Prior to cloning, pMF111 vector and precursor miR-7 were digested with *EcoR*I and *Not*I. A further 101bp of flanking sequences were also included either side (not shown). The sequence shown consists in mature miR-7 sequence (red letters) and flanking sequences (including the stem-loop, in black letters) from CHO genomic DNA (black letters).

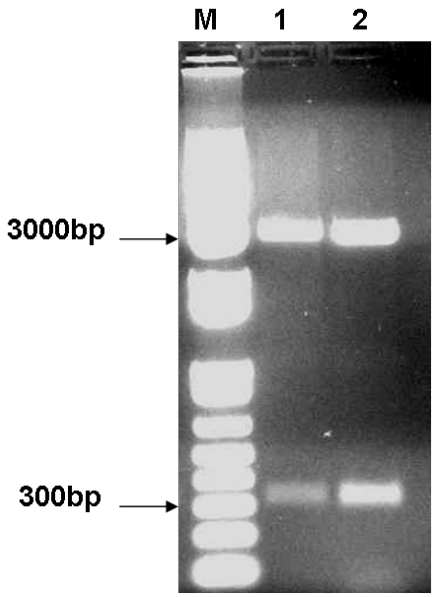

Figure 6.7.1.B: Digestion of pMF111-miR-7 with *EcoR*I and *Not*I.

The vector pMF111-miR-7 (3181bp) was digested with *EcoR*I and *Not*I. Following digestion, samples were run on a 1% agarose gel. Two bands were expected at 2833bp for pMF111 vector and at 348bp for precursor miR-7. M: 1kb Plus DNA ladder. Lane 1&2: two positive clones showing the two bands expected.

6.7.1.1 Investigation of pMF111-miR-7 transfection on CHO1.14 growth and viability

To study the impact of miR-7 up-regulation, cell growth and cell viability were monitored at day 1, day 4 and day 6 after transfection in CHO1.14 and CHO2B6 cell lines. The negative control used in this assay was pMF111 empty vector and pMF-GEO to assess inducible GFP expression by fluorescence microscopy.

The growth profile of non-transfected cells was usual and viability was maintained at high levels until the end of culture (**Figures 6.7.1.1.A&B**). In presence of doxycline, the transfection negatively impacted on cell proliferation in all samples particularly at day 4. Following removal of doxycyline, cell growth was further reduced above all four days after transfection (**Figure 6.7.1.1.A**). For some of the samples, this non-specific effect was abated by day 6 but for the others it was still detectable. In most cases, cell viability was decreased in presence and in absence of doxycyline (**Figures 6.7.1.1. B**).

Thus the non-specific reduction of proliferation observed upon transfection of the controls did not facilitate the analysis of these results. In an attempted to detect any changes following pMF111-miR-7 transfection, we repeated this assay in another cell line.

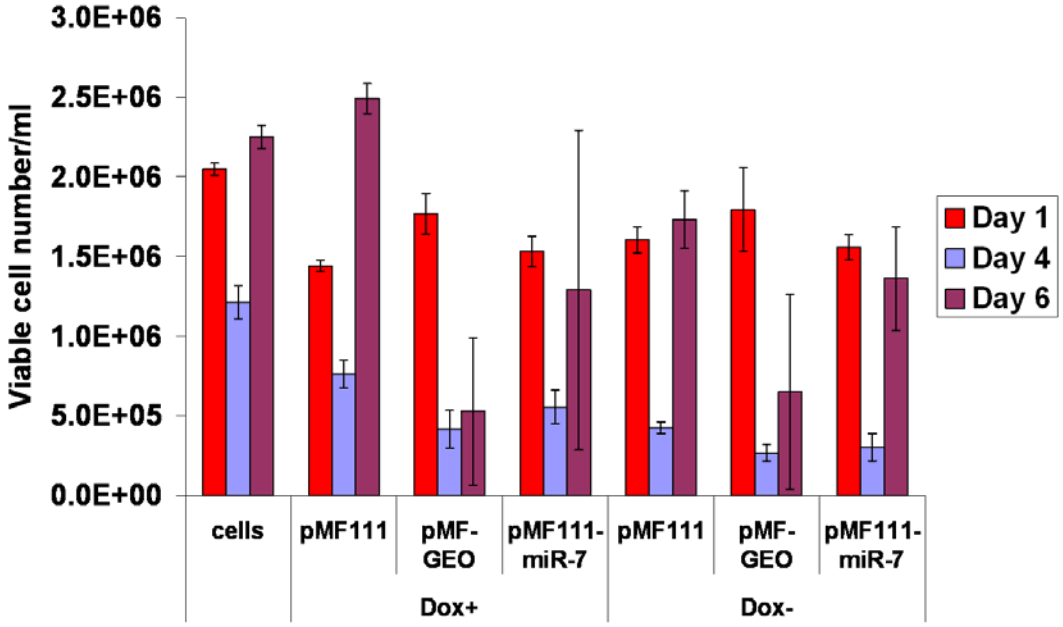

Figure 6.7.1.1.A: Impact of pMF111-miR-7 transfection on CHO 1.14 growth.

Transfection was performed in suspension with 2µl of lipofectamine 2000 reagent (Invitrogen), using 1µg of plasmids, in cells seeded at a concentration of $1x10^6$cells/ml in 1ml final volume. Doxycyline was added six hours after transfection, at a final concentration of 1µg/ml. Bars represent standard deviations of three biological replicates. In this study, pMF111-miR-7/Dox+ was compared to pMF111/Dox+ and pMF111-miR-7/Dox - was compared to pMF111/Dox-. Dox+: Culture with doxycyline; Dox-: Culture without doxycyline.

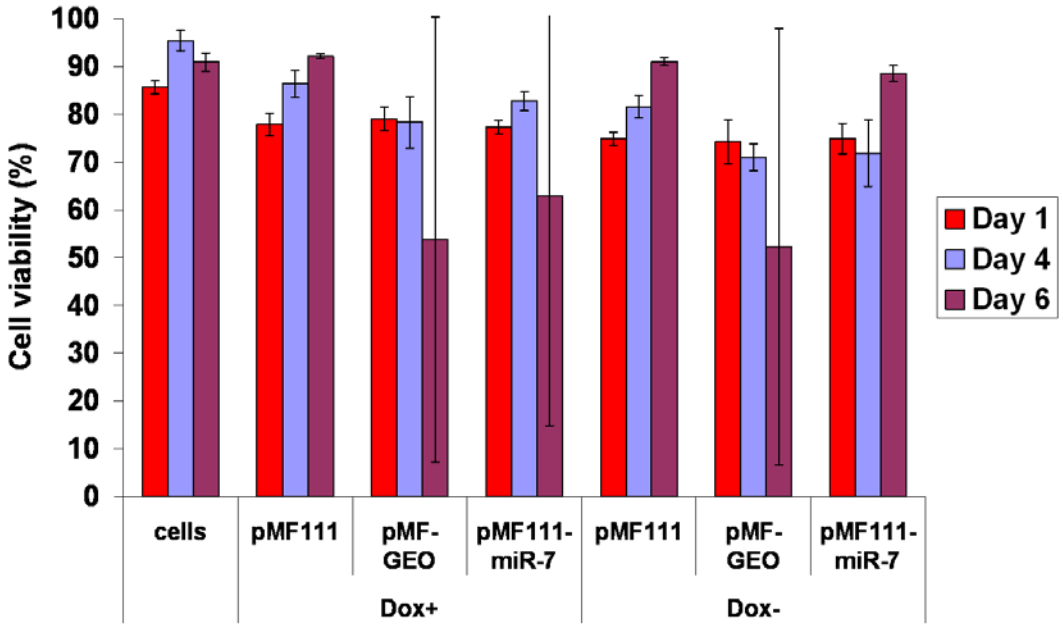

Figure 6.7.1.1.B: Impact of pMF111-miR-7 transfection on CHO 1.14 viability. Transfection was performed in suspension with 2µl of lipofectamine 2000 reagent (Invitrogen), using 1µg of plasmids, in cells seeded at a concentration of $1x10^6$cells/ml in 1ml final volume. Doxycyline was added six hours after transfection, at a final concentration of 1µg/ml. Bars represent standard deviations of three biological replicates. In this study, pMF111-miR-7/Dox+ was compared to pMF111/Dox+ and pMF111-miR-7/Dox - was compared to pMF111/Dox-. Dox+: Culture with doxycyline; Dox-: Culture without doxycyline.

6.7.1.2 Investigation of pMF111-miR-7 transfection on CHO2B26 growth and viability

In CHO1.14 cells, the transfection of pMF111-miR-7 induced cell proliferation reduction as well as the transfection of the controls. Therefore we performed a second assay to try to capture any specific changes correlated to pMF111-miR-7 transfection**.**

The non-transfected cells showed an unusual cell proliferation pattern. At day 4 cell growth decreased and increased again by day 7 (**Figure 6.7.1.2.A**). However, cells showed high levels of viability so this is possibly a technical error (**Figure 6.7.1.2.B**). In the presence of doxycyline, all the controls as well as pMF111-miR-7 induced a non-specific impact on cell growth (**Figure 6.7.1.2.A**). In the absence of doxycyline, the growth reduction was maintained in all controls but in contrast to the previous assay in CHO1.14 cells, it was not diminished four days after transfection. By day 7 cells had recovered from this effect. Surprisingly, the cell growth of pMF111-miR-7 transfected cells was enhanced by day 4 after withdrawal of doxycyline, when we would have expected a reduction of cell growth. Cell viability was maintained at high levels across all samples in presence and absence of doxycycline (**Figure 6.7.1.2.B**). Several repeats were performed to verify the influence of pMF111-miR-7 on cell proliferation (decrease or increase). The results obtained across the assays were inconsistent though the reduction of cell proliferation was observed in most cases, but no overall conclusions could be made.

These results are similar to the observations made in the previous assay (section 6.3.2 for miR-24). The transfection impacted negatively on cell proliferation and often on cell viability. Doxycyline removal prevented further cell growth and usually promoted cell death increase. In most cases, the non-specific impact diminished at day 6 likely due to the loss of the plasmid and recovery from the transfection process. To verify whether precursor miR-7 was processed into the mature form by the cellular machinery, we investigated the levels of expression of miR-7 in these cells.

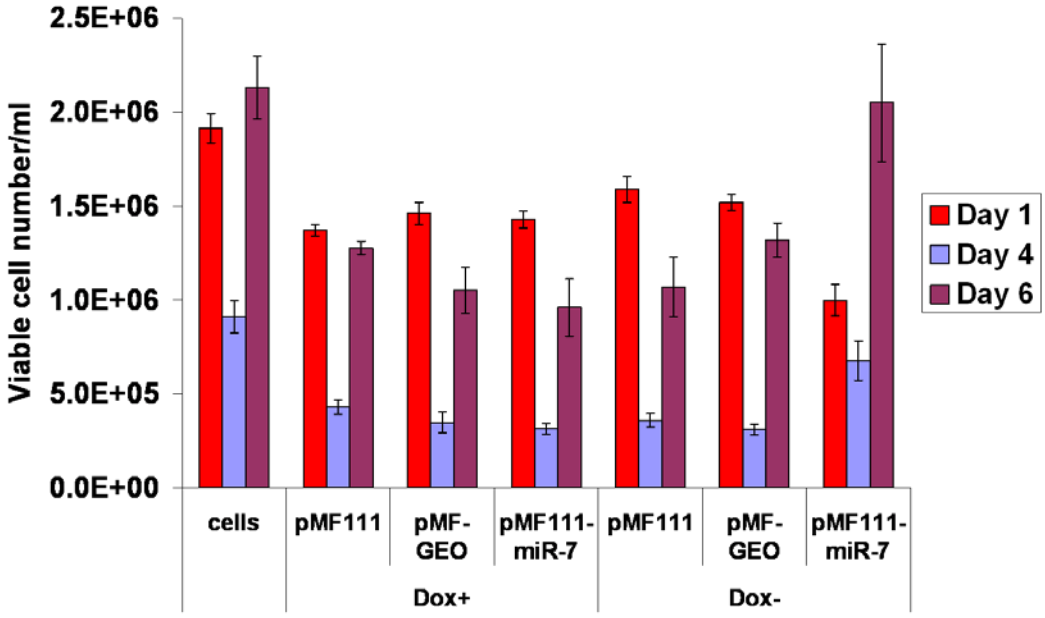

Figure 6.7.1.2.A: Impact of pMF111-miR-7 transfection on CHO 2B6 growth.

Transfection was performed in suspension with 2µl of lipofectamine 2000 reagent (Invitrogen), using 1µg of plasmids, in cells seeded at a concentration of $1x10^6$cells/ml in 1ml final volume. Doxycyline was added six hours after transfection, at a final concentration of 1µg/ml. Bars represent standard deviations of three biological replicates. In this study, pMF111-miR-7/Dox+ was compared to pMF111/Dox+ and pMF111-miR-7/Dox - was compared to pMF111/Dox-. Dox+: Culture with doxycyline; Dox-: Culture without doxycyline.

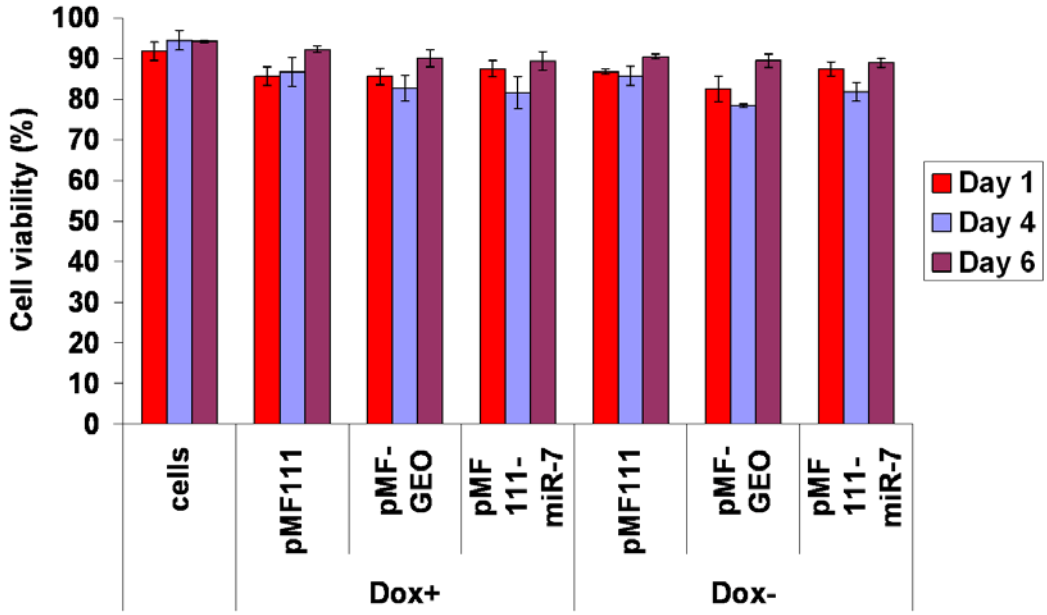

Figure 6.7.1.2.B: Impact of pMF111-miR-7 transfection on CHO2B6 viability.

Transfection was performed in suspension with 2µl of lipofectamine 2000 reagent (Invitrogen), using 1µg of plasmids, in cells seeded at a concentration of $1x10^6$cells/ml in 1ml final volume. Doxycyline was added six hours after transfection, at a final concentration of 1µg/ml. Bars represent standard deviations of three biological replicates. In this study, pMF111-miR-7/Dox+ was compared to pMF111/Dox+ and pMF111-miR-7/Dox - was compared to pMF111/Dox-. Dox+: Culture with doxycyline; Dox-: Culture without doxycyline.

6.7.1.3 Investigation of miR-7 levels in pMF111-miR-7 transfected cells

To verify whether miR-7 precursor was processed correctly into the mature form and overexpressed following transfection of pMF111-miR-7 in absence of doxycylin, the levels of miR-7 expression were assessed using qPCR in CHO1.14 and CHO2B6 cells (**Figure 6.7.1.3**).

The levels of miR-7 expression were increased by 1.83-fold and 7.81-fold in absence of doxycyline in CHO1.14 and CHO2B6 cells respectively.

This indicated that precursor miR-7 was processed into mature miR-7 in both cell lines though the increase was to a lower extent in CHO1.14 cells. The processing of precursor miR-7 may be more efficient in CHO2B6 cells. It is also possible that pMF111-miR-7 was transfected at higher copies in this cell line.

At the time of the study, we could not improve the outcomes of these assays so we considered another system of expression.

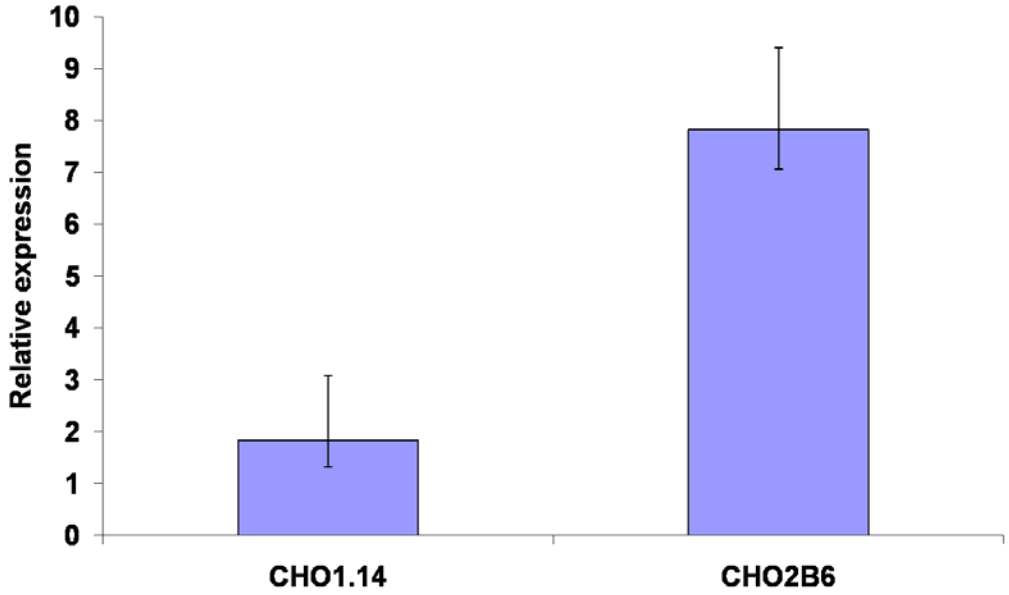

Figure 6.7.1.3: Levels of miR-7 expression in pMF111-miR-7 expressing CHO1.14 and CHO2B6 cells. Changes in miR-7 expression were assessed after removal of doxycyline in pMF111-miR-7 expressing cells at day 4 after transfection compared to cultures containing doxycyline. The expression of miR-7 was normalised to U6 snRNA as an endogenous control to correct for variation of RNA input. Analysis was performed using AB7500 Real Time PCR instrument. Bars represent the minimum and maximum of two biological samples run in technical triplicates.

6.7.2 Overexpression of miR-7 using a tetracycline inducible system: pTet /Hyg vector

6.7.2.1 Description of pTet /Hyg vector

The first attempt to overexpress miR-7 using the inducible system pMF111/pSAM00 presented some issues that could not be resolved at the time. Another inducible system named pTet /Hyg vector was used instead (**Figure 6.7.2.1**). Two constructs were designed pTet-miR-7 (for up-regulation of miR-7) and pTet-neg (negative control) (design and cloning were done by Dr Nga Lao). In this system, the tetracycline-controlled transactivator (tTA) binds to the tetracycline-response element (TRE) and activates transcription in the absence of tetracycline or doxyxycline. An EGFP reporter was driven by the TRE-minimal CMV promoter. mir-7 was placed downstream of the EGFP (**Figure 6.7.2.1**). The mature miR-7 (the guide strand loaded in the RISC complex) and minor mir-7 (miR-7*, known as passenger strand or star strand) sequences were inserted between *Xho*I and *EcoR*I sites. Several RNA interference studies have demonstrated that the stem loop structure and the flanking sequences of human miR-30 precursor trigger optimal miRNA processing by the endogenous RNAi machinery (Zeng, Wagner and Cullen 2002, Boden, et al. 2004). Therefore the loop of the miR-30 precursor was cloned between the miR-7 and miR-7* sequences and the 5'/3'arms of miR-30 precursor were inserted between the *Not*I and *Nhe*I sites. The negative control was designed in the same way except that miR-7 sequence was replaced with a random sequence. Prior to transfection, different concentrations of hygromycin were tested on non-transfected cells to find the minimum concentration required for selection. The concentration applied was 350µg/ml.

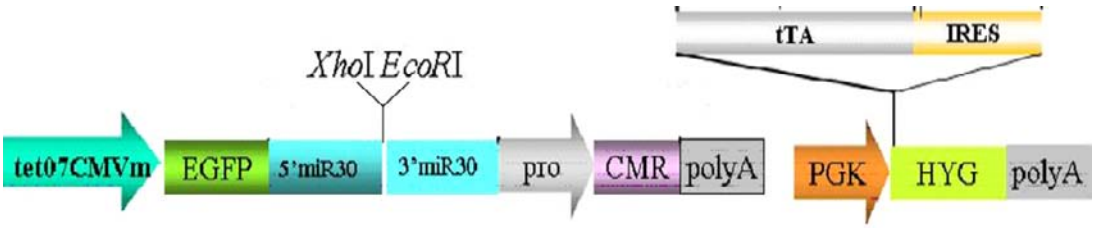

Figure 6.7.2.1: Map of pTet /Hyg vector.

Tet07CMV: TRE-minimal promoter with seven direct repeats of the tetracycline operator sequences; EGFP: enhanced Green Fluorescent Proteint; 5'miR-30/3'miR-30: human flanking sequences of miR-30. pro: promoter; CMR: cmr gene that confers resistance to chloramphenicol. polyA: signal of polyadenylation for transcription termination; PGK: human phosphoglycerate promoter; tTA: tetracycline activator that consists of the fusion of the Tet repressor protein and Herpes simplex virus VP16 activation domain; IRES: internal ribosome entry site for translation of tTA; HYG: gene that confers resistance to hygromycin.

6.7.2.2 Overexpression of miR-7

Stable transfection was performed in a 6-well plate using 11µl lipofectamine and 5µg of pTet-miR-7 plasmid or 5µg of the control vector pTet-neg. A control vector, peGFP-C1 was used to estimate transfection efficiency. GFP expression was observed by fluorescence miscroscopy. Doxycyline was added six hours after transfection at a final concentration of 1µg/ml. The next day, the medium was replaced by fresh medium. Transfection efficiency was estimated at 70% (**Figure 6.7.2.2**).

As expected, the expression of GFP in pTet-NC and pTet-miR-7 transfected cells was blocked in presence of doxycyline. There was a small leak of GFP expression which did not interfere with the study (**Figure 6.7.2.2**). Although GFP expression levels increased following withdrawal of doxycyline, the levels were lower than the positive control (**Figure 6.7.2.2**). This observation suggested that the tet07-CMV promoter was not as strong as the wild-type CMV in the peGFP control.

At day 2, cells were transferred to a T-25 flask in 5ml culture and selection was applied using 350µg/ml of hygromycin. However, the cells did not survive the selection process. The concentration of hygromycin was not seen as an issue as it was tested

previously in non-transfected cells. In addition, even at a low concentration, hygromycin triggered cell death indicating that cells were not resistant to hygromycin. Doxycylin was not an issue as cells died either in presence or in absence of doxycylin.

Thus besides the tet07-CMV promoter being quite weak, we suspected the PGK promoter/ IRES may not have been correctly driving transcription/ translation of the hygromycin resistance marker. The integrity of the construct was checked by sequencing to ensure there was no issue with the design and cloning of the vector. No errors could be detected and we were unable to successfully resolve this issue.

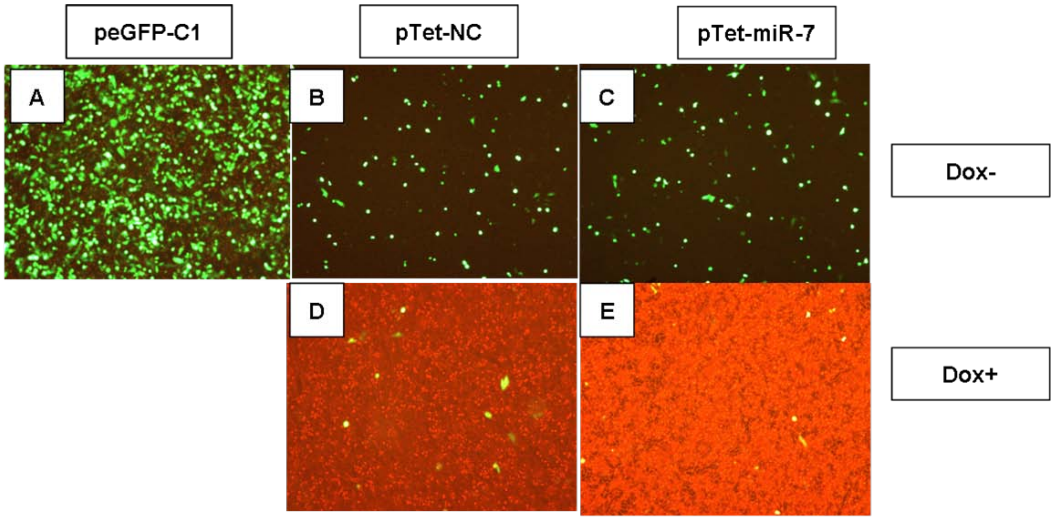

Figure 6.7.2.2: Investigation of GFP positivity in peGFP-C1, pTet-NC and pTet-miR-7 expressing cells. GFP positivity was appreciated by fluorescence microscopy in peGFP-C1 (A, positive control), pTet-NC (B&D, negative control) and pTet-miR-7 (C&E) expressing cells, in absence (Dox-) or presence (Dox+) of doxycyline at day 1 after transfection. Magnification x10.

6.7.3 Stable knockdown of miR-7 using miRNA "sponge" technology

6.7.3.1 Description of miRNA "sponge" technology

In a bioprocessing context, we were interested in improving the cell growth rate of CHO cells. We demonstrated that transient miR-7 overexpression led to cell growth reduction. Higher cell density was achieved successfully only with high levels of miR-7 inhibitors and it was not consistent and reproducible. We thought that a stable system would be more appropriate to increase the cell proliferation rate and to monitor the specificity and efficiency of the inhibition. The "sponge"system was first described by Ebert and co-workers in 2007 (Ebert, Neilson and Sharp 2007). This system was developed to induce efficient endogenous miRNA inhibition by competing with the mRNA target for the miRNA binding site. Endogenously, a mature miRNA recognizes its mRNA target by sequence complementarity. The "seed region" of a miRNA, located at the position 2-8 nt of the 5' end, binds to the 3'UTR of the mRNA target and induces post-transcriptional repression.

Herein, four miR-7 binding sites were inserted in tandem in the 3'UTR of a destabilised enhanced GFP gene (dEGFP). This modified EGFP consists of the fusion of the ornithine decarboxylase degradation domain from mouse (MODC) and the C-terminal of an enhanced variant of GFP (EGFP). The resulting protein is very unstable with a short half-life of 2 hrs. The change of dEGFP fluorescence induced by the binding of the miRNA to the sponge can be correlated to the change in miRNA expression. By binding to the sponge, the miRNA prevents dEGFP from being translated so the dEGFP reporter acts as reporter of miRNA depletion. Once the miRNA is bound to the sponge, it is sequestered and less miRNA molecules are available to bind to their cognate mRNA targets. More than ten binding sites have been shown to promote sponge degradation (Ebert, Neilson and Sharp 2007, Ebert and Sharp 2010). To avoid RNAi-type cleavage by Argonaute 2 and consequent degradation, the sponge system was designed to include a bulge at position 9-11. The characteristics of this system make it a very attractive tool, as miRNAs that belong to the same family share a common seed region thus the entire miRNA family can be inactivated. This tool provides the opportunity to synergistically target miRNAs potentially involved in common cellular

pathways. Thus this 'sponge' technology might be a valuable tool for cell growth manipulation. Cloning of miR-7 binding sites in pCMV-d_2EGFP was performed by Dr Nga Lao (see section 6.5.1 for description of the vector). The four miR-7 binding sites arranged in tandem were cloned at *Xho*I and *Eco*RI sites. The resulting vector was called miR-7 sponge (**Figure 6.7.3.1**). A negative control was engineered in the same manner but non-specific sequences replaced the miR-7 binding sites; this construct was called control sponge. At the time of the study, the CHO genome was not available therefore the sequence of this construct was aligned against non-redundant database (NCBI) using BLAST to ensure there was no match between the negative control and other miRNAs existing in several species including mouse, rat and human. miR-7 sponge and control sponge cassettes were sequence to verify the design and cloning of the vectors.

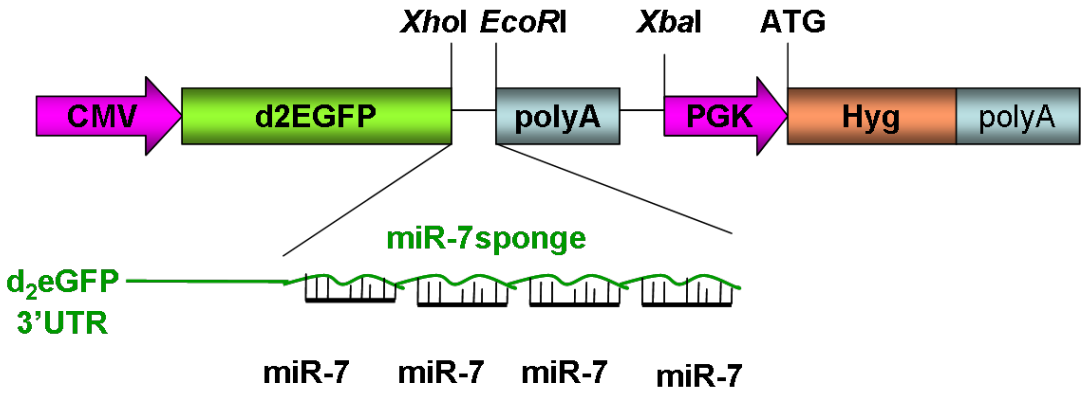

Figure 6.7.3.1: miR-7 sponge cassette

CMV: cytomegalovirus promoter; d2EGFP: destabilized enhanced Green Fluorescent Protein (2 hrs life time); polyA: signal of polyadenylation for transcription termination; PGK: human phosphoglycerate kinase promoter; Hyg: hygromycin (antibiotic for selection of positive clones). *Xho*I/*Eco*RI: restriction enzyme sites for cloning.

6.7.3.2 Transfection of control and miR-7 sponge

Transfection was performed in a 6-well plate using 2µl lipofectamine reagent, with 1µg/well of miR-7 or control sponge vector in CHO-K1 SEAP cells. The vector pEGFP-C1 was included as a control for transfection efficiency. The transfection was performed in biological triplicates. The day after transfection, two wells were used to collect cell pellets for miR-7 expression evaluation by qPCR. Surprisingly, the expression of miR-7 in miR-7 sponge expressing cells was only slightly reduced in comparison to its expression in the control sponge expressing cells (**Figure 6.7.3.2**). This suggested that miR-7 is not degraded immediately following its sequestration by miR-7 sponge and is released upon exposure to the denaturing conditions during lysis and total RNA extraction.

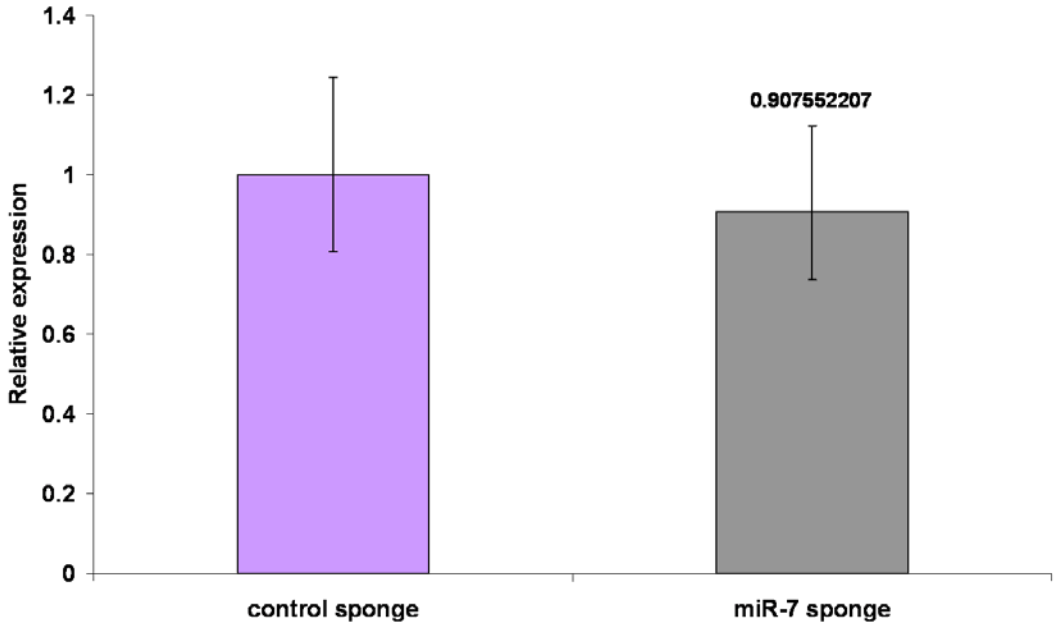

Figure 6.7.3.2: Expression of endogenous mature miR-7 levels in control and miR-7 sponge transfected cells. The changes in the levels of miR-7 expression were investigated the day after transfection using the AB7500 Real Time PCR instrument. The expression of miR-7 was normalised to snRNAu6 to correct for RNA input. Bars represent the minimum and maximum expression levels of biological duplicates. Each biological sample was run in technical triplicates.

6.7.3.3 Impact of miR-7 sponge in a stable mixed population

Two days after transfection, cells were transferred into a T-25 monolayer flask in 5ml adherent culture for three days and drugs were applied to the culture for selection (G418 at 1000µg/ml to maintain SEAP protein production and hygromycin at 350µg/ml for the sponge cassette selection). After selection, cells were cultured in a T-75 monolayer flask in 10ml adherent culture for another three days. At this stage, samples from the mixed population were harvested for GFP expression evaluation using FACS (BD Bioscences) and for cell growth analysis using a Guava flow cytometry. In theory, cells that express the negative control (designed with a non-specific sequence) should have higher GFP positivity than cells transfected with miR-7 sponge because no sequence should bind to it.

GFP positivity was 56.1% in the control sponge expressing cells in comparison to 34.9% in sponge miR-7 expressing cells (**Figure 6.7.3.3.A**). This result was a positive indication that miR-7 was repressing reporter expression via binding to the miR-7 sponge.

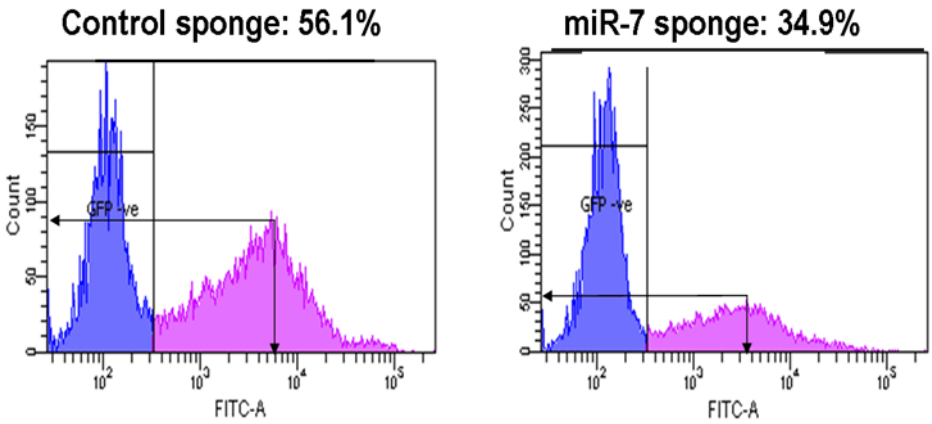

Figure 6.7.3.3.A: GFP positivity in miR-7 sponge (a) and control sponge (b) expressing cells from mixed populations. GFP expression was analysed using FITC channel (Emission: 525nm; Excitation: 488nm) by flow cytometry (FACS, BD Biosciences) using a strict cut-off gate for GFP negative cells versus GFP positive cells.

Cell growth and cell viability were monitored every day for six days. miR-7 sponge expressing cells showed an increase in cell density in comparison to the control sponge transfected cells by 1.45-fold at day 2 ($1.6x10^6$cells/ml versus $1.1x10^6$cells/ml) and by 1.14-fold at day 3 ($3.4x10^6$cells/ml versus $2.98x10^6$cells/ml) (**Figure 6.7.3.3.B**). Cell growth rate was significantly higher at day 2 (0.0431 hr^{-1} versus 0.0352 hr^{-1}) and slightly at day 3 in miR-7 sponge expressing cells (**Figure 6.7.3.3.C**). We also calculated the integrated viable cell density and the accumulated viable cell density. At day 2 and day 3, the IVCD of miR-7 sponge expressing cells was significantly higher by 1.28- and 1.11-fold in comparison to the control cells (**Figure 6.7.3.3.D**). Regarding the AIVCD, it was significantly higher in miR-7 sponge expressing cells from day 2 to day 4 (**Figure 6.7.3.3.E)**. miR-7 sponge expressing cells seemed to have a small advantage on cell survival over the culture but it was not statistically significant (**Figure 6.7.3.3.F**). Although this work was still at a preliminary stage and more validation was required, these results were positive indications that the sponge system worked inducing lower levels of active miR-7 by endogenous miR-7 sequestration and increasing cell density.

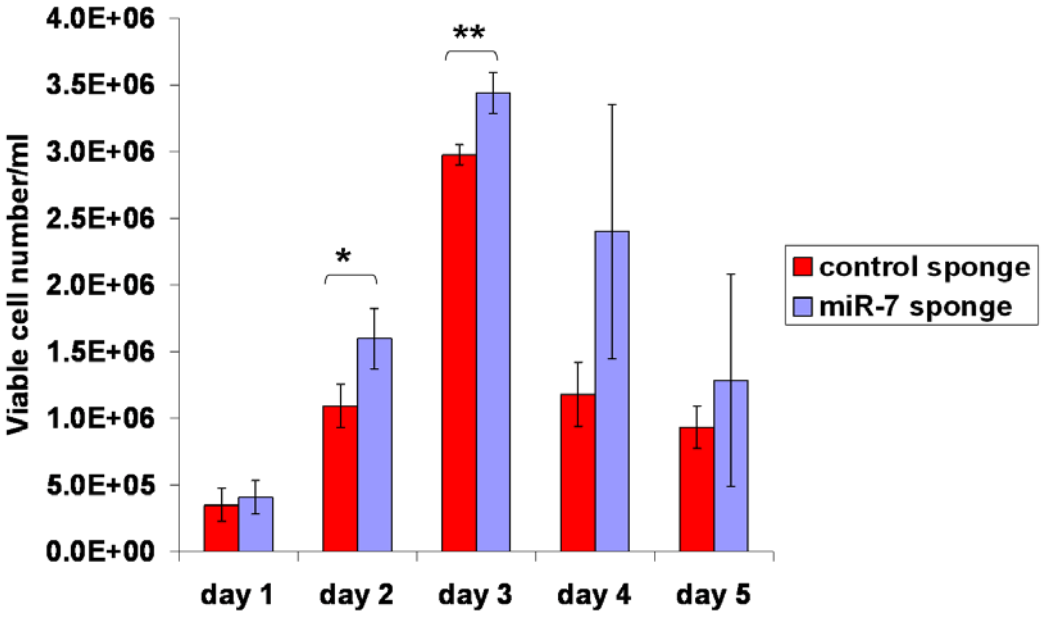

Figure 6.7.3.3.B: Cell density of control sponge and miR-7 sponge expressing cells in mixed populations. The cell growth rate is the increase in cell biomass per unit of time (hour). Cells were seeded at $2x10^5$cells/ml in T-75 flaks in biological triplicates in serum-free medium. Samples were harvested every day for five days and resuspended into GuavaViacount reagent to monitor cell growth using Guava Flow cytometry technology. Bars represent standard deviations from three biological samples. Statistical significance of the data was analysed using a Student t-test. *: p-value<0.05; **: p-value<0.01.

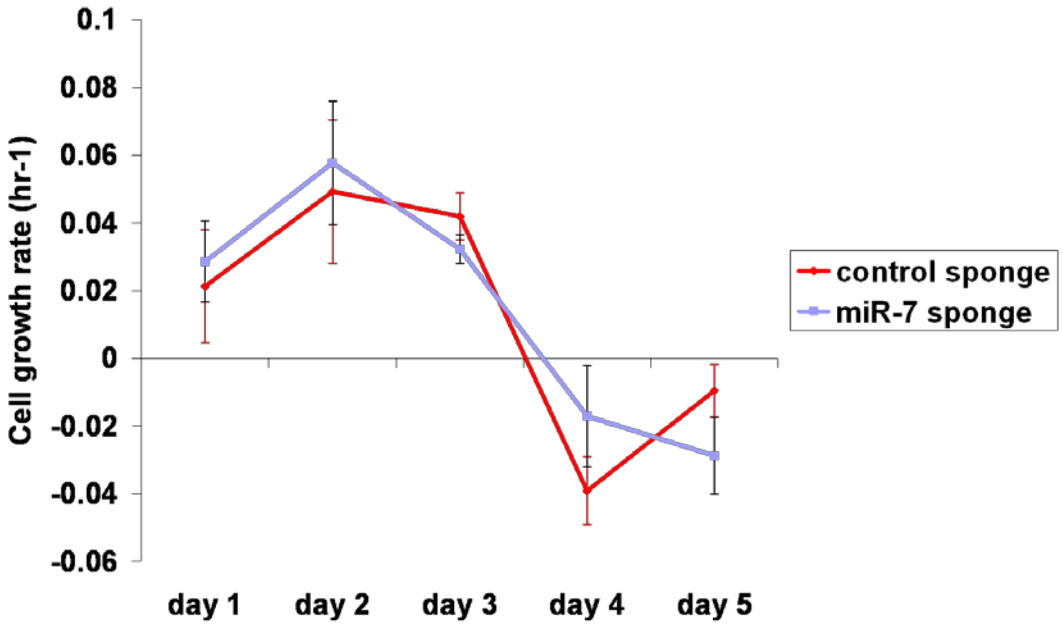

Figure 6.7.3.3.C: Cell growth rate of control sponge and miR-7 sponge expressing cells in mixed populations. The cell growth rate is the increase in cell biomass per unit of time (hour). Cells were seeded at $2x10^5$cells/ml in T-75 flaks in biological triplicates. Samples were harvested everyday for five days and resuspended into GuavaViacount reagent to monitor cell growth using Guava Flow cytometry technology. Bars represent standard deviations from three biological samples.

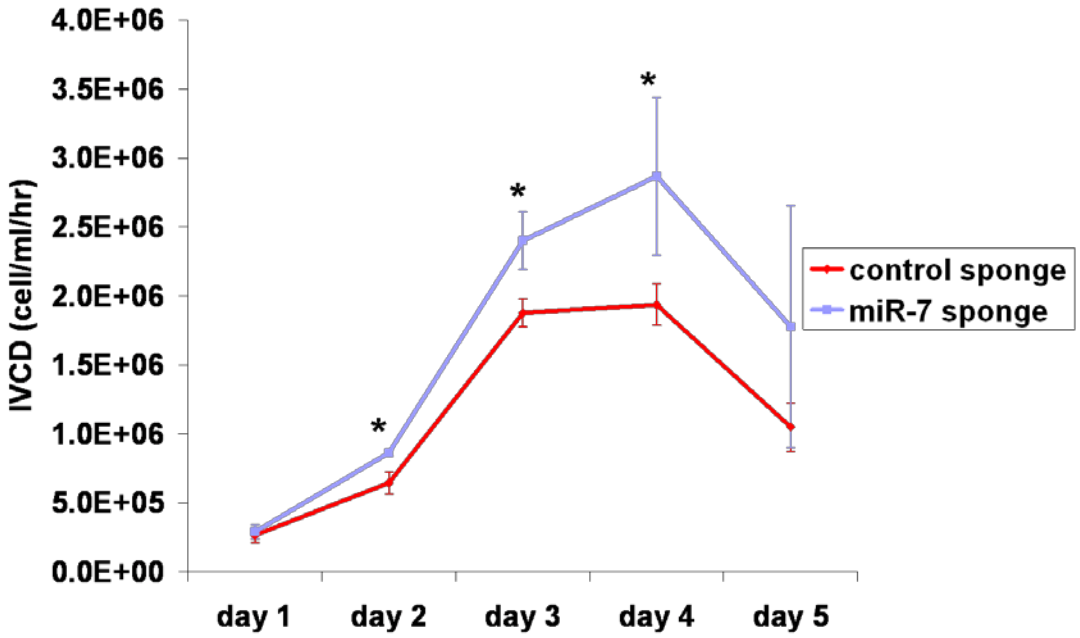

Figure 6.7.3.3.D: Integral viable cell density (IVCD) of control sponge and miR-7 sponge expressing cells in mixed populations. Cells were seeded at $2x10^5$cells/ml in T-75 flaks in biological triplicates. Samples were harvested every day for five days and resuspended into GuavaViacount reagent to monitor cell growth. The IVCD is represented by the area under the curve when the concentration of viable cells is plotted against the culture time. Bars represent standard deviations from three biological samples. Statistical significance of the data was analysed using a Student t-test. *: p-value<0.05

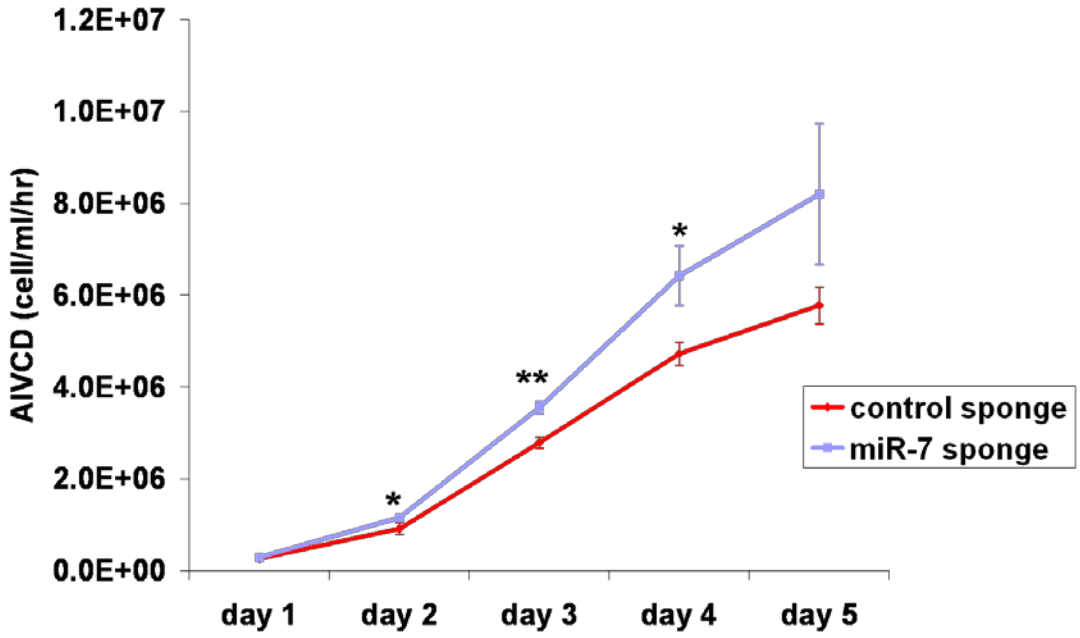

Figure 6.7.3.3.E: Accumulated integral cell density (AIVCD) of control sponge and miR-7 sponge expressing cells in mixed populations. Cells were seeded at $2x10^5$cells/ml in T-75 flaks in biological triplicates. Samples were harvested every day for five days and resuspended into GuavaViacount reagent to monitor cell growth using Guava Flow cytometry technology. Bars represent standard deviations from three biological samples. Statistical significance of the data was analysed using a Student t-test. *: p-value<0.05; **: p-value<0.01.

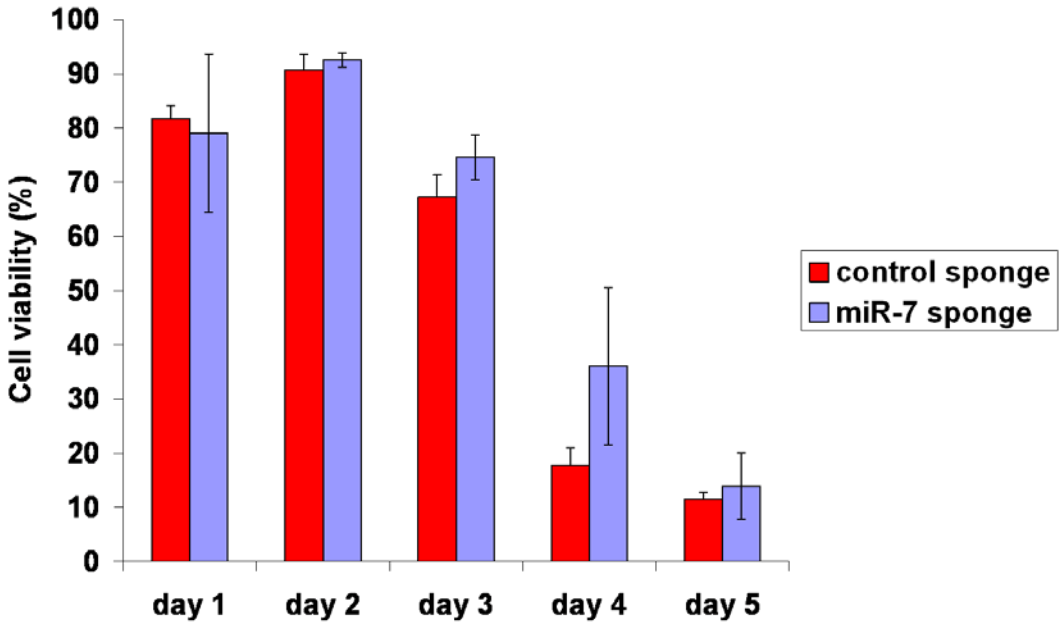

Figure 6.7.3.3.F: Cell viability of control sponge and miR-7 sponge expressing cells in mixed populations. Cells were seeded at $2x10^5$cells/ml in T-75 flaks in biological triplicates. Samples were harvested every day for five days and resuspended into GuavaViacount reagent to monitor cell viability using Guava Flow cytometry technology.

6.7.3.4 Impact of miR-7 sponge in single cell clones

To validate knockdown of miR-7, the original transfection was repeated in CHO-K1 SEAP and CHO1.14 cells using 5µg of plasmid DNA and 11µl of lipofectamine to increase the transfection efficiency and the copy number. The concentration of hygromycin for positive clone selection was kept at 350µg/ml in CHO-K1 SEAP cells and applied at 200µg/ml after optimisation in CHO1.14 cells. Single cell sorting using FACS flow cytometry was carried out. A range of clones with high and medium GFP expression were chosen for further investigation. When confluency reached 90%, 24 single clones from the high GFP expression group and 24 single clones from the medium GFP expression group were transferred to 24-well plates in adherent culture. After drug selection, 23 clones per group from CHO-K1 SEAP population were seeded at $2x10^5$cells/ml in a 24-well plate in suspension and serum-free medium. The selection applied in CHO1.14 cells resulted in 9 clones from the control sponge and 13 clones from miR-7 sponge group surviving and which were transferred to a 24-well plate in suspension, in serum-free medium. Cells were maintained in this format for several weeks. At day 3 after cell passaging, samples were harvested to monitor cell growth, cell viability and GFP fluorescence.

6.7.3.4.1 Impact of miR-7 sponge in CHO-K1 SEAP single cell clones cultured in 24-well plates

In CHO-K1 SEAP cells, the data distribution of 23 clones for each group (control and miR-7 sponge) showed that the median cell density (represented by the 50^{th} percentile-band in the middle of the box) showed a 1.31-fold increase in miR-7 sponge expressing clones (**Figure 6.7.3.4.A**). The 25^{th} and 75^{th} percentiles of the data (bottom and top of the box) confirmed the cell growth advantage of miR-7 sponge expressing cells between the two groups. The analysis of the mean showed that this difference was statistically significant (p-value= 0.0024). Cell viability was slightly lower in miR-7 sponge expressing cells (**Figure 6.7.3.4.A**). However, there was no statistical significance.
The median of GFP fluorescence representing the 50^{th} percentile was 31.8% lower in miR-7 sponge expressing clones than in the control cells (**Figure 6.7.3.4.A**). The 25^{th}

and 75th percentiles of the data confirmed the difference of GFP fluorescence between the two groups. In addition, the analysis of the mean showed that this difference was statistically significant (p-value= 0.0053).

Thus the low levels of GFP fluorescence in miR-7 sponge expressing clones confirmed the results observed in the mixed population. All together these results suggested that active endogenous miR-7 was sequestered by the sponge leading to reduction of its levels of expression. Consequently, miR-7 inhibition triggered significant cell density increase.

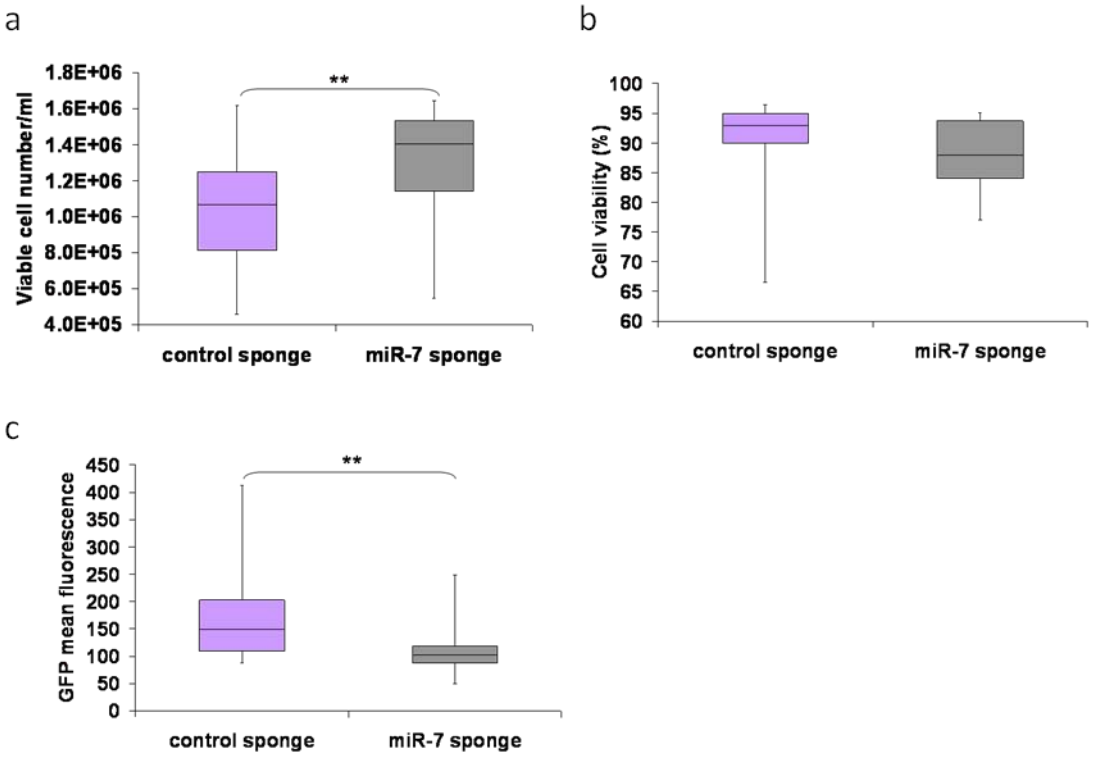

Figure 6.7.3.4.A: Distribution of cell growth (a), cell viability (b) and GFP fluorescence (c) in control sponge and miR-7 sponge expressing CHO-K1 SEAP cells. Cells were seeded at $2x10^5$cells/ml in a 24-well plate in 1ml suspension. Cells were harvested at day 3 and stained with GuavaViacount reagent to monitor cell growth and viability using Guava Flow cytometry. GFP expression was also assessed using Guava Flow cytometry. Distribution of all data was analysed for each group using the minimum, the 25%, the 75% and the maximum of all the data. The bottom and top of the boxes represent the 25th and 75th percentiles (the lower and upper quartiles, respectively), the band near the middle of the boxes is the 50th percentile (the median) and the ends of the whiskers represent the minimum and the maximum of all 23 data. Student t-test was performed to check the statistical significance of the average values of 23 clones.

**: p-value <0.01.

6.7.3.4.2 Impact of miR-7 sponge in CHO-K1 SEAP single cell clones cultured in 5ml spin tubes

CHO-K1 SEAP cell culture was scaled-up to 5ml suspension in CHO-S-SFMII serum-free medium. 12 clones were transferred to this culture. Samples from each group were harvested for four days to monitor GFP expression, cell growth and viability. The cell growth phenotype observed in the miR-7 sponge expressing cells cultured in a 24-well plate was reproducible in the 5ml culture. The mean cell density was statistically increased by 1.5-fold ($p= 0.048$) at day 2 of the culture (**Figure 6.7.3.4.B**). The median of all clones was higher from day 1 to day 3 by 1.09-fold, 1.73-fold and 1.58-fold in miR-7 sponge expressing cells. The cell viability of miR-7 sponge expressing cells dropped suddenly the third day (**Figure 6.7.3.4.C**). The difference in GFP fluorescence between control sponge and miR-7 sponge expressing cells was not as clear as the assay in 24-well plate. There was a lot of variation between clones from the same group and between the different days over the period of the culture (**Figure 6.7.3.4.D**). The median GFP fluorescence of all data was higher in miR-7 sponge expressing cells. In addition, the whiskers showed high variation of GFP fluorescence in the different clones at 24 hrs and 48 hrs. The assay was repeated several times and the variability in GFP fluorescence was present in all the assays, between clones in the same group and for the same clone at different time points. This variability could be due to the inherent genetic heterogeneity of CHO cells or the site of integration in the genome. As we did not use a directed recombination method, the vector would have been integrated randomly at different sites in the genome in each of these clones. It may also be related to fluctuations in endogenous miR-7 expression over the duration of the culture, though it is not apparent why this would be the case in 5ml cultures and not in 24-well plates.

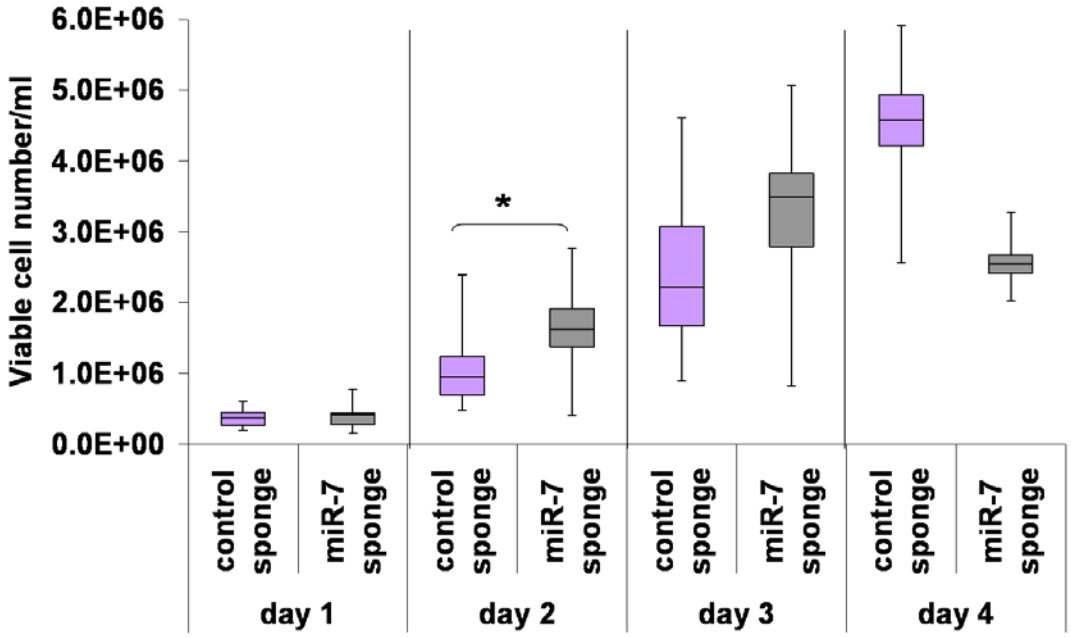

Figure 6.7.3.4.B: Distribution of cell growth in control sponge and miR-7 sponge expressing CHO-K1 SEAP cells. Cells were seeded at $2x10^5$cells/ml in 5ml suspension. Cells were harvested at day 1 to day 4 and stained with GuavaViacount reagent to monitor cell growth using Guava Flow cytometry. Distribution of the 12 clones was analysed for each group using the minimum, the 25%, the 75% and the maximum of all the data. The bottom and top of the boxes represent the 25th and 75th percentiles (the lower and upper quartiles, respectively), the band near the middle of the boxes is the 50th percentile (the median) and the ends of the whiskers represent the minimum and the maximum of all the 12 clones. Student t-test was performed for the analysis of the statistical significance of the average values of 12 clones.*: p-value<0.05.

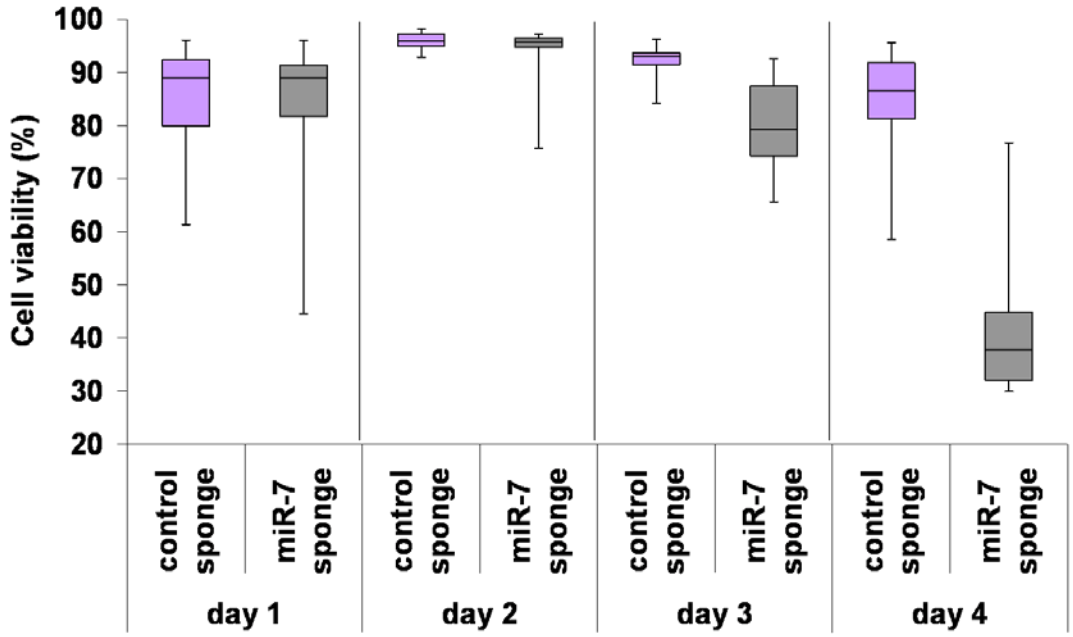

Figure 6.7.3.4.C: Distribution of cell viability in control sponge and miR-7 sponge expressing CHO-K1 SEAP cells. Cells were seeded at $2x10^5$cells/ml in 5ml suspension. Cells were harvested at day 1 to day 4 and stained with GuavaViacount reagent to monitor cell viability using Guava Flow cytometry. Distribution of the 12 clones was analysed for each group using the minimum, the 25%, the 75% and the maximum of all the data. The bottom and top of the boxes represent the 25th and 75th percentiles (the lower and upper quartiles, respectively), the band near the middle of the boxes is the 50th percentile (the median) and the ends of the whiskers represent the minimum and the maximum of all the 12 clones.

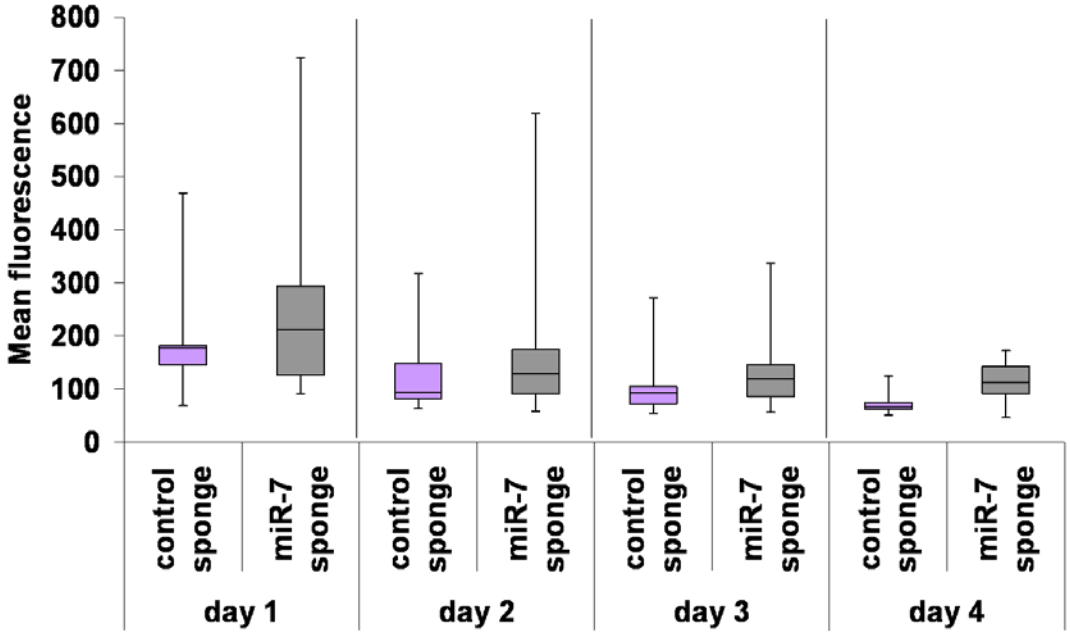

Figure 6.7.3.4.D: Distribution of GFP fluorescence in control sponge and miR-7 sponge expressing CHO-K1 SEAP cells. Cells were seeded at $2x10^5$cells/ml in 5ml suspension. Cells were harvested at day 3 to monitor GFP fluorescence by Guava Flow cytometry. Distribution of 12 clones was analysed for each group using the minimum, the 25%, the 75% and the maximum of all the data. The bottom and top of the boxes represent the 25th and 75th percentiles (the lower and upper quartiles, respectively), the band near the middle of the boxes is the 50th percentile (the median) and the ends of the whiskers represent the minimum and the maximum of all the 12 clones.

6.7.3.4.3 Impact of miR-7 sponge in CHO1.14 single cell clones cultured in 24-well plates

In CHO1.14 cells, the data distribution for each group demonstrated that the median of cell density showed a 2.26-fold increase in miR-7 sponge expressing clones (**Figure 6.7.3.4.E**). The 25^{th} and 75^{th} percentiles of the data confirmed the cell growth advantage of miR-7 sponge expressing cells between the two groups. The analysis of the mean showed that this difference was statistically significant (p-value=0.01814). The levels of cell viability were similar in both groups (**Figure 6.7.3.4.E).**

The median of GFP expression was higher in miR-7 sponge expressing clones (**Figure 6.7.3.4.E**). However, the distribution of GFP fluorescence was in the same range in both groups indicating a high variability of GFP expression independent of control or miR-7 sponge. Despite the observed GFP signal, these data suggested that the sponge system was efficient in depleting endogenous miR-7 and inducing significant cell growth increase in miR-7 sponge expressing CHO1.14 cells.

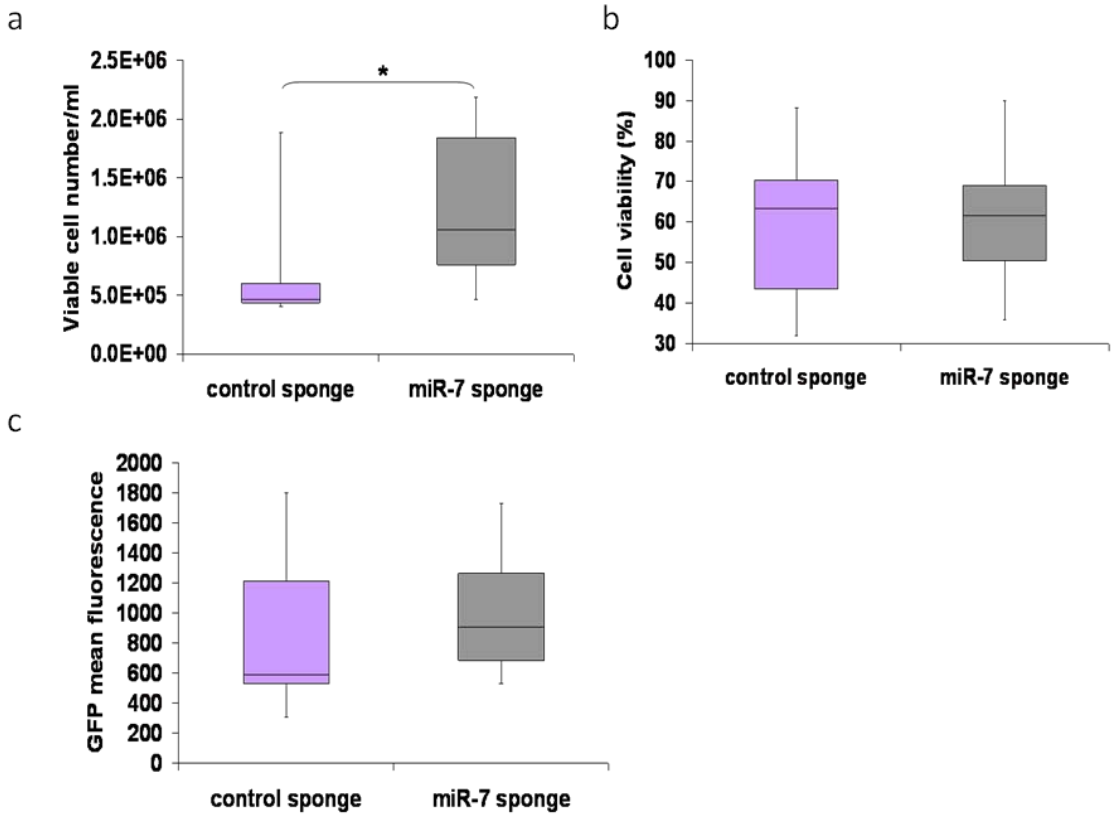

Figure 6.7.3.4.E: Distribution of cell growth (a), cell viability (b) and GFP fluorescence (c), in control sponge and miR-7 sponge expressing CHO1.14 cells. Cells were seeded at $2x10^5$cells/ml in a 24-well plate in 1ml suspension. Cells were harvested at day 3 and stained with GuavaViacount reagent to monitor cell growth and cell viability using Guava Flow cytometry. GFP expression was also assessed using Guava Flow cytometry. Distribution of all data was analysed for each group using the minimum, the 25%, the 75% and the maximum of all the data. The bottom and top of the boxes represent the 25th and 75th percentiles (the lower and upper quartiles, respectively), the band near the middle of the boxes is the 50th percentile (the median) and the ends of the whiskers represent the minimum and the maximum of all the 9 and 13 clones from the control and miR-7 sponge group respectively. A Student t-test was performed to investigate the statistical significance of the mean value of the clones from each group. *: p-value <0.05.

6.7.3.4.4 Impact of miR-7 sponge in CHO1.14 single cell clones cultured in 5ml spin tubes

The same assay was performed in CHO1.14 cells where 7 clones from each group were transferred to a 5ml suspension culture in serum-free medium. The median cell density was higher in miR-7 sponge expressing clones at day 1 by 1.17-fold, at day 2 by 1.35-fold (p-value= 0.005742) and by 1.19-fold both at day 3 and day 4 (**Figure 6.7.3.4.F**)**.** The cell viability was slightly improved at day 1 and day 2 in miR-7 sponge expressing cells (**Figure 6.7.3.4.G**). Although the whiskers indicated high variability of GFP expression, the median of all data was lower in miR-7 sponge expressing cells from day 1 to day 5 (**Figure 6.7.3.4.H**)**.**

Thus stable knockdown of miR-7 enhanced cell growth significantly in CHO-K1 SEAP and CHO1.14 cultured in 5ml. However, the observed impact was significant at one or two time points only. This was likely due to the waste accumulation that triggered early cell death and reduction of cell density.

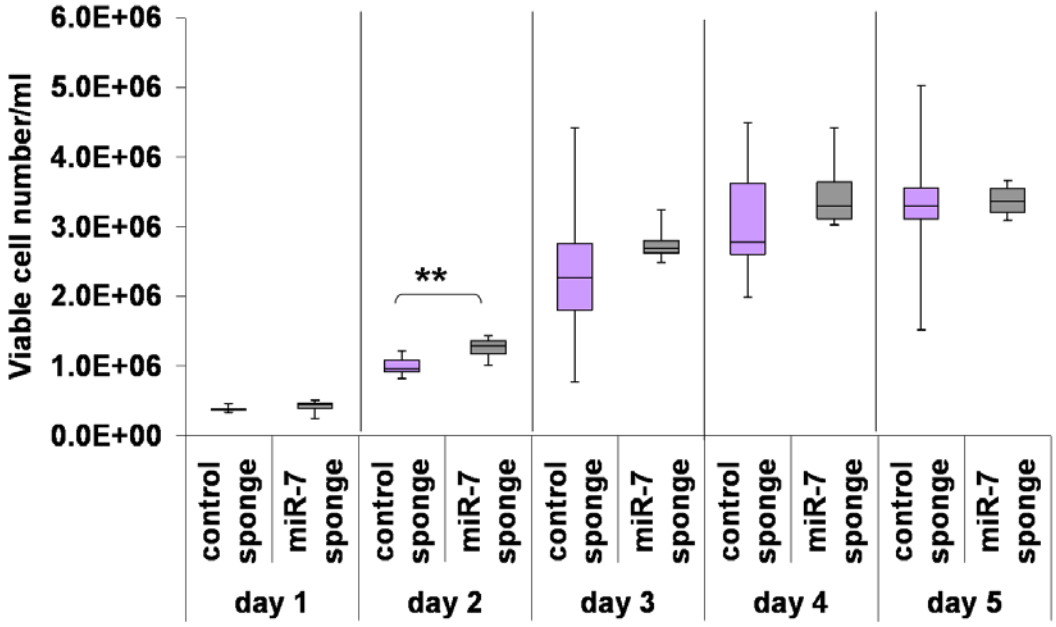

Figure 6.7.3.4.F: Distribution of cell growth in control sponge and miR-7 sponge expressing CHO1.14 cells. Cells were seeded at $2x10^5$cells/ml in 24-well plate in 1ml suspension. Cells were harvested at day 3 and stained with GuavaViacount reagent to monitor cell growth using Guava Flow cytometry. Distribution of all data was analysed for each group using the minimum, the 25%, the 75% and the maximum of all the data. The bottom and top of the boxes represent the 25th and 75th percentiles (the lower and upper quartiles, respectively), the band near the middle of the boxes is the 50th percentile (the median) and the ends of the whiskers represent the minimum and the maximum of 7 clones in each group. A Student t-test was performed to investigate the statistical significance of the mean value of 7 clones from each group. **: p-value <0.01.

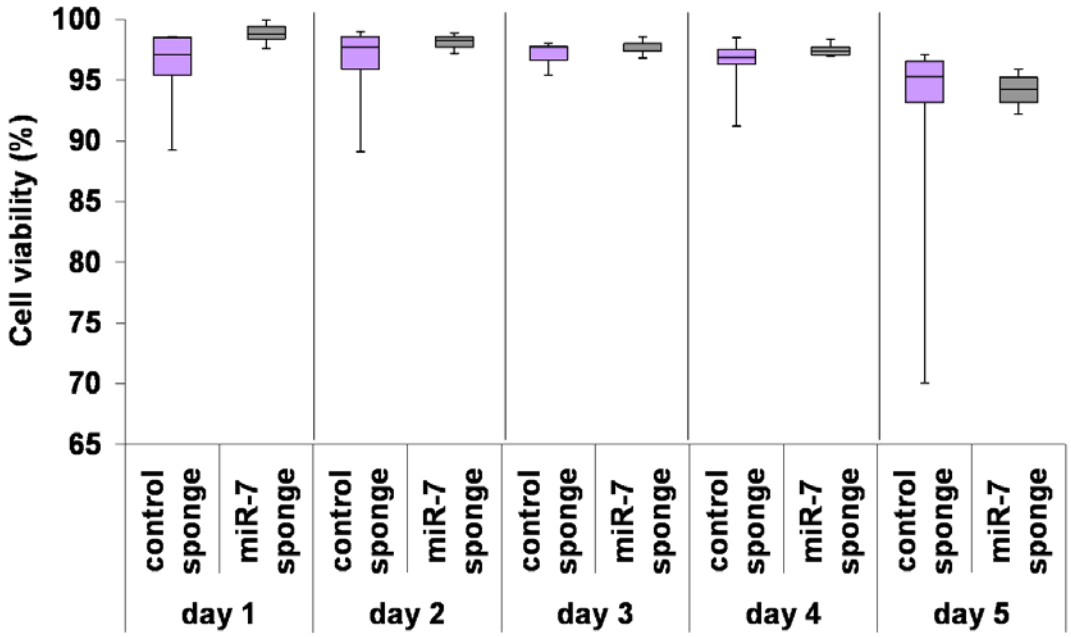

Figure 6.7.3.4.G: Distribution of cell viability in control sponge and miR-7 sponge expressing CHO1.14 cells. Cells were seeded at $2x10^5$cells/ml in 24-well plate in 1ml suspension. Cells were harvested at day 3 and stained with GuavaViacount reagent to monitor cell viability using Guava Flow cytometry. Distribution of all data was analysed for each group using the minimum, the 25%, the 75% and the maximum of all the data. The bottom and top of the boxes represent the 25th and 75th percentiles (the lower and upper quartiles, respectively), the band near the middle of the boxes is the 50th percentile (the median) and the ends of the whiskers represent the minimum and the maximum of 7 clones in each group.

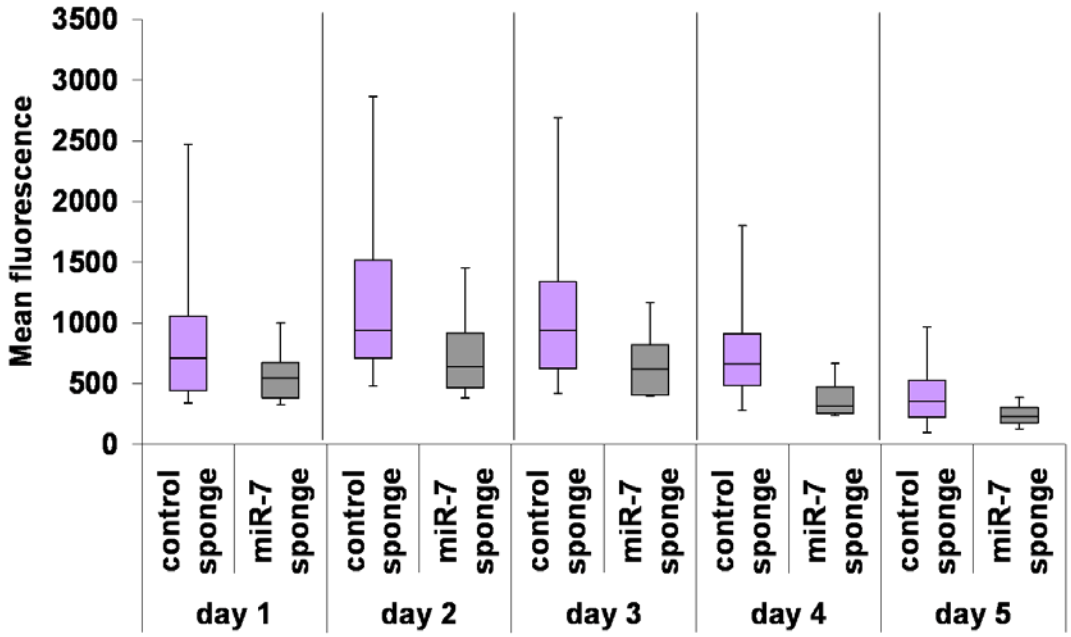

Figure 6.7.3.4.H: Distribution of GFP fluorescence in control sponge and miR-7 sponge expressing CHO1.14 cells. Cells were seeded at $2x10^5$cells/ml in 5ml suspension. Cells were harvested at day 3 to monitor GFP fluorescence by Guava Flow cytometry. Distribution of 7 clones was analysed for each group using the minimum, the 25%, the 75% and the maximum of all the data. The bottom and top of the boxes represents the 25th and 75th percentiles (the lower and upper quartiles, respectively), the band near the middle of the boxes is the 50th percentile (the median) and the ends of the whiskers represent the minimum and the maximum of all the 7 clones.

6.7.3.5 Cell cycle analysis

To investigate whether the increase of cell growth observed in miR-7 sponge expressing cells was due to a rapid progression through the cell cycle control analysis was done 72 hrs after passaging. At this time point, miR-7 sponge expressing cells showed a significant increase in proliferation compared to the control expressing cells.

Cell cycle analysis revealed that control sponge expressing cells displayed a normal distribution with high percentage of cells in G1 and S phase (**Figure 6.7.3.5**) whereas miR-7 sponge cells showed a similar distribution in the different phases (**Figure 6.7.3.5**). The ratio of cells detected in G1 phase was not very different in miR-7 sponge expressing cells and the control cells (34.34% vs 39.32%) (**Figure 6.7.3.5**).

However, there was more miR-7 sponge expressing cells accumulated in the G2 phase (35.04% vs 16.64%), indicating that miR-7 sponge expressing cells progressed faster in the cell cycle. To verify that these results were not specific to one clone, we performed a cell cycle analysis in 12 clones from the control groups and 10 clones from miR-7 sponge group. We found that the average ratio of cells accumulated in the different phases was very similar to what we observed in the first two clones. Control expressing cells were more frequently in the S phase compared to miR-7 sponge expressing cells (41.67% vs 33.39%; p-value= 0.00040) which in turn showed higher proportion in G2 phase (32.04% vs 18.62%; p-value= 8.70623E-06) (**Figure 6.7.3.5**). Thus the advantage of miR-7 sponge expressing cells in proliferation can be explained by the rapid progression of these cells through the cell cycle.

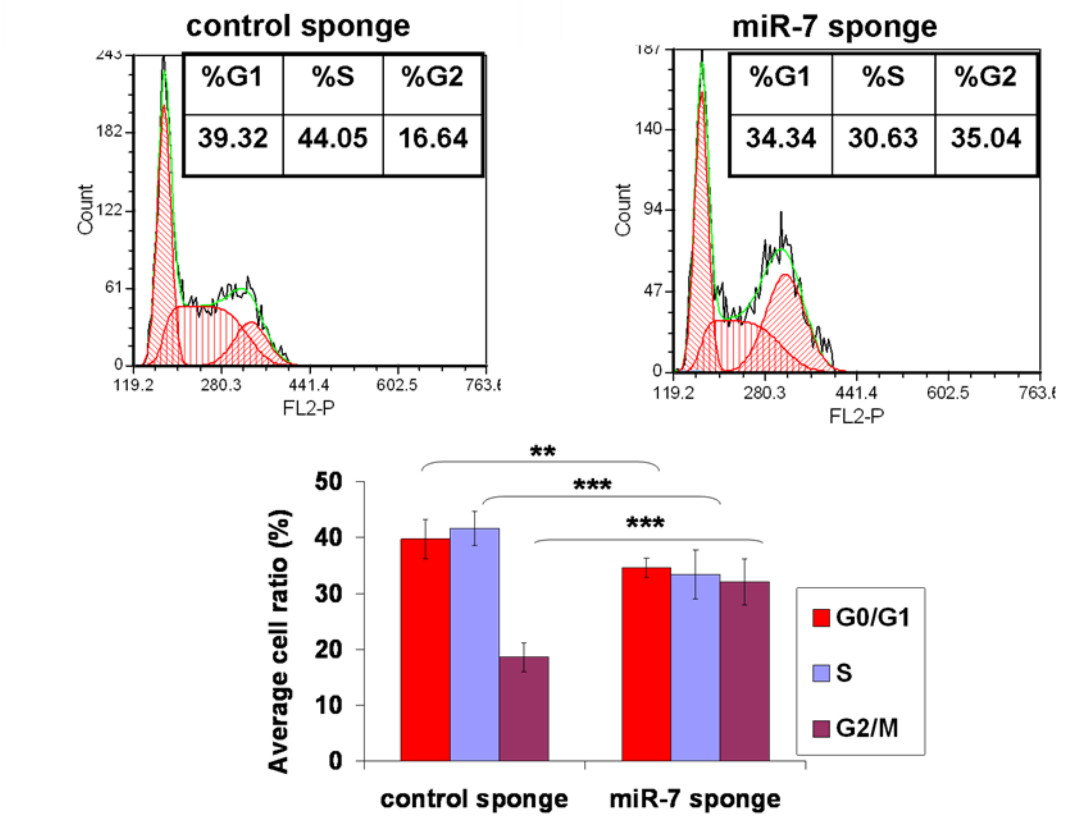

Figure 6.7.3.5: Cell cycle analysis of control sponge and miR-7 sponge expressing CHO-K1 SEAP cells. Control sponge (a) and miR-7 sponge expressing clones (b) were harvested 72 hrs after passaging and stained with Guava Cell Cycle reagent (FL2-P, Propidium Iodide). Cell cycle analysis was carried out using a Guava Flow cytometry. The data enclosed in FCS files were extracted and analysed using FCS Express Plus software. The average of cell ratio for 12 control and 10 miR-7 sponge expressing clones was calculated and represented in c. Bars represent standard deviations between the clones (n=12 and n=10). For statistical significance of the mean value, a Student t-test was performed. **: p-value<0.01; ***: p-value<0.001.

6.7.3.6 Validation of miR-7 sponge technology

Before pursuing our investigation of the impact of miR-7 sponge in larger-scale and fed-batch culture, it was important to ensure that the cell growth phenotype observed in miR-7 sponge expressing cells was specific to endogenous miR-7. In this regard, levels of miR-7 expression were investigated in CHO-K1 SEAP cells. Surprisingly, the levels of mature miR-7 were significantly higher (by 5.11-fold) in miR-7 sponge expressing clones (p-value=0.000864) (**Figure 6.7.3.6.A**), suggesting that cells were possibly compensating for the lack of miR-7 by increasing pre-miR-7 transcription.

To verify this hypothesis, cellular levels of precursor miR-7 were analysed. Although not significant, there appeared to be a slight decrease in pre-miR-7 expression in the miR-7 sponge clones (**Figure 6.7.3.6.A**). Thus the hypothesis that cells may be compensating for the perceived lack of miR-7 by activating transcription was unfounded. Another possibility could be the recently described phenomenon of target mediated miRNA protection (TMMP) whereby the miRNAs shielded from degradation by being bound to its target (Chatterjee, et al. 2011). This prevents exonucleases such as XRN-2 from accessing miRNA. By providing a large number of targets (the miR-7 sponge transcript), mature miR-7 may be protected by TMMP and upon lysis the interaction is disrupted, releasing the miR-7 molecules and resulting in an apparent up-regulation when analysed by qPCR.

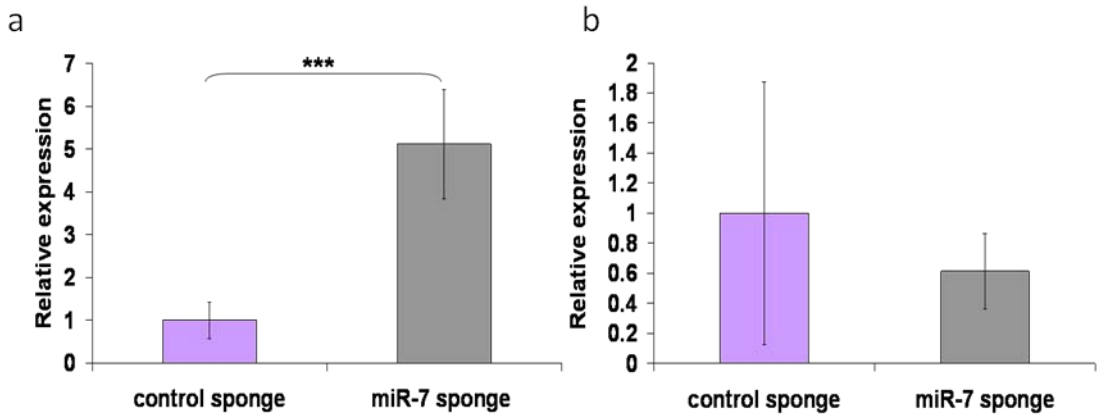

Figure 6.7.3.6.A: Expression of mature miR-7 (a) and precursor miR-7 (b) in control and miR-7 sponge expressing clones. Changes in the levels of expression of miR-7 were analysed using AB7500 Real Time PCR instrument. Bars represent standard deviations of four biological replicates in figure a and triplicates in figure b. Each sample was run with three technical replicates. A Student t-test was carried out to investigate the statistical significance of the changes in miR-7 expression. ***: p-value<0.001. The levels of expression of miR-7 were normalised to snRNAu6 and the levels of expression of precursor miR-7 were normalised to 18S rRNA.

To better understand the mode of action of the miRNA sponge and to verify whether the sponge protected miR-7 against degradation, a siRNA against dEGFP was transfected into miR-7 sponge expressing cells. Inhibition of dEGFP protein was confirmed by the low fluorescence of GFP (**Figure 6.7.3.6.B**).

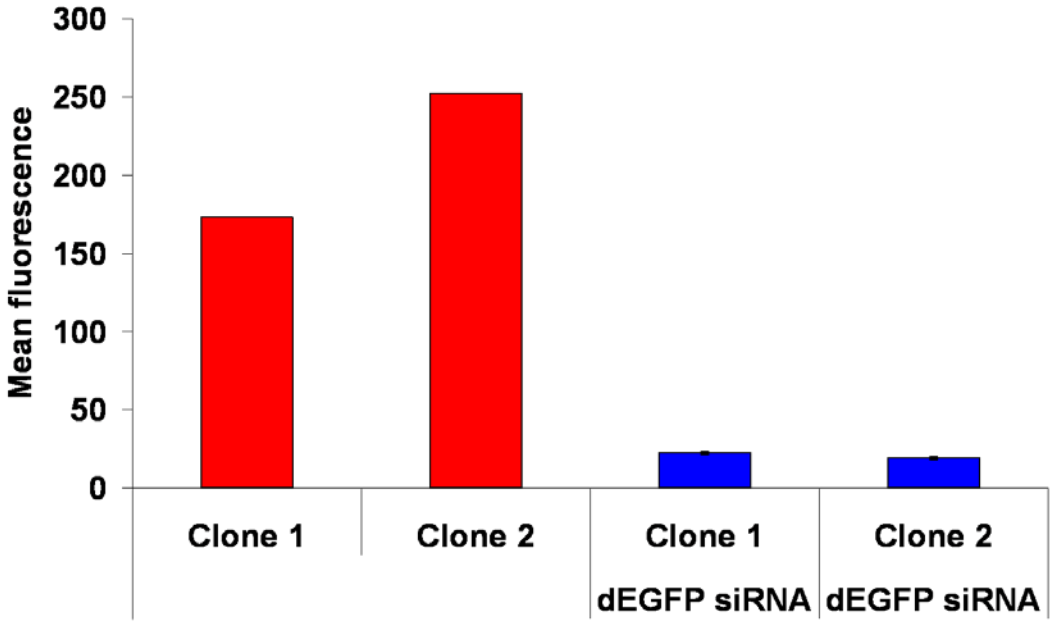

Figure 6.7.3.6.B: Knockdown of dEGFP by RNAi in miR-7 sponge expressing clones. GFP mean fluorescence was analysed using GFP Express Plus software by Guava flow cytometry. Bars represent standard deviations of three technical replicates for clones 1&2 treated with dEGFP siRNA (in blue). The control clones 1&2 (in red) represent one biological sample. The levels of GFP expression were normalised to the levels of 18S rRNA.

Following inhibition of dEGFP, the levels of miR-7 expression in miR-7 sponge expressing cells were similar to the levels of expression in the control cells. The range of Ct values were from 31.8 to 32.4 (**Figure 6.7.3.6.C**). The levels of precursor miR-7 were also investigated after knockdown of dEGFP. There was no difference of expression between the control and miR-7 sponge expressing clones (**Figure 6.7.3.6.C**). Thus knockdown of dEGFP by RNAi may have promoted the degradation of the sponge cassette thus leading to reduction of miR-7 levels in the cells. These results suggested that the the sponge may have protected miR-7 against degradation resulting in apparently high levels of miR-7 in miR-7 sponge expressing clones (**Figure 6.7.3.6.C**).

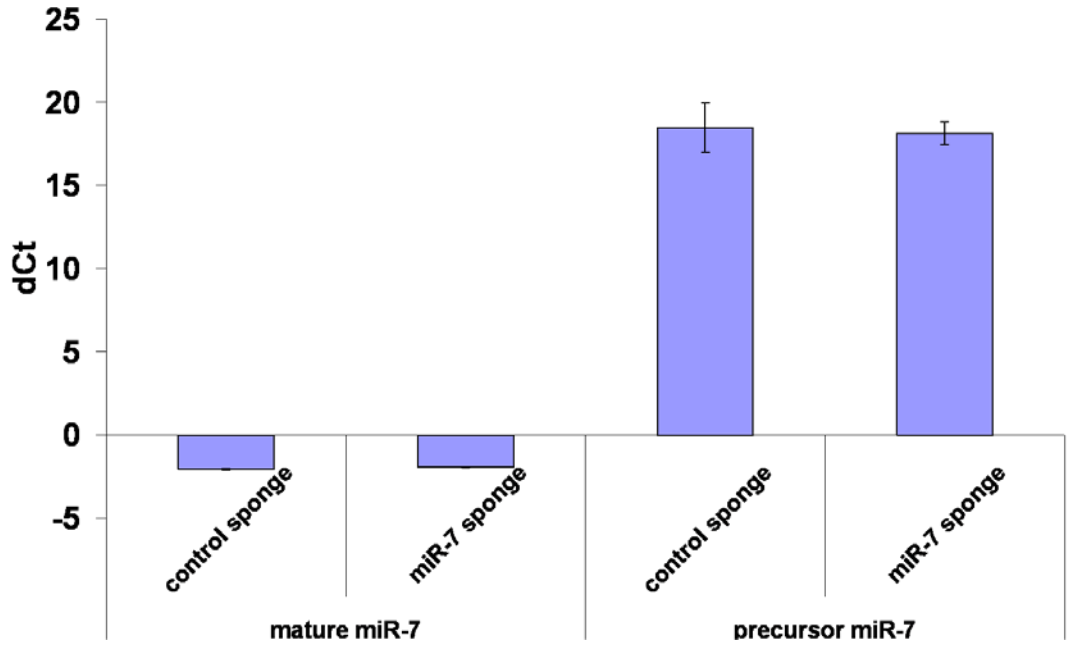

Figure 6.7.3.6.C: Expression of mature miR-7 (a) and precursor miR-7 (b) in control and miR-7 sponge expressing clones after dEGFP knockdown. Change in expression of miR-7 was analysed using the AB7500 Real Time PCR instrument. The levels of expression of miR-7 and precursor miR-7 were normalised to U6 snRNA and to 18S rRNA respectively. Bars represent the ΔCt standard errors of three clones.

To verify that the sponge was soaking up endogenous miR-7 in an efficient manner, a transient transfection was performed with pm-neg, am-neg and pm-7 molecules at a concentration of 30nM in control and miR-7 sponge expressing CHO-K1 SEAP cultures. Ten different clones expressing either control sponge or miR-7 sponge were subjected to this treatment. One day after transfection, transient up-regulation of miR-7 induced further reduction in GFP signal fluorescence only in the miR-7 sponge expressing cells, indicating that the sponge worked appropriately to target not only endogenous miR-7 but also exogenous miR-7 (**Figure 6.7.3.6.D**). As expected, following transient miR-7 up-regulation, cell density dropped in the control treated cells (**Figure 6.7.3.6.E**). In theory, up-regulation of miR-7 should antagonize the positive impact of the miR-7 sponge on cell proliferation so no difference should be seen between pm-neg and pm-7 treated cells. This was verified for two clones that showed similar cell number after pm-neg and pm-7 treatment (**Figure 6.7.3.6.E**). However, the three other clones had a lower cell density after transient miR-7 overexpression. These clones may have a lower copy numbers of the sponge cassette resulting in less efficiency to counteract the excess of pm-7 molecules.

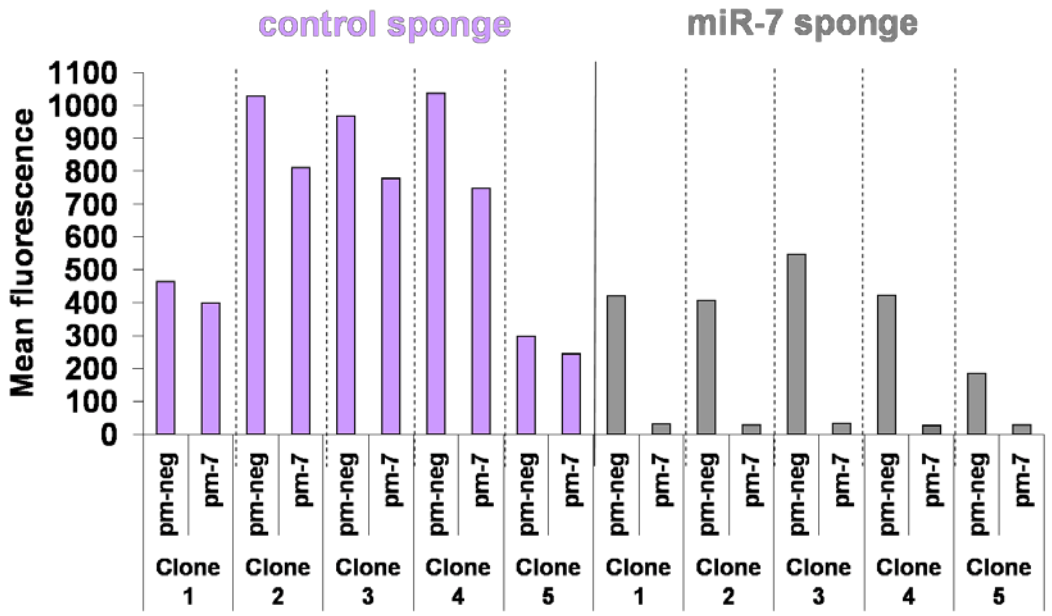

Figure 6.7.3.6.D: Analysis of GFP fluorescence after transfection of pm-neg or pm-7 in control and miR-7 sponge expressing cells. Cells were seeded at $1*10^5$cells/ml prior to transfection with pm-neg and pm-7 molecules at a concentration of 30nM in serum-free medium. GFP mean fluorescence was analysed using GFP Express Plus software by Guava flow cytometry 24 hrs after transfection. pm-neg: control for mimics; pm-7: mimic of miR-7.

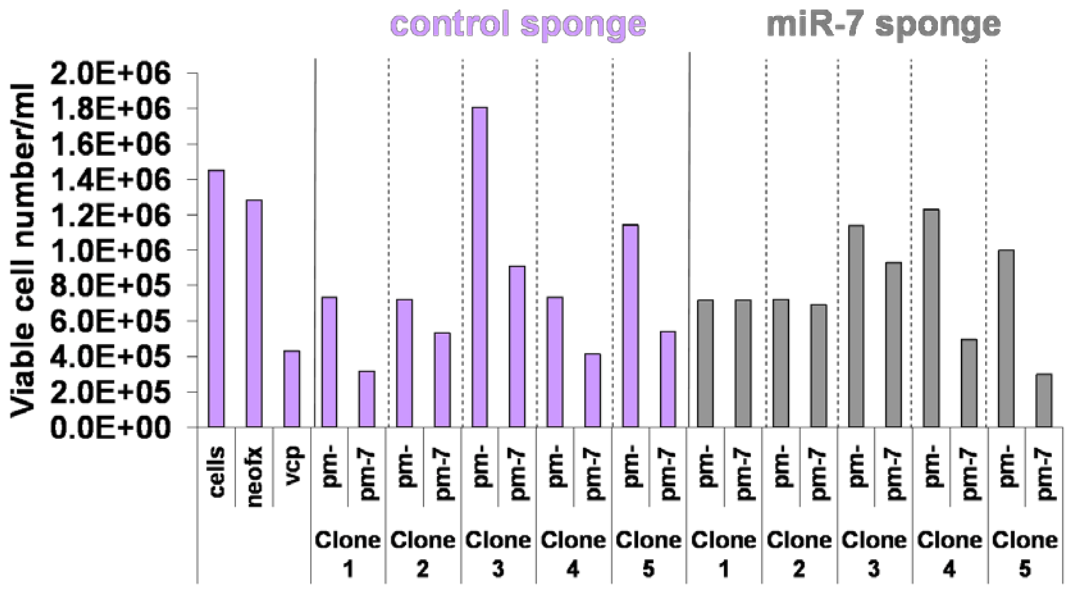

Figure 6.7.3.6.E: Analysis of cell density after transfection of pm-neg or pm-7 in control and miR-7 sponge expressing cells. Cells were seeded at $1*10^5$cells/ml prior to transfection with pm-neg and pm-7 molecules at a concentration of 30nM in serum-free medium. Cells were stained with GuavaViacount reagent and cell density was analysed by Guava Flow Cytometry three days after transfection. cells: non-transfected cells; neofx: transfection reagent in its own; vcp: siRNA against Valosin-containing protein; pm-neg: control for mimics; pm-7: mimic of miR-7.

Another transfection was performed at higher concentration to investigate the efficiency of miR-7 sponge and its levels of saturation. Although the miR-7 sponge was efficient at sequestering the exogenous miRNAs at 30nM, the same profile was observed at 50nM (**Figure 6.7.3.6.F**). As expected GFP fluorescence was reduced after pm-7 treatment in miR-7 sponge expressing cells. Inhibitor molecules were also transfected at 50 nM to investigate whether their presence in the cells would trigger competitive binding between these molecules and the sponge for miR-7. Transient inhibition of miR-7 slightly increased GFP fluorescence in four of the miR-7 sponge expressing clones (**Figure 6.7.3.6.F**).

Together these results confirmed that the miR-7 sponge was highly expressed in the cells to efficiently sequester not only endogenous miR-7 but also exogenous miR-7 molecules. This confirmed that the improvement in cell proliferation was a direct consequence of miR-7 sequestration.

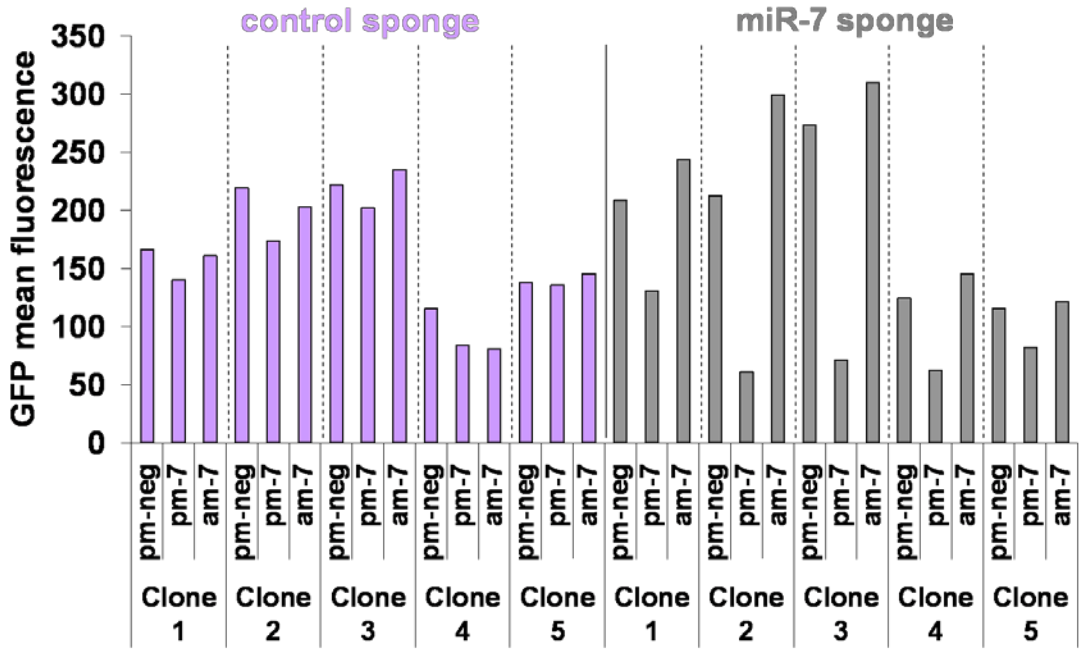

Figure 6.7.3.6.F: Analysis of GFP fluorescence after transfection of pm-neg, pm-7 or am-7 in control and miR-7 sponge expressing cells. Cells were seeded at $1*10^5$cells/ml prior to transfection with pm-neg, pm-7 and am-7 molecules at a concentration of 50 nM in serum-free medium. GFP mean fluorescence was analysed using GFP Express Plus software by Guava flow cytometry one day after transfection. pm-neg: control for mimics; pm-7: mimic of miR-7; am-7: inhibitor for miR-7;

To verify whether the sponge cassette was degraded or not, mRNA levels of GFP were monitored after transient up-regulation of miR-7 in control and miR-7 sponge expressing cells. In theory, the GFP-sponge transcript should not be targeted for degradation as it was designed with a bulge.

Surprisingly, there was a 27.67-fold reduction of GFP expression in miR-7 sponge expressing clones (p-value=0.009881) (**Figure 6.7.3.6.G**) thus suggesting that the sponge cassette underwent degradation. However, we postulated previously that the sponge may protect miR-7 from exonuclease-dependent degradation. Thus the bulge may be not effective in preventing destabilization of the transcript when miR-7 molecules are in excess in the cells.

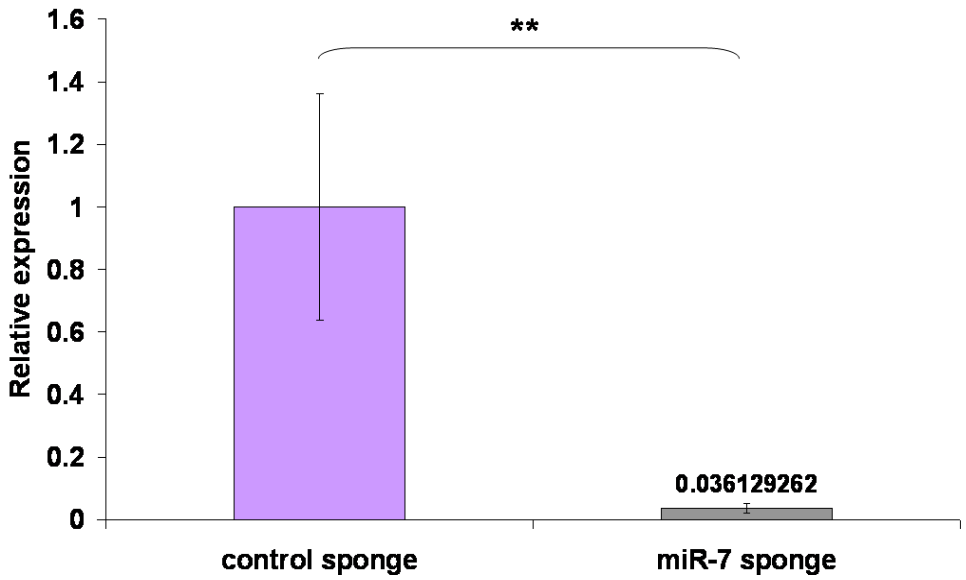

Figure 6.7.3.6.G: Levels of dEGFP expression following pm-7 transfection in control and miR-7 sponge expressing cells. GFP expression was evaluated 24 hrs after transfection by qPCR using the AB7500 Real Time PCR instrument. The levels of miR-7 expression were normalised to U6 snRNA for correction of RNA input. Bars represent standard deviations of three clones. Statistical significance of dEGFP knockdown was investigated using a Student t-test. **: p-value< 0.01

6.7.3.7 Impact of stable miR-7 knockdown in CHO-K1 SEAP cell cultured in fed-batch culture

6.7.3.7.1 Investigation of miR-7 sponge impact on CHO-K1 SEAP growth and viability

To further verify the advantage of miR-7 sponge expressing cells on cell growth, a fed-batch assay was performed for 13 days at 37°C, in 30 ml starting volume with the two best performing clones from the control and miR-7 sponge expressing CHO-K1 SEAP cells. 4.5ml of Fed CHO CD EfficientFeed A™ (Invitrogen) medium was added to the culture at day 0. Then 3ml were added every three days to extend the culture period. Samples were harvested every day to assess cell growth, cell viability and cell productivity.

miR-7 sponge expressing clone 2 and clone 7 showed a higher cell density from day 5 of the culture (control sponge 2: $54.4x10^5$cells/ml; control sponge 13: $47.04x10^5$cells/ml; miR-7 sponge 2: $58.32x10^5$cells/ml; miR-7 sponge 7: $56.74x10^5$cells/ml) (**Figure 6.7.3.7.A**). This difference was increased at day 6 (control sponge 2: $62.74x10^5$cells/ml; control sponge 13: $53.45x10^5$cells/ml; miR-7 sponge 2: $81.81x10^5$cells/ml; miR-7 sponge 7: $69.82x10^5$cells/ml). Although cell density dropped in the four cultures the following day, cell density in miR-7 sponge expressing cells dropped more slowly resulting in an extended period of culture while maintaining high cell viability at later stages of culture (control sponge 2: 56.36%; control sponge 13: 52.54%; miR-7 sponge 2: 83.32%; miR-7 sponge 7: 81.89%) (**Figures 6.7.3.7.A&D**). Cell growth rate (change in cell concentration per minute) and accumulated integral viable cell density (AIVCD; cell per time per unit volume accumulated over the culture) confirmed the advantage of miR-7 sponge expressing clones (**Figures 6.7.3.7.B&C**).

Thus miR-7 knockdown significantly improved cell growth rate and maintained high viability in fed-batch culture. These results confirmed the value of the miR-7 sponge as a tool to improve CHO proliferation in culture.

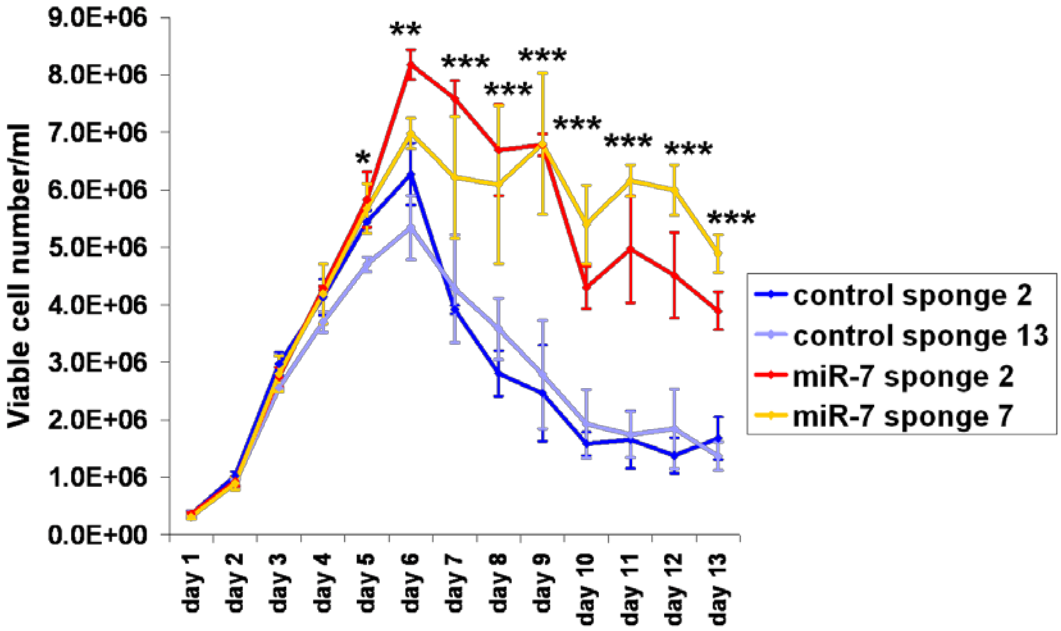

Figure 6.7.3.7.A: Evaluation of cell density in control and miR-7 sponge expressing in fed-batch culture. Two clones from the control sponge population and two clones from the miR-7 sponge group were seeded at $2x10^5$cells/ml and cultured in 30ml in serum-free medium. Clones were run in biological triplicates for 13 days. 4.5ml of Fed CHO CD EfficientFeed A™ (Invitrogen) medium was added to the culture at day 0. Then 3ml were added every three days to extend the culture period. Cells were harvested every day and stained with trypan blue solution to monitor cell density by Cedex Automated Cell Counter (Roche). Bars represent standard deviations of three biological replicates. Two clones from the control sponge population and two clones from the miR-7 sponge group were seeded at $2x10^5$cells/ml and cultured in 30ml in serum-free medium. A Student t-test was performed to evaluate the statistical significance between the density average of the control sponge clones with the density average of the miR-7 sponge clones. *: p-value< 0.05; **: p-value< 0.01; ***: p-value< 0.001.

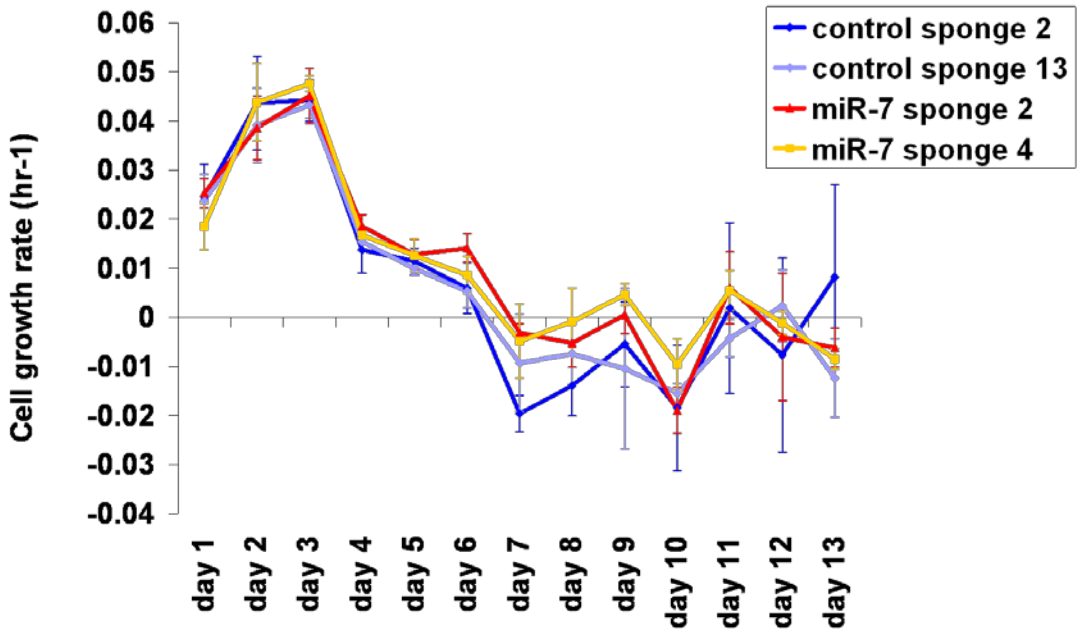

Figure 6.7.3.7.B: Evaluation of cell growth rate in control and miR-7 sponge expressing in fed-batch culture. Two clones from the control sponge population and two clones from the miR-7 sponge group were seeded at $2x10^5$cells/ml and cultured in 30ml in serum-free medium. Clones were run in biological triplicates for 13 days. 4.5ml of Fed CHO CD EfficientFeed A™ (Invitrogen) medium was added to the culture at day 0. Then 3ml were added every three days to extend the culture period. Cells were harvested every day and stained with trypan blue solution to monitor cell density by Cedex Automated Cell Counter (Roche). Bars represent standard deviations of three biological replicates. A Student t-test was performed to evaluate the statistical significance between the cell growth rate average of the control sponge clones with the average cell growth rate average of the miR-7 sponge clones. There was no statistical significance.

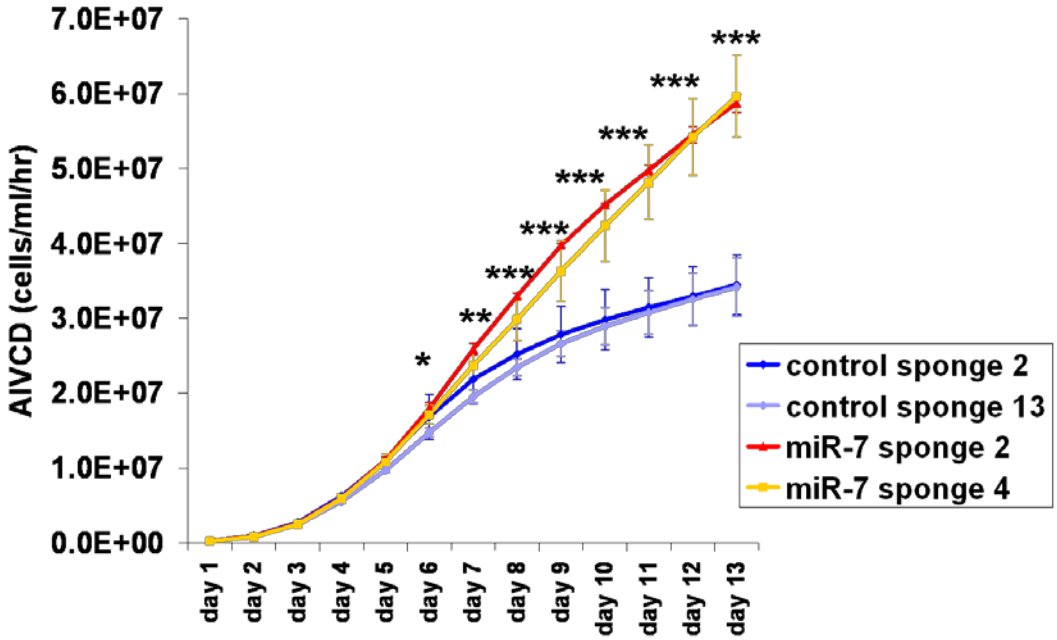

Figure 6.7.3.7.C: Evaluation of accumulated integrated viable cell density in control and miR-7 sponge expressing in fed-batch culture. Two clones from the control sponge population and two clones from the miR-7 sponge group were seeded at $2x10^5$cells/ml and cultured in 30ml in serum-free medium. Clones were run in biological triplicates for 13 days. 4.5ml of Fed CHO CD EfficientFeed A™ (Invitrogen) medium was added to the culture at day 0. Then 3ml were added every three days to extend the culture period. Cells were harvested every day and stained with trypan blue solution to monitor cell density by Cedex Automated Cell Counter (Roche). Bars represent standard deviations of three biological replicates. A Student t-test was performed to evaluate the statistical significance between the AIVCD average of the control sponge clones with the AIVCD average of the miR-7 sponge clones. *: p-value< 0.05; **: p-value< 0.01; ***: p-value< 0.001.

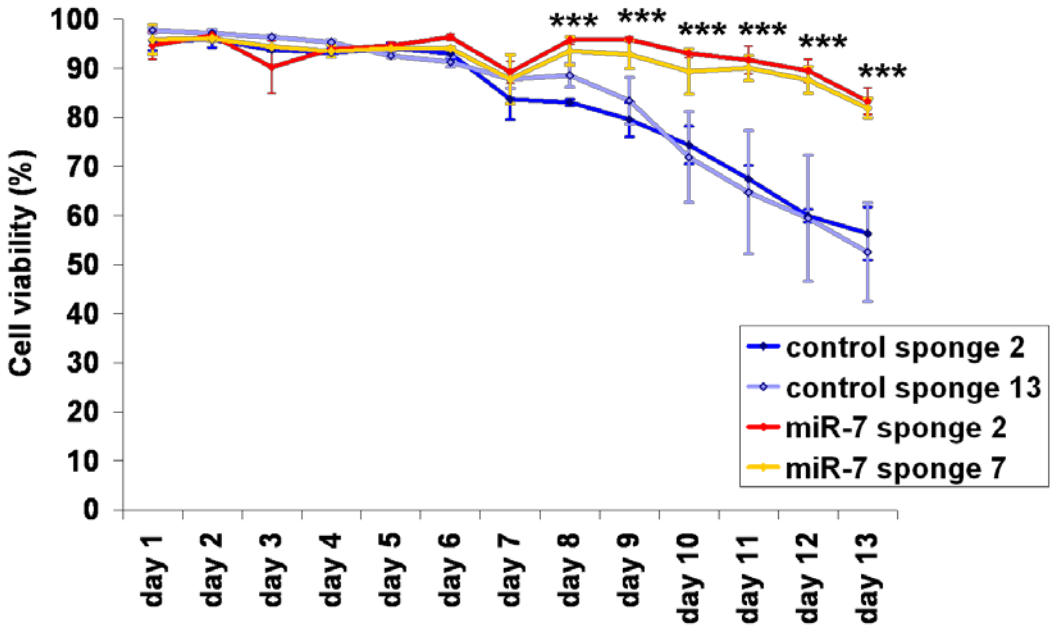

Figure 6.7.3.7.D: Evaluation of cell viability in control and miR-7 sponge expressing in fed-batch culture. Two clones from the control sponge population and two clones from the miR-7 sponge group were seeded at $2x10^5$cells/ml and cultured in 30ml in serum-free medium. Clones were run in biological triplicates for 13 days. 4.5ml of Fed CHO CD EfficientFeed A™ (Invitrogen) medium was added to the culture at day 0. Then 3ml were added every three days to extend the culture period. Cells were harvested every day and stained with trypan blue solution to monitor cell viability by Cedex Automated Cell Counter (Roche). Bars represent standard deviations of three biological replicates. A Student t-test was performed to evaluate the statistical significance between the cell viability average of the control sponge clones with the cell viability average of the miR-7 sponge clones. *: p-value< 0.05; **: p-value< 0.01; ***: p-value< 0.001.

6.7.3.7.2 Investigation of miR-7 sponge impact on SEAP total yield and normalised productivity

To investigate the impact of miR-7 sponge on SEAP productivity, in the same fed-batch culture, supernatants of samples were harvested every day to evaluate normalised productivity and total yield.

Control sponge expressing clone 2 had the highest total yield over the culture period, followed by miR-7 sponge expressing clone 2 and clone 7 (**Figure 6.7.3.7.E**). Control sponge expressing clone 2 also had the highest normalised productivity. This impact was further increased from day 6 and prolonged until later stages of culture (**Figure 6.7.3.7.F**). miR-7 sponge did not improve normalised productivity.

Taken all together, these results suggested that sponge miR-7 is an efficient tool to extend the longevity of the culture as well as to improve cell growth rate, AIVCD and cell viability. The monitoring of more clones in culture would validate these results and would provide more information on the impact of miR-7 on protein production.

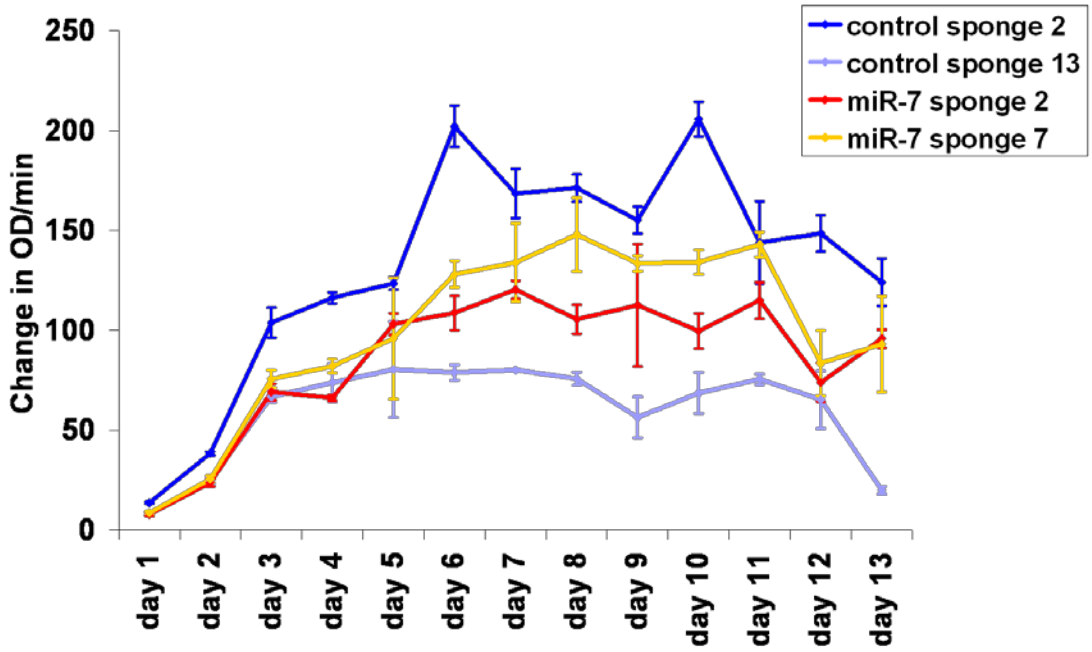

Figure 6.7.3.7.E: Evaluation of SEAP total yield in control and miR-7 sponge expressing cells cultured in fed-batch. Supernatants of samples were harvested every day for 13 days**.** Change in absorbance of SEAP substrate, p-nitrophenolphosphate, was analysed using a kinetic assay. Bars represent standard deviations of three biological replicates.

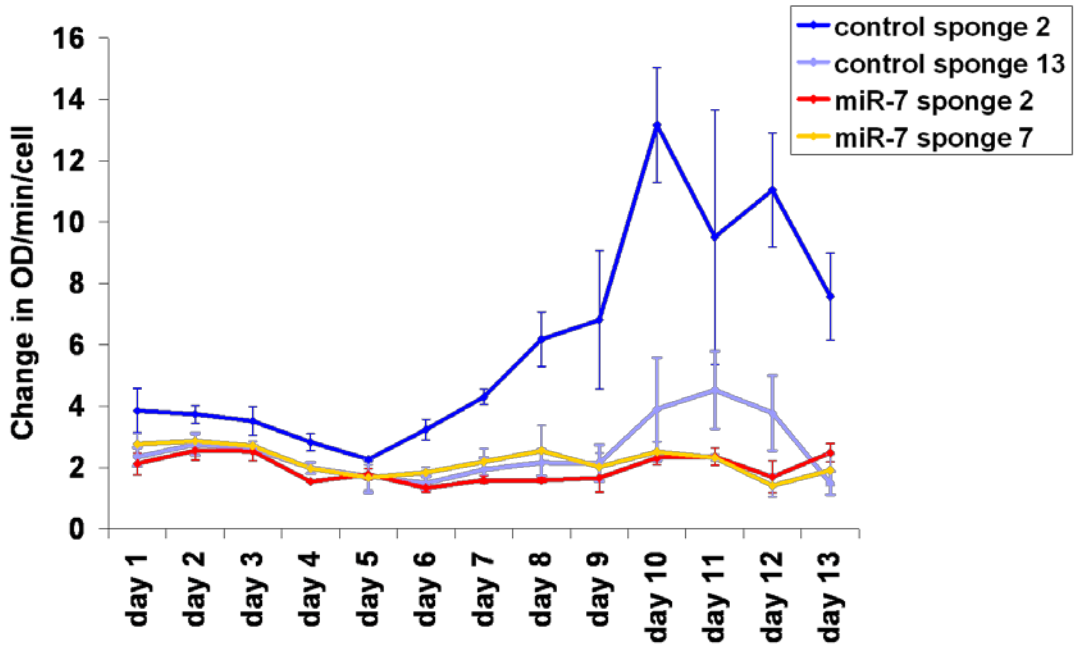

Figure 6.7.3.7.F: Evaluation of normalised productivity in control and miR-7 sponge expressing cells cultured in fed-batch. Supernatants of samples were harvested every day for 13 days**.** Change in absorbance of SEAP substrate, p-nitrophenolphosphate, was analysed using a kinetic assay. Bars represent standard deviations of three biological replicates.

6.8 The role of miR-7 in CHO cells

6.8.1 Investigation of the role of miR-7 in cell cycle and apoptosis

Previously, we showed that subsequent to pm-7 transfection cell growth was significantly reduced and cell viability was maintained. Once the effect of the transfection diminishes the cells re-enter the cell cycle and proliferate normally.

To establish the role of miR-7 in the regulation of cell cycle, we performed cell cycle analysis 72 hrs after transfection. High levels of miR-7 triggered cell accumulation in G1 phase (59.73%) compared to pm-neg (31.86%) thus reducing the proportion of cells in S and G2 phases (**Figure 6.8.1.A).** There was no indication of cells in sub-G1 population suggesting that cells did not undergo apoptosis while arrested. Thus pm-7 treated cells were arrested in G0/G1 phase compared to pm-neg treated cells which progressed normally through the cell cycle.

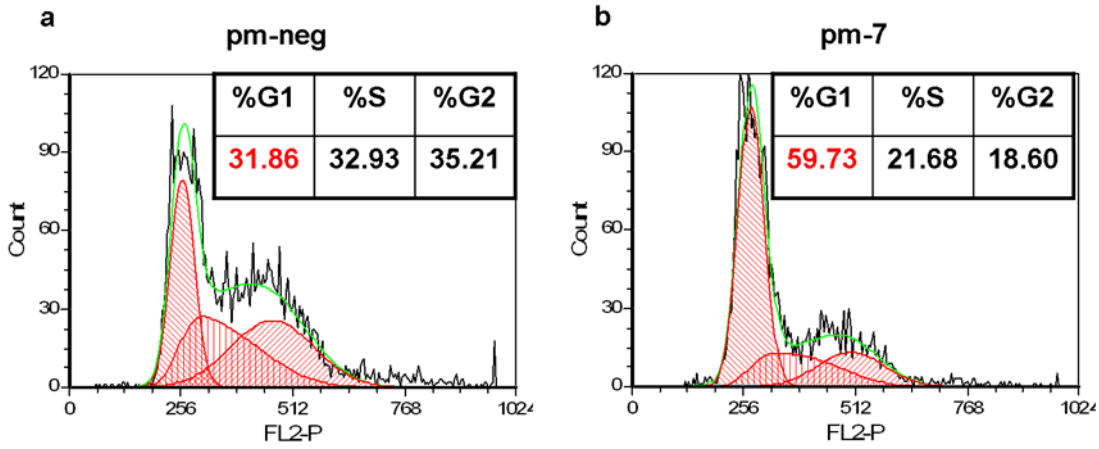

Figure 6.8.1.A: Cell cycle analysis after pm-7 transfection.

Cells were stained with Guava Cell Cycle reagent at day 3 following treatment with pm-neg (a) or pm-7 (b). The data were captured using a Guava Flow cytometry. FCS files from cell cycle assay were extracted and analysed using FCS Express Plus, a curve fitting software. FL2-P: fluorescent light of the DNA dye, Propidium iodide.

We measured the apoptosis levels specifically using Nexin assay in the cells and found that there was no significant change 72hrs after transfection (**Figure 6.8.1.B**). However, at 120hrs after transfection the apoptotic percentage was very slightly but significantly increased in miR-7 treated cells (**Figure 6.8.1.B**).

Thus the high cell viability and the lack of sub-G1 population observed in pm-7 treated cells suggested that the low cell densities observed were not due to increased levels of apoptosis.

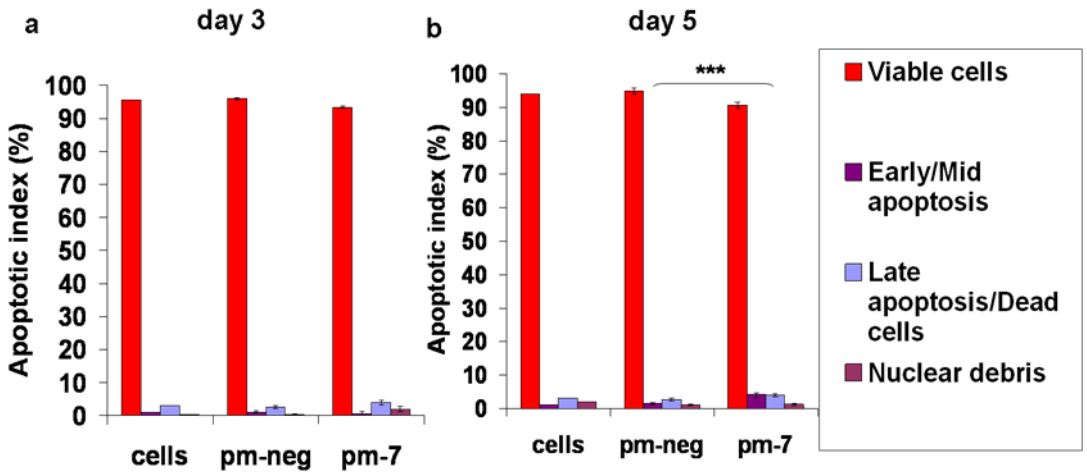

Figure 6.8.1.B: Analysis of the levels of apoptosis after pm-7 transfection.

Apoptosis rate was evaluated with the Nexin assay reagent at day 3 (a) and day 5 (b) after pm-neg or pm-7 transfection. The data were captured using a Guava Flow cytometry. Bars represent standard deviations of five biological replicates in pm-neg and pm-7 treated cells. The statistical significance of these data was analysed using a Student t-test. ***: p-value< 0.001.

6.8.2 Investigation of the molecular mechanisms beyond the growth arrest in G1 phase

We then investigated the possibility of senescence occurring subsequent to G1 arrest of cells by analysis of senescence-associated β-galactosidase activity. As a positive control, different concentrations of BrDU were used in an attempt to induce senescence in CHO cells (**Figure 6.8.2.A**). However, CHO cells did not become senescent even at high concentration of BrdU. CHO cells are known to replicate indefinitely and are likely to carry mutations in senescence-specific genes so it is possible that senescence cannot be induced in these cells. Another explanation is that senescence in CHO cells is not associated with β-galactosidase.

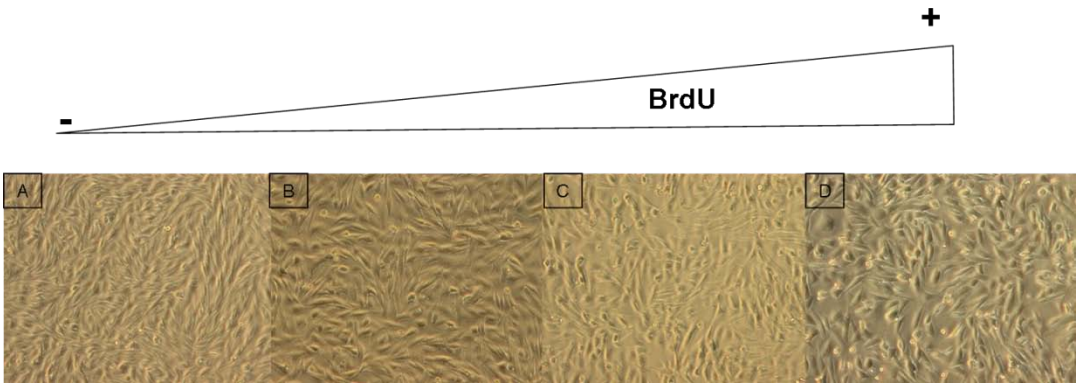

Figure 6.8.2.A: Treatment of BrDU in CHO cells. A: non-treated cells; B: cells treated with 250 µM; C: cells treated with 500 µM; D: cells treated with 1mM.

As a positive control of senescence, a breast cancer cell line, HCC1419 cells, was treated with 50µM of BrDU. A blue color indicated the presence of β-galactosidase thus confirming that senescence was efficiently induced in this cell line (**Figure 6.8.2.B**). Treatment with a non-specific control or exogenous miR-7 molecules did not activate β-galactosidase in CHO cells (**Figure 6.8.2.B**). We also previously showed that the impact of transient miR-7 transfection on cell growth was diminished at day 5 and lost at day 7 after transfection presumably allowing cells to re-enter the cell cycle. This would not be the case in senescent cells as their arrest is irreversible. Thus the cell growth arrest observed in G1 phase is not likely to be a result of senescence indicating that other mechanisms are responsible for the arrest of CHO cells in G1.

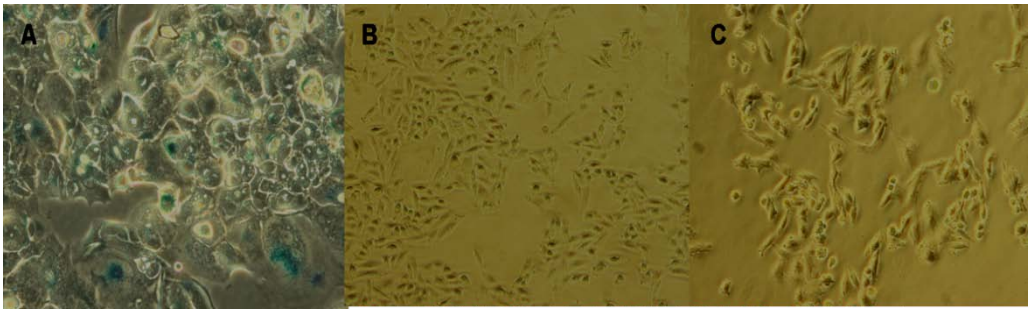

Figure 6.8.2.B: miR-7 does not trigger senescence.

β-galactosidase was assayed after 96 hrs using a senescence β-galactosidase staining kit in cells treated with BrdU, pm-neg or pm-7 treatment. Cells were observed using microscopy at 20X. A: HCC1419 cells treated with 50 µM BrdU as positive control; **B**: pm-neg-treated CHO cells; **C**: pm-7-treated cells.

6.8.3 Investigation of miR-7 targets

6.8.3.1.1 Identification of miR-7 targets

To further investigate the molecular mechanisms by which miR-7 influences cell growth, we performed gene expression profiling using CHO specific oligonucleotide arrays. The identification of direct miRNA targets presents some challenges in mammals. Unlike miRNAs in plants which have near-perfect complementarity with their targets, the specific binding between the seed region of a miRNA and the 3'UTR of its cognate mRNA target has different degrees of complementarity in mammals. In addition, the miRNA-mRNA binding can also occur elsewhere including in the 5'UTR, in the ORF or in multiple binding sites. At the time of the assay, the other challenge was the lack of genomic sequences publicly available for Cricetulus griseus or CHO. Therefore a custom CHO oligonucleotide WyeHamster3a microarray (Affymetrix) was used in this study. It contained a total of 19,809 CHO-specific transcripts, combining library-derived CHO and publicly-available hamster sequences, as well as 92 (non-CHO) array quality control sequences (Housekeeping and Spike Controls) and 22 product/process specific sequences, covering an estimated 85% of the CHO genome (unpublished at the time of the assay). The CHO-specific microarrays were provided by Pfizer (Pfizer Grange Castle, Dublin and Pfizer Andover, Massachussets). Cells were treated with non-specific control (pm-neg) or with mimic molecules of endogenous miR-7 (pm-7). Non-transfected cells were also included as a control. The changes in gene expression upon pm-neg treatment were compared to the changes in the non-transfected cells to assess the impact of the transfection itself. Non-transfected cells were al so compared to pm-7 transfected cells and this latter was compared to pm-neg treated cells. All samples were run in biological triplicates.

A heat map was generated using unsupervised hierarchical clustering and showed that the replicates clustered together but also that the pm-neg and non-transfected cells were more similar than the miR-7 transfected cells (**Figure 6.8.3.A**). Genes were considered to be differentially expressed and statistically significant if a 1.2 fold change in either direction was observed with a p-value<0.05.

Overall, the heat map showed that the gene expression data from the non-transfected cells and pm-neg treated cells were more similar than pm-7 (**Figure 6.8.3.A**). This observation was confirmed by the number of differentially expressed genes in each comparison. In fact, only a very small number of genes were detected as differentially regulated after transfection with pm-neg compared to non-transfected cells (13 up-regulated and 39 down-regulated genes (**Figure 6.8.3.A**). On an array with >19,000 probesets, we would expect more than this by chance. In addition, the comparison between pm7/pm-neg and pm-neg/cells showed no overlap between the two groups. Taken together these results indicated that the changes observed upon pm-7 transfection were specific to the increase in miR-7 levels and not due to the transfection itself. Also the changes in gene expression of the biological replicates of pm-7 transfected cells were in the same direction (up-regulation or knockdown) and to a very similar extent (**Figure 6.8.3.A**). This was also observed in the non-tranfected cells. Although, the three replicates in pm-neg treated cells showed some variation in the extent of the expression variation, the direction of the changes was the same. This consistency between biological replicates added more strength and confidence to our results and demonstrated that the array experiment performed well.

Among the differentially regulated genes upon pm-7 transfection, 341 probesets were found to be significantly down-regulated and 219 were found to be up-regulated (1.2-fold cut-off filter, $p < 0.05$) (**Figure 6.8.3.A**) (refer to appendices 2&3 for the full list of up- and down-regulated genes). This generated a list of 355 annotated, non-redundant, differentially expressed gene transcripts. This number is in line with the fact that miRNAs are known to typically target hundreds of genes (Bartel 2004). The magnitude of down- and up-regulation did not exceed fourfold (**Appendices 2&3 respectively**) which is also consistent with what has been reported previously (Baek, et al. 2008, Selbach, et al. 2008).

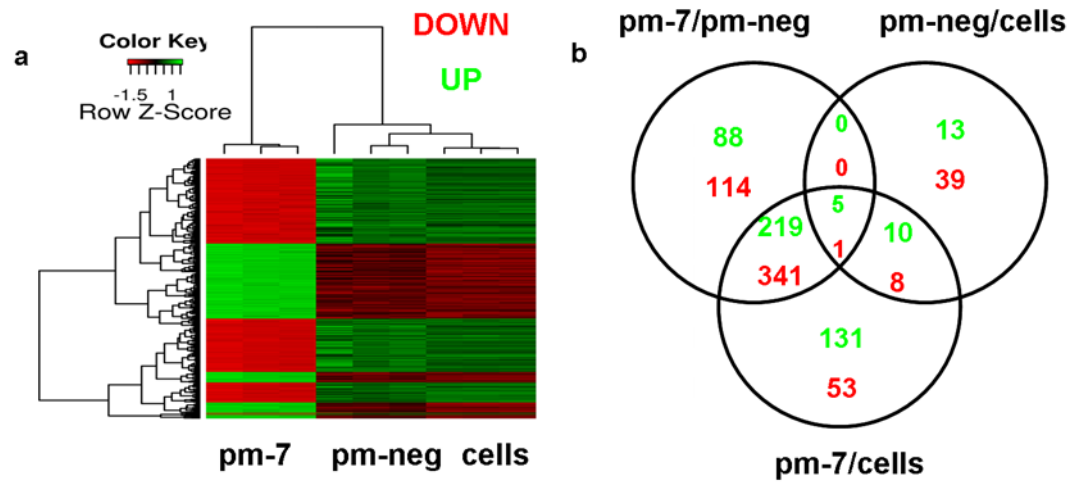

Figure 6.8.3.A: Heat map (a) and venn diagram representing the changes in CHO-specific gene expression upon miR-7 up-regulation.

Following pm-7 or pm-neg transfection, gene expression profiling was performed on biological triplicates using CHO specific oligonucleotide arrays. Genes were considered to be differentially expressed and statistically significant if a 1.2 fold change in either direction was observed along with a Bonferroni adjusted p-value <0.05. Using the LIMA method and Bonferroni algorithm, gene expression between the three groups was evaluated and compared. A heat map was generated using unsupervised hierarchical clustering (a). The relative expression of each gene is represented by the red colour for down-regulation and by the green colour for up-regulation. pm-7: mimic of miR-7; pm-neg: negative control for pm-7; cells: non-transfected cells.

A venn diagram was created (b) to identify the number of genes differentially regulated in three conditions pm-neg/cells, pm-7/cells and pm-7/pm-neg and the overlap between these groups.

To identify the cellular pathways affected by the transient overexpression of miR-7, we conducted a Gene ontology analysis using PANTHER on the diffentially regulated genes found on the array. This revealed that apoptosis, cell cycle, cell proliferation, and DNA repair were in the first 30 overrepresented cellular processes (**Figure 6.8.3.B; Table 4.8.3, Appendices 2-4**).

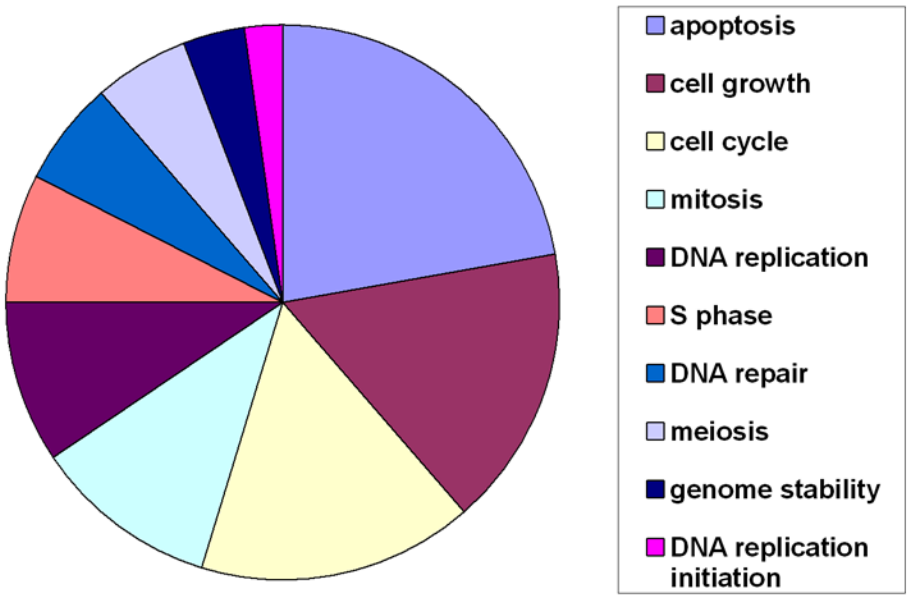

Figure 6.8.3.B: Gene ontology analysis using PANTHER software.
The 10 most represented cellular pathways are displayed in this figure.

6.8.3.1.2 Validation of the array data

To validate the quality of the array data, we checked for proven miR-7 targets. Spata2 was found to be down-regulated by 3.16-fold in the array. This gene has been experimentally validated to be a miR-7 target using next-generation sequencing (Hafner M, 2010). Psme3, Ckap4, Cnot8, Cnn3, Pfn2 were also found to be down-regulated upon miR-7 transfection in A549 cells using also microarray analysis (Webster, et al. 2009). However, the authors did not validate these genes by reporter assay. Although these genes were not validated as direct targets by a reporter assay, there was some overlap with our findings.

To further confirm the array results, we selected 39 genes that were found to be down-regulated in the array and verified their levels of expression by qPCR. Only down-regulated genes were chosen due to the usual mode of action of miRNAs which is the repression of their targets by binding to the 3'UTR. These genes were all significantly down-regulated, with the exception of HDAC1 which was found significantly up-regulated. This inconsistency between the array and the qRT-PCR methods could be the result of a poor quality probeset thus giving a wrong indication of the direction changes. Out of the 39 targets, 16 were predicted as miR-7 targets by different databases (**Table 6.8.3)**. Among these genes, 22 genes have been shown to be involved in the G1/S phase of the cell cycle including Cdk1/2 (down by 4.07-fold and 2.24-fold respectively) and Cyclin D1/3 (down by 4.67-fold and 2.11-fold respectively) (**Figure 6.8.3.C**). Others were associated with replication like the Mcm family (Mcm 2,3,5,7 down between 2.78-fold and 5.33-fold), or with the DNA damage/repair pathway such as Rad52/Rad54l (down by 10.71-fold and 21.64-fold respectively), Psme3 (down by 19.20-fold) or Bcl-2 associated factor (down by 7.27-fold) (**Figure 6.8.3.C**, **Table 6.8.3**). Thus these results confirmed the quality of the array data as well as the cellular pathways identified *in silico*.

Table 6.8.3: Validation of genes down-regulated in the microarray data

Gene ID	**Fold change**		**Prediction**
	Microarray	**qPCR**	
Psme3	-3.924	-19.197	Diana, miranda, mirwalk, targetscan
Apex1	-3.493	-2.510	No
Skp2	-3.267	-2.739	Diana
Cno	-3.236	-3.943	Diana, miranda, mirwalk,targetscan
Spata2	-3.167	-4.747	Diana, miranda, miRwalk, pictar, targetscan
Rad54l	-3.148	-21.642	Mirwalk, pictar
Ccnd3	-3.137	-2.109	No
Peo1	-2.874	-8.863	Diana
Ckap4	-2.871	-2.828	Diana,miranda, mirwalk, pictar, targetscan
Plp2	-2.815	-4.569	Diana, miranda, mirwalk, pictar, targetscan
DHFR	-2.764	-5.126	No
Setd8	-2.667	-2.648	Diana, miranda, pictar, targetscan
Ccnd1	-2.555	-4.669	No
H2afx	-2.552	-8.238	No
Tmem55b	-2.510	-3.493	No
Slc7a5	-2.506	-4.710	No
Mcm2	-2.493	-4.190	No
Lig1	-2.485	-5.998	No
Orc1l	-2.424	-4.730	No
Cdk2	-2.413	-2.245	MiRwalk
Aup1	-2.399	-3.118	No
Mcm5	-2.391	-5.332	No
Mcm3	-2.251	-3.765	No
Aplp2	-2.166	-5.207	No
Bclaf1	-2.005	-7.266	No
Slc39a9	-1.963	-3.434	No
Cdc6	-1.861	-15.770	No
Cnot8	-1.851	-2.622	Diana, miranda, pictar,

			targetscan
Mcm7	-1.847	-2.779	No
Cenpo	-1.783	-4.238	Diana, miranda
Fen1	-1.767	-2.997	No
Cdc25b	-1.752	-3.706	No
TFDP1	-1.544	-2.624	Miranda
Pabpn1	-1.311	-2.005	Diana
Cdc7	-1.244	-1.625	No
Rad52	-0.851	-10.708	No
Cdk1	-0.754	-4.071	Diana, targetscan
BCL10	-0.737	-3.968	No
Hdac1	2.529	2.920	Diana, targetscan

Table 6.8.3: Validation of down-regulated genes

Several genes found to be differentially regulated in the oligonucleotide array study were validated using the AB7500 Real Time PCR instrument. Gene expression was normalised to β-actin, the endogenous control. Different databases including DIANA LAB, Micro.org, miRWalk, PicTar and TargetScan (Grimson, et al. 2007, Krek, et al. 2005, Maragkakis, et al. 2009, Dweep, et al. 2011, Friedman, et al. 2009, Betel, et al. 2008) were used to identify predicted binding sites between miR-7 and its mRNA targets in mammals.

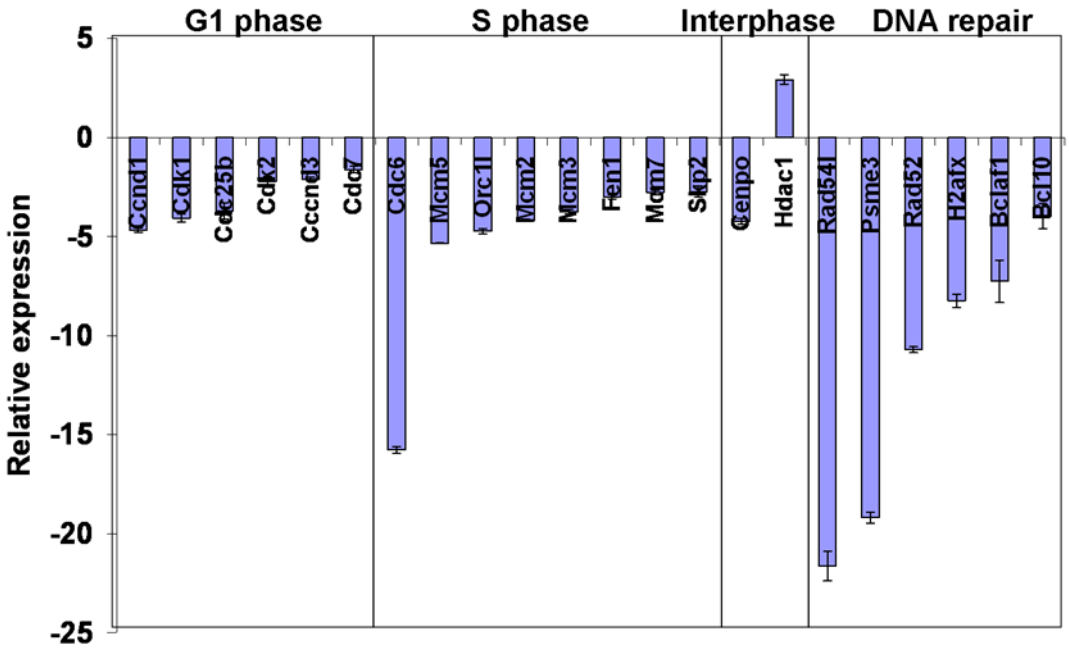

Figure 6.8.3.C: Validation of arrays results using qRT-PCR

Genes involved in cell cycle regulation and DNA repair were validated using SYBR green qPCR in an AB7500 Real Time PCR instrument. Relative expression analysis was calculated using the $2^{-\Delta\Delta Ct}$ method. Gene expression was normalised to β-actin as an endogenous control.

6.8.4 Investigation of other down-regulated genes upon pm-7 treatment

The computational identification of the cellular pathways affected upon miR-7 transfection indicated that cell proliferation, DNA repair and cell cycle were over represented. We checked in the list of down-regulated genes in the array whether we could find other genes involved in these pathways.

The gene encoding for mitogen-activated protein kinase associated protein 1 (Mapkap1) was down-regulated by 2.18-fold (**Appendix 2**). Mapkap1 is a subunit of mTORC2, which regulates cell growth and survival in response to hormonal signals. The levels of expression of the gene encoding the cell division cycle-associated protein (Cdca4) were reduced by 3.52-fold. This gene may participate in the regulation of cell proliferation through the E2F/RB pathway. The cell division cycle associated 7 (Cdca7) protein-encoding gene showed a 2.33-fold decrease. Cdca7 participates in MYC-mediated cell transformation. Eif4ebp2, a gene encoding the eukaryotic translation initiation factor 4E binding protein family was found to be down-regulated by 2.32-fold. Eif4ebp2 regulates the production of proteins implicated in cell proliferation. Together, these results gave some indication of how miR-7 may exert a control on cell proliferation.

Other genes were involved in chromatin remodelling as well as cell proliferation including ATP-dependent DNA ligase I (Lig1), H4-K20-specific histone methyltransferase (Setd8), nucleus accumbens-associated protein 1 (NACC1). Following miR-7 transfection their levels of expression were reduced by 2.41-fold to 2.66-fold. Thus miR-7 may be involved in chromatin remodelling.

MYST2 and USP10, two genes which play a role in DNA damage/repair pathway, were found to be down-regulated by 2.02-fold to 2.31-fold. MYST2, a histone acetyltransferase may regulate DNA replication through chromatin acetylation and may act as a coactivator of TP53-dependent transcription. USP10, a ubiquitin specific peptidase acts as an essential regulator of p53/TP53 stability in unstressed cells, specifically deubiquitinating p53/TP53 in the cytoplasm to counteract MDM2 action and stabilize p53/TP53. These data suggested a role for miR-7 in p53 regulation.

6.8.5 Investigation of up-regulated genes upon pm-7 transfection

Vasudevan and co-workers have demonstrated that miRNAs can induce translation up-regulation of target mRNAs by AGO_2-3'UTR interaction in non-proliferating cells that are in cell cycle arrest but on the other hand, miRNAs induce repression of translation in proliferating cells (Vasudevan, Tong and Steitz 2007a) . These authors proposed that translation regulation can switch between these two antagonistic mechanisms of repression and activation, depending on the cell cycle phase.

In the list of up-regulated genes, we found that the levels of expression of TGFBR3 (transforming growth factor, beta receptor III) were increased by 2.55-fold upon pm-7 overexpression (**Appendix 3**). TGFBR3 is a member of the TGF-beta superfamily signaling pathways, which have essential roles in mediating cell proliferation, apoptosis, differentiation, and migration. This gene undergoes mutations in cancers and usually acts as a tumor suppressor. The role of TGFBR3 and its high levels of expression in miR-7 transfected cells corroborated our previous results which showed that cells were arrested in G0/G1 phase upon pm-7 treatment.

Another gene Hbp1 was also found to be down-regulated by twofold. This gene is involed in cell growth regulation. It binds to the $p16^{INK4A}$ promoter to activate $p16^{INK4A}$ expression. This latter induces cell cycle arrest in G1 phase through inhibition of MDM2 and prevents MDM2-induced degradation of p53.

Again these data fit nicely with the results from the array and qPCR assays and reinforces the idea that miR-7 triggers cell cycle arrest and is involved in apoptosis regulation. In addition, these results give more insight into the protein network involved in this regulation.

6.8.6 Validation of Psme3, Rad54l and Skp2 as direct targets of miR-7

6.8.6.1 Computational prediction of Psme3, Rad54l and Skp2 in CHO cells

Having established that several growth and DNA replication-related genes were deregulated upon miR-7 treatment, we wished to verify whether they were primary binding targets or secondary targets downstream of miR-7. We focused on three targets, Psme3 (REGγ or PA28γ), Rad54L and Skp2 which were representative of the cell proliferation and DNA repair pathways. None of them had previously been shown to be directly regulated by miRNAs, but were predicted to bind miR-7 through either their 3'UTR (Psme3, Skp2) or coding sequence (Rad54L).

The CHO mRNA sequences of these genes were aligned with the mature sequence of CHO miR-7 (cgr-miR-7) using RNA Hybrid (Rehmsmeier, et al. 2004). The predicted 3'UTR binding sites of Psme3 and Skp2 were found to be conserved in Chinese Hamster (**Figure 6.8.6.1**). The non-canonical miR-7 binding site with the CDS of Rad54l was also conserved in Chinese Hamster and showed a high binding score (**Figure 6.8.6.1**).

a

```
TARGET : Psme3
length: 140
MIRNA  : cgr-miR-7
length: 23

mfe: -19.3 kcal/mol
p-value: undefined

position  59
target 5'  U   UU       CCUCU        A 3'
            GGC    UUAUU     GUCUUCCA
            UUG    AGUGA     CAGAAGGU
miRNA  3' UG   UUUU     U             5'
```

b

```
TARGET : Skp2
length: 418
MIRNA  : cgr-miR-7
length: 23

mfe: -21.4 kcal/mol
p-value: undefined

position  258
target 5'  A         UG   CCAAC       A 3'
            AGCGAAAUU   AG     UCUUCCA
            UUGUUUUAG   UC     AGAAGGU
miRNA  3' UG         UGA               5'
```

c

```
TARGET : Rad54l
length: 2790
MIRNA  : cgr-miR-7
length: 23

mfe: -25.8 kcal/mol
p-value: undefined

position  2473
target 5' U     C       CUUC        U 3'
           ACAGC   AUCAC    GUCUUCCA
           UGUUG   UAGUG    CAGAAGGU
miRNA  3'       UUU     AU            5'
```

Figure 6.8.6.1: Binding of miR-7 and its predicted targets Psme3, Rad54l and Skp2. The mature sequence of cgr-miR-7 was aligned with the sequences of its CHO mRNA targets, Psme3 (a), Skp2 (b) and Rad54l (c) using RNAhybrid (Rehmsmeier, et al. 2004), a tool to evaluate the score of the binding by calculating the minimum free energy of hybridisation (mfe).

6.8.6.2 Experimental validation of Psme3, Rad54l and Skp2

6.8.6.2.1 Isolation and cloning of the 3'UTR of Psme3, Rad54l and Skp2

Experimental validation of Psme3, Rad54l and Skp2 as direct targets of miR-7 was performed using a dEGFP reporter assay. The 3'UTR of Psme3 and Skp2 was PCR-amplified using the primers described in section 6.3.4 of the materials and method. These 1760 bp and 417 bp amplicons were subcloned downstream of the dEGFP reporter gene in the pd_2EGFP-Hyg2 vector (**Figure 6.8.6.2.A**) to create the pd2EGFP-Psme3 and pd2EGFP-Skp2 plasmids (**Figure 6.8.6.2.A**). In the case of Rad54L we deliberately included 65 bp upstream of the translational stop codon in order to incorporate the RNA Hybrid-predicted miR-7 seed binding site. The size of Rad54L amplicon including the CDS sequence and the 3'UTR was 319 bp (**Figure 6.8.6.2.A**). The 319 bp fragment of Rad54L was cloned into the reporter vector to create the pd2EGFP-Rad54L plasmid (**Figure 6.8.6.2.A**).

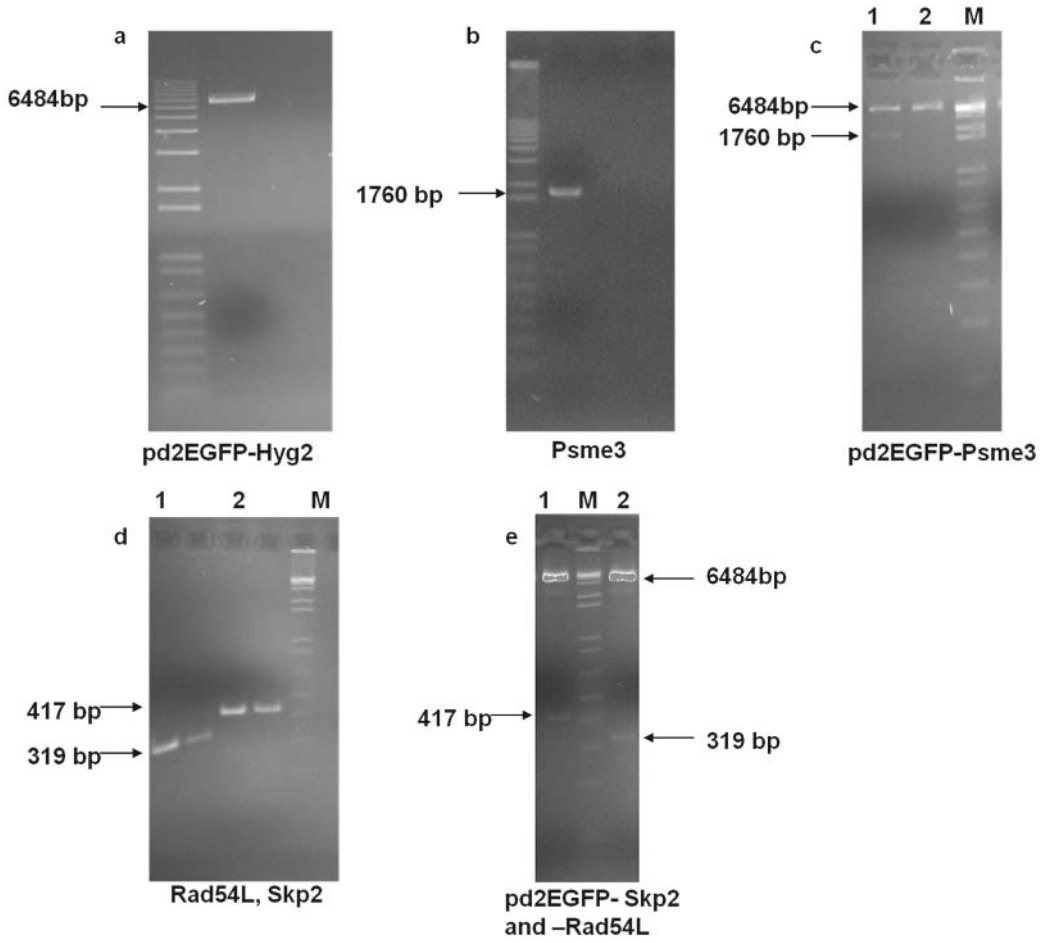

Figure 6.8.6.2.A: Cloning steps of Psme3, Skp2 and Rad54L into pd$_2$EGFP-Hyg2 vector.

a: Double digestion of pd2EGFP-Hyg2 vector with *Xho*I and *Eco*RI; b: Amplification of the 3'UTR of Psme3 in CHO cells; c: Double digestion of pd2EGFP-Psme3 vector with *Xho*I and *Eco*RI (Lane 1: positive clone; Lane 2 negative clone); d: Amplification of the 3'UTR of Rad54L (Lane 1) and Skp2 (Lane 2) in CHO cells; e: Double digestion of pd2EGFP-Skp2 (Lane 1) and pd2EGFP-Rad54L (Lane 2) vectors with *Xho*I and *Eco*RI.

6.8.6.2.2 Validation of Psme3, Rad54l and Skp2 at the transcriptional level

Following cloning, these plasmids were transfected into CHO cells in combination with either a pm-neg or pm-7. A GFP reporter without any UTR sequence was included as a negative control. The GFP signal in cells receiving this control was unchanged in the presence of either pm-neg or pm-7 (**Figure 6.8.6.2.B**). Addition of a GFP specific siRNA efficiently blocked fluorescence and provided a strong positive control for the assay. GFP fluorescence was significantly reduced for all three targets (**Figure 6.8.6.2.B**).

The reporter containing the Psme3 UTR showed a 21.97% reduction in mean fluorescence when co-transfected with pm-7 compared to pm-neg (p-value= 0.0029). The mean fluorescence of p2dEGFP-Rad54L and p2dEGFP-Skp2 was reduced by 23% (p-value= 0.0002) and 18.81% (p-value= 0.0123) respectively in comparison to the control. This reporter assay provided positive indications that Psme3, Skp2 and Rad54L may be direct targets of miR-7.

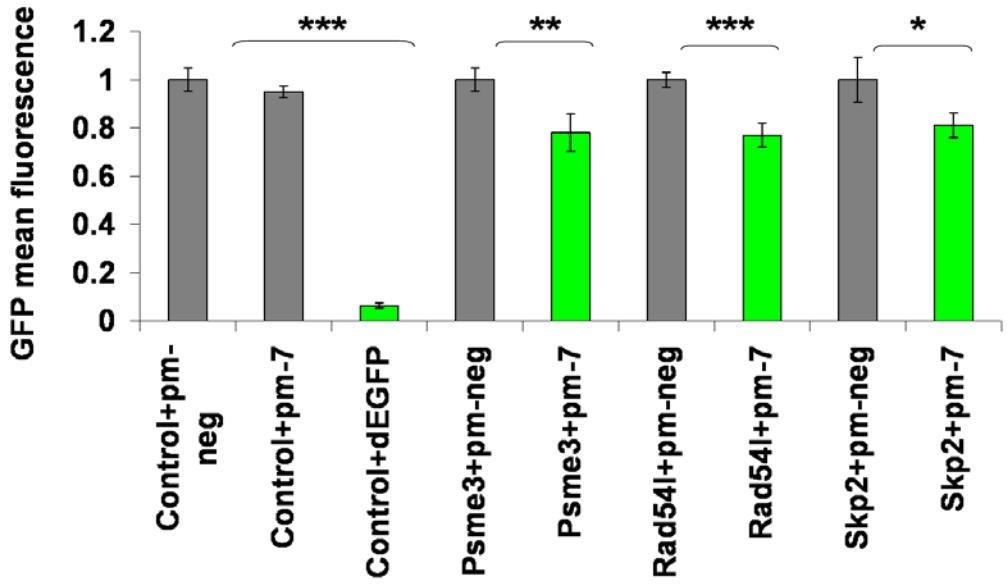

Figure 6.8.6.2.B: Validation of Psme3, Rad54l and Skp2 as direct targets of miR-7 in a GFP reporter assay. The 3'UTR sequences of Psme3, Skp2 and Rad54l (including 65bp of CDS sequence) were inserted between *Xho*I and *EcoR*I restriction sites of the CMV-d2 sponge vector. Following co-transfection of 1µg of reporter with 50nM of miR-7 and 2µl of lipofectamine, GFP signal fluorescence was analysed using Guava Flow cytometry. control: pd_2EGFP-Hyg2 vector backbone with no UTR sequence. dEGFP: siRNA against dEGFP (dEGFP) as a positive control of GFP fluorescence reduction. pm-neg: negative control for miR-7 mimic; pm-7: mimic of miR-7; Psme3: pd_2EGFP-Hyg2 containing Psme3 3'UTR; Skp2: pd_2EGFP-Hyg2 containing Skp2 3'UTR; Rad54L: pd_2EGFP-Hyg2 containing Rad54L 3' CDS/UTR. Bars represent standard deviations of four biological replicates. Statistical significance of the d2EGFP expression reduction was assessed by a Student t-test.*: p-value<0.05; **: p-value< 0.01; ***: p-value<0.001.

6.8.6.2.3 Validation of Psme3, Skp2 and Rad54L at the protein level

To continue the validation of Psme3, Skp2 and Rad54L as true targets of miR-7, we investigated their protein expression using western blotting.

Upon miR-7 treatment, the endogenous protein levels of SKP2 were strongly down-regulated (**Figure 6.8.6.2.C**). PSME3 protein levels were also confirmed to be down-regulated but to a lesser extent. A recent study done in our laboratory showed that PSME3 protein levels were reduced by 11-fold and by 30-fold at 48hours and 96 hours after treatment with miR-7, though it did not pass some of the selection filters (Meleady, et al. 2012). The validation of Rad54L could not be verified at the protein levels due to the unspecificity of the antibody tested in CHO cells.

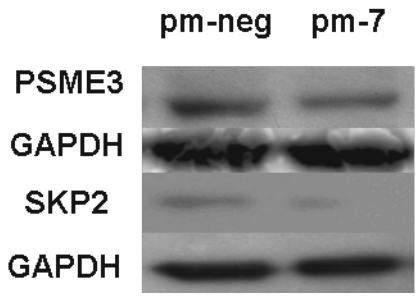

Figure 6.8.6.2.C: Validation of Psme3 and Skp2 protein levels upon pm-7 transfection

Levels of endogenous PSME3 and SKP2 proteins were investigated by western blotting following transfection with pm-neg or pm-7. GAPDH was used as a loading control.

6.8.7 Investigation of the impact of Psme3 and Skp2 on cell proliferation

To establish to what extent the phenotypic impact of miR-7 transfection was due to targeting these genes, we depleted PSME3 and SKP2 individually using two siRNAs for each target.

To confirm the knockdown of PSME3 and SKP2 following siRNA transfection, their protein levels were monitored by western blotting. Depletion of PSME3 was achieved with both siRNA a&b, though it was more efficient with siRNA a (**Figure 6.8.7.A**). The protein levels of SKP2 were dramatically down-regulated, particularly with siRNA b.

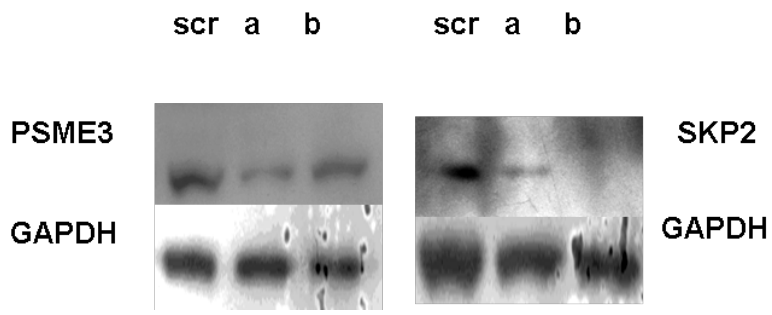

Figure 6.8.7.A: Depletion of PSME3 and SKP2 by RNAi

Following siRNA transfection, the protein levels of PSME3 and SKP2 were investigated by western blotting. Two siRNAs (a&b) were tested for each target. A negative control (scr) was included for comparison of the protein expression levels before and after treatment with siRNA. GAPDH was used as a loading control.

Psme3 knockdown led to a 22% reduction in cell density using siRNA b (p-value= 0.0016) (**Figure 6.8.7.B**). Skp2 knockdown reduced cell density by 44% using siRNA a (p-value= 0.0001) and 36% using siRNA b (p-value= 0.0003). Although the cell viability was significantly reduced, knockdown of Psme3 and Skp2 had little impact on this phenotype (<3%) (**Figure 6.8.7.B**).

To investigate the simultaneous effect of Psme3 and Skp2 depletion, the best siRNA was chosen for each target. The two siRNAs were co-transfected at a combined concentration of 50nM to avoid saturation of the RNAi machinery. The combined effects of Psme3 and Skp2 siRNAs had a small but significant impact on cell density (**Figure 6.8.7.C**). This observation may be the result of the lower concentration used for each co-transfected siRNA.

Together, these results suggested that Skp2 plays a unique and important role in G1 arrest. Although Psme3 showed lower impact on cell density than Skp2, Psme3 may also be involved in G1 arrest. This might be explained by compensation via redundant proteins in the same family or it may also be the result of a less effective siRNA leading to moderate depletion of Psme3 and consequently moderate impact of Psme3 on cell proliferation.

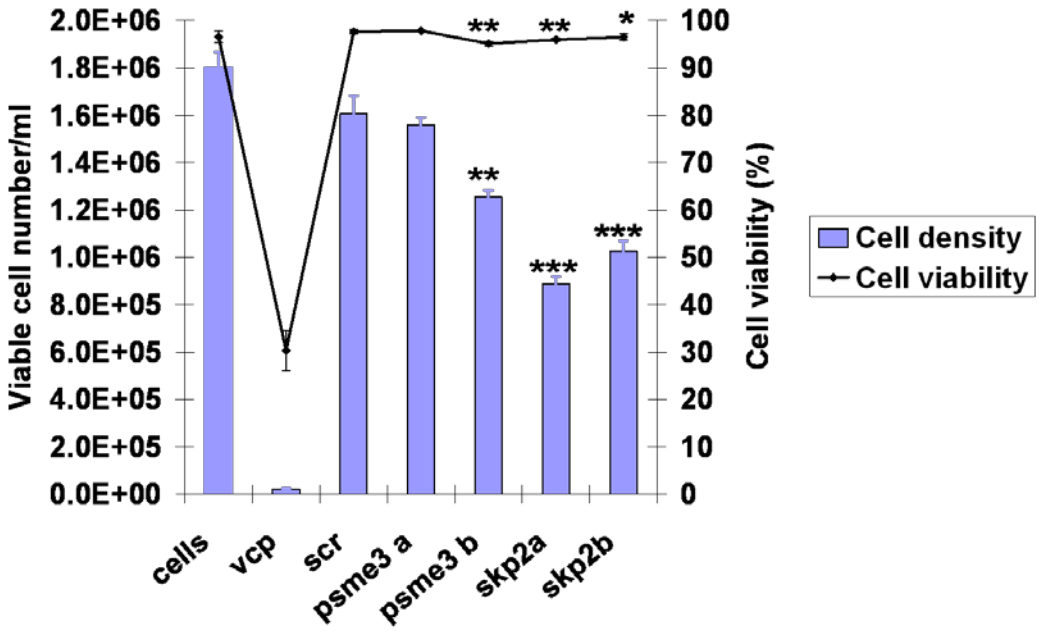

Figure 6.8.7.B: Impact of individual Psme3 and Skp2 depletion on cell proliferation.

Two siRNAs (a&b) for Psme3 and Skp2 were transfected separately at a final concentration of 50nM. Non-transfected cells were included as a negative control and siRNA against Valosin-containing protein (VCP) was included as a positive control. Cell growth and viability were assessed at day 3 after transfection using GuavaViacount staining with a Guava Flow Cytometry. Standard deviations represent biological triplicates. A Student t-test was performed to analyse the statistical significance of the data. *: p-value<0.05; **: p-value< 0.01; ***: p-value<0.001

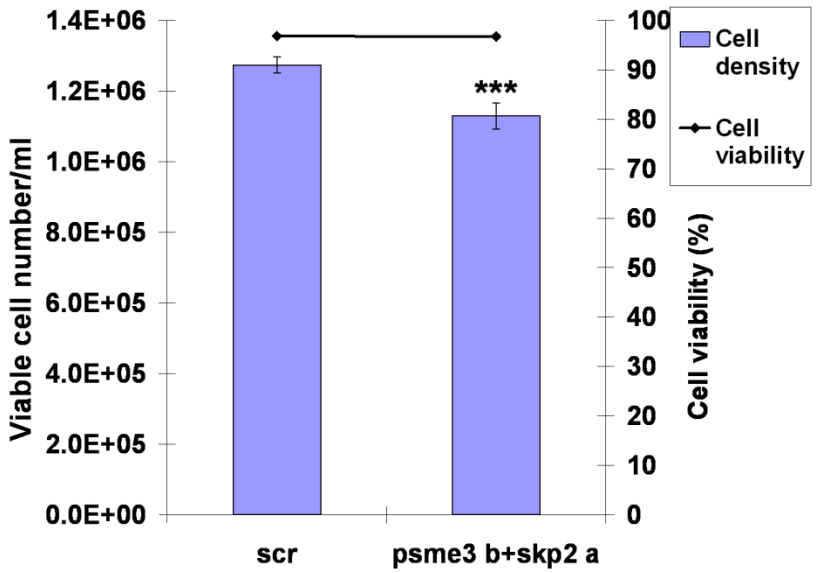

Figure 6.8.7.C: Impact of the simultaneous depletion of Psme3 and Skp2 on cell proliferation.

The best performing siRNA was chosen for Psme3 as well as for Skp2 and were co-transfected at a final concentration of 50nM. Cell growth and viability were assessed at day 3 after transfection using GuavaViacount staining with a Guava Flow Cytometry. Standard deviations represent biological triplicates. A Student t-test was performed to analyse the statistical significance of the data. ***: p-value<0.001

6.8.8 Investigation of other proteins involved in cell growth arrest response and impairment of apoptosis initiation

To better understand the mechanisms related to miR-7-dependent cell growth arrest, we investigated the change in expression of well studied proteins involved in cell proliferation, cell cycle and apoptosis including Igf1-R, c-Myc, p53, $p27^{KIP1}$ and p-Akt. The levels of Igf1-R protein were not affected despite Igf1-R having previously been shown to be a target of miR-7 in other cell type (Jiang, et al. 2010)·(Zhao, et al. 2012) (**Figure 6.8.8**). The levels of $p27^{KIP1}$ were increased after miR-7 transfection. This is consistent with reduction of Skp2 which is known to stabilise p27 thus impairing G1 to S transition**.** The proto-oncogene c-Myc was reduced significantly. Skp2 has been reported to interact directly with c-Myc promoting its degradation by ubiquitination thus regulating its turnover at the G1/S transition phase (von der Lehr, et al. 2003). Interestingly, p53, a key molecule in cell cycle and apoptosis regulation as well as other processes, was significantly down-regulated. Psme3 is known to promote Mdm2-p53 interaction which triggers ubiquitination and degradation of p53 consequently leading to apoptosis inhibition (Zhang and Zhang 2008). One might expect that the down-regulation of Psme3 would result in an increase in p53 levels. The levels of p-Akt, also known to rescue cells from apoptosis, were slightly increased after miR-7 transfection possibly explaining why miR-7 transfected cells do not become apoptotic despite growth arrest. Taken together, these results indicate that as well as Psme3 and Skp2, miR-7 also targets, either directly or indirectly, critical proteins including $p27^{KIP1}$, c-Myc, p53 and p-Akt in order to control cell fate.

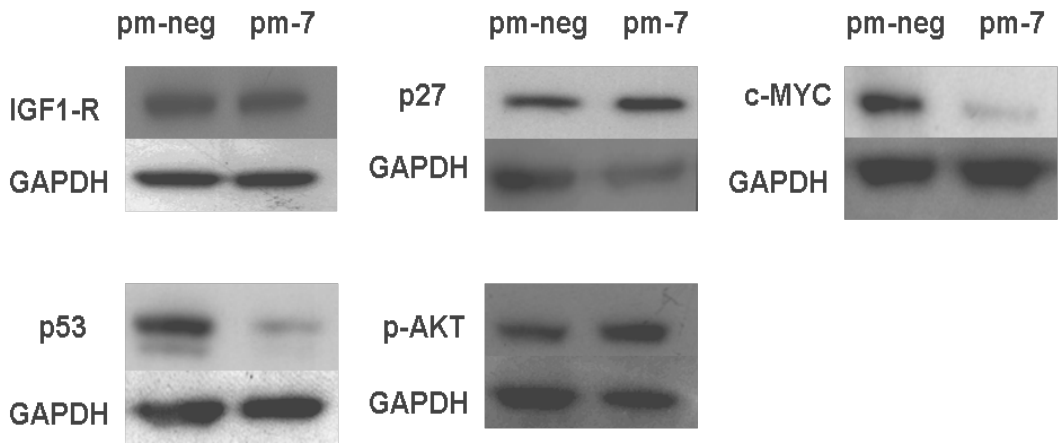

Figure 6.8.8: Investigation of the expression levels of other potential miR-7 targets. Levels of IGF1-R, p27, c-Myc, p53 and p-AKT were analysed using western blotting. GAPDH was used as a loading control.

6.8.9 Identification of miR-7 responsive miRNAs

miRNAs have an established role in modifying the levels of proteins as well as mRNAs in cells. Having identified a number of important genes deregulated in response to miR-7 as well as proteins, we were interested to discover whether increasing miR-7 levels impacted on the cellular levels of other miRNAs. To this end, we identified differentially expressed miRNAs as a consequence of miR-7 transfection using TaqMan Low Density Array (TLDA). Unfortunately two of the six TLDA cards displayed poor QC upon analysis (<50miRNAs detected) making the data somewhat inconclusive. However, there was some indication that several well-studied miRNAs previously implicated in cell proliferation and apoptosis were differentially regulated, including miR-15b~16 cluster, miR-17~92 cluster, miR-21, miR-24 and let-7 family (**Figure 6.8.9.A**). Thus these miRNAs may be involved in miR-7 network to regulate cell growth arrest and apoptosis avoidance in CHO cells.These results highlight the fact that miRNAs not only impact on mRNA targets but can instigate a coordinated response via the recruitment of other miRNAs in order to regulate cellular pathways via very complex interactions. A hypothetical and simplified miR-7 network was designed using the data we obtained from this study and the literature (**Figure 6.8.9.B**).

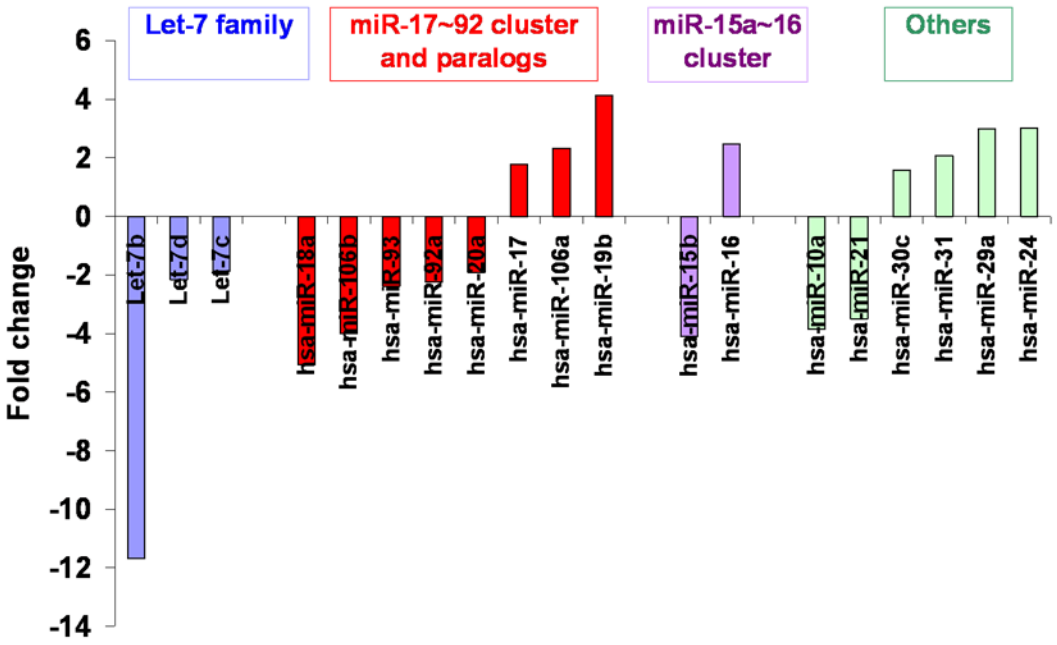

Figure 6.8.9.A: Identification of differentially regulated miRNAs following miR-7 transfection.

TaqMan Low Density Assay was performed in three biological triplicates following treatment with pm-neg or pm-7. A list of down- and up-regulated miRNAs was generated. Blue: let-family; red: miR-17~92 cluster; purple: miR-15a~16 cluster; green: other miRNAs reported to be associated with cell proliferation in the literature and found to be differentially regulated in different studies conducted in our laboratory.

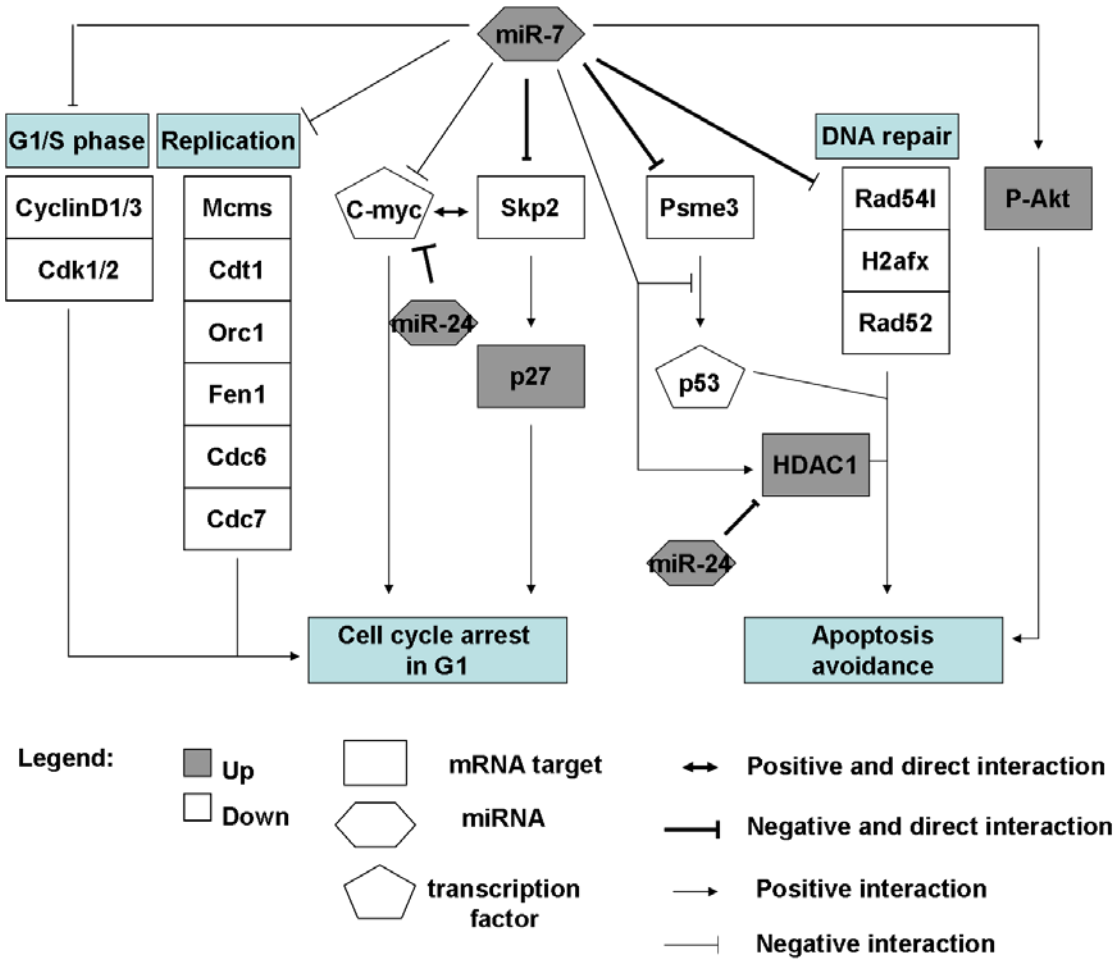

Figure 6.8.9.B: Hypothetical model of miR-7 network in CHO cells.

DISCUSSION

7 Discussion

In the past three decades, a great deal of effort has been put into answering the increasing demand for biopharmaceutical products. Improvements in medium formulation, vector design and process control have been responsible for major increases in product titer (Butler 2005, Wurm 2004, Kim, Kim and Lee 2012). However, to meet the needs of an increasing number of patients with chronic diseases (Kim, Kim and Lee 2012), other strategies will be necessary to further enhance the production of drugs for these indications. New approaches have focused particularly on the improvement of Chinese Hamster Ovary (CHO) cell growth and productivity capacities. For their ease of genetic manipulation, safety reasons and, most importantly, for their ability to synthesize and secrete glycoproteins with similar carbohydrate structures to those found in human, CHO cells are the most commonly used host in the production of complex recombinant proteins. Recently, single gene engineering approaches have proven to be an efficient method of enhancing individual cellular functions including cell proliferation, secretion capacities, specific productivity and to inhibit apoptosis (Hacker, De Jesus and Wurm 2009, Wu 2009). However, several studies have reported that targeting one single gene in one specific pathway does not necessarily benefit other pathways (Kim, et al. 2009, Lee and Lee 2003) or can result in negative side-effects (Davis, et al. 2000, Mohan, et al. 2008, Borth, et al. 2005).

Therefore omics-based approaches (transcriptomics, proteomics and metabolomics) have been developed. The aim of these approaches compared to single-gene engineering is to understand how genetic manipulation can globally affect an entire pathway at the levels of DNA, RNA and protein. Currently, there is a particular interest in miRNAs and manipulation of their expression to achieve this objective. These small non-coding RNAs are attractive as tools as they display some unique characteristics: 1) they are capable of targeting hundreds of genes; 2) they are involved in the regulation of many cellular pathways including cell proliferation, apoptosis, cell metabolism, development and differentiation; 3) they are highly conserved between species and 4) they are not processed by the translational machinery (Bartel 2004). These characteristics have persuaded several research groups in the CHO area, including ours that miRNAs might

prove to be beneficial tools in the search for more efficient engineering targets. With this ambition in mind this project focused on characterising the function of several of these molecules in relation to their impact on CHO cell growth and recombinant protein production.

7.1 Functional validation of miRNAs as potential candidates to improve bioprocess-relevant CHO characteristics

7.1.1 Screening of miRNAs in fast growing cells

A miRNA profiling study had been performed in our laboratory to identify differentially expressed miRNAs in temperature-shifted culture (from 37°C to 31°C) (Gammell, et al. 2007). The aim of this study was to investigate the changes in miRNA expression associated with temperature reduction and the concurrent cell growth decrease. Several miRNAs with significant fold-changes in expression were selected including miR-490, miR-34a/c, miR-30e-5p, miR-10a, miR-29a and let-7e. The potential of these miRNAs in improving the phenotypes mentioned above was studied in functional assays using mimic and inhibitor molecules in several CHO cell lines cultured in serum-free medium. Despite the lack of publicly available Chinese Hamster genomic sequences at the time of the study, these molecules were deemed suitable for screening in CHO cells as they target the mature form of the miRNA which tends to be well conserved between species including human, rat and mouse (Bartel 2004). In the intervening period, the sequence homology of miRNAs has been confirmed to be well conserved in CHO cells (Hammond, et al. 2012, Johnson, et al. 2011).

7.1.1.1 miR-490

Based on Ct values after qRT-PCR, endogenous levels of miR-490 were low in CHO cells and increased at the middle of the logarithmic phase at 37°C. We anticipated that miR-490 overexpression using mimics might improve cell growth. However, transient up-regulation of miR-490 had the opposite effect, reducing proliferation by 1.28-fold.

One recent paper reported high levels of miR-490 in human uterine Leiomyoma, a female genital tract neoplasm, using high-throughput sequencing (Georgieva, et al. 2012). This endorses the data from our profiling study which showed up-regulation of miR-490 levels at the exponential growth phase. Along with this report, there was no experimental validation using other approaches. In addition, the role of miR-490 has not been extensively described in the literature and the inconsistency of the phenotypes observed across repeats in our functional validation did not give additional information on the impact of miR-490 on cell proliferation. This suggests that in our profiling study, higher levels of miR-490 were probably a consequence of the enhanced cell growth rather than the cause.

Transient transfection of miR-490 increased viability by 9.39% at early and later stages of culture as well as normalised productivity by 1.5-fold in CHO-K1 SEAP cells. As for the impact on cell proliferation, these effects were not observed consistently in the different transfection assays performed. Baek and co-workers demonstrated that the impact of miRNA on protein levels is usually less than twofold (Baek, et al. 2008). It has been suggested that this small change can also originate from random fluctuations in mRNA or protein level (Ebert and Sharp 2012). The subtle phenotypic impact can also be caused by off-target effects. Khan et al reported that the transfection of siRNA/miRNA perturbs the transcriptome by inducing the expression of genes that are normally repressed by endogenous miRNAs (Khan, et al. 2009). This may be caused by the excess of exogenous miRNA which competes with the endogenous miRNA to be loaded into the RISC complex or downstream of it for binding to the same target and leads to unexpected phenotype consequent to loss-of-function of the endogenous miRNA.

In the aim to find promising targets, we sought for more convincing and reproducible impact.

7.1.1.2 miR-34a and miR-34c

miR-34a and miR-34c were found to be down-regulated upon temperature-shift from 37°C to 31°C and to be associated with reduction in proliferation. However, the miR-34 family has been reported as a tumor suppressor family which blocks proliferation and induces apoptosis following oxidative stress and DNA damage (He, et al. 2007b, He, et

al. 2007c, Yamakuchi and Lowenstein 2009, Yamakuchi, Ferlito and Lowenstein 2008). Therefore, despite the profiling results, we followed the reported findings and considered the depletion of these miR-34 family members to increase cell growth and prevent apoptosis. Despite the established role of miR-34 family in cell proliferation and DNA damage, knockdown of miR-34a/c did not affect significantly cell proliferation or cell viability in CHO cells. The Ct values from the array data indicated that miR-34a and miR-34c were expressed at low and moderate levels respectively in CHO cells. Due to the low levels of miR-34a, further inhibition of its expression might not result in further impact. The moderate levels of miR-34c expression made it a more suitable target for inhibition but, following am-34c transfection, there was no effect on proliferation or viability. However, total yield was slightly increased upon am-34a and am-34c transfection and normalised productivity was significantly improved upon am-34a treatment. Thus miR-34a/c knockdown may be more impactful on total yield and productivity than cell proliferation or viability in CHO cells. Cheng and co-workers reported that the functional role of miRNAs is dependent of cell line, tissue and environmental conditions thus it is not surprising that miR-34a/c display distinct functions in CHO cells and in mouse embryonic fibroblasts or human cancer cells (Cheng, et al. 2005). To add more confidence to our data, this assay was repeated twice but showed variability and led to inconclusive results. As discussed for mimic molecules, the difference in the phenotype observed following transfection repeats may be due to off-target effects or compensation of the subtle change in mRNA target expression. The inhibitor molecules showed a transient impact therefore in contrast to dominant negative tools, their impact can be more easily compensate by other miRNAs sharing the same target so little impact might be seen (Ebert and Sharp 2012). On the other hand, inhibitors can also compete with endogenous miRNAs reducing the repression of their mRNA targets but instead repressing non-specific targets (Khan, et al. 2009). Vankoningsloo and co-workers showed that the non-psecific silencing of gene trancripts can be dependent of the cell line, the siRNA sequence, the duration of the transfection, transfection reagent and the time of the analysis following transfection. It has also been shown that the issue may not come from the synthetic molecules but from the mRNA target site accessibility (Cullen 2006). In vivo, the RISC complex can not access mRNA target sites if the RNA displays secondary structure or if there is protein binding thus the antisense miRNA may not be effective for this reason (Overhoff, et al. 2005, Brown, Chu and Rana 2005).

Although the functional validation of miR-34a/c was not pursued, we believe that the impact of these two miRNAs would be interesting to follow up.

7.1.1.3 miR-30e-5p

In a recent report, we showed that miR-30e expression was activated upon temperature-shift from 37°C to 31°C (Barron, et al. 2011). Under these conditions, it has been demonstrated that cell growth is arrested and the cellular machinery is directed towards protein production (Kaufmann, et al. 1999). Therefore we investigated whether miR-30e-5p was an effector of arrest in response to temperature-shift. It has been shown that miR-30e-5p suppresses cell growth in cancer (Wu 2009). In agreement with this paper, transient overexpression of miR-30e-5p induced cell growth decrease in CHO-K1 SEAP cells. However, it increased the growth in CHO1.14 cells. It has been demonstrated that one miRNA can have antagonising effects of the same biological function in two different cell lines (Cheng, et al. 2005). Thus it is possible that the impact of miR-30e-5p is CHO cell line dependent. To verify this statement, transient transfection of pm-30e-5p was carried out several times but resulted in contradictory results. Thus we could not affirm that the changes in expression of miR-30e observed at low temperature were merely a consequence of the shift in temperature and were not a mediator of the associated cell growth reduction.

Li and colleagues reported that miR-30 family members can inhibit apoptosis by suppressing p53 expression (Li, et al. 2010). However, we found that the viability of CHO1.14 was reduced by 20.4% at later stages of culture and to a lesser extent in CHO-K1 SEAP. Nonetheless, this phenotype was not reproducible. Thus a role for miR-30e-5p in apoptosis regulation was not apparent.

Besides its role in cell proliferation and apoptosis, miR-30-family might be involved in secretion regulation in CHO cells. Joglekar and co-workers showed that low levels of miR-30 were associated with the loss of insulin during epithelial-mesenchymal transition (Joglekar, et al. 2009). Tang et al., reported that miR-30d was up-regulated by glucose and increased insulin gene expression in pancreatic β-cell line MIN6 (Tang, et al. 2009). In CHO cells, we found that transient overexpression of miR-30e-5p enhanced total yield by 1.37-fold in CHO-K1 SEAP but no detectable improvement was observed in CHO1.14 cells or in normalised productivity in any of the two cell lines.

Also, this advantage in total yield was not clear in other repeats. Thus they were not enough valid indication to conclude on a role of miR-30e-5p in protein secretion.

Double-stranded mimic molecules have to be processed into a mature single-strand through the RNAi machinery. It is possible that, during a transient transfection, the excess of mimic molecules may block endogenous miRNAs from being processed and lead to deregulation of their targets, which in turn may impact other phenotypes unintentionally (Khan, et al. 2009, Jackson, et al. 2006). Besides saturation of the RISC complex or downstream processing, the excess of exogenous miRNAs could trigger saturation of the P-bodies and/or stress granules by endogenous miRNA. Endogenous miRNAs, mRNAs and other molecules of the RNAi machinery are found in the P-bodies or they may be also retained in the stress granules like AGO proteins in stress situations. Therefore this could accelerate endogenous miRNA degradation leading to attenuation of their function.

Due to the erratic results from these assays, we discontinued the investigation of miR-30e-5p. Approaches other than use of synthetic mimics/inhibitors might give additional information on the precise function of miR-30e-5p.

7.1.1.4 miR-29a

One of the members of miR-29 family, miR-29a was found to be down-regulated upon temperature shift in our previous miRNA profiling. In the literature, miR-29 family is often described as a tumor suppressor family (Muniyappa MK, et al. , Zhao, et al. 2010). Due to its anti-proliferative role, we thought to deplete miR-29a to consequently improve cell proliferation. Surprisingly, knockdown of miR-29a did not impact on either CHO-K1 SEAP or CHO1.14 cell growth thus suggesting that low levels of miR-29a were not directly associated with cell growth reduction but were probably just a consequence of the shift of temperature.

Cell viability was enhanced by 9.91% in CHO-K1 SEAP but not in CHO1.14. Desjobert and co-workers reported that inhibition of miR-29a impaired apoptosis induction through ovexpression of the anti-apoptotic protein myeloid cell leukemia 1 (MCL-1) (Desjobert, et al. 2011). This may imply that the inhibition of miR-29a in CHO-K1 SEAP may promote viability maintenance and also that the possible anti-apoptotic role of miR-29a may be cell line dependent.

In addition to its impact on cell viability, miR-29a knockdown enhanced SEAP total yield by 1.2- to 1.4-fold and normalised productivity by 4.93-fold. However, it did not increase the production of IgG1 in CHO1.14. High levels of miR-29a have been found to be associated with insulin resistance in diabetic rats (He, et al. 2007a) and its depletion promoted higher glucose-stimulated insulin-secretion in pancreatic β-cells (Bagge, et al. 2012). To confirm the increase of SEAP secretion observed upon am-29a transfection, this assay was performed again but resulted in variable impact.

The data from these assays were again confusing and did not lead to a convincing impact thus the impact of miR-29a on CHO cell characteristics was not further investigated. The contrasting results may have been caused by the efficiency of the antisense oligonucleotides. These molecules work differently from the mimics. They are single-stranded molecules that are thought to bind competitively to the mature miRNA after it was selected as the guide strand to assemble into the RISC complex (Davis, et al. 2006). To ensure an efficient knockdown, the dose of antisense oligonucleotides should be dependent on the levels of the targeted miRNA. If a miRNA is highly expressed in the cells then a higher dose of antimiRs may be necessary. If the miRNA is expressed at moderate levels its knockdown would require less antisense molecules. In the case of a low expressed miRNA it could be challenging to down-regulate its expression further. The data collected from the profiling study revealed that the endogenous levels of miR-29a were in the average range so in theory the concentration of inhibitors used (50nM) should have been sufficient to ensure significant knockdown. It has also been reported that many cells both in vitro and in vivo are resistant to the uptake of oligonucleotides (Ebert and Sharp 2010). However, the CHO cell lines used in this assay as well as the transfection protocol proved to be efficient for miR-7 mimics in a recent study conducted in our laboratory (Barron, et al. 2011). It is possible that despite their chemical modifications, these single-stranded inhibitors are susceptible to degradation, though this has not been reported previously. It is more likely than these molecules can be diluted and lost after few cell divisions leading to poor efficiency of inhibition and small phenotype. As discussed previously, the accumulation of the molecules in the cytoplasm of the cells could lead to competition with the endogenous miRNA for mRNA binding leading to unexpected phenotypes.

Despite inconclusive results, miR-29a seems an interesting candidate to improve viability and productivity but further investigation would require other tools than synthetic antisense molecules.

7.1.1.5 miR-10a

Upon low-temperature culture, levels of expression of miR-10a were reduced compared to culture at 37°C. miR-10a is involved in cell proliferation, apoptosis and in various tumor pathologies (Ma, et al. 2010, Ovcharenko, et al. 2007, Sirotkin, et al. 2010). It is has been reported that miR-10a can have antagonising roles for a same biological function (i.e. pro- or anti-proliferative) depending on the cell types (Cheng, et al. 2005). To see whether we could reproduce the impact observed in temperature-shifted culture, we considered the inhibition of miR-10a. We found that transient knockdown of miR-10a led to higher cell density (1.8-fold) as well as enhanced viability four days after transfection in CHO-K1 SEAP cells but little impact was detected on CHO1.14 growth. The reproducibility of these results was not convincing despite every effort to perform the assays in a routine, standard manner. However, a recent global expression profiling study using different technologies including qPCR, microarray and quantitative LC-MS/MS was carried out in our laboratory on a set of Mab producing clones with varying growth rates (Clarke, et al. 2012). In this study, miR-10a was both up-regulated by 2.12-fold and positively correlated with cellular growth rate. This finding is consistent with the reduced expression of miR-10a detected following shift of temperature culture. As previously discussed, we were unsure about the efficiency of the inhibitor molecules and their reproducible impact. Thus other approaches using shRNA or a sponge in a transient assay might be more suitable to reveal the impact of miR-10a. The use of shRNA may not guarantee the loss of off-target effects including saturation of the RNAi machinery (unprocessed shRNA or accumulation of shRNA) and the effective inhibition of the miRNA (Grimm, et al. 2006, McBride, et al. 2008). To be effective, the shRNA design must be optimised depending of the cell lines, the endogenous levels of miRNA and the application of transfection for in vivo or in vitro studies (Cullen 2006).
Interestingly miR-10a has been reported to enhance ribosomal protein translation via binding to the 5' UTR of their mRNAs and so via this regulation, miR-10a may impact on global protein synthesis (Orom, Nielsen and Lund 2008). Depletion of miR-10a increased total yield by 1.2- to 2-fold in both CHO1.14 and CHO-K1 SEAP cells as well as normalised productivity though it was not statistically significant.

Again repeats were not convincing enough to pursue the further validation of this miRNA. However, there was an impact on proliferation and productivity that was not negligible even if the directions were contrasting between the repeats and the approaches. Instead of synthetic molecules, other strategies may verify if miR10a is worth further investigation.

7.1.1.6 let-7e

let-7 (lethal-7) was one of the first miRNAs discovered in the nematode *C.elegans*. Let-7 is conserved across species (Lee and Ambros 2001, Lagos-Quintana, et al. 2001, Pasquinelli, et al. 2000) and has an essential role in the development of C.elegans and other organisms (Thomson, et al. 2006, Sempere, et al. 2002, Reinhart, et al. 2000, Liu, et al. 2007). Let-7 family acts as a tumor suppressor family in many cancers (Roush and Slack 2008). We found that let-7e was expressed at low levels in CHO cells and its expression increased upon temperature-shift. Therefore to verify whether the tumor suppressor role of let-7e was conserved in CHO cells, we forced its expression using mimic molecules. Following transient up-regulation of let-7e cell density was dramatically reduced by 3- to 4-fold in CHO-K1 SEAP and CHO1.14 cells and CHO2B6 cells were growth arrested for five days. Thus the anti-proliferative role of let-7e was conserved in CHO cells and across cell lines though the impact was to different extents.

The cell viability in the three CHO cell lines was significantly decreased. In opposition to this finding, transfection of pm-let-7e has been shown to reduce the levels of expression of Caspase-3 protein as well as cellular apoptosis in PC12 cells upon anoxia/reoxygenation injury (Peng, et al. 2011). These contrasting results can be explained by the different conditions of transfection used which in this report was carried out in cells exposed to anoxia (depletion of oxygen) whereas in our study the viability of cells was assessed under normal conditions of culture. Thus let-7e may be a critical regulator of cell growth and viability in CHO cells and it may be a promising tool to improve these two phenotypes following its stable knockdown.

To explore the potential of let-7e in impacting on total yield and productivity, we investigated the levels of SEAP and IgG1 expression in pm-let-7e transfected-CHO cells. Overexpression of let-7e resulted in reduced total yield in the three cell lines. This

is due to the anti-proliferative effect of let-7e which resulted in very few cells remaining in culture thus less protein produced than the controls. Normalised productivity was improved by 4- to 14.47-fold in CHO1.14 and CHO2B6 cells but it was negatively impacted in CHO-K1-SEAP at later stages of culture. This result is surprising as we expected the same behaviour from the three cell lines. They all exhibited lower cell density, viability as well as total yield thus we expected an increased normalised productivity in the three cell lines.

It is worth noting that Dicer, the endonuclease requires for processing of precursor miRNA into mature miRNA form, is a direct target of miR-let-7a, c&d. The up-regulation of miR-let-7 has been shown to reduce the levels of Dicer leading to knockdown of many miRNAs (Tokumaru, et al. 2008). Thus targeting any member of the miR-let-7 family in CHO cells may be an advantage to control several cellular pathways simultaneously. However, it could also be a problem if it impacts negatively on other pathways. Its overexpression might be used to enhance total yield when using an inducible system in a biphasic culture. However, the negative impact of up-regulated let-7e would have to be prevented by the use of an anti-apoptotic miRNA.

7.1.2 Screening in fast versus slow cell lines

The miRNAs derived from the temperature-shift profiling study yielded very mixed results in terms of impacting CHO behaviour in our functional assays. In a separate but related study which focused on cell proliferation, we had identified another group of miRNAs whose expression was correlated or anti-correlated with specific growth rate. This particular experiment was designed to minimize confounding parameters in order to maximize the possibility of filtering out non-growth related miRNAs. The clones in the study were all derived from the same transfection (in this case a cell line development project in our collaborators laboratories from Pfizer) of an antibody-encoding plasmid. Subsequently the clones chosen had distinct growth rates (Slow< $0.02hr^{-1}$ or Fast>$0.025hr^{-1}$) but identical specific productivity (Qp). A group of differentially expressed miRNAs were chosen from the list generated after experimental profiling (Clarke, et al. 2012).

7.1.2.1 miR-23b*

Recent studies have revealed that in contradiction with what was initially thought, miRNA* (also known as passenger strand) do not always undergo degradation but can be functional and expressed in an abundant manner in cells (Okamura, et al. 2008, Guo and Lu 2010). The selection between miRNA and miRNA* strand to incorporate into the RISC complex, may be tissue and developmental stage dependent (Ro, et al. 2007, Chiang, et al. 2010, Ruby, Jan and Bartel 2007). From the data generated in the miRNA profiling study described above, we found that miR-23b* was relatively abundant in fast growing cells and not present in slow growing cells. To our knowledge, there have been no reports to date focusing on the functions of miR-23b*. In contrast cancer research has been focused on the other strand of the hairpin miR-23b, which is more commonly selected by the RNAi machinery to be loaded into the RISC complex. Inhibition of miR-23a/b by c-Myc has been proven to enhance mitochondria glutaminase expression and glutamine metabolism (Gao, et al. 2009). miR-23b has also been associated with cell growth, apoptosis, cell migration and invasion in human colon cancer ((Zhang, et al. 2011). The linked between Myc and miR-23b has been highlighted in the altered glucose metabolism of cancer cells, which is known as the Warburg effect (or aerobic glycolysis). In this condition, cancer cells can take up excessive amounts of glucose and convert it to lactate even in the presence of oxygen (Vander Heiden, Cantley and Thompson 2009). Interestingly, Dang and co-workers reported that Myc stimulates glycolysis, glutamine oxidation and mitochondria biogenesis (Dang 2012, Dang 2010). Using a human B-cell lymphoma model carrying an inducible c-Myc, cells consume glucose and glutamine in presence of oxygen. In deprivation of oxygen (known as hypoxia), c-Myc cooperates with HIF-1 (Hypoxia-Inducible Factor-1) to promote the conversion of glucose to lactate. Thus this gives great sources of energy to cancerous cells by providing ATP and NADPH to promote their proliferation in the hypoxic as well as the more oxygenated regions of the tumor environment. As c-Myc is involved in the Warburg effect and it increases the expression of mitochondria glutaminase by repression of miR23a/b in transformed cells, we thought that as well as miR-23b, miR-23b* would be an interesting target to investigate in CHO cells with a view to altering their metabolism. In fact, the production of recombinant protein is an energy-intensive process so an increase of metabolism should help to produce more building blocks to increase proliferation and product secretion.

Although miR-23b* and miR-23b derived from the same hairpin sequence, miR-23b was not differentially regulated in our profiling despite the large range of growth rates across clones and its reported role in proliferation. In addition, in the temperature-shift profiling study the expression of miR-23b was detected at low levels based on Ct-values and did not vary after the shift of temperature to 31°C. First, this suggests that miR-23b may not be involved in the regulation of CHO cell growth as it is the case in cancer cells. Secondly, the levels of miR-23b* were high in the fast growing cells indicating that in CHO cells miR-23b* is more abundant than miR-23b and is more likely to be involved in cell proliferation. In support of this statement, Okumar and co-workers demonstrated that from cloning data in drosophila S2 cells some miRNA* species were more abundant than the miRNA species including miR-276a*, bantam*, miR-34*, miR-2a-2* miR-282*, miR-996* and miR-306* (Okamura, et al. 2008). In addition, they validated this accumulation by northern blot to prove that the levels of expression of these miRNA* species were indicative of miRNAs with proper biological function.

To validate the correlation between high levels of miR-23b* and fast proliferating cells, we forced the expression of miR-23b* using mimic molecules in CHO-K1 SEAP, a fast growing CHO cell line. Transient overexpression of miR-23b* resulted in a significant reduction in cell density over two days as well as viability. A 44% improvement of cell viability was detected at later stages of culture likely due to the reduction of cell number at earlier time points. We observed across the different transfection assays of this screening study that the impact of the transient molecules was often abated by day 7. Thus in this case, cells could recover by day 7 due to the loss of pm-23b* molecules explaining the higher cell density and viability compared to the non-specific treated cells. The expected phenotype consequent to transient overexpression was the improvement of cell growth. However, the opposite effect was observed suggesting that the fast proliferation rate increased the levels of miR-23b* and not the other way around. Although these results were statistically significant and a repeated experiment showed the same profiles, only one CHO cell lines was tested. Repeats in different cell lines would confirm if the overexpression of miR-23b* triggers cell growth reduction and if the validation of miR-23* deserves further investigation.

7.1.2.2 miR-216b

miR-216b was found to be down-regulated in fast growing cells. In agreement with this finding, miR-216 has been shown to be inversely correlated with Insulin-Growth Factor (IGF) activation in hepatocellular carcinoma (Tovar, et al. 2010). IGF signalling is a key regulator of cell proliferation and survival and its deregulation is often described in malignancies (Harris and Westwood 2012, Pollak 2008). To improve CHO proliferation, we used inhibitors of miR-216b which slightly enhanced cell density three and five days after transfection and provoked a 1.45-fold increase at day 7. These results are consistent with the profiling data and the reported role of miR-216 in the literature. In addition, cell viability was improved at later stages of culture by 16.57%. Peruzzi and co-workers showed that the activation of IGF receptor by its ligands protects different cell types from apoptosis (Peruzzi, et al. 1999). As miR-216 has been shown to anti-correlate with IGF activation and its expression levels are down in fast growing CHO cells, its knockdown may suppress apoptosis through IGF activation.

7.1.2.3 miR-409-5p

In the miRNA profiling, expression levels of miR-409-5p were generally high in the cell lines and were reduced in fast growing cells. Little is known about the role of miR-409. Recently, miR-409-3p, but not miR-409-5p, has been reported to suppress gastric cancer invasion and metastasis (Zheng, et al. 2012). However, miR-409-3p was not detected as a differentially regulated miRNA in our profiling. As discussed earlier, mature miRNA (in this case miR-409-3p) and miRNA* (miR-409-5p) have been shown to have different fates. Generally mature miRNA are more abundant in the cells than miRNA* species due to their presumably rapid turnover. However, though it is more rare, miRNA* can be also functional and accumulate at the same levels or even be, in rare cases, more abundant than the major miRNA species particularly when their seed sequences are well-conserved across species (Okamura, et al. 2008, Guo and Lu 2010). It is possible that miR-409-3p is more abundant in human cells and miR-409-5p is the dominant selected strand in CHO cells. Thus miR-409-5-p may be functional in CHO cells and involved in the regulation of cell proliferation whereas miR-409-3p might be considered as the passenger strand and so be degraded rapidly. The transient

knockdown of this miRNA showed no impact on either CHO cell growth or productivity. Thus it is likely that the variation of miR-409-5p levels in fast and slow growing cells was a consequence of the cell growth rate changes and not the opposite.

7.1.2.4 miR-874

miR-874 has been described as a tumor suppressor in maxillary sinus squamous cell carcinoma (Nohata, et al. 2011). This is in the same direction as our data which indicated low levels of miR-874 in fast growing cells. However, in the functional assay knockdown of miR-874 reduced cell proliferation to a small extent at day 3 and significantly five days after transfection. Cells recovered by day 7 likely due to the loss of am-874 at this stage. These contrasting outcomes suggest that miR-874 would influence positively cell proliferation after its induction. This could be verified in other transfection assays with different cell lines.

Following miR-874 knockdown, cell viability was improved by 12.32 % at later stages of culture. miR-874 has been found to be a temperature-sensitive miRNA in human hypothermia conditions (Truettner, et al. 2011). It was highly expressed at 37°C after traumatic brain injury in rats and its levels of expression decreased after hypothermia treatment at 33°C, leading to protection of these injured and vulnerable cells against negative signals. Thus by analogy, miR-874 may be involved in the homeostasis of CHO cells and may protect them against perturbation fluctuations thus leading to an increase of viability as observed in the functional validation. The transfection of am-874 did not impact significantly on total yield and normalised productivity.

Summary of miRNA screening data

In summary, our results from screening individual miRNAs were mixed and somewhat disappointing. The most striking observation was that in many cases the impact was the opposite to what would be expected based on either our own expression profiling experiments or from studies performed by others in other systems. It is difficult to identify the reasons for this. It may be that CHO, as a cell line or group of cell lines, is already well adapted to growth in vitro after many years of culture under these conditions. Mayr and Bartel reported an existing alternative cleavage and polyadenylation (APA) mechanism in cancer cell lines, which results in the expression

of multiple proto-oncogene isoforms which exhibit shorter 3'UTRs (Mayr and Bartel 2009). The shorter mRNAs were more stable than the homolog mRNAs in the non-transformed cells leading to the production of ten-fold more proteins, though the two cell lines had similar proliferation rates. This difference proved to be in part due to the loss of miRNA-mediated repression which generally occurs at the 3'UTRs of the mRNA targets thus conferring an advantage to the transformed cells through repression attenuation of oncogenes. Another study identified shorter 3'UTRs in activated T cells compared to resting T cells, and found that in general shorter 3'UTRs were associated with cell proliferation (Sandberg, et al. 2008). Previous reports showed that shorter 3'UTR can also be caused by genomic deletions or substitutions at the 3'UTR site (Wiestner, et al. 2007). Therefore it is possible that similar mechanisms occur in CHO cells which are also transformed cells and undergo mutations to prevent for instance apoptosis through the aberrant expression of p53 (Hu, et al. 1999, Lee, Larner and Hamlin 1997).

Alternatively, it may be the nature of the role that miRNAs, or many of them at least, play in the cell, ie to counteract genetic fluctuations across entire pathways using feedback loops and posttranscriptional repression (Ebert and Sharp 2012). To buffer these variations, miRNAs may work in unison with other miRNAs in a complex network so perturbing one maybe futile if compensation by other family members can occur.

The timing of expression could also be critical during the phase of culture or during the phase of the cell cycle. Vaseduvan and co-workers have shown that depending on the cell cycle phase, miRNAs can induce translational up-regulation of target mRNAs in non-proliferating cells and on the other hand miRNA promoted posttranscriptional repression in proliferating cells (Vasudevan, Tong and Steitz 2007a).

Transient transfection may not be the most suitable approach in a rapidly proliferating cell line like CHO. For instance, it is uneasy to measure apoptosis which occurs later in culture if mina levels are being diluted out. The transient transfection of mimics causes huge increase beyond what would be normal physiologically with unpredictable consequences so we were unsure if the phenotypes observed were due in part to off-target effects.

With these observations in mind we decided to pursue some alternative approaches – multiple knockdown of miRNAs from a cluster, 'miRNA sponge' to attenuate the

expression of an entire miRNA family and inducible systems for miRNA overexpression.

7.2 Investigation of the individual miR-23a~miR-27a~24-2 cluster member potential in improving CHO cell characteristics

7.2.1 Screening of miR-24

The microarray profiling study carried out following temperature-shifted culture indicated that high levels of miR-24 were associated with cell growth inhibition (Gammell, et al. 2007). The role of miR-24 in cell growth, cell cycle and DNA repair has been well described (Lal, et al. 2009a, Lal, et al. 2008, Lin, et al. 2010, Liu, et al. 2010, Mishra, et al. 2007). However, miR-24 has also been reported to be differentially regulated in different cell lines and in different conditions (Cheng, et al. 2005). This peculiarity applies to many miRNAs which have a unique expression level depending on the cell or tissue type as well as environmental conditions (Bartel 2004).

With the intention to validate the anti-proliferative impact of miR-24 in CHO cells, we transiently overexpressed miR-24 using mimic molecules at moderate (50nM) and high concentrations (100nM). As anticipated with the data from the profiling study, the anti-proliferative role of miR-24 was reproducible and consistent in different CHO cells lines, though the extent was dependent of the cell-line and on the exogenous miRNA concentration. At high concentrations, mimics of miR-24 led to a 1.68-fold decrease of CHO1.14 cell growth four days after transfection and arrested cell growth for five days in CHO2B6 cells. At lower concentrations, transient overeexpression of miR-24 induced a 1.27-fold growth reduction in CHO-K1 SEAP cells. We confirmed up-regulation of miR-24 levels using qRT-PCR to verify that cell growth reduction was caused directly by high levels of miR-24.

To support these results, we aimed to promote cell growth through miR-24 inhibition using transient molecules. When using synthetic inhibitors of miR-24 at a high concentration, cell growth was improved by more than twofold in CHO1.14 cells but no impact was observed in CHO2B6 cells. At lower concentration, CHO-K1 SEAP growth was also increased by 1.27-fold. Surprisingly, the investigation of the expression levels

of miR-24 revealed only a small reduction in CHO2B6 whereas there was no noticeable phenotypic impact in these cells. On the other hand, it showed a small increase of miR-24 levels in CHO1.14, though there was distinct increase in cell density in CHO1.14 cells upon am-24 transfection. It is possible that antimiR molecules which are single-stranded molecules may be dissociated from their target miRNA during RNA extraction process so the levels of miRNA would still be detectable. In addition, across the different transient assays performed in the different screening, it seems more difficult to observe a reproducible impact with the inhibitor molecules suggesting again that inhibitors might be less efficient than the mimics due to the nature of their binding. In fact, they compete with mRNA targets to bind to endogenous miR-24 which is expressed at high levels in CHO cells.

The repeated attempts of pm-24 and am-24 transfection at different concentrations showed contrasting results. Based on Ct-values, miR-24 is expressed at high levels in CHO cells (Gammell 2007) so further overexpression might not be impactful. It is also possible that further exogenous addition of this miRNA merely results in saturation of the RNAi machinery and leads to off-target effects. Khan and co-workers proposed that siRNA transfection perturbs global gene regulation by endogenous miRNAs (Khan, et al. 2009). They postulated that exogenous molecules compete with endogenous miRNAs for miRISC complex, thus perturbing the levels of endogenous miRNAs and their many transcripts. In another study they showed that cells would have limited capacities to assemble the RISC complex for exogenous molecules (Jackson, et al. 2006, Jackson and Linsley 2010). This could explain that the impact of mimic miR-24 on CHO-K1 SEAP cells was not as striking as in CHO1.14 and CHO2B6 cells due to lower concentration of these transient molecules.

On the other hand, if miR-24 is expressed at high levels then its knockdown may be achievable. Transient knockdown of miR-24 using moderate concentration of inhibitors promoted only a slight increase in cell growth and high concentration proved to be more efficient. However, there was no impact on CHO2B6 cells. The excess of exogenous inhibitor miRNAs which are single-stranded molecules and not processed by the RNAi machinery, could lead to accumulation in the cells and trigger unspecific targeting on mRNA transcripts thus little impact might be observed due to possible antagonizing signals from different transcripts. Another possibility, though never reported, is their rapid degradation or storage in P-bodies or stress granules caused by the excess of exogenous molecules present in the cells.

Having observed an impact on cell growth, we were interested to investigate the influence of miR-24 on SEAP total yield and normalised productivity. SEAP total yield was improved by 1.6-fold as well as normalised productivity though it was not statistically significant following miR-24 knockdown. The up-regulation of miR-24 impacted negatively on total yield likely due to the lower cell number in culture.

Thus these findings revealed positive indications that miR-24 was involved in cell proliferation but the issues with the mimic and inhibitor molecules posed some questions about their utility. The well established role of miR-24 in cell proliferation, cell cycle and its deregulation in many cancers convinced us to pursue the validation of miR-24.

7.2.2 Investigation of the functional role of miR-24 in CHO cells

Many reports have established a role for miR-24 in cell proliferation, cell cycle, apoptosis and DNA repair genes (Lal, et al. 2009a, Qin, et al. 2010, Mishra, et al. 2009, Lal, et al. 2009b, Lin, et al. 2010, Liu, et al. 2010, Mishra, et al. 2007). We showed that manipulation of mir-24 impacted on cell proliferation and cell viability though there was some inconsistency in the data. To ensure that the impact on cell proliferation and viability was specific to the up- or down-regulation of miR-24, we checked the levels of expression of validated mRNA targets upon pm-24 and am-24 transfection.

Overexpression of miR-24 has been reported to trigger cell cycle arrest in G1 phase via targeting key nodes of the cell cycle like MYC and E2F2, and their downstream targets including CCNB1, CDC2, CDK4, $p27^{KIP1}$ (Lal, et al. 2009a). Genes involved in other phases of the cell cycle were also down-regulated including FEN1, MCM4, MCM10, PCNA (S-phase) and AURKB (M-phase). A particularly interesting finding in this report was that miR-24 interaction with its mRNA targets did not involve canonical seed pairing binding. In addition, these targets were not predicted by seed recognition computational methods. However, miR-24 is a well conserved miRNA across species (Lal, et al. 2009a) so we considered validating the same targets using real-time PCR in CHO cells. PABPNI, a gene involved in polyA synthesis (Kuhn and Wahle 2004), was chosen as endogenous control for this study. It was identified as a non-varying gene in a microarray gene expression profiling study and validated by qPCR in CHO cells (Bahr, et al. 2009). This gene had a lower expression variability (CV=23.8%) than the usual

endogenous control used in qPCR including ACTINB (CV=27.13%), GAPDH (CV=44.97%) and B2M (β-2-microglobulin) (CV=38.23%). However, we observed that transient up-regulation or knockdown of miR-24 impacted significantly on the levels of expression of PABPNI therefore we used ACTINB instead as it showed lower variability between our samples. It is worth noting that the median %CV of the candidate housekeeping genes identified in the profiling was 23.8% (Bahr, et al. 2009). This value is quite high considering the application of these genes as endogenous controls for qPCR studies especially in the case of miRNA manipulation and the investigation of changes in the expression of their targets. Since miRNAs are able to target hundreds of genes, it has been demonstrated that they often cause moderate changes of gene expression (Krutzfeldt, et al. 2005, Lim, et al. 2005). If the endogenous control is also targeted by a miRNA, the difference in expression of its true targets may be hard to detect. Thus it may be quiet challenging to find an appropriate endogenous control in these conditions. To improve the accuracy of normalisation, it has been suggested to use the mean of several endogenous genes that have been selected prior to the experiment (Persson, Hamby and Ugozzoli 2005, Vandesompele, et al. 2002).

To validate a role of miR-24 in cell proliferation and cell cycle in CHO cells, we focused on five of its established targets, MCM4, MYC, PCNA, CYCLIN A and FEN1. Transient knockdown of miR-24 led to increase of PCNA expression levels and slight down-regulation of FEN1. On the other hand, transient up-regulation of miR-24 induced knockdown of FEN1 and slight increase of PCNA. This was not statistically proven as only two biological samples were run in technical triplicates. PCNA is known to interact with FEN1 and to stimulate its activity in many FEN1 dependent DNA metabolic pathways including DNA replication (Li Zheng 2011). Disruption of the FEN1/PCNA interaction leads to DNA replication defects and newborn lethality in mice (Zheng, et al. 2007). PCNA stimulates DNA synthesis and is involved in DNA damage (Kannouche, Wing and Lehmann 2004, Haracska, et al. 2002). FEN1 is a member of the Rad2 structure-specific nuclease family and it processes the 5' ends of Okazaki fragments in lagging strand DNA synthesis and has an essential role in base excision repair (BER) (Lieber 1997, Liu, Kao and Bambara 2004). These two miRNAs seem to cooperate in the regulation of cellular function like DNA damage and replication thus the levels of expression of both genes PCNA and FEN1 might be linked together and fluctuate upon changes in miR-24 expression.

The expression levels of MCM4, MYC, PABPNI were increased following transfection with am-24. On the other hand, up-regulation of miR-24 induced knockdown of MCM4, MYC, PABPNI. Again these results were not supported by statistical significance due to the restricted number of biological replicates. However, the direction of the changes in expression of these targets was consistent between the data from the up-and down-regulation of miR-24. MCM4 belongs to the mini-chromosome maintenance proteins (MCM) family and is involved in the initiation of replication in eukaryotes (Bochman and Schwacha 2009, Forsburg 2004). MYC is involved in many cellular pathways including cell proliferation, apoptosis, cell metabolism and is a key regulator of the G1/S transition phase (Obaya, Mateyak and Sedivy 1999, Dang 1999) (Herold, Herkert and Eilers 2009). Thus this indicates that MCM4 and MYC may be conserved targets of miR-24 in CHO cells as well as PABPNI.

Further validation using a reporter assay would demonstrate the direct relationship between miR-24 and these targets and validate its role in cell cycle.

7.2.3 Inducible overexpression of miR-24 using a tetracycline-inducible cassette

Although there were some indications that manipulating the levels of miR-24 could lead to positive impact on growth, the variability in the results observed in the transient assays was unsatisfactory. In an attempt to gain greater control over the levels of miR-24 expression in the cells, we decided to implement an inducible, plasmid-based system. The miR-24 precursor was cloned into pmF111, a tetracycline-inducible vector. Although transfection of pmF111-miR-24 reduced cell proliferation in CHO1.14 and CHO2B6 cells, this decrease was also observed following transfection of pmF111 and other controls of transfection in presence of doxycyline. Addition of doxycyline should prevent the expression of the gene of interest and in absence of this drug it should release its control and allow the gene to switch its expression. Upon withdrawal of doxycyline, cell growth was further reduced particularly four days after transfection in all samples. Cell viability was also negatively impacted in both conditions. This non-specific impact was abated at day 7 likely due to the loss of plasmid. Thus the process of transfection had detrimental impact on all samples and could not allow comparison between the samples. If any small changes occurred it might not be noticeable.

We verified that the inducible system allowed the overexpression of miR-24, by investigating the levels of miR-24. Higher miR-24 levels were detected in pmF111-miR-24 transfected CHO1.14 cells, indicating that precursor miR-24 was processed into mature miR-24 and this latter was up-regulated. However, the fold-change was quite small (4-fold). Recently, Jadhav and co-workers reported that following transfection of precursor miR-17 and other miRNA precursors using a shRNA approach in CHO cells, miRNA expression did not exceed 2.3-fold and the increase of growth rate reached a maximum of 15.4% (Jadhav, et al. 2012). However, in this study they used a chimeric precursor that consisted in CHO miRNA mature sequences inserted into a design pre-miRNA sequence of murine miR-155. It has been reported that the stem-loop of a precursor miRNA may be critical and sufficient for miRNA processing (McManus and Sharp 2002). Thus it might be possible that the murine flanking and stem-loop sequences/structure, which are critical for processing was not properly recognised by the RNAi machinery in CHO cells. Zeng and co-workers reported that the flanking and loop sequences of miR-30 have important features and are sufficient to enhance siRNA/miRNA precursor processing into the mature form (Zeng, Wagner and Cullen 2002, Boden, et al. 2004). In this study, they tested their approach by replacing the stem sequence of the human miR-30 with a drosophila-specific gene sequence which was not conserved in human and the chimeric sequence was successful expressed. However, they also inserted the predicted *C. elegans* lin-4 precursor as well as the human mir-27 and let-7a3 precursors into the same expression vector but they could not detect up-regulation of these three miRNAs. This suggests that miRNA processing might be dependent not only of structural features, for instance secondary structures/RNA folding but other mechanisms that could be species-related.

In addition, transfection of shRNA has been reported to trigger competition with endogenous miRNAs and inhibit their function as they undergo the same processing by saturating the RNAi machinery (Yi, et al. 2005). In addition, Grimm and co-workers showed that oversaturation of shRNA molecules induced lethality in mice (Grimm, et al. 2006). Thus it is also possible that unexpected impact was seen due to off-target effects. If precursor miR-24 was processed in excess, the other miRNAs could not be processed and therefore would not regulate their targets leading to perturbation of other cellular functions. In addition, miR-24 is already expressed at high levels in CHO cells so the excess of mature miR-24 could also trigger binding to undesirable targets. These

undesirable effects may have masked the phenotype expected, in this case reduction of cell growth, by compensation of other routes.

In CHO2B6 cells there was no indication of miR-24 up-regulation suggesting that precursor miR-24 was not processed into a mature strand in this cell line. The flanking sequences inserted on either sides of mature miR-24 were amplified from CHO cells thus we anticipated the correct processing of precursor miR-24 in both CHO cell lines. It has been reported that mature miRNAs are well conserved between species but it is not the case for precursor miRNAs (Bartel 2004). Thus it is possible that between cell lines that derived from a same parental clone, they might be some mutations in the precursor sequence that prevent its processing. Another explanation is that precursor miR-24 was processed into an isomiR form of miR-24 thus in this case it may be difficult to evaluate its levels of expression using miR-24 primers that would be non-specific. IsomiRs have been described by Morin and co-workers as variants of the mature form of miRNAs induced by the variability in either Dicer1 or Drosha cleavage positions within the pre-miRNA hairpin (Morin, et al. 2008) . Using Illumina sequencing technology, they showed that miR-24 had several isomiRs expressed at low abundance in differentiating human embryonic stem cells (90 counts for isomiRs vs 787counts for the miR-24 used as reference). Finally, to eliminate the possibility of an issue in the vector design and cloning, we verified the sequences of these constructs by sequencing and did not find secondary structures or nucleotide changes or deletions.

Thus the issues encountered at the transfection levels and miRNA processing levels discouraged us from continuing in this direction. The optimisation of the transfection protocol, the concentration of plasmids as well as transfection reagent and the time of transfection might improve the success of this assay.

7.2.4 Investigation of the simultaneous impact of miR-23a~miR-27a~24-2 cluster members on CHO cell characteristics

Many miRNAs are transcribed as polycistronic transcripts due to their organization in clusters. In humans, out of 721 miRNAs known, 247 of them are arranged within 64 clusters at an inter-miRNA distance of less than 5000bp and most of these clusters are highly conserved across species (Griffiths-Jones, et al. 2008, Altuvia, et al. 2005). miRNAs within a genomic cluster are often related to each others but it is not always

the case (Lau, et al. 2001, Lagos-Quintana, et al. 2001). Due to the nature of their binding, miRNA sequence homology gives the possibility of targeting the same transcripts and the same cellular pathways (Bartel 2004, Olena and Patton 2010). Examples in the literature show that even when clustered miRNAs have no apparent sequence homology they may share a functional role (Bashirullah, et al. 2003, Sempere, et al. 2003, Aravin, et al. 2003). On the other hand, they may share homology and have different targets (Lau, et al. 2001). miR-24-2 is co-transcribed with miR-23a and miR-27a as part of miR-23a~27a~24-2 cluster. In humans, miR-23a~27a~24-2 cluster is intergenic and localized on chromosome 9q22 and its paralogous intronic cluster, miR-23b~27b~24-1, is localized on chromosome 19p13 (Chhabra, et al. 2009). Yu and co-workers have reported that it is not uncommon for miRNA clusters to have homologs and paralogs (Yu, et al. 2006). It has been suggested that targeting only one miRNA of a cluster could lead to compensation from its co-transcribed miRNAs particularly in the case of clustered miRNAs sharing sequence homology and/or functions (Lu, et al. 2009). This counteraction may result in restoring the original function and so little or no effect might be seen. Druz and co-workers reported the up-regulation of miR-297~669 cluster upon nutrient-depleted medium and investigated the anti-apoptotic role of miR-466h in CHO cells, which showed the highest levels of expression among the cluster members (Druz, et al. 2011). The inhibition of miR-466h using synthetic antisense oligonucleotides induced the up-regulation of genes invovled in apoptosis in nutrient-depleted medium. Two mediators of the apoptosis pathways, caspase-3/7 were found to be down-regulated and the viability increased. However, this was not enough to rescue cells from apoptosis thus suggesting that the other miR-297~669 cluster members that were also found to be differentially expressed upon nutrient-depletion, may act in unison with miR-466h to regulate apoptosis.

Therefore the single and synergic impact of the three miRNAs from miR-23a~27a~24-2 cluster was investigated in transient assays.

7.2.4.1 Screening of miR-23a

miR-23a was not previously detected as differentially regulated in our miRNA profiling studies so there was no indication of the functional role of this miRNA in CHO cells. miR-23a has been shown to promote cell growth in gastric adenocarcinoma cell lines

(Zhu, et al. 2010). c-Myc is also involved in cell cycle progression, apoptosis and its deregulation is associated with cancers (Cascon and Robledo 2012, Dang 2012) suggesting that miR-23a/b might also contribute to the regulation of the same cellular pathways. As discussed previously, the Warburg effect, an altered glucose metabolism, stimulates cancer cells to promote the conversion of glucose to lactate and to induce glutamine metabolism changes (Dang 2010). It has been reported that inhibition of miR-23a/b by c-Myc enhances mitochondria glutaminase expression and glutamine metabolism (Gao, et al. 2009). This is a really interesting characteristic of the regulation between c-Myc and miR-23a/b which might be exploited to increase the levels of energy in cells and activate further the metabolism and the proliferation of cells.

The forced expression of miR-23a provoked a 1.61-fold growth reduction in CHO-K1 SEAP cells whereas its inhibition did not reverse this phenotype. Cell viability was negatively impacted four days after pm-23a transfection and no impact was observed in am-23a transfected cells. As observed previously, in contrast to pm molecules the inhibitor molecules did not resulted in noticeable phenotypic impact. Based on the data obtained from previous study in our laboratory, miR-23a was expressed at low levels in CHO cells. Therefore further knockdown might be challenging to achieve. Despite the absence of a phenotype upon am-23 transfection, there were positive indications that, like miR-24, miR-23a may influence CHO cell proliferation. This suggested that the up-/down-regulation of the entire cluster might lead to a stronger impact.

7.2.4.2 Screening of miR-27a

Similarly to miR-23a, the data from our profiling studies did not indicate that miR-27a was differentially regulated in temperature-shifted culture or fast growing cells. miR-27 participates in the regulation of cell metabolism. PPARγ, a key regulator of adipogenesis has been validated as miR-27 target (Lin, et al. 2009) and miR-27 has been shown to affect cholesterol homeostasis, fatty acid metabolism and lipogenesis (Lin, et al. 2009, Fernandez-Hernando, et al. 2011, Fernandez-Hernando, et al. 2011). miR-27 is also involved in the G2/M checkpoint of the cell cycle in breast cancer cells (Mertens-Talcott, et al. 2007) and acts as an oncogene in gastric adenocarcinoma (Liu, et al. 2009). Thus miR-27 may influence cell proliferation and cell metabolism in CHO cells.

Transient manipulation of miR-27a expression using mimics/inhibitors at high concentration (100nM) led to contrasting results in CHO1.14 and CHO2B6 cells. Overexpression of miR-27a in CHO1.14 cells induced significant growth reduction for two days and improved viability by 8.23% at later stages of culture. In CHO2B6 cells, high levels of miR-27a induced cell growth increase at two and four days after transfection and reduced cell viability by 4.67% to 7.52%. Surprisingly, knockdown of miR-27a led to decrease in CHO1.14 growth at day 2, increase at day 4 and improve viability at the same time but it did not impact on CHO2B6 cells. Although we observed opposing results in these assay, there was phenotypic changes in the pm-27/am-27 transfected cells compared to the controls. Therefore we continued the validation of this miRNA by considering the manipulation of miR-23a~27a~24-2 cluster expression in a transient assay.

7.2.5 Investigation of the simultaneous impact of miR-23a~miR-27a~24-2 cluster members on CHO cell characteristics

The individual manipulation of miR-24, miR-23a and miR-27a resulted in contrasting phenotypes in CHO cells. As mentioned previously, targeting only one miRNA of a cluster could lead to compensation from its co-transcribed miRNAs so little or no effect might be seen (Lu, et al. 2009). Interestingly, the miR-23a~27a~24-2 cluster seems to be present only in vertebrates (Chhabra, Dubey and Saini 2010). Despite this, the functional role of the cluster in cell proliferation and apoptosis has been reported to be cell-line dependent. Up-regulation of miR-23a~27a~24-2 cluster has been shown to stimulate apoptosis in human embryonic kidney cells upon endoplasmic reticulum (ER) stress (Chhabra, Dubey and Saini 2010, Chhabra, et al. 2009, Chhabra, Dubey and Saini 2011, Huang, et al. 2008)

In CHO cells, we showed that transient up-regulation of the entire cluster induced a 2.11-fold reduction of cell growth, 30% improvement in cell viability and enhanced total yield and normalised productivity by 1.44-fold and 1.84-fold respectively. Knockdown of the cluster did not impact on CHO cell growth at early time points and had little impact on viability. However, it did improve total and normalised productivity at later stages of culture by 1.35-fold and 1.71-fold respectively. To avoid saturation of

the RNAi machinery, the final concentration of the co-transfected molecules used was 50nM thus reducing the concentration of each individual mimic and inhibitor to 16.66 nM. Using this concentration, clear phenotypes could be observed suggesting that the synergic manipulation of the three miRNAs is a better approach than the manipulation of single miRNA. It is also possible that a lower concentration of synthetic molecules reduced the risk of off-target effects by allowing endogenous miRNAs to be processed normally and exert their control on their cognate mRNAs. Together these results confirmed that miR-23a~27a~24-2 cluster influences proliferation and productivity in CHO cells. Previous studies in our laboratory indicated that miR-24 was highly expressed, miR-27 was moderately expressed and miR-23a had a lower level of expression in CHO cells. Thus it would be interesting to use different combinations of mimic/inhibitor concentrations to investigate the simultaneous impact of miR-23a, miR-27a and miR-24-2 within the cluster on different CHO characteristics.

7.3 Generation of CHO cell clones with improved characteristics by stable knockdown of miR-23a~miR-27a~24-2 cluster

Single or multiple knockdown of miR-24-2, miR-23a or miR-27a using inhibitor molecules did not impact significantly on cell proliferation or cell viability in contrast to its up-regulation which reduced cell proliferation by 2-fold and enhanced cell viability by 30%. In an attempt to improve cell proliferation we decided to try depleting all three cluster members simultaneously using a stable antisense approach named ‘multi-antisense cluster’. One potential advantage of reducing cellular miRNA levels rather than increasing them is that it does not require processing via the RNAi machinery. In this attempt, two stable cell lines were generated; one expressing a multi-antisense cluster to target miR-23a~27a~24-2 cluster (wt cluster) and the other one with a random sequence (mut cluster).

In a mixed population, wt cluster transfected cells showed 20-30% lower GFP signal fluorescence than in the control cells indicating that miR-23a~27~24-2 cluster miRNAs were binding to the multi-antisense cluster and blocking translation/catalyzing degradation of the reporter transcript. Although the median GFP fluorescence was generally lower in wt cluster expressing clones, there was a lot of variability between clones in both wt and mut cluster expressing clones. This is to be expected and is caused

by genetic heterogeneity induced by random integration of the vector DNA. It has been documented that this clonal heterogeneity is due to gene dosage/number of integrated copies and random integration of exogenous DNA affecting other cell traits (Wurtele, Little and Chartrand 2003). Pilbroug and co-workers suggested that in addition to clonal genetic heterogeneity, cells undergo random expression fluctuations leading to phenotypic differences between clones (Pilbrough, Munro and Gray 2009). It is this heterogeneity that is routinely exploited to select clones showing an advantage for a particular phenotype (Pichler, et al. 2011).

Further evidence that the multi-antisense cluster was successfully binding the miRNAs of interest was found when the clones were transfected with mimics of miR-23a, miR-27a or miR-24-2, resulting in lower reporter expression in the targeted multi-antisense cluster but not the control. This decrease was stronger when using mimics of miR-24-2 or miR-27a. It is possible that mimics of miR-23a were not processed efficiently when loading to the RISC complex thus leading to less mimic molecules to bind to the multi-antisense cluster. This may also be due to the endogenous levels of expression of these miRNAs. miR-24 and miR-27a have high and moderate levels of expression in CHO cells whereas miR-23a is expressed at low levels. Therefore more molecules of endogenous miR-24-2 and miR-27 may be bound to the multi-antisense cluster leading to further GFP reduction compared to less endogenous miR-23a inducing smaller reduction of GFP. If the concentration of miR-23a is not increased by the transfection of exogenous miR-23a molecules then the reduction of GFP would appear smaller. This difference in levels of expression between clustered miRNAs is not uncommon. Although these miRNAs are transcribed from the same promoter and belong to the same cluster, their subsequent biogenesis into mature form are likely to be regulated by very complex mechanisms (Lee et al;. 2004). Following overexpression of miR-23a~27a~24-2 cluster in HEK293T cells, levels of miR-24-2 and miR-27a were increased but not miR-23a levels (Chhabra, et al. 2009). In another study, knockdown of miR-27a was independent of miR-23a and miR-24-2 (Buck, et al. 2010). This suggests that due to low levels of miR-23a, less endogenous and exogenous miR-23a molecules were bound to the multi-antisense cluster compared to miR-24-2 and miR-27a which are more abundant in the cells. The processing of endogenous miR-23a into mature miR-23a could also be blocked as reported in HEK293T cells (Lee, et al. 2008). Surprisingly, one clone out of the three tested in this assay did not show a reduction in GFP fluorescence. Although the impact on cell growth in this clone was not as obvious as in the two other

clones, there was a significant improvement in cell density in comparison to the control cells.

Following validation the multi-antisense cluster approach, we focused on the impact of the simultaneous knockdown miR-23a, miR-27a and miR-24. Depletion of the miR-23a~27~24-2 cluster resulted in cell density increase by 2.5-fold to 2.87-fold in mixed population and by 1.4-fold in single cell clones in batch-culture. Cell viability was also improved by 12.5% at day 5. One of the features of batch culture is waste accumulation and nutrient depletion which may explain the reduction in cell viability and cell density by day 5. To overcome this and to investigate the potential of miR-23a~27~24-2 cluster knockdown at later time points, fresh medium was added to the culture at day 3. In this culture, an increase in cell density was observed at day 3/day 4 and this improvement was extended until day 6. At day 5, the average cell density between the three clones was enhanced by 1.71-fold. There were no changes in cell viability between the two groups. The increase of cell density seems to be limited by the nature of the batch culture and it may be possible to further extent this potential in fed-batch culture. Thus we demonstrated that the multi-antisense cluster is an efficient approach to simultaneously target clustered miRNAs and in contrast to transient molecules, reproducible phenotypic impacts could be achieved. In addition, we proved that knockdown of miR-23a~27~24-2 cluster members resulted in significant cell growth increase in a batch-culture.

Thus this suggests that the three miRNAs cooperate to strengthen the control of cell proliferation. Chabra and co-workers investigate the predicted targets of all three miRNAs using TargetScan program and found that these miRNAs shared only few predicted targets (Chhabra, Dubey and Saini 2010). However they also showed that these miRNAs are often differentially expressed in the same direction in several diseases.

Thus the manipulation of the expression of the 23a~27~24-2 cluster members is a promising tool to improve CHO cell proliferation and possibly cell viability. The improvement of culture conditions (i.e; fed-batch culture) might further enhance the potential of this approach.

7.4 Investigation of miR-7 potential in improving CHO cell phenotypes

7.4.1 Screening of miR-7

miR-7 is involved in cell proliferation and apoptosis regulation and its deregulation has been reported in many cancers including breast, pancreatic, glioblastoma, lung and tongue squamous cell carcinoma (Chou, et al. 2010, Kefas, et al. 2008, Ikeda, et al. 2012, Jiang, et al. 2010, McInnes, et al. 2011). In most of these studies, miR-7 plays a role of tumor suppressor, with its induction causing inhibition of tumor progression. miR-7 was previously identified as differentially regulated upon low temperature exposure in a miRNA profiling conducted in our laboratory (Gammell, et al. 2007). These findings led us to investigate the role of miR-7 in cell proliferation. Recently, we reported that cells were growth arrested for 96hrs and maintained high cell viability following treatment with miR-7 mimics in low-serum culture (Barron, et al. 2011). In the same study, normalised productivity was significantly improved but the total yield remained low consequent to impairment of cell proliferation. The impact of miR-7 on protein production is consistent with high levels of miR-7 reported in endocrine tissues including in the developing and adult human pancreas (Correa-Medina, et al. 2009, Joglekar, Joglekar and Hardikar 2009, Kredo-Russo, et al. 2012), in human pancreatic islets (Landgraf, et al. 2007), in the islets of zebrafish (Wienholds, et al. 2005), the neurosecretory cells of the annelid *Platynereis dumerillii* and zebra-fish (Tessmar-Raible, et al. 2007) and in the pituitary gland (Landgraf, et al. 2007). As high levels of miR-7 has been reported in these endocrine tissues, which are gland systems that produce and secrete hormones, in different species, it is likely that in CHO cells miR-7 might also influence the regulation of secretory pathways to improve the production of proteins.

To continue the detailed study of miR-7 in CHO cells, we investigated whether the anti-proliferative role of miR-7 was reproducible in serum-free culture and in different CHO cell lines. To engineer CHO cells, the ideal tool would be one which displays a ubiquitous phenotypic impact across all CHO cell lines. The suppressive role of miR-7 on cell growth proved to be reproducible in serum-free culture and in different CHO cell

lines though the extent of growth reduction was cell line-dependent. At high concentrations of miR-7 mimics, CHO2B6 growth was reduced by 2.5-to 3-fold and CHO1.14 were growth arrested for five days. At lower concentrations, transfection of exogenous miR-7 impacted to a lesser extent but still induced a 1.8-fold reduction in CHO-K1 SEAP cell density. This is possibly related to the concentration of mimics used in the two different assays. Using miR-7 inhibitor molecules, we expected to observe the opposite phenotype. However, improvement of cell proliferation was only present in CHO1.14 cells at high concentrations. There was no impact on CHO2B6 or on CHO-K1 SEAP cells. From previous miRNA profiling studies, we knew that the levels of expression of miR-7 in CHO cells were quite low. Therefore significant impact of miR-7 upon further knockdown may be difficult to detect. It is also possible that an excess of synthetic single-stranded miRNAs (inhibitors) might trigger a stress response leading to recognition by nucleases and rapid degradation of these molecules before they could impact on their mRNA targets.

Although the impact on cell proliferation was reproducible in the three cell lines upon pm-7 treatment, maintenance of cell viability was not observed in all repeats and in all cell lines. In CHO1.14, viability was slightly improved and in CHO-K1 SEAP cells, it was 37% higher than in the control treated cells at later stages of culture. To verify that the enhancement of cell viability was directly caused by high levels of miR-7 or due to a lower number of cells present in culture, the transient transfection assay was repeated at high density in CHO-K1 SEAP and CHO1.14 cells. First, the anti-proliferative role of miR-7 was not reproducible in every assay and there was no indication of cell viability improvement. In addition, non-transfected cells cultured at 31°C, as positive control, did not show the phenotype expected as their cell growth was not reduced and the viability was not prolonged. Many reports have demonstrated the use of low-temperature in biphasic culture to trigger cell growth arrest and extend cell viability, while more proteins are being produced (Kaufmann, et al. 1999, Oguchi, et al. 2006, Al-Fageeh, et al. 2006, Yoon, Kim and Lee 2003). We recently reported that CHO-K1 SEAP cells exposed to low temperature also display this behaviour (Barron, et al. 2011). To ensure that the transfection protocol was optimised at high density, a siRNA against Valosin Containing Protein (VCP) was included as a positive control. VCP has been previously reported to be a housekeeping gene in CHO cells, its deregulation leading to harmful effects on CHO cell growth and survival (Doolan, et al. 2010). The impact of VCP knockdown was reproducible in CHO-K1 SEAP and CHO1.14 cells cultured at high

density indicating that the transfection process performed well. Together these results suggest that the higher rate of cell viability observed in the previous transient transfection experiments was likely due to a lower cell number leading to healthier culture environment and not directly specific to miR-7 induction.

This assay was done at high density in a batch culture leading to rapid waste accumulation and nutrient depletion (Butler 1987, Newland, et al. 1994, Butler 1985). Thus we cannot rule out that the impact of miR-7 up-regulation on cell growth and viability might have been perturbed in those suboptimal conditions. This is supported by the significant drop in cell viability in most of the samples only three days after transfection. Usually in a healthy culture, miR-7 starts to reveal its impact on cell growth at day 2/3 while cells maintain high cell viability.

Regarding protein production, upon pm-7 transfection normalised productivity was slightly but not significantly improved in comparison to the non-specific control. We previously demonstrated that transient overexpression of miR-7 did significantly impact on normalised productivity in low serum-supplemented CHO-K1 SEAP culture (Barron, et al. 2011). In the present study, the cells were maintained in serum-free culture so the difference in culture conditions may affect the productivity of the cells (Cheng, et al. 2005).

Thus we confirmed the anti-proliferative role of miR-7 in CHO cells cultured in serum-free medium and continued the validation of this miRNA as candidate to improve CHO cell growth.

7.4.2 miR-7 as a tool for CHO cell engineering

Transient pm-neg and am-neg molecules were used for screening to reveal the impact of miR-7 expression manipulation on CHO phenotypes. These molecules are useful in short-term studies however, their transient effect, the low reproducibility between assays and cell lines, and the time consuming nature of these assays are major drawbacks for long-term studies.

7.4.2.1 Inducible overexpression of miR-7

Due to the significant negative impact of miR-7 overexpression on cell growth, an inducible system would be more suitable to allow cells to grow until the middle of the logarithmic phase. At this stage, the system would trigger cell growth arrest and turn the cellular machinery towards protein production. The first system tested was a Tet OFF system that allows tight regulation of gene expression by responding to the presence or absence of doxycycline, a tetracycline analogue. The removal of the drug allows the expression of a specific gene of interest and its presence prevents any expression. The precursor of miR-7 was inserted with its CHO flanking sequences into the vector pmF111 to allow processing into mature sequence by the endogenous machinery. In presence of doxycycline, reduction of cell density was observed not only following pmF111-miR-7 transfection but also in all transfection controls in CHO1.14 and CHO2B6 cells. Cell growth was further decreased after withdrawal of doxycyline in all samples. Thus the transfection itself had such a dramatic impact on cell proliferation that any gene or miR-7 specific effects would not be detected.

Zeng and co-workers reported the successful overexpression of miR-30 using a short hairpin RNA (shRNA) (Zeng, Wagner and Cullen 2002). This consisted of the insertion of precursor miR-30 (71nt) in a plasmid with a CMV promoter. They also demonstrated that the backbone of miR-30 that consists of the stem-loop was sufficient to enter the processing machinery therefore they created artificial miRNAs that were processed by the endogenous machinery into mature miRNAs. Thus the stem-loop of the precursor miRNA may be critical and sufficient for miRNA processing (McManus, et al. 2002). Since this report, many papers have reported efficient expression of miRNA or siRNA using miR-30 backbone in gene function studies but also for gene therapy applications (Boden, et al. 2004, Bauer, et al. 2009). In our study, the flanking sequences of miR-7 were amplified from CHO cells so due to this specificity, we expected processing of the miR-7 precursor into mature form. In addition, the length of the sequences inserted into the plasmid pmF111 was more than 100 nt. Chang et al 2006 reported that primary sequences provide the highest levels of mature miRNA after processing thus our design was suitable for the expression of mature miRNA. In absence of doxycycline, the levels of miR-7 expression were increased by 7.81-fold in CHO2B6 cells but only by 1-83-

fold in CHO1.14. As the conditions of transfection and the concentrations of plasmids were similar, we anticipated the same levels of expression in both cell lines. Recently, Jadhav and co-workers reported that following transfection of precursor miR-17 and other miRNA precursors using a shRNA approach in CHO cells, the increase in miRNA total levels did not exceed 2.3-fold (Jadhav, et al. 2012). The authors postulated that the small increase in miRNA expression was due to regulatory feedback loops which prevent saturation of the RNAi machinery by down-regulating the expression of endogenous miRNAs in the presence of artificial overexpression. However, in this study they used a chimeric precursor that consisted in CHO miRNA mature sequences inserted into a design pre-miRNA sequence of murine miR-155. Thus it might be possible that the murine flanking and stem-loop sequences/structure, which are critical for processing was not properly recognised by the RNAi machinery in CHO cells and this subtle change in miRNA levels could be due to random fluctuations (Ebert and Sharp 2012). This could also be the case in our study or it may be the transfection process which was possibly less efficient in CHO1.14 cells compared to CHO2B6 cells and less copies of the vector were delivered into the cells. Similarly, the transient expression of the plasmid did not allow integration in the genome so it could have been lost more rapidly in these cells after several cell doublings. Optimisation of the concentration of plasmids, the concentration of doxycyline and the transfection process might help to improve the outcome of this assay.

In an attempt to overexpress miR-7 in an inducible manner, another Tet OFF system named pTet-Hyg was developed in the laboratory. The human flanking and stem-loop sequences of miR-30 were inserted into the pTet-Hyg vector. The expression of GFP following removal of doxycyline in pTet-Hyg transfected cells was lower than in the peGFP-C1 that constitutively expressed GFP, but it was sufficient for what we tried to achieve and indicated there was induction upon doxycyline withdrawal. In presence of doxycyline, minimal GFP fluorescence was detected suggesting that the system was under control of this drug. The hygromycin selection of positive cells transfected with pTet /Hyg vector resulted in cell death thus indicating that cells were not resistant to hygromycin. The PGK promoter and/or the Internal Ribosome Entry Site (IRES) might not have been sufficient to allow transcription/ translation of hygromycin. It would be interesting to verify whether the human flanking sequences containing the stem-loop of

miR-30 would be recognised by the CHO cell machinery and to which extent the expression of miR-7 would increased.

7.4.2.2 Generation of CHO cell clones with improved characteristics by stable knockdown of miR-7

The up-regulation of miR-7 using mimics revealed its anti-proliferative role in CHO cell lines. In a bioprocess context, we were interested in improving cell proliferation. Therefore we considered the inhibition of miR-7 to increase the cell growth rate (change in cell concentration per unit time). The efficiency of inhibitor molecules were not convincing in achieving knockdown of miR-7. To get a better control of endogenous miRNA inhibition and to minimise off-target effects, we thought to generate CHO cell clones stably expressing artificial miR-7 targets. In contrast to overexpression, knockdown of a miRNA does not require miRNA processing thus there is no risk of saturating the RNAi machinery. The 'miRNA sponge' technology was previously described to induce efficient endogenous miRNA inhibition by competing with endogenous mRNA targets for miRNA binding (Ebert, Neilson and Sharp 2007). A miRNA sponge sequesters the miRNA of interest through complementarity to its seed region.

The application of miRNA sponges in transient and stable transfections has been extensively used since the technology has been described in 2007 (Ebert, Neilson and Sharp 2007, Ebert and Sharp 2010). Among a long list of assays performed in different cell lines, with different vector types, transient knockdown of individual miRNAs such as miR-155 (Bolisetty, et al. 2009) or large seed families like let-7 (Kumar, et al. 2008), have been successfully achieved using the sponge approach (Ebert and Sharp 2010). Stable expression of the sponge has also been extensively reported *in vitro* (Ma, et al. 2010, Ma, et al. 2010, Valastyan, et al. 2009, Scherr, et al. 2007, Bonci, et al. 2008) as well as *in vivo* in plants, drosophila and mice (Loya, et al. 2009, Franco-Zorrilla, et al. 2007).

Three years after the development of this approach, endogenous miRNA decoys were discovered in plants. A non-coding RNA IPS1 (Induced by Phosphate Starvation 1) which displays sequence complementarity for miR-399 (a phosphate (Pi) starvation-induced miRNA) presents a mismatch at the site of canonical miRNA cleavage. Its

overexpression induces sequestration of miR-399 which leads to release of PHO2 mRNA and consequently lowers the shoot phosphate content (M. Franco-Zorrilla;2007). Posileno and co-workers reported that PTEN1, the pseudogene of PTEN, was biologically active (Poliseno, et al. 2010). For a long time, pseudogenes have been described as DNA genomic sequences, which derived from genetic duplication or retrotransposition and have no function due to the presence of premature stop-codons and/or mutations in their sequences (D'Errico, Gadaleta and Saccone 2004, Harrison, et al. 2005). PTEN1 has conserved seed matches for several miRNAs including miR-17, miR-21, miR-214, miR-19 and miR-26 families. Among these miRNAs, miR-17-5p/miR-20-p and miR-19 are able to repress both PTENP1 and PTEN RNA levels to a similar degree. Knockdown of PTEN1 reduced the mRNA and protein levels of expression of PTEN in prostate cancer and concomitantly increased cell proliferation through competitive binding to these miRNAs.

Thus the information released in these reports, led us to take the same approach as miRNA sponge seemed an ideal tool to inhibit an entire miRNA family and to target a specific function regulated by these miRNAs as reported for let-7 family (Kumar, et al. 2008).

To inhibit mature miRNAs, the affinity of antisense sequence is critical. The decoy target should be able to compete with the endogenous miRNA targets. Therefore, four miR-7 binding sites were tandemly inserted in the 3'UTR of a destabilised enhanced GFP (dEGFP) gene to increase the efficacy of sequestration. Ebert et al., speculated that if seven binding sites were inserted in the sponge and all seven targeted endogenous miRNAs, the levels of expression of the sponge would allow inhibition of most miRNAs in most cell types (estimated number at approximately 10^4) (Ebert, Neilson and Sharp 2007). To avoid a risk of saturation and degradation no more than ten binding sites are generally inserted in the sponge vector. The dEGFP is a very unstable protein with a half life of ~2hrs so once translation of new proteins is repressed by the binding of a miRNA to the sponge, there is a rapid drop in cellular fluorescence. The change in dEGFP fluorescence therefore, provides a read-out of miRNA binding to the sponge. To increase the stability of the sponge and avoid RNAi-type cleavage, a bulge region was included at the position 9-11, which is often recognised for degradation by Argonaute 2 (Ebert, Neilson and Sharp 2007). The characteristics of the sponge, which binds to the seed region of a miRNA (positions 2-8), made it a very attractive tool as miRNAs that belong to a same family share a common seed region thus the entire miRNA family

could be inactivated. For the same reasons, the sponge might be more efficient than synthetic antisense oligonucleotides which are known to target one single miRNA with full sequence complementarity. The decoy mRNA would target miRNAs that share common targets so the concomitant phenotypic impact may be accentuated and more effective.

CHO-K1 SEAP and CHO1.14 cells were engineered with a miRNA sponge to target specifically endogenous mature miR-7 (miR-7 sponge) or with a control sponge which consisted instead, of a random sequence inserted in the same cassette. In mixed populations, GFP fluorescence was 20% lower in miR-7 sponge transfected cells suggesting that miRNA sponge was expressed by the cells and recognised endogenous mature miR-7 for sequestration. miR-7 sponge expressing cells showed increased cell density compared to the control sponge transfected cells by 1.45-fold at day 2 and by 1.14-fold at day 3. Cell growth rate was higher at day 2 (0.0577 hr^{-1} versus 0.0492 hr^{-1}) in miR-7 sponge expressing cells, though it was not statistically significant due to high standard deviations. The advantage of cell growth was also confirmed by the statistical significant improvement of both integral viable cell density (IVCD; cell per time per unit volume) and accumulated integral viable cell density (AIVCD). The IVCD is represented by the area under the curve when the concentration of viable cells is plotted against the culture time. The integral of viable cell density is the most frequently used method to compare the average viable cell density among different gene expression systems. The AIVCD is the IVCD accumulated over culture duration. Thus both measurements are good indicators of cell proliferation improvement and the amount of 'work' a culture can perform.

miR-7 sponge expressing cells seemed to have a small advantage on cell survival in the first three days of culture but it was not statistically significant. Cell viability decreased at 72hrs in both control and miR-7 sponge transfected cells, likely due to the nature of the batch-culture. Despite that drop, miR-7 sponge expressing cells maintained higher cell viability compared to the control sponge treated cells in the next two days. Thus the sponge miR-7 might confer an advantage to these cells from being more resistant to cell death.

Using a flow cytometry to sort single cells with high and medium levels of GFP expression, many positive clones were selected for further investigation. By choosing these clones, we eliminated the possibility to select only clones with low GFP

expression in the miR-7 sponge group and clones with high GFP in the control sponge. However, by doing so we also eliminated the possibility of selecting clones with very high copies of the transgene in miR-7 sponge and less importantly, clones from the control sponge group with very low copies of the cassette. The selection of clones with high and medium GFP expression allowed the monitoring of a wide range of clones therefore the elimination of miR-7 sponge expressing clones with low GFP fluorescence was not an issue. In contrast to transient expression, the generation of a stable population could allow us to monitor the impact of miR-7 over a longer period of time, to assess the different parameters we were interested in improving and to change the conditions of culture in order to have more impactful effect.

To validate the preliminary results observed in mixed population, the impact of miR-7 sponge on cell growth was monitored in different culture formats. In CHO-K1 SEAP cells, the median of GFP signal fluorescence of 23 clones cultured in 1ml suspension was also significantly reduced. The median of cell density showed a 1.31-fold increase in miR-7 sponge expressing clones at day 3. This confirmed the preliminary results and suggested that stable miR-7 knockdown is accountable for cell growth increase.

The improvement of cell growth was reproducible in CHO1.14 cells. The median of cell density of 12 clones showed a 2.26-fold increase in miR-7 sponge expressing clones. Thus the impact of miR-7 knockdown on cell proliferation was also conserved in another CHO cell lines. The median of cell viability in both cell lines was slightly lower than in the control expressing cells. As expected with a randomly integrated vector, there was a high variability in GFP expression between the clones. The variation of GFP was likely due to genetic heterogeneity induced by random integration of the vector DNA. As discussed previously, the vector could be integrated in epigenetically regulated regions for instance by methylation or acetylation, leading to chromatin condensation and transcription repression. Although this technique of DNA delivery is an illegitimate integration and we cannot control the site of integration, it has been reported that this homology-independent integration occurs 1000–10,000 times more frequently than targeted integration (Smith 2001). Thus this technique of integration and the selection of GFP positive clones by flow cytometry are favourable to increase the number of positive clones and the choice of clones for selection. It has also been reported that rodent cells can integrate exogenous DNA 30–100 times more than human cells (Colbere-Garapin, et al. 1986, Hoeijmakers, Odijk and Westerveld 1987). This peculiarity is an advantage for recombinant protein production in CHO cells, which

have been used for the past 50 years for their easiness in genetic manipulation (Jayapal, et al. 2007).

However, a random integration can have negative impact on the miRNA sponge inserted downstream of the GFP gene. The transfected gene can undergo mutations, complex rearrangements or form concatamers which can be truncated, deleted or amplified (Wurtele, Little and Chartrand 2003). Despite these drawbacks it has been shown that after homology-independent integration in cell culture, mutations and rearrangements are less frequent after expansion of cells (Merrihew, et al. 2001, Hoglund, Siden and Rohme 1992) and that even if the expression of the sponge is affected and concomitant miRNA inhibition is partial, the impact is still detectable and can result in interesting phenotypes (Ebert and Sharp 2010). Optimising the dose of transfected miRNA sponge may increase the number of integrated and fully functional copies into the genome.

In addition to clonal genetic heterogeneity, CHO cells have been reported to undergo random expression fluctuations leading to phenotypic differences between clones (Pilbrough, Munro and Gray 2009, Ramunas, et al. 2007, Neildez-Nguyen, et al. 2008, Kaern, et al. 2005). In this context, if mRNAs and proteins undergo expression fluctuation due to intrinsic variability then miRNAs may also have their expression changed. It might be that miRNAs are responsible in some part for these fluctuations changes. Most miRNAs regulate their mRNA targets by fine-tuning (rather than switching their expression on or off) through feed-forward and feedback loops thus it is thought that they are involved in promoting homeostasis (Milo, et al. 2002, Hornstein and Shomron 2006). One of the miRNAs particularly studied for its role in this process is miR-7. Lin X and co-workers (Li, et al. 2009) showed that under temperature fluctuation (between 31°C and 18°C), miR-7 is able to buffer specific gene expression and ultimately cell fate in the development of *Drosophila* larvae (Li, et al. 2009). Upon temperature fluctuation in presence of miR-7, there were no changes in expression of two miR-7 targets, Ato and Yan. This latter is a critical factor for the development of insect sensory organs and Ato (atonal) is expressed in precursor cells of proprioceptor and olfactory organs. Under the same conditions, miR-7 mutants showed strong repression of Ato and high expression of Yan leading to development defects. It would be interesting to follow the fluctuation of miR-7 concomitant to fluctuations of GFP and also during the time course of the cell culture in both miR-7 and control sponge

expressing clones to have more insight in its levels of expression in the cells and its role in directing stability during environmental changes.

Scale-up in 5ml suspension and a longer culture period confirmed the improvement in cell growth by 1.35-fold to 1.58-fold in both cell lines. This was significantly different from the control at day 2 and/or day 3 of the culture. Cell growth was maintained until day 4/day 5 then cell viability dropped dramatically. This can be explained by the culture conditions in a batch culture that consists of cells growing in suspension with limited nutrient supply and no replacement of fresh medium (Butler 1987, Newland, et al. 1994). The lack of nutrient and the waste accumulation was caused by the rapid growth of mir-7 sponge expressing clones thus leading to rapid cell density and viability decline. In this culture the variability of GFP expression was also present in both cell lines. The GFP varied between the clones of a same group (control or miR-7 sponge) but also for an individual clone at different time points.

Cell cycle analysis confirmed the fast progression of miR-7 sponge expressing clones through the cell cycle. While control cells were accumulated in S phase (44.05%), miR-7 sponge expressing cells progressed through the cell cycle and showed similar ratio in the different phases of the cell cycle. miR-7 sponge expressing cells were present at 35.04% in G2 phase, in contrast to 16.64% of the controls cells. G2 phase is described as a period of rapid cell growth and protein synthesis which prepares for the segregation of chromosomes in mitosis (Yang, Hitomi and Stacey 2006). In addition, the fact that cells are not accumulated in the G2/M phase which is often used as a DNA damage checkpoint added more confidence that cells proliferate more rapidly when expressing the miR-7 sponge. Using bioinformatics approaches, John A. Foekens and co-workers showed that mir-7 was associated with the G2/M checkpoint in human breast cancer (Foekens, et al. 2008). Transfection with miR-7 induced cell cycle arrest at G_1 and caused a significant decrease in A549 cell numbers and cell viability (Webster, et al. 2009). This was also reported by Jiand and colleagues (Jiang, et al. 2010). However, when using anti-miR-7, cell proliferation and viability were restored and surprisingly there were no changes in the cell cycle. In ovarian cancer cells, following miR-7 up-regulation there was a significant increase in the proportion of cells in G0/G1 and a significant decrease in the proportion of cells in the S and G2/M stages (Shahab, et al. 2012). This is consistent with our findings and indicated that miR-7 may regulate the cell progression through cell cycle to decrease cell growth rate.

Simple batch culture is typically only used as a screening tool in research and development therefore we wanted to measure the performance of these clones in a more realistic fed-batch experiment more in line with what is employed commercially. Although there was still no control over parameters such as pH or dissolved O2, we wanted to see if providing a nutrient feed would improve the conditions of culture and lead to an extended viable period of culture.

Two clones from the control group and two clones from miR-7 sponge expressing CHO-K1 SEAP cells were transferred to shaker flasks in 30ml final volume using a fed-batch mode for 13 days. Fed-batch culture is a simple and reliable method consisting of the addition of nutrients at appropriate concentration (Bibila and Robinson 1995, Xie and Wang 2006). Unlike the batch culture, miR-7 sponge expressing cells had a very similar cell growth profile to control sponge expressing cells in the first six days of culture. Thus the feed extended the period of culture in both groups, keeping the control sponge as healthy as miR-7 sponge clones for six days compared to four in the batch-culture. The impact of stable miR-7 knockdown on cell proliferation was revealed by day 7. Cell density and viability dropped in the control clones whereas miR-7 sponge clones continued their proliferation. Cell density was improved from day 3 and this enhancement was extended until the next ten days. At day 11, cell density was significantly increased by 3.27-fold. The advantage of miR-7 sponge expressing cells was confirmed by the higher cell growth rate, IVCD and accumulated IVCD. Consequently, cell viability was significantly improved from day 8 and increased by 28.9% at later stages of culture. The improvement in miR-7 sponge clone proliferation in association with non-optimal culture conditions for more than six days suggested that depletion of miR-7 may protect cells from environmental stresses or, perhaps, fail to react to them. Thus the role of miR-7 in controlling homeostasis regulation may be conserved in CHO cells.

Besides cell proliferation, we were also interested in improving cell productivity. Using a fed-batch culture, we intended to achieve high volumetric productivity (Li, et al. 2005, Dorka, et al. 2009). Herein, stable miR-7 knockdown had a moderate impact on total productivity. It was enhanced in comparison to one of the control sponge clones but the other control showed higher protein titers. Normalised productivity was not improved in these conditions but it was not negatively impacted. This has also been reported previously by Jadhav and co-workers who transiently overexpressed miR-17 using a shRNA approach and showed that the speed of cell proliferation was increased but there

was no improvement and no negative impact on cell productivity in CHO cells (Jadhav, et al. 2012). On the other hand, they reported a 20% reduction of specific productivity (Q_p) without affecting growth rate upon miR-21-5p overexpression. Recent work from colleagues in our laboratory showed that the final volumetric titre of a product is tightly associated with high cell density, this latter being in some cases more important than the intrinsic productivity rate (Clarke, et al. 2011).

The optimisation of feeding conditions might further prolong the culture period and improve the fed-batch conditions leading to further increase of cell growth rate and cell viability. Although waste accumulation cannot be avoided with this method, it can be minimized by slow feeding and low concentrations of essential components including glucose and glutamine (Butler 2004). Low levels of glucose and glutamine or replacement by other carbon sources prevent lactate and ammonia accumulation by improving oxidation of glucose to CO^2 (Duval, et al. 1992, Altamirano, et al. 2004, Zhou, et al. 2011, De Alwis, et al. 2007).

An attempt to improve productivity using inducible overexpression of miR-7 or at least ceasing down-regulation might be suitable at day 7 when the culture reached high density and viability remained high. The viability may be sustained if the suspected role of miR-7 in imparting robustness appears to be real.

Thus we demonstrated that miR-7 sponge is a powerful tool to extend the longevity of the culture leading to improvement of cell density as well as cell viability in fed-batch culture. Metabolite measurement would add information regarding the role of miR-7 in keeping the culture active and healthy and its impact on other pathways.

7.4.2.3 Validation of the sponge effect

Different methods of validation were conducted to ensure that the improvement in cell growth rate and viability was specific to miR-7 knockdown. The levels of expression of endogenous miR-7 were analysed in control sponge and miR-7 sponge expressing cells in mixed population and single clones. Following transfection of miR-7 sponge, miR-7 levels were only slightly reduced in comparison to its levels in the control sponge in mixed population. Surprisingly, we found that the levels of miR-7 were 5.11-fold higher in the single clones. Endogenous mature miR-7 molecules are single-stranded molecules and could be dissociated from the sponge during the RNA extraction process or during

the reverse transcription (RT) step. The specific miR-7 primer used in the RT might compete with the sponge, which could lose its sequestration capability outside the cellular context, resulting in primer-miR-7 binding and so the level of this miRNA would be detectable. From these results, it is tempting to speculate that miR-7 is not degraded immediately following its sequestration by miR-7 sponge.

Measurement of precursor miR-7 levels indicated that there was no increase of expression thus it was unlikely that the transcription rate of miR-7 caused higher levels of mature miR-7 upon its sequestration. Another possibility is that the sponge may protect miR-7 from degradation leading to accumulation of mature form of miR-7 bound to the sponge transcript and consequently higher levels would be detected upon cell lysis. Recently, Chatterjee and co-workers showed that miRNA turnover is regulated by the exoribonuclease XRN-2, via a new mechanism, known as target-mediated miRNA protection (TMMP) (Chatterjee and Grosshans 2009, Chatterjee, et al. 2011). TMMP may enable miRNA targets to protect their cognate miRNAs against XRN-2 induced degradation therefore leading to mature miRNA accumulation. To test this hypothesis, we investigated the levels of miR-7 in dEGFP depleted cells. Following inhibition of dEGFP, the levels of mature miR-7 detected in miR-7 sponge expressing cells were similar to the levels of miR-7 in control cells. The levels of miR-7 precursor were unchanged between the control and miR-7 sponge expressing clones. Thus an EGFP-specific siRNA not only promoted the degradation of the GFP-sponge transcript but reduced the detectable levels of mature miR-7. This suggests that by binding to the sponge, miR-7 not only is prevented from binding its endogenous mRNA targets but is stabilised and protected from degradation.

The addition of exogenous miR-7 at two different concentrationsm, 30nM and 50nM, induced further repression of GFP expression in miR-7 sponge-expressing clones. If the miR-7 sponge was expressed abundantly enough to sequester additional exogenous miR-7 it would suggest that it was efficiently sequestering all endogenous miR-7. Inhibitor molecules were also added to the culture at 50nM causing a slight derepression of GFP expression for some of the clones. This suggests that inhibitors were competing with miR-7 sponge for endogenous miR-7 binding. Only a slight release of GFP expression was observed likely due to the high level of expression of miR-7 sponge.

Having observed the apparent protection of mature miR-7 while bound to the sponge and the further reduction in GFP fluorescence upon pm-7 transfection we assumed that this must be due to translational repression. This would be in keeping with the initial

sponge design strategy which included a 2 nucleotide mismatch at positions 10-11 to create a bulge in the bound duplex in order to minimise cleavage. In addition, deliberately degrading the sponge via GFP-siRNA treatment returned the detectable level of miR-7 to that of the control, ie reversing the protective phenomenon. Based on these findings one would expect that the sponge transcript levels should therefore remain relatively constant upon pm-7 transfection. However, qPCR revealed a considerable reduction in sponge mRNA after transfection indicating destabilisation/degradation rather than translational repression.

This suggests that very high levels of exogenous pm-7 combined with the multiple (4) binding sites in each sponge transcript might result in destabilisation of the mRNA. It would seem that under normal conditions however, the amount of sponge expressed in the clones was sufficient to 'soak up' endogenous miR-7 without excessive degradation occurring.

7.5 The role and network of miR-7 in CHO cells

Recently there have been several reports on a role for miR-7 in cell proliferation and its deregulation leading to various cancers (Kefas, et al. 2008, Ikeda, et al. 2012, McInnes, et al. 2012, Fang, et al. 2012, McInnes, et al. 2011). Herein, we showed that transfection with miR-7 induced cell growth reduction while maintaining high cell viability. Cell cycle and apoptosis analysis revealed that cells were arrested in G1 phase without exhibiting sign of apoptosis. In cancer cells the epidermal growth factor receptor (EGFR) and the insulin-like growth factor receptor 1 (IGF1-R) signalling, have been reported to be the routes regulated upon miR-7 induction to trigger proliferation inhibition (Chou, et al. 2010, Jiang, et al. 2010, Nieto, et al. 2011, Duex, et al. 2011, Lee, Choi and Kim 2011). However, EGFR signalling is not likely to be the pathway by which miR-7 regulates cell proliferation in CHO cells as these cells do not express EGFR (Shi, et al. 2000). In addition, we found that there was no difference in IGF1-R expression at the mRNA and protein levels following miR-7 transfection in CHO cells. To investigate other possible mechanisms of action by which miR-7 might control cell growth, we used CHO-specific oligonucleotide arrays to profile miR-7 mimic-treated cells. Many of the identified targets, including CylinD1/D3, Cdk1/2, Psme3, Rad52/54l and Skp2 are reported to be involved in cell cycle, DNA repair and are often

deregulated in cancers (Kanaar, et al. 1996, Bretones, et al. 2011, Roessler, et al. 2006, Zhang, et al. 2012a, Malumbres and Barbacid 2009, Shi, et al. 2012). We focused on three targets, Psme3 (REGγ or PA28γ), Rad54L and Skp2, none of which had previously been shown to be directly regulated by miRNAs but were predicted to bind miR-7 through either their 3'UTR (Psme3, Skp2) or coding sequence (Rad54L) and were representative of the cell proliferation and DNA repair pathways (Zhang and Zhang 2008, Kanaar, et al. 1996, Roessler, et al. 2006, Sistrunk, et al. 2011, Fang and Rajewsky 2011, Rajewsky 2011). Although miRNA binding sites in open reading frames are less common than UTR-based sites (Fang and Rajewsky 2011, Rajewsky 2011) the predicted miR-7 target in Rad54L was highly complementary and considered worthy of investigation. A reporter assay indicated a direct interaction between this sequence and miR-7 though the reduction in signal was not as striking as the reduction in endogenous Rad54L mRNA levels observed by qPCR. This may be in part due to the fact that the reporter assay was restricted to only contain this predicted site plus the 3'UTR downstream. There is actually a second predicted miR-7 binding site (in human as well as CHO cells) near the 5' end of the coding sequence which may also contribute to the regulation of the endogenous transcript. In addition, GFP-based reporter assays tend to be more qualitative than quantitative. Unfortunately, there was no suitable antibody available to establish the levels of Rad54L protein in CHO cells in response to miR-7. Both Psme3 and Skp2 were found to be direct targets of miR-7 via their respective 3'UTRs and subsequent individual depletion of these genes using siRNA inhibited cell proliferation, in particular when Skp2 was knocked down. The more modest impact of Psme3 on proliferation might be explained by compensation via redundant proteins in the same family (Masson, Lundgren and Young 2003, Murata, et al. 1999) or possibly the less effective depletion of the target by RNAi.

The role of Skp2 in miR-7-mediated G1/S block was confirmed by the observation that several of its downstream targets were also deregulated including an increase in $p27^{KIP1}$ (a cyclin D inhibitor) and reduced Cks1, Cdk1/2 and CyclinD1/3, all indicative of G1 arrested cell (Kossatz, et al. 2004, Zhang, et al. 1995, Yu, Gervais and Zhang 1998). In addition, the levels of phospho-Akt, another substrate of Skp2, were increased upon miR-7 transfection. Akt is known to play a central role in the regulation of cell proliferation, cell viability and cell cycle arrest in G1 phase by indirect regulation of CyclinD1 inhibition (Brazil, Park and Hemmings 2002, Diehl, et al. 1998). In contrast to our findings, Skp2 knockdown has been shown to impair activation of Akt in

response to ErbB signalling (Chan, et al. 2012, Lin, et al. 2009). However, EGFR is not expressed in CHO cells thus the activation of Akt in the presence of reduced Skp2 must be via another pathway or another member of the EGFR family. c-Myc levels have also been reported to be regulated by Skp2 to promote cell cycle progression at the G1/S transition (Lal, et al. 2009a, Bretones, et al. 2011, Kim, et al. 2003) and in its turn, Myc is able to induce Skp2 transcription (Bretones, et al. 2011). We show that the levels of Myc were dramatically reduced in response to miR-7 upregulation, as would be expected in quiescent cells, and further re-enforcing the down-regulation of Skp2. Interestingly, Myc has been reported to be directly regulated by miR-24 through a seedless recognition element (Lal, et al. 2009a). In the same study, high levels of miR-24 induce cell accumulation in G1 compartment. c-Myc degradation can also be promoted through the recruitment of miR-24 by a ribosomal protein L11 (Challagundla, et al. 2011).

We identified several miRNAs to be down-regulated in miR-7 treated cells, including miR-24, suggesting that miR-7 might co-ordinate several molecular networks in order to mediate a temporary arrest in G1. Furthermore the interaction of Skp2 with DNA replication proteins including ORC1, Cdt1(Mendez, et al. 2002, Li, et al. 2003) and the depletion of other regulators of the S phase including Fen1, cdc6 and the MCM family (MCM2, MCM3, MCM5 and MCM7) would strengthen the blockage of G1/S transition.

In normal cells, arrest in the G1/S phase and the inhibition of the replication machinery can be initiated by Chk1 or Chk2 in response to DNA damage and frequently results in initiation of apoptosis (Sancar, et al. 2004). However, in our study cells treated with miR-7 remained as viable as the control treated cells. Low Psme3 expression would normally be associated with elevated levels of p53, reduced proliferation and induction of apoptosis (Vousden and Prives 2009, Vousden and Lu 2002). Herein, we found p53 levels to be suppressed despite miR-7-dependent reduction in Psme3, cell growth arrest and no apoptosis. Although miR-7 is acting to arrest cell growth, its role may be to simultaneously ensure that the response is not catastrophic (apoptosis) by directly or indirectly targeting p53 for degradation. Phosphorylation of Akt can also impair apoptosis initiation via subsequent inhibition of pro-apoptotic proteins including Bad and Foxo3a. On the other hand, Akt can act in synergy with p53 and c-Myc promote cell survival (Cantley 2002, Datta, Brunet and Greenberg 1999, Alessi, et al. 1996, Alessi and Cohen 1998, Mayo and Donner 2001). Interestingly, Foxo3a promotes Myc

post-transcriptional regulation via miR-34b and miR-34c induction (Kress, et al. 2011). Recently, Foxp3, another member of the Fork-head family of transcription factors, has been reported to induce miR-7, causing suppression of STAB1 by a feed-forward loop (McInnes, et al. 2011). Foxp3 is also known to directly repress Skp2 and c-Myc (Zuo, et al. 2007, Dehan and Pagano 2005, Wang, et al. 2009a). It is induced by p53 following DNA damage contributing to the growth suppressive activity of p53 (Jung, et al. 2010). Thus miR-7 might regulate the knockdown of Skp2 and c-Myc via induction of Fox3p by positive feedback loop (Gottlob, et al. 2001, Kim, Sasaki and Chao 2003, Yamaguchi and Wang 2001). The down-regulation of BCLAF1,a pro-apoptotic factor that induces p53, BAX and triggers downregulation of MDM2 (Sarras, Alizadeh Azami and McPherson 2010), again points toward a co-ordinating role of miR-7 in preventing apoptosis induction. Likewise, the up-regulation of HDAC, a histone deacetylase involved in p53 degradation is in keeping with the observed response (Ito, et al. 2002, Brooks and Gu 2003, Tang, et al. 2008).

In addition, several miRNAs found differentially regulated upon miR-7 transfection, including let-7 family, miR-31, miR-15b~16 cluster, miR-17 and miR-106a may contribute to the regulation of p53. All have predicted binding sites for p53 and are often deregulated in cancer. Most importantly, the let-7 family, miR-17~92 cluster and miR-16 have been previously reported to be repressed by p53 (Saleh, et al. 2011, Suzuki, et al. 2009, Yan, et al. 2009) . Three let-7 family members, let-7b/c/d were found to be down-regulated upon pm-7 transfection which is associated with cell growth arrest. In our screen, we showed that transient up-regulation of let-7e impacted negatively on cell proliferation and viability in three CHO cell lines. In keeping with the protective role of miR-7 against detrimental perturbation, it is probable that miR-7 influences the expression of let-7 family members to overcome major changes in viability and avoid apoptosis induction by negative feedback loop.

The low levels of DNA repair proteins including H_2af, Rad52, Rad54L and Parp1/2 as well as the regulation of H_2afx by miR-24 are likely to strengthen the anti-apoptotic response (Lal, et al. 2009a). Thus we suggest that miR-7 has a dual role which counteracts pro-apoptotic signals and activates anti-apoptotic factors to prevent cells undergoing apoptosis-dependent cell death while simultaneously arresting growth in G1. Therefore in this context, miR-7 seems to act as a rheostat to maintain cellular homeostasis. This is supported by previous reports that demonstrated a role of miR-7 in fine-tuning development-specific genes to avoid major cell perturbation and to maintain

robustness during environmental flux (Aboobaker, et al. 2005, Li, et al. 2009). This is also supported by the fact that the stable knockdown of miR-7 promoted high cell growth and extended viability despite harmful conditions.

7.6 Regulation of cell cycle and proliferation by miRNA network in CHO cells

miRNAs have been reported to target hundreds of genes therefore it follows that some must share common targets (Bartel 2009). In addition, this property would suggest that they should also impact on the expression of other miRNAs – not necessarily by direct interaction but via secondary effects. For example the expression of one miRNA might repress a transcription factor that is involved in activating transcription of another miRNA. To identify downstream members of the miR-7 network, we conducted a miRNA profiling study following pm-7 transfection.

Let-7b, let-7c and let-7d were found to be down-regulated upon miR-7 treatment which is associated with cell growth reduction. However, in our functional validation studies of candidates miRNAs, we showed that the anti-proliferative potential of let-7 family reported in cancers (Roush and Slack 2008), was conserved in CHO cells. Thus impairment of cell proliferation was expected to be associated with up-regulation of these three miRNAs.

Similarly, miR-10a was also found down-regulated in this profiling but in the transient assay, miR-10a knockdown led to increased cell density by 1.8-fold. Despite the established role of miR-29 family in cancers (Pekarsky, et al. 2006), knockdown of miR-29a using inhibitor molecules did not impact on CHO cell proliferation. Upon pm-7 transfection, miR-29a was found up-regulated. It is possible that in the functional study, miR-29a inhibitors were not efficient enough to impact on cell growth or that in CHO cells, miR-29 alone is not sufficient to impact on this phenotype.

miR-21 expression has been correlated with slow growth in CHO cells continuously cultured at 31˚C (Gammell, et al. 2007, Gammell 2007). Upon miR-7 treatment, miR-21 was found to be down-regulated. Similarly, miR-17 was found up-regulated following miR-7 overexpression. miR-17 belongs to the oncogenic miR-17~92 cluster (He, et al. 2005, Volinia, et al. 2010, Hayashita, et al. 2005) and it has been shown to increase cell proliferation following its overexpression in CHO cells (Jadhav, et al. 2012). Taken

together these results suggest that miR-7 exerts a tight regulation on cell proliferation by modulating the expression not only of several important protein-encoding genes but also the expression of let-7 family, miR-10a, miR-21, miR-17 and possibly miR-29a. miR-7 may repress or activate targets which in turn control the regulation of these miRNAs. We could imagine that if these miRNAs were not regulated by feed-forward and/or feed-back loops, cells would stop their growth for a longer period of time eventually leading to cell death. Thus this miRNA profiling study reinforces the hypothesis on the role of miR-7 in robustness.

Conversely, miR-16 and miR-24 were found up-regulated. These two miRNAs have been shown to play critical roles in cell cycle regulation (Lal, et al. 2009a, Liu, et al. 2008). Consistent with our study, miR-16 and miR-24 induced down-regulation of key regulators of the G1/S transition including CCND1, Myc and E2F to arrest cell growth in G1 without inducing apoptosis. Thus miR-16 and miR-24 may cooperate with miR-7 to strengthen the block at the G1/S transition as the well as the avoidance of apoptosis.

From individual studies in miR-7 and miR-23a~27~24-2 cluster, we found common cellular pathways that may be regulated by these miRNAs. Herein, the expression levels of Myc, one of the key nodes involved in cell cycle regulation was strongly down-regulated by miR-24 and by miR-7 induction. Myc has been show to regulate glucose metabolism by promoting glycolysis in transformed cells (Osthus, et al. 2000, Kim, et al. 2004b). We discussed earlier that through the Warbug effect, glucose and glutamine are great sources of energy and provide ATP and NAPDH to promote the formation of new cancer cells (Dang 2012). By targeting Myc via miR-7 and miR-23a in CHO cells, the metabolism of the cells would be further activated thus leading to less accumulated waste and providing new ways to take-up energy and cell proliferation may be increased.

In addition, overexpression of miR-7 led to cell growth arrest in G1 in CHO cells and induction of miR-24 also perturbs the G1 phase in hepatocellular carcinoma cells (Lal, et al. 2009a). Both miRNAs are able to arrest the cell cycle via targeting genes involved in cell cycle and DNA repair, including the CyclinD inhibitor $p27^{kip1}$, CDC2, CDCA7, members of the MCM family, FEN1 and H2AX. This suggests that cell proliferation and cell cycle are regulated through cooperative activities of both miR-7 and miR-24 in CHO cells. Further validation of miR-24 targets would verify this hypothesis. In addition, we showed that the up-regulation of miR-7 was associated with the up-regulation of miR-24 levels leading to knockdown of their common target H2AX.

H2AX is involved in double strand-break response for DNA repair. The up-regulation of miR-24 triggers knockdown of H2AX and induces cell sensitivity to DNA damage in differentiated blood cells (Lal, et al. 2009a). On the other hand, miR-7 up-regulation led to H2AX decrease maybe protect the cells against damage to avoid apoptosis induction thus reinforcing the cellular environment against stress. Analysis of apoptosis would verify the role of miR-24 in apoptosis induction in normal conditions and in miR-7 depleted CHO cells and would give more information on the axis of regulation of apoptosis with these two miRNAs.

7.7 miRNAs as promising targets for CHO cell engineering

The use of single-gene engineering as an approach to improve bioprocess-relevant CHO characteristics has been extensively described and focused in improving cell growth rate, increasing apoptosis resistance and enhancing specific productivity (Kim, Kim and Lee 2012). Some of these studies resulted in successful impact on cell proliferation and/or cell viability maintenance but did not improve cell productivity. E2F-1 overexpression has been reported to increase viable cell density by 20% and prolonged the batch culture for an additional day (Majors, et al. 2008). There was no impact on protein production. In the same manner, c-Myc increased maximal cell density by more than 70% through reduction of cell size as well as a significant decrease in glucose and amino acid consumption rate. Again, there was no improvement of cell productivity (Kuystermans and Al-Rubeai 2009). Up-regulation of bcl-2 expression also increased maximum viable cell by 75% (Tey, et al. 2000). In the same study, cells were growth arrested following addition of thymidine leading to a 40% increase in cell viability compared to the control. Under these conditions, the antibody titers were not enhanced (Tey, et al. 2000). Using RNAi, knockdown of caspase-8 and caspase-9 also increased cell viability by 30% and prolonged the period of high cell viability for 1.5-2 days in batch and fed-batch culture in CHO cells (Yun, et al. 2007).

This is similar to what we observed following stable knockdown of miR-7. Despite the significant increase of cell growth rate and IVCD, normalised productivity was not impacted and total yield was moderate. The overexpression of other regulators involved in apoptosis and cell cycle improved cell viability as well as cell productivity. The overexpression of Bcl-x(L) enhanced cell viability by 20%, antibody titers by 80% and

specific productivities by almost two-fold on scale-up to bioreactors. In addition, cell viability and product titer were further increased when cells were cultured in a chemically defined media without impacting on product quality (Chiang and Sisk 2005). Cyclin-dependent kinase inhibitor p27 expressing CHO cells had their proliferation arrested over a 5-day period and consequently showed a 10-15-fold increase in SEAP specific productivity (Mazur, et al. 1998). The combination of single-gene approach and site-specific integration using zinc-finger nucleases was applied to deletion of BAK and BAX. It proved to be efficient in impairing apoptosis and produced two- to fivefold more IgG than wild-type CHO cells under serum-starvation conditions (Cost, et al. 2010). The addition of sodium butyrate (NaBu) to the culture is an efficient approach to enhance protein expression. However, it causes toxicity leading to cell proliferation inhibition and promotion of apoptosis. Inhibition of caspase-3 using RNAi was reported to successfully enhance apoptosis resistance. Cell culture was extended by more than 2 days and cell viability was increased by 50%. However, the final antibody concentration was not improved (Kim and Lee 2002).

In comparison to the other studies which addressed the improvement of one or two CHO characteristics, Dreesen and co-workers reported the promising potential of mammalian target of rapamycin (mTOR) to simultaneously improve key bioprocess-relevant phenotypes of CHO cells (Dreesen and Fussenegger 2011). Overexpression of mTOR resulted in a twofold increase of viable cell density by increasing cell-cycle progression, improved apoptosis resistance and robustness, increased cell size and protein content, enhanced specific productivity of therapeutic IgG and antibody titers by four-fold (50pg/cell/day).

In contrast to single-gene engineering, miRNA are involved in the regulation of entire networks thus providing the possibility to target entire pathways individually and simultaneously. Yet, there has been only one study on the manipulation of miRNA which reported a modest increase of 15.4% in cell proliferation (Jadhav, et al. 2012).

The overexpression of miRNA from a vector does not require the translational machinery thus does not lead to stress responses (i.e; UPR response) or compete with translation of a trangene. Identification of miRNA targets may increase the discovery of important cellular targets for CHO cell engineering like mTOR which improved simultaneously multiple bioprocess-relevant phenotypes of CHO cells. The simultaneous overexpression or knockdown of multiple miRNAs involved in the same

function can reinforce the impact on this function for instance to improve cell proliferation or to stop cell growth and enhance product titers.

However, the fact that miRNAs regulate hundred of targets can be a major advantage but also a drawback. Manipulating one miRNA to improve a specific function could impact negatively on other pathways. On the other hand, the manipulation of multiple miRNAs involved in different pathways may help to counteract negative impact. In the same manner, using inducible system, multiple miRNAs can be switched on and off at different stages of the cell culture. In the first days of culture, a miRNA capable of increasing cell growth rate would be turned on and at maximum cell density, it would be switched off. At that same time point, another miRNA proven to arrest cell growth would be turned on as well as another miRNA efficient in improving productivity. Although the manipulation of miRNAs as tool to engineer CHO cells in large-scale is still in its infancy, the possibility of simultaneously manipulating several miRNAs at different stages of culture makes miRNAs promising tools to improve all bioprocess-relevant CHO characteristics in a same culture thus reducing the cost and the timeline of protein production.

The accumulation of information from the miR-7 sponge study proved that miRNA as tools to improve CHO characteristics are as efficient as single-gene engineering approaches. The optimisation of culture conditions including medium formulation in a fed-batch, removal of waste accumulation and the control of DNA integration may further improve the potential of miRNAs in enhancing cell proliferation and apoptosis resistance.

CONCLUSIONS

8 Conclusions

8.1 Screening of candidate miRNAs as potential candidates to improve bioprocess-relevant CHO characteristics

- The use of synthetic mimics and inhibitors as tools for functional validation was not convincing due to the lack of reproducibility and inconsistency in the phenotypes observed following transfection.

- We believe that miR-30e-5p, miR-29a, miR-10a and let-7e would be worth further investigation.

- We showed that miR-23b* and miR-409-5p, two miRNA* species were functional and expressed at high levels in CHO cells.

8.2 Investigation of the individual miR-23a~miR-27a~24-2 cluster member potential in improving CHO cell characteristics

- Functional validation assays using mimic and inhibitor molecules indicated that miR-24, miR-23a and miR-27a impacted on growth, viability and/or productivity.

- Simultaneous transient overexpression or knockdown of the miR-23~27a~24-2 cluster members proved to be a relevant approach to investigate the influence of the miR-23~27a~24-2 cluster on CHO characteristics,

- We conclude that 1) the impact of the miR-23~27a~24-2 cluster members on CHO phenotypes appeared to be cooperative, 2) miR-23~27a~24-2 cluster did influence these CHO phenotypes in a substantial manner.

8.3 Generation of CHO cell clones with improved characteristics by stable knockdown of miR-23a~miR-27a~24-2 cluster

- We showed that 1) the 'multi-antisense cluster' was a reliable strategy to simultaneously knockdown clustered miRNAs, 2) the resulting phenotypic impact was significant and reproducible in contrast to synthetic antisense oligonucleotides and 3) the miR-23a~27~24-2 cluster members acted cooperatively to improve cell density by 71% compared to the control. Thus we demonstrated that miR-23a~27~24-2 cluster is a good candidate to improve CHO cell proliferation.

8.4 Investigation of miR-7 potential in improving CHO cell phenotypes

- We demonstrated that the anti-proliferative role of miR-7 was reproducible in serum-free medium in different CHO cell lines.

- Knockdown of miR-7 using synthetic antisense oligonucleotides resulted in little or no impact on proliferation.

- At low density, overexpression of miR-7 levels led to extended viability at later stages of culture. The apparent benefits of increased miR-7 levels to viability were not reproducible at higher densities.

8.5 Generation of CHO cell clones with improved characteristics by stable knockdown of miR-7

- We showed that 1) the ‘miRNAsponge’approach was an effective strategy to deplete the levels of miR-7 in the cells, 2) the resulting phenotypic impact was significant and reproducible in contrast to synthetic antisense oligonucleotides and 3) upon stable knockdown of miR-7, cell growth was successfully improved by 130% as well as cell viability by 45% compared to the control.

- We suggested that knockdown of miR-7 may promote a ‘cancer type-phenotype’ to the cells allowing uncontrolled growth and extended survival.

- We conclude that stable knockdown of miR-7 is a potent strategy to affect global changes in cells and improve bioprocess-relevant CHO characteristics.

8.6 Investigation of the functional role of miR-7 in CHO cells

- We showed that high levels of miR-7 induced cell growth arrest in G1 phase of the cell cycle and did not induce apoptosis.

- Profiling of miR-7 targets using CHO-specific oligonucleotide arrays upon pm-7 transfection and gene ontology analysis indicated a role for miR-7 in G1/S phase of the cell cycle, DNA replication and DNA damage/repair pathways.

- Three representative targets of these pathways, Psme3, Rad54L and Skp2, were validated as direct targets of miR-7. The validation of other key regulators of the G1 to S phase transition, including $p27^{KIP}$ and Myc as well as critical apoptotic regulators such as p53 and p-Akt confirmed the role of miR-7 in the regulation of cell proliferation and apoptosis.

- A miRNA profiling using TaMan Low Density arrays upon overexpression of miR-7 indicated that miR-7 exerts a tight regulation on cell proliferation and apoptosis by modulating the expression of not only protein-encoding genes but also other miRNAs in a complex regulatory network.

- Finally we speculated that the phenotypes observed upon overexpression of miR-7- cell growth arrest and apoptosis avoidance- might mimic the response caused by environment stress. On the other hand, depletion of miR-7 may prevent a stress response and induce uncontrolled proliferation of cells. Thus we conclude that miR-7 acts as a sensor to control homeostasis regulation in CHO cells.

FUTURE WORK

9 Future work

9.1 Screening of candidate miRNAs as potential candidates to improve bioprocess-relevant CHO characteristics

- The use of synthetic molecules in the manipulation of miR-30e-5p miR-29a, miR-10a and let-7e expression suggested a possible impact on cell proliferation, cell survival and protein production/secretion. Future work would include the functional validation of transient overexpression and knockdown of miRNAs using a shRNA vector instead of synthetic molecules. The use of shRNA might help to control the amount of exogenous molecules to minimise off-target effects due to RNAi machinery saturation.

- Few miRNA* species have been shown to be functional and little has been reported on their role and their regulation. It would be interesting to pursue the investigation of miR-23b* in a functional validation using a shRNA vector for overexpression as well as the combined impact of miR-23b* and miR-23b.

9.2 Generation of CHO cell clones with improved characteristics by stable knockdown of miR-23a~miR-27a~24-2 cluster

- We demonstrated that the ‘multi-antisense cluster’ was a reliable strategy to simultaneously knockdown miR-23a~27~24-2 cluster members and also that miR-23a~27~24-2 cluster was a good candidate to improve CHO cell proliferation at later stages of a batch culture. Further validation would include the stable expression of the multi-antisense cluster in a fed-batch culture to assess cell proliferation, viability, total yield as well as normalised productivity.

9.3 Investigation of the functional role of miR-23a~27~24-2 cluster in CHO cells

- The identification of miR-24, miR-23a and miR-27a targets could be investigated using CHO-specific oligonucleotide arrays following stable knockdown of the miR-23a~27~24-2 cluster members and validation would involve qPCR, western blotting and siRNA transfection.

9.4 Generation of CHO cell clones with improved characteristics by stable manipulation of miR-7

- We showed that stable depletion of miR-7 is a potent tool to improve cell proliferation and extent viability in CHO-K1 SEAP cells. To validate these findings, future work would include the fed-batch culture of a human recombinant IgG1-secreting cell line using CHO1.14 cells that are stably engineered to knockdown miR-7.

- It would be interesting to take measurement of metabolites including glucose/glutamine to assess nutrients consumption and lactate/ammonia to monitor waste accumulation in these cultures in both the control and miR-7 sponge expressing clones.

- Larger scale-culture in 2L bioreactors may help to confirm the promising possibility of using miR-7 in large-scale culture in biopharmaceutical production.

9.5 Investigation of the network of factors involved in miR-7-dependent regulation of cell proliferation, cell cycle and DNA repair

- To further investigate miR-7 network and its interactions, future work would involve the validation of Rad54L at the protein levels.

- To validate the role of miR-7 in apoptosis resistance, it would be interesting to induce apoptosis in normal condition culture, in miR-7-depleted cells and in miR-7-overexpressing cells.

- To validate the impact of miR-7 overexpression on let-7 family, miR-31, miR-21, miR-24, miR-15b~16 cluster, miR-17~92 cluster and its paralog mir-106a-363, future work would involve to repeat the TLDA array study combined with functional validation assays.

- miR-7 and miR-24 may cooperate tightly to regulate similar cellular pathways in CHO cells including cell cycle, cell proliferation and apoptosis. Cell proliferation, cell cycle and apoptosis assays following simultaneous transient knockdown of miR-7 and miR-24 expression would add information on this statement.

10 Bibliography

Aboobaker, A.A., Tomancak, P., Patel, N., Rubin, G.M. and Lai, E.C. 2005. Drosophila microRNAs exhibit diverse spatial expression patterns during embryonic development. *Proceedings of the National Academy of Sciences of the United States of America,* 102(50), pp.18017-18022.

Abston, L.R. and Miller, W.M. 2005. Effects of NHE1 expression level on CHO cell responses to environmental stress. *Biotechnology Progress,* 21(2), pp.562-567.

Afonina, I., Zivarts, M., Kutyavin, I., Lukhtanov, E., Gamper, H. and Meyer, R.B. 1997. Efficient priming of PCR with short oligonucleotides conjugated to a minor groove binder. *Nucleic Acids Research,* 25(13), pp.2657-2660.

Alessi, D.R., Caudwell, F.B., Andjelkovic, M., Hemmings, B.A. and Cohen, P. 1996. Molecular basis for the substrate specificity of protein kinase B; comparison with MAPKAP kinase-1 and p70 S6 kinase. *FEBS Letters,* 399(3), pp.333-338.

Alessi, D.R. and Cohen, P. 1998. Mechanism of activation and function of protein kinase B. *Current Opinion in Genetics & Development,* 8(1), pp.55-62.

Alexiou, P., Maragkakis, M., Papadopoulos, G.L., Reczko, M. and Hatzigeorgiou, A.G. 2009. Lost in translation: an assessment and perspective for computational microRNA target identification. *Bioinformatics,* 25(23), pp.3049-3055.

Al-Fageeh, M.B., Marchant, R.J., Carden, M.J. and Smales, C.M. 2006. The cold-shock response in cultured mammalian cells: Harnessing the response for the improvement of recombinant protein production. *Biotechnology and Bioengineering,* 93(5), pp.829-835.

Alon, U. 2007. Network motifs: theory and experimental approaches. *Nature Reviews.Genetics,* 8(6), pp.450-461.

Altamirano, C., Paredes, C., Illanes, A., Cairo, J.J. and Godia, F. 2004. Strategies for fed-batch cultivation of t-PA producing CHO cells: substitution of glucose and

glutamine and rational design of culture medium. *Journal of Biotechnology,* 110(2), pp.171-179.

Altuvia, Y., Landgraf, P., Lithwick, G., Elefant, N., Pfeffer, S., Aravin, A., Brownstein, M.J., Tuschl, T. and Margalit, H. 2005. Clustering and conservation patterns of human microRNAs. *Nucleic Acids Research,* 33(8), pp.2697-2706.

Aravin, A.A., Hannon, G.J. and Brennecke, J. 2007. The Piwi-piRNA pathway provides an adaptive defense in the transposon arms race. *Science (New York, N.Y.),* 318(5851), pp.761-764.

Aravin, A.A., Lagos-Quintana, M., Yalcin, A., Zavolan, M., Marks, D., Snyder, B., Gaasterland, T., Meyer, J. and Tuschl, T. 2003. The small RNA profile during Drosophila melanogaster development. *Developmental Cell,* 5(2), pp.337-350.

Arden, N. and Betenbaugh, M.J. 2004. Life and death in mammalian cell culture: strategies for apoptosis inhibition. *Trends in Biotechnology,* 22(4), pp.174-180.

Arden, N., Majors, B.S., Ahn, S.H., Oyler, G. and Betenbaugh, M.J. 2007. Inhibiting the apoptosis pathway using MDM2 in mammalian cell cultures. *Biotechnology and Bioengineering,* 97(3), pp.601-614.

Baek, D., Villen, J., Shin, C., Camargo, F.D., Gygi, S.P. and Bartel, D.P. 2008. The impact of microRNAs on protein output. *Nature,* 455(7209), pp.64-U38.

Bagge, A., Clausen, T.R., Larsen, S., Ladefoged, M., Rosenstierne, M.W., Larsen, L., Vang, O., Nielsen, J.H. and Dalgaard, L.T. 2012. MicroRNA-29a is up-regulated in beta-cells by glucose and decreases glucose-stimulated insulin secretion. *Biochemical and Biophysical Research Communications,* 426(2), pp.266-272.

Bahr, S.M., Borgschulte, T., Kayser, K.J. and Lin, N. 2009. Using microarray technology to select housekeeping genes in Chinese hamster ovary cells. *Biotechnology and Bioengineering,* 104(5), pp.1041-1046.

Barad, O., Meiri, E., Avniel, A., Aharonov, R., Barzilai, A., Bentwich, I., Einav, U., Gilad, S., Hurban, P., Karov, Y., Lobenhofer, E.K., Sharon, E., Shiboleth, Y.M., Shtutman, M., Bentwich, Z. and Einat, P. 2004. MicroRNA expression detected by

oligonucleotide microarrays: system establishment and expression profiling in human tissues. *Genome Research,* 14(12), pp.2486-2494.

Barron, N., Kumar, N., Sanchez, N., Doolan, P., Clarke, C., Meleady, P., O'Sullivan, F. and Clynes, M. 2011. Engineering CHO cell growth and recombinant protein productivity by overexpression of miR-7. *Journal of Biotechnology,* 151(2), pp.204-211.

Bartel, D.P. 2009. MicroRNAs: Target Recognition and Regulatory Functions. *Cell,* 136(2), pp.215-233.

Bartel, D.P. 2004. MicroRNAs: genomics, biogenesis, mechanism, and function. *Cell,* 116(2), pp.281-297.

Bashirullah, A., Pasquinelli, A.E., Kiger, A.A., Perrimon, N., Ruvkun, G. and Thummel, C.S. 2003. Coordinate regulation of small temporal RNAs at the onset of Drosophila metamorphosis. *Developmental Biology,* 259(1), pp.1-8.

Baskerville, S. and Bartel, D.P. 2005. Microarray profiling of microRNAs reveals frequent coexpression with neighboring miRNAs and host genes. *RNA (New York, N.Y.),* 11(3), pp.241-247.

Bauer, M., Kinkl, N., Meixner, A., Kremmer, E., Riemenschneider, M., Forstl, H., Gasser, T. and Ueffing, M. 2009. Prevention of interferon-stimulated gene expression using microRNA-designed hairpins. *Gene Therapy,* 16(1), pp.142-147.

Behm-Ansmant, I., Rehwinkel, J., Doerks, T., Stark, A., Bork, P. and Izaurralde, E. 2006. MRNA degradation by miRNAs and GW182 requires both CCR4 : NOT deadenylase and DCP1 : DCP2 decapping complexes. *Genes & Development,* 20(14), pp.1885-1898.

Benton, T., Chen, T., McEntee, M., Fox, B., King, D., Crombie, R., Thomas, T.C. and Bebbington, C. 2002. The use of UCOE vectors in combination with a preadapted serum free, suspension cell line allows for rapid production of large quantities of protein. *Cytotechnology,* 38(1-3), pp.43-46.

Bentwich, I. 2005. Prediction and validation of microRNAs and their targets. *FEBS Letters*, 579(26), pp.5904-5910.

Berezikov, E., Chung, W.J., Willis, J., Cuppen, E. and Lai, E.C. 2007. Mammalian mirtron genes. *Molecular Cell,* 28(2), pp.328-336.

Berezikov, E., Guryev, V., van de Belt, J., Wienholds, E., Plasterk, R.H. and Cuppen, E. 2005. Phylogenetic shadowing and computational identification of human microRNA genes. *Cell*, 120(1), pp.21-24.

Berger, J., Hauber, J., Hauber, R., Geiger, R. and Cullen, B.R. 1988. Secreted placental alkaline phosphatase: a powerful new quantitative indicator of gene expression in eukaryotic cells. *Gene,* 66(1), pp.1-10.

Betel, D., Wilson, M., Gabow, A., Marks, D.S. and Sander, C. 2008. The microRNA.org resource: targets and expression. *Nucleic Acids Research*, 36(Database issue), pp.D149-53.

Bibila, T.A., Ranucci, C.S., Glazomitsky, K., Buckland, B.C. and Aunins, J.G. 1994. Monoclonal antibody process development using medium concentrates. *Biotechnology Progress*, 10(1), pp.87-96.

Bibila, T.A. and Robinson, D.K. 1995. In pursuit of the optimal fed-batch process for monoclonal antibody production. *Biotechnology Progress,* 11(1), pp.1-13.

Blow, M.J., Grocock, R.J., van Dongen, S., Enright, A.J., Dicks, E., Futreal, P.A., Wooster, R. and Stratton, M.R. 2006. RNA editing of human microRNAs. *Genome Biology*, 7(4),

Bochman, M.L. and Schwacha, A. 2009. The Mcm complex: unwinding the mechanism of a replicative helicase. *Microbiology and Molecular Biology Reviews : MMBR*, 73(4), pp.652-683.

Boden, D., Pusch, O., Silbermann, R., Lee, F., Tucker, L. and Ramratnam, B. 2004. Enhanced gene silencing of HIV-1 specific siRNA using microRNA designed hairpins. *Nucleic Acids Research,* 32(3), pp.1154-1158.

Bolisetty, M.T., Dy, G., Tam, W. and Beemon, K.L. 2009. Reticuloendotheliosis virus strain T induces miR-155, which targets JARID2 and promotes cell survival. *Journal of Virology,* 83(23), pp.12009-12017.

Bonci, D., Coppola, V., Musumeci, M., Addario, A., Giuffrida, R., Memeo, L., D'Urso, L., Pagliuca, A., Biffoni, M., Labbaye, C., Bartucci, M., Muto, G., Peschle, C. and De Maria, R. 2008. The miR-15a-miR-16-1 cluster controls prostate cancer by targeting multiple oncogenic activities. *Nature Medicine,* 14(11), pp.1271-1277.

Borchert, G.M., Lanier, W. and Davidson, B.L. 2006. RNA polymerase III transcribes human microRNAs. *Nature Structural & Molecular Biology,* 13(12), pp.1097-1101.

Borel, C. and Antonarakis, S.E. 2008. Functional genetic variation of human miRNAs and phenotypic consequences. *Mammalian Genome,* 19(7-8), pp.503-509.

Borth, N., Mattanovich, D., Kunert, R. and Katinger, H. 2005. Effect of increased expression of protein disulfide isomerase and heavy chain binding protein on antibody secretion in a recombinant CHO cell line. *Biotechnology Progress,* 21(1), pp.106-111.

Borys, M.C., Linzer, D.I. and Papoutsakis, E.T. 1993. Culture pH affects expression rates and glycosylation of recombinant mouse placental lactogen proteins by Chinese hamster ovary (CHO) cells. *Bio/technology (Nature Publishing Company),* 11(6), pp.720-724.

Boyer, L.A., Lee, T.I., Cole, M.F., Johnstone, S.E., Levine, S.S., Zucker, J.P., Guenther, M.G., Kumar, R.M., Murray, H.L., Jenner, R.G., Gifford, D.K., Melton, D.A., Jaenisch, R. and Young, R.A. 2005. Core transcriptional regulatory circuitry in human embryonic stem cells. *Cell,* 122(6), pp.947-956.

Boyerinas, B., Park, S.M., Hau, A., Murmann, A.E. and Peter, M.E. 2010. The role of let-7 in cell differentiation and cancer. *Endocrine-Related Cancer,* 17(1), pp.F19-36.

Bravo-Egana, V., Rosero, S., Molano, R.D., Pileggi, A., Ricordi, C., Dominguez-Bendala, J. and Pastori, R.L. 2008. Quantitative differential expression analysis reveals miR-7 as major islet microRNA. *Biochemical and Biophysical Research Communications,* 366(4), pp.922-926.

Brazil, D.P., Park, J. and Hemmings, B.A. 2002. PKB binding proteins. Getting in on the Akt. *Cell,* 111(3), pp.293-303.

Bretones, G., Acosta, J.C., Caraballo, J.M., Ferrandiz, N., Gomez-Casares, M.T., Albajar, M., Blanco, R., Ruiz, P., Hung, W.C., Albero, M.P., Perez-Roger, I. and Leon, J. 2011. SKP2 oncogene is a direct MYC target gene and MYC down-regulates p27(KIP1) through SKP2 in human leukemia cells. *The Journal of Biological Chemistry,* 286(11), pp.9815-9825.

Brooks, C.L. and Gu, W. 2003. Ubiquitination, phosphorylation and acetylation: the molecular basis for p53 regulation. *Current Opinion in Cell Biology,* 15(2), pp.164-171.

Brown, B.D. and Naldini, L. 2009. INNOVATION Exploiting and antagonizing microRNA regulation for therapeutic and experimental applications. *Nature Reviews Genetics,* 10(8), pp.578-585.

Brown, K.M., Chu, C.Y. and Rana, T.M. 2005. Target accessibility dictates the potency of human RISC. *Nature Structural & Molecular Biology,* 12(5), pp.469-470.

Brueckner, B., Stresemann, C., Kuner, R., Mund, C., Musch, T., Meister, M., Sultmann, H. and Lyko, F. 2007. The human let-7a-3 locus contains an epigenetically regulated microRNA gene with oncogenic function. *Cancer Research,* 67(4), pp.1419-1423.

Buck, A.H., Perot, J., Chisholm, M.A., Kumar, D.S., Tuddenham, L., Cognat, V., Marcinowski, L., Doelken, L. and Pfeffer, S. 2010. Post-transcriptional regulation of miR-27 in murine cytomegalovirus infection. *Rna-a Publication of the Rna Society,* 16(2), pp.307-315.

Butler, M. 2006. Optimisation of the cellular metabolism of glycosylation for recombinant proteins produced by Mammalian cell systems. *Cytotechnology,* 50(1-3), pp.57-76.

Butler, M. 2005. Animal cell cultures: recent achievements and perspectives in the production of biopharmaceuticals. *Applied Microbiology and Biotechnology,* 68(3), pp.283-291.

Butler, M. 1987. Growth limitations in microcarrier cultures. *Advances in Biochemical Engineering/Biotechnology*, 34pp.57-84.

Butler, M. 1985. Growth limitations in high density microcarrier cultures. *Developments in Biological Standardization,* 60pp.269-280.

Butler, M., Imamura, T., Thomas, J. and Thilly, W.G. 1983. High yields from microcarrier cultures by medium perfusion. *Journal of Cell Science,* 61pp.351-363.

Cannell, I.G. and Bushell, M. 2010. Regulation of Myc by miR-34c: A mechanism to prevent genomic instability? *Cell Cycle (Georgetown, Tex.),* 9(14), pp.2726-2730.

Cantley, L.C. 2002. The phosphoinositide 3-kinase pathway. *Science (New York, N.Y.),* 296(5573), pp.1655-1657.

Cascon, A. and Robledo, M. 2012. MAX and MYC: a heritable breakup. *Cancer Research,* 72(13), pp.3119-3124.

Chakrabarti, A., Chen, A.W. and Varner, J.D. 2011. A review of the mammalian unfolded protein response. *Biotechnology and Bioengineering,* 108(12), pp.2777-2793.

Challagundla, K.B., Sun, X.X., Zhang, X., DeVine, T., Zhang, Q., Sears, R.C. and Dai, M.S. 2011. Ribosomal protein L11 recruits miR-24/miRISC to repress c-Myc expression in response to ribosomal stress. *Molecular and Cellular Biology,* 31(19), pp.4007-4021.

Chan, C.H., Li, C.F., Yang, W.L., Gao, Y., Lee, S.W., Feng, Z., Huang, H.Y., Tsai, K.K., Flores, L.G., Shao, Y., Hazle, J.D., Yu, D., Wei, W., Sarbassov, D., Hung, M.C., Nakayama, K.I. and Lin, H.K. 2012. The Skp2-SCF E3 ligase regulates Akt ubiquitination, glycolysis, herceptin sensitivity, and tumorigenesis. *Cell,* 149(5), pp.1098-1111.

Chan, J.A., Krichevsky, A.M. and Kosik, K.S. 2005. MicroRNA-21 is an antiapoptotic factor in human glioblastoma cells. *Cancer Research,* 65(14), pp.6029-6033.

Chang, J., Hsu, Y., Kuo, P., Kuo, Y., Chiang, L. and Lin, C. 2005. Increase of Bax/ Bcl-XL ratio and arrest of cell cycle by luteolin in immortalized human hepatoma cell line. *Life Sciences,* 76(16), pp.1883-1893.

Chang, S., Johnston, R.J., Frokjaer-Jensen, C., Lockery, S. and Hobert, O. 2004. MicroRNAs act sequentially and asymmetrically to control chemosensory laterality in the nematode. *Nature,* 430(7001), pp.785-789.

Chang, T.C., Zeitels, L.R., Hwang, H.W., Chivukula, R.R., Wentzel, E.A., Dews, M., Jung, J., Gao, P., Dang, C.V., Beer, M.A., Thomas-Tikhonenko, A. and Mendell, J.T. 2009. Lin-28B transactivation is necessary for Myc-mediated let-7 repression and proliferation. *Proceedings of the National Academy of Sciences of the United States of America,* 106(9), pp.3384-3389.

Chatterjee, S., Fasler, M., Bussing, I. and Grosshans, H. 2011. Target-mediated protection of endogenous microRNAs in C. elegans. *Developmental Cell,* 20(3), pp.388-396.

Chatterjee, S. and Grosshans, H. 2009. Active turnover modulates mature microRNA activity in Caenorhabditis elegans. *Nature,* 461(7263), pp.546-U120.

Chaudhuri, K. and Chatterjee, R. 2007. MicroRNA detection and target prediction: Integration of computational and experimental approaches. *DNA and Cell Biology,* 26(5), pp.321-337.

Cheloufi, S., Dos Santos, C.O., Chong, M.M.W. and Hannon, G.J. 2010. A Dicer-independent miRNA biogenesis pathway that requires Ago catalysis. *Nature,* 465(7298), pp.584-U76.

Chen, C., Ridzon, D.A., Broomer, A.J., Zhou, Z., Lee, D.H., Nguyen, J.T., Barbisin, M., Xu, N.L., Mahuvakar, V.R., Andersen, M.R., Lao, K.Q., Livak, K.J. and Guegler, K.J. 2005. Real-time quantification of microRNAs by stem-loop RT-PCR. *Nucleic Acids Research,* 33(20), pp.e179.

Chendrimada, T.P., Gregory, R.I., Kumaraswamy, E., Norman, J., Cooch, N., Nishikura, K. and Shiekhattar, R. 2005. TRBP recruits the Dicer complex to Ago2 for microRNA processing and gene silencing. *Nature,* 436(7051), pp.740-744.

Cheng, A.M., Byrom, M.W., Shelton, J. and Ford, L.P. 2005. Antisense inhibition of human miRNAs and indications for an involvement of miRNA in cell growth and apoptosis. *Nucleic Acids Research,* 33(4), pp.1290-1297.

Chhabra, R., Adlakha, Y.K., Hariharan, M., Scaria, V. and Saini, N. 2009. Upregulation of miR-23a-27a-24-2 cluster induces caspase-dependent and -independent apoptosis in human embryonic kidney cells. *PloS One,* 4(6), pp.e5848.

Chhabra, R., Dubey, R. and Saini, N. 2011. Gene expression profiling indicate role of ER stress in miR-23a~27a~24-2 cluster induced apoptosis in HEK293T cells. *RNA Biology,* 8(4), pp.648-664.

Chhabra, R., Dubey, R. and Saini, N. 2010. Cooperative and individualistic functions of the microRNAs in the miR-23a~27a~24-2 cluster and its implication in human diseases. *Molecular Cancer,* 9pp.232.

Chi, S.W., Zang, J.B., Mele, A. and Darnell, R.B. 2009. Argonaute HITS-CLIP decodes microRNA-mRNA interaction maps. *Nature,* 460(7254), pp.479-486.

Chiang, G.G. and Sisk, W.P. 2005. Bcl-x(L) mediates increased production of humanized monoclonal antibodies in Chinese hamster ovary cells. *Biotechnology and Bioengineering,* 91(7), pp.779-792.

Chiang, H.R., Schoenfeld, L.W., Ruby, J.G., Auyeung, V.C., Spies, N., Baek, D., Johnston, W.K., Russ, C., Luo, S., Babiarz, J.E., Blelloch, R., Schroth, G.P., Nusbaum, C. and Bartel, D.P. 2010. Mammalian microRNAs: experimental evaluation of novel and previously annotated genes. *Genes & Development,* 24(10), pp.992-1009.

Chivukula, R.R. and Mendell, J.T. 2008. Circular reasoning: microRNAs and cell-cycle control. *Trends in Biochemical Sciences,* 33(10), pp.474-481.

Choi, S.S., Rhee, W.J., Kim, E.J. and Park, T.H. 2006. Enhancement of recombinant protein production in chinese hamster ovary cells through anti-apoptosis engineering using 30Kc6 gene. *Biotechnology and Bioengineering,* 95(3), pp.459-467.

Chou, Y.T., Lin, H.H., Lien, Y.C., Wang, Y.H., Hong, C.F., Kao, Y.R., Lin, S.C., Chang, Y.C., Lin, S.Y., Chen, S.J., Chen, H.C., Yeh, S.D. and Wu, C.W. 2010. EGFR promotes lung tumorigenesis by activating miR-7 through a Ras/ERK/Myc pathway that targets the Ets2 transcriptional repressor ERF. *Cancer Research,* 70(21), pp.8822-8831.

Cifuentes, D., Xue, H., Taylor, D.W., Patnode, H., Mishima, Y., Cheloufi, S., Ma, E., Mane, S., Hannon, G.J., Lawson, N.D., Wolfe, S.A. and Giraldez, A.J. 2010. A novel miRNA processing pathway independent of Dicer requires Argonaute2 catalytic activity. *Science (New York, N.Y.),* 328(5986), pp.1694-1698.

Clarke, C., Doolan, P., Barron, N., Meleady, P., O'Sullivan, F., Gammell, P., Melville, M., Leonard, M. and Clynes, M. 2011. Predicting cell-specific productivity from CHO gene expression. *Journal of Biotechnology*, 151(2), pp.159-165.

Clarke, C., Henry, M., Doolan, P., Kelly, S., Aherne, S., Sanchez, N., Kelly, P., Kinsella, P., Breen, L., Madden, S.F., Zhang, L., Leonard, M., Clynes, M., Meleady, P. and Barron, N. 2012. Integrated miRNA, mRNA and protein expression analysis reveals the role of post-transcriptional regulation in controlling CHO cell growth rate. *BMC Genomics,* 13(1), pp.656.

Cohen, S.N., Chang, A.C., Boyer, H.W. and Helling, R.B. 1973. Construction of biologically functional bacterial plasmids in vitro. *Proceedings of the National Academy of Sciences of the United States of America,* 70(11), pp.3240-3244.

Colbere-Garapin, F., Ryhiner, M.L., Stephany, I., Kourilsky, P. and Garapin, A.C. 1986. Patterns of integration of exogenous DNA sequences transfected into mammalian cells of primate and rodent origin. *Gene,* 50(1-3), pp.279-288.

Corcoran, D.L., Pandit, K.V., Gordon, B., Bhattacharjee, A., Kaminski, N. and Benos, P.V. 2009. Features of mammalian microRNA promoters emerge from polymerase II chromatin immunoprecipitation data. *PloS One*, 4(4), pp.e5279.

Correa-Medina, M., Bravo-Egana, V., Rosero, S., Ricordi, C., Edlund, H., Diez, J. and Pastori, R.L. 2009. MicroRNA miR-7 is preferentially expressed in endocrine cells of the developing and adult human pancreas. *Gene Expression Patterns : GEP*, 9(4), pp.193-199.

Cost, G.J., Freyvert, Y., Vafiadis, A., Santiago, Y., Miller, J.C., Rebar, E., Collingwood, T.N., Snowden, A. and Gregory, P.D. 2010. BAK and BAX deletion using zinc-finger nucleases yields apoptosis-resistant CHO cells. *Biotechnology and Bioengineering*, 105(2), pp.330-340.

Crea, F., Sarti, D., Falciani, F. and Al-Rubeai, M. 2006. Over-expression of hTERT in CHO K1 results in decreased apoptosis and reduced serum dependency. *Journal of Biotechnology*, 121(2), pp.109-123.

Cudna, R.E. and Dickson, A.J. 2003. Endoplasmic reticulum signaling as a determinant of recombinant protein expression. *Biotechnology and Bioengineering*, 81(1), pp.56-65.

Cullen, B.R. 2006. Induction of stable RNA interference in mammalian cells. *Gene Therapy*, 13(6), pp.503-508.

Czech, B., Zhou, R., Erlich, Y., Brennecke, J., Binari, R., Villalta, C., Gordon, A., Perrimon, N. and Hannon, G.J. 2009. Hierarchical rules for Argonaute loading in Drosophila. *Molecular Cell*, 36(3), pp.445-456.

Dang, C.V. 2012. MYC on the path to cancer. *Cell*, 149(1), pp.22-35.

Dang, C.V. 2010. Rethinking the Warburg effect with Myc micromanaging glutamine metabolism. *Cancer Research*, 70(3), pp.859-862.

Dang, C.V. 1999. c-Myc target genes involved in cell growth, apoptosis, and metabolism. *Molecular and Cellular Biology*, 19(1), pp.1-11.

Danial, N.N. and Korsmeyer, S.J. 2004. Cell death: critical control points. *Cell*, 116(2), pp.205-219.

Datta, S.R., Brunet, A. and Greenberg, M.E. 1999. Cellular survival: a play in three Akts. *Genes & Development*, 13(22), pp.2905-2927.

Davies, J., Jiang, L., Pan, L.Z., LaBarre, M.J., Anderson, D. and Reff, M. 2001. Expression of GnTIII in a recombinant anti-CD20 CHO production cell line: Expression of antibodies with altered glycoforms leads to an increase in ADCC through higher affinity for FC gamma RIII. *Biotechnology and Bioengineering,* 74(4), pp.288-294.

Davis, R., Schooley, K., Rasmussen, B., Thomas, J. and Reddy, P. 2000. Effect of PDI overexpression on recombinant protein secretion in CHO cells. *Biotechnology Progress,* 16(5), pp.736-743.

Davis, S., Lollo, B., Freier, S. and Esau, C. 2006. Improved targeting of miRNA with antisense oligonucleotides. *Nucleic Acids Research,* 34(8), pp.2294-2304.

De Alwis, D.M., Dutton, R.L., Scharer, J. and Moo-Young, M. 2007. Statistical methods in media optimization for batch and fed-batch animal cell culture. *Bioprocess and Biosystems Engineering,* 30(2), pp.107-113.

Dehan, E. and Pagano, M. 2005. Skp2, the FoxO1 hunter. *Cancer Cell,* 7(3), pp.209-210.

D'Errico, I., Gadaleta, G. and Saccone, C. 2004. Pseudogenes in metazoa: origin and features. *Briefings in Functional Genomics & Proteomics,* 3(2), pp.157-167.

Desjobert, C., Renalier, M.H., Bergalet, J., Dejean, E., Joseph, N., Kruczynski, A., Soulier, J., Espinos, E., Meggetto, F., Cavaille, J., Delsol, G. and Lamant, L. 2011. MiR-29a down-regulation in ALK-positive anaplastic large cell lymphomas contributes to apoptosis blockade through MCL-1 overexpression. *Blood,* 117(24), pp.6627-6637.

Diehl, J.A., Cheng, M., Roussel, M.F. and Sherr, C.J. 1998. Glycogen synthase kinase-3beta regulates cyclin D1 proteolysis and subcellular localization. *Genes & Development,* 12(22), pp.3499-3511.

Ding, X.C., Weiler, J. and Grosshans, H. 2009. Regulating the regulators: mechanisms controlling the maturation of microRNAs. *Trends in Biotechnology,* 27(1), pp.27-36.

Doe, M.R., Ascano, J.M., Kaur, M. and Cole, M.D. 2012. Myc posttranscriptionally induces HIF1 protein and target gene expression in normal and cancer cells. *Cancer Research,* 72(4), pp.949-957.

Doench, J.G., Petersen, C.P. and Sharp, P.A. 2003. siRNAs can function as miRNAs. *Genes & Development,* 17(4), pp.438-442.

Doench, J.G. and Sharp, P.A. 2004. Specificity of microRNA target selection in translational repression. *Genes & Development,* 18(5), pp.504-511.

Doolan, P., Meleady, P., Barron, N., Henry, M., Gallagher, R., Gammell, P., Melville, M., Sinacore, M., McCarthy, K., Leonard, M., Charlebois, T. and Clynes, M. 2010. Microarray and Proteomics Expression Profiling Identifies Several Candidates, Including the Valosin-Containing Protein (VCP), Involved in Regulating High Cellular Growth Rate in Production CHO Cell Lines. *Biotechnology and Bioengineering,* 106(1), pp.42-56.

Dorka, P., Fischer, C., Budman, H. and Scharer, J.M. 2009. Metabolic flux-based modeling of mAb production during batch and fed-batch operations. *Bioprocess and Biosystems Engineering,* 32(2), pp.183-196.

Dreesen, I.A. and Fussenegger, M. 2011. Ectopic expression of human mTOR increases viability, robustness, cell size, proliferation, and antibody production of chinese hamster ovary cells. *Biotechnology and Bioengineering,* 108(4), pp.853-866.

Dresios, J., Aschrafi, A., Owens, G.C., Vanderklish, P.W., Edelman, G.M. and Mauro, V.P. 2005. Cold stress-induced protein Rbm3 binds 60S ribosomal subunits, alters rnicroRNA levels, and enhances global protein synthesis. *Proceedings of the National Academy of Sciences of the United States of America,* 102(6), pp.1865-1870.

Druz, A., Chu, C., Majors, B., Santuary, R., Betenbaugh, M. and Shiloach, J. 2011. A novel microRNA mmu-miR-466h affects apoptosis regulation in mammalian cells. *Biotechnology and Bioengineering,* 108(7), pp.1651-1661.

Duex, J.E., Comeau, L., Sorkin, A., Purow, B. and Kefas, B. 2011. Usp18 regulates epidermal growth factor (EGF) receptor expression and cancer cell survival via microRNA-7. *The Journal of Biological Chemistry,* 286(28), pp.25377-25386.

Duval, D., Demangel, C., Miossec, S. and Geahel, I. 1992. Role of metabolic waste products in the control of cell proliferation and antibody production by mouse hybridoma cells. *Hybridoma,* 11(3), pp.311-322.

Dweep, H., Sticht, C., Pandey, P. and Gretz, N. 2011. miRWalk--database: prediction of possible miRNA binding sites by "walking" the genes of three genomes. *Journal of Biomedical Informatics,* 44(5), pp.839-847.

Ebert, M.S., Neilson, J.R. and Sharp, P.A. 2007. MicroRNA sponges: competitive inhibitors of small RNAs in mammalian cells. *Nature Methods,* 4(9), pp.721-726.

Ebert, M.S. and Sharp, P.A. 2012. Roles for microRNAs in conferring robustness to biological processes. *Cell,* 149(3), pp.515-524.

Ebert, M.S. and Sharp, P.A. 2010. MicroRNA sponges: progress and possibilities. *RNA (New York, N.Y.),* 16(11), pp.2043-2050.

Elbashir, S.M., Harborth, J., Lendeckel, W., Yalcin, A., Weber, K. and Tuschl, T. 2001. Duplexes of 21-nucleotide RNAs mediate RNA interference in cultured mammalian cells. *Nature,* 411(6836), pp.494-498.

Elmen, J., Lindow, M., Schutz, S., Lawrence, M., Petri, A., Obad, S., Lindholm, M., Hedtjarn, M., Hansen, H.F., Berger, U., Gullans, S., Kearney, P., Sarnow, P., Straarup, E.M. and Kauppinen, S. 2008. LNA-mediated microRNA silencing in non-human primates. *Nature,* 452(7189), pp.896-U10.

Esquela-Kerscher, A. and Slack, F.J. 2006. Oncomirs - microRNAs with a role in cancer. *Nature Reviews.Cancer,* 6(4), pp.259-269.

Even, M.S., Sandusky, C.B. and Barnard, N.D. 2006. Serum-free hybridoma culture: ethical, scientific and safety considerations. *Trends in Biotechnology,* 24(3), pp.105-108.

Fan, L., Kadura, I., Krebs, L.E., Hatfield, C.C., Shaw, M.M. and Frye, C.C. 2012. Improving the efficiency of CHO cell line generation using glutamine synthetase gene knockout cells. *Biotechnology and Bioengineering,* 109(4), pp.1007-1015.

Fang, Y.X., Xue, J.L., Shen, Q., Chen, J. and Tian, L. 2012. miR-7 inhibits tumor growth and metastasis by targeting the PI3K/AKT pathway in hepatocellular carcinoma. *Hepatology (Baltimore, Md.),*

Fang, Z. and Rajewsky, N. 2011. The impact of miRNA target sites in coding sequences and in 3'UTRs. *PloS One,* 6(3), pp.e18067.

Farh, K.K.H., Grimson, A., Jan, C., Lewis, B.P., Johnston, W.K., Lim, L.P., Burge, C.B. and Bartel, D.P. 2005. The widespread impact of mammalian microRNAs on mRNA repression and evolution. *Science,* 310(5755), pp.1817-1821.

Fazi, F., Rosa, A., Fatica, A., Gelmetti, V., De Marchis, M.L., Nervi, C. and Bozzoni, I. 2005. A minicircuitry comprised of microRNA-223 and transcription factors NFI-A and C/EBPalpha regulates human granulopoiesis. *Cell,* 123(5), pp.819-831.

Fernandez-Hernando, C., Suarez, Y., Rayner, K.J. and Moore, K.J. 2011. MicroRNAs in lipid metabolism. *Current Opinion in Lipidology,* 22(2), pp.86-92.

Figueroa, B.,Jr, Ailor, E., Osborne, D., Hardwick, J.M., Reff, M. and Betenbaugh, M.J. 2007. Enhanced cell culture performance using inducible anti-apoptotic genes E1B-19K and Aven in the production of a monoclonal antibody with Chinese hamster ovary cells. *Biotechnology and Bioengineering,* 97(4), pp.877-892.

Fire, A., Albertson, D., Harrison, S.W. and Moerman, D.G. 1991. Production of antisense RNA leads to effective and specific inhibition of gene expression in C. elegans muscle. *Development (Cambridge, England),* 113(2), pp.503-514.

Fire, A., Xu, S.Q., Montgomery, M.K., Kostas, S.A., Driver, S.E. and Mello, C.C. 1998. Potent and specific genetic interference by double-stranded RNA in Caenorhabditis elegans. *Nature,* 391(6669), pp.806-811.

Foekens, J.A., Sieuwerts, A.M., Smid, M., Look, M.P., de Weerd, V., Boersma, A.W., Klijn, J.G., Wiemer, E.A. and Martens, J.W. 2008. Four miRNAs associated with aggressiveness of lymph node-negative, estrogen receptor-positive human breast cancer. *Proceedings of the National Academy of Sciences of the United States of America,* 105(35), pp.13021-13026.

Forman, J.J., Legesse-Miller, A. and Coller, H.A. 2008. A search for conserved sequences in coding regions reveals that the let-7 microRNA targets Dicer within its coding sequence. *Proceedings of the National Academy of Sciences of the United States of America,* 105(39), pp.14879-14884.

Forman, M.S., Lee, V.M. and Trojanowski, J.Q. 2003. 'Unfolding' pathways in neurodegenerative disease. *Trends in Neurosciences,* 26(8), pp.407-410.

Forsburg, S.L. 2004. Eukaryotic MCM proteins: beyond replication initiation. *Microbiology and Molecular Biology Reviews : MMBR,* 68(1), pp.109-131.

Franco-Zorrilla, J.M., Valli, A., Todesco, M., Mateos, I., Puga, M.I., Rubio-Somoza, I., Leyva, A., Weigel, D., Garcia, J.A. and Paz-Ares, J. 2007. Target mimicry provides a new mechanism for regulation of microRNA activity. *Nature Genetics,* 39(8), pp.1033-1037.

Frankel, L.B., Christoffersen, N.R., Jacobsen, A., Lindow, M., Krogh, A. and Lund, A.H. 2008. Programmed cell death 4 (PDCD4) is an important functional target of the microRNA miR-21 in breast cancer cells. *The Journal of Biological Chemistry,* 283(2), pp.1026-1033.

Friedman, R.C., Farh, K.K.H., Burge, C.B. and Bartel, D.P. 2009. Most mammalian mRNAs are conserved targets of microRNAs. *Genome Research,* 19(1), pp.92-105.

Fu, H.J., Zhu, J., Yang, M., Zhang, Z.Y., Tie, Y., Jiang, H., Sun, Z.X. and Zheng, X.F. 2006. A novel method to monitor the expression of microRNAs. *Molecular Biotechnology,* 32(3), pp.197-204.

Fussenegger, M., Mazur, X. and Bailey, J.E. 1997. A novel cytostatic process enhances the productivity of Chinese hamster ovary cells. *Biotechnology and Bioengineering,* 55(6), pp.927-939.

Fussenegger, M., Schlatter, S., Datwyler, D., Mazur, X. and Bailey, J.E. 1998. Controlled proliferation by multigene metabolic engineering enhances the productivity of Chinese hamster ovary cells. *Nature Biotechnology,* 16(5), pp.468-472.

Gaidatzis, D., van Nimwegen, E., Hausser, J. and Zavolan, M. 2007. Inference of miRNA targets using evolutionary conservation and pathway analysis. *BMC Bioinformatics,* 8pp.69.

Gammell, P. 2007. MicroRNAs: recently discovered key regulators of proliferation and apoptosis in animal cells. *Cytotechnology,* 53(1), pp.55-63.

Gammell, P., Barron, N., Kumar, N. and Clynes, M. 2007. Initial identification of low temperature and culture stage induction of miRNA expression in suspension CHO-K1 cells. *Journal of Biotechnology,* 130(3), pp.213-218.

Gammell, P. 2007. MicroRNAs: recently discovered key regulators of proliferation and apoptosis in animal cells - Identification of miRNAs regulating growth and survival. *Cytotechnology,* 53(1-3), pp.55-63.

Gammell, P., Barron, N., Kumar, N. and Clynes, M. 2007. Initial identification of low temperature and culture stage induction of miRNA expression in suspension CHO-K1 cells. *Journal of Biotechnology,* 130(3), pp.213-218.

Gandor, C., Leist, C., Fiechter, A. and Asselbergs, F.A. 1995. Amplification and expression of recombinant genes in serum-independent Chinese hamster ovary cells. *FEBS Letters,* 377(3), pp.290-294.

Gao, P., Tchernyshyov, I., Chang, T., Lee, Y., Kita, K., Ochi, T., Zeller, K.I., De Marzo, A.M., Van Eyk, J.E., Mendell, J.T. and Dang, C.V. 2009. c-Myc suppression of miR-23a/b enhances mitochondrial glutaminase expression and glutamine metabolism. *Nature,* 458(7239), pp.762-U100.

Gawlitzek, M., Conradt, H.S. and Wagner, R. 1995. Effect of different cell culture conditions on the polypeptide integrity and N-glycosylation of a recombinant model glycoprotein. *Biotechnology and Bioengineering,* 46(6), pp.536-544.

Georgieva, B., Milev, I., Minkov, I., Dimitrova, I., Bradford, A.P. and Baev, V. 2012. Characterization of the uterine leiomyoma microRNAome by deep sequencing. *Genomics,* 99(5), pp.275-281.

Ghildiyal, M. and Zamore, P.D. 2009. Small silencing RNAs: an expanding universe. *Nature Reviews Genetics,* 10(2), pp.94-108.

Giles, K.M., Barker, A., Zhang, P.M., Epis, M.R. and Leedman, P.J. 2011. MicroRNA regulation of growth factor receptor signaling in human cancer cells. *Methods in Molecular Biology (Clifton, N.J.),* 676pp.147-163.

Girod, P.A., Zahn-Zabal, M. and Mermod, N. 2005. Use of the chicken lysozyme 5' matrix attachment region to generate high producer CHO cell lines. *Biotechnology and Bioengineering,* 91(1), pp.1-11.

Goeddel, D.V. 1990. Systems for heterologous gene expression. *Methods in Enzymology,* 185pp.3-7.

Goochee, C.F. 1992. Bioprocess factors affecting glycoprotein oligosaccharide structure. *Developments in Biological Standardization,* 76pp.95-104.

Gossen, M. and Bujard, H. 1992. Tight control of gene expression in mammalian cells by tetracycline-responsive promoters. *Proceedings of the National Academy of Sciences of the United States of America,* 89(12), pp.5547-5551.

Goto, M. 2007. Protein O-glycosylation in fungi: diverse structures and multiple functions. *Bioscience, Biotechnology, and Biochemistry,* 71(6), pp.1415-1427.

Gottlob, K., Majewski, N., Kennedy, S., Kandel, E., Robey, R.B. and Hay, N. 2001. Inhibition of early apoptotic events by Akt/PKB is dependent on the first committed step of glycolysis and mitochondrial hexokinase. *Genes & Development,* 15(11), pp.1406-1418.

Gregory, R.I., Chendrimada, T.P., Cooch, N. and Shiekhattar, R. 2005. Human RISC couples microRNA biogenesis and posttranscriptional gene silencing. *Cell,* 123(4), pp.631-640.

Griffiths-Jones, S. 2006. miRBase: the microRNA sequence database. *Methods in Molecular Biology (Clifton, N.J.),* 342pp.129-138.

Griffiths-Jones, S., Grocock, R.J., van Dongen, S., Bateman, A. and Enright, A.J. 2006. miRBase: microRNA sequences, targets and gene nomenclature. *Nucleic Acids Research,* 34(Database issue), pp.D140-4.

Griffiths-Jones, S., Hui, J.H., Marco, A. and Ronshaugen, M. 2011. MicroRNA evolution by arm switching. *EMBO Reports,* 12(2), pp.172-177.

Griffiths-Jones, S., Saini, H.K., van Dongen, S. and Enright, A.J. 2008. miRBase: tools for microRNA genomics. *Nucleic Acids Research,* 36(Database issue), pp.D154-8.

Grimm, D., Streetz, K.L., Jopling, C.L., Storm, T.A., Pandey, K., Davis, C.R., Marion, P., Salazar, F. and Kay, M.A. 2006. Fatality in mice due to oversaturation of cellular microRNA/short hairpin RNA pathways. *Nature,* 441(7092), pp.537-541.

Grimson, A., Farh, K.K.H., Johnston, W.K., Garrett-Engele, P., Lim, L.P. and Bartel, D.P. 2007. MicroRNA targeting specificity in mammals: Determinants beyond seed pairing. *Molecular Cell,* 27(1), pp.91-105.

Guo, L. and Lu, Z. 2010. The fate of miRNA* strand through evolutionary analysis: implication for degradation as merely carrier strand or potential regulatory molecule? *PloS One,* 5(6), pp.e11387.

Hacker, D.L., De Jesus, M. and Wurm, F.M. 2009. 25 Years of Recombinant Proteins from Reactor-Grown Cells - Where do we Go from Here? *Biotechnology Advances,* 27(6), pp.1023-1027.

Hackl, M., Jadhav, V., Jakobi, T., Rupp, O., Brinkrolf, K., Goesmann, A., Puhler, A., Noll, T., Borth, N. and Grillari, J. 2012. Computational identification of microRNA gene loci and precursor microRNA sequences in CHO cell lines. *Journal of Biotechnology,* 158(3), pp.151-155.

Hackl, M., Jakobi, T., Blom, J., Doppmeier, D., Brinkrolf, K., Szczepanowski, R., Bernhart, S.H., Honer Zu Siederdissen, C., Bort, J.A., Wieser, M., Kunert, R., Jeffs, S., Hofacker, I.L., Goesmann, A., Puhler, A., Borth, N. and Grillari, J. 2011. Next-generation sequencing of the Chinese hamster ovary microRNA transcriptome:

Identification, annotation and profiling of microRNAs as targets for cellular engineering. *Journal of Biotechnology*, 153(1-2), pp.62-75.

Hamilton, A.J. and Baulcombe, D.C. 1999. A species of small antisense RNA in posttranscriptional gene silencing in plants. *Science (New York, N.Y.)*, 286(5441), pp.950-952.

Hammell, M., Long, D., Zhang, L., Lee, A., Carmack, C.S., Han, M., Ding, Y. and Ambros, V. 2008. mirWIP: microRNA target prediction based on microRNA-containing ribonucleoprotein-enriched transcripts. *Nature Methods*, 5(9), pp.813-819.

Hammond, S., Swanberg, J.C., Polson, S.W. and Lee, K.H. 2012. Profiling conserved microRNA expression in recombinant CHO cell lines using Illumina sequencing. *Biotechnology and Bioengineering*, 109(6), pp.1371-1375.

Hammond, S.M., Bernstein, E., Beach, D. and Hannon, G.J. 2000. An RNA-directed nuclease mediates post-transcriptional gene silencing in Drosophila cells. *Nature*, 404(6775), pp.293-296.

Han, J., Pedersen, J.S., Kwon, S.C., Belair, C.D., Kim, Y.K., Yeom, K.H., Yang, W.Y., Haussler, D., Blelloch, R. and Kim, V.N. 2009. Posttranscriptional crossregulation between Drosha and DGCR8. *Cell*, 136(1), pp.75-84.

Hanson, M.A., Ge, X., Kostov, Y., Brorson, K.A., Moreira, A.R. and Rao, G. 2007. Comparisons of optical pH and dissolved oxygen sensors with traditional electrochemical probes during mammalian cell culture. *Biotechnology and Bioengineering*, 97(4), pp.833-841.

Haracska, L., Unk, I., Johnson, R.E., Phillips, B.B., Hurwitz, J., Prakash, L. and Prakash, S. 2002. Stimulation of DNA synthesis activity of human DNA polymerase kappa by PCNA. *Molecular and Cellular Biology*, 22(3), pp.784-791.

Harraghy, N., Buceta, M., Regamey, A., Girod, P.A. and Mermod, N. 2012. Using matrix attachment regions to improve recombinant protein production. *Methods in Molecular Biology (Clifton, N.J.)*, 801pp.93-110.

Harris, L.K. and Westwood, M. 2012. Biology and significance of signalling pathways activated by IGF-II. *Growth Factors (Chur, Switzerland)*, 30(1), pp.1-12.

Harrison, P.M., Zheng, D., Zhang, Z., Carriero, N. and Gerstein, M. 2005. Transcribed processed pseudogenes in the human genome: an intermediate form of expressed retrosequence lacking protein-coding ability. *Nucleic Acids Research*, 33(8), pp.2374-2383.

Hartig, J.S., Grune, I., Najafi-Shoushtari, S.H. and Famulok, M. 2004. Sequence-specific detection of MicroRNAs by signal-amplifying ribozymes. *Journal of the American Chemical Society*, 126(3), pp.722-723.

Hayashita, Y., Osada, H., Tatematsu, Y., Yamada, H., Yanagisawa, K., Tomida, S., Yatabe, Y., Kawahara, K., Sekido, Y. and Takahashi, T. 2005. A polycistronic microRNA cluster, miR-17-92, is overexpressed in human lung cancers and enhances cell proliferation. *Cancer Research*, 65(21), pp.9628-9632.

Hayter, P.M., Curling, E.M., Baines, A.J., Jenkins, N., Salmon, I., Strange, P.G., Tong, J.M. and Bull, A.T. 1992. Glucose-limited chemostat culture of Chinese hamster ovary cells producing recombinant human interferon-gamma. *Biotechnology and Bioengineering*, 39(3), pp.327-335.

He, A., Zhu, L., Gupta, N., Chang, Y. and Fang, F. 2007a. Overexpression of micro ribonucleic acid 29, highly up-regulated in diabetic rats, leads to insulin resistance in 3T3-L1 adipocytes. *Molecular Endocrinology (Baltimore, Md.)*, 21(11), pp.2785-2794.

He, L., He, X., Lim, L.P., de Stanchina, E., Xuan, Z., Liang, Y., Xue, W., Zender, L., Magnus, J., Ridzon, D., Jackson, A.L., Linsley, P.S., Chen, C., Lowe, S.W., Cleary, M.A. and Hannon, G.J. 2007b. A microRNA component of the p53 tumour suppressor network. *Nature*, 447(7148), pp.1130-1134.

He, L., He, X., Lowe, S.W. and Hannon, G.J. 2007c. microRNAs join the p53 network--another piece in the tumour-suppression puzzle. *Nature Reviews.Cancer*, 7(11), pp.819-822.

He, L., Thomson, J.M., Hemann, M.T., Hernando-Monge, E., Mu, D., Goodson, S., Powers, S., Cordon-Cardo, C., Lowe, S.W., Hannon, G.J. and Hammond, S.M. 2005. A microRNA polycistron as a potential human oncogene. *Nature,* 435(7043), pp.828-833.

Heale, B.S.E., Keegan, L.P., McGurk, L., Michlewski, G., Brindle, J., Stanton, C.M., Caceres, J.F. and O'Connell, M.A. 2009. Editing independent effects of ADARs on the miRNA/siRNA pathways. *Embo Journal,* 28(20), pp.3145-3156.

Hermeking, H. 2010. The miR-34 family in cancer and apoptosis. *Cell Death and Differentiation,* 17(2), pp.193-199.

Hermeking, H. 2007. p53 enters the microRNA world. *Cancer Cell,* 12(5), pp.414-418.

Herold, S., Herkert, B. and Eilers, M. 2009. Facilitating replication under stress: an oncogenic function of MYC? *Nature Reviews.Cancer,* 9(6), pp.441-444.

Hertel, J., Lindemeyer, M., Missal, K., Fried, C., Tanzer, A., Flamm, C., Hofacker, I.L., Stadler, P.F. and Students of Bioinformatics Computer Labs 2004 and 2005. 2006. The expansion of the metazoan microRNA repertoire. *BMC Genomics,* 7pp.25.

Hobert, O. 2004. Common logic of transcription factor and microRNA action. *Trends in Biochemical Sciences,* 29(9), pp.462-468.

Hoeijmakers, J.H., Odijk, H. and Westerveld, A. 1987. Differences between rodent and human cell lines in the amount of integrated DNA after transfection. *Experimental Cell Research,* 169(1), pp.111-119.

Hoglund, M., Siden, T. and Rohme, D. 1992. Different pathways for chromosomal integration of transfected circular pSVneo plasmids in normal and established rodent cells. *Gene,* 116(2), pp.215-222.

Hornstein, E. and Shomron, N. 2006. Canalization of development by microRNAs. *Nature Genetics,* 38pp.S20-S24.

Horwich, M.D. and Zamore, P.D. 2008. Design and delivery of antisense oligonucleotides to block microRNA function in cultured Drosophila and human cells. *Nature Protocols,* 3(10), pp.1537-1549.

Hu, T., Miller, C.M., Ridder, G.M. and Aardema, M.J. 1999. Characterization of p53 in Chinese hamster cell lines CHO-K1, CHO-WBL, and CHL: implications for genotoxicity testing. *Mutation Research,* 426(1), pp.51-62.

Hu, W., Chan, C.S., Wu, R., Zhang, C., Sun, Y., Song, J.S., Tang, L.H., Levine, A.J. and Feng, Z. 2010. Negative regulation of tumor suppressor p53 by microRNA miR-504. *Molecular Cell,* 38(5), pp.689-699.

Huang, S., He, X., Ding, J., Liang, L., Zhao, Y., Zhang, Z., Yao, X., Pan, Z., Zhang, P., Li, J., Wan, D. and Gu, J. 2008. Upregulation of miR-23a approximately 27a approximately 24 decreases transforming growth factor-beta-induced tumor-suppressive activities in human hepatocellular carcinoma cells. *International Journal of Cancer.Journal International Du Cancer,* 123(4), pp.972-978.

Huang, Y., Li, Y., Wang, Y.G., Gu, X., Wang, Y. and Shen, B.F. 2007. An efficient and targeted gene integration system for high-level antibody expression. *Journal of Immunological Methods,* 322(1-2), pp.28-39.

Hutvagner, G., Simard, M.J., Mello, C.C. and Zamore, P.D. 2004. Sequence-specific inhibition of small RNA function. *Plos Biology,* 2(4), pp.465-475.

Ifandi, V. and Al-Rubeai, M. 2005. Regulation of cell proliferation and apoptosis in CHO-K1 cells by the coexpression of c-Myc and Bcl-2. *Biotechnology Progress,* 21(3), pp.671-677.

Ikeda, Y., Tanji, E., Makino, N., Kawata, S. and Furukawa, T. 2012. MicroRNAs Associated with Mitogen-Activated Protein Kinase in Human Pancreatic Cancer. *Molecular Cancer Research : MCR,* 10(2), pp.259-269.

Imai-Nishiya, H., Mori, K., Inoue, M., Wakitani, M., Iida, S., Shitara, K. and Satoh, M. 2007. Double knockdown of alpha1,6-fucosyltransferase (FUT8) and GDP-mannose 4,6-dehydratase (GMD) in antibody-producing cells: a new strategy for generating fully non-fucosylated therapeutic antibodies with enhanced ADCC. *BMC Biotechnology,* 7pp.84.

Inui, M., Martello, G. and Piccolo, S. 2010. MicroRNA control of signal transduction. *Nature Reviews Molecular Cell Biology*, 11(4), pp.252-263.

Irani, N., Beccaria, A.J. and Wagner, R. 2002. Expression of recombinant cytoplasmic yeast pyruvate carboxylase for the improvement of the production of human erythropoietin by recombinant BHK-21 cells. *Journal of Biotechnology*, 93(3), pp.269-282.

Ito, A., Kawaguchi, Y., Lai, C.H., Kovacs, J.J., Higashimoto, Y., Appella, E. and Yao, T.P. 2002. MDM2-HDAC1-mediated deacetylation of p53 is required for its degradation. *The EMBO Journal*, 21(22), pp.6236-6245.

Ivanovska, I., Ball, A.S., Diaz, R.L., Magnus, J.F., Kibukawa, M., Schelter, J.M., Kobayashi, S.V., Lim, L., Burchard, J., Jackson, A.L., Linsley, P.S. and Cleary, M.A. 2008. MicroRNAs in the miR-106b family regulate p21/CDKN1A and promote cell cycle progression. *Molecular and Cellular Biology*, 28(7), pp.2167-2174.

Izant, J.G. and Weintraub, H. 1984. Inhibition of thymidine kinase gene expression by anti-sense RNA: a molecular approach to genetic analysis. *Cell*, 36(4), pp.1007-1015.

Jackson, A.L., Burchard, J., Schelter, J., Chau, B.N., Cleary, M., Lim, L. and Linsley, P.S. 2006. Widespread siRNA "off-target" transcript silencing mediated by seed region sequence complementarity. *RNA (New York, N.Y.)*, 12(7), pp.1179-1187.

Jackson, A.L. and Linsley, P.S. 2010. Recognizing and avoiding siRNA off-target effects for target identification and therapeutic application. *Nature Reviews.Drug Discovery*, 9(1), pp.57-67.

Jadhav, V., Hackl, M., Bort, J.A., Wieser, M., Harreither, E., Kunert, R., Borth, N. and Grillari, J. 2012. A screening method to assess biological effects of microRNA overexpression in Chinese hamster ovary cells. *Biotechnology and Bioengineering*, 109(6), pp.1376-1385.

Jagadeeswaran, G., Zheng, Y., Sumathipala, N., Jiang, H., Arrese, E.L., Soulages, J.L., Zhang, W. and Sunkar, R. 2010. Deep sequencing of small RNA libraries reveals

dynamic regulation of conserved and novel microRNAs and microRNA-stars during silkworm development. *BMC Genomics*, 11pp.52.

Jakymiw, A., Pauley, K.M., Li, S., Ikeda, K., Lian, S., Eystathioy, T., Satoh, M., Fritzler, M.J. and Chan, E.K. 2007. The role of GW/P-bodies in RNA processing and silencing. *Journal of Cell Science,* 120(Pt 8), pp.1317-1323.

Jaluria, P., Betenbaugh, M., Konstantopoulos, K. and Shiloach, J. 2007. Enhancement of cell proliferation in various mammalian cell lines by gene insertion of a cyclin-dependent kinase homolog. *BMC Biotechnology*, 7pp.71.

Jayapal, K.R., Wlaschin, K.F., Hu, W. and Yap, M.G.S. 2007. Recombinant protein therapeutics from CHO cells - 20 years and counting. *Chemical Engineering Progress,* 103(10), pp.40-47.

Jenkins, N. and Curling, E.M. 1994. Glycosylation of recombinant proteins: problems and prospects. *Enzyme and Microbial Technology*, 16(5), pp.354-364.

Jenkins, N., Parekh, R.B. and James, D.C. 1996. Getting the glycosylation right: Implications for the biotechnology industry. *Nature Biotechnology,* 14(8), pp.975-981.

Jensen, S., Gassama, M.P. and Heidmann, T. 1999. Taming of transposable elements by homology-dependent gene silencing. *Nature Genetics*, 21(2), pp.209-212.

Jeong, D.W., Cho, I.T., Kim, T.S., Bae, G.W., Kim, I.H. and Kim, I.Y. 2006. Effects of lactate dehydrogenase suppression and glycerol-3-phosphate dehydrogenase overexpression on cellular metabolism. *Molecular and Cellular Biochemistry*, 284(1-2), pp.1-8.

Jiang, L., Liu, X., Chen, Z., Jin, Y., Heidbreder, C.E., Kolokythas, A., Wang, A., Dai, Y. and Zhou, X. 2010. MicroRNA-7 targets IGF1R (insulin-like growth factor 1 receptor) in tongue squamous cell carcinoma cells. *The Biochemical Journal,* 432(1), pp.199-205.

Joglekar, M.V., Joglekar, V.M. and Hardikar, A.A. 2009. Expression of islet-specific microRNAs during human pancreatic development. *Gene Expression Patterns : GEP,* 9(2), pp.109-113.

Joglekar, M.V., Patil, D., Joglekar, V.M., Rao, G.V., Reddy, D.N., Mitnala, S., Shouche, Y. and Hardikar, A.A. 2009. The miR-30 family microRNAs confer epithelial phenotype to human pancreatic cells. *Islets,* 1(2), pp.137-147.

Johnson, K.C., Jacob, N.M., Nissom, P.M., Hackl, M., Lee, L.H., Yap, M. and Hu, W.S. 2011. Conserved microRNAs in Chinese hamster ovary cell lines. *Biotechnology and Bioengineering,* 108(2), pp.475-480.

Johnston, R.J.,Jr, Chang, S., Etchberger, J.F., Ortiz, C.O. and Hobert, O. 2005. MicroRNAs acting in a double-negative feedback loop to control a neuronal cell fate decision. *Proceedings of the National Academy of Sciences of the United States of America,* 102(35), pp.12449-12454.

Jung, D.J., Jin, D.H., Hong, S.W., Kim, J.E., Shin, J.S., Kim, D., Cho, B.J., Hwang, Y.I., Kang, J.S. and Lee, W.J. 2010. Foxp3 expression in p53-dependent DNA damage responses. *The Journal of Biological Chemistry,* 285(11), pp.7995-8002.

Kaern, M., Elston, T.C., Blake, W.J. and Collins, J.J. 2005. Stochasticity in gene expression: from theories to phenotypes. *Nature Reviews.Genetics,* 6(6), pp.451-464.

Kameyama, Y., Kawabe, Y., Ito, A. and Kamihira, M. 2010. An accumulative site-specific gene integration system using Cre recombinase-mediated cassette exchange. *Biotechnology and Bioengineering,* 105(6), pp.1106-1114.

Kanaar, R., Troelstra, C., Swagemakers, S.M., Essers, J., Smit, B., Franssen, J.H., Pastink, A., Bezzubova, O.Y., Buerstedde, J.M., Clever, B., Heyer, W.D. and Hoeijmakers, J.H. 1996. Human and mouse homologs of the Saccharomyces cerevisiae RAD54 DNA repair gene: evidence for functional conservation. *Current Biology : CB,* 6(7), pp.828-838.

Kannouche, P.L., Wing, J. and Lehmann, A.R. 2004. Interaction of human DNA polymerase eta with monoubiquitinated PCNA: a possible mechanism for the polymerase switch in response to DNA damage. *Molecular Cell,* 14(4), pp.491-500.

Kantardjieff, A., Nissom, P.M., Chuah, S.H., Yusufi, F., Jacob, N.M., Mulukutla, B.C., Yap, M. and Hu, W. 2009. Developing genomic platforms for Chinese hamster ovary cells. *Biotechnology Advances,* 27(6), pp.1028-1035.

Kaufmann, H., Mazur, X., Fussenegger, M. and Bailey, J.E. 1999. Influence of low temperature on productivity, proteome and protein phosphorylation of CHO cells. *Biotechnology and Bioengineering,* 63(5), pp.573-582.

Kawamata, T. and Tomari, Y. 2010. Making RISC. *Trends in Biochemical Sciences,* 35(7), pp.368-376.

Kedersha, N., Stoecklin, G., Ayodele, M., Yacono, P., Lykke-Andersen, J., Fritzler, M.J., Scheuner, D., Kaufman, R.J., Golan, D.E. and Anderson, P. 2005. Stress granules and processing bodies are dynamically linked sites of mRNP remodeling. *The Journal of Cell Biology,* 169(6), pp.871-884.

Kefas, B., Godlewski, J., Comeau, L., Li, Y.Q., Abounader, R., Hawkinson, M., Lee, J.W., Fine, H., Chiocca, E.A., Lawler, S. and Purow, B. 2008. microRNA-7 inhibits the epidermal growth factor receptor and the Akt pathway and is down-regulated in glioblastoma. *Cancer Research,* 68(10), pp.3566-3572.

Kennard, M.L., Goosney, D.L., Monteith, D., Roe, S., Fischer, D. and Mott, J. 2009a. Auditioning of CHO host cell lines using the artificial chromosome expression (ACE) technology. *Biotechnology and Bioengineering,* 104(3), pp.526-539.

Kennard, M.L., Goosney, D.L., Monteith, D., Zhang, L., Moffat, M., Fischer, D. and Mott, J. 2009b. The generation of stable, high MAb expressing CHO cell lines based on the artificial chromosome expression (ACE) technology. *Biotechnology and Bioengineering,* 104(3), pp.540-553.

Kennerdell, J.R. and Carthew, R.W. 1998. Use of dsRNA-mediated genetic interference to demonstrate that frizzled and frizzled 2 act in the wingless pathway. *Cell,* 95(7), pp.1017-1026.

Kertesz, M., Iovino, N., Unnerstall, U., Gaul, U. and Segal, E. 2007. The role of site accessibility in microRNA target recognition. *Nature Genetics,* 39(10), pp.1278-1284.

Khan, A.A., Betel, D., Miller, M.L., Sander, C., Leslie, C.S. and Marks, D.S. 2009. Transfection of small RNAs globally perturbs gene regulation by endogenous microRNAs. *Nature Biotechnology*, 27(6), pp.549-555.

Kim, A.H., Sasaki, T. and Chao, M.V. 2003. JNK-interacting protein 1 promotes Akt1 activation. *The Journal of Biological Chemistry,* 278(32), pp.29830-29836.

Kim, D.H. and Rossi, J.J. 2007. Strategies for silencing human disease using RNA interference. *Nature Reviews.Genetics,* 8(3), pp.173-184.

Kim, D.Y., Chaudhry, M.A., Kennard, M.L., Jardon, M.A., Braasch, K., Dionne, B., Butler, M. and Piret, J.M. 2012. Fed-batch CHO cell t-PA production and feed glutamine replacement to reduceammonia production. *Biotechnology Progress,*

Kim, J.M., Kim, J.S., Park, D.H., Kang, H.S., Yoon, J., Baek, K. and Yoon, Y. 2004a. Improved recombinant gene expression in CHO cells using matrix attachment regions. *Journal of Biotechnology*, 107(2), pp.95-105.

Kim, J.W., Zeller, K.I., Wang, Y., Jegga, A.G., Aronow, B.J., O'Donnell, K.A. and Dang, C.V. 2004b. Evaluation of myc E-box phylogenetic footprints in glycolytic genes by chromatin immunoprecipitation assays. *Molecular and Cellular Biology,* 24(13), pp.5923-5936.

Kim, J.Y., Kim, Y.G. and Lee, G.M. 2012. CHO cells in biotechnology for production of recombinant proteins: current state and further potential. *Applied Microbiology and Biotechnology*, 93(3), pp.917-930.

Kim, N.S., Chang, K.H., Chung, B.S., Kim, S.H., Kim, J.H. and Lee, G.M. 2003. Characterization of humanized antibody produced by apoptosis-resistant CHO cells under sodium butyrate-induced condition. *Journal of Microbiology and Biotechnology,* 13(6), pp.926-936.

Kim, N.S. and Lee, G.M. 2002. Inhibition of sodium butyrate-induced apoptosis in recombinant Chinese hamster ovary cells by constitutively expressing antisense RNA of caspase-3. *Biotechnology and Bioengineering,* 78(2), pp.217-228.

Kim, S.H. and Lee, G.M. 2007. Down-regulation of lactate dehydrogenase-A by siRNAs for reduced lactic acid formation of Chinese hamster ovary cells producing thrombopoietin. *Applied Microbiology and Biotechnology*, 74(1), pp.152-159.

Kim, S.Y., Herbst, A., Tworkowski, K.A., Salghetti, S.E. and Tansey, W.P. 2003. Skp2 regulates Myc protein stability and activity. *Molecular Cell*, 11(5), pp.1177-1188.

Kim, V.N., Han, J. and Siomi, M.C. 2009. Biogenesis of small RNAs in animals. *Nature Reviews Molecular Cell Biology*, 10(2), pp.126-139.

Kim, V.N. and Nam, J.W. 2006. Genomics of microRNA. *Trends in Genetics*, 22(3), pp.165-173.

Kim, Y.G., Cha, J. and Chandrasegaran, S. 1996. Hybrid restriction enzymes: zinc finger fusions to Fok I cleavage domain. *Proceedings of the National Academy of Sciences of the United States of America*, 93(3), pp.1156-1160.

Kim, Y.G., Kim, J.Y., Mohan, C. and Lee, G.M. 2009. Effect of Bcl-xL overexpression on apoptosis and autophagy in recombinant Chinese hamster ovary cells under nutrient-deprived condition. *Biotechnology and Bioengineering*, 103(4), pp.757-766.

Kim, Y.K. and Kim, V.N. 2007. Processing of intronic microRNAs. *Embo Journal*, 26(3), pp.775-783.

Kiriakidou, M., Nelson, P.T., Kouranov, A., Fitziev, P., Bouyioukos, C., Mourelatos, Z. and Hatzigeorgiou, A. 2004. A combined computational-experimental approach predicts human microRNA targets. *Genes & Development*, 18(10), pp.1165-1178.

Kito, M., Itami, S., Fukano, Y., Yamana, K. and Shibui, T. 2002. Construction of engineered CHO strains for high-level production of recombinant proteins. *Applied Microbiology and Biotechnology*, 60(4), pp.442-448.

Klaue, Y., Kallman, A.M., Bonin, M., Nellen, W. and Ohman, M. 2003. Biochemical analysis and scanning force microscopy reveal productive and nonproductive ADAR2 binding to RNA substrates. *RNA (New York, N.Y.)*, 9(7), pp.839-846.

Kloosterman, W.P., Wienholds, E., Ketting, R.F. and Plasterk, R.H. 2004. Substrate requirements for let-7 function in the developing zebrafish embryo. *Nucleic Acids Research,* 32(21), pp.6284-6291.

Koh, T.C., Lee, Y.Y., Chang, S.Q. and Nissom, P.M. 2009. Identification and expression analysis of miRNAs during batch culture of HEK-293 cells. *Journal of Biotechnology,* 140(3-4), pp.149-155.

Koralov, S.B., Muljo, S.A., Galler, G.R., Krek, A., Chakraborty, T., Kanellopoulou, C., Jensen, K., Cobb, B.S., Merkenschlager, M., Rajewsky, N. and Rajewsky, K. 2008. Dicer ablation affects antibody diversity and cell survival in the B lymphocyte lineage. *Cell,* 132(5), pp.860-874.

Kossatz, U., Dietrich, N., Zender, L., Buer, J., Manns, M.P. and Malek, N.P. 2004. Skp2-dependent degradation of p27kip1 is essential for cell cycle progression. *Genes & Development,* 18(21), pp.2602-2607.

Kredo-Russo, S., Ness, A., Mandelbaum, A.D., Walker, M.D. and Hornstein, E. 2012. Regulation of pancreatic microRNA-7 expression. *Experimental Diabetes Research,* 2012pp.695214.

Krek, A., Grun, D., Poy, M.N., Wolf, R., Rosenberg, L., Epstein, E.J., MacMenamin, P., da Piedade, I., Gunsalus, K.C., Stoffel, M. and Rajewsky, N. 2005. Combinatorial microRNA target predictions. *Nature Genetics,* 37(5), pp.495-500.

Kress, T.R., Cannell, I.G., Brenkman, A.B., Samans, B., Gaestel, M., Roepman, P., Burgering, B.M., Bushell, M., Rosenwald, A. and Eilers, M. 2011. The MK5/PRAK kinase and Myc form a negative feedback loop that is disrupted during colorectal tumorigenesis. *Molecular Cell,* 41(4), pp.445-457.

Krol, J., Loedige, I. and Filipowicz, W. 2010. The widespread regulation of microRNA biogenesis, function and decay. *Nature Reviews.Genetics,* 11(9), pp.597-610.

Krutzfeldt, J., Poy, M.N. and Stoffel, M. 2006. Strategies to determine the biological function of microRNAs. *Nature Genetics,* 38pp.S14-S19.

Krutzfeldt, J., Rajewsky, N., Braich, R., Rajeev, K.G., Tuschl, T., Manoharan, M. and Stoffel, M. 2005. Silencing of microRNAs in vivo with 'antagomirs'. *Nature,* 438(7068), pp.685-689.

Kuhn, D.E., Martin, M.M., Feldman, D.S., Terry Jr., A.V., Nuovo, G.J. and Elton, T.S. 2008. Experimental validation of miRNA targets. *Methods,* 44(1), pp.47-54.

Kuhn, U. and Wahle, E. 2004. Structure and function of poly(A) binding proteins. *Biochimica Et Biophysica Acta,* 1678(2-3), pp.67-84.

Kumar, M.S., Erkeland, S.J., Pester, R.E., Chen, C.Y., Ebert, M.S., Sharp, P.A. and Jacks, T. 2008. Suppression of non-small cell lung tumor development by the let-7 microRNA family. *Proceedings of the National Academy of Sciences of the United States of America,* 105(10), pp.3903-3908.

Kunkel, J.P., Jan, D.C., Jamieson, J.C. and Butler, M. 1998. Dissolved oxygen concentration in serum-free continuous culture affects N-linked glycosylation of a monoclonal antibody. *Journal of Biotechnology,* 62(1), pp.55-71.

Kurano, N., Leist, C., Messi, F., Kurano, S. and Fiechter, A. 1990. Growth behavior of Chinese hamster ovary cells in a compact loop bioreactor: 1. Effects of physical and chemical environments. *Journal of Biotechnology,* 15(1-2), pp.101-111.

Kutyavin, I.V., Lukhtanov, E.A., Gamper, H.B. and Meyer, R.B. 1997. Oligonucleotides with conjugated dihydropyrroloindole tripeptides: base composition and backbone effects on hybridization. *Nucleic Acids Research,* 25(18), pp.3718-3723.

Kuystermans, D. and Al-Rubeai, M. 2009. cMyc increases cell number through uncoupling of cell division from cell size in CHO cells. *BMC Biotechnology,* 9pp.76.

Lagos-Quintana, M., Rauhut, R., Lendeckel, W. and Tuschl, T. 2001. Identification of novel genes coding for small expressed RNAs. *Science (New York, N.Y.),* 294(5543), pp.853-858.

Lai, E.C., Tomancak, P., Williams, R.W. and Rubin, G.M. 2003. Computational identification of Drosophila microRNA genes. *Genome Biology,* 4(7), pp.R42.

Lakowicz, J.R. and Maliwal, B.P. 1983. Oxygen quenching and fluorescence depolarization of tyrosine residues in proteins. *The Journal of Biological Chemistry*, 258(8), pp.4794-4801.

Lal, A., Kim, H.H., Abdelmohsen, K., Kuwano, Y., Pullmann, R.,Jr, Srikantan, S., Subrahmanyam, R., Martindale, J.L., Yang, X., Ahmed, F., Navarro, F., Dykxhoorn, D., Lieberman, J. and Gorospe, M. 2008. p16(INK4a) translation suppressed by miR-24. *PloS One*, 3(3), pp.e1864.

Lal, A., Navarro, F., Maher, C.A., Maliszewski, L.E., Yan, N., O'Day, E., Chowdhury, D., Dykxhoorn, D.M., Tsai, P., Hofmann, O., Becker, K.G., Gorospe, M., Hide, W. and Lieberman, J. 2009a. miR-24 Inhibits Cell Proliferation by Targeting E2F2, MYC, and Other Cell-Cycle Genes via Binding to "Seedless" 3 ' UTR MicroRNA Recognition Elements. *Molecular Cell*, 35(5), pp.610-625.

Lal, A., Pan, Y., Navarro, F., Dykxhoorn, D.M., Moreau, L., Meire, E., Bentwich, Z., Lieberman, J. and Chowdhury, D. 2009b. miR-24-mediated downregulation of H2AX suppresses DNA repair in terminally differentiated blood cells. *Nature Structural & Molecular Biology*, 16(5), pp.492-498.

Landgraf, P., Rusu, M., Sheridan, R., Sewer, A., Iovino, N., Aravin, A., Pfeffer, S., Rice, A., Kamphorst, A.O., Landthaler, M., Lin, C., Socci, N.D., Hermida, L., Fulci, V., Chiaretti, S., Foa, R., Schliwka, J., Fuchs, U., Novosel, A., Muller, R.U., Schermer, B., Bissels, U., Inman, J., Phan, Q., Chien, M., Weir, D.B., Choksi, R., De Vita, G., Frezzetti, D., Trompeter, H.I., Hornung, V., Teng, G., Hartmann, G., Palkovits, M., Di Lauro, R., Wernet, P., Macino, G., Rogler, C.E., Nagle, J.W., Ju, J., Papavasiliou, F.N., Benzing, T., Lichter, P., Tam, W., Brownstein, M.J., Bosio, A., Borkhardt, A., Russo, J.J., Sander, C., Zavolan, M. and Tuschl, T. 2007. A mammalian microRNA expression atlas based on small RNA library sequencing. *Cell*, 129(7), pp.1401-1414.

Lau, N.C., Lim, L.P., Weinstein, E.G. and Bartel, D.P. 2001. An abundant class of tiny RNAs with probable regulatory roles in Caenorhabditis elegans. *Science (New York, N.Y.)*, 294(5543), pp.858-862.

Lee, H., Larner, J.M. and Hamlin, J.L. 1997. Cloning and characterization of Chinese hamster p53 cDNA. *Gene*, 184(2), pp.177-183.

Lee, I., Ajay, S.S., Yook, J.I., Kim, H.S., Hong, S.H., Kim, N.H., Dhanasekaran, S.M., Chinnaiyan, A.M. and Athey, B.D. 2009. New class of microRNA targets containing simultaneous 5 '-UTR and 3 '-UTR interaction sites. *Genome Research,* 19(7), pp.1175-1183.

Lee, J.Y., Kim, S., Hwang do, W., Jeong, J.M., Chung, J.K., Lee, M.C. and Lee, D.S. 2008. Development of a dual-luciferase reporter system for in vivo visualization of MicroRNA biogenesis and posttranscriptional regulation. *Journal of Nuclear Medicine : Official Publication, Society of Nuclear Medicine,* 49(2), pp.285-294.

Lee, K.M., Choi, E.J. and Kim, I.A. 2011. microRNA-7 increases radiosensitivity of human cancer cells with activated EGFR-associated signaling. *Radiotherapy and Oncology : Journal of the European Society for Therapeutic Radiology and Oncology,* 101(1), pp.171-176.

Lee, R.C. and Ambros, V. 2001. An extensive class of small RNAs in Caenorhabditis elegans. *Science,* 294(5543), pp.862-864.

Lee, R.C., Feinbaum, R.L. and Ambros, V. 1993. The C-Elegans Heterochronic Gene Lin-4 Encodes Small Rnas with Antisense Complementarity to Lin-14. *Cell,* 75(5), pp.843-854.

Lee, S.K. and Lee, G.M. 2003. Development of apoptosis-resistant dihydrofolate reductase-deficient Chinese hamster ovary cell line. *Biotechnology and Bioengineering,* 82(7), pp.872-876.

Lee, Y., Jeon, K., Lee, J.T., Kim, S. and Kim, V.N. 2002. MicroRNA maturation: stepwise processing and subcellular localization. *Embo Journal,* 21(17), pp.4663-4670.

Leung, A.K.L., Calabrese, J.M. and Sharp, P.A. 2006. Quantitative analysis of Argonaute protein reveals microRNA-dependent localization to stress granules. *Proceedings of the National Academy of Sciences of the United States of America,* 103(48), pp.18125-18130.

Lewis, B.P., Burge, C.B. and Bartel, D.P. 2005a. Conserved seed pairing, often flanked by adenosines, indicates that thousands of human genes are microRNA targets. *Cell,* 120(1), pp.15-20.

Lewis, B.P., Burge, C.B. and Bartel, D.P. 2005b. Conserved seed pairing, often flanked by adenosines, indicates that thousands of human genes are microRNA targets. *Cell,* 120(1), pp.15-20.

Li, J., Donath, S., Li, Y., Qin, D., Prabhakar, B.S. and Li, P. 2010. miR-30 regulates mitochondrial fission through targeting p53 and the dynamin-related protein-1 pathway. *PLoS Genetics,* 6(1), pp.e1000795.

Li, L., Mi, L., Feng, Q., Liu, R., Tang, H., Xie, L., Yu, X. and Chen, Z. 2005. Increasing the culture efficiency of hybridoma cells by the use of integrated metabolic control of glucose and glutamine at low levels. *Biotechnology and Applied Biochemistry,* 42(Pt 1), pp.73-80.

Li, X. and Carthew, R.W. 2005. A microRNA mediates EGF receptor signaling and promotes photoreceptor differentiation in the Drosophila eye. *Cell,* 123(7), pp.1267-1277.

Li, X., Cassidy, J.J., Reinke, C.A., Fischboeck, S. and Carthew, R.W. 2009. A MicroRNA Imparts Robustness against Environmental Fluctuation during Development. *Cell,* 137(2), pp.273-282.

Li, X., Zhao, Q., Liao, R., Sun, P. and Wu, X. 2003. The SCF(Skp2) ubiquitin ligase complex interacts with the human replication licensing factor Cdt1 and regulates Cdt1 degradation. *The Journal of Biological Chemistry,* 278(33), pp.30854-30858.

Li, Z.Y., Na, H.M., Peng, G., Pu, J. and Liu, P. 2011. Alteration of microRNA expression correlates to fatty acid-mediated insulin resistance in mouse myoblasts. *Molecular bioSystems,* 7(3), pp.871-877.

Licatalosi, D.D., Mele, A., Fak, J.J., Ule, J., Kayikci, M., Chi, S.W., Clark, T.A., Schweitzer, A.C., Blume, J.E., Wang, X., Darnell, J.C. and Darnell, R.B. 2008. HITS-

CLIP yields genome-wide insights into brain alternative RNA processing. *Nature,* 456(7221), pp.464-469.

Lieber, M.R. 1997. The FEN-1 family of structure-specific nucleases in eukaryotic DNA replication, recombination and repair. *BioEssays : News and Reviews in Molecular, Cellular and Developmental Biology,* 19(3), pp.233-240.

Lim, L.P., Lau, N.C., Garrett-Engele, P., Grimson, A., Schelter, J.M., Castle, J., Bartel, D.P., Linsley, P.S. and Johnson, J.M. 2005. Microarray analysis shows that some microRNAs downregulate large numbers of target mRNAs. *Nature,* 433(7027), pp.769-773.

Lim, L.P., Lau, N.C., Weinstein, E.G., Abdelhakim, A., Yekta, S., Rhoades, M.W., Burge, C.B. and Bartel, D.P. 2003. The microRNAs of Caenorhabditis elegans. *Genes & Development,* 17(8), pp.991-1008.

Lim, S.F., Chuan, K.H., Liu, S., Loh, S.O., Chung, B.Y., Ong, C.C. and Song, Z. 2006. RNAi suppression of Bax and Bak enhances viability in fed-batch cultures of CHO cells. *Metabolic Engineering,* 8(6), pp.509-522.

Lim, Y., Mantalaris, A., Yap, M.G. and Wong, D.C. 2010. Simultaneous targeting of Requiem & Alg-2 in Chinese hamster ovary cells for improved recombinant protein production. *Molecular Biotechnology,* 46(3), pp.301-307.

Lin, H.K., Wang, G., Chen, Z., Teruya-Feldstein, J., Liu, Y., Chan, C.H., Yang, W.L., Erdjument-Bromage, H., Nakayama, K.I., Nimer, S., Tempst, P. and Pandolfi, P.P. 2009. Phosphorylation-dependent regulation of cytosolic localization and oncogenic function of Skp2 by Akt/PKB. *Nature Cell Biology,* 11(4), pp.420-432.

Lin, N., Davis, A., Bahr, S., Borgschulte, T., Achtien, K. and Kayser, K. 2010. Profiling highly conserved microrna expression in recombinant IgG-producing and parental chinese hamster ovary cells. *Biotechnology Progress,*

Lin, Q., Gao, Z., Alarcon, R.M., Ye, J. and Yun, Z. 2009. A role of miR-27 in the regulation of adipogenesis. *Febs Journal,* 276(8), pp.2348-2358.

Lin, S.C., Liu, C.J., Lin, J.A., Chiang, W.F., Hung, P.S. and Chang, K.W. 2010. miR-24 up-regulation in oral carcinoma: positive association from clinical and in vitro analysis. *Oral Oncology,* 46(3), pp.204-208.

Lindstrom, M.S. 2009. Emerging functions of ribosomal proteins in gene-specific transcription and translation. *Biochemical and Biophysical Research Communications,* 379(2), pp.167-170.

Lipscomb, M.L., Palomares, L.A., Hernandez, V., Ramirez, O.T. and Kompala, D.S. 2005. Effect of production method and gene amplification on the glycosylation pattern of a secreted reporter protein in CHO cells. *Biotechnology Progress,* 21(1), pp.40-49.

Liu, C.G., Calin, G.A., Volinia, S. and Croce, C.M. 2008. MicroRNA expression profiling using microarrays. *Nature Protocols,* 3(4), pp.563-578.

Liu, J., Rivas, F.V., Wohlschlegel, J., Yates, J.R.,3rd, Parker, R. and Hannon, G.J. 2005. A role for the P-body component GW182 in microRNA function. *Nature Cell Biology,* 7(12), pp.1261-1266.

Liu, Q., Fu, H., Sun, F., Zhang, H., Tie, Y., Zhu, J., Xing, R., Sun, Z. and Zheng, X. 2008. miR-16 family induces cell cycle arrest by regulating multiple cell cycle genes. *Nucleic Acids Research,* 36(16), pp.5391-5404.

Liu, S., Gao, S., Zhang, D., Yin, J., Xiang, Z. and Xia, Q. 2010. MicroRNAs show diverse and dynamic expression patterns in multiple tissues of Bombyx mori. *BMC Genomics,* 11pp.85.

Liu, S., Xia, Q., Zhao, P., Cheng, T., Hong, K. and Xiang, Z. 2007. Characterization and expression patterns of let-7 microRNA in the silkworm (Bombyx mori). *BMC Developmental Biology,* 7pp.88.

Liu, T., Tang, H., Lang, Y., Liu, M. and Li, X. 2009. MicroRNA-27a functions as an oncogene in gastric adenocarcinoma by targeting prohibitin. *Cancer Letters,* 273(2), pp.233-242.

Liu, X., Wang, A., Heidbreder, C.E., Jiang, L., Yu, J., Kolokythas, A., Huang, L., Dai, Y. and Zhou, X. 2010. MicroRNA-24 targeting RNA-binding protein DND1 in tongue squamous cell carcinoma. *FEBS Letters,* 584(18), pp.4115-4120.

Liu, Y., Kao, H.I. and Bambara, R.A. 2004. Flap endonuclease 1: a central component of DNA metabolism. *Annual Review of Biochemistry,* 73pp.589-615.

Loya, C.M., Lu, C.S., Van Vactor, D. and Fulga, T.A. 2009. Transgenic microRNA inhibition with spatiotemporal specificity in intact organisms. *Nature Methods,* 6(12), pp.897-903.

Lu, J., Getz, G., Miska, E.A., Alvarez-Saavedra, E., Lamb, J., Peck, D., Sweet-Cordero, A., Ebert, B.L., Mak, R.H., Ferrando, A.A., Downing, J.R., Jacks, T., Horvitz, H.R. and Golub, T.R. 2005. MicroRNA expression profiles classify human cancers. *Nature,* 435(7043), pp.834-838.

Lu, Y., Thomson, J.M., Wong, H.Y., Hammond, S.M. and Hogan, B.L. 2007. Transgenic over-expression of the microRNA miR-17-92 cluster promotes proliferation and inhibits differentiation of lung epithelial progenitor cells. *Developmental Biology,* 310(2), pp.442-453.

Lu, Y.J., Xiao, J.N., Lin, H.X., Bai, Y.L., Luo, X.B., Wang, Z.G. and Yang, B.F. 2009. A single anti-microRNA antisense oligodeoxyribo-nucleotide (AMO) targeting multiple microRNAs offers an improved approach for microRNA interference. *Nucleic Acids Research,* 37(3),

Lynn, F.C., Skewes-Cox, P., Kosaka, Y., McManus, M.T., Harfe, B.D. and German, M.S. 2007. MicroRNA expression is required for pancreatic islet cell genesis in the mouse. *Diabetes,* 56(12), pp.2938-2945.

Lytle, J.R., Yario, T.A. and Steitz, J.A. 2007. Target mRNAs are repressed as efficiently by microRNA-binding sites in the 5' UTR as in the 3' UTR. *Proceedings of the National Academy of Sciences of the United States of America,* 104(23), pp.9667-9672.

Ma, L., Reinhardt, F., Pan, E., Soutschek, J., Bhat, B., Marcusson, E.G., Teruya-Feldstein, J., Bell, G.W. and Weinberg, R.A. 2010. Therapeutic silencing of miR-10b inhibits metastasis in a mouse mammary tumor model. *Nature Biotechnology,* 28(4), pp.341-U67.

Majors, B.S., Arden, N., Oyler, G.A., Chiang, G.G., Pederson, N.E. and Betenbaugh, M.J. 2008. E2F-1 overexpression increases viable cell density in batch cultures of Chinese hamster ovary cells. *Journal of Biotechnology*, 138(3-4), pp.103-106.

Majors, B.S., Betenbaugh, M.J. and Chiang, G.G. 2007. Links between metabolism and apoptosis in mammalian cells: applications for anti-apoptosis engineering. *Metabolic Engineering*, 9(4), pp.317-326.

Malumbres, M. and Barbacid, M. 2009. Cell cycle, CDKs and cancer: a changing paradigm. *Nature Reviews.Cancer,* 9(3), pp.153-166.

Mann, M. 2006. Functional and quantitative proteomics using SILAC. *Nature Reviews Molecular Cell Biology*, 7pp.952-958.

Maragkakis, M., Reczko, M., Simossis, V.A., Alexiou, P., Papadopoulos, G.L., Dalamagas, T., Giannopoulos, G., Goumas, G., Koukis, E., Kourtis, K., Vergoulis, T., Koziris, N., Sellis, T., Tsanakas, P. and Hatzigeorgiou, A.G. 2009. DIANA-microT web server: elucidating microRNA functions through target prediction. *Nucleic Acids Research*, 37(Web Server issue), pp.W273-6.

Martinez, N.J., Ow, M.C., Barrasa, M.I., Hammell, M., Sequerra, R., Doucette-Stamm, L., Roth, F.P., Ambros, V.R. and Walhout, A.J. 2008. A C. elegans genome-scale microRNA network contains composite feedback motifs with high flux capacity. *Genes & Development,* 22(18), pp.2535-2549.

Maselli, V., Di Bernardo, D. and Banfi, S. 2008. CoGemiR: a comparative genomics microRNA database. *BMC Genomics*, 9pp.457.

Masson, P., Lundgren, J. and Young, P. 2003. Drosophila proteasome regulator REGgamma: transcriptional activation by DNA replication-related factor DREF and

evidence for a role in cell cycle progression. *Journal of Molecular Biology,* 327(5), pp.1001-1012.

Matranga, C., Tomari, Y., Shin, C., Bartel, D.P. and Zamore, P.D. 2005. Passenger-strand cleavage facilitates assembly of siRNA into Ago2-containing RNAi enzyme complexes. *Cell,* 123(4), pp.607-620.

Mayo, L.D. and Donner, D.B. 2001. A phosphatidylinositol 3-kinase/Akt pathway promotes translocation of Mdm2 from the cytoplasm to the nucleus. *Proceedings of the National Academy of Sciences of the United States of America,* 98(20), pp.11598-11603.

Mayr, C. and Bartel, D.P. 2009. Widespread shortening of 3'UTRs by alternative cleavage and polyadenylation activates oncogenes in cancer cells. *Cell,* 138(4), pp.673-684.

Mazur, X., Fussenegger, M., Renner, W.A. and Bailey, J.E. 1998. Higher productivity of growth-arrested Chinese hamster ovary cells expressing the cyclin-dependent kinase inhibitor p27. *Biotechnology Progress,* 14(5), pp.705-713.

McBride, J.L., Boudreau, R.L., Harper, S.Q., Staber, P.D., Monteys, A.M., Martins, I., Gilmore, B.L., Burstein, H., Peluso, R.W., Polisky, B., Carter, B.J. and Davidson, B.L. 2008. Artificial miRNAs mitigate shRNA-mediated toxicity in the brain: implications for the therapeutic development of RNAi. *Proceedings of the National Academy of Sciences of the United States of America,* 105(15), pp.5868-5873.

McInnes, N., Sadlon, T.J., Brown, C.Y., Pederson, S., Beyer, M., Schultze, J.L., McColl, S., Goodall, G.J. and Barry, S.C. 2012. FOXP3 and FOXP3-regulated microRNAs suppress SATB1 in breast cancer cells. *Oncogene,* 31(8), pp.1045-1054.

McInnes, N., Sadlon, T.J., Brown, C.Y., Pederson, S., Beyer, M., Schultze, J.L., McColl, S., Goodall, G.J. and Barry, S.C. 2011. FOXP3 and FOXP3-regulated microRNAs suppress SATB1 in breast cancer cells. *Oncogene,*

McManus, M.T., Petersen, C.P., Haines, B.B., Chen, J. and Sharp, P.A. 2002. Gene silencing using micro-RNA designed hairpins. *RNA (New York, N.Y.),* 8(6), pp.842-850.

McManus, M.T. and Sharp, P.A. 2002. Gene silencing in mammals by small interfering RNAs. *Nature Reviews.Genetics,* 3(10), pp.737-747.

Meents, H., Enenkel, B., Eppenberger, H.M., Werner, R.G. and Fussenegger, M. 2002. Impact of coexpression and coamplification of sICAM and antiapoptosis determinants bcl-2/bcl-x(L) on productivity, cell survival, and mitochondria number in CHO-DG44 grown in suspension and serum-free media. *Biotechnology and Bioengineering,* 80(6), pp.706-716.

Meister, G., Landthaler, M., Dorsett, Y. and Tuschl, T. 2004. Sequence-specific inhibition of microRNA- and siRNA-induced RNA silencing. *Rna-a Publication of the Rna Society,* 10(3), pp.544-550.

Meister, G., Landthaler, M., Peters, L., Chen, P.Y., Urlaub, H., Luhrmann, R. and Tuschl, T. 2005. Identification of novel argonaute-associated proteins. *Current Biology : CB,* 15(23), pp.2149-2155.

Meleady, P., Gallagher, M., Clarke, C., Henry, M., Sanchez, N., Barron, N. and Clynes, M. 2012. Impact of miR-7 over-expression on the proteome of Chinese hamster ovary cells. *Journal of Biotechnology,* 160(3-4), pp.251-262.

Mendez, J., Zou-Yang, X.H., Kim, S.Y., Hidaka, M., Tansey, W.P. and Stillman, B. 2002. Human origin recognition complex large subunit is degraded by ubiquitin-mediated proteolysis after initiation of DNA replication. *Molecular Cell,* 9(3), pp.481-491.

Merrihew, R.V., Clay, W.C., Condreay, J.P., Witherspoon, S.M., Dallas, W.S. and Kost, T.A. 2001. Chromosomal integration of transduced recombinant baculovirus DNA in mammalian cells. *Journal of Virology,* 75(2), pp.903-909.

Mertens-Talcott, S.U., Chintharlapalli, S., Li, X. and Safe, S. 2007. The oncogenic microRNA-27a targets genes that regulate specificity protein transcription factors and the G2-M checkpoint in MDA-MB-231 breast cancer cells. *Cancer Research,* 67(22), pp.11001-11011.

Michienzi, A., Cagnon, L., Bahner, I. and Rossi, J.J. 2000. Ribozyme-mediated inhibition of HIV 1 suggests nucleolar trafficking of HIV-1 RNA. *Proceedings of the National Academy of Sciences of the United States of America,* 97(16), pp.8955-8960.

Milo, R., Shen-Orr, S., Itzkovitz, S., Kashtan, N., Chklovskii, D. and Alon, U. 2002. Network motifs: Simple building blocks of complex networks. *Science,* 298(5594), pp.824-827.

Min, H. and Yoon, S. 2010. Got target?: computational methods for microRNA target prediction and their extension. *Experimental and Molecular Medicine,* 42(4), pp.233-244.

Mishra, P.J., Humeniuk, R., Mishra, P.J., Longo-Sorbello, G.S.A., Banerjee, D. and Bertino, J.R. 2007. A miR-24 microRNA binding-site polymorphism in dihydrofolate reductase gene leads to methotrexate resistance. *Proceedings of the National Academy of Sciences of the United States of America,* 104(33), pp.13513-13518.

Mishra, P.J., Song, B., Mishra, P.J., Wang, Y., Humeniuk, R., Banerjee, D., Merlino, G., Ju, J. and Bertino, J.R. 2009. MiR-24 Tumor Suppressor Activity Is Regulated Independent of p53 and through a Target Site Polymorphism. *Plos One,* 4(12), pp.e8445.

Mohan, C., Kim, Y.G., Koo, J. and Lee, G.M. 2008. Assessment of cell engineering strategies for improved therapeutic protein production in CHO cells. *Biotechnology Journal,* 3(5), pp.624-630.

Mori, K., Kuni-Kamochi, R., Yamane-Ohnuki, N., Wakitani, M., Yamano, K., Imai, H., Kanda, Y., Niwa, R., Iida, S., Uchida, K., Shitara, K. and Satoh, M. 2004. Engineering Chinese hamster ovary cells to maximize effector function of produced antibodies using FUT8 siRNA. *Biotechnology and Bioengineering,* 88(7), pp.901-908.

Morin, R.D., O'Connor, M.D., Griffith, M., Kuchenbauer, F., Delaney, A., Prabhu, A.L., Zhao, Y., McDonald, H., Zeng, T., Hirst, M., Eaves, C.J. and Marra, M.A. 2008. Application of massively parallel sequencing to microRNA profiling and discovery in human embryonic stem cells. *Genome Research,* 18(4), pp.610-621.

Morozova, O. and Marra, M.A. 2008. Applications of next-generation sequencing technologies in functional genomics. *Genomics*, 92(5), pp.255-264.

Mourelatos, Z., Dostie, J., Paushkin, S., Sharma, A., Charroux, B., Abel, L., Rappsilber, J., Mann, M. and Dreyfuss, G. 2002. miRNPs: a novel class of ribonucleoproteins containing numerous microRNAs. *Genes & Development,* 16(6), pp.720-728.

Muller, D., Katinger, H. and Grillari, J. 2008. MicroRNAs as targets for engineering of CHO cell factories. *Trends in Biotechnology*, 26(7), pp.359-365.

Muniyappa MK, FAU - Dowling, P., Dowling P, FAU - Henry, M., Henry M, FAU - Meleady, P., Meleady P, FAU - Doolan, P., Doolan P, FAU - Gammell, P., Gammell P, FAU - Clynes, M., Clynes M, FAU - Barron, N. and Barron N. MiRNA-29a regulates the expression of numerous proteins and reduces the invasiveness and proliferation of human carcinoma cell lines. - *Eur J Cancer.2009 Nov;45(17):3104-18.Epub 2009 Oct 7.*, (1879-0852 (Electronic); 0959-8049 (Linking)),

Murata, S., Kawahara, H., Tohma, S., Yamamoto, K., Kasahara, M., Nabeshima, Y., Tanaka, K. and Chiba, T. 1999. Growth retardation in mice lacking the proteasome activator PA28gamma. *The Journal of Biological Chemistry*, 274(53), pp.38211-38215.

Neildez-Nguyen, T.M., Parisot, A., Vignal, C., Rameau, P., Stockholm, D., Picot, J., Allo, V., Le Bec, C., Laplace, C. and Paldi, A. 2008. Epigenetic gene expression noise and phenotypic diversification of clonal cell populations. *Differentiation; Research in Biological Diversity*, 76(1), pp.33-40.

Nelson, A.L., Dhimolea, E. and Reichert, J.M. 2010. Development trends for human monoclonal antibody therapeutics. *Nature Reviews.Drug Discovery,* 9(10), pp.767-774.

Newland, M., Kamal, M.N., Greenfield, P.F. and Nielsen, L.K. 1994. Ammonia inhibition of hybridomas propagated in batch, fed-batch, and continuous culture. *Biotechnology and Bioengineering*, 43(5), pp.434-438.

Newman, M.A. and Hammond, S.M. 2010. Lin-28: an early embryonic sentinel that blocks Let-7 biogenesis. *The International Journal of Biochemistry & Cell Biology*, 42(8), pp.1330-1333.

Nieto, M., Hevia, P., Garcia, E., Klein, D., Alvarez-Cubela, S., Bravo-Egana, V., Rosero, S., Molano, R.D., Vargas, N., Ricordi, C., Pileggi, A., Diez, J., Dominguez-Bendala, J. and Pastori, R.L. 2011. Anti sense miR-7 impairs insulin expression in developing pancreas and in cultured pancreatic buds. *Cell Transplantation,*

Nishiyama, H., Higashitsuji, H., Yokoi, H., Itoh, K., Danno, S., Matsuda, T. and Fujita, J. 1997a. Cloning and characterization of human CIRP (cold-inducible RNA-binding protein) cDNA and chromosomal assignment of the gene. *Gene,* 204(1-2), pp.115-120.

Nishiyama, H., Itoh, K., Kaneko, Y., Kishishita, M., Yoshida, O. and Fujita, J. 1997b. A glycine-rich RNA-binding protein mediating cold-inducible suppression of mammalian cell growth. *Journal of Cell Biology,* 137(4), pp.899-908.

Nobuta, K., McCormick, K., Nakano, M. and Meyers, B.C. 2010. Bioinformatics analysis of small RNAs in plants using next generation sequencing technologies. *Methods in Molecular Biology (Clifton, N.J.),* 592pp.89-106.

Nohata, N., Hanazawa, T., Kikkawa, N., Sakurai, D., Fujimura, L., Chiyomaru, T., Kawakami, K., Yoshino, H., Enokida, H., Nakagawa, M., Katayama, A., Harabuchi, Y., Okamoto, Y. and Seki, N. 2011. Tumour suppressive microRNA-874 regulates novel cancer networks in maxillary sinus squamous cell carcinoma. *British Journal of Cancer,* 105(6), pp.833-841.

Obaya, A.J., Mateyak, M.K. and Sedivy, J.M. 1999. Mysterious liaisons: the relationship between c-Myc and the cell cycle. *Oncogene,* 18(19), pp.2934-2941.

O'Connell, M.A. and Keegan, L.P. 2006. Drosha versus ADAR: wrangling over pri-miRNA. *Nature Structural & Molecular Biology,* 13(1), pp.3-4.

O'Donnell, K.A., Wentzel, E.A., Zeller, K.I., Dang, C.V. and Mendell, J.T. 2005. c-Myc-regulated microRNAs modulate E2F1 expression. *Nature,* 435(7043), pp.839-843.

Oguchi, S., Saito, H., Tsukahara, M. and Tsumura, H. 2006. pH Condition in temperature shift cultivation enhances cell longevity and specific hMab productivity in CHO culture. *Cytotechnology,* 52(3), pp.199-207.

Ohya, T., Hayashi, T., Kiyama, E., Nishii, H., Miki, H., Kobayashi, K., Honda, K., Omasa, T. and Ohtake, H. 2008. Improved production of recombinant human antithrombin III in Chinese hamster ovary cells by ATF4 overexpression. *Biotechnology and Bioengineering*, 100(2), pp.317-324.

Okamura, K., Phillips, M.D., Tyler, D.M., Duan, H., Chou, Y.T. and Lai, E.C. 2008. The regulatory activity of microRNA* species has substantial influence on microRNA and 3' UTR evolution. *Nature Structural & Molecular Biology*, 15(4), pp.354-363.

Olena, A.F. and Patton, J.G. 2010. Genomic organization of microRNAs. *Journal of Cellular Physiology*, 222(3), pp.540-545.

Omasa, T., Takami, T., Ohya, T., Kiyama, E., Hayashi, T., Nishii, H., Miki, H., Kobayashi, K., Honda, K. and Ohtake, H. 2008. Overexpression of GADD34 enhances production of recombinant human antithrombin III in Chinese hamster ovary cells. *Journal of Bioscience and Bioengineering*, 106(6), pp.568-573.

Orlando, S.J., Santiago, Y., DeKelver, R.C., Freyvert, Y., Boydston, E.A., Moehle, E.A., Choi, V.M., Gopalan, S.M., Lou, J.F., Li, J., Miller, J.C., Holmes, M.C., Gregory, P.D., Urnov, F.D. and Cost, G.J. 2010. Zinc-finger nuclease-driven targeted integration into mammalian genomes using donors with limited chromosomal homology. *Nucleic Acids Research*, 38(15), pp.e152.

Orom, U.A., Nielsen, F.C. and Lund, A.H. 2008. MicroRNA-10a binds the 5'UTR of ribosomal protein mRNAs and enhances their translation. *Molecular Cell*, 30(4), pp.460-471.

Osthus, R.C., Shim, H., Kim, S., Li, Q., Reddy, R., Mukherjee, M., Xu, Y., Wonsey, D., Lee, L.A. and Dang, C.V. 2000. Deregulation of glucose transporter 1 and glycolytic gene expression by c-Myc. *The Journal of Biological Chemistry*, 275(29), pp.21797-21800.

Ovcharenko, D., Kelnar, K., Johnson, C., Leng, N. and Brown, D. 2007. Genome-scale microRNA and small interfering RNA screens identify small RNA modulators of TRAIL-induced apoptosis pathway. *Cancer Research*, 67(22), pp.10782-10788.

Overhoff, M., Alken, M., Far, R.K., Lemaitre, M., Lebleu, B., Sczakiel, G. and Robbins, I. 2005. Local RNA target structure influences siRNA efficacy: a systematic global analysis. *Journal of Molecular Biology*, 348(4), pp.871-881.

Pallavicini, M.G., DeTeresa, P.S., Rosette, C., Gray, J.W. and Wurm, F.M. 1990. Effects of methotrexate on transfected DNA stability in mammalian cells. *Molecular and Cellular Biology*, 10(1), pp.401-404.

Pan, X., Wang, Z.X. and Wang, R. 2011. MicroRNA-21: a novel therapeutic target in human cancer. *Cancer Biology & Therapy*, 10(12), pp.1224-1232.

Papageorgiou, N., Tousoulis, D., Androulakis, E., Siasos, G., Briasoulis, A., Vogiatzi, G., Kampoli, A.M., Tsiamis, E., Tentolouris, C. and Stefanadis, C. 2012. The role of microRNAs in cardiovascular disease. *Current Medicinal Chemistry*, 19(16), pp.2605-2610.

Papagiannakopoulos, T., Shapiro, A. and Kosik, K.S. 2008. MicroRNA-21 targets a network of key tumor-suppressive pathways in glioblastoma cells. *Cancer Research*, 68(19), pp.8164-8172.

Park, H., Kim, I.H., Kim, I.Y., Kim, K.H. and Kim, H.J. 2000. Expression of carbamoyl phosphate synthetase I and ornithine transcarbamoylase genes in Chinese hamster ovary dhfr-cells decreases accumulation of ammonium ion in culture media. *Journal of Biotechnology*, 81(2-3), pp.129-140.

Pasquinelli, A.E., Reinhart, B.J., Slack, F., Martindale, M.Q., Kuroda, M.I., Maller, B., Hayward, D.C., Ball, E.E., Degnan, B., Muller, P., Spring, J., Srinivasan, A., Fishman, M., Finnerty, J., Corbo, J., Levine, M., Leahy, P., Davidson, E. and Ruvkun, G. 2000. Conservation of the sequence and temporal expression of let-7 heterochronic regulatory RNA. *Nature*, 408(6808), pp.86-89.

Pavletich, N.P. and Pabo, C.O. 1991. Zinc finger-DNA recognition: crystal structure of a Zif268-DNA complex at 2.1 A. *Science (New York, N.Y.)*, 252(5007), pp.809-817.

Pekarsky, Y., Santanam, U., Cimmino, A., Palamarchuk, A., Efanov, A., Maximov, V., Volinia, S., Alder, H., Liu, C.G., Rassenti, L., Calin, G.A., Hagan, J.P., Kipps, T. and

Croce, C.M. 2006. Tcl1 expression in chronic lymphocytic leukemia is regulated by miR-29 and miR-181. *Cancer Research,* 66(24), pp.11590-11593.

Peng, G., Yuan, Y., He, Q., Wu, W. and Luo, B.Y. 2011. MicroRNA let-7e regulates the expression of caspase-3 during apoptosis of PC12 cells following anoxia/reoxygenation injury. *Brain Research Bulletin,* 86(3-4), pp.272-276.

Peng, R.W. and Fussenegger, M. 2009. Molecular engineering of exocytic vesicle traffic enhances the productivity of Chinese hamster ovary cells. *Biotechnology and Bioengineering,* 102(4), pp.1170-1181.

Persson, K., Hamby, K. and Ugozzoli, L.A. 2005. Four-color multiplex reverse transcription polymerase chain reaction--overcoming its limitations. *Analytical Biochemistry,* 344(1), pp.33-42.

Peruzzi, F., Prisco, M., Dews, M., Salomoni, P., Grassilli, E., Romano, G., Calabretta, B. and Baserga, R. 1999. Multiple signaling pathways of the insulin-like growth factor 1 receptor in protection from apoptosis. *Molecular and Cellular Biology,* 19(10), pp.7203-7215.

Peter, M.E. 2010. Targeting of mRNAs by multiple miRNAs: the next step. *Oncogene,* 29(15), pp.2161-2164.

Peters, L. and Meister, G. 2007. Argonaute proteins: mediators of RNA silencing. *Molecular Cell,* 26(5), pp.611-623.

Petrocca, F., Visone, R., Onelli, M.R., Shah, M.H., Nicoloso, M.S., de Martino, I., Iliopoulos, D., Pilozzi, E., Liu, C.G., Negrini, M., Cavazzini, L., Volinia, S., Alder, H., Ruco, L.P., Baldassarre, G., Croce, C.M. and Vecchione, A. 2008. E2F1-regulated microRNAs impair TGFbeta-dependent cell-cycle arrest and apoptosis in gastric cancer. *Cancer Cell,* 13(3), pp.272-286.

Pichler, J., Galosy, S., Mott, J. and Borth, N. 2011. Selection of CHO host cell subclones with increased specific antibody production rates by repeated cycles of transient transfection and cell sorting. *Biotechnology and Bioengineering,* 108(2), pp.386-394.

Pilbrough, W., Munro, T.P. and Gray, P. 2009. Intraclonal protein expression heterogeneity in recombinant CHO cells. *PloS One,* 4(12), pp.e8432.

Pillai, R.S. 2005. MicroRNA function: multiple mechanisms for a tiny RNA? *RNA (New York, N.Y.),* 11(12), pp.1753-1761.

Poliseno, L., Salmena, L., Zhang, J., Carver, B., Haveman, W.J. and Pandolfi, P.P. 2010. A coding-independent function of gene and pseudogene mRNAs regulates tumour biology. *Nature,* 465(7301), pp.1033-U90.

Pollak, M. 2008. Insulin and insulin-like growth factor signalling in neoplasia. *Nature Reviews.Cancer,* 8(12), pp.915-928.

Pothof, J., Verkaik, N.S., van IJcken, W., Wiemer, E.A.C., Ta, V.T.B., van der Horst, G.T.J., Jaspers, N.G.J., van Gent, D.C., Hoeijmakers, J.H.J. and Persengiev, S.P. 2009. MicroRNA-mediated gene silencing modulates the UV-induced DNA-damage response. *Embo Journal,* 28(14), pp.2090-2099.

Prochnik, S.E., Rokhsar, D.S. and Aboobaker, A.A. 2007. Evidence for a microRNA expansion in the bilaterian ancestor. *Development Genes and Evolution,* 217(1), pp.73-77.

PUCK, T.T. 1957. The genetics of somatic mammalian cells. *Advances in Biological and Medical Physics,* 5pp.75-101.

Qin, W., Shi, Y., Zhao, B., Yao, C., Jin, L., Ma, J. and Jin, Y. 2010. miR-24 regulates apoptosis by targeting the open reading frame (ORF) region of FAF1 in cancer cells. *PloS One,* 5(2), pp.e9429.

Rajewsky, N. 2011. MicroRNAs and the Operon paper. *Journal of Molecular Biology,* 409(1), pp.70-75.

Ramachandran, V. and Chen, X. 2008. Degradation of microRNAs by a family of exoribonucleases in Arabidopsis. *Science (New York, N.Y.),* 321(5895), pp.1490-1492.

Ramunas, J., Montgomery, H.J., Kelly, L., Sukonnik, T., Ellis, J. and Jervis, E.J. 2007. Real-time fluorescence tracking of dynamic transgene variegation in stem cells.

Molecular Therapy : The Journal of the American Society of Gene Therapy, 15(4), pp.810-817.

Rand, T.A., Petersen, S., Du, F. and Wang, X. 2005. Argonaute2 cleaves the anti-guide strand of siRNA during RISC activation. *Cell,* 123(4), pp.621-629.

Ratcliff, F.G., MacFarlane, S.A. and Baulcombe, D.C. 1999. Gene silencing without DNA. rna-mediated cross-protection between viruses. *The Plant Cell,* 11(7), pp.1207-1216.

Rehmsmeier, M., Steffen, P., Hochsmann, M. and Giegerich, R. 2004. Fast and effective prediction of microRNA/target duplexes. *RNA (New York, N.Y.),* 10(10), pp.1507-1517.

Reinhart, B.J., Slack, F.J., Basson, M., Pasquinelli, A.E., Bettinger, J.C., Rougvie, A.E., Horvitz, H.R. and Ruvkun, G. 2000. The 21-nucleotide let-7 RNA regulates developmental timing in Caenorhabditis elegans. *Nature,* 403(6772), pp.901-906.

Ren, J., Wang, Y., Liang, Y., Zhang, Y., Bao, S. and Xu, Z. 2010. Methylation of ribosomal protein S10 by protein-arginine methyltransferase 5 regulates ribosome biogenesis. *The Journal of Biological Chemistry,* 285(17), pp.12695-12705.

Renner, W.A., Lee, K.H., Hatzimanikatis, V., Bailey, J.E. and Eppenberger, H.M. 1995. Recombinant cyclin E expression activates proliferation and obviates surface attachment of chinese hamster ovary (CHO) cells in protein-free medium. *Biotechnology and Bioengineering,* 47(4), pp.476-482.

Restelli, V., Wang, M.D., Huzel, N., Ethier, M., Perreault, H. and Butler, M. 2006. The effect of dissolved oxygen on the production and the glycosylation profile of recombinant human erythropoietin produced from CHO cells. *Biotechnology and Bioengineering,* 94(3), pp.481-494.

Reuter, G. and Gabius, H.J. 1999. Eukaryotic glycosylation: whim of nature or multipurpose tool? *Cellular and Molecular Life Sciences : CMLS,* 55(3), pp.368-422.

Rhoades, M.W., Reinhart, B.J., Lim, L.P., Burge, C.B., Bartel, B. and Bartel, D.P. 2002. Prediction of plant microRNA targets. *Cell,* 110(4), pp.513-520.

Ritchie, W., Flamant, S. and Rasko, J.E.J. 2009. Predicting microRNA targets and functions: traps for the unwary. *Nature Methods,* 6(6), pp.397-398.

Ro, S., Park, C., Young, D., Sanders, K.M. and Yan, W. 2007. Tissue-dependent paired expression of miRNAs. *Nucleic Acids Research,* 35(17), pp.5944-5953.

Rodrigues, M.E., Costa, A.R., Henriques, M., Azeredo, J. and Oliveira, R. 2010. Technological progresses in monoclonal antibody production systems. *Biotechnology Progress,* 26(2), pp.332-351.

Rodriguez, A., Griffiths-Jones, S., Ashurst, J.L. and Bradley, A. 2004. Identification of mammalian microRNA host genes and transcription units. *Genome Research,* 14(10A), pp.1902-1910.

Roessler, M., Rollinger, W., Mantovani-Endl, L., Hagmann, M.L., Palme, S., Berndt, P., Engel, A.M., Pfeffer, M., Karl, J., Bodenmuller, H., Ruschoff, J., Henkel, T., Rohr, G., Rossol, S., Rosch, W., Langen, H., Zolg, W. and Tacke, M. 2006. Identification of PSME3 as a novel serum tumor marker for colorectal cancer by combining two-dimensional polyacrylamide gel electrophoresis with a strictly mass spectrometry-based approach for data analysis. *Molecular & Cellular Proteomics : MCP,* 5(11), pp.2092-2101.

Romano, N. and Macino, G. 1992. Quelling: transient inactivation of gene expression in Neurospora crassa by transformation with homologous sequences. *Molecular Microbiology,* 6(22), pp.3343-3353.

Roush, S. and Slack, F.J. 2008. The let-7 family of microRNAs. *Trends in Cell Biology,* 18(10), pp.505-516.

Ruby, J.G., Jan, C.H. and Bartel, D.P. 2007. Intronic microRNA precursors that bypass Drosha processing. *Nature,* 448(7149), pp.83-86.

Ruby, J.G., Stark, A., Johnston, W.K., Kellis, M., Bartel, D.P. and Lai, E.C. 2007. Evolution, biogenesis, expression, and target predictions of a substantially expanded set of Drosophila microRNAs. *Genome Research,* 17(12), pp.1850-1864.

Rutkowski, D.T. and Kaufman, R.J. 2004. A trip to the ER: coping with stress. *Trends in Cell Biology,* 14(1), pp.20-28.

Sacco, J. and Adeli, K. 2012. MicroRNAs: emerging roles in lipid and lipoprotein metabolism. *Current Opinion in Lipidology,* 23(3), pp.220-225.

Sadowski, P.D. 1993. Site-specific genetic recombination: hops, flips, and flops. *FASEB Journal : Official Publication of the Federation of American Societies for Experimental Biology,* 7(9), pp.760-767.

Saini, H.K., Enright, A.J. and Griffiths-Jones, S. 2008. Annotation of mammalian primary microRNAs. *BMC Genomics,* 9pp.564.

Saini, H.K., Griffiths-Jones, S. and Enright, A.J. 2007. Genomic analysis of human microRNA transcripts. *Proceedings of the National Academy of Sciences of the United States of America,* 104(45), pp.17719-17724.

Saleh, A.D., Savage, J.E., Cao, L., Soule, B.P., Ly, D., DeGraff, W., Harris, C.C., Mitchell, J.B. and Simone, N.L. 2011. Cellular stress induced alterations in microRNA let-7a and let-7b expression are dependent on p53. *PloS One,* 6(10), pp.e24429.

Sancar, A., Lindsey-Boltz, L.A., Unsal-Kacmaz, K. and Linn, S. 2004. Molecular mechanisms of mammalian DNA repair and the DNA damage checkpoints. *Annual Review of Biochemistry,* 73pp.39-85.

Sandberg, R., Neilson, J.R., Sarma, A., Sharp, P.A. and Burge, C.B. 2008. Proliferating cells express mRNAs with shortened 3' untranslated regions and fewer microRNA target sites. *Science (New York, N.Y.),* 320(5883), pp.1643-1647.

Sandelin, A., Carninci, P., Lenhard, B., Ponjavic, J., Hayashizaki, Y. and Hume, D.A. 2007. Mammalian RNA polymerase II core promoters: insights from genome-wide studies. *Nature Reviews.Genetics,* 8(6), pp.424-436.

Sarras, H., Alizadeh Azami, S. and McPherson, J.P. 2010. In search of a function for BCLAF1. *TheScientificWorldJournal,* 10pp.1450-1461.

Sato, G., Fisher, H.W. and Puck, T.T. 1957. Molecular Growth Requirements of Single Mammalian Cells. *Science (New York, N.Y.),* 126(3280), pp.961-964.

Sauerwald, T.M., Betenbaugh, M.J. and Oyler, G.A. 2002. Inhibiting apoptosis in mammalian cell culture using the caspase inhibitor XIAP and deletion mutants. *Biotechnology and Bioengineering,* 77(6), pp.704-716.

Sauerwald, T.M., Oyler, G.A. and Betenbaugh, M.J. 2003. Study of caspase inhibitors for limiting death in mammalian cell culture. *Biotechnology and Bioengineering,* 81(3), pp.329-340.

Saydam, O., Senol, O., Wurdinger, T., Mizrak, A., Ozdener, G.B., Stemmer-Rachamimov, A.O., Yi, M., Stephens, R.M., Krichevsky, A.M., Saydam, N., Brenner, G.J. and Breakefield, X.O. 2011. miRNA-7 attenuation in Schwannoma tumors stimulates growth by upregulating three oncogenic signaling pathways. *Cancer Research,* 71(3), pp.852-861.

Scadden, A.D. and Smith, C.W. 2001. Specific cleavage of hyper-edited dsRNAs. *The EMBO Journal,* 20(15), pp.4243-4252.

Scherr, M., Venturini, L., Battmer, K., Schaller-Schoenitz, M., Schaefer, D., Dallmann, I., Ganser, A. and Eder, M. 2007. Lentivirus-mediated antagomir expression for specific inhibition of miRNA function. *Nucleic Acids Research,* 35(22), pp.e149.

Schmittgen, T.D., Jiang, J., Liu, Q. and Yang, L. 2004. A high-throughput method to monitor the expression of microRNA precursors. *Nucleic Acids Research,* 32(4), pp.e43.

Schmittgen, T.D., Lee, E.J., Jiang, J., Sarkar, A., Yang, L., Elton, T.S. and Chen, C. 2008. Real-time PCR quantification of precursor and mature microRNA. *Methods (San Diego, Calif.),* 44(1), pp.31-38.

Schweikart, F., Jones, R., Jaton, J.C. and Hughes, G.J. 1999. Rapid structural characterisation of a murine monoclonal IgA alpha chain: heterogeneity in the oligosaccharide structures at a specific site in samples produced in different bioreactor systems. *Journal of Biotechnology,* 69(2-3), pp.191-201.

Selbach, M., Schwanhausser, B., Thierfelder, N., Fang, Z., Khanin, R. and Rajewsky, N. 2008. Widespread changes in protein synthesis induced by microRNAs. *Nature*, 455(7209), pp.58-63.

Sempere, L.F., Dubrovsky, E.B., Dubrovskaya, V.A., Berger, E.M. and Ambros, V. 2002. The expression of the let-7 small regulatory RNA is controlled by ecdysone during metamorphosis in Drosophila melanogaster. *Developmental Biology*, 244(1), pp.170-179.

Sempere, L.F., Freemantle, S., Pitha-Rowe, I., Moss, E., Dmitrovsky, E. and Ambros, V. 2004. Expression profiling of mammalian microRNAs uncovers a subset of brain-expressed microRNAs with possible roles in murine and human neuronal differentiation. *Genome Biology*, 5(3), pp.R13.

Sempere, L.F., Sokol, N.S., Dubrovsky, E.B., Berger, E.M. and Ambros, V. 2003. Temporal regulation of microRNA expression in Drosophila melanogaster mediated by hormonal signals and broad-Complex gene activity. *Developmental Biology*, 259(1), pp.9-18.

Sen, G.L. and Blau, H.M. 2005. Argonaute 2/RISC resides in sites of mammalian mRNA decay known as cytoplasmic bodies. *Nature Cell Biology*, 7(6), pp.633-636.

Sethi, P. and Lukiw, W.J. 2009. Micro-RNA abundance and stability in human brain: specific alterations in Alzheimer's disease temporal lobe neocortex. *Neuroscience Letters*, 459(2), pp.100-104.

Shahab, S.W., Matyunina, L.V., Hill, C.G., Wang, L., Mezencev, R., Walker, L.D. and McDonald, J.F. 2012. The effects of MicroRNA transfections on global patterns of gene expression in ovarian cancer cells are functionally coordinated. *BMC Medical Genomics*, 5(1), pp.33-8794-5-33.

Shalgi, R., Lieber, D., Oren, M. and Pilpel, Y. 2007. Global and local architecture of the mammalian microRNA-transcription factor regulatory network. *PLoS Computational Biology*, 3(7), pp.e131.

Sheeley, D.M., Merrill, B.M. and Taylor, L.C. 1997. Characterization of monoclonal antibody glycosylation: comparison of expression systems and identification of terminal alpha-linked galactose. *Analytical Biochemistry,* 247(1), pp.102-110.

Shendure, J. and Church, G.M. 2002. Computational discovery of sense-antisense transcription in the human and mouse genomes. *Genome Biology,* 3(9), pp.RESEARCH0044.

Shen-Orr, S.S., Milo, R., Mangan, S. and Alon, U. 2002. Network motifs in the transcriptional regulation network of Escherichia coli. *Nature Genetics,* 31(1), pp.64-68.

Shi, J., Chatterjee, N., Rotunno, M., Wang, Y., Pesatori, A.C., Consonni, D., Li, P., Wheeler, W., Broderick, P., Henrion, M., Eisen, T., Wang, Z., Chen, W., Dong, Q., Albanes, D., Thun, M., Spitz, M.R., Bertazzi, P.A., Caporaso, N.E., Chanock, S.J., Amos, C.I., Houlston, R.S. and Landi, M.T. 2012. Inherited variation at chromosome 12p13.33, including RAD52, influences the risk of squamous cell lung carcinoma. *Cancer Discovery,* 2(2), pp.131-139.

Shi, W., Fan, H., Shum, L. and Derynck, R. 2000. The tetraspanin CD9 associates with transmembrane TGF-alpha and regulates TGF-alpha-induced EGF receptor activation and cell proliferation. *The Journal of Cell Biology,* 148(3), pp.591-602.

Shin, C., Nam, J.W., Farh, K.K., Chiang, H.R., Shkumatava, A. and Bartel, D.P. 2010. Expanding the microRNA targeting code: functional sites with centered pairing. *Molecular Cell,* 38(6), pp.789-802.

Silva, G., Poirot, L., Galetto, R., Smith, J., Montoya, G., Duchateau, P. and Paques, F. 2011. Meganucleases and other tools for targeted genome engineering: perspectives and challenges for gene therapy. *Current Gene Therapy,* 11(1), pp.11-27.

Sirotkin, A.V., Laukova, M., Ovcharenko, D., Brenaut, P. and Mlyncek, M. 2010. Identification of microRNAs controlling human ovarian cell proliferation and apoptosis. *Journal of Cellular Physiology,* 223(1), pp.49-56.

Sistrunk, C., Macias, E., Nakayama, K., Kim, Y. and Rodriguez-Puebla, M.L. 2011. Skp2 is necessary for Myc-induced keratinocyte proliferation but dispensable for Myc

oncogenic activity in the oral epithelium. *The American Journal of Pathology,* 178(6), pp.2470-2477.

Slack, F.J. and Weidhaas, J.B. 2006. MicroRNAs as a potential magic bullet in cancer. *Future Oncology (London, England),* 2(1), pp.73-82.

Smith, K. 2001. Theoretical mechanisms in targeted and random integration of transgene DNA. *Reproduction, Nutrition, Development,* 41(6), pp.465-485.

Soutschek, J., Akinc, A., Bramlage, B., Charisse, K., Constien, R., Donoghue, M., Elbashir, S., Geick, A., Hadwiger, P., Harborth, J., John, M., Kesavan, V., Lavine, G., Pandey, R.K., Racie, T., Rajeev, K.G., Rohl, I., Toudjarska, I., Wang, G., Wuschko, S., Bumcrot, D., Koteliansky, V., Limmer, S., Manoharan, M. and Vornlocher, H.P. 2004. Therapeutic silencing of an endogenous gene by systemic administration of modified siRNAs. *Nature,* 432(7014), pp.173-178.

Stark, A., Brennecke, J., Bushati, N., Russell, R.B. and Cohen, S.M. 2005. Animal microRNAs confer robustness to gene expression and have a significant impact on 3 ' UTR evolution. *Cell,* 123(6), pp.1133-1146.

Stark, A., Brennecke, J., Russell, R.B. and Cohen, S.M. 2003. Identification of Drosophila MicroRNA targets. *PLoS Biology,* 1(3), pp.E60.

Sun, J., Gong, X., Purow, B. and Zhao, Z. 2012. Uncovering MicroRNA and Transcription Factor Mediated Regulatory Networks in Glioblastoma. *PLoS Computational Biology,* 8(7), pp.e1002488.

Sung, Y.H., Hwang, S.J. and Lee, G.M. 2005. Influence of down-regulation of caspase-3 by siRNAs on sodium-butyrate-induced apoptotic cell death of Chinese hamster ovary cells producing thrombopoietin. *Metabolic Engineering,* 7(5-6), pp.457-466.

Sung, Y.H., Lee, J.S., Park, S.H., Koo, J. and Lee, G.M. 2007. Influence of co-down-regulation of caspase-3 and caspase-7 by siRNAs on sodium butyrate-induced apoptotic cell death of Chinese hamster ovary cells producing thrombopoietin. *Metabolic Engineering,* 9(5-6), pp.452-464.

Suryawanshi, H., Scaria, V. and Maiti, S. 2010. Modulation of microRNA function by synthetic ribozymes. *Molecular bioSystems,* 6(10), pp.1807-1809.

Suzuki, H.I., Yamagata, K., Sugimoto, K., Iwamoto, T., Kato, S. and Miyazono, K. 2009. Modulation of microRNA processing by p53. *Nature,* 460(7254), pp.529-533.

Svoboda, P., Stein, P., Hayashi, H. and Schultz, R.M. 2000. Selective reduction of dormant maternal mRNAs in mouse oocytes by RNA interference. *Development (Cambridge, England),* 127(19), pp.4147-4156.

Sylvestre, Y., De Guire, V., Querido, E., Mukhopadhyay, U.K., Bourdeau, V., Major, F., Ferbeyre, G. and Chartrand, P. 2007. An E2F/miR-20a autoregulatory feedback loop. *The Journal of Biological Chemistry,* 282(4), pp.2135-2143.

Takada, S., Berezikov, E., Yamashita, Y., Lagos-Quintana, M., Kloosterman, W.P., Enomoto, M., Hatanaka, H., Fujiwara, S., Watanabe, H., Soda, M., Choi, Y.L., Plasterk, R.H., Cuppen, E. and Mano, H. 2006. Mouse microRNA profiles determined with a new and sensitive cloning method. *Nucleic Acids Research,* 34(17), pp.e115.

Tang, F., Hajkova, P., Barton, S.C., Lao, K. and Surani, M.A. 2006. MicroRNA expression profiling of single whole embryonic stem cells. *Nucleic Acids Research,* 34(2), pp.e9.

Tang, X., Muniappan, L., Tang, G. and Ozcan, S. 2009. Identification of glucose-regulated miRNAs from pancreatic {beta} cells reveals a role for miR-30d in insulin transcription. *RNA (New York, N.Y.),* 15(2), pp.287-293.

Tang, Y., Zhao, W., Chen, Y., Zhao, Y. and Gu, W. 2008. Acetylation is indispensable for p53 activation. *Cell,* 133(4), pp.612-626.

Tarasov, V., Jung, P., Verdoodt, B., Lodygin, D., Epanchintsev, A., Menssen, A., Meister, G. and Hermeking, H. 2007. Differential regulation of microRNAs by p53 revealed by massively parallel sequencing: miR-34a is a p53 target that induces apoptosis and G1-arrest. *Cell Cycle (Georgetown, Tex.),* 6(13), pp.1586-1593.

Tessmar-Raible, K., Raible, F., Christodoulou, F., Guy, K., Rembold, M., Hausen, H. and Arendt, D. 2007. Conserved sensory-neurosecretory cell types in annelid and fish forebrain: insights into hypothalamus evolution. *Cell*, 129(7), pp.1389-1400.

Tey, B.T., Singh, R.P., Piredda, L., Piacentini, M. and Al-Rubeai, M. 2000. Influence of bcl-2 on cell death during the cultivation of a Chinese hamster ovary cell line expressing a chimeric antibody. *Biotechnology and Bioengineering*, 68(1), pp.31-43.

Thatcher, E.J., Bond, J., Paydar, I. and Patton, J.G. 2008. Genomic organization of zebrafish microRNAs. *BMC Genomics*, 9pp.253.

Thommes, J., Gatgens, J., Biselli, M., Runstadler, P.W. and Wandrey, C. 1993. The influence of dissolved oxygen tension on the metabolic activity of an immobilized hybridoma population. *Cytotechnology*, 13(1), pp.29-39.

Thompson, S.R., Goodwin, E.B. and Wickens, M. 2000. Rapid deadenylation and Poly(A)-dependent translational repression mediated by the Caenorhabditis elegans tra-2 3' untranslated region in Xenopus embryos. *Molecular and Cellular Biology*, 20(6), pp.2129-2137.

Thomson, J.M., Newman, M., Parker, J.S., Morin-Kensicki, E.M., Wright, T. and Hammond, S.M. 2006. Extensive post-transcriptional regulation of microRNAs and its implications for cancer. *Genes & Development*, 20(16), pp.2202-2207.

Tigges, M. and Fussenegger, M. 2006. Xbp1-based engineering of secretory capacity enhances the productivity of Chinese hamster ovary cells. *Metabolic Engineering*, 8(3), pp.264-272.

Tokashiki, M. and Takamatsu, H. 1993. Perfusion culture apparatus for suspended mammalian cells. *Cytotechnology*, 13(3), pp.149-159.

Tokumaru, S., Suzuki, M., Yamada, H., Nagino, M. and Takahashi, T. 2008. let-7 regulates Dicer expression and constitutes a negative feedback loop. *Carcinogenesis*, 29(11), pp.2073-2077.

Toonen, R.F. and Verhage, M. 2003. Vesicle trafficking: pleasure and pain from SM genes. *Trends in Cell Biology*, 13(4), pp.177-186.

Tovar, V., Alsinet, C., Villanueva, A., Hoshida, Y., Chiang, D.Y., Sole, M., Thung, S., Moyano, S., Toffanin, S., Minguez, B., Cabellos, L., Peix, J., Schwartz, M., Mazzaferro, V., Bruix, J. and Llovet, J.M. 2010. IGF activation in a molecular subclass of hepatocellular carcinoma and pre-clinical efficacy of IGF-1R blockage. *Journal of Hepatology,* 52(4), pp.550-559.

Truettner, J.S., Alonso, O.F., Bramlett, H.M. and Dietrich, W.D. 2011. Therapeutic hypothermia alters microRNA responses to traumatic brain injury in rats. *Journal of Cerebral Blood Flow and Metabolism : Official Journal of the International Society of Cerebral Blood Flow and Metabolism,*

Umana, P., Jean-Mairet, J., Moudry, R., Amstutz, H. and Bailey, J.E. 1999. Engineered glycoforms of an antineuroblastoma IgG1 with optimized antibody-dependent cellular cytotoxic activity. *Nature Biotechnology,* 17(2), pp.176-180.

Valastyan, S., Benaich, N., Chang, A., Reinhardt, F. and Weinberg, R.A. 2009. Concomitant suppression of three target genes can explain the impact of a microRNA on metastasis. *Genes & Development,* 23(22), pp.2592-2597.

Valencia-Sanchez, M.A., Liu, J., Hannon, G.J. and Parker, R. 2006. Control of translation and mRNA degradation by miRNAs and siRNAs. *Genes & Development,* 20(5), pp.515-524.

Vander Heiden, M.G., Cantley, L.C. and Thompson, C.B. 2009. Understanding the Warburg effect: the metabolic requirements of cell proliferation. *Science (New York, N.Y.),* 324(5930), pp.1029-1033.

Vandesompele, J., De Preter, K., Pattyn, F., Poppe, B., Van Roy, N., De Paepe, A. and Speleman, F. 2002. Accurate normalization of real-time quantitative RT-PCR data by geometric averaging of multiple internal control genes. *Genome Biology,* 3(7), pp.RESEARCH0034.

Varghese, J. and Cohen, S.M. 2007. microRNA miR-14 acts to modulate a positive autoregulatory loop controlling steroid hormone signaling in Drosophila. *Genes & Development,* 21(18), pp.2277-2282.

Vasudevan, S., Tong, Y. and Steitz, J.A. 2007a. Switching from repression to activation: microRNAs can up-regulate translation. *Science (New York, N.Y.)*, 318(5858), pp.1931-1934.

Vasudevan, S., Tong, Y.C. and Steitz, J.A. 2007b. Switching from repression to activation: MicroRNAs can up-regulate translation. *Science*, 318(5858), pp.1931-1934.

Vehar, G.A., Spellman, M.W., Keyt, B.A., Ferguson, C.K., Keck, R.G., Chloupek, R.C., Harris, R., Bennett, W.F., Builder, S.E. and Hancock, W.S. 1986. Characterization studies of human tissue-type plasminogen activator produced by recombinant DNA technology. *Cold Spring Harbor Symposia on Quantitative Biology*, 51 Pt 1pp.551-562.

Vinther, J., Hedegaard, M.M., Gardner, P.P., Andersen, J.S. and Arctander, P. 2006. Identification of miRNA targets with stable isotope labeling by amino acids in cell culture. *Nucleic Acids Research*, 34(16),

Viswanathan, S.R. and Daley, G.Q. 2010. Lin28: A microRNA regulator with a macro role. *Cell*, 140(4), pp.445-449.

Volinia, S., Galasso, M., Costinean, S., Tagliavini, L., Gamberoni, G., Drusco, A., Marchesini, J., Mascellani, N., Sana, M.E., Abu Jarour, R., Desponts, C., Teitell, M., Baffa, R., Aqeilan, R., Iorio, M.V., Taccioli, C., Garzon, R., Di Leva, G., Fabbri, M., Catozzi, M., Previati, M., Ambs, S., Palumbo, T., Garofalo, M., Veronese, A., Bottoni, A., Gasparini, P., Harris, C.C., Visone, R., Pekarsky, Y., de la Chapelle, A., Bloomston, M., Dillhoff, M., Rassenti, L.Z., Kipps, T.J., Huebner, K., Pichiorri, F., Lenze, D., Cairo, S., Buendia, M.A., Pineau, P., Dejean, A., Zanesi, N., Rossi, S., Calin, G.A., Liu, C.G., Palatini, J., Negrini, M., Vecchione, A., Rosenberg, A. and Croce, C.M. 2010. Reprogramming of miRNA networks in cancer and leukemia. *Genome Research*, 20(5), pp.589-599.

von der Lehr, N., Johansson, S., Wu, S., Bahram, F., Castell, A., Cetinkaya, C., Hydbring, P., Weidung, I., Nakayama, K., Nakayama, K.I., Soderberg, O., Kerppola, T.K. and Larsson, L.G. 2003. The F-box protein Skp2 participates in c-Myc proteosomal degradation and acts as a cofactor for c-Myc-regulated transcription. *Molecular Cell*, 11(5), pp.1189-1200.

Vousden, K.H. and Lu, X. 2002. Live or let die: the cell's response to p53. *Nature Reviews.Cancer,* 2(8), pp.594-604.

Vousden, K.H. and Prives, C. 2009. Blinded by the Light: The Growing Complexity of p53. *Cell,* 137(3), pp.413-431.

Walsh, G. 2006. Biopharmaceutical benchmarks 2006. *Nature Biotechnology,* 24(7), pp.769-776.

Wang, H., Zhao, L.N., Li, K.Z., Ling, R., Li, X.J. and Wang, L. 2006. Overexpression of ribosomal protein L15 is associated with cell proliferation in gastric cancer. *BMC Cancer,* 6pp.91.

Wang, J., Lu, M., Qiu, C. and Cui, Q. 2010. TransmiR: a transcription factor-microRNA regulation database. *Nucleic Acids Research,* 38(Database issue), pp.D119-22.

Wang, K. and Li, P.F. 2010. Foxo3a regulates apoptosis by negatively targeting miR-21. *The Journal of Biological Chemistry,* 285(22), pp.16958-16966.

Wang, L., Liu, R., Li, W., Chen, C., Katoh, H., Chen, G.Y., McNally, B., Lin, L., Zhou, P., Zuo, T., Cooney, K.A., Liu, Y. and Zheng, P. 2009a. Somatic single hits inactivate the X-linked tumor suppressor FOXP3 in the prostate. *Cancer Cell,* 16(4), pp.336-346.

Wang, P., Zou, F., Zhang, X., Li, H., Dulak, A., Tomko, R.J.,Jr, Lazo, J.S., Wang, Z., Zhang, L. and Yu, J. 2009b. microRNA-21 negatively regulates Cdc25A and cell cycle progression in colon cancer cells. *Cancer Research,* 69(20), pp.8157-8165.

Warner, J.R. and McIntosh, K.B. 2009. How common are extraribosomal functions of ribosomal proteins? *Molecular Cell,* 34(1), pp.3-11.

Webster, R.J., Giles, K.M., Price, K.J., Zhang, P.M., Mattick, J.S. and Leedman, P.J. 2009. Regulation of Epidermal Growth Factor Receptor Signaling in Human Cancer Cells by MicroRNA-7. *Journal of Biological Chemistry,* 284(9), pp.5731-5741.

Weterings, E. and van Gent, D.C. 2004. The mechanism of non-homologous end-joining: a synopsis of synapsis. *DNA Repair,* 3(11), pp.1425-1435.

Wettenhall, J.M. and Smyth, G.K. 2004. limmaGUI: a graphical user interface for linear modeling of microarray data. *Bioinformatics (Oxford, England)*, 20(18), pp.3705-3706.

Wianny, F. and Zernicka-Goetz, M. 2000. Specific interference with gene function by double-stranded RNA in early mouse development. *Nature Cell Biology*, 2(2), pp.70-75.

Wiberg, F.C., Rasmussen, S.K., Frandsen, T.P., Rasmussen, L.K., Tengbjerg, K., Coljee, V.W., Sharon, J., Yang, C.Y., Bregenholt, S., Nielsen, L.S., Haurum, J.S. and Tolstrup, A.B. 2006. Production of target-specific recombinant human polyclonal antibodies in mammalian cells. *Biotechnology and Bioengineering*, 94(2), pp.396-405.

Wienholds, E., Kloosterman, W.P., Miska, E., Alvarez-Saavedra, E., Berezikov, E., de Bruijn, E., Horvitz, H.R., Kauppinen, S. and Plasterk, R.H. 2005. MicroRNA expression in zebrafish embryonic development. *Science (New York, N.Y.)*, 309(5732), pp.310-311.

Wiestner, A., Tehrani, M., Chiorazzi, M., Wright, G., Gibellini, F., Nakayama, K., Liu, H., Rosenwald, A., Muller-Hermelink, H.K., Ott, G., Chan, W.C., Greiner, T.C., Weisenburger, D.D., Vose, J., Armitage, J.O., Gascoyne, R.D., Connors, J.M., Campo, E., Montserrat, E., Bosch, F., Smeland, E.B., Kvaloy, S., Holte, H., Delabie, J., Fisher, R.I., Grogan, T.M., Miller, T.P., Wilson, W.H., Jaffe, E.S. and Staudt, L.M. 2007. Point mutations and genomic deletions in CCND1 create stable truncated cyclin D1 mRNAs that are associated with increased proliferation rate and shorter survival. *Blood*, 109(11), pp.4599-4606.

Wirth, D., Gama-Norton, L., Riemer, P., Sandhu, U., Schucht, R. and Hauser, H. 2007. Road to precision: recombinase-based targeting technologies for genome engineering. *Current Opinion in Biotechnology*, 18(5), pp.411-419.

Woods, K., Thomson, J.M. and Hammond, S.M. 2007. Direct regulation of an oncogenic micro-RNA cluster by E2F transcription factors. *The Journal of Biological Chemistry*, 282(4), pp.2130-2134.

Wu, L., Zhou, H., Zhang, Q., Zhang, J., Ni, F., Liu, C. and Qi, Y. 2010a. DNA Methylation Mediated by a MicroRNA Pathway. *Molecular Cell*, 38(3), pp.465-475.

Wu, S., Huang, S., Ding, J., Zhao, Y., Liang, L., Liu, T., Zhan, R. and He, X. 2010b. Multiple microRNAs modulate p21Cip1/Waf1 expression by directly targeting its 3 ' untranslated region. *Oncogene,* 29(15), pp.2302-2308.

Wu, S.C. 2009. RNA interference technology to improve recombinant protein production in Chinese hamster ovary cells. *Biotechnology Advances,* 27(4), pp.417-422.

Wurm, F.M. 2004. Production of recombinant protein therapeutics in cultivated mammalian cells. *Nature Biotechnology,* 22(11), pp.1393-1398.

Wurtele, H., Little, K.C. and Chartrand, P. 2003. Illegitimate DNA integration in mammalian cells. *Gene Therapy,* 10(21), pp.1791-1799.

Xie, L. and Wang, D.I. 2006. Fed-batch cultivation of animal cells using different medium design concepts and feeding strategies. 1994. *Biotechnology and Bioengineering,* 95(2), pp.270-284.

Xiong, S., Zheng, Y., Jiang, P., Liu, R., Liu, X. and Chu, Y. 2011. MicroRNA-7 inhibits the growth of human non-small cell lung cancer A549 cells through targeting BCL-2. *International Journal of Biological Sciences,* 7(6), pp.805-814.

Xu, X., Nagarajan, H., Lewis, N.E., Pan, S., Cai, Z., Liu, X., Chen, W., Xie, M., Wang, W., Hammond, S., Andersen, M.R., Neff, N., Passarelli, B., Koh, W., Fan, H.C., Wang, J., Gui, Y., Lee, K.H., Betenbaugh, M.J., Quake, S.R., Famili, I., Palsson, B.O. and Wang, J. 2011. The genomic sequence of the Chinese hamster ovary (CHO)-K1 cell line. *Nature Biotechnology,* 29(8), pp.735-741.

Yamaguchi, H. and Wang, H.G. 2001. The protein kinase PKB/Akt regulates cell survival and apoptosis by inhibiting Bax conformational change. *Oncogene,* 20(53), pp.7779-7786.

Yamakuchi, M., Ferlito, M. and Lowenstein, C.J. 2008. miR-34a repression of SIRT1 regulates apoptosis. *Proceedings of the National Academy of Sciences of the United States of America,* 105(36), pp.13421-13426.

Yamakuchi, M. and Lowenstein, C.J. 2009. MiR-34, SIRT1 and p53: the feedback loop. *Cell Cycle (Georgetown, Tex.),* 8(5), pp.712-715.

Yan, H.L., Xue, G., Mei, Q., Wang, Y.Z., Ding, F.X., Liu, M.F., Lu, M.H., Tang, Y., Yu, H.Y. and Sun, S.H. 2009. Repression of the miR-17-92 cluster by p53 has an important function in hypoxia-induced apoptosis. *The EMBO Journal*, 28(18), pp.2719-2732.

Yang, J.S. and Lai, E.C. 2010. Dicer-independent, Ago2-mediated microRNA biogenesis in vertebrates. *Cell Cycle (Georgetown, Tex.),* 9(22), pp.4455-4460.

Yang, K., Hitomi, M. and Stacey, D.W. 2006. Variations in cyclin D1 levels through the cell cycle determine the proliferative fate of a cell. *Cell Division,* 1pp.32.

Yang, W., Chendrimada, T.P., Wang, Q., Higuchi, M., Seeburg, P.H., Shiekhattar, R. and Nishikura, K. 2006. Modulation of microRNA processing and expression through RNA editing by ADAR deaminases. *Nature Structural & Molecular Biology,* 13(1), pp.13-21.

Yi, R., Doehle, B.P., Qin, Y., Macara, I.G. and Cullen, B.R. 2005. Overexpression of exportin 5 enhances RNA interference mediated by short hairpin RNAs and microRNAs. *RNA (New York, N.Y.),* 11(2), pp.220-226.

Yoo, A.S., Staahl, B.T., Chen, L. and Crabtree, G.R. 2009. MicroRNA-mediated switching of chromatin-remodelling complexes in neural development. *Nature,* 460(7255), pp.642-U112.

Yoon, S.K., Kim, S.H. and Lee, G.M. 2003. Effect of low culture temperature on specific productivity and transcription level of anti-4-1BB antibody in recombinant Chinese hamster ovary cells. *Biotechnology Progress,* 19(4), pp.1383-1386.

Yoon, S.K., Song, J.Y. and Lee, G.M. 2003. Effect of low culture temperature on specific productivity, transcription level, and heterogeneity of erythropoietin in chinese hamster ovary cells. *Biotechnology and Bioengineering,* 82(3), pp.289-298.

Yu, J., Wang, F., Yang, G.H., Wang, F.L., Ma, Y.N., Du, Z.W. and Zhang, J.W. 2006. Human microRNA clusters: genomic organization and expression profile in leukemia cell lines. *Biochemical and Biophysical Research Communications,* 349(1), pp.59-68.

Yu, Z.K., Gervais, J.L. and Zhang, H. 1998. Human CUL-1 associates with the SKP1/SKP2 complex and regulates p21(CIP1/WAF1) and cyclin D proteins. *Proceedings of the National Academy of Sciences of the United States of America,* 95(19), pp.11324-11329.

Yuan, X., Liu, C., Yang, P., He, S., Liao, Q., Kang, S. and Zhao, Y. 2009. Clustered microRNAs' coordination in regulating protein-protein interaction network. *BMC Systems Biology,* 3pp.65.

Yun, C.Y., Liu, S., Lim, S.F., Wang, T., Chung, B.Y., Jiat Teo, J., Chuan, K.H., Soon, A.S., Goh, K.S. and Song, Z. 2007. Specific inhibition of caspase-8 and -9 in CHO cells enhances cell viability in batch and fed-batch cultures. *Metabolic Engineering,* 9(5-6), pp.406-418.

Zahn-Zabal, M., Kobr, M., Girod, P.A., Imhof, M., Chatellard, P., de Jesus, M., Wurm, F. and Mermod, N. 2001. Development of stable cell lines for production or regulated expression using matrix attachment regions. *Journal of Biotechnology,* 87(1), pp.29-42.

Zeng, Y., Wagner, E.J. and Cullen, B.R. 2002. Both natural and designed micro RNAs can inhibit the expression of cognate mRNAs when expressed in human cells. *Molecular Cell,* 9(6), pp.1327-1333.

Zhang, F., Sun, X., Yi, X. and Zhang, Y. 2006. Metabolic characteristics of recombinant Chinese hamster ovary cells expressing glutamine synthetase in presence and absence of glutamine. *Cytotechnology,* 51(1), pp.21-28.

Zhang, H., Hao, Y., Yang, J., Zhou, Y., Li, J., Yin, S., Sun, C., Ma, M., Huang, Y. and Xi, J.J. 2011. Genome-wide functional screening of miR-23b as a pleiotropic modulator suppressing cancer metastasis. *Nature Communications,* 2pp.554.

Zhang, H., Kobayashi, R., Galaktionov, K. and Beach, D. 1995. p19Skp1 and p45Skp2 are essential elements of the cyclin A-CDK2 S phase kinase. *Cell,* 82(6), pp.915-925.

Zhang, J.G., Wang, J.J., Zhao, F., Liu, Q., Jiang, K. and Yang, G.H. 2010. MicroRNA-21 (miR-21) represses tumor suppressor PTEN and promotes growth and invasion in

non-small cell lung cancer (NSCLC). *Clinica Chimica Acta; International Journal of Clinical Chemistry*, 411(11-12), pp.846-852.

Zhang, L.Q., Jiang, F., Xu, L., Wang, J., Bai, J.L., Yin, R., Wu, Y.Q. and Meng, L.J. 2012a. The role of cyclin D1 expression and patient's survival in non-small-cell lung cancer: a systematic review with meta-analysis. *Clinical Lung Cancer*, 13(3), pp.188-195.

Zhang, P., Haryadi, R., Chan, K.F., Teo, G., Goh, J., Pereira, N.A., Feng, H. and Song, Z. 2012b. Identification of functional elements of the GDP-fucose transporter SLC35C1 using a novel Chinese hamster ovary mutant. *Glycobiology*, 22(7), pp.897-911.

Zhang, R. and Su, B. 2009. Small but influential: the role of microRNAs on gene regulatory network and 3 ' UTR evolution. *Journal of Genetics and Genomics*, 36(1), pp.1-6.

Zhang, Z. and Zhang, R. 2008. Proteasome activator PA28 gamma regulates p53 by enhancing its MDM2-mediated degradation. *The EMBO Journal*, 27(6), pp.852-864.

Zhao, J., Lin, J., Lwin, T., Yang, H., Guo, J., Kong, W., Dessureault, S., Moscinski, L.C., Rezania, D., Dalton, W.S., Sotomayor, E., Tao, J. and Cheng, J.Q. 2010. microRNA expression profile and identification of miR-29 as a prognostic marker and pathogenetic factor by targeting CDK6 in mantle cell lymphoma. *Blood*, 115(13), pp.2630-2639.

Zhao, X., Dou, W., He, L., Liang, S., Tie, J., Liu, C., Li, T., Lu, Y., Mo, P., Shi, Y., Wu, K., Nie, Y. and Fan, D. 2012. MicroRNA-7 functions as an anti-metastatic microRNA in gastric cancer by targeting insulin-like growth factor-1 receptor. *Oncogene*,

Zheng, B., Liang, L., Huang, S., Zha, R., Liu, L., Jia, D., Tian, Q., Wang, Q., Wang, C., Long, Z., Zhou, Y., Cao, X., Du, C., Shi, Y. and He, X. 2012. MicroRNA-409 suppresses tumour cell invasion and metastasis by directly targeting radixin in gastric cancers. *Oncogene*, 31(42), pp.4509-4516.

Zheng, L., Dai, H., Qiu, J., Huang, Q. and Shen, B. 2007. Disruption of the FEN-1/PCNA interaction results in DNA replication defects, pulmonary hypoplasia,

pancytopenia, and newborn lethality in mice. *Molecular and Cellular Biology,* 27(8), pp.3176-3186.

Zhou, M., Crawford, Y., Ng, D., Tung, J., Pynn, A.F., Meier, A., Yuk, I.H., Vijayasankaran, N., Leach, K., Joly, J., Snedecor, B. and Shen, A. 2011. Decreasing lactate level and increasing antibody production in Chinese Hamster Ovary cells (CHO) by reducing the expression of lactate dehydrogenase and pyruvate dehydrogenase kinases. *Journal of Biotechnology*, 153(1-2), pp.27-34.

Zhu, L.H., Liu, T., Tang, H., Tian, R.Q., Su, C., Liu, M. and Li, X. 2010. MicroRNA-23a promotes the growth of gastric adenocarcinoma cell line MGC803 and downregulates interleukin-6 receptor. *The FEBS Journal*, 277(18), pp.3726-3734.

Zhu, S., Wu, H., Wu, F., Nie, D., Sheng, S. and Mo, Y.Y. 2008. MicroRNA-21 targets tumor suppressor genes in invasion and metastasis. *Cell Research,* 18(3), pp.350-359.

Zuo, T., Liu, R., Zhang, H., Chang, X., Liu, Y., Wang, L., Zheng, P. and Liu, Y. 2007. FOXP3 is a novel transcriptional repressor for the breast cancer oncogene SKP2. *The Journal of Clinical Investigation,* 117(12), pp.3765-3773.

11 Appendices

11.1 Appendix 1: List of primers used for real-time PCR

MCM4 F: GCAGTGCTGAAGGACTACATAGCA
MCM4 R: GGCTGGCCTCCTCACTCA

MYC F: TCAAGAACATCATTCATCCAAGATT
MYC R: AAGCCAGCTTCTCGGAGAC

FEN1 F: TGGTGAAGGCTGGCAAAGTT
FEN1 R: GTACAGGGCTGCCAAAAGTGA

PCNA F: GCTGTGTGGTAAAGATGCCTTCT
PCNA R: CAGGATATTACAACAGCATCTCCAA

Psme3 F: TAT CCC ACC TTG AGC CTG AC
Psme3 R: TGC AGG AAG GAA GGC TAT GT

Apex1 F: ACAGCAAGATCCGCTCCAAA
Apex1 R: GGGCCTAAAGGACACTGGAC

Skp2 F: GGT CCT TTA TGG AGC AAC CA
Skp2 R: CCA CTG CAG ATT CGG AAA AT

Cno F: ACC CAG TTT GGC TGT CTT GA
Cno R: TGC AAT ATG GCA GAG CTG TT

Spata2 F: TCT GGC CCA CAT ACT TCT CC
Spata2 R: GAG TCT GCC CTC TCC AAG TG

Rad54 F: CCA TTA AGA AGC GAG CCA AG
Rad54 R: GGG TTC CAG TCA GGA TCA AA

Ccnd3 F: CCC CAC TAT GGT CAG AGG AA
Ccnd3 R: CCA AGC TCA GTC CCT CAC TC

Peo1 F: ATGTGGAGCAAGCAGCTGGT
Peo1 R: CTCTTCCAGCCGTGTCACAG

Ckap4 F: TGA CTC CAC TTG GCT CAC TG
Ckap4 R: ACA GTG AAG AGC CTG GAG GA

Plp2 F: TCA GGT AGA GGA TGG CTG CT
Plp2 R: TGC TTC AGT GCT TCG ACA TC

Dhfr F: AAT GAC CAC CAC CTC CTC AG
Dhfr R: AGG CAT CGT CCA GAC TTT TG

Setd8 F: GAG GCC ACA TGG TTA ATG CT
Setd8 R: TAA GTG GGG AAT TGG CAG AC

Ccnd1 F: CAC AAC GCA CTT TCT TTC CA
Ccnd1 R: CTC CCT CTG CTT CTC CCT CT

H2afx F: CTG AGG AAA GGC CAC TAT GC
H2afx R: CTT GTT GAG CTC CTC GTC GT

Slc7a5 F: CCA AAG AGC AGG GAC TCT TG
Slc7a5 R: CCA AAA TGC AAA GCA CTG AA

Mcm2 F: ACT TCC TAC CTG AGG CAC CA
Mcm2 R: ACC TCA GTG AAC GCA ACT CC

Lig1 F: CCC TTT CTC TTT GTC CAC CA
Lig1 R: AGG AGC ATC ACC AGA GCC TA

Orc1l F: TGC CTG ACT CTC TTC CCT GT
Orc1l R: TGC AGA CAG CGT ATG ACC TC

Cdk2 F: AGT GGA GGC ACA ACT TTG CT
Cdk2 R: GTG GAC TGA CGT CAA TGT GG

Aup1 F: TTG TCT GAC GGA GTG AGT CG
Aup1 R: TCC TGG GTC TCA GAA CTG CT

Mcm5 F: ACA CTG GCT CCA CTG CTC TT
Mcm5 R: TGT GTT TGG ATG CCT GAG AG

Mcm3 F: CAG CCT CCA TCA GTG AAA CA
Mcm3 R: TGT GTT TGG ATG CCT GAG AG

Bclaf1 F: CAC CGG AAT ACT GAG GAG GA
Bclaf1 R: TTT TGC AGT GCT AGG CCT TT

Slc39a9 F: GCA GAC AGG TCC CTT GAA AA
Slc39a9 R: GGA CCT GTA CCC AAA CGA GA

Cdc6 F: TCT GTG CCC GAA AAG TAT CC
Cdc6 R: CCG CTG AGA AAC AAG TCC TC

Cnot8 F: ATC AGA GCA AAC CCC CTT CT
Cnot8 R: ATG TGA ATT TTG CCC AGG AG

Mcm7 F: AAG TCA AAC CTC GGA TGG TG

Mcm7 R: ATT TGG AAC CAC GAG TCT GC

Cenpo F: CTG GTG TCC CTG ATC CAC TT
Cenpo R: CTG ATA TCC AGC GCT TCC TC

Fen1 F: AACCCCGAACCAAGCTTTAG
Fen1 R: GGGCCACATCAGCAATTAGT

Cdc25b F: AGA CGG GTA GCC AAG GTT TT
Cdc25b R: AGC CAC TCT TCA GGT GCA TT

Tfdp1 F: CCA AAC TTC TGG CCA CCT TA
Tfdp1 R: GAC TGC AGC ATC TCC AAT GA

PabpnI F: GTGGCCATCCTAAAGGGTTT
PabpnI R: CGGGAGCTGTTGTAATTGGT

Cdc7 F: CAT CTG ACC TTC CCT CCA AA
Cdc7 R: GAT ACG GCA TGG CAA TAA CC

Rad52 F: GGA GGC CAG AAG GTG TGT TA
Rad52 R: CCC ACG TAG AAT TTG CCA TT

Cdk1 F: CTC CAC CCC TGT TGA CAT CT
Cdk1 R: CGT TGT TAG GAG TCC CCA GA

Bcl10 F: TCT CCT CAG GCA CAC TTC CT
Bcl10 R: CGT GAT CGT AAG GGG AGA AA

Hdac1 F: GGA TGG CCA GAG ACA CTC AT
Hdac1 R: AGC ATC CGG TTT CTG TTA CG

11.2 Appendix 2: List of down-regulated genes upon pm-7 treatment

mouse	human	rat	pm-7/pm-neg	pm-neg /cells	pm-7/cells	P.Value
Crtap	**NA**	**Crtap**	**-3,94**	0,24	-3,71	5,75E-08
Psme3	**PSME3**	**Psme3**	**-3,92**	0,32	-3,61	1,57E-08
Rnf26	**RNF26**	**Rnf26**	**-3,70**	0,78	-2,92	5,39E-08
NA	**NA**	**Cdca4**	**-3,58**	0,65	-2,93	3,74E-08
Pdk3	**NA**	**Pdk3**	**-3,57**	0,34	-3,23	1,60E-09
NA	**NA**	**Rfng**	**-3,56**	0,42	-3,13	1,80E-07
NA	**NA**	**NA**	**-3,43**	0,01	-3,42	6,10E-08
Nadk	**NA**	**Nadk**	**-3,42**	0,54	-2,88	1,08E-07
Mosc2	**NA**	**NA**	**-3,40**	0,21	-3,19	2,67E-10
Tex261	**NA**	**NA**	**-3,34**	0,74	-2,60	2,17E-07
Tk1	**NA**	**NA**	**-3,33**	0,35	-2,98	1,34E-07
Ado	**NA**	**NA**	**-3,28**	0,26	-3,02	6,24E-09
Skp2	**SKP2**	**Skp2**	**-3,27**	0,06	-3,21	5,36E-12
NA	**NA**	**NA**	**-3,26**	0,81	-2,45	5,54E-09
Ppif	**PPIF**	**Ppif**	**-3,26**	0,55	-2,71	3,77E-09
Rcc2	**NA**	**NA**	**-3,24**	0,25	-2,99	1,39E-08
Cno	**CNO**	**Cno**	**-3,24**	0,54	-2,69	8,50E-08
5930416I 19Rik	**NA**	**MGC94282**	**-3,23**	0,20	-3,02	6,09E-09
Zdhhc3	**NA**	**Zdhhc3**	**-3,22**	0,69	-2,53	1,05E-07
Mosc2	**MOSC2**	**Mosc2**	**-3,17**	0,22	-2,96	1,02E-08
Spata2	**SPATA2**	**NA**	**-3,17**	0,69	-2,47	6,26E-08
Rad54l	**RAD54L**	**Rad54l**	**-3,15**	-0,02	-3,17	1,32E-10
Ccnd3	**CCND3**	**Ccnd3**	**-3,14**	0,49	-2,65	2,40E-07
Ado	**ADO**	**NA**	**-3,06**	0,25	-2,81	2,44E-09
Ubqln4	**UBQLN4**	**NA**	**-3,01**	0,34	-2,68	9,33E-09
Gins1	**NA**	**Gins1**	**-3,01**	0,26	-2,75	1,38E-09
Heg1	**HEG1**	**NA**	**-3,01**	0,20	-2,80	2,34E-10
Tpbg	**NA**	**Tpbg**	**-3,00**	0,04	-2,96	4,77E-07
NA	**NA**	**NA**	**-3,00**	0,46	-2,54	3,41E-07
Grk6	**GRK6**	**Grk6**	**-2,98**	0,43	-2,54	5,08E-07
Slc39a11	**NA**	**NA**	**-2,93**	0,64	-2,29	3,37E-07
NA	**NA**	**NA**	**-2,92**	0,42	-2,49	2,22E-07
Dhx16	**DHX16**	**Dhx16**	**-2,89**	0,38	-2,52	1,09E-07
Timm50	**TIMM50**	**NA**	**-2,87**	0,40	-2,47	1,87E-07
Peo1	**NA**	**NA**	**-2,87**	0,23	-2,65	9,57E-08

Ckap4	**CKAP4**	**Ckap4**	**-2,87**	0,09	-2,78	9,36E-08
Emp1	**NA**	**Emp1**	**-2,83**	0,25	-2,58	9,41E-11
NA	**NA**	**NA**	**-2,83**	-0,14	-2,97	9,31E-13
NA	**PHF5A**	**Phf5a**	**-2,82**	0,61	-2,20	5,19E-08
Plp2	**NA**	**Plp2**	**-2,81**	0,17	-2,64	3,37E-09
Mesdc2	**NA**	**Mesdc2**	**-2,81**	0,34	-2,47	1,03E-08
NA	**NA**	**NA**	**-2,80**	-0,07	-2,86	3,26E-10
Dhfr	**NA**	**NA**	**-2,76**	-0,17	-2,94	2,59E-08
NA	**NA**	**NA**	**-2,75**	0,61	-2,14	1,23E-07
Ak3	**NA**	**NA**	**-2,74**	0,41	-2,33	8,14E-09
NA	**NA**	**NA**	**-2,73**	-0,09	-2,82	5,97E-11
Mfsd5	**MFSD5**	**Mfsd5**	**-2,68**	0,57	-2,11	6,19E-07
NA	**NA**	**NA**	**-2,68**	-0,19	-2,87	1,71E-07
Setd8	**SETD8**	**Setd8**	**-2,67**	0,52	-2,15	4,71E-10
1810055 G02Rik	**C11orf24**	**RGD1311 946**	**-2,65**	0,17	-2,48	3,11E-08
Lancl1	**NA**	**NA**	**-2,63**	0,75	-1,88	8,19E-09
1110034 A24Rik	**C14orf10 4**	**RGD1310 311**	**-2,63**	0,10	-2,53	1,30E-08
NA	**NA**	**NA**	**-2,61**	-0,35	-2,96	1,49E-10
NA	**NA**	**NA**	**-2,56**	0,46	-2,10	1,09E-06
NA	**NA**	**Ccnd1**	**-2,56**	0,47	-2,09	5,38E-08
H2afx	**NA**	**H2afx**	**-2,55**	0,47	-2,08	2,84E-08
Wipf1	**WIPF1**	**NA**	**-2,55**	0,43	-2,12	1,69E-10
NA	**NA**	**NA**	**-2,55**	-0,14	-2,69	1,24E-10
NA	**NA**	**NA**	**-2,53**	-0,08	-2,61	1,64E-09
Hdac1	**HDAC1**	**Hdac1l**	**-2,53**	-0,31	-2,84	1,56E-07
Emp1	**EMP1**	**Emp1**	**-2,53**	0,34	-2,18	3,93E-10
Tmem55 b	**APEX1**	**Apex1**	**-2,51**	0,17	-2,34	5,32E-09
Slc7a5	**NA**	**NA**	**-2,51**	0,58	-1,93	1,71E-07
Slc7a5	**NA**	**Slc7a5**	**-2,50**	0,48	-2,02	1,33E-07
Mcm2	**NA**	**Mcm2**	**-2,49**	0,37	-2,12	5,87E-08
Lig1	**LIG1**	**Lig1**	**-2,49**	0,28	-2,20	1,43E-06
NA	**NA**	**Slc7a5**	**-2,48**	0,57	-1,91	3,25E-07
Rela	**RELA**	**Rela**	**-2,48**	0,53	-1,96	3,21E-07
Hdlbp	**NA**	**Hdlbp**	**-2,43**	0,20	-2,22	6,86E-09
Orc1l	**ORC1L**	**Orc1l**	**-2,42**	-0,27	-2,69	1,52E-08
Nacc1	**NA**	**NA**	**-2,42**	0,60	-1,81	6,62E-07
NA	**NA**	**Cdk2**	**-2,41**	0,51	-1,90	4,33E-07

Aup1	**AUP1**	**Aup1**	**-2,40**	0,44	-1,96	1,03E-06
LOC1001 35765	**DYX1C1**	**NA**	**-2,39**	-0,06	-2,46	2,07E-07
NA	**NA**	**Mcm5**	**-2,39**	0,44	-1,95	2,51E-07
NA	**NA**	**NA**	**-2,39**	0,01	-2,37	1,73E-08
NA	**NA**	**NA**	**-2,38**	0,26	-2,12	1,99E-08
NA	**NA**	**NA**	**-2,38**	0,44	-1,94	2,23E-07
Dhdds	**DHDDS**	**NA**	**-2,38**	0,56	-1,81	6,24E-07
Klhl5	**KLHL5**	**Klhl5**	**-2,36**	-0,14	-2,51	8,51E-10
Nolc1	**NOLC1**	**Nolc1**	**-2,35**	-0,34	-2,69	4,07E-07
NA	**NA**	**Cdca7**	**-2,34**	-0,22	-2,56	3,64E-10
Tnfaip3	**NA**	**NA**	**-2,33**	0,25	-2,09	3,22E-09
Cmtm6	**NA**	**Cmtm6**	**-2,33**	-0,20	-2,53	3,59E-07
Eif4ebp2	**NA**	**NA**	**-2,33**	0,31	-2,02	4,25E-07
Usp10	**USP10**	**Usp10**	**-2,32**	0,01	-2,30	1,98E-08
Sigmar1	**SIGMAR1**	**Sigmar1**	**-2,31**	0,00	-2,31	6,40E-07
NA	**NA**	**NA**	**-2,29**	0,19	-2,10	2,21E-08
Mcm3	**NA**	**LOC367976**	**-2,25**	0,04	-2,21	1,30E-09
NA	**NA**	**NA**	**-2,24**	-0,61	-2,84	1,96E-07
NA	**UBQLN4**	**Ubqln4**	**-2,23**	0,19	-2,05	1,93E-07
Dhfr	**DHFR**	**Dhfr**	**-2,23**	-0,48	-2,71	3,07E-07
Exosc2	**NA**	**Exosc2**	**-2,21**	-0,08	-2,29	3,72E-08
Tada2b	**TADA2B**	**Tada2b**	**-2,21**	0,66	-1,55	4,93E-08
Mllt6	**LOC100129395**	**NA**	**-2,20**	0,64	-1,56	2,30E-07
Mapkap1	**NA**	**NA**	**-2,19**	0,65	-1,54	9,87E-09
Derl1	**DERL1**	**Derl1**	**-2,19**	0,60	-1,59	4,69E-07
Aplp2	**NA**	**Aplp2**	**-2,17**	0,26	-1,91	7,41E-08
Prps1	**PRPS1**	**Prps1**	**-2,15**	-0,14	-2,28	4,16E-08
Usp10	**USP10**	**Usp10**	**-2,14**	0,07	-2,07	9,85E-10
NA	**NA**	**NA**	**-2,11**	0,13	-1,98	2,04E-08
NA	**NA**	**NA**	**-2,10**	0,02	-2,08	8,76E-09
Ubr7	**NA**	**Ubr7**	**-2,09**	0,00	-2,09	2,98E-07
Lrrc8a	**LRRC8A**	**NA**	**-2,08**	0,50	-1,58	6,40E-07
A730085K08Rik	**ABHD5**	**Abhd5**	**-2,07**	0,32	-1,75	2,44E-09
A730071L15Rik	**NA**	**NA**	**-2,06**	0,45	-1,61	3,00E-07
Lrrc59	**LRRC59**	**Lrrc59**	**-2,06**	0,18	-1,88	1,72E-07

Urb2	**NA**	**Urb2**	**-2,06**	0,09	-1,97	3,88E-09
Myst2	**MYST2**	**Myst2**	**-2,03**	0,30	-1,73	4,32E-09
Naa40	**NA**	**Nat11**	**-2,01**	0,01	-2,01	2,48E-06
H2afx	**NA**	**H2afx**	**-2,01**	0,28	-1,73	1,94E-08
NA	**NA**	**NA**	**-2,01**	0,58	-1,43	3,98E-07
NA	**NA**	**Bclaf1**	**-2,01**	0,01	-2,00	9,05E-08
NA	**LOC1001 31735**	**Rbmx**	**-2,00**	-0,20	-2,20	2,94E-11
Ykt6	**NA**	**Ykt6**	**-1,99**	0,29	-1,70	3,67E-08
NA	**NA**	**NA**	**-1,99**	-0,12	-2,11	1,85E-08
NA	**PFN2**	**Pfn2**	**-1,98**	0,11	-1,87	2,20E-07
NA	**NA**	**NA**	**-1,97**	0,65	-1,32	4,37E-08
Tmed9	**TMED9**	**Tmed9**	**-1,96**	0,19	-1,77	4,88E-07
Slc39a9	**SLC39A9**	**NA**	**-1,96**	0,27	-1,70	4,07E-08
Cat	**CAT**	**Cat**	**-1,96**	0,01	-1,95	1,05E-06
Derl1	**NA**	**NA**	**-1,95**	0,36	-1,59	2,70E-07
NA	**NA**	**NA**	**-1,94**	0,43	-1,51	2,62E-09
Znrf3	**ZNRF3**	**NA**	**-1,94**	0,19	-1,75	3,18E-07
NA	**NA**	**NA**	**-1,94**	0,07	-1,87	2,62E-08
Bysl	**BYSL**	**Bysl**	**-1,94**	0,27	-1,66	1,12E-06
NA	**NA**	**NA**	**-1,93**	-0,13	-2,06	8,20E-08
Trub1	**NA**	**NA**	**-1,93**	0,10	-1,83	1,53E-10
Ormdl2	**ORMDL2**	**Ormdl2**	**-1,93**	0,63	-1,30	3,87E-07
Atpaf1	**NA**	**Atpaf1**	**-1,91**	-0,53	-2,44	8,90E-07
Rqcd1	**RQCD1**	**NA**	**-1,90**	0,41	-1,49	2,41E-07
Tmed9	**NA**	**Tmed9**	**-1,88**	0,14	-1,74	1,03E-07
Pole2	**POLE2**	**Pole2**	**-1,88**	-0,53	-2,42	4,54E-07
Kpna6	**KPNA6**	**NA**	**-1,88**	0,02	-1,86	7,59E-10
Lig3	**NA**	**NA**	**-1,86**	-0,14	-2,00	1,15E-07
Cdc6	**CDC6**	**Cdc6**	**-1,86**	-0,47	-2,33	3,82E-07
Derl1	**NA**	**NA**	**-1,86**	0,48	-1,38	1,09E-07
Nfkbia	**NFKBIA**	**Nfkbia**	**-1,86**	0,17	-1,69	1,87E-08
NA	**NA**	**Pfn2**	**-1,86**	0,12	-1,74	3,28E-07
Ppib	**PPIB**	**Ppib**	**-1,85**	0,01	-1,84	2,27E-08
Cnot8	**CNOT8**	**Cnot8**	**-1,85**	0,18	-1,67	5,25E-09
NA	**MCM7**	**Mcm7**	**-1,85**	0,13	-1,71	5,87E-09
NA	**NA**	**Racgap1**	**-1,85**	0,41	-1,44	9,05E-09
Ubqln1	**UBQLN1**	**Ubqln1**	**-1,84**	0,47	-1,37	1,68E-09
Rnf114	**NA**	**NA**	**-1,83**	-0,09	-1,92	7,83E-07
Pqlc3	**NA**	**Pqlc3**	**-1,82**	0,57	-1,25	7,26E-11

NA	**NA**	**NA**	**-1,82**	0,21	-1,61	2,03E-07
Nfkbia	**NFKBIA**	**Nfkbia**	**-1,82**	0,20	-1,62	6,47E-08
NA	**NUDT21**	**Nudt21**	**-1,81**	-0,13	-1,95	4,07E-10
Clp1	**CLP1**	**Clp1**	**-1,81**	0,20	-1,61	1,91E-10
Rtel1	**NA**	**NA**	**-1,81**	0,01	-1,79	6,09E-08
NA	**NA**	**Cenpa**	**-1,81**	0,24	-1,57	2,02E-10
Uhrf1bp1	**NA**	**NA**	**-1,81**	0,34	-1,47	8,67E-10
NA	**NA**	**NA**	**-1,80**	0,23	-1,57	1,16E-07
Parp1	**NA**	**NA**	**-1,80**	-0,04	-1,84	2,50E-08
NA	**NA**	**Usp39**	**-1,79**	-0,45	-2,23	1,26E-08
Pole	**POLE**	**Pole**	**-1,78**	-0,44	-2,23	9,47E-08
	CENPO	**NA**	**-1,78**	-0,51	-2,29	4,48E-08
NA	**NA**	**NA**	**-1,78**	0,21	-1,57	1,82E-08
NA	**NA**	**NA**	**-1,77**	-0,18	-1,95	3,20E-11
Fen1	**NA**	**Fen1**	**-1,77**	0,21	-1,56	1,30E-06
NA	**NA**	**NA**	**-1,76**	0,34	-1,43	1,51E-07
Exo1	**EXO1**	**Exo1**	**-1,76**	-0,28	-2,04	1,68E-07
Hip1	**HIP1**	**Hip1**	**-1,76**	0,26	-1,50	4,23E-08
Pes1	**NA**	**Pes1**	**-1,75**	0,19	-1,56	2,71E-08
Cdc25b	**CDC25B**	**Cdc25b**	**-1,75**	0,24	-1,51	6,72E-07
NA	**ABHD2**	**NA**	**-1,74**	0,25	-1,49	1,24E-06
Snx9	**SNX9**	**NA**	**-1,74**	-0,07	-1,81	4,30E-09
NA	**ABHD2**	**NA**	**-1,74**	0,24	-1,50	1,63E-08
Cirh1a	**NA**	**Cirh1a**	**-1,74**	-0,36	-2,09	5,17E-08
NA	**NA**	**NA**	**-1,73**	0,38	-1,35	6,53E-11
Ccl2	**NA**	**Ccl2**	**-1,72**	-0,78	-2,50	4,80E-08
NA	**NA**	**NA**	**-1,71**	-0,19	-1,90	1,57E-09
Cat	**NA**	**Cat**	**-1,71**	0,03	-1,68	5,81E-07
1110008	**C20orf24**	**RGD1307**	**-1,71**	-0,03	-1,74	8,00E-09
F13Rik		**752**				
Dnajc5	**NA**	**NA**	**-1,71**	0,40	-1,30	1,42E-07
Cnn3	**CNN3**	**Cnn3**	**-1,70**	-0,11	-1,81	4,00E-10
NA	**NA**	**NA**	**-1,69**	0,34	-1,35	1,17E-07
F3	**F3**	**F3**	**-1,69**	0,10	-1,58	7,66E-08
Snap29	**NA**	**Snap29**	**-1,67**	-0,04	-1,71	7,93E-07
NA	**NA**	**NA**	**-1,67**	0,13	-1,54	9,48E-07
9530053	**NA**	**Ndufaf4**	**-1,63**	0,09	-1,54	1,49E-07
P14Rik						
5830485	**NA**	**NA**	**-1,63**	-0,47	-2,10	6,32E-08
P09Rik						

Cirh1a	**CIRH1A**	**Cirh1a**	**-1,63**	-0,40	-2,03	5,27E-09
Rnf111	**RNF111**	**Rnf111**	**-1,62**	0,15	-1,47	2,56E-09
Bri3bp	**NA**	**NA**	**-1,62**	0,39	-1,23	4,59E-08
Fam82a2	**NA**	**Fam82a2**	**-1,62**	0,38	-1,24	6,40E-07
Ddx39	**DDX39**	**Ddx39**	**-1,62**	-0,09	-1,70	2,48E-09
Ahcy	**AHCY**	**Ahcy**	**-1,61**	0,01	-1,61	1,45E-06
NA	**NA**	**Strap**	**-1,61**	0,15	-1,46	1,64E-07
NA	**NA**	**Wipf1**	**-1,61**	0,24	-1,37	3,04E-07
Tbc1d1	**NA**	**NA**	**-1,60**	0,34	-1,26	1,90E-09
NA	**NA**	**NA**	**-1,58**	0,47	-1,11	5,46E-08
NA	**FSTL1**	**NA**	**-1,57**	-0,19	-1,77	2,10E-09
Rpp30	**RPP30**	**NA**	**-1,56**	-0,15	-1,71	2,62E-07
NA	**NA**	**NA**	**-1,56**	0,08	-1,48	1,14E-07
Tsn	**NA**	**NA**	**-1,55**	-0,40	-1,94	1,96E-07
LOC674691	**TFDP1**	**MGC112830**	**-1,54**	-0,12	-1,66	7,46E-08
Ykt6	**YKT6**	**Ykt6**	**-1,54**	-0,08	-1,62	1,40E-09
Nucks1	**NA**	**Nucks1**	**-1,53**	-0,05	-1,58	1,45E-09
NA	**NA**	**MGC112830**	**-1,53**	0,18	-1,35	6,03E-10
Mgat2	**MGAT2**	**Mgat2**	**-1,51**	0,14	-1,37	6,78E-08
Clns1a	**NA**	**Clns1a**	**-1,50**	0,04	-1,46	1,68E-08
Ppp1r7	**NA**	**Ppp1r7**	**-1,50**	0,03	-1,46	2,37E-08
Mcm7	**MCM7**	**Mcm7**	**-1,49**	-0,04	-1,53	3,50E-08
NA	**NA**	**NA**	**-1,49**	0,52	-0,97	1,07E-09
NA	**NA**	**NA**	**-1,49**	-0,30	-1,79	1,82E-07
Amotl1	**NA**	**Amotl1**	**-1,49**	0,45	-1,04	2,73E-07
Rbbp5	**RBBP5**	**Rbbp5**	**-1,47**	-0,37	-1,84	1,89E-07
Uqcr10	**NA**	**LOC685322**	**-1,46**	0,33	-1,13	1,28E-07
NA	**NA**	**Slc35f2**	**-1,46**	0,17	-1,29	1,61E-06
NA	**NA**	**Kif2c**	**-1,46**	-0,03	-1,48	4,51E-07
NA	**NA**	**Trip13**	**-1,45**	-0,05	-1,50	6,05E-07
Uqcr10	**NA**	**LOC685322**	**-1,44**	0,33	-1,11	7,09E-08
NA	**NA**	**NA**	**-1,43**	0,51	-0,92	1,99E-07
Cxcl1	**NA**	**Cxcl1**	**-1,43**	-0,39	-1,82	8,64E-08
Serp1	**NA**	**Serp1**	**-1,42**	0,40	-1,02	2,28E-08
NA	**NA**	**Slc25a30**	**-1,42**	0,29	-1,13	2,70E-08
Enc1	**ENC1**	**Enc1**	**-1,40**	0,17	-1,23	1,91E-07

Thada	**NA**	**NA**	**-1,40**	-0,06	-1,46	4,38E-08
2610036 L11Rik	**NA**	**NA**	**-1,40**	0,33	-1,07	7,34E-07
Ncapd2	**NCAPD2**	**NA**	**-1,39**	0,03	-1,36	1,60E-07
Parp2	**PARP2**	**Parp2**	**-1,39**	-0,34	-1,73	4,05E-07
Tsn	**NA**	**NA**	**-1,38**	-0,19	-1,57	3,82E-10
NA	**NA**	**NA**	**-1,37**	0,02	-1,35	1,17E-06
Atic	**ATIC**	**Atic**	**-1,36**	-0,32	-1,68	8,11E-09
Tomm22	**TOMM22**	**Tomm22**	**-1,36**	0,22	-1,14	9,77E-07
Bzw2	**BZW2**	**Bzw2**	**-1,36**	-0,07	-1,43	1,74E-09
Cnot8	**NA**	**Cnot8**	**-1,33**	0,15	-1,18	1,23E-06
Zfp259	**NA**	**Zfp259**	**-1,32**	0,09	-1,24	6,80E-08
Crkl	**NA**	**NA**	**-1,32**	0,05	-1,27	1,09E-06
1500003 O03Rik	**CHP**	**Chp**	**-1,32**	0,10	-1,22	1,24E-06
Celf1	**CELF1**	**NA**	**-1,32**	0,63	-0,69	1,97E-08
Pabpn1	**PABPN1**	**Pabpn1**	**-1,31**	-0,05	-1,36	7,66E-08
NA	**NA**	**NA**	**-1,31**	0,12	-1,19	1,78E-08
NA	**SMS**	**Sms**	**-1,30**	-0,05	-1,35	1,26E-09
Tfam	**NA**	**NA**	**-1,30**	-0,13	-1,43	4,99E-07
NA	**NA**	**NA**	**-1,29**	0,16	-1,13	1,71E-06
Nedd8	**NEDD8**	**Nedd8**	**-1,28**	0,27	-1,01	3,28E-08
Atxn7l1	**ATXN7L1**	**Atxn7l4**	**-1,27**	-0,22	-1,49	1,32E-08
Kdm2a	**LOC100131150**	**Kdm2a**	**-1,27**	0,15	-1,11	3,88E-07
NA	**NA**	**NA**	**-1,26**	-0,07	-1,34	2,30E-08
Mbnl3	**NA**	**Mbnl3**	**-1,26**	-0,01	-1,27	5,04E-07
Cdc7	**NA**	**NA**	**-1,24**	-0,07	-1,31	2,02E-06
NA	**KIAA0174**	**RGD1307799**	**-1,23**	0,41	-0,81	1,78E-09
NA	**NA**	**NA**	**-1,23**	0,12	-1,10	2,47E-07
NA	**GLI3**	**NA**	**-1,22**	-0,21	-1,42	9,20E-09
Atl1	**SAV1**	**Sav1**	**-1,22**	0,12	-1,10	3,41E-09
NA	**NA**	**NA**	**-1,21**	0,17	-1,05	1,15E-08
Dbr1	**DBR1**	**Dbr1**	**-1,20**	-0,22	-1,43	4,84E-08
NA	**NA**	**NA**	**-1,20**	-0,38	-1,58	1,35E-08
Paxip1	**PAXIP1**	**Paxip1**	**-1,20**	-0,02	-1,21	1,44E-06
Bicd2	**BICD2**	**Bicd2**	**-1,18**	0,38	-0,80	9,88E-09
NA	**NA**	**NA**	**-1,18**	0,03	-1,15	1,01E-09
Nr2c1	**NA**	**NA**	**-1,17**	-0,01	-1,18	2,54E-06

Nup93	**NUP93**	**Nup93**	**-1,17**	0,00	-1,17	9,70E-07
Ift52	**NA**	**Ift52**	**-1,16**	0,14	-1,02	1,13E-07
Dscc1	**DSCC1**	**NA**	**-1,14**	-0,20	-1,34	2,88E-07
Rbm17	**RBM17**	**Rbm17**	**-1,14**	-0,15	-1,29	4,95E-09
Thbd	**NA**	**Thbd**	**-1,13**	-0,76	-1,90	2,23E-08
Prmt5	**NA**	**Prmt5**	**-1,13**	0,23	-0,89	3,45E-07
Cd44	**NA**	**Cd44**	**-1,11**	0,17	-0,94	1,30E-07
NA	**NA**	**Hdhd2**	**-1,11**	-0,09	-1,19	2,15E-08
6720463	**C13orf34**	**RGD1309**	**-1,10**	-0,14	-1,24	2,34E-07
M24Rik		**522**				
Gtl3	**C16orf80**	**Gtl3**	**-1,10**	0,23	-0,87	2,27E-08
Ptch1	**PTCH1**	**NA**	**-1,09**	0,18	-0,91	2,81E-08
Polr1e	**POLR1E**	**Polr1e**	**-1,08**	0,12	-0,96	5,79E-07
Snx9	**SNX9**	**Snx9**	**-1,07**	-0,13	-1,20	1,20E-08
Ncaph	**NA**	**Ncaph**	**-1,06**	-0,12	-1,18	9,67E-08
Mthfd1l	**MTHFD1**	**Mthfd1l**	**-1,05**	-0,06	-1,11	3,71E-07
	L					
NA	**NA**	**NA**	**-1,05**	0,34	-0,71	2,71E-07
Gins4	**GINS4**	**Gins4**	**-1,04**	-0,18	-1,23	1,33E-06
NA	**NA**	**NA**	**-1,04**	0,07	-0,96	5,27E-07
Dclre1b	**DCLRE1**	**Dclre1b**	**-1,03**	-0,40	-1,43	1,21E-07
	B					
Crkl	**NA**	**NA**	**-1,03**	-0,15	-1,18	8,41E-08
Cep72	**NA**	**NA**	**-1,01**	0,13	-0,88	2,34E-07
Eif4b	**EIF4B**	**Eif4b**	**-1,01**	0,17	-0,84	1,08E-06
Zfp276	**FANCA**	**Zfp276**	**-0,99**	-0,08	-1,07	2,55E-07
Sfrs2	**SFRS2**	**Sfrs2**	**-0,99**	0,00	-0,99	1,44E-06
Impdh2	**IMPDH2**	**Impdh2**	**-0,99**	-0,16	-1,15	7,16E-09
Dnmt1	**DNMT1**	**Dnmt1**	**-0,97**	-0,22	-1,19	1,11E-08
Ppil2	**NA**	**NA**	**-0,95**	0,18	-0,77	3,42E-07
NA	**NA**	**NA**	**-0,94**	0,22	-0,73	4,74E-07
NA	**NA**	**Prdx3**	**-0,93**	-0,04	-0,97	8,56E-07
Cks1b	**CKS1B**	**RGD1561**	**-0,93**	0,27	-0,66	8,24E-08
		797				
Gtl3	**NA**	**Gtl3**	**-0,93**	0,16	-0,76	3,68E-08
NA	**NA**	**NA**	**-0,92**	-0,04	-0,96	1,21E-08
Soat1	**NA**	**Soat1**	**-0,92**	0,01	-0,90	2,37E-06
Zfp207	**ZNF207**	**Zfp207**	**-0,92**	0,16	-0,75	2,66E-08
Rnf4	**RNF4**	**NA**	**-0,92**	0,15	-0,77	7,06E-08
D9Mgi32	**NOP56**	**Nop56**	**-0,91**	-0,37	-1,29	3,44E-08

Hbxip	**HBXIP**	**Hbxip**	**-0,90**	0,41	-0,50	5,06E-08
NA	**NA**	**Atp10a**	**-0,90**	0,01	-0,89	1,98E-07
NA	**NA**	**Odc1**	**-0,89**	0,13	-0,76	6,95E-07
Pnp2	**NA**	**Np**	**-0,89**	0,10	-0,79	2,88E-07
A130006I 12Rik	**PDSS1**	**NA**	**-0,89**	-0,22	-1,11	7,50E-07
NA	**CYB5R4**	**Cyb5r4**	**-0,88**	-0,16	-1,04	3,04E-08
NA	**NA**	**NA**	**-0,88**	0,13	-0,74	9,58E-07
1110005 A03Rik	**SFRS2**	**Sfrs2**	**-0,87**	0,01	-0,86	1,27E-07
NA	**SCD**	**Scd1**	**-0,85**	-0,11	-0,97	3,85E-09
Rad52	**NA**	**Rad52**	**-0,85**	-0,02	-0,87	3,81E-07
NA	**NA**	**NA**	**-0,85**	-0,07	-0,92	7,04E-08
Csnk2a2	**CSNK2A 2**	**Csnk2a2**	**-0,84**	-0,08	-0,93	1,35E-06
NA	**NA**	**NA**	**-0,84**	0,21	-0,63	6,07E-08
Ptma	**PTMA**	**NA**	**-0,83**	-0,14	-0,98	7,28E-08
Gins2	**NA**	**Gins2**	**-0,81**	0,08	-0,72	1,39E-08
Gm9079	**TMEM5**	**Tmem5**	**-0,80**	0,12	-0,68	9,34E-08
Pa2g4	**PA2G4**	**Pa2g4**	**-0,80**	-0,26	-1,06	4,85E-08
Cnn3	**CNN3**	**Cnn3**	**-0,80**	-0,27	-1,06	3,07E-08
Lpl	**LPL**	**Lpl**	**-0,79**	-0,37	-1,16	3,77E-07
Scd1	**NA**	**Scd1**	**-0,79**	-0,15	-0,94	1,44E-07
Gar1	**GAR1**	**Gar1**	**-0,78**	-0,07	-0,85	2,32E-07
Racgap1	**RACGAP 1**	**Racgap1**	**-0,76**	0,14	-0,62	3,15E-07
Cdk1	**CDK1**	**Cdc2**	**-0,75**	-0,03	-0,79	3,56E-07
2610028 A01Rik	**PINX1**	**Pinx1**	**-0,75**	-0,06	-0,81	2,42E-07
NA	**NA**	**NA**	**-0,74**	-0,16	-0,91	4,25E-08
NA	**BCL10**	**NA**	**-0,74**	0,02	-0,72	6,84E-08
NA	**FAM120A**	**NA**	**-0,71**	0,13	-0,58	1,41E-07
NA	**NA**	**NA**	**-0,71**	0,21	-0,50	2,42E-07
NA	**NA**	**NA**	**-0,70**	-0,13	-0,83	1,41E-07
NA	**NA**	**LOC2903 41**	**-0,69**	0,15	-0,54	7,87E-07
Spin1	**SPIN1**	**NA**	**-0,69**	-0,14	-0,83	1,01E-06
Gars	**GARS**	**Gars**	**-0,69**	-0,15	-0,84	2,91E-07
Eif3d	**EIF3D**	**Eif3d**	**-0,68**	-0,20	-0,89	8,43E-07
Rpl26	**RPL26**	**Rpl26**	**-0,68**	0,07	-0,61	3,76E-07

Mat2a	**MAT2A**	**NA**	**-0,65**	-0,29	-0,94	3,79E-08
Mat2a	**MAT2A**	**Mat2a**	**-0,64**	-0,24	-0,88	3,39E-07
Eif3d	**EIF3D**	**Eif3d**	**-0,64**	0,01	-0,63	1,73E-06
LOC677086	**NA**	**Pa2g4**	**-0,63**	-0,18	-0,81	1,82E-07
Ssrp1	**NA**	**Ssrp1**	**-0,62**	-0,01	-0,63	8,05E-08
Traf3ip1	**NA**	**NA**	**-0,62**	-0,04	-0,67	9,48E-07
NA	**RPS26**	**Rps26**	**-0,60**	0,06	-0,54	7,09E-07
NA	**SLBP**	**Slbp**	**-0,59**	-0,33	-0,92	2,62E-07
NA	**NA**	**Psat1**	**-0,59**	-0,12	-0,71	2,56E-07
Rbmxrt	**LOC100131735**	**Rbmxrtl**	**-0,57**	-0,13	-0,70	2,28E-07
NA	**NA**	**NA**	**-0,57**	0,08	-0,49	5,00E-07
Tmem156	**TMEM156**	**NA**	**-0,57**	-0,16	-0,73	5,81E-07
NA	**NA**	**Psat1**	**-0,55**	-0,16	-0,72	5,84E-07
Shq1	**NA**	**Shq1**	**-0,55**	-0,04	-0,59	9,67E-07
Zfp207	**ZNF207**	**Zfp207**	**-0,51**	0,03	-0,48	1,40E-06
Acsl5	**ACSL5**	**Acsl5**	**-0,50**	0,01	-0,49	2,52E-06

11.3 Appendix 3: List of up-regulated genes upon pm-7 treatment

mouse	human	rat	pm-7/pm-neg	pm-neg/cells	pm-7/cells	P.Value
NA	NA	NA	3,65	0,13	3,77	1,22E-11
NA	NA	NA	3,49	0,15	3,64	3,07E-10
Ntn4	NTN4	NA	3,43	-0,03	3,39	8,13E-10
Slc40a1	NA	Slc40a1	3,20	-0,16	3,04	1,54E-08
NA	NA	NA	3,11	0,91	4,02	5,77E-09
Mmp12	MMP12	Mmp12	2,96	0,17	3,13	2,25E-08
Ccdc67	NA	Ccdc67	2,94	0,10	3,05	8,43E-09
NA	NA	NA	2,86	-0,01	2,85	1,47E-08
Tmprss6	NA	NA	2,71	0,65	3,36	5,59E-07
Tgfbr3	TGFBR3	NA	2,55	-1,53	1,02	1,26E-09
Slc40a1	SLC40A1	Slc40a1	2,52	0,59	3,12	7,01E-09
Armcx3	ARMCX3	Armcx3	2,35	-0,75	1,60	1,50E-11
Ypel5	YPEL5	Ypel5	2,33	0,62	2,95	4,26E-10
Ypel3	YPEL3	RGD1564579	2,25	0,44	2,69	3,77E-08
6430548M08Rik	NA	NA	2,16	0,75	2,91	4,50E-08
2810407C02Rik	LOC100133398	Selt	2,15	-1,60	0,55	8,84E-11
Vldlr	VLDLR	Vldlr	2,13	0,34	2,46	1,15E-07
Hbp1	HBP1	Hbp1	2,07	-0,02	2,06	1,01E-06
Ptprg	PTPRG	Ptprg	2,03	-0,09	1,94	1,34E-07
Mx2	MX1	Mx2	1,99	0,27	2,26	4,77E-08
Pde4dip	PDE4DIP	Pde4dip	1,99	-0,32	1,67	2,02E-07
Arhgef16	NA	LOC687105	1,96	0,66	2,63	1,95E-07
NA	COG5	Hbp1	1,95	0,05	2,00	1,95E-06
NA	NA	NA	1,94	0,67	2,61	1,22E-09
NA	NA	NA	1,93	0,18	2,11	2,47E-08
NA	SLC1A4	Slc1a4	1,91	0,24	2,15	4,08E-08
Osgin1	NA	Osgin1	1,91	0,87	2,78	8,60E-08

Mut	**MUT**	**NA**	**1,90**	-0,66	1,24	5,90E-08
Synm	**NA**	**Synm**	**1,88**	0,03	1,91	6,39E-08
Myo10	**NA**	**NA**	**1,88**	0,28	2,15	2,27E-09
Zpbp2	**ZPBP2**	**Zpbp2**	**1,85**	-0,28	1,57	1,23E-08
Ctla2b	**NA**	**Ctla2a**	**1,81**	-0,42	1,39	3,60E-08
NA	**NA**	**NA**	**1,80**	-0,44	1,36	7,25E-07
C03004	**TXNDC1**	**Txndc1**	**1,77**	-1,05	0,72	5,64E-10
3A13Rik	**2**	**2**				
Riok3	**RIOK3**	**Riok3**	**1,75**	0,03	1,78	3,51E-07
Col4a3b	**COL4A3**	**Col4a3b**	**1,73**	-0,25	1,48	6,27E-08
p	**BP**	**p**				
Ndfip2	**NDFIP2**	**Ndfip2**	**1,71**	-0,88	0,83	1,73E-09
Nqo1	**NQO1**	**NA**	**1,69**	-0,12	1,57	2,58E-10
Taok3	**TAOK3**	**Taok3**	**1,69**	-0,18	1,51	1,21E-07
NA	**NA**	**NA**	**1,69**	-0,01	1,67	5,28E-10
Fth1	**BEST1**	**NA**	**1,67**	0,19	1,86	9,13E-08
1110003	**C4orf34**	**RGD131**	**1,65**	0,01	1,66	2,28E-08
E01Rik		**1122**				
NA	**NA**	**NA**	**1,65**	-0,08	1,57	5,26E-09
NA	**NA**	**NA**	**1,64**	0,04	1,68	5,73E-07
Tmem1	**TMEM1**	**Tmem1**	**1,64**	0,23	1,87	5,44E-09
35	**35**	**35**				
Anxa3	**ANXA3**	**Anxa3**	**1,64**	-0,04	1,59	8,23E-07
NA	**NA**	**NA**	**1,60**	-0,02	1,59	1,54E-06
Ccdc93	**CCDC93**	**Ccdc93**	**1,60**	-0,31	1,30	3,01E-09
Nt5c2	**NT5C2**	**NA**	**1,59**	-0,27	1,32	5,94E-10
Vwa5a	**VWA5A**	**Vwa5a**	**1,58**	0,40	1,98	5,94E-10
NA	**TCEAL4**	**NA**	**1,58**	0,56	2,13	5,87E-07
NA	**NA**	**NA**	**1,57**	0,52	2,09	6,52E-10
Abcc5	**ABCC5**	**Abcc5**	**1,57**	0,04	1,61	6,72E-10
Rab8b	**NA**	**NA**	**1,56**	-0,17	1,38	9,06E-07
Rcan1	**NA**	**Rcan1**	**1,56**	0,25	1,81	2,85E-09
NA	**NA**	**NA**	**1,56**	-0,09	1,47	6,57E-07
Nt5c2	**NT5C2**	**NA**	**1,56**	-0,22	1,34	1,89E-07
NA	**NA**	**NA**	**1,54**	-0,10	1,44	4,76E-07
Rit1	**RIT1**	**Rit1**	**1,54**	0,25	1,79	7,22E-09
Rufy3	**NA**	**NA**	**1,53**	-0,31	1,22	8,51E-07
Gmpr2	**GMPR2**	**Gmpr2**	**1,53**	-0,61	0,91	1,23E-09
NA	**NA**	**NA**	**1,52**	-0,33	1,20	9,29E-07
2210403	**NA**	**NA**	**1,52**	0,11	1,63	7,02E-07

K04Rik						
Zfp455	**ZNF99**	**Zfp455**	**1,52**	0,00	1,52	2,77E-06
Sqrdl	**NA**	**Sqrdl**	**1,51**	0,15	1,65	1,31E-08
Dusp3	**NA**	**Dusp3**	**1,48**	1,04	2,52	4,79E-08
Adam23	**ADAM23**	**Adam23**	**1,46**	0,18	1,65	2,86E-08
Hsdl2	**HSDL2**	**Hsdl2**	**1,45**	-0,38	1,07	5,47E-07
Dusp16	**NA**	**Dusp16**	**1,42**	0,01	1,43	7,39E-07
Sri	**SRI**	**LOC683667**	**1,42**	-0,28	1,14	9,95E-09
Clu	**NA**	**Clu**	**1,41**	-0,02	1,40	6,73E-08
Ndrg3	**NDRG3**	**Ndrg3**	**1,41**	-0,04	1,37	3,87E-07
Clic4	**CLIC4**	**Clic4**	**1,39**	0,02	1,41	7,22E-07
Nit1	**NIT1**	**Nit1**	**1,39**	-0,22	1,17	8,67E-07
1110003E01Rik	**NA**	**NA**	**1,39**	0,16	1,55	1,19E-08
Nit1	**NIT1**	**Nit1**	**1,39**	-0,08	1,30	5,62E-07
NA	**NA**	**NA**	**1,38**	0,66	2,03	9,85E-09
Ccnd2	**NA**	**NA**	**1,37**	0,16	1,53	2,83E-08
Ptpdc1	**NA**	**NA**	**1,36**	0,34	1,70	1,01E-09
Irf9	**IRF9**	**Irf9**	**1,36**	0,35	1,71	1,61E-07
Taok3	**TAOK3**	**Taok3**	**1,35**	-0,25	1,11	3,79E-08
NA	**OSTM1**	**NA**	**1,35**	-0,56	0,79	1,13E-07
Appl2	**APPL2**	**Appl2**	**1,34**	0,03	1,38	6,72E-07
Rab4a	**NA**	**Rab4a**	**1,34**	0,09	1,43	3,46E-07
Car5b	**CA5B**	**Car5b**	**1,32**	0,37	1,69	9,68E-07
Xdh	**NA**	**Xdh**	**1,32**	0,59	1,91	1,81E-07
Fundc1	**FUNDC1**	**Fundc1**	**1,31**	0,04	1,35	5,74E-09
Pdyn	**NA**	**NA**	**1,30**	0,40	1,70	1,22E-09
Gpnmb	**NA**	**Gpnmb**	**1,29**	0,38	1,68	2,24E-07
Glcci1	**GLCCI1**	**RGD1563612**	**1,29**	-0,29	1,00	4,93E-07
Lpin1	**LPIN1**	**NA**	**1,29**	0,03	1,32	4,69E-07
Gyg	**NA**	**Gyg1**	**1,29**	0,00	1,28	1,52E-08
Fbxl4	**FBXL4**	**Fbxl4**	**1,28**	0,32	1,61	1,05E-06
Ahnak2	**NA**	**NA**	**1,28**	0,48	1,75	3,17E-08
Acaa2	**ACAA2**	**Acaa2**	**1,28**	-0,68	0,60	1,17E-09
NA	**NA**	**Tes**	**1,28**	0,12	1,40	1,04E-06
Nova1	**NOVA1**	**Nova1**	**1,28**	-0,31	0,97	4,89E-08

Kpna1	**KPNA1**	**Kpna1**	**1,27**	-0,16	1,11	3,92E-07
Rcan1	**NA**	**Rcan1**	**1,24**	0,32	1,57	5,95E-08
Zpbp2	**ZPBP2**	**Zpbp2**	**1,23**	-0,62	0,61	2,50E-08
Plcd3	**NA**	**Plcd3**	**1,21**	0,27	1,49	8,58E-07
Il18bp	**IL18BP**	**Il18bp**	**1,21**	-0,13	1,08	1,03E-06
Chmp2b	**CHMP2B**	**NA**	**1,20**	0,24	1,44	1,68E-08
NA	**NA**	**NA**	**1,19**	0,36	1,55	9,37E-07
NA	**NA**	**NA**	**1,19**	0,42	1,62	1,87E-08
Ap2b1	**AP2B1**	**NA**	**1,19**	0,04	1,23	5,50E-07
NA	**NA**	**NA**	**1,19**	0,32	1,51	2,01E-08
NA	**NA**	**Abcc3**	**1,18**	0,37	1,54	8,25E-08
Sh3glb1	**SH3GLB1**	**Sh3glb1**	**1,17**	-0,29	0,88	5,59E-09
Zfand2a	**NA**	**NA**	**1,17**	0,17	1,33	1,49E-06
Aig1	**NA**	**NA**	**1,15**	0,20	1,34	1,47E-07
NA	**NA**	**NA**	**1,14**	0,51	1,65	5,07E-08
2210013O21Rik	**LOC550643**	**NA**	**1,14**	0,45	1,58	1,59E-07
Lgmn	**LGMN**	**Lgmn**	**1,14**	0,26	1,40	3,37E-09
Ptgr1	**PTGR1**	**Ptgr1**	**1,13**	0,05	1,18	4,89E-07
NA	**NA**	**NA**	**1,13**	0,14	1,27	8,04E-09
Ppcs	**NA**	**NA**	**1,12**	0,23	1,35	4,61E-07
Anxa7	**ANXA7**	**Anxa7**	**1,12**	0,12	1,24	3,06E-07
Scarb2	**SCARB2**	**Scarb2**	**1,11**	0,04	1,16	6,74E-07
Gbas	**GBAS**	**NA**	**1,10**	-0,18	0,93	3,75E-07
Akt3	**AKT3**	**NA**	**1,10**	0,40	1,50	6,15E-10
Smcr8	**NA**	**NA**	**1,10**	-0,14	0,95	7,32E-09
NA	**RECK**	**Reck**	**1,09**	-0,19	0,90	8,35E-08
NA	**NA**	**NA**	**1,08**	0,67	1,75	7,09E-08
Btbd1	**BTBD1**	**Btbd1**	**1,07**	-0,04	1,04	1,29E-06
NA	**NA**	**NA**	**1,07**	0,13	1,20	7,04E-09
Wdr26	**WDR26**	**Wdr26**	**1,07**	0,07	1,14	1,51E-08
Usp13	**USP13**	**Usp13**	**1,04**	0,19	1,23	2,34E-08
Lactb2	**LACTB2**	**Lactb2**	**1,03**	0,18	1,21	6,59E-09
Rab7	**NA**	**Rab7a**	**1,03**	0,09	1,12	8,09E-09
Elmo1	**ELMO1**	**Elmo1**	**1,03**	-0,04	0,99	5,20E-07
Hars	**HARS**	**Hars**	**1,02**	-0,13	0,88	4,42E-09
Sdf2	**SDF2**	**Sdf2**	**1,01**	0,24	1,25	1,25E-07

Galk2	**GALK2**	**Galk2**	**1,01**	0,17	1,19	1,15E-07
NA	**NA**	**NA**	**1,01**	0,33	1,34	5,35E-07
Clu	**NA**	**Clu**	**1,01**	0,33	1,34	1,24E-09
NA	**INPP4A**	**Inpp4a**	**1,01**	0,24	1,25	2,33E-08
Pex12	**NA**	**Pex12**	**1,00**	0,13	1,13	7,65E-07
NA	**NA**	**NA**	**0,99**	0,19	1,18	1,07E-07
Tmeff2	**TMEFF2**	**Tmeff2**	**0,98**	0,10	1,08	9,71E-07
Ube2w	**LOC729696**	**NA**	**0,98**	-0,02	0,96	8,22E-08
Nhlrc3	**NA**	**NA**	**0,98**	0,16	1,14	1,46E-07
NA	**LOC732229**	**Zfand5**	**0,98**	0,13	1,11	2,27E-08
Cyp2j13	**CYP2J2**	**Cyp2j13**	**0,97**	0,22	1,19	6,44E-07
Gypc	**NA**	**Gypc**	**0,97**	0,36	1,33	2,28E-08
Rnase4	**NA**	**Rnase4**	**0,97**	0,64	1,61	2,34E-08
Prdm2	**NA**	**Prdm2**	**0,95**	0,16	1,11	8,45E-07
Yipf4	**YIPF4**	**Yipf4**	**0,94**	-0,12	0,82	1,26E-06
Nit2	**NA**	**NA**	**0,93**	-0,15	0,78	1,23E-06
Ppip5k1	**PPIP5K1**	**Hisppd2a**	**0,93**	0,14	1,07	2,77E-07
Rnf19a	**RNF19A**	**Rnf19a**	**0,92**	-0,17	0,75	5,77E-07
Ptgr1	**PTGR1**	**Ptgr1**	**0,91**	0,08	0,99	1,94E-06
Gm10652	**RWDD3**	**Rwdd3**	**0,90**	0,15	1,05	8,14E-07
Cd109	**CD109**	**NA**	**0,90**	0,11	1,01	8,39E-07
Sccpdh	**SCCPDH**	**Sccpdh**	**0,89**	0,11	0,99	4,56E-07
Tmed10	**TMED10**	**Tmed10**	**0,88**	-0,10	0,78	4,42E-08
Fgf18	**NA**	**Fgf18**	**0,87**	0,41	1,28	1,70E-07
Psmd11	**PSMD11**	**Psmd11**	**0,87**	-0,12	0,75	8,40E-07
Rab7	**NA**	**Rab7a**	**0,86**	0,20	1,06	3,15E-08
Minpp1	**NA**	**NA**	**0,85**	-0,02	0,83	1,89E-06
Fundc1	**NA**	**Fundc1**	**0,85**	0,21	1,05	1,45E-07
Dusp16	**DUSP16**	**NA**	**0,85**	0,31	1,16	6,44E-08
Pacsin2	**PACSIN2**	**Pacsin2**	**0,84**	0,01	0,85	5,69E-07
Pcnx	**PCNX**	**Pcnx**	**0,84**	0,21	1,05	3,62E-08
Bdnf	**BDNF**	**Bdnf**	**0,82**	-0,01	0,81	3,06E-07
Scpep1	**NA**	**Scpep1**	**0,80**	0,25	1,06	8,64E-07
NA	**NA**	**NA**	**0,80**	0,29	1,09	9,15E-08

Ugt1a1	**NA**	**NA**	**0,80**	-0,01	0,80	2,77E-07
NA	**NA**	**NA**	**0,80**	0,01	0,81	2,50E-06
Plekhb2	**NA**	**Plekhb2**	**0,80**	0,36	1,16	7,60E-08
Nras	**NRAS**	**Nras**	**0,80**	-0,11	0,68	1,25E-06
NA	**NA**	**NA**	**0,80**	0,08	0,87	2,53E-07
Prdxdd1	**PRDXDD1P**	**Ncrna00117**	**0,79**	0,09	0,89	4,15E-07
NA	**TMEM66**	**Tmem66**	**0,79**	0,16	0,95	3,39E-07
Rab11a	**RAB11A**	**Rab11a**	**0,78**	0,08	0,86	7,48E-08
Cox16	**NA**	**Cox16**	**0,78**	-0,01	0,77	1,39E-06
Map1lc3b	**NA**	**NA**	**0,78**	0,36	1,14	9,22E-08
Ddx59	**DDX59**	**Ddx59**	**0,78**	-0,07	0,71	1,27E-06
Dhrs7	**DHRS7**	**NA**	**0,77**	0,16	0,93	1,22E-06
Usp4	**NA**	**Usp4**	**0,76**	0,22	0,99	2,48E-07
Sod1	**SOD1**	**Sod1**	**0,76**	0,14	0,90	9,80E-09
App	**APP**	**App**	**0,76**	0,08	0,84	1,67E-07
Dennd5a	**DENND5A**	**Dennd5a**	**0,75**	0,44	1,19	2,24E-07
Dctn5	**DCTN5**	**Dctn5**	**0,75**	0,10	0,85	1,31E-07
Gne	**GNE**	**Gne**	**0,75**	0,14	0,89	1,18E-06
4930535I16Rik	**NA**	**NA**	**0,74**	0,23	0,98	6,78E-07
Clu	**NA**	**Clu**	**0,74**	0,24	0,98	4,42E-07
Mark1	**MARK1**	**Mark1**	**0,74**	0,15	0,89	1,27E-07
NA	**VAPA**	**Vapa**	**0,71**	-0,10	0,61	1,53E-07
NA	**NA**	**NA**	**0,71**	0,28	0,99	6,60E-08
Arl6ip5	**ARL6IP5**	**Arl6ip5**	**0,70**	0,22	0,92	1,40E-08
Psap	**NA**	**Psap**	**0,69**	0,44	1,14	4,39E-08
LOC100233175	**NA**	**LOC100233176**	**0,68**	0,12	0,80	1,34E-06
Mgst1	**NA**	**NA**	**0,67**	0,10	0,77	6,93E-08
LOC100043810	**NA**	**Rin2**	**0,67**	0,20	0,87	2,98E-07
Pts	**PTS**	**Pts**	**0,66**	-0,07	0,59	1,99E-06
NA	**NA**	**NA**	**0,64**	-0,04	0,60	1,20E-06
8430410K20Rik	**KIAA1826**	**MGC105560**	**0,64**	0,23	0,87	7,04E-07

Itgb1bp1	**ITGB1BP1**	**Itgb1bp1**	**0,62**	0,08	0,71	1,36E-07
Cetn3	**CETN3**	**Cetn3**	**0,62**	-0,01	0,61	2,72E-06
NA	**NA**	**NA**	**0,62**	0,05	0,67	2,06E-07
Tmed4	**TMED4**	**Tmed4**	**0,60**	0,04	0,64	1,48E-06
Tmem50a	**TMEM50A**	**Tmem50a**	**0,59**	0,15	0,75	1,43E-07
Ghitm	**GHITM**	**Ghitm**	**0,59**	0,09	0,68	1,81E-07
Parl	**PARL**	**Parl**	**0,59**	0,03	0,62	7,59E-07
Mbtps1	**MBTPS1**	**Mbtps1**	**0,59**	-0,04	0,55	9,35E-07
App	**APP**	**App**	**0,59**	0,27	0,86	1,89E-08
Lactb2	**LACTB2**	**Lactb2**	**0,58**	0,37	0,95	1,05E-07
Leprot	**LEPROT**	**Leprot**	**0,57**	0,46	1,04	3,87E-08
Ctps2	**CTPS2**	**Ctps2**	**0,57**	0,14	0,71	5,07E-07
Mgst1	**MGST1**	**Mgst1**	**0,57**	0,10	0,66	4,59E-07
Gclm	**GCLM**	**Gclm**	**0,56**	0,03	0,59	4,76E-07
Tsc22d1	**TSC22D1**	**Tsc22d1**	**0,56**	0,03	0,59	7,83E-07
Gpbp1l1	**GPBP1L1**	**NA**	**0,53**	0,05	0,58	1,28E-06
Gla	**GLA**	**Gla**	**0,51**	0,46	0,97	4,02E-08
Degs1	**DEGS1**	**Degs1**	**0,50**	0,05	0,55	6,70E-07
AF085738	**NA**	**Gnas**	**0,47**	0,14	0,61	2,21E-07
Pdia6	**PDIA6**	**Pdia6**	**0,46**	0,06	0,52	7,92E-07
Ostf1	**OSTF1**	**NA**	**0,41**	0,34	0,75	8,05E-08